CHEMISTRY OF INOSITOLS: INVESTIGATION ON THE SOLID-STATE ACYL TRANSFER REACTIONS OF INOSITOL DERIVATIVES

AND

THE USE OF SULFONATE PROTECTING GROUPS FOR THE SYNTHESIS OF CYCLITOL DERIVATIVES

Thesis

Submitted to the

UNIVERSITY OF PUNE

for the degree of

Doctor of philosophy

in Chemistry

by

Manash Pratim Sarmah

Division of Organic Chemistry (Synthesis)
National Chemical Laboratory
Pune-411008
April 2005

Dedicated to my parents

CERTIFICATE

This is to certify that the work incorporated in the thesis entitled "**Chemistry of inositols: Investigation on the solid-state acyl transfer reactions of inositol derivatives and the use of sulfonate protecting groups for the synthesis of cyclitol derivatives**" submitted by **Manash Pratim Sarmah** was carried out by him under my supervision at the National Chemical Laboratory, Pune, India. Such materials, obtained from other sources have been duly acknowledged in the thesis.

Date:

(Dr. M. S. SHASHIDHAR)

Research Guide

Division of Organic Chemistry (Synthesis)

National Chemical Laboratory

Pune-411 008

DECLARATION

I hereby declare that the thesis entitled "**Chemistry of inositols: Investigation on the solid-state acyl transfer reactions of inositol derivatives and the use of sulfonate protecting groups for the synthesis of cyclitol derivatives**" submitted for Ph. D. degree to the University of Pune has not been submitted by me for a degree to any other University.

Date: **(MANASH PRATIM SARMAH)**

Division of Organic Chemistry (Synthesis)

National Chemical Laboratory

Pune-411 008

Acknowledgement

This thesis is the result of five years of work whereby I have been accompanied and supported by many people. It is a pleasant aspect that I have now the opportunity to express my gratitude for all of them.

The first person I would like to thank is my research supervisor, Dr. M. S. Shashidhar. I have known Dr. Shashidhar as a sympathetic and principle-centered person. His integral view on research and his mission for providing 'only high-quality work and training and not less', has made a deep impression on me. I owe him lots of gratitude for having me shown this way of research. Besides of being an excellent supervisor, Dr. Shashidhar was a good friend to me during my stay in NCL.

I am thankful to Dr. K. N. Ganesh, Head, OCS division and Director, NCL for providing me an opportunity to work in the OCS division of NCL and for providing the required infrastructure. I also thank Dr. Ganesh Pandey, Dr. B.G. Hazra, Dr. T. Pathak and Dr. N. N. Joshi for their encouragement.

I would like to thank Dr. Mohan M. Bhadbhade and Mr. Rajesh G. Gonnade of the single crystal X-ray crystallography group for the fruitful discussions, suggestions and for providing me with the crystal data in time. Besides of being a good crystallographer, Rajesh is also a very good friend to me, who was available for help and advices both within and outside NCL whenever needed. I would also like to thank Dr. (Mrs.) V. G. Puranik and Mrs. Renu Pasricha for their constant encouragement.

*My colleagues, Dr. T. Praveen, Dr. K. M. Sureshan, Dr. Aditya Kunar Sanki, Sachin, Devaraj, Shailesh, Murali, Manoj, Gaurav and Madhuri, all gave me the feeling of being at home at work by maintaining a cheerful atmosphere in the laboratory. I take this opportunity to thank them for their kind co-operation during my stay in NCL. I also thank Suni*ji *and More*ji *for their regular help in the laboratory maintenance.*

I would like to thank my friends Dr. Meena, Dr. B. N. Tosh, Dr. Santosh, Akhilesh, Anupam, Anuj, Ashwani, Govindaraju, Nagendra, Pallavi, Rani, Ramalingam, Dinesh, Umasankara, Raman, Khirud, Gitali, Deepak, Bapu, Namdev, Nilkanth, Sudhir, Anamitra, Kartick, Balakrishna, Prabal, Sanjay, Subhasini, Arindam, Rahul, Ankur, Pranjal Baruah, Pranjal Kalita, Sasanka, Jadab, Sanjib, Lakshi, Vaneet, Upendra, Diganta, Shivanand, Satyajyoti, Sofia and many others for being with me whenever I needed. I must acknowledge the encouragements from Mani (Ranju) from the day one she is known to me.

I wish to thank Prof. B. C. Goswami and Dr. P. Phukan of Gauhati University, Dr. R. C. Deka of Tezpur University, Prof. B. C. Bhuyan of Assam Engineering College and Mrs. Bidyavati Bhuyan of Cotton College for their all time encouragement. I feel great sense of gratitude for Mr. Khiradhar Baruah and Mr. Nabajyoti Sharma Baruah of Biswanath College, where I did my intermediate and graduation, who has introduced me to this fascinating subject and inspired me to come for research.

I am grateful to my parents, who formed part of my vision and taught me the good things that really matter in life. The love and affection of my brother and other family members are also gratefully acknowledges.

Financial support from CSIR, New Delhi in the form of my junior and senior research fellowships is gratefully acknowledged.

The chain of my gratitude would be definitely incomplete if I would forget to thank the first cause of this chain, using Aristotle's words, The Prime Mover. My deepest and sincere gratitude for inspiring and guiding this humble being.

April 11, 2005; Pune, India. (**Manash Pratim Sarmah**)

CONTENTS

Part B.
Use of sulfonate protecting groups for the synthesis of cyclitol derivatives

Section 1. Sulfonate groups as hydroxyl protecting groups: A Review

Section 2. Synthesis of cyclitol derivatives with the aid of *p*-toluenesulfonyl group for the protection of inositol hydroxyl groups

ABBREVIATIONS

Ac	Acetyl
All	Allyl
Als	Allyl sulfonyl
aq.	Aqueous
Bn	Benzyl
bp	Boiling point
Bu	Butyl
Bz	Benzoyl
Calcd	Calculated
Cat.	Catalytic
Conc.	Concentration
CS	1*S*-(+)-camphorsulfonyl
d	Day
DABCO	1,4-diazabicyclo [2,2,2]-octane
DBU	1,8-diaza bicycle [5,4,0]-undecane
DCC	N, N-dicyclohexyl carbodiimide
DCM	Dichloromethane
DEAD	Diethyl azodicarboxylate
dia	Diastereomer
DMAP	4-(dimethylamino)-pyridine
DME	1,2-dimethoxy ethane
DMF	N, N–dimethyl formamide
DMEU	1,3-dimethyl-2-imidazolidinone
DMPU	N, N'-dimethylpropyleneurea
DMN	1,5-dimethoxynaphthalene
DMNP	(4,8-dimethoxynaphathyl) propionic acid
DMSO	Dimethyl sulfoxide

DMTr	Dimethoxy trityl or dimethoxy triphenylmethyl
DSC	Differential scanning calorimetry
DTA	Differential thermal analysis
EI-MS	Electron impact mass spectrometry
El	Electrophile
ent	Enantiomer
Et	Ethyl
eq.	Equivalent
EWG	Electron withdrawing group
FT	Fourier Transformed
g	Gram
GC-MS	Gas chromatography-mass spectrometry
GPI	Glycosidylphospatidylinositol
h	Hour
HPLC	High performance liquid chromatography
i-Bu	*iso*-Butyl
IC	Inhibition constant
Ins(1,2,4)P_3	*myo*-Inositol-1,2,4-trisphosphate
Ins(1,2,5)P_3	*myo*-Inositol-1,2,5-trisphosphate
Ins(1,2,6)P_3	*myo*-Inositol-1,2,6-trisphosphate
Ins(1,3,4,5)P_4	*myo*-Inositol-1,3,4,5-tetrakisphosphate
i-Pr	*iso*-Propyl
IR	Infrared
LDA	Lithium diisopropylamide
LVT	Low valent titanium
m-CPBA	*meta*-Chloroperbenzoic acid
Me	Methyl

min	Minute
mL	Milli liter
mM	Milli Molar
mmol	Milli mole
mp	Melting point
Ms	Mesyl or methanesulfonyl
MS	Molecular sieves
N	Normal
n-Bu	Normal butyl
NMO	N-methylmorpholin-N-oxide
NMP	N-methyl-2-pyrrolidone
NMR	Nuclear magnetic resonance
Npes	2-(4-nitrophenyl)ethylsulfonyl
Nu	Nucleophile
ORTEP	Oak Ridge thermal ellipsoid plot
PCC	Pyridinium chlorocromate
PDC	Pyridinium dichromate
Ph	Phenyl
PI-PLC	Phospatidylinositol specific phospholipase C
Piv	Pivaloyl
PMB	*para*-Methoxy benzyl
PMP	Pentamethyl pipyridine
PMPh	*para*-Methoxy phenyl
PPL	Pig Pancreas Lipase
PPTS	Pyridinium *para*-toluene sulfonate
psi	Per square inch
Pyr	Pyridine
RHT	Reverse hydrogen transfer
rt	Room temperature (23-30 ºC)
scyllo-Ins(1,2)P_2	*scyllo*-Inositol 1,2-bisphosphate

scyllo-Ins(1,3)P_2	*scyllo*-Inositol 1,3-bisphosphate
scyllo-Ins(1,2,3,5)P_4	*scyllo*-Inositol 1,2,3,5-tetrakisphosphate
scyllo-Ins(1,2,4,5)P_4	*scyllo*-Inositol 1,2,4,5-tetrakisphosphate
t-Bu	Tertiary butyl
TBS	Tertiary butyl dimethyl silyl
TEAB	Tetraethyl ammonium bromide
Tempr.	Temperature
Tf	Triflate or trifluoromethane sulfonate
TFA	Trifluoroacetic acid
TG	Thermo gravimetry
THF	Tetrahydrofuran
TLC	Thin layer chromatography
Ts	Tosyl or toluene 4-sulfonyl
UV	Ultraviolate
µL	Micro liter

Synopsis of the thesis

The thesis entitled '**Chemistry of inositols: Investigation on the solid state acyl transfer reactions of inositol derivatives and the use of sulfonate protecting groups for the synthesis of cyclitol derivatives**' consists of two parts. Part A: Investigation on the acyl transfer reactions of inositol derivatives in the solid state. Part B: Use of sulfonate protecting groups for the synthesis of cyclitol derivatives. Part A consists of two sections; Section 1 gives an account of solid state group transfer reactions reported in the literature relevant to the work described in Section 2. The work done on the solid state acyl transfer reactions of inositol derivatives is presented in Section 2. Part B also consists of two sections; Section 1 is a review of the literature on the use of sulfonate protecting groups for the synthesis of various organic compounds. Section 2 presents the work done on the synthesis of cyclitol derivatives with the aid of sulfonate groups for the protection of hydroxyl groups. Both Part A and Part B also have experimental sections and appendices, which give detailed experimental procedures, spectroscopic, crystallographic and other analytical data on the compounds prepared during the course of this investigation.

Part A: Investigation on the solid state acyl transfer reactions of inositol derivatives.

Section 1. An illustrative review on the solid state group transfer reactions.

This section reviews the literature on organic group transfer reactions in the solid state. Reports on group transfer reactions of organic compounds are very common in solution, but are rare in the solid state. Solid-state reactions are gaining interest among organic chemists because the product selectivity of reactions in the solid state is often different from their selectivity in solution. In the solid state, the reactivity depends on steric packing factors in crystals and perhaps on electronic properties of molecules. While, in solution the reactivity is mainly dependent on the electronic and steric properties of the reactant molecules. Also, since solvents are not needed to carry out reactions in the solid state, such reactions have the potential to be developed as green reactions. Solid state reactions coupled with the X-ray crystal structure data (of reactants and / or products) can also provide valuable information on the mechanisms of reactions that cannot be obtained by observing the corresponding reactions in solution. For example, good understanding of the mechanisms of reactions like addition to C=C, S_N2 displacement reactions and Chapman rearrangement-like reactions, have resulted because

of studies conducted in the solid state. Although addition to C=C in the solid state is well investigated, these are not covered in the present review as they have been discussed extensively in the literature.

Section 2. Solid state acyl transfer reactions in inositol derivatives

Inositols and their derivatives have continued to attract the attention of chemists and biologists due to their ubiquitous presence in animals and plants as well as their involvement in several biological processes in eukaryotic cells. Solution state acyl migration reactions among the hydroxyl groups of inositol derivatives have been used for the preparation of phosphoinositols in the last two decades. Most of these acyl migration reactions however, resulted in the formation of a mixture of isomeric esters, which are not easy to separate and consequently in poor isolated yield of the required *O*-protected cyclitol intermediates. The first example of a facile acyl transfer reaction in the solid state (**Scheme 1**) was reported from our laboratory[1] few years ago. Hydrogen bonding interaction between the carbonyl oxygen of the C-2-*O*-benzoyl group of one molecule of **1** and the hydrogen atom of C-6-hydroxyl group of another molecule in the same crystal, as well as electrophile (C=O) – nucleophile (OH) interactions between the two reacting molecules were thought to be responsible for the facile reaction in the solid state.

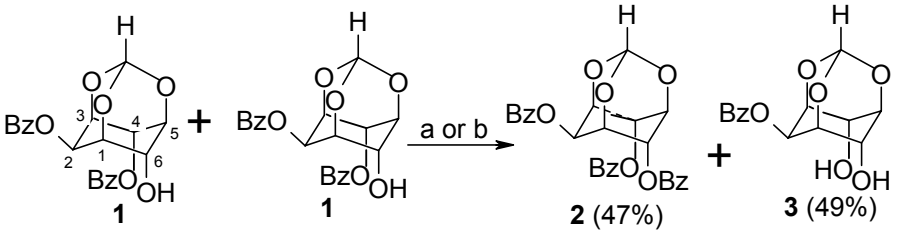

Scheme 1. Reagents and conditions: a) Na_2CO_3 (8 eq), 140 °C, 60 h; b) Na_2CO_3 (8 eq), microwave, 25 min.

Encouraged by the discovery of a clean solid-state acyl transfer reaction (**Scheme 1**) we sought out to explore such reactions further with the following objectives. (a) Can we find other inositol derivatives that exhibit solid-state acyl transfer reaction and if so could they be used for the preparation of protected *myo*-inositol derivatives? (b) How do minor modifications in the molecular structure reflect in their reactivity in the solid state? (c) Can we utilize the non-bonded intermolecular interaction parameters, similar to those observed in the crystals of the dibenzoate **1** that were used to rationalize its reactivity, to predict the reactivity of other hydroxyl esters? Accordingly, this section describes

preparation of several inositol based hydroxyl esters (**Scheme 2**) and study of their acyl transfer reactivity in the solid state. Acyl transfer reactions of some of the esters were carried out in the solution and molten states for comparison. Correlation of the observed reactivity in the solid state with the crystal structure of the reactants was also attempted. Since crystals of **1**, **8** and **19** were found to be isostructural, we tried to crystallize them together from different solvents. We were able to obtain 1:1 molecular complex crystals of **1** and **8** (**1.8**) which also showed good acyl transfer reactivity in the sold state.

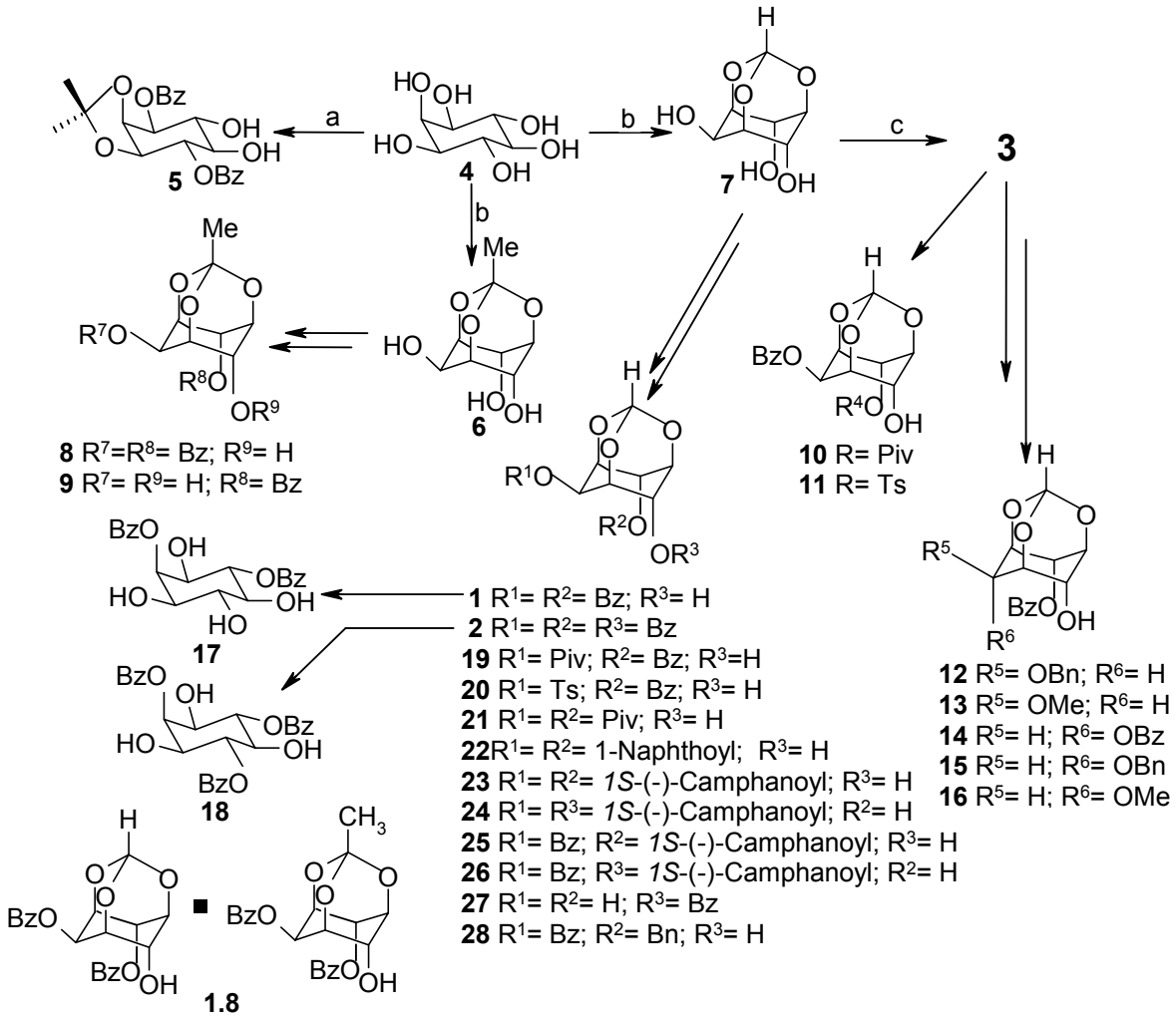

Scheme 2. Reagents and conditions: as in a) reference 2; b) reference 3; c) reference 4.

From the results obtained it was observed that structurally similar hydroxyl esters show widely different reactivity under similar conditions. An interesting observation was that minor modification in the molecular structure (for example changing from orthoformate **1** to orthoacetate **8**) resulted in considerable change in the solid state

reactivity. Results of the solid state reactivity of the inositol derivatives and their crystal structures suggested that three types of intermolecular interactions in the crystals of *myo*-inositol orthoester derivatives played crucial role to decide the facility of acyl transfer. (a) Hydrogen bonding interaction between the carbonyl oxygen of C-2-*O*-benzoyl group of one molecule and the hydrogen atom of C-6-hydroxyl group of another molecule (b) electrophile – nucleophile interactions between the two reacting molecules (c) CH…π interaction between the phenyl ring of the migrating benzoyl group and a hydrogen of the inositol ring.

Usually chemical reactions in crystals lead to distortion of the crystal lattice due to appearance of products, only exceptions to this being single crystal to single crystal transformations. Distortion of the crystal structure is usually high enough to cause a collapse which result in rather low conversion to the product due to loss of topochemical control. However, if the reaction proceeds in a domino fashion along an axis in the crystal of the reactant, higher conversion and better yield of the products can be expected. The transesterification of **1** and **1.8** having very good facility of the heterogeneous reaction that proceeds to high conversion to products could be categorized in the above class. Based on their crystal structure a mechanism for the reaction was suggested. A part of this work has been communicated for publication.

Part B: Use of sulfonate protecting groups for the synthesis of cyclitol derivatives.

Section 1. A review on the use of sulfonates as hydroxyl protecting groups

This section reviews the literature on the use of alkyl / aryl sulfonyl groups for the protection of alcohols with a bias towards cyclitol hydroxyl groups. Protection and deprotection of functional groups like OH, NH_2, C=O are very common in organic synthesis. Protection of alcohols as their carboxylic acid esters, ethers etc. are encountered very often in the literature; but reports on their protection as sulfonates are very rare (**Scheme 3**). The main reason behind this is that sulfonates function as good leaving groups and result in nucleophilic substitution at the carbon carrying the sulfonate group (which could result in inversion or racemization in optically active alcohols) or elimination to form unsaturated compounds (**Scheme 4**). Hence deprotection of sulfonates to regenerate the parent alcohol is not easily achievable or needs conditions that could affect other functional groups in the same molecule.

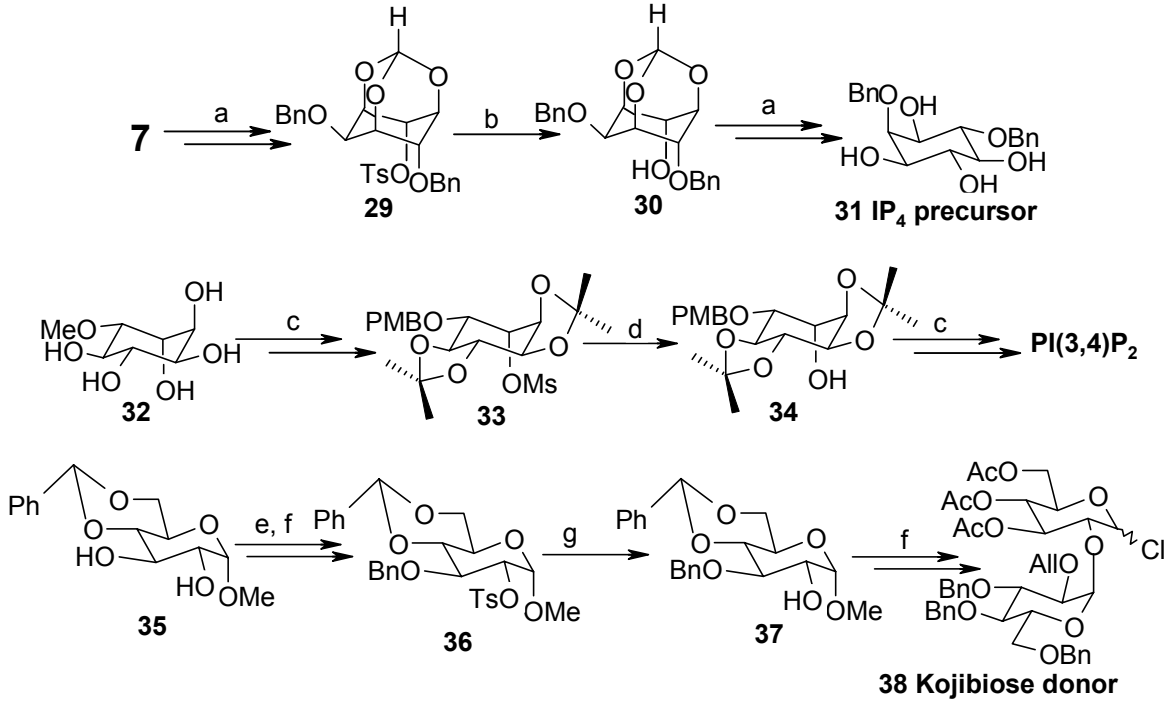

Scheme 3. Reagents and conditions: a) reference 5; b) NaOMe, MeOH, reflux, 12 h, 99%; c) reference 6; d) $LiAlH_4$ (3 eq), THF, 0 ^oC-rt, 2 h, 63%; e) reference 7; f) reference 8; g) $NaBH_4$, DMSO, 150 ^oC, 24 h, 71%.

Although there are many reports in the literature on the sulfonates (mesylates, tosylates, camphorsulfonates) of cyclitols, most of them were used for the further

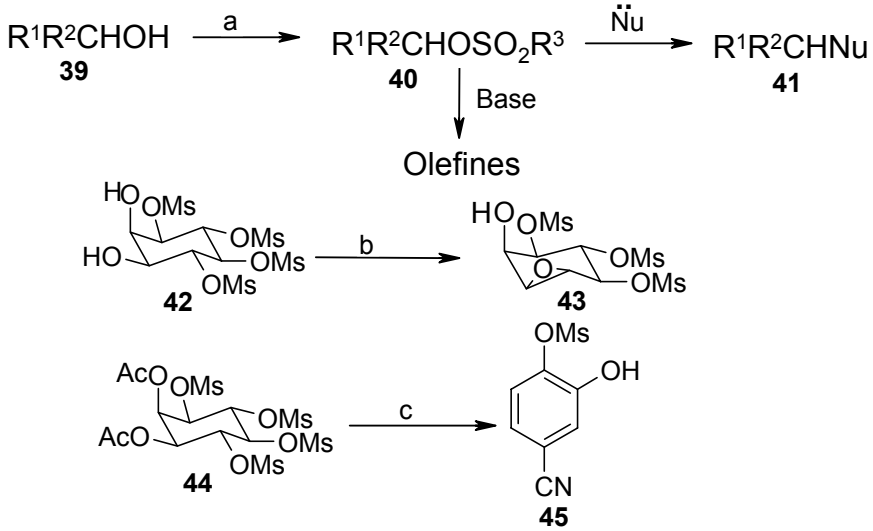

Scheme 4. Reagents and conditions: a)R^3SO_2Cl, base; b) NaOMe (1 eq), MeOH, reflux, 15 min, 91%; c) KCN (4 eq), 2-methoxyethanol, 100 ^oC, 42%.

functionalization of the cyclitol moiety by nucleophilic substitution or deoxygenation. Accordingly this section provides a survey of the literature (that is relevant to the work described in the next section) illustrating the points mentioned above.

Section 2. Synthesis of cyclitol derivatives with the aid of sulfonyl groups for the protection of *myo*-inositol hydroxyl groups.

Previous work in our laboratory[5] had shown that the three hydroxyl groups of *myo*-inositol orthoesters (**6**, **7**) can be sulfonylated with very good regioselectivity and the resulting sulfonates can be cleaved efficiently with retention of configuration of the *myo*-inositol ring. This is mainly because these orthoesters are trioxaadamantanes. In the present work, we have used sulfonate protection in *myo*-inositol orthoesters for the synthesis of isomeric cyclitols, their methylated derivatives and aminocyclitols. Some of the cyclitol derivatives synthesized in the present work are shown in **Scheme 5**.

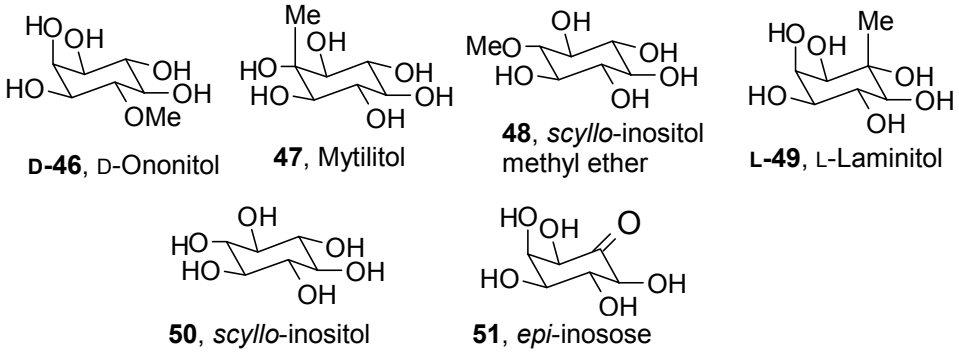

Scheme 5

Synthesis of methylated derivatives of cyclitols. *O*-methylated derivatives of inositols are present in grains and forage legumes and are known to take part in many biological phenomena in the plant kingdom. Natural *O*-methyl ethers of *myo*-inositol such as (+)-bornesitol (1D-3-*O*-methyl-*myo*-inositol), (+)-ononitol (1D-4-*O*-methyl-*myo*-inositol), sequoyitol (5-*O*-methyl-*myo*-inositol) are all present, albeit in small amount, in many plants and frequently in combination with one another, which makes it difficult to isolate them from plant sources. *O*-methyl-*scyllo*-inositol was isolated from the seeds of *Phaselous vidissimus* (mung bean). Among the *O*-methylated inositols (-)-quebrachitol (1L-2-*O*-methyl-*chiro*-inositol) and (+)-pinitol (1D-3-*O*-methyl-*chiro*-inositol) are commercially available but most of the other inositol methyl ethers are scarce. Laminitol and mytilitol are the two known naturally occurring *C*-methyl inositols, mostly found in algae. Synthesis of (+)- & (-)-ononitol, racemic & (-)-laminitol and mytilitol are reported

in the literature; but in all of the literature procedures the isolated yields were very low (3-18%). There is no report in the literature on the synthesis of the unnatural isomer, (+)-laminitol, till date. We have developed high yielding procedures (overall yield in parenthesis) for the synthesis of both (+)- & (-)-ononitol (32%), *scyllo*-inositol methyl ether (60%), mytilitol (48%), racemic laminitol (63%), (-)- & (+)- laminitol (30%) and *scyllo*-inositol (64%) from *myo*-inositol using sulfonate (tosylate) as protecting group. The synthetic route for (+)- and (-)-ononitol (**D-46** & **L-46**) is shown in **Scheme 6**. Configuration of **D-53** and **L-53** were established by X-ray crystallography. Synthetic route for mytilitol (**47**) and *scyllo*-inositol methyl ether (**48**) are shown in the **Scheme 7**. Configuration of **61** and **66** were established by X-ray crystallography.

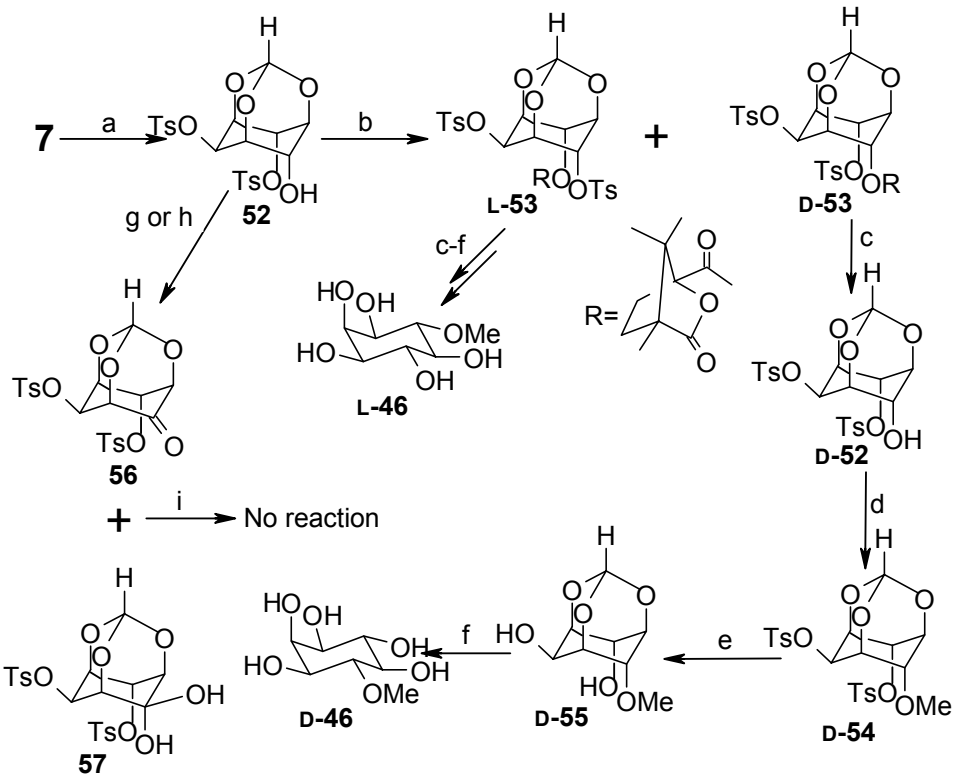

Scheme 6.Reagents and conditions: a) TsCl (2.1 eq), pyr, 80-100 ^{o}C, 48 h, 90%; b) RCl (1.5 eq), DMAP, pyr, 80-100 ^{o}C, 12 h, 97%; (**D-53**, 43% ; **L-53**, 44%); c) *iso*-But-NH_2, MeOH, reflux, 12 h, 98%; d) MeI (1.2 eq), NaH (1.1 eq), DMF, rt, 5 min, 95%; e) NaOMe, MeOH, reflux, 12 h, 100%; f) TFA-H_2O (4:1), rt, 1 h, 98%; g) DMSO (3 eq), $(COCl)_2$ (1.5 eq), DCM, -78 ^{o}C, 1 h then Et_3N (5 eq), rt, 3 h, 82%; h) DMSO-Ac_2O, 40 h, 94%; i) MeMgI, Et_2O, 0 ^{o}C-rt, 24 h.

We tried to execute the synthesis of racemic laminitol from the ditosylate **52**. Oxidation of **52** gave a mixture of ketone **56** and gem diol **57**, where gem diol was found

to be the major product. Unfortunately, our efforts to convert **57** to **56** and Grignard reaction on a mixture of **56** and **57** failed (**Scheme 6**).

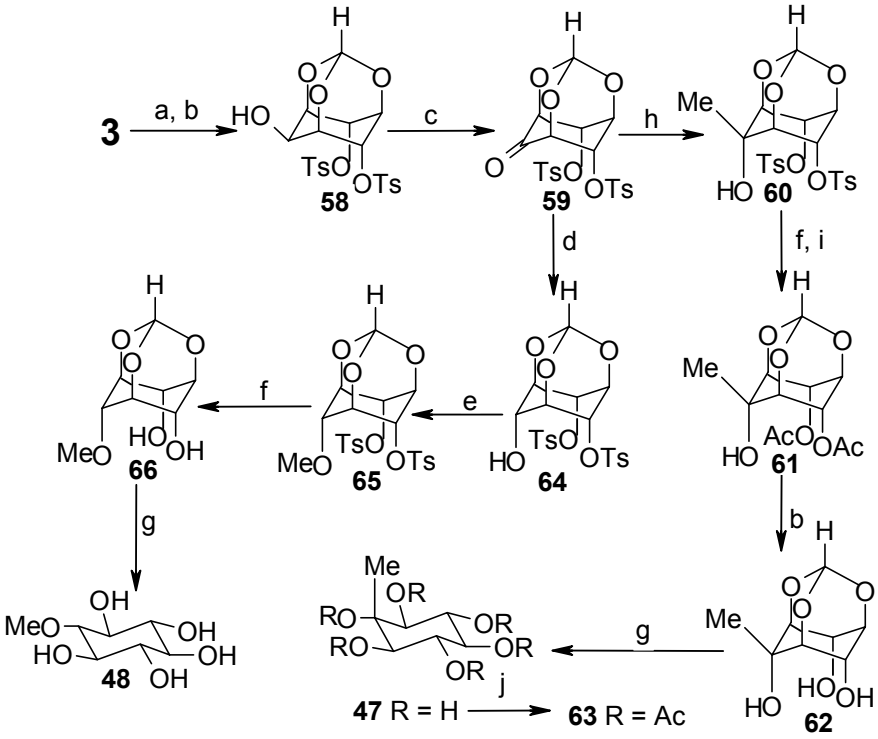

Scheme 7. Reagents and conditions: a) TsCl (3 eq), pyr, 80-100 ^{o}C, 12 h; b) *iso*-But-NH_2, MeOH, reflux, 12 h, 95% in two steps for **58** and 94% for **62**; c) DMSO (2 eq), $(COCl)_2$ (1.1 eq), DCM, -78 ^{o}C, 1 h then Et_3N (5 eq), rt, 3 h, 100%; d) $NaBH_4$ (3 eq), MeOH-THF (4 : 1), 30 min, rt, 99%; e) MeI (1.3 eq), NaH (1.1 eq), DMF, rt, 5 min, 92%; f) NaOMe, MeOH, reflux, 8 h, 94% ; g) TFA-H_2O (4 : 1), rt, 1 h, 100% for **47** and 96% for **48**; h) MeMgI (5 eq), Et_2O-THF (3 : 1), 0^{o}C-rt, 6 h, 74%; i) Ac_2O, pyr., 24 h, rt, 98%; j) Ac_2O, pyr., DMAP, rt, 24 h, 96%.

Since the reaction of **56** + **57** with methyl magnesium iodide failed, we synthesized racemic laminitol (**Scheme 8**) from unsymmetrical dibenzyl ether **30**. Structure of **69** was established by X-ray crystallography. After successful synthesis of racemic laminitol (**49**), both (-)- and (+)- laminitol (**D-49 & L-49)** were synthesized, by using same reaction sequence (as shown in **Scheme 8**) on enantiomeric dibenzyl ethers **D-30 & L-30**. For this purpose, the dibenzyl ether **30** was resolved by converting it to its diastereomeric *1S*-(-)-camphanoate esters according to procedure previously developed in our laboratory.[5] Part of this work has been published in *Trends in Carbohydrate Chemistry*.

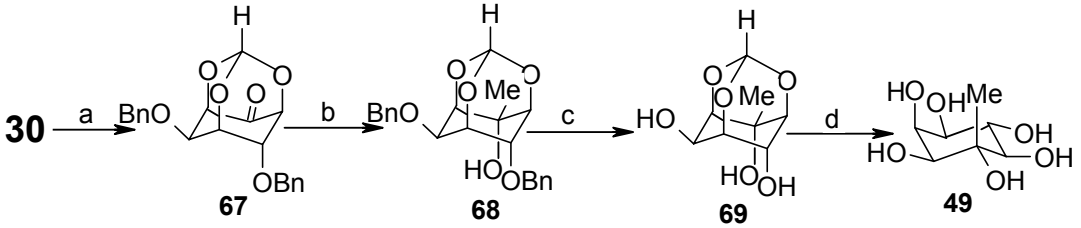

Scheme 8. Reagents and conditions: a) DMSO (2 eq), $(COCl)_2$ (1.1 eq), DCM, -78 ^oC, 1 h then Et_3N (5 eq), rt, 3 h, 85-90%; b) MeMgI (5 eq), Et_2O, 0 ^oC-rt, 30 min, 88%; c) $Pd(OH)_2$ (20 mol%), H_2/ 30 psi, MeOH, 6 h, rt, 98%; d) TFA : H_2O (4 : 1), rt, 1 h, 100%.

Synthesis of isomeric cyclitols from *myo*-inositol. *scyllo*-Inositol (**50**), the inositol having six equatorial hydroxyl groups, is found in many plants and animals. It has been suggested that certain human diseases are associated with *scyllo*-inositol depletion. Among the nine isomers of inositols known, the *myo*-isomer, having five equatorial and one axial hydroxyl group is the most abundant in nature and hence there have been efforts to convert *myo*-inositol to other isomers. Isomeric inositols have also been synthesized from carbohydrates as well as from benzene and its derivatives. There are reports on the conversion of *myo*-inositol to *scyllo*-inositol or its derivatives in overall yields of 10-40%. In the present work, *scyllo*-inositol was prepared from the ditosylate **64** without the involvement of chromatography (**Scheme 9**). Configuration of **71** was established by X-ray crystallography. This work was published in *Carbohydr*. *Res*. **2003**, *338*, 999-1001.

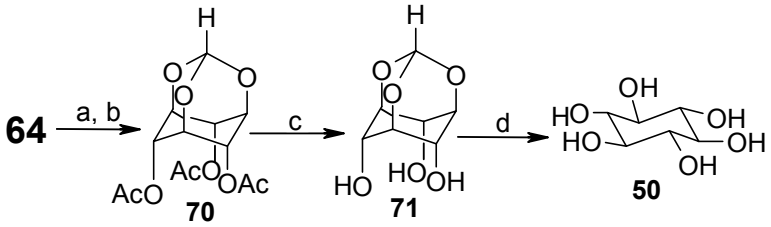

Scheme 9. Reagents and conditions: a) NaOMe, MeOH, reflux, 12 h; b) Ac_2O, pyr, rt, 12 h, 96% in two steps; c) *iso*-But-NH_2, MeOH, reflux, 12 h, 98%; d) TFA-H_2O (4:1), rt, 1 h, 98%.

epi-Inositol (**76**, **Scheme 10**) is one of the members of the cyclitol family having two axial and four equatorial hydroxyl groups. Several synthetic routes for *epi*-inositol, starting from different starting materials like D-glucose, D-galactose, *myo*-inositol and benzene are known in the literature. We investigated the possibility of obtaining *epi*-inositol from the ketone **67** and the gem-diol **57.** The ketone **67** was subjected to acid hydrolysis in a mixture of trifluoroacetic acid and water to obtain the *epi*-inosose

derivative **72**. Since **72** was unstable, we attempted to prepare its tribenzoate derivative. But benzoylation of **72** in pyridine gave a mixture of products that could not be separated by flash chromatography. One of the products **73** (yield 23%) could be isolated by crystallization from dichloromethane - light petroleum mixture. Structure of **73** was confirmed by X-ray crystallography. After our approach to synthesize *epi*-inositol from ketone **67** met with failure, we attempted synthesis of *epi*-inositol from gem diol **57** (**Scheme 10**). Attempts for the conversion of **51** to **76** are in progress.

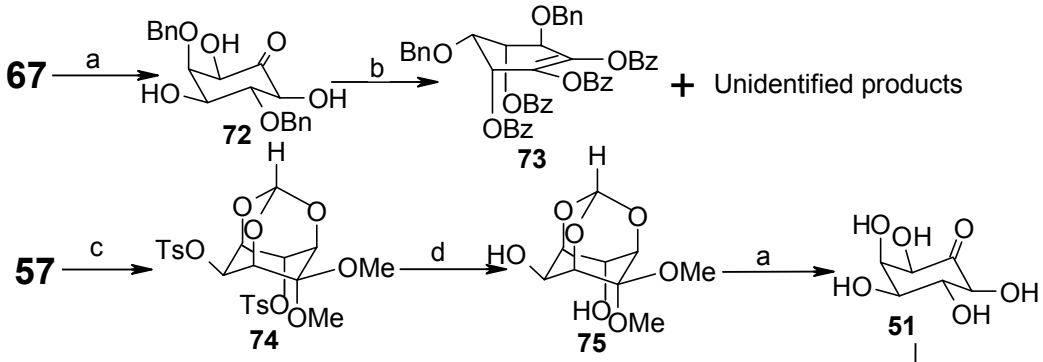

Scheme 10. Reagents and conditions: a) TFA-H_2O (4:1), rt, 2-3 h, 94% for **72** and 98% for **51**; b) BzCl, pyr, rt, 12 h, 23%; c) MeI (3.0 eq), NaH (2.2 eq), DMF, rt, 5 min, 74%; d) NaOMe, MeOH, reflux, 12 h, 75%.

Synthesis of aminocyclitols. Free and conjugated amino derivatives of inositols are capable of inhibiting glycosidases and also play an active role in antibiotic action. Azido- and amino-*myo*-inositol derivatives are known to inhibit cell growth. To study biological and physical properties of isomeric inositols and aminocyclitols, sufficient supply of these compounds is required. However, only a few syntheses of amino derivatives of *myo*-inositol are reported in the literature till date. After successful synthesis of isomeric cyclitols and some *O*- and *C*-methylated cyclitol derivatives in high yield by using sulfonate protecting groups, we took up the synthesis of aminocyclitols from *myo*-inositol. Racemic 4-deoxy-4-amino-*myo*-inositol (isolated as hexaacetate, **78**) was prepared from the ketone **67**, with an overall yield of 50% from *myo*-inositol (**Scheme 11**). The *myo*- configuration of racemic **78** was established by X-ray crystallography. Following the same sequence but starting from the enantiomeric ketones **D-67** and **L-67**, enantiomers **D-78** and **L-78**, were prepared, with overall yields 25% from *myo*-inositol.

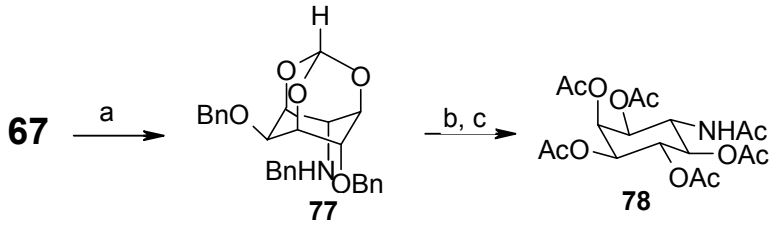

Scheme 11. Reagents and conditions: a) $BnNH_2$ (3 eq), MeOH, 50 °C, 3 h followed by $NaBH_3CN$ (3 eq), rt, 1 h 90%; b) $Pd(OH)_2$ (50 mol%), TFA-MeOH (1 : 1), H_2 / 60 psi, 8 h; c) Ac_2O, pyr., DMAP, rt, 12 h, 81% in two steps.

References:

1. Praveen, T.; Samanta, U.; Das, T.; Shashidhar, M. S.; Chakrabarti, P. *J. Am. Chem. Soc*. **1998**, *120*, 3842-3845.
2. Chung, S-K.; Chang, Y-T. *J. Chem. Soc., Chem. Commun*. **1995**, 11-12.
3. Praveen, T.; Shashidhar, M. S. *Carbohydr. Res*. **2001**, *330*, 409-411.
4. Sureshan, K. M.; Shashidhar, M. S. *Tetrahedron Lett*. **2000**, *41*, 4185-4188.
5. Sureshan, K. M.; Shashidhar, M. S.; Praveen, T.; Gonnade, R. G.; Bhadbhade, M. M.; *Carbohydr. Res*. **2002**, *337*, 2399-2411.
6. Qiao, L.; Hu, Y.; Nan, F.; Powis, G.; Kozikowski, A. P. *Org. Lett*. **2000**, *2*, 115-117.
7. Jenkins, D. J.; Potter, B. V. L. *Carbohydr. Res*. **1994**, *265*, 145-149.
8. Pozsgay, V.; Dubois, E. P.; Pannell, L. *J. Org. Chem*. **1997**, *62*, 2832-2846.

List of Publications:

Papers published in Journals:

1. Sulfonate protecting groups. Improved synthesis of *scyllo*-inositol and its orthoformate from *myo*-inositol.

   Sarmah, M. P.; Shashidhar, M. S. *Carbohydr. Res*. **2003**, *338*, 999-1001.

2. Benzoyl transfer reactivities of racemic 2,4-di-*O*-acyl-*myo*-inosityl 1,3,5-orthoesters in the solid state: molecular packing and intermolecular interactions correlate with the facility of the reaction.

   Sarmah, M. P.; Gonnade, R. G.; Shashidhar, M. S.; Bhadbhade, M. M. *Chem*. *Eur*. *J*. **2005**, *11*, 2103-2110.

3. Sulfonate protecting groups. Synthesis of O- and C-methylated inositols: D- and L-ononitol, D- and L-laminitol, mytilitol and *scyllo*-inositol methyl ether.

   Sarmah, M. P.; Shashidhar, M. S.; Sureshan, K. M.; Gonnade, R. G.; Bhadbhade, M. M. *Tetrahedron* **2005**, *61*, 4437-4446.

4. Use of sulfonate protecting groups: synthesis of *scyllo*-inositol and mytilitol from *myo*-inositol.

   Sarmah, M. P.; Shashidhar, M. S. *Trends in Carbohydr. Chem*. (in press).

5. Solvent induced polymorphism in *myo*-inositol 1,3,5-orthoesters: X-ray structure of four triols and their polymorphs.

   Sarmah, M. P.; Murali, C.; Bhosekar, G.; Gonnade, R. G.; Sureshan, K. M.; Shashidhar, M. S.; Bhadbhade, M. M. (*Manuscript to be communicated*).

Papers presented in conferences:

Oral presentations in conferences:

1. Role of C-H….π interactions in intermolecular reactions: transesterification of helically self assembled *myo*-inositol 1,3,5-orhtoesters in the solid state.

   Sarmah, M. P.; Gonnade, R. G.; Shashidhar, M. S.; Bhadbhade, M. M

   Presented at the XXXIII National Seminar on Crystallography, Jan. 8-10, 2004 (organized by Indian Crystallographic Association); National Chemical Laboratory; Pune- 411 008; Maharashtra, India.

2. Sulfonate protecting groups: efficient synthesis of (+) & (-) Laminitol, *scyllo*-inositol and mytilitol from *myo*-inositol.

Sarmah, M. P.; Shashidhar, M. S.

Presented at the National Symposium on Current Trends in Chemical Research; Feb.27-28, 2004; Department of Chemistry; Gauhati University;

Guwahati- 781 014; Assam, India.

Posters presented in conferences:

1. Acyl transfer reactions of *myo*-inositol derivatives in the solid state.

   Sarmah, M. P.; Shashidhar, M. S.

   Poster presented at National Bioorganic Symposium-7, Nov. 9-10, 2001 (organized by Indian Society for BioOrganic Chemists); Department of Chemistry; Guru Nanak Dev University; Amritsar- 143 005; Punjab, India.

2. Acyl transfer reactions of *myo*-inositol derivatives in the solid state: correlation with their crystal structures.

   Sarmah, M. P.; Gonnade, R. G.; Bhadbhade, M. M; Shashidhar, M. S.

   Poster presented at the Fourth National Symposium in Chemistry, Feb.1-3, 2002 (organized by Chemical Research Society of India); National Chemical Laboratory; Pune- 411 008; Maharashtra, India.

3. Role of weak interactions in controlling the rate of intermolecular acyl transfer in the solid state: X-ray structure and reactivity correlation in 2,4-di-*O*-benzoyl-*myo*-inositol 1,3,5-orhtoesters.

   Sarmah, M. P.; Gonnade, R. G.; Shashidhar, M. S.; Bhadbhade, M. M

   Poster presented at the XXXII National Seminar on Crystallography, Oct. 24-26, 2002 (organized by Indian Crystallographic Association); Regional Research Laboratory, Jammu, Jammu & Kashmir, India.

4. Sulfonate protecting groups: synthesis of *scyllo*-inositol and mytilitol from *myo*-inositol.

   Sarmah, M. P.; Shashidhar, M. S.

   Poster presented at the XVII National Carbohydrate Conference, Nov. 21-22, 2002 (organized by Association of Carbohydrate Chemists and Technologists of India); Central Food Technology Research Institute; Mysore, Karnataka, India.

5. Solvent induced polymorphism in *myo*-inositol triols: Synthesis and X-ray structure of three triols and their polymorphs.

Bhosekar, G.; Gonnade, R. G.; **Sarmah, M. P.**; Murali, C.; Shashidhar, M. S.; Bhadbhade, M. M.

Poster presented at the XXXIII National Seminar on Crystallography, Jan. 8-10, 2004 (organized by Indian Crystallographic Association); National Chemical Laboratory; Pune- 411 008; Maharashtra, India.

6. Sulfonate protecting groups: efficient synthesis of (+) & (-)-Laminitol and (+) & (-) Ononitol from *myo*-Inositol.

Sarmah, M. P.; Sureshan, K. M.; Shashidhar, M. S.

Poster presented at the 6th National Symposium in Chemistry, Feb.6-8, 2004 (organized by Chemical Research Society of India); Department of Chemistry; Indian Institute of Technology; Kanpur; Uttar Pradesh, India.

Part A

Investigation on the solid-state acyl transfer reactions of inositol derivatives

Section 1

An illustrative review on the solid-state group transfer reactions

A1.1. Introduction

Crushed grapes give wine by fermentation, milk turns sour and meat soup putrefies; but dried grapes, dried milk and dried meat can be stored for longer periods of time. By observing these phenomena one of the most famous ancient philosophers in Greece, Aristotle, concluded '*No Coopora Nisi Fluida*' which means 'No reaction occurs in the absence of solvent'. From these day-to-day observations it appears that conversion of one material into another does not occur as efficiently in the solid-state as compared to the liquid state. This could be the reason why organic reactions were generally carried out in the solution state. In the solid-state most organic compounds are generally stable and do not undergo chemical transformation at an observable rate. For years, chemical reactivity studies have been focused on two states, gaseous and liquid, that allow molecular freedom, relying on the principle that reaction requires mobility.

Over the years, some reactions, such as photo-induced reactions of olefins were found to occur quite efficiently in the solid-state. Reactions in highly condensed media, in which the molecules are held in fixed orientation, often display product selectivity that is unimaginable in solution or gas phases. Consequently, solid-state reactions began gaining interest among organic chemists. Also, since solid-state reactions do not require solvents, they have the potential to be developed as green reactions. Low costs and simplicity in process and handling are among the other advantages of the solid-state organic reactions, which are especially relevant in industry. In the solid-state, the reactivity depends on steric packing factors in crystals and perhaps to some extent on electronic properties of molecules. While in solution, the reactivity is mainly dependent on electronic and steric properties of the reactant molecules. Solid-state reactions coupled

with the X-ray crystal data (of reactants and / or of products) can also provide valuable information on the mechanisms of reaction that cannot be obtained by observing the corresponding reactions in solution.[1-3] The science of solid-state chemistry, and particularly the effect of crystal lattice control over reaction pathways, now seems to be entering a period of rapid growth.[4] Techniques such as X-ray crystallography, high-resolution electron microscopy[5] and solid-state magic angle spinning NMR spectroscopy[6] have opened up entirely new dimensions in organic solid-state chemistry. Although considerable progress has been made in this area in the last two decades, scope of solid-state reactions is still expanding. With a deeper understanding of crystal packing effects and of topochemistry, perhaps solid-state organic reactions could be planned and exploited for organic synthesis in the future.

Most well studied reactions among the solid-state organic reactions are, addition to C=C bonds. Photodimerization of several olefinic compounds (for example cinnamic acids, Scheme A1.1) were studied by Schmidt and Cohen in the 1960s.[7-9]

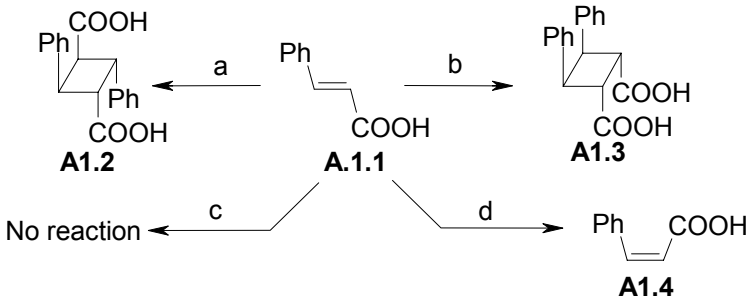

Scheme A1.1. a) hν, α crystals b) hν, β crystals, c) hν, γ crystals d) hν, solution

Photochemical reactions in organic crystals were reviewed by Ramamurthy and Venkatesan.[4] Solid-state polymerization reactions have also been studied by many groups.[10-14]

Several decades ago, Kohlschütter proposed that reactions in crystals had to proceed with minimum atomic and molecular motion.[15] This idea led to the topochemical postulate that constituted the basis of Schmidt and co-workers on the solid-state [2+2] cyclo-addition reactions.[7,16-19] However, the discovery of other solid-state reactions[20-23] made it clear that the topochemical postulate could only account for some of the solid-state reactions observed. Although the topochemical control explains most cycloaddition reactions, it cannot explain many solid-gas and solid-solid reactions that seem to require the molecules to travel through the reactant crystals. It has also been argued that crystal homogeneity (for example, the absence of amorphous material) could be much more relevant for the success of a solid-state processes.[24]

Subsequent to Schmidt and co-workers' pioneering attempts,[7-9] Toda[21] and Kaup[25-28] were among the first to investigate non-photochemical organic solid-state reactions in a systematic manner. They attempted to develop preparative scale solid-state reactions. It has been observed that many solid-state reactions gave near quantitative yield of a single product. In many such reactions yields and selectivities were found to be better than their solution state reaction counterparts. Many reactions such as Baeyer-Villiger oxidation,[29] hydride reduction,[30-32] hydrogenation,[33] halogenation,[34] Michael addition,[35,36] aldol addition,[37,38] aldol condensation,[39] Dieckmann condensation,[40] Wittig-Horner reaction,[41] Grignard reaction,[42] Reformatsky reaction,[43] Luche reaction,[43] ylide reaction,[44] oxidative coupling of phenols with ferric chloride,[45] Meyer-Schuster rearrangement, etherification,[46,47] pinacol rearrangement,[48] pinacol coupling reaction,[49] Glaser and Eglinton coupling of acetylinic compounds,[50] benzilic acid rearrangement,[51] Beckmann rearrangement,[52,53] Chapman rearrangement[2,54] were studied under solvent

free conditions. A selection of assorted solid-state reactions reported in the literature is listed in Scheme A1.2.

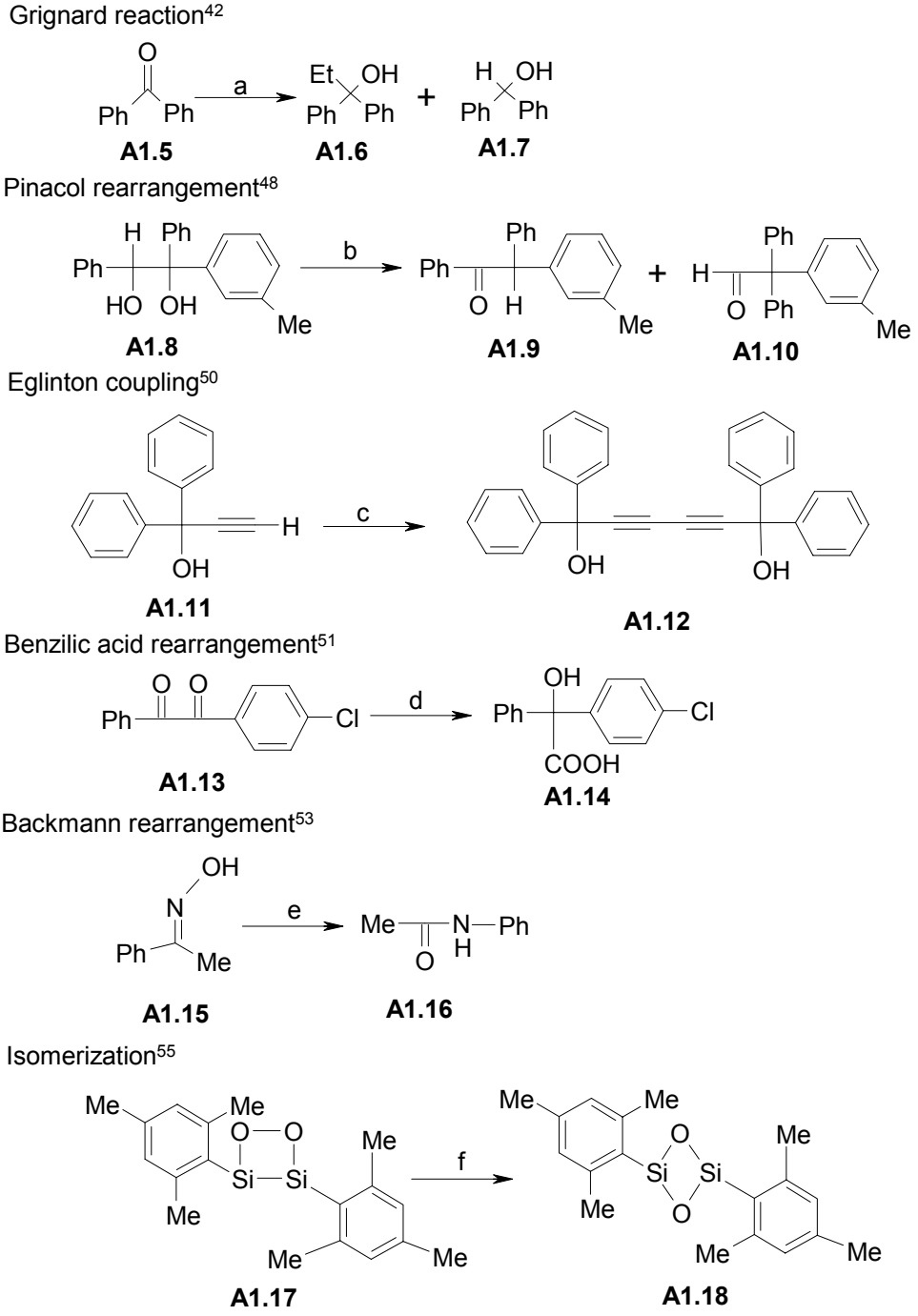

Scheme A1.2. a) EtMgBr, rt, 30 min, 30% **A1.6**, 31% **A1.7**; b) TsOH (3 eq), 60 °C, 20 min, 89% **A1.9**, 8% **A1.10**; c) $CuCl_2(Pyr)_2$, heat, 70%; d) KOH, 80 °C, 30 min, 92%; e) Montmorillonite K10, microwave, 7 min, 91%; f) rt.

Solvent free reactions have been reviewed by Toda[21] and Tanaka[20, 21] and solvent free mechanochemical reactions were reviewed by Braga and Grepioni.[22] In many of the solvent free reactions (such as Baeyer-Villiger oxidation, oxidative coupling of naphthols, condensation of amines and aldehydes, aldol condensation) mixing of the solid reactants gave rise to liquid phases or eutectic mixtures even below the ambient temperature, that facilitated product formation.[56] However, even among the truly solid-state reactions, it appears, attempt was made to understand the solid-state reactivity using X-ray crystallography or other advanced techniques, only in a few cases. Remaining part of this section will be devoted to solid-state group transfer reactions which are of rare occurrence in the solid-state. We have categorized solid-state group transfer reactions as follows: (i) atom transfer reactions; (ii) methyl transfer reactions and (iii) other group-transfer reactions.

A1.2. Atom transfer reactions in the solid-state

The simplest and most prevalent among the atom transfer reactions are those that involve hydrogen transfer; [30-32,57-63] three of the examples are given below (Scheme A1.3). Crystalline complexes of certain quinones and hydroquinones undergo redox reaction at ambient or elevated temperature.[57] For example, a 1:1 complex of benzoquinone and naphthadiol (**A1.19·A1.21** and **A1.20·A1.21**) was found to rearrange to a 1:1 complex of naphthoquinone and hydroquinone (**A1.22·A1.23** and **A1.22·A1.24**). These reactions were studied by X- ray powder diffraction, FT-IR and differential scanning calorimetry (DSC) techniques. Construction of phase diagrams by determining melting behavior of mixtures of quinones and hydroquinones gave evidence for the anticipated complex formation.

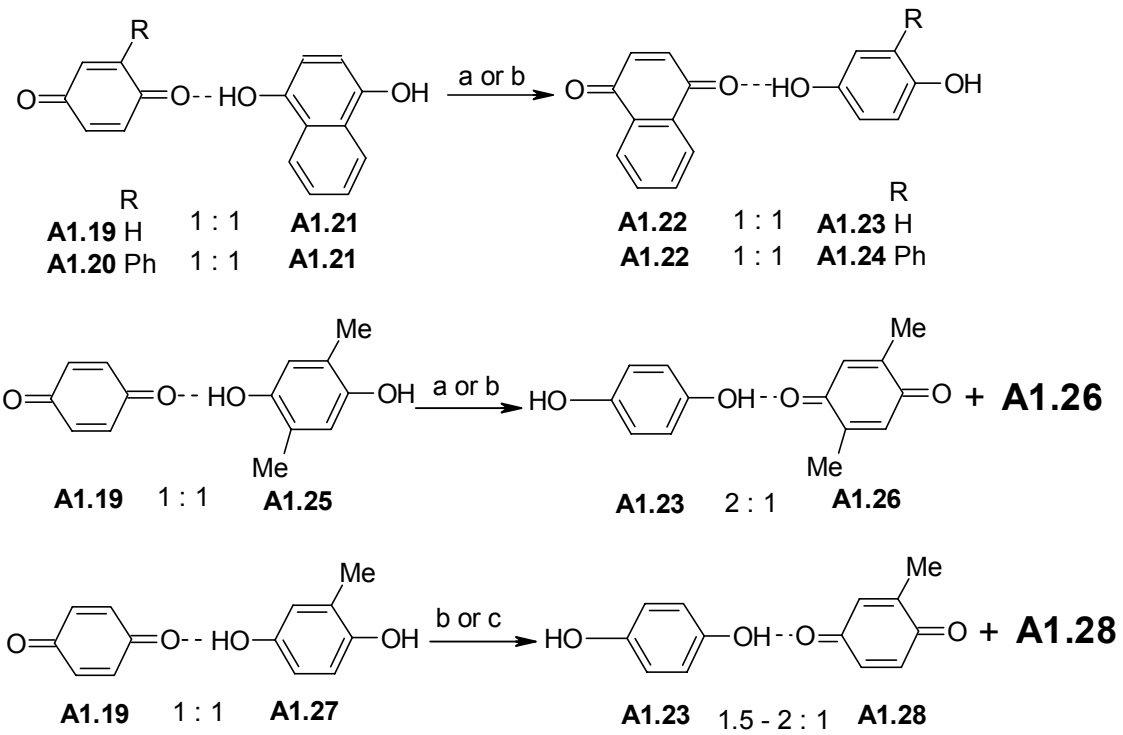

Scheme A1.3. a) 80-85 °C, 6-10 h; b) rt, prolonged standing; c) 70-75 °C, 8-10 h.

The redox reaction involved, in the simplest formulation, a series of hydrogen transfers converting each hydroquinone to a quinone and *vice versa* (Scheme A1.4).

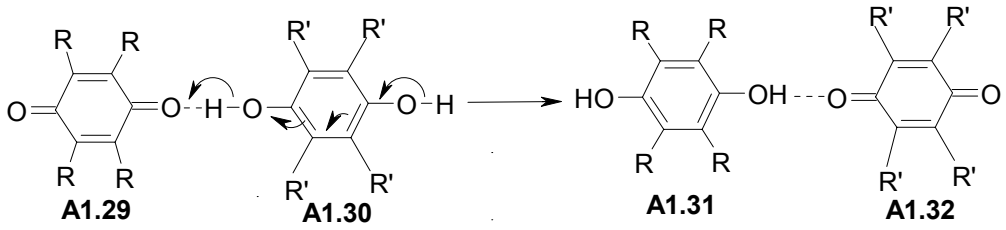

Scheme A1.4

Ketones such as **A1.33** (Scheme A1.5) undergo C-C bond cleavage or Yang type II cyclization, on photolysis. These intramoleular hydrogen atom transfer reactions were studied in detail in the solid-state by Scheffer and his co-workers.[62-63] They observed

three types of reactions depending on the structure of the triplet 1,4-hydroxy biradicals (**A1.34**) initially formed in the photochemical Norrish / Yang type II reactions: (a) cleavage of the central carbon-carbon bond to form an enol (**A1.35**) and an alkene (**A1.36**); (b) Yang cyclization to form a cyclobutanol derivative **A1.37**; (c) reverse hydrogen transfer to regenerate the starting ketone **A1.33** in its ground state. The structure of the 1,4-hydroxybiradicals was inferred from the X-ray crystal structures of the parent ketones which provided valuable information regarding the path of reactions leading to different products.

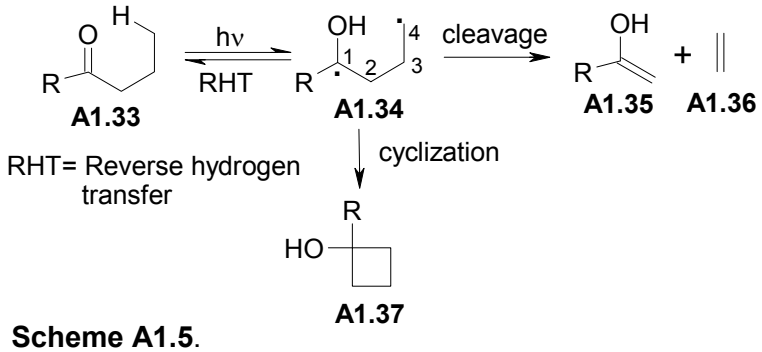

Scheme A1.5.

Another example of solid-state hydride transfer reaction is the reduction of ketones with sodium borohydride.[30-32] Often the observed selectivity for such reactions is different in solid and solution states.[31, 32] Two examples are shown in Scheme A1.6. X-ray structure analysis of **A1.38** showed that C1-C7-C4 bridge was tilted by 6° toward the C5-C6 bond in the crystal, thus rendering the double bond side face of the carbonyl group more open which facilitated the *syn* approach of the hydride ion.[31]

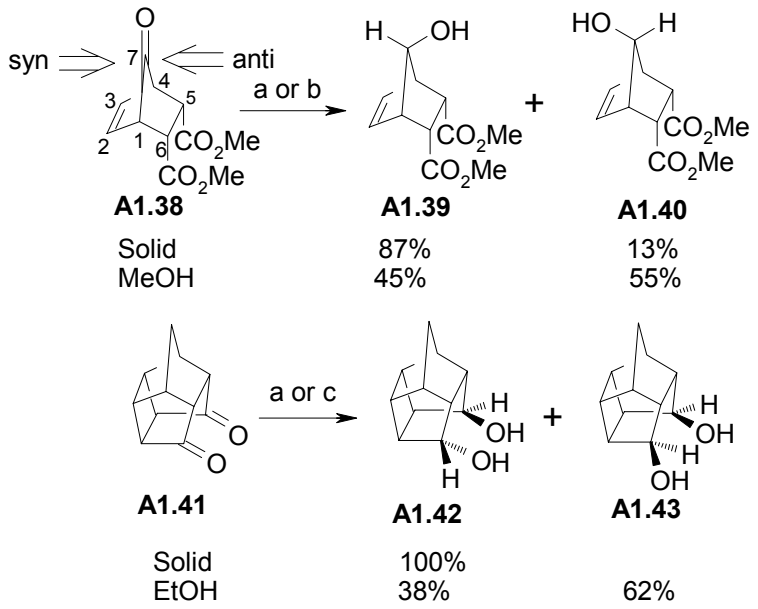

Scheme A1.6. a) $NaBH_4$, solid; b) $NaBH_4$, MeOH; c) $NaBH_4$, EtOH.

Halogen atom transfer reactions in the solid-state have been observed in enones under thermal as well as photochemical conditions (Scheme A1.7).[23] Microscopic observations on single crystals of **A1.44** under UV irradiation as well as during thermal transformation suggested these reactions to be homogeneous. The preferential migration of a fluorine atom over a chlorine atom during the reaction in **A1.46** and **A1.48** was explained based on electronic factors as well as steric effects due to crystal packing.

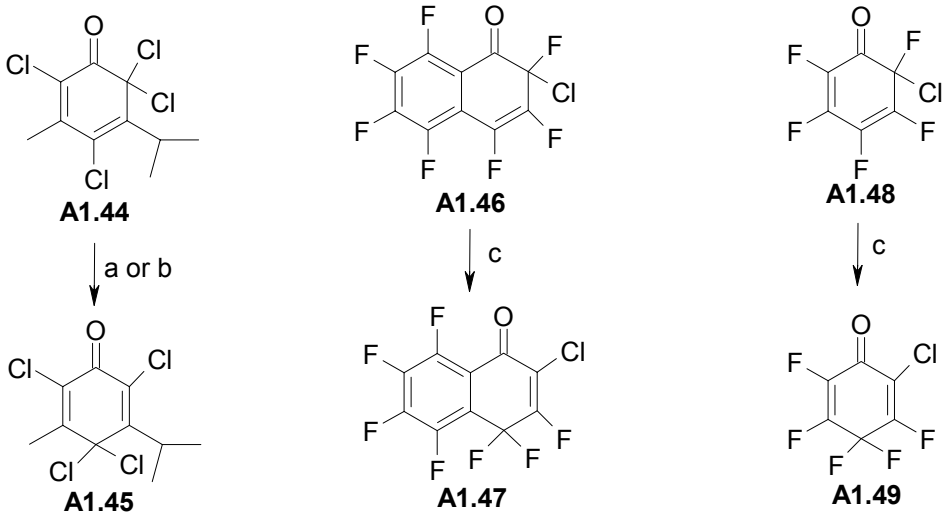

Scheme A1.7. a) heat; b) UV radiation; c) Celite, heat.

Photochemical oxygen transfer reactions were reviewed by Ramamurthy and Venkatesan;[4] one example is shown in Scheme A1.8.

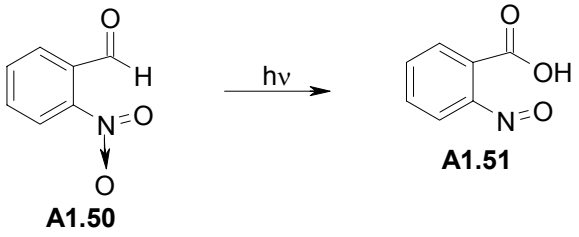

A1.50 **A1.51**

Scheme A1.8.

A1.3. Methyl group transfer reactions in the solid-state

The first systematically studied methyl group transfer reaction in the solid-state[1] was the rearrangement of methyl *p*-dimethylaminobenzenesulfonate (**A1.52**) to the zwitterionic product, *p*-trimethylammoniumbenzenesulfonate (**A1.53**, Scheme A1.9).

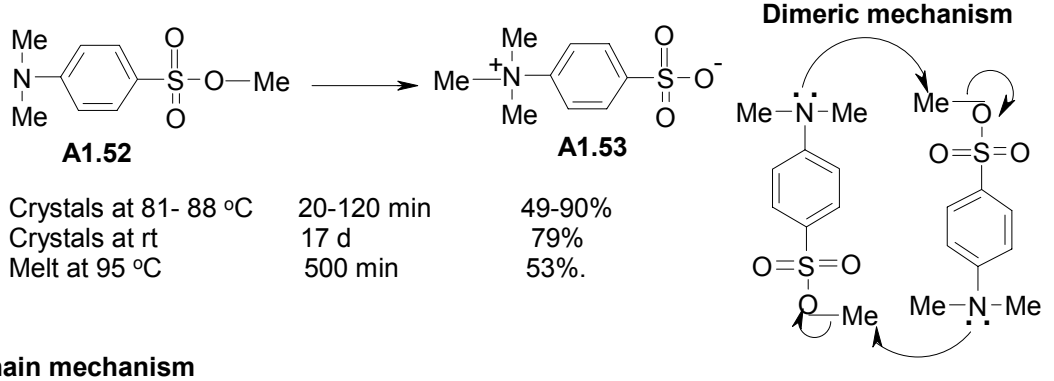

Chain mechanism

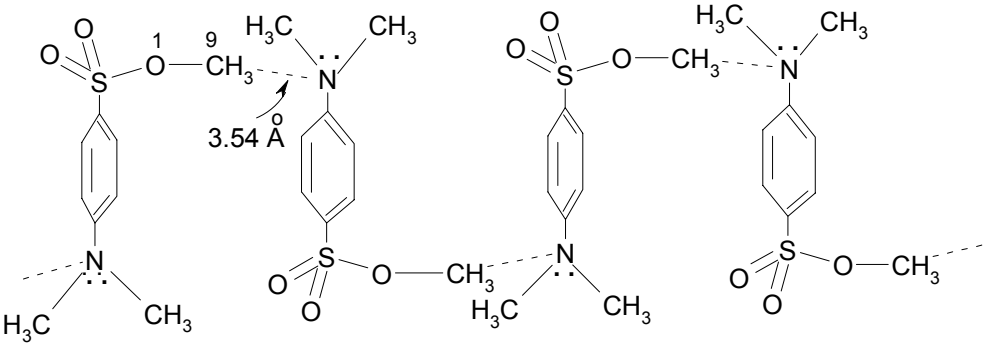

Alignment of the migrating methyl group and the nitrogen in crystals of **A1.52**.

Scheme A1.9.

This reaction was first reported by Kuhn and Ruelius[64] and later confirmed by Brand and Rutherford.[65] It was observed that **A1.54** remained unchanged in concentrated solutions, at room temperature for long periods of time (months or more). However, solid **A1.52** on standing at room temperature was cleanly converted to the zwitterion **A1.53**. Later studies on this reaction[66] revealed that the reaction proceeded faster in the bulk solid than on the surface.

The possibility of an intramolecular process for the observed methyl group transfer was ruled out, as this would require the methyl sulfonate ester to undergo severe molecular distortion. Also, a 'double label scrambling' experiment confirmed the reaction to be intermolecular. Hence two intermolecular pathways possible for this transformation, (1) a dimeric process and (2) an intermolecular chain reaction were proposed (Scheme A1.9). The role of crystal structure of the starting material on the reaction was suggested by the fact that the observed rate of the reaction in crystals was faster than the reaction in melt (mp of **A1.52** = 91 °C). The crystal structure of **A1.53** revealed stacking of molecules with alternating diaminomethyl and sulfonate groups within a chain (Scheme A1.9). Each nitrogen was in alignment with a methyl carbon of the sulfonate group about 3.54 Å away (the sum of the van der Waals radii for carbon and nitrogen is 3.5 Å) and the O1-C9----N angle was 147°, close to linear alignment needed for the S_N2 like transition state. The system could therefore readily transfer the sulfonate methyl group to its neighboring N-atom by a chain reaction sequence (Scheme A1.9). Thus from the crystal structure analysis it was understood that the reaction proceeded via S_N2 like transition state and involved the chain mechanism.

5-Methoxy-2-aryl-1,3,4-oxadiazoles are known to undergo Chapman-like thermal rearrangements (1,3-O to N methyl transfer) to give the corresponding N-alkyl amides, (Scheme A1.10).[2,54,67,68] relatively faster in the crystalline state than in solution or melt. The thermal rearrangement of a 1 : 1 mixture of **A1.56** and **A1.58**, gave a mixture of four

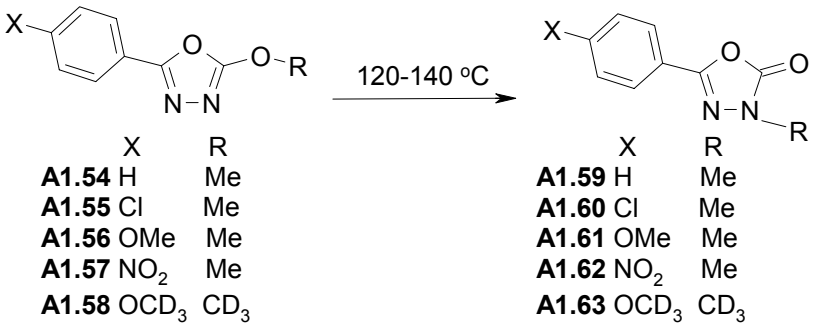

	X	R
A1.54	H	Me
A1.55	Cl	Me
A1.56	OMe	Me
A1.57	NO_2	Me
A1.58	OCD_3	CD_3

	X	R
A1.59	H	Me
A1.60	Cl	Me
A1.61	OMe	Me
A1.62	NO_2	Me
A1.63	OCD_3	CD_3

Scheme A1.10

products (with R = Me or CD_3; X = OMe or OCD_3), under both solid-state and molten conditions, which confirmed the reaction to be intermolecular. In general, Chapman-like rearrangements take place at very high temperature (about 200 °C), but the oxadiazoles **A1.54**-**A1.58**, reacted at relatively low temperatures. This facile rearrangement in the solid-state was attributed to very favorable geometry as revealed by the crystal packing of **A1.58**.[2] The O, C and N atoms involved in the transfer of the methyl group from a given oxadiazole molecule to its neighbor were aligned (Figure A1.1), with the distance C3----N2 equal to 2.9 Å, a value lower than the sum of the corresponding van der Waals radii (3.55 Å).

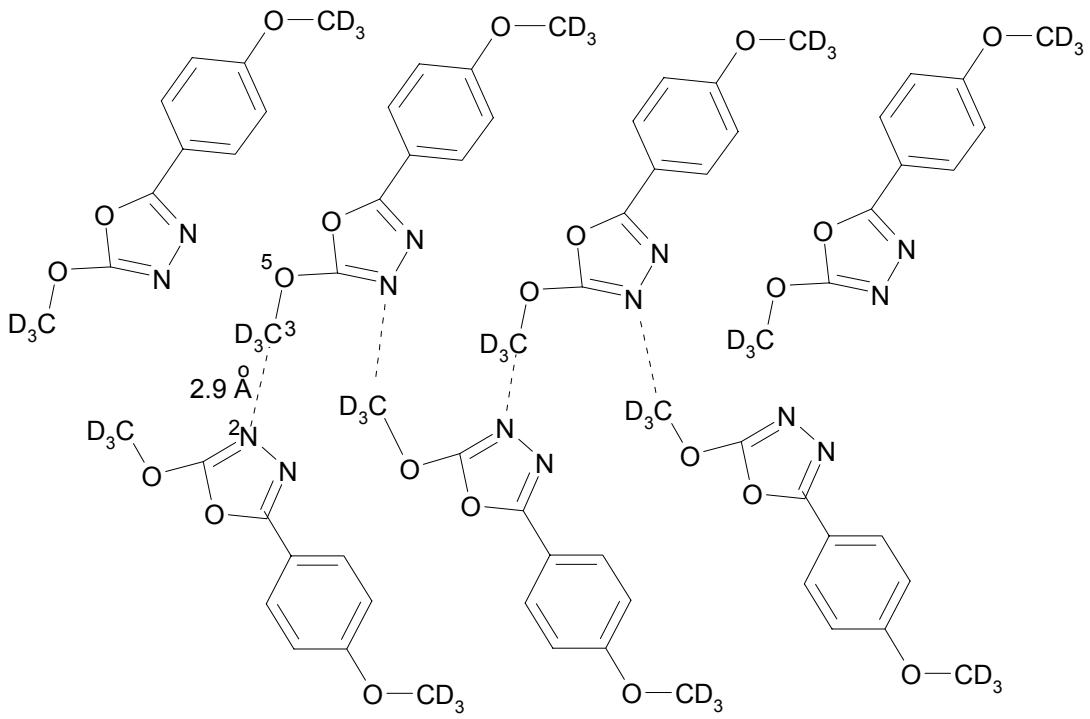

Figure A1.1. Schematic representation of the alignment of methyl group and the nitrogen atom in crystals of **A1.58**.

In addition, the crystal structure of **A1.58** showed a characteristic average intermediate state with a long O5-C3 distance (1.60 Å). A double ionic mechanism was proposed (Scheme A1.11) for this methyl group transfer reaction based on kinetic studies (by NMR spectroscopy) and computational studies.

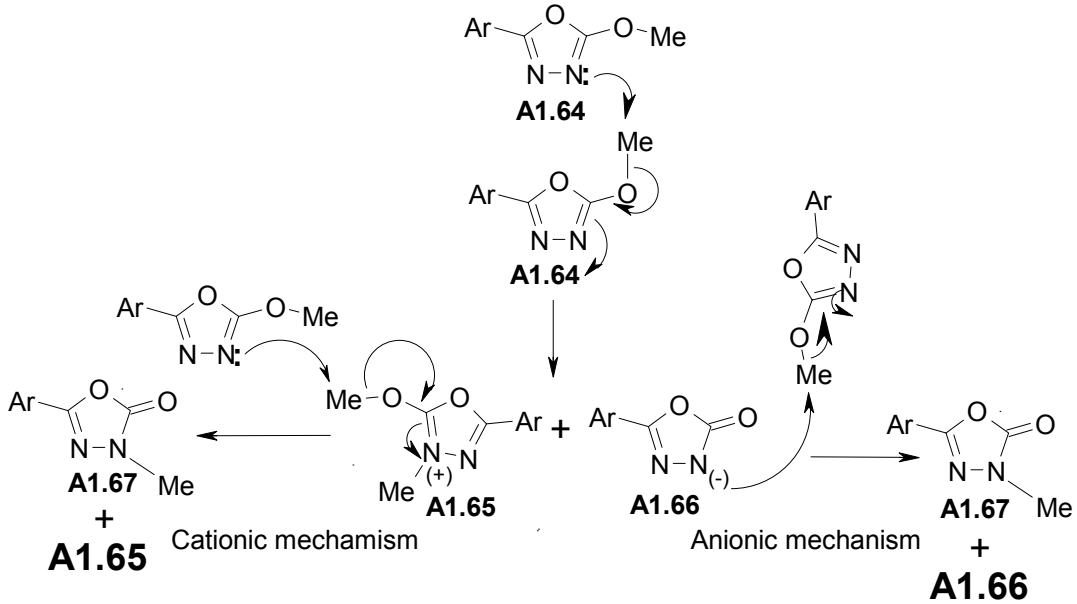

Scheme A1.11

A O → N methyl group transfer reaction in binaphthol derivative **A1.68** was reported by Smrčina and co-workers.[3] They observed that heating crystals of **A1.68** at 150 °C for 15 min, gave **A1.69** in almost quantitative yield (Scheme A1.12) while refluxing **A1.68** in xylene for 3 h left it unchanged. The single crystal X-ray analysis showed that in crystals of **A1.68** the amine nitrogen group of one molecule was 3.20 Å away from the methyl carbon of another homochiral molecule, related by a two-fold screw axis. The angle N-Me----O was (173.2°) suitable for an S_N2 type reaction. Hence the reaction was thought to occur between the homochiral pairs *R*-*R* and *S*-*S* and not between *R* and *S* molecules (which formed a centrosymmetric unit cell). The double isotope labeling experiment with CD_3 in one enantiomer and ^{18}O in the other gave rigorous proof for the enantioselectivity of this reaction, where no product having label with both deuterium and ^{18}O was obtained.

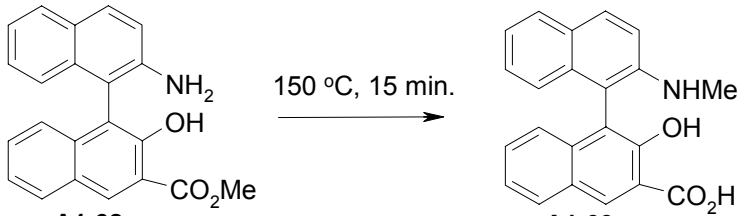

A1.68 **A1.69**

Scheme A1.12

Clue for the occurrence of this solid-state methyl transfer reaction was provided by the fact that the IR and NMR spectra of the product of the coupling reaction between 2-amino naphthalene (**A1.70**) and **A1.71** corresponded to structure **A1.68**[69] (Scheme A1.13) whereas the fragmentation pattern in the EI-MS suggested structure **A1.69**.

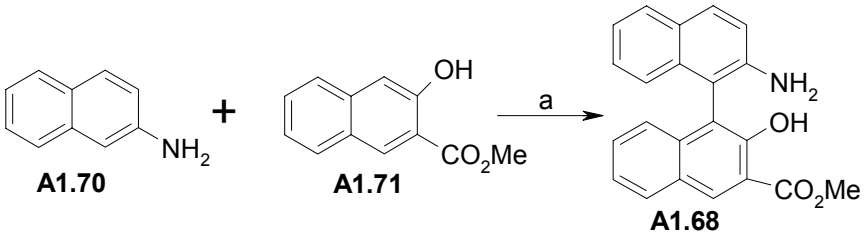

A1.70 **A1.71** **A1.68**

Scheme A1.13. a) $CuCl_2$, *t*-$BuNH_2$, MeOH, 36 h, 71%.

In all the methyl transfer reactions discussed so far, a common feature observed was that the reactions in crystals were faster than the corresponding reaction in solution and / or melt. Hence the crystal structure could explain the experimental observations. An interesting non-topochemical methyl transfer reaction was studied by Venugopalan and co-workers.[70] The relative rate of methyl transfer (Scheme A1.14) was faster in amorphous **A1.72** and melt, as compared to the reaction in crystalline **A1.72**. The crystal structure of **A1.72** showed no structural features to support the observed reaction. Results of double isotope labeling experiments ruled out the possibility of an intermolecular process. It was finally concluded that the reaction was a non-topochemical methyl transfer, which might start at some defects such as micro cavities, surfaces or other irregularities in crystals.

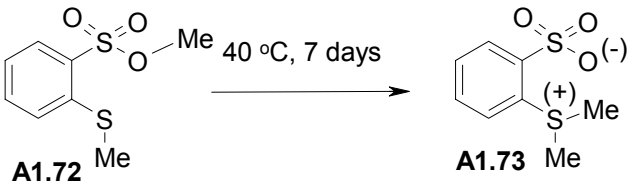

A1.72 **A1.73**

Scheme A1.14

Kinetics of solid-state methyl transfer reaction of tetraglycin methyl ester (**A1.74**) was investigated recently.[71-73] HPLC and powder X-ray diffraction analysis of the reaction mixture at different stages revealed that the rate of the reaction was accelerated

after an initial incubation period.[71] The reaction was postulated to proceed via intermediacy of **A1.75** and **A1.76** and involve intermolecular methyl transfer.[72] It is not clear whether the characteristics of the reaction in Scheme A1.15 can be correlated to the crystal structure since this appears to involve more than one parallel reactions occurring

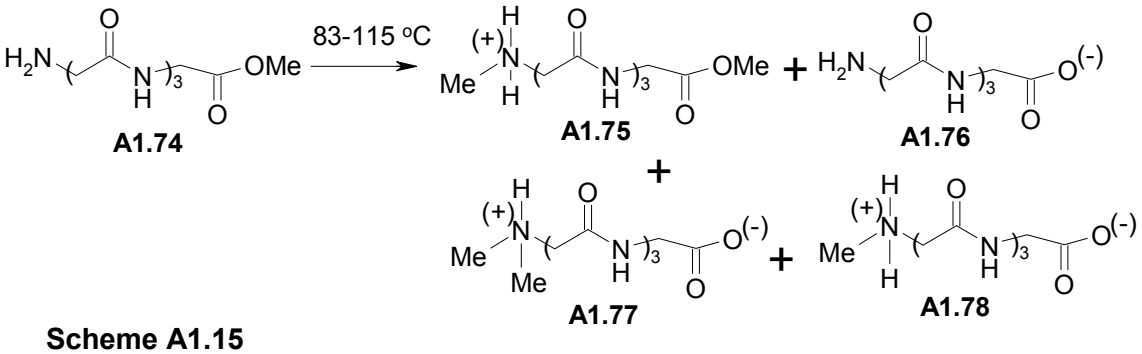

Scheme A1.15

simultaneously and hence the reaction mixture could consists of more than one phase.

A1.4. Other group transfer reactions in the solid-state

Although group transfer reactions, other than methyl and hydrogen transfer, are rare in the solid-state, some interesting examples are reported. One such reaction is the photochemical rearrangement of enone A1.79[74,75] involving transfer of a phenyl group. The photoreaction of A1.79 in benzene solution gave a mixture of two products arising from the migration of both the phenyl groups (Scheme A1.16); migration of *p*-cyanophenyl group was preferred over the unsubstituted phenyl group.[76]

It was observed that **A1.79** crystallized in two different modifications ($P2_1/c$ - type A, and $C2/c$ - type B). Photolysis of type A crystals afforded *p*-cyanophenyl migration product **A1.80** as the major product, (similar to that observed in solution). On the other hand, photolysis of type B crystals led exclusively to phenyl migration to form

A1.81 at conversion below 15%.[77] At higher conversions (monitored up to 66%) 1:1 mixture of **A1.80** and **A1.81** was observed for 'type B' while for 'type A' this ratio was 3:1. The preferential migration of the phenyl group in type B crystals of **A1.79** was

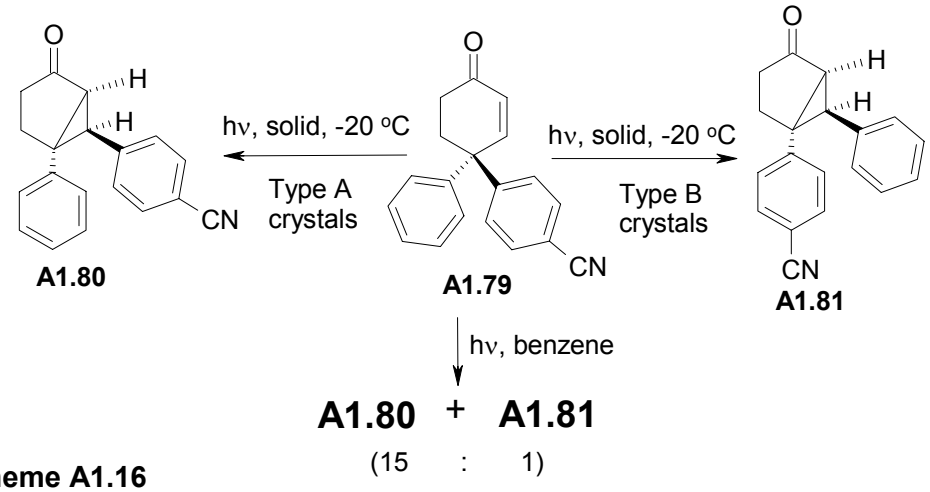

Scheme A1.16

attributed to disorders in crystals.

Salicyl amides, **A1.82**-**A1.84** were reported to undergo O- to N- acyl migration in the solid-state (Scheme A1.17).[78] X-ray crystallography of **A1.82-A1.84** revealed that the intramolecular N---C=O distances and the relative orientation of the nitrogen and the ester carbonyl group were suitable for the intramolecular acyl transfer to take place. The authors also carried out thermal motion analysis by using the anisotropic displacement parameters obtained by X-ray crystallography, to understand the mechanism of the reaction.

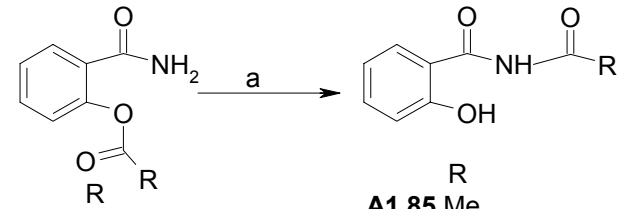

Scheme A1.17. a) solid, heat (100 °C for **A1.82** & **A1.83**, 85 °C for **A1.84**).

Very recently the first solid-state transketalization reaction in an inositol derivative was reported (Scheme A1.18).[79] It was observed that the melting point of racemic diisopropylidine ketal **A1.88** varied from 137 °C to 155 °C, for samples obtained in different experiments. ^{1}H NMR spectrum of a molten sample of **A1.88** revealed the presence of the isomeric racemic ketal **A1.89**. Heating **A1.88** at 110 °C for 10 min affected 92-95% isomerization and the reaction was found to follow a sigmoidal kinetics. Equilibration of DMF or benzene solution of **A1.88** with *p*-toluenesulfonic acid resulted in the formation of a mixture of three possible diketals (**A1.88**, **A1.89** and **A1.90**) and the 1,2-isopropylidene-*myo*-inositol (**A1.91**),[79] which confirmed that the isomerization was more selective in the solid-state. Surprisingly, the isomerization of **A1.88** to **A1.89** in the solid-state does not require an acid. The occurrence of this transketalization reaction in the solid-state in the absence of an acid was attributed to the

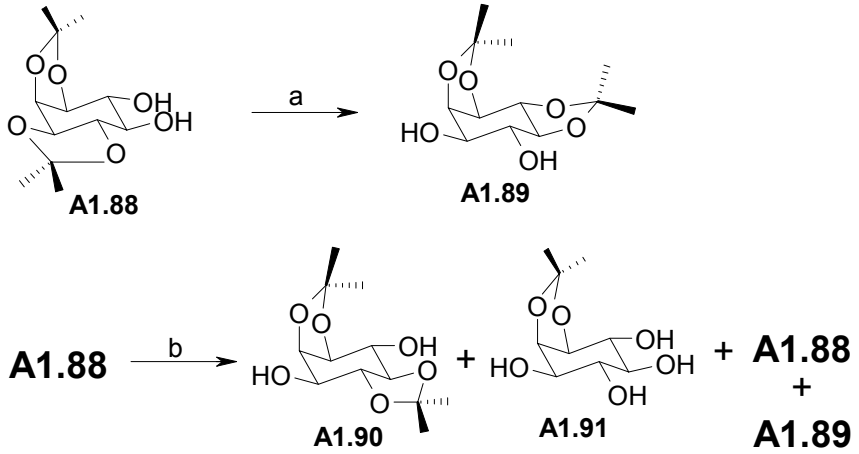

Scheme A1.18. a) 110 °C, 10 min, solid, 92-95%; b) TsOH, DMF or Benzene.

proper juxtaposition of the reacting molecules in the crystal lattice. Analysis of the crystal structure of **A1.88** showed that each asymmetric unit contained

two types of molecules which were associated with strong intermolecular hydrogen bonding. On the basis of crystal packing (Figure A1.2) it was thought that the transketalization reaction took place via initial nucleophilic attack of the C5 hydroxyl group on the *trans*-ketal carbon of a neighboring molecule to form a ketal-bridged polymeric intermediate.

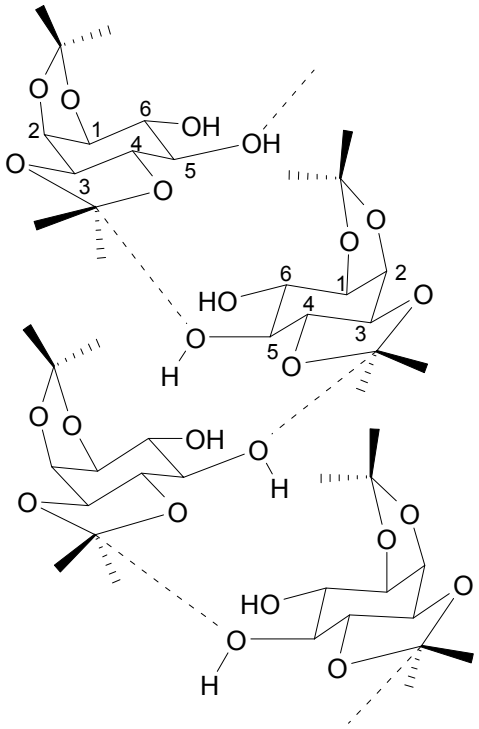

Figure A1.2. Schemetic representation of the relative orientation **A1.88** molecules in its crystal showing the proximity of the C-5 hydroxyl group of one moleucle and the *trans* acetal carbon of the other.

Another group transfer reaction known to occur in the solid-state is the diazo transfer from tosylazide or 4-carboxybenzenesulfonly azide to active methylene compounds.[80] Examples of this reaction are shown in Scheme A1.19. Diazo compounds were obtained by mixing a solid active methylene compound, tosyl azide or 4-carboxybenzenesulfonyl azide and calcined potassium carbonate. It was proposed that the reaction proceeded through host-guest interaction mechanism, although there was no

experimental data to support this statement. Furthermore, the authors state that mixing of the reactants resulted in a pasty mass. This observation does suggest the possibility of this multi component reaction not taking place in the solid-state. In any case, this reaction is one of the high yielding and convenient methods for synthesis of diazo compounds and does not require a solvent.

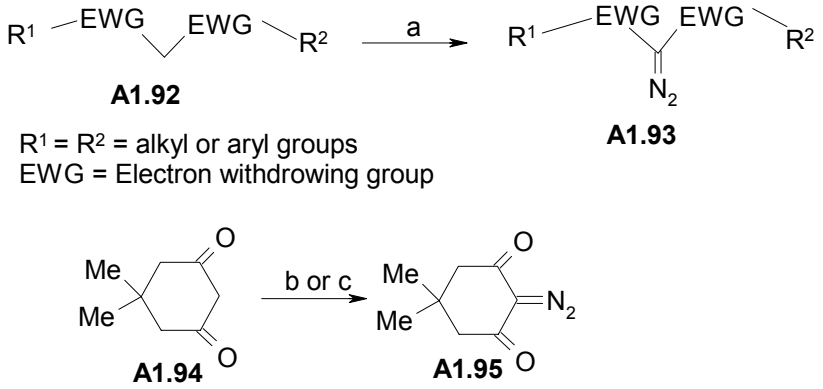

Scheme A1.19. a) TsN_3 or 4-carboxybenzenesulfonyl azide, K_2CO_3, 5-20 min, 75-95%; b) TsN_3, K_2CO_3, 5 min, 96%; c) 4-carboxybenzenesulfonyl azide, K_2CO_3, 15 min, 84%.

Another facile solid-state group transfer reaction is the disproportionation of racemic 2,4-di-*O*-benzoyl-*myo*-inositol 1,3,5-orthoformate (**A1.96**, Scheme A1.20).[81] Under similar conditions, racemic 2-*O*-benzoyl-4-*O*-acetyl-*myo*-inositol 1,3,5-orthoformate (**A1.97**) did not react. The crystal structure analysis of **A1.96** revealed that two crystallographic symmetry related molecules of **A1.96** were held together by a

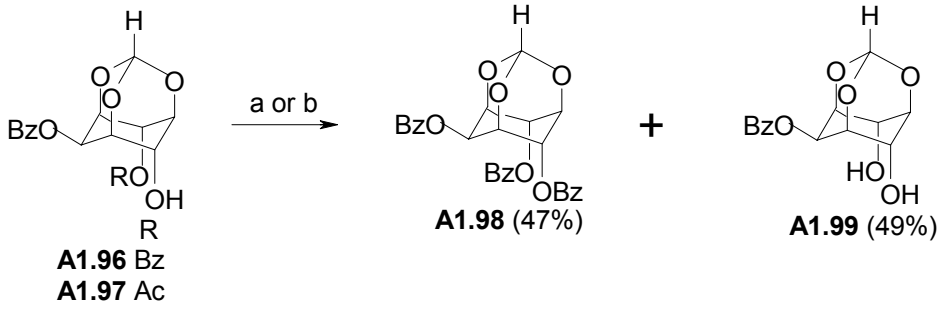

Scheme A1.20. a) Na_2CO_3 (8 eq), 140 °C, 60 h; b) Na_2CO_3 (8 eq), microwave, 25 min.

hydrogen bond between the C4 hydroxyl group of one molecule and the carbonyl oxygen of the C2 benzoyl group of the other molecule (Figure A1.3).

O4….C15 = 3.226 Å
< O4….C15-O8 = 88.1º

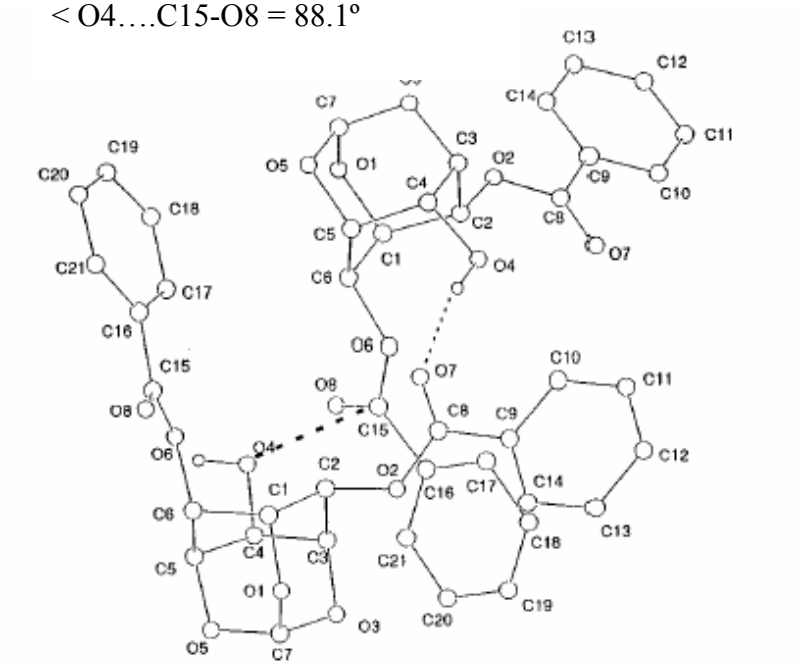

Figure A1.3. Two crystallographic symmetry related molecules of **A1.96** held together by hydrogen bond O4-H----O7.

The difference in reactivity observed between the dibenzoate **A1.96** and the acetate **A1.97** was rationalized based on electrophile (El) – nuclephile (Nu) interaction in their crystal structures. The distance between the hydroxyl group (Nu) and the carbonyl carbon (El) was 3.226 Å (3.249 Å for the second molecule in the unit cell) and 3.748 Å in the crystals of **A1.96** and **A1.97** respectively. The corresponding angles of approach of the nucleophile were 88.1º (89.9º for the second molecule in the unit cell) and 33.1º respectively for **A1.98** and **A1.99**. Therefore it was suggested that the acyl transfer took place where the geometry was good for nucleophilic addition to the carbonyl group.

A survey of the literature on structure correlation[82-85] suggests that the 'pre-organization' of the El (C=O) and Nu (OH, NH_2 etc.) close to the tetrahedral angle (Nu…C=O ~ 110º) and a distance of about 3.2-3.5 Å between the El and the Nu (Figure A1.4) is an essential pre-requisite for the addition of the Nu to a carbonyl group. This conclusion was arrived at by a study of the crystal structure of simple organic compounds (**A1.100** – **A1.103**)[86] containing a carbonyl group and an amino group.

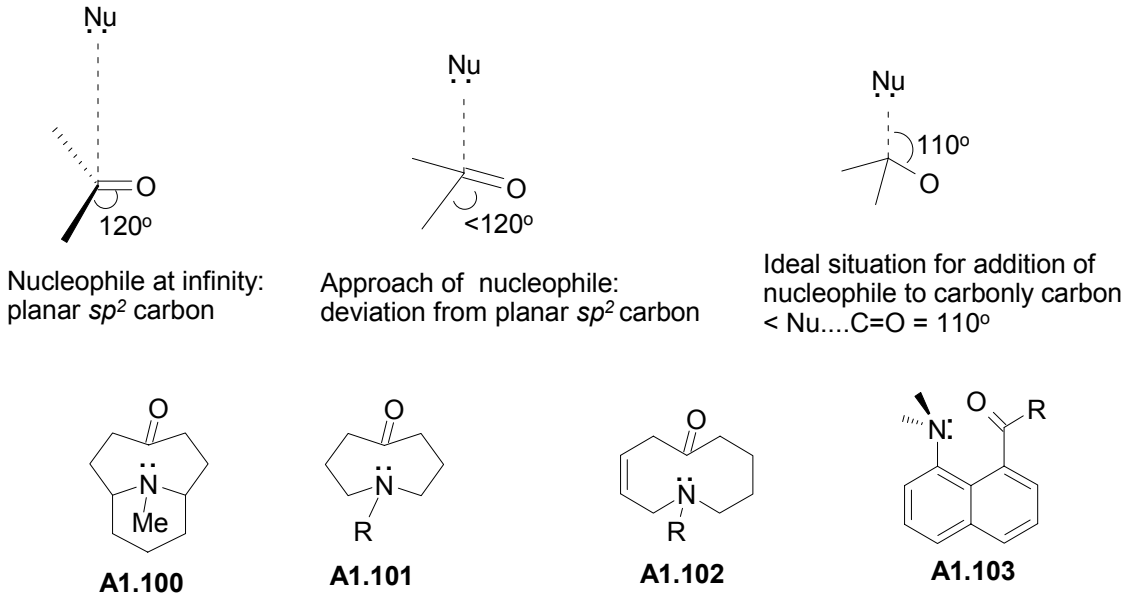

Figure A1.4

Computational[87] and experimental studies[81] of solid-state reactions which involve addition of a nucleophile to a carbonyl group support these observations. Further results on systems which undergo acyl transfer reaction in the solid-state and involve addition of a hydroxyl group to a carbonyl group are discussed in the subsequent section of this thesis.

A1.5. Conclusions

In this section, solid-state group transfer reactions reported in the literature have been reviewed. Although there are few reports available on the solid-state group transfer reactions, a survey of the literature shows that in some cases the reactions in the solid-state are more facile than the corresponding reaction in solution. By analyzing the crystal structure of the starting material, the mechanism of many of these reactions were understood and found to be topochemical in nature. Only one non-topochemical methyl migration is reported.[70] Since most synthetically useful organic reactions involve intermolecular group transfer, there seems to be a need to discover and study the scope of other group transfer reactions in the solid-state.

A1.6. References

1. Sukenik, C. N.; Bonapace, J. A. P.; Mandel, N. S.; Lau, P-Y.; Wood, G.; Bergman, R. G. *J. Am. Chem. Soc.*, **1977**, *99*, 851.
2. Dessolin, M.; Eisenstein, O.; Golfier, M.; Prangé, T.; Sautet, P. *J. Chem. Soc., Chem. Commun.*, **1992**, 132.
3. Smrčina, M.; Vyskočil, Š.; Hanuš, V.; Polášek, M.; Langer, V.; Chew, B. G. M.; Zax, D. B.; Verrier, H.; Harper, K.; Claxton, T. A.; Kočovoský, P. *J. Am. Chem. Soc.*, **1996**, *118*, 487.
4. Ramamurthy, V.; Venkatesan, K. *Chem. Rev.*, **1987**, *87*, 433.
5. Kaupp, G.; Haak, M.; Toda, F. *J. Phys. Chem.*, 1995, *8*, 545.
6. Gan, Z.; Ernst, R. R. *J. Chem. Phys.*, **1998**, *108*, 9444.
7. Cohen, M. D.; Schmidt, G. M. J. *J. Chem. Soc.*, **1964**, 1996.
8. Cohen, M. D.; Schmidt, G. M. J.; Sonntag, F. I. *J. Chem. Soc.*, **1964**, 2000.

9. Schmidt, G. M. J. *J. Chem. Soc.*, **1964**, 2014.
10. James, N.; Ramesh, C.; Sivaram, S. *Polymer International*, **2004**, *53*, 664.
11. Furukawa, A.; Imanishi, Y.; Tanihara, M. *J. Polymer Sci., Part A: Polymer Chem.*, **2003**, *41*, 3227.
12. Yukio, I.; Irngartinger, H. Skipinski, M. *Tetrahedron*, **2000**, *56*, 6781.
13. Irngartinger, H. Skipinski, M. *Eur. J. Org. Chem.*, **1999**, 917.
14. Epple, M.; Kirschnick, H. *Chem. Ber.*, **1996**, *129*, 1123 and references cited theirin.
15. Kohlschütter, V. *Z. Anorg. Allg. Chem.*, **1918**, *105*, 121.
16. Schmidt, G. M. J. *Pure Appl. Chem.*, **1971**, *43*, 647.
17. Cohen, M. D. *Angew. Chem.*, **1975**, *87*, 439.
18. Cohen, M. D. *Angew. Chem. Int. Ed. Engl.*, **1975**, *14*, 1386.
19. Elgavi, G. A.; Green, B. S.; Schmidt, G. M. J. *J. Am. Chem. Soc.*, **1973**, *95*, 2058.
20. Tanaka, K. in *Solvent-free Organic Synthesis*, Wiley-VCH, Weinheim, 2003.
21. Tanaka, K.; Toda, F. *Chem. Rev.*, **2000**, *100*. 1025.
22. Braga, D.; Grepioni, F. *Angew. Chem. Int. Ed. Engl.*, **2004**, *43*, 4002.
23. Singh, N. B.; Singh, R. J.; Singh, N. P. *Tetrahedron*, **1994**, *50*, 6441 and references cited therein.
24. Garcia-Garibay, M. A. *Acc. Chem. Res.*, **2003**, *36*, 491.
25. Kaup, G.; Matthis, D.; *Chem. Ber.*, **1986**, *119*, 2387.
26. Kaup, G.; Schmeyer, J.; Boy, J. *Chemosphere*, **2001**, *43*, 55.
27. Kaup, G.; Schmeyer, J.; Boy, J. *Tetrahedron*, **2000**, *51*, 6899.
28. Kaup, G. in *Comprehensive Supramolecular Chemistry*, *Vol. 8* (Davies, J. E. D. ed.), Elsevier, Oxford 1996, p. 381.

29. Toda, F.; Yagi, M.; Kiyoshige, K. *J. Chem. Soc., Chem. Commun.*, **1988**, 958.

30. Toda, F.; Kiyoshige, K.; Yagi, M *Angew. Chem. Int. Ed. Engl.*, **1989**, *28*, 320.

31. Mehta, G.; Khan, F. A.; Lakshmi, K. A. *Tetrahedron Lett.*, **1992**, *33*, 7977.

32. Marhand, A. P.; Reddy, G. M. *Tetrahedron*, **1991**, *47*, 6571.

33. Sabra, F.; Bassus, J.; Lamartiue, R. *Mol. Cryst. Liq. Cryst.*, **1990**, *186*, 69.

34. Hamazaki, H.; Ohba, S.; Toda, F.; Takumi, H. *Acta Crystallogr.*, **1997**, *C53*, 620.

35. Satish, B.; Panneerselvam, K.; Zacharias, D.; Desiraju, G. R. *J. Chem. Soc., Perkin Trans. 2*, **1995**, 325.

36. Deiz-Barra, E.; de la Hoz, A.; Merino, S.; Sanchez-Verdu, P. *Tetrahedron Lett.*, **1997**, *38*, 2359.

37. Wei, Y.; Bakthavatchalam, R. *Tetrahedron Lett.*, **1991**, *32*, 1535.

38. Khruscheva, N. S.; Loins, N. M.; Sokolov, V. I.; Makhaev, V. D. *J. Chem. Soc., Perkin Trans. 1*, **1997**, 2425.

39. Toda, F.; Tanaka, K.; Hamai, K. *J. Chem. Soc., Perkin Trans. 1*, **1990**, 3207.

40. Toda, F.; Suzuki, T.; Higa, S. *J. Chem. Soc., Perkin Trans. 1*, **1998**, 3521.

41. Toda, F.; Akai, H.; *J. Org. Chem.*, **1990**, *55*, 3446.

42. Toda, F.; Takumi, H.; Yamaguchi, H.; *Chem. Exp.*, **1989**, *4*, 507.

43. Tanaka, H.; Kishigami, S.; Toda, F. *J. Org. Chem.*, **1991**, *56*, 4333.

44. Toda, F.; Imai, N. *J. Chem. Soc., Perkin Trans. 1*, **1994**, 2673.

45. Toda, F.; Tanaka, K.; Iwata, S.; *J. Org. Chem.*, **1989**, *54*, 3007.

46. Toda, F.; Takumi, H.; Akehi, M. *J. Chem. Soc., Chem. Commun.*, **1990**, 1270.

47. Toda, F.; Okuda, K.; *J. Chem. Soc., Chem. Commun.*, **1991**, 1212.

48. Toda, F.; Shigemasa, T. *J. Chem. Soc., Perkin Trans. 1*, **1989**, 209.

49. Tanaka, H.; Kishigami, S.; Toda, F. *J. Org. Chem.*, **1990**, *55*, 2982.

50. Toda, F.; Tokumaru, Y. *Chem. Lett.*, **1990**, 987.

51. Toda, F.; Tanaka, K.; Hagawa, Y.; Sakaino, Y. *Chem. Lett.*, **1990**, 373.

52. Toda, F.; Akai, H *J. Org. Chem.*, **1990**, *55*, 4973.

53. Almena, I.; Diaz-Ortiz, A.; Diez-Barra, E.; Hoz, A.; Loupy, A. *Chem. Lett.*, **1996**, 333.

54. Dessolin, M.; Golfier, M. *J. Chem. Soc., Chem. Commun.*, **1986**, 38.

55. McKillop, K.; Gillette, G. R.; Powell, D. R.; West, R. *J. Am. Chem. Soc.*, **1992**, *114*, 5203.

56. Rothenberg, G.; Downie, A. P.; Raston, C. L.; Scott, J. L. *J. Am. Chem. Soc.*, **2001**, *123*, 8701.

57. Patil, A. O.; Curtin, D. Y.; Paul, I. C. *J. Am. Chem. Soc.*, **1984**, *106*, 4010.

58. Buchachenko, A. L.; Motyakin, M. V.; Aliev, I. I. in *Mol. Solid State* (Ed.: Boldyreva, E.; Boldyreva, V), John Wiley and Sons Ltd., Chichester, UK, 1999, *Vol. 3*, p. 221.

59. Scheurer, C.; Saalfrank, P. *Chem. Phys. Lett.*, **1995**, *245*, 201.

60. Flomenblit, V. Sh.; Trakhtenberg, L. I. *Khim. Fiz.*, **1992**, *11*, 1324.

61. Koshima, H.; Hessler, B.; Diane, P.; Miyoshi, F.; Wang, Y.; Matsuura, T. *J. Photochem. Photobiol. A*, **1995**, *86*, 171.

62. Cheung, E.; Netherton, M. R; Scheffer, J. R.; Trotter, J. *Org. Lett.*, **2000**, *2*, 77.

63. Braga, D.; Chen, S.; Filson, H.; Maini, L.; Netherton, M .R.; Patrick, B. O.; Scheffer, J. R.; Scott, C.; Xia, W. *J. Am. Chem. Soc.*, **2004**, *126*, 3511.

64. Kuhn, R.; Ruelius, H. W. *Chem. Ber.*, **1950**, *83*, 420.

65. Brand, J. C. D.; Rutherford, A. *J. Chem. Soc.*, **1952**, 3927.

66. Menger, F. M.; Kaiserman, H. B.; Scotchie, L. J. *Tetrahedron Lett.*, **1984**, *25*, 2311.

67. Schulenberg, J. W.; Archer, S.; *Org. React.*, **1965**, *14*, 24.

68. Lander, G. D.; *J. Chem. Soc.*, **1903**, *83*, 406.

69. Smrčina, M.; Vyskočil, Š.; Máca, B.; Polášek, M.; Claxton, T. A.; Abbott, D. P.; Kočovoský, P. *J. Org. Chem.*, **1994**, *59*, 2156.

70. Venugopalan, P.; Venkatesan, K.; Klausen, J.; Novotny-Bregger, E.; Leumann, C.; Eschenmoser, A.; Dunitz, J. D. *Helv. Chim. Acta.*, **1991**, *74*, 662.

71. Shalaeva, M.: Byrn, S. R.; Zografi, G. *Int. J. Pharm.*, **1997**, *152*, 75.

72. Shalaev, E. Y.; Byrn, S. R.; Zografi, G. *Int. J. Chem. Kinet.*, **1997**, *29*, 339.

73. Shalaev, E. Y.; Shalaeva, M.; Zografi, G. *J. Pharm. Sci.*, **2002**, *91*, 584.

74. Zimmerman, H. E.; Wilson, J. W. *J. Am. Chem. Soc.*, **1964**, *86*, 4036.

75. Zimmerman, H. E.; Hancock, K. G. *J. Am. Chem. Soc.*, **1968**, *90*, 3749.

76. Zimmerman, H. E.; Rieke, R. D.; Scheffer, J. R. *J. Am. Chem. Soc.*, **1967**, *89*, 2033.

77. Zimmerman, H. E.; Alabugin, I. V.; Chen, W.; Zhu, Z. *J. Am. Chem. Soc.*, **1999**, *121*, 11930.

78. Vyas, K.; Manohar, H.; Venkateshan, K. *J. Phys. Chem.*, **1990**, *94*, 6069.

79. Sureshan, K. M.; Murakami, T.; Miyasou, T.; Watanabe, Y. *J. Am. Chem. Soc.*, **2004**, *126*, 9174.

80. Ghosh, S.; Datta, I. *Synth. Commun.*, **1991**, *21*, 191.

81. Praveen, T.; Samanta, U.; Das, T.; Shashidhar, M. S.; Chakrabarti, P. *J. Am. Chem. Soc.*, **1998**, *120*, 3842.

82. Bürgi, H. B. *Perspective in Coordination Chemistry*; Williams, A. F., Floriani, C.; Mercbach, A. E., Eds.; VCH: Weinheim, 1993; p. 1.

83. Bürgi, H. B.; Dunitz, J. D. In *Structure Correlation*; Bürgi, H. B.; Dunitz, J. D., Eds.; VCH: Weinheim, 1994; Vol. 2, p. 767.

84. Ferretti, V.; Gilli, P.; Bertolasi, V.; Gilli, G. *Cryst. Rev.*, **1996**, *5*, 3.

85. O'Leary, J.; Bell, P. C.; Wallis, J. D.; Schweizer, W. B. *J. Chem. Soc. Perkin Trans. 2*, **2001**, 133.

86. Bürgi, H. B.; Dunitz, J. D. *Acc. Chem. Res.*, **1983**, *16*, 153.

87. Bruice, T. C. *Acc. Chem. Res.*, **2002**, *35*, 139.

Section 2

Solid-tate acyl transfer reactions in inositol derivatives

A2.1. Introduction

myo-Inositol and its phosphorylated derivatives play major roles in many cellular functions like cellular signal transduction,[1] and anchoring of proteins to cell membranes.[2-4] Some inositol derivatives have been shown to be inhibitors of cell proliferation and phosphatidylinositol 3-kinase signaling.[5] The developments in biology and medicine implicating the involvement of phosphoinsoitols in several biological processes in eukaryotic cells, necessitated simpler methods for the synthesis of various inositol derivatives. Synthesis of biologically relevant inositol derivatives involves a series of protection-deprotection reactions of its six-hydroxyl groups.[6] Protection of inositol hydroxyl groups as the corresponding carboxylic acid esters is frequently encountered in the literature.[7-17]

Acyl transfer reactions, ubiquitous in natural systems[18,19] have been extensively studied in the solution state.[20] Acyl transfer reactions in cyclitol derivatives have been known for decades.[21-23] Way back in 1965, Angyal and Melrose studied the migration of acetates among the hydroxyl groups of partially acetylated *myo*-inositol derivatives (Scheme A2.1).[21,22]

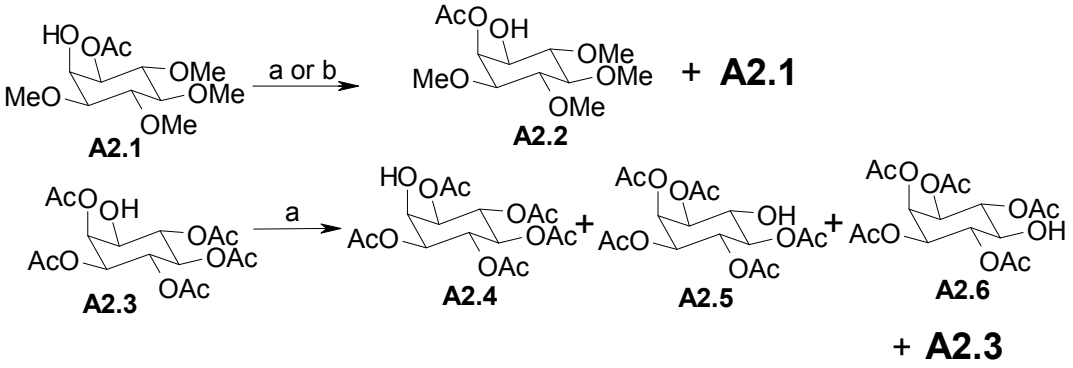

Scheme A2.1. a) Pyr-H_2O (1 : 1), 100 ^oC, 7 h. b) Ag_2O, $CHCl_3$, rt, 3 weeks.

Meek and co-workers[24] obtained racemic 2,4-di-*O*-benzoyl-*myo*-inositol (**A2.9**) as the major product by the base catalyzed isomerization of racemic 1,4-di-*O*-benzoyl-*myo*-inositol (**A2.8**). The dibenzoate **A2.9** was used to synthesize *myo*-inositol 1,3,4,5-tetrakis phosphate (Scheme A2.2). This constituted the first report of exploiting benzoyl migration for the synthesis of *myo*-inositol phosphates.

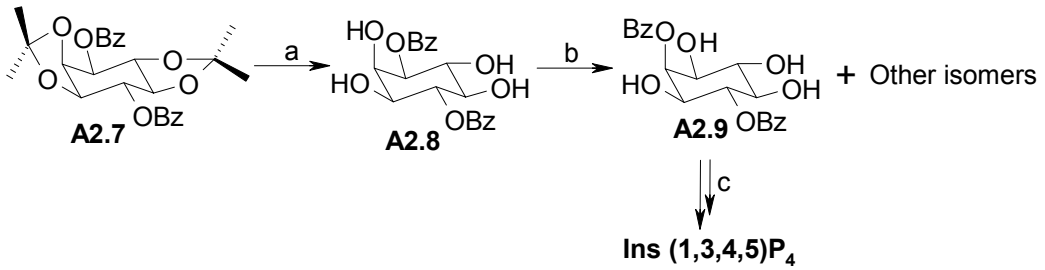

Scheme A2.2. a) TFA-H_2O (10 : 1), $CHCl_3$, reflux, 94%; b) Pyr.-H_2O (3 : 2), 100 ^oC, 2 h; c) As in reference 24.

Chung and co-workers synthesized both racemic[25-27] and optically active[28] *myo*-inositol phosphates by exploiting base catalyzed benzoyl migration among the hydroxyl groups of *myo*-inositol (Scheme A2.3).

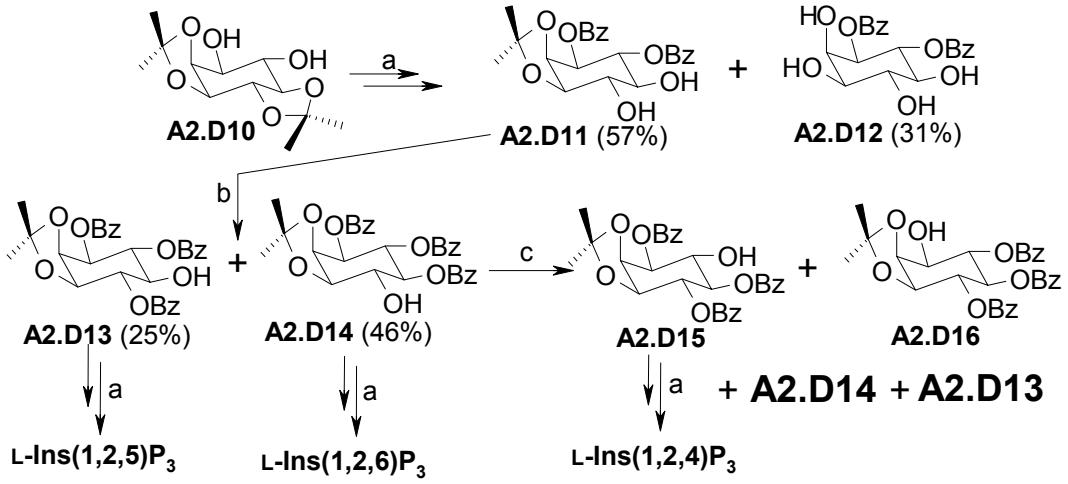

Scheme A2.3. a) as in reference 28; b) BzCl (1.2 eq), Pyr, 0 ^oC-rt, 3 h; c) Pyr-H_2O (3 : 2), 100 ^oC, 3 h.

From kinetic studies on these systems it was shown that the benzoyl group migration to an adjacent *cis*-hydroxyl group was faster than to an adjacent *trans*-hydroxyl

group.[26] *scyllo*-Inositol phosphates have also been synthesized by using benzoyl migration technique (Scheme A2.4).[29] Most of these acyl migration reactions resulted in the formation of a mixture of isomeric esters which were separated by HPLC.

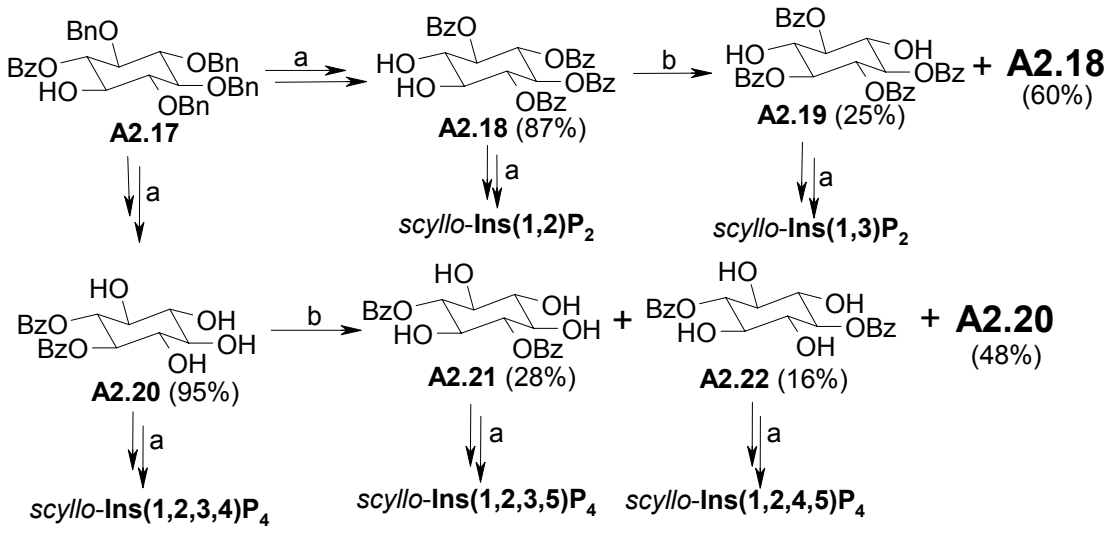

Scheme A2.4. a) as in reference 29; b) Pyr-H_2O (3 : 2), 100 °C, 1.5 h.

Clean migration of acyl groups in 4-O-acyl-*myo*-inositol orthoformates has been reported although the mechanism of this unusual isomerization remains unclear (Scheme A2.5).[30] These literature reports suggest that controlled migration of the acyl groups in inositol could provide preparative routes for certain partially protected inositol derivatives useful for the synthesis of phosphoinositols.

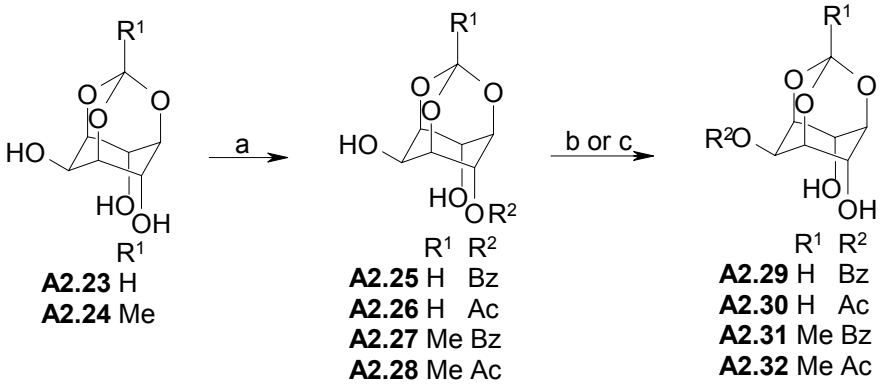

Scheme A2.5. a) R^2Cl (1 eq), NaH (1 eq), DMF, rt, 5 min, 86-89%; b) NaH (1 eq), DMF, rt, 5 min, 85-97%; c) *t*-BuOK, DMF, rt, 5 min, 90-96%.

As discussed in the previous section (Section A1), often solid-state reactions show regioselectivities different than that observed for the corresponding reaction in solution. Hence we wondered whether acyl migration in inositol derivatives in the solid-state could result in migration to specific hydroxyl groups. The discovery of the facile solid-state transesterification reaction in our laboratory[31] also encouraged us to explore the acyl migration in the solid-state, for the preparation of protected cyclitol derivatives. Hence we undertook a study of acyl migration reaction of inositol derivatives in the solid state with the objectives as below:

(a) To see if we can find any solid-state acyl transfer reaction in inositol derivatives, other than the one reported.[31]

(b) If so, whether we can use these reactions for the synthesis of cyclitol derivatives of biological significance.

(c) To see how minor modifications in the molecular structure of *myo*-inositol orthoformate derived esters reflect in their reactivity in the solid state.

(d) To understand the mechanism of the acyl migration reaction in the dibenzoate **A2.33** (Scheme A1.20).

Accordingly several inositol esters were prepared and their ability to undergo transesterification in the solid-state was examined. An attempt was made to correlate the observed reactivity of some of the inositol esters with their crystal structures.

A2.2. Results

A2.2.1. Preparation of ester derivatives of *myo*-inositol

The *myo*-inositol 1,3,5-orthoesters **A2.23** and **A2.24** were prepared according to literature procedure.[32] Racemic 2,4-di-*O*-benzoyl-*myo*-inositol 1,3,5-orthoformate

(**A2.33**),[12] 2,4,6-tri-*O*-benzoyl-*myo*-inositol 1,3,5-orthoformate (**A2.34**),[32] racemic 4-*O*-benzoyl-*myo*-inositol 1,3,5-orthoformate (**A2.25)**,[30] racemic 4-*O*-benzoyl-*myo*-inositol 1,3,5-orthoacetate (**A2.27)**,[30] racemic 2-*O*-benzoyl-4-*O*-benzyl-*myo*-inisitol 1,3,5-orthoformate (**A2.35)**,[33] D- and L-2-*O*-benzoyl-[(-)-*ω*-camphanoyl]-*myo*-inositol 1,3,5-orthoformate (**A2.D36** & **A2.L36)**,[34] D- and L-di-*O*-[(-)-*ω*-camphanoyl]-*myo*-inositol 1,3,5-orthoformate (**A2.D37** & **A2.L37**),[13] and racemic 1,2-*O*-isopropylidine-3,6-di-*O*-benzoyl-*myo*-inositol (**A2.38)**[25] were prepared according to literature procedures.

Racemic 2,4-di-*O*-pivaloyl-*myo*-inositol 1,3,5-orthoformate (**A2.41**, Scheme A2.6) and racemic 2,4-di-*O*-naphthoyl-*myo*-inositol 1,3,5-orthoformate (**A2.42**) were obtained, in good yield (60-80%), by acylation of the triol **A2.23** with pivaloyl chloride and naphthoyl chloride respectively. Racemic 2,4-di-*O*-benzoyl-*myo*-inositol 1,3,5-orthoacetate (**A2.43**) was prepared by the sequential reaction of *myo*-inositol with triethylorthoacetate and benzoylchloride using a procedure similar to that used for the preparation of racemic 2,4-di-*O*-benzoyl-*myo*-inositol 1,3,5-orthoformate **A2.33**.[12] The intermediate triol **A2.24** was not isolated during this experiment.[12,35] The unsymmetric nature of all these *myo*-inositol orthoester derived diesters were revealed by their NMR spectra. *myo*-Inositol derived esters **A2.9** and **A2.39** were prepared from **A2.33** and **A2.34** respectively by cleaving the orthoformate with aqueous trifluoroacetic acid.

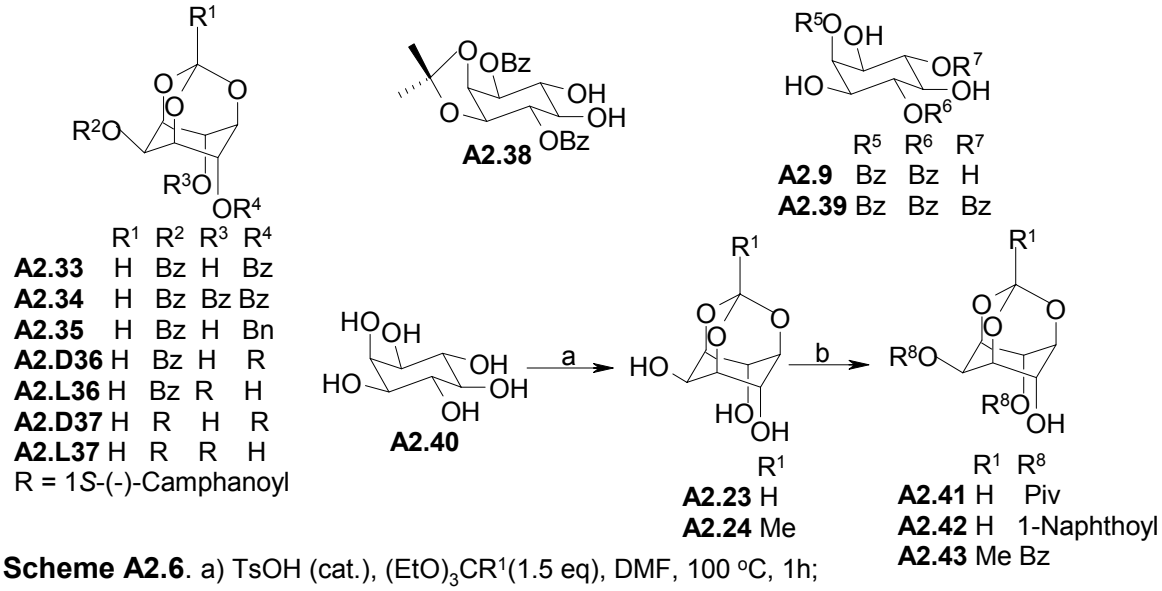

Scheme A2.6. a) TsOH (cat.), $(EtO)_3CR^1$(1.5 eq), DMF, 100 ^oC, 1h; b) R^8Cl (2.1 eq), Pyr., 0 ^oC-rt, 12h.

The benzoates **A2.49** and **A2.50** (Scheme A2.7) were prepared from the symmetrical ditosylate **A2.44** (see Section 2, Part B of this thesis). Alkylation of the ditosylate **A2.44** with benzyl bromide and methyl iodide in the presence of sodium hydride in DMF gave the benzyl ether **A2.45** and the methyl ether **A2.46** respectively. The tosyl groups in these ditosylates were cleaved by treatment with magnesium in a mixture of methanol and THF to obtain the diols **A2.47** and **A2.48** respectively. Benzoylation of these diols with one equivalent of benzoyl chloride afforded the benzoates **A2.49** and **A2.50**.

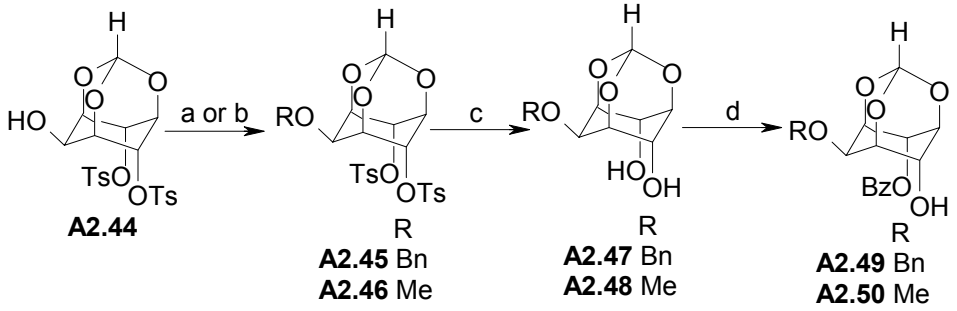

Scheme A2.7. a) NaH (1.1 eq), BnBr (1.2 eq), DMF, rt, 5 min, 100%; b) NaH (1.1 eq), MeI (1.3 eq), DMF, rt, 5 min, 100%; c) Mg turnings, MeOH-THF (3 :1), rt, 6 h, 95% for **A2.47** and 94% for **A2.48**; d) BzCl (1.1 eq), Pyr., 0 ^oC-rt, 12 h, 75-80% for **A2.49** and 70-75% for **A2.50**.

The preparation of racemic benzoate **A2.51** and racemic pivalate **A2.53** are shown in the Scheme A2.8. Tosylation of the triol **A2.23** in pyridine followed by benzoylation with benzoyl chloride in a one-pot procedure gave the benzoate **A2.51**. Similarly the pivalate **A2.52** was obtained by pivaloylation of **A2.23**, [30,36] benzoylation which gave the racemic **A2.53**. It is known in the literature that acylation[12] and sulfonylation[37] of *myo*-inositol 1,3,5-orthoesters with one equivalent of the corresponding acid chloride in pyridine results in the acylation and sulfonylation of the C-2 hydroxyl group of **A2.23**. The structures of **A2.51** and **A2.52** were also confirmed by X-ray crystallography.

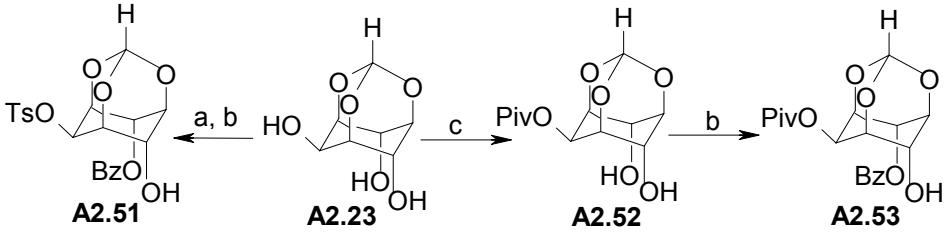

Scheme A2.8. a) TsCl (1.1 eq), Pyr., rt, 18 h; b) BzCl (1.1 eq), Pyr., rt, 12 h, 65% for **A2.51** and 62% for **A2.53**; c) PivCl (1.2 eq), Pyr.,0 °C-rt, 12 h.

The 4-pivalate **A2.54** and the 4-tosylate **A2.55** were synthesized by pivaloylation and tosylation of the known diol **A2.29**[35] with pivaloyl chloride and tosyl chloride in pyridine respectively.

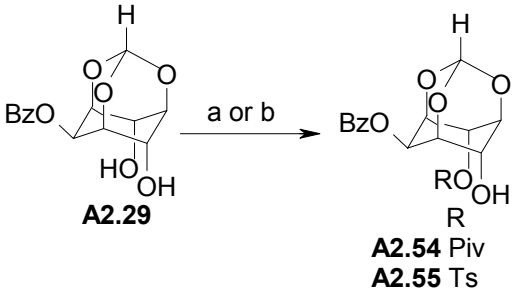

Scheme A2.9. a) PivCl (1.2 eq), Pyr., 0 °C-rt, 12 h, 70%; b) TsCl (1.1 eq), Pyr., rt, 12 h, 84%.

Since the crystal structures of **A2.33**, **A2.43** and **A2.53** looked similar (discussed in the next section), and also the study of co-crystallization of organic molecules is of current research interest[38-41] we attempted the cocrystallization of mixtures of **A2.33** and **A2.43**, **A2.33** and **A2.53**, **A2.43** and **A2.53** and the ternary mixture of **A2.33**, **A2.43** and **A2.53**. Of all the trials, we were fortunate to obtain crystals of mixture of **A2.33** and **A2.43**, where, the unit cell consisted of one molecule of **A2.33** and **A2.43** each. It was interesting to observe that, irrespective of the ratio of **A2.33** and **A2.43** in solution, the "molecular adduct" (hereafter **A2.33·43**) always crystallized with 1 : 1 ratio of **A2.33** and **A2.43**.

A2.2.2. Preparation of ester derivatives of *scyllo*-inositol

scyllo-Inositol orthoformate (**A2.56**,[42] Scheme A2.10) was prepared from *myo*-inositol as described in Part B, Section 2 of this thesis. The dibenzoate **A2.57** was prepared by benzoylation of the triol **A2.56** with two equivalents of benzoyl chloride in pyridine in the presence of catalytic amount of DMAP. The racemic benzoates **A2.63** and **A2.64** were synthesized from the ditosylate **A2.58** as shown in Scheme A2.10. The ditosylate **A2.58** was alkylated with benzyl bromide or methyl iodide in the presence of sodium hydride in DMF to obtain the benzyl ether **A2.59** and the methyl ether **A2.60** respectively. Removal of the tosylates from **A2.59** and **A2.60** by refluxing them with sodium methoxide in methanol gave the diols **A2.61** and **A2.62** respectively. The benzoates **A2.63** and **A2.64** were obtained by acylation of the diols **A2.61** and **A2.62** with benzoyl chloride in pyridine in the presence of catalytic amount of DMAP.

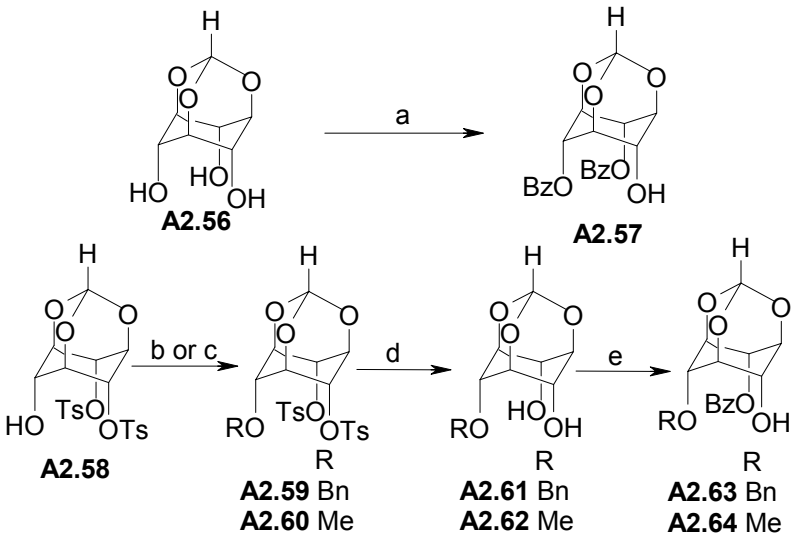

Scheme A2.10. a) BzCl (2.1 eq), DMAP (cat.), Pyr., 0 ^{o}C-rt, 12 h, 63%; b) NaH (1.1 eq), BnBr (1.2 eq), DMF, rt, 5 min, 100%; c) NaH (1.1 eq), MeI (1.5 eq), DMF, rt, 5 min, 92%; d) NaOMe, MeOH, reflux, 8 h, 98% for **A2.61** and 93% for **A2.62**; e) BzCl (1.1 eq), DMAP (cat.), Pyr., 0 ^{o}C-rt, 12 h, 72% for **A2.63** and 69% for **A2.64**.

A2.2.3. Solid-state transesterification reactivity *myo*-inositol derivatives

The *myo*-inositol derivatives **A2.9**, **A2.25**, **A2.27**, **A2.33**, **A2.35**-**A2.39**, **A2.41**-**A2.43**, **A2.49**, **A2.50**, **A2.51**, **A2.53**-**A2.55** and the co-crystal **A2.33·43** were heated with sodium carbonate below their melting points for 60-192 h and the products obtained were isolated and characterized. Although the solid-state transesterification reactions were carried out at temperatures well below the melting point of the reactants, to examine if any liquid phases were involved below the melting points of the reactants and products in these multi-component reaction mixtures, we examined the reactivity of some of the hydroxy esters in the molten state. We also carried out the transeterification reaction of some of the hydroxyesters in solution for comparison with their reaction in the solid state. In experiments wherein a mixture of many products was obtained, no attempt was made to isolate the products.

Chung and co-workers studied benzoyl migration in inositol derivatives and used the various benzoates for the synthesis of *myo*- and *scyllo*-inositol phosphates.[25-29] (Schemes A2.3 & A2.4). We investigated the solid-state reactivity of *myo*-inositol esters **A2.9**, **A2.38** and **A2.39** (Scheme A2.11) hoping to achieve selectivity during acyl migration, leading to precursors for the preparation of inositol phosphate in high yield. However, our attempts to obtain good crystals of these solids were not successful.

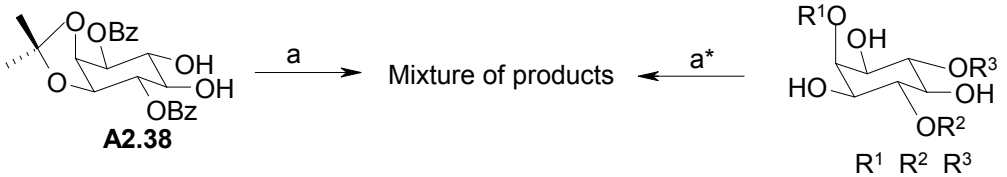

A2.38

Scheme A2.11. a) Na_2CO_3 (8 eq), 100 °C, 1 h;
* reaction time was 172 h.

	R^1	R^2	R^3
A2.9	Bz	Bz	H
A2.39	Bz	Bz	Bz

Although crystal structure of one of these hydroxy esters (**A2.38**) containing THF is reported, these THF adducts could not be obtained consistently by the reported method of crystallization.[43] Heating these amorphous solid esters with sodium carbonate led to the formation of a mixture of many products (by TLC). Since these reactions did not appear to be of any synthetic utility, no attempt was made to isolate the products.

Transesterification of *myo*-inositol orthoformate derivatives **A2.D36**, **A2.L36**, **A2.D37** and **A2.L37** was also investigated to look for selectivity in acyl migration and a possibility of synthetic utility. These diesters have been used as precursors for Ins(1,3,4,5)P_4.[13,34] Since the diesters **A2.D36**, **A2.L36**, **A2.D37** and **A2.L37** are diastereomeric and are obtained from 1,3-diaxial diols, intramolecular migration of the camphanoyl group between the two axial hydroxyl groups is a possibility. Heating of **A2.D36** and **A2.L36** with sodium carbonate (Scheme A2.12), led to the formation of a

mixture of many products (by TLC). Since these reactions did not appear to be of any synthetic utility, no attempt was made to isolate the products from the reaction mixture. Treatment of **A2.D37** and **A2.L37** with sodium carbonate even at 170°C did not result in any tansesterification. We also investigated the transesterification of **A2.D37** and **A2.L37** in solution (acetonitrile / triethylamine and DMF / sodium hydride), but under these conditions also no transesterification was observed. These experiments were found to be unsuitable for the synthesis of cyclitol derivatives.

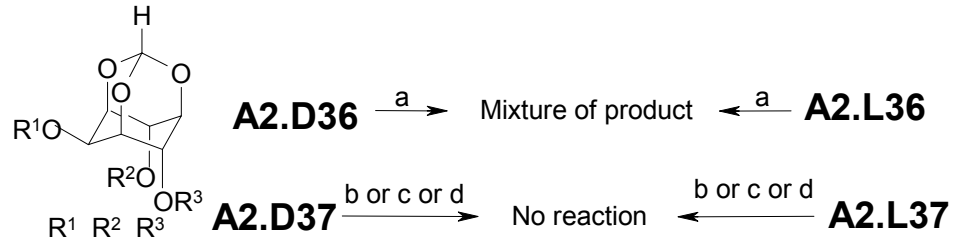

	R^1	R^2	R^3
A2.D36	Bz	H	R
A2.L36	Bz	R	H
A2.D37	R	H	R
A2.L37	R	R	H

R = 1*S*-(-)-camphanoyl

Scheme A2.12. a) Na_2CO_3 (8 eq), 140 °C for 48 h; b) Na_2CO_3 (8 eq), 170 °C, 48 h; c) Et_3N (10 eq), MeCN, rt, 48 h; d) NaH (4.5 eq), DMF, rt, 48 h.

The solid-state transesterification reaction of *myo*-inositol orthoester derivatives **A2.54** and **A2.55** (Scheme A2.13) in the presence of sodium carbonate gave inseparable mixture of products; no attempt was made to isolate the products. The hydroxy esters **A2.35** and **A2.42** remained unchanged on heating with Na_2CO_3. The compound A2.**27** underwent hydrolysis on heating with Na_2CO_3 in the solid state. This could be due to the presence of water in crystals of **A2.27** (see page 53 for crystal packing and page 111 for ORTEP).

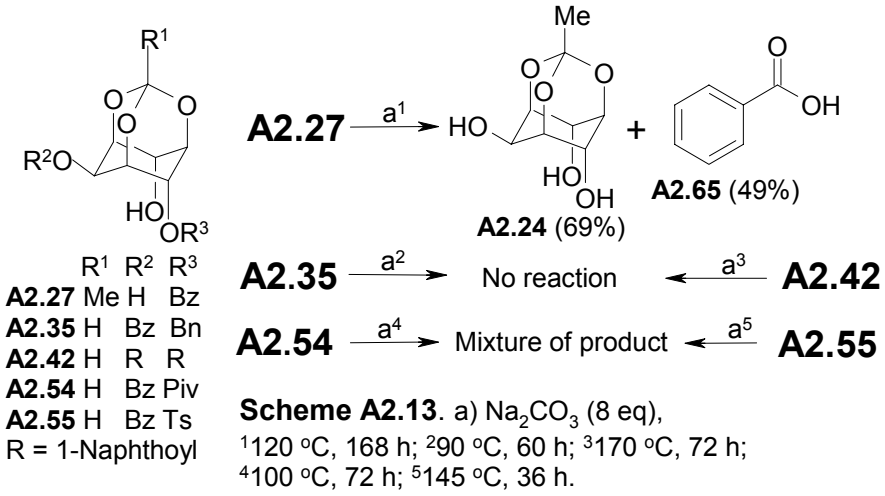

Scheme A2.13. a) Na_2CO_3 (8 eq), [1]120 °C, 168 h; [2]90 °C, 60 h; [3]170 °C, 72 h; [4]100 °C, 72 h; [5]145 °C, 36 h.

A2.2.3.1. Transesterification of racemic 4-*O*-benzoyl-*myo*-inositol 1,3,5-orthoformate (A2.25)

Transesterification of **A2.25** (Scheme A2.14) with sodium carbonate in the solid state afforded a mixture of triester **A2.34** (24%), the diesters **A2.33** (<2%) and **A2.66** (<2%), the diol **A2.29** (<2%), triol **A2.23** (56%) and benzoic acid (**A2.65**, 20%). Formation of the tribenzoate **A2.34** might be due to the transesterification of the initially formed dibenzoate **A2.33**.[31] The appearance of benzoic acid suggested that the transesterification reaction was accompanied by hydrolysis of some of the components present in the reaction mixture.

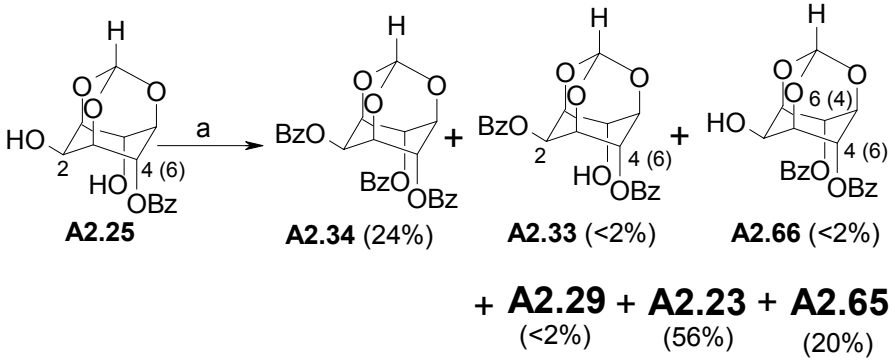

Scheme A2.14. a) Na_2CO_3 (8 eqv.), 120 °C, 80 h.

A2.2.3.2. Transesterification of racemic 2, 4-di-*O*-benzoyl-*myo*-inositol 1,3,5-orthoformate (**A2.33**)

On heating with sodium carbonate, in the solid-state, **A2.33** gave the tribenzoate **A2.34** (47%) and the diol **A2.29** (49%, Scheme A2.15) as reported earlier.[31] Treatment of **A2.33** with triethylamine in acetonitrile solution at ambient temperature for 144 h gave **A2.34** (32%) and **A2.29** (31%).[31] Reaction of **A2.33** with sodium carbonate in the molten state (180 °C) afforded mixture of products consisting of **A2.34**, **A2.25**, **A2.29** and **A2.66**. This suggested the migration of both the C-6 axial benzoyl group and the C-2 equatorial benzoyl group to other hydroxyl groups. The difference in the reactivity of **A2.33** in the solid-state and in the molten state ruled out the involvement of a liquid phase below the melting point of **A2.33** during its solid-state reaction.

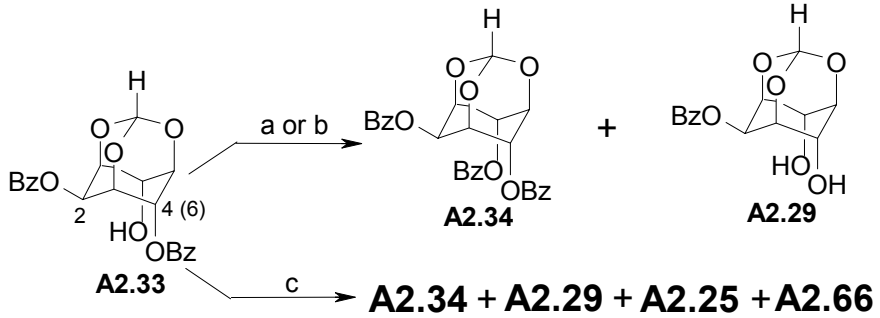

Condition	Product (% yield)			
Solid-state	**A2.34** (47)	**A2.29** (49)	**A2.25** (0)	**A2.66** (0)
Solution	**A2.34** (32)	**A2.29** (31)	**A2.25** (0)	**A2.66** (0)
Melt	**A2.34** (16)	**A2.29** (15)	**A2.25** (9)	**A2.66** (13)

Scheme A2.15. a) Na_2CO_3 (8 eq), 140 °C, 60 h; b) Et_3N (10 eq), MeCN, rt, 144 h; c) Na_2CO_3 (8 eq), 180 °C, 36 h.

A2.2.3.3. Transesterification of racemic 2,4-di-*O*-pivaloyl-*myo*-inositol 1,3,5-orthoformate (A2.41)

Transesterification of **A2.41** (Scheme A2.16) in the solid-state afforded the dipivalate **A2.67** (23%), the diol **A2.52** (61%) and pivalic acid (detected by ^{1}H NMR spectroscopy). On refluxing with triethylamine in acetonitrile solution, **A2.41** afforded **A2.67** (19%) and **A2.52** (18%).

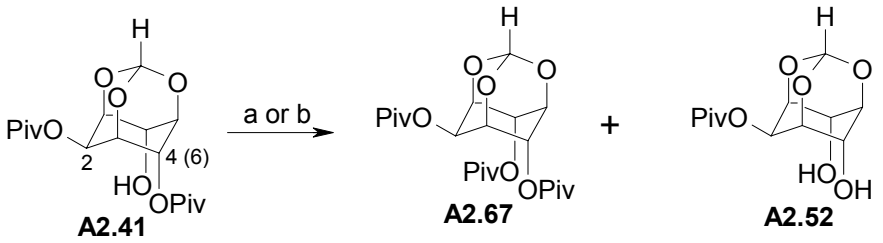

Condition	Product (% yield)	
Solid-state	**A2.67**(23)	**A2.52**(61)
Solution	**A2.67**(19)	**A2.52**(18)

Scheme A2.16. a) Na_2CO_3 (8 eq), 125 ^oC, 192 h; b) Et_3N (10 eq), MeCN, reflux, 144 h.

A2.2.3.4. Transesterification of racemic 2,4-di-*O*-benzoyl-*myo*-inositol 1,3,5-orthoacetate (A2.43)

When heated with sodium carbonate in the solid state (Scheme A2.17), **A2.43** gave the tribenzoate **A2.68** (19%), the diol **A2.31** (21%), the dibenzoate **A2.69** (8%) and the racemic monobenzoate **A2.27** (16%). Transesterification of **A2.43** in the presence of triethylamine in acetonitrile solution at ambient temperature for 144 h gave **A2.68** (30%) and **A2.31** (29%). Reaction of **A2.43** with sodium carbonate in the molten state (180 °C) also afforded a mixture of products resulting from transesterification not only from the C-6 axial ester, but also from the C-2 equatorial ester, leading to the formation of **A2.68**,

A2.31, **A2.69** and **A2.27** (confirmed by TLC by comparison with authentic samples), no attempt was made to isolate the products of the reaction in melt.

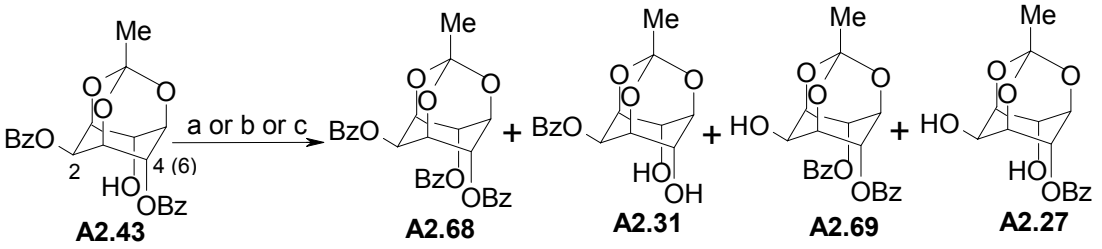

Condition	Product (% yield)			
Solid-state	**A2.68**(19)	**A2.31**(21)	**A2.69**(8)	**A2.27**(16)
Solution	**A2.68**(30)	**A2.31**(29)	**A2.69**(0)	**A2.27**(0)
Melt	Products not isolated			

Scheme A2.17. a) Na_2CO_3 (8 eq), 140 °C, 168 h; b) Et_3N (10 eq), MeCN, rt; c) Na_2CO_3 (8 eq),180 °C, 36 h.

A2.2.3.5. Transesterification of the molecular complex A2.33·43

When heated with sodium carbonate in the solid-state, the complex **A2.33·43** afforded tribenzoates **A2.34**, **A2.68** and the diols **A2.29**, **A2.31** (Scheme A2.18). The proportion of the individual tribenzoates and the diols were estimated by ^{1}H NMR spectroscopy. The ^{1}H NMR spectrum of the mixture of **A2.34** and **A2.68** (see page 166) showed peaks at δ 5.75 (corresponding to orthoformate proton of **A2.34**) and at δ 1.55 (corresponding to the orthoacetate methyl protons of **A2.68**) bearing integration ratio 1 : 1.5, which showed that **A2.34** and **A2.68** were formed in 2 : 1 ratio. Similarly, ^{1}H NMR spectrum of the mixture of **A2.29** and **A2.31** (see page 166) showed peaks at δ 5.55 (corresponding to the orthoformate proton and C-2 proton of **A2.29**) and δ 1.45 (corresponding to the orthoacetate methyl protons of **A2.31**) with integration ratio 1 : 3. This suggested the ratio of **A2.29** and **A2.31** I the mixture to be 1 : 2. Triethylamine catalyzed transesterification of the molecular complex **A2.33·43** in acetonitrile solution

also afforded the triesters **A2.34**, **A2.68** and the diols **A2.29**, **A2.31** in 1 : 1 ratio (estimated by by ^{1}H NMR spectroscopy as above, see pages 167 and 168). Heating a melt of **A2.33·43** with solid sodium carbonate gave a mixture of many products (revealed by a comparison of TLC of the products with authentic samples) arising from the migration of benzoyl groups at C6(4)- and C2 positions of both **A2.33** and **A2.43**. No attempt was made to isolate products from this experiment.

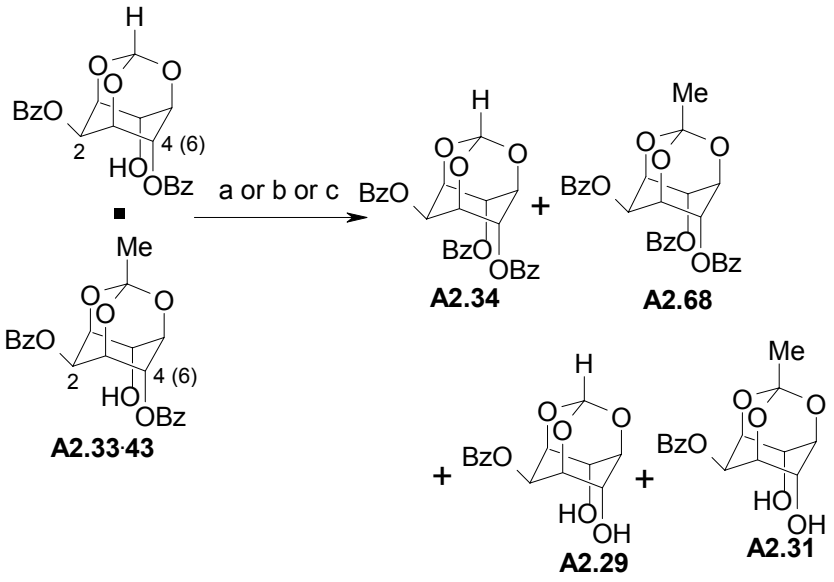

Condition	Product (% yield, ratio)	
Solid-state	**A2.34** + **A2.68**(41, 2 : 1)	**A2.29** + **A2.31**(39, 1 : 2)
Solution	**A2.34** + **A2.68**(32, 1 : 1)	**A2.29** + **A2.31**(28, 1 : 1)
Melt	Products not isolated	

Scheme A2.18. a) Na_2CO_3 (8 eq), 120 °C, 168 h; b) Et_3N (10 eq), MeCN, rt, 144 h; c) Na_2CO_3 (8 eq), 180 °C, 36 h.

A2.2.3.6. Transesterification of racemic 2-*O*-benzyl-4-*O*-benzoyl-*myo*-inositol 1,3,5-orthoformate (A2.49)

Transesterification of **A2.49** (Scheme A2.19) in the presence of sodium carbonate in the solid state at 100 °C afforded the dibenzoate **A2.70** (42%) and the diol **A2.47**

(45%). Heating of **A2.49** with sodium carbonate in the molten state also resulted in the formation of **A2.70** (41%) and **A2.47** (42%).

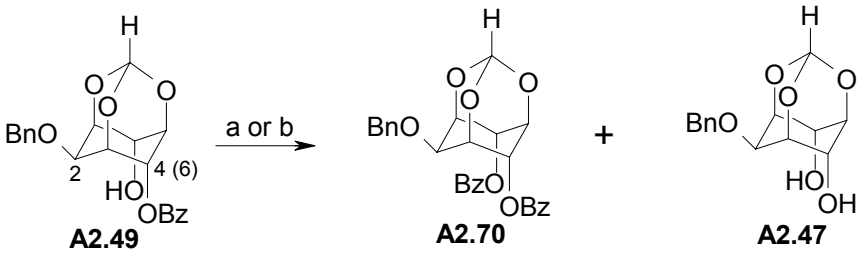

Condition	Product (% yield)	
Solid-state	**A2.70**(42)	**A2.47**(45)
Melt	**A2.70**(41)	**A2.47**(42)

Scheme A2.19. a) Na_2CO_3 (8 eq), 100 ^oC, 192 h; b) Na_2CO_3 (8 eq), 140 ^oC, 192 h.

A2.2.3.7. Transesterification of racemic 2-*O*-methyl-4-*O*-benzoyl-*myo*-inositol 1,3,5-orthoformate (A2.50)

Transesterification of **A2.50** (Scheme A2.20) in the solid-state afforded the dibenzoate **A2.71** (15%), the diol **A2.48** (55%) and benzoic acid (**A2.65**). Heating of **A2.50** with sodium carbonate in the molten state led to decomposition and charring of **A2.50**.

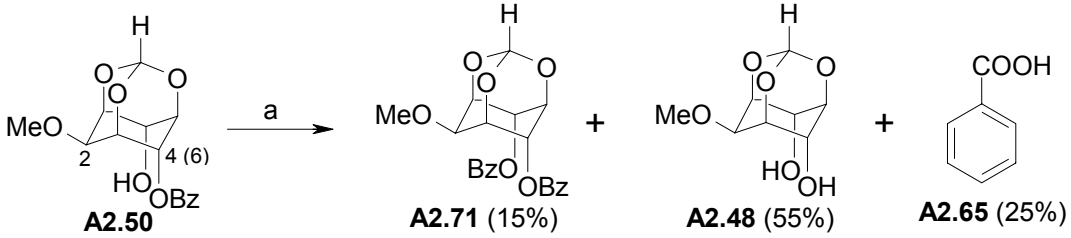

Scheme A2.20. a) Na_2CO_3 (8 eq), 125 ^oC, 144 h.

A2.2.3.8. Transesterification of racemic 2-*O*-tosyl-4-*O*-benzoyl-*myo*-inositol 1,3,5-orthoformate (A2.51)

Transesterification of **A2.51** in the solid-state (Scheme A2.21) afforded the dibenzoate **A2.72** (17%) and the diol **A2.73** (10%). This reaction was accompanied by

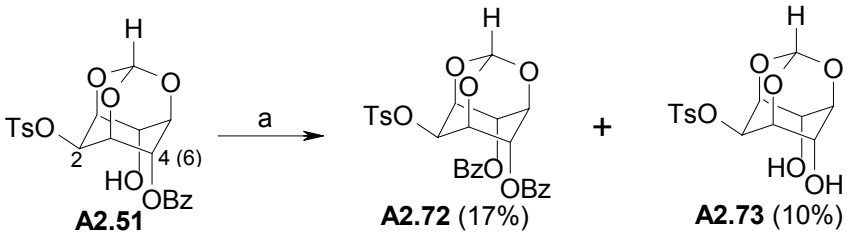

Scheme A2.21. a) Na_2CO_3 (8 eq), 100 °C, 192 h.

decomposition and charring of **A2.51,** which could be the reason for low recovery of products. The benzoate **A2.51** did not react at lower temperatures.

In case of *myo*-inositol orthoester derivatives **A2.25, A2.41** and **A2.50**, the transesterification was accompanied by hydrolysis, reason for which was not fully understood. It is likely that in the solid state there is a competition between transesterification and hydrolysis of the ester groups due to water present in solid sodium carbonate. When the crystal structure allows facile transesterification reaction it occurs predominantly whereas when the crystal structure is not conducive for transesterification, hydrolysis could become predominant.

A2.2.3.9. Transesterification of racemic 2-*O*-pivaloyl-4-*O*-benzoyl-*myo*-inositol 1,3,5-orthoformate (A2.53)

The racemic pivalate **A2.53** on heating with sodium carbonate in the solid-state afforded a mixture of products (Scheme **A2.22**). Only the triester **A2.74** (14%) was

isolated from the reaction mixture. No attempt was made to isolate the other products formed during this reaction. On treatment with triethylamine in acetonitrile solution, **A2.53** afforded the triester **A2.74** (23%) and the diol **A2.52** (25%).

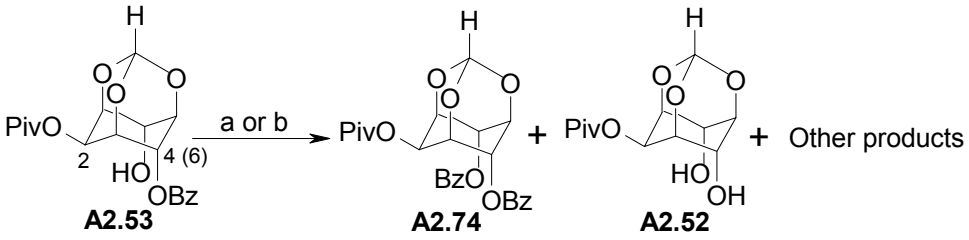

A2.53 **A2.74** **A2.52**

Condition		Product (% yield)
Solid-state	**A2.74**(14)	Other products not isolated
Solution	**A2.74**(23)	**A2.52**(25)

Scheme A2.22. a) Na_2CO_3 (8 eq), 140 °C, 168 h; b) Et_3N (10 eq), MeCN, rt, 144 h.

Although, the solid-state transesterification reaction of **A2.33**, **A2.43**, **A2.53** and **A2.33·43** were carried out at temperatures well below the melting point of the reactants, to ensure that the reactions took place in the crystalline state only and not in their molten forms and to rule out the possibility of liquid phases being involved below the melting points of the reactants and products in these multi-component reaction mixtures, we examined the reactivities of diesters at comparable temperatures. For instance, at 100 °C, the dibenzoate **A2.33** underwent clean reaction while **A2.43** and **A2.33·43** were unreactive. At 110 °C and above, crystals of **A2.43** and **A2.33·43** began to react (although slowly) to give the transesterified products. At still higher temperatures, **A2.43** gave a mixture of products as described earlier. None of the diesters underwent any reaction in the molten state (~ 180 °C) in the absence of sodium carbonate. Reaction of **A2.33**, **A2.43** and **A2.33·43** in melt with sodium carbonate afforded mixture of products resulting from the transesterification not only from the C6-axial ester but also from C2-

equatorial ester. These results exclude the possibility of formation of any molten phases during the reaction of crystals below their melting points. Such an occurrence would have resulted in the loss of specificity of the transesterification reaction below the melting point of the reactants.

A2.2.3.10. Solid-state transesterification of *scyllo*-inositol 1.3.5-orthoformate derivatives

Since variations in the molecular structure of the *myo*-inositol 1,3,5-orthoester derivatives showed major differences in the solid-state transesterification reactivity of these compounds, we examined the solid state reactivity of *scyllo*-inositol derivatives **A2.57**, **A2.63** and **A2.64** as these differ only in the orientation of the hydroxyl group at the 2-position of the *myo*-inositol ring. The solid monoesters **A2.63** and **A2.64** remained unchanged on heating with sodium carbonate, but the diester **A2.57** gave the tribenzoate **A2.75** (69%) and the triol **A2.56** (17%).

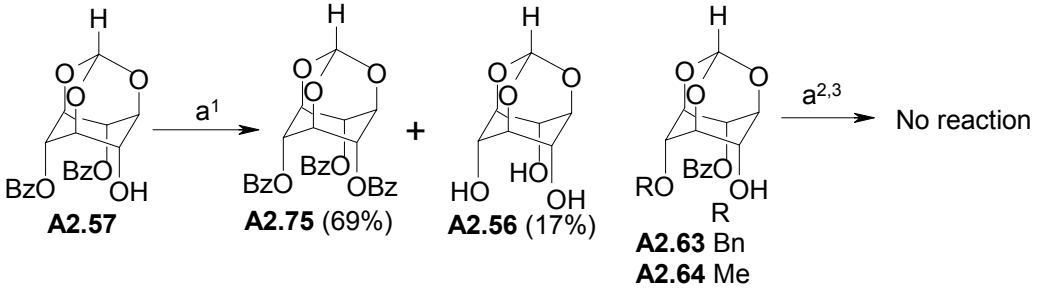

Scheme A2.23. a) Na_2CO_3 (8 eq), 48 h, [1]160 °C ; [2]115 °C for **A2.63**; [3]125 °C for **A2.64**.

A2.3. Discussion

Inositol orthoester derivatives tested for transesterification in the solid state and / or solution can be categorized into two groups; those containing one acyl group or two acyl groups. In the case of compounds having one acyl group, only one transesterification product arising from the intermolecular migration of the axial acyl

group is possible (Scheme A2.24). While in those with two acyl groups, intermolecular migration of both the axial and the equatorial acyl groups resulting in the formation of four products are possible. Furthermore, in this case, acyl migration in the monoesters produced can take place, giving rise to a number of products. This was evident from the results of some of the solid state experiments described above.

Another possibility in both the mono and diesters is the intramolecular migration of the acyl group among the two 4,6-axial positions. The reactant (**A2.D79**) and the product (**A2.L79**) in this intramolecular reaction are enantiomers. However, since all the acylated inositol orthoester derivatives (except the camphanoates **A2.36** and **A2.37**) in

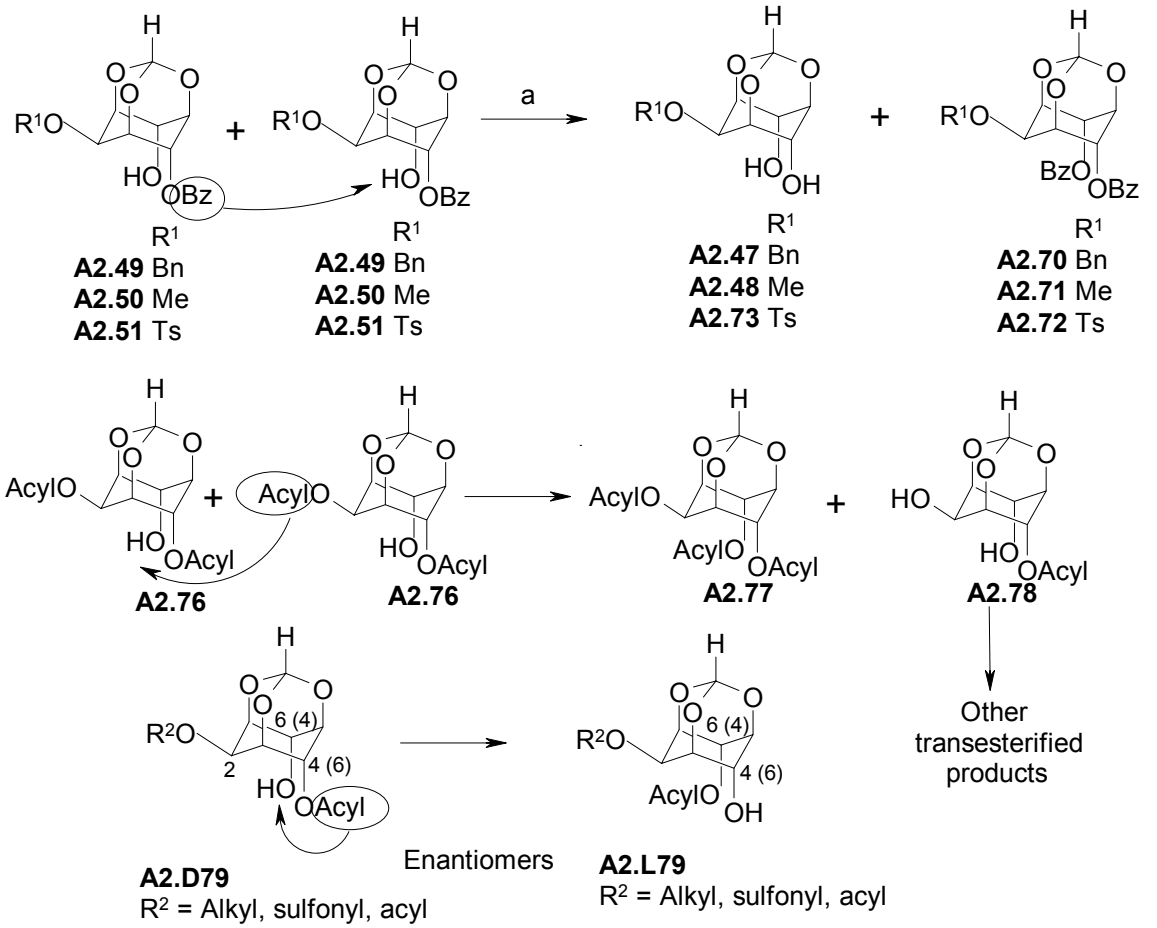

Scheme A2.24. a) Na_2CO_3 (8 eq), heat, 60-192 h.

the present study are racemic, this intramolecular reaction is not detectable. Hence the possibility of intramolecular acyl migration will not be considered during the discussion of results. In the case of the dicamphanoates **A2.D37** and **A2.L37**, there was no appreciable reaction either in the solid state or in solution (in this case the possible product **A2.D37** is a diastereomer of **A2.L37** and *vice-versa*, hence the reaction is detectable). This could be due to the large size of the acyl group. The lesser reactivity of the dipivalate **A2.41** towards base catalyzed transesterification also supports this view.

The base catalyzed transesterification of **A2.33**, **A2.41**, **A2.43**, **A2.33·43** and **A2.53** in solution involves specific transfer of the C4(6)-O- acyl group of one molecule of the diester to the C6(4)-hydroxyl group of another (Schemes A2.15-A2.18 and Scheme A2.22). Earlier work from our laboratory[12] had shown that this specific transesterification reaction in solution is due to the intramolecular catalysis of the C6(4)-axial hydroxyl group for the transfer of the C4(6)-O-benzoyl group. Hence of the two possible transesterification reactions (migration of 2-*O*- and 4 (6)-*O*- acyl groups), only that assisted by intramolecular catalysis prevails.

A2.3.1. Correlation of crystal structure of inositol orthoester derivatives with their solid-state reactivity

All the inositol orthoester derivatives examined for solid-state transesterification reactivity except **A2.35**, **A2.42**, **A2.54** and **A2.55** gave crystals suitable for X-ray diffraction analysis. Hence, the reactivity of **A2.35**, **A2.42**, **A2.54** and **A2.55** will not be considered for further discussion. Among the other inositol orthoester derivatives tested for solid-state transesterification reaction, **A2.25**, **A2.27**, **A2.41** and **A2.50** underwent

hydrolysis. Since the source of water in these reactions cannot be specified clearly, these results cannot be rationalized based on the crystal structure of the reactants.

The acyl transfer reaction in the crystalline state involves the transfer of the C4(6)-O- benzoyl group (Electrophile, El = C=O) of one molecule of the diester (**A2.33**, **A2.43**, **A2.53**, **A2.33·43**) to the C6(4)-hydroxyl group (Nucleophile, Nu = OH) of another. A comparison of the yields of transesterified products in solution and the solid-state reactions reveal significant variations in the reactivities of **A2.33**, **A2.43**, **A2.53**, and **A2.33·43.** The reactivity of these esters is similar in the solution state as regards nature of the products formed, although relative rates appear to be different. Hence the observed differences in their reactivity in the solid state can be attributed to the differences in the molecular packing in crystals. It was observed that minor changes in the molecular structure, like changing of orthoformate (in **A2.33**) to orthoacetate (in **A2.43**) and replacement of the benzoyl group at O-2 (in **A2.33**) with pivaloyl group (in **A2.53**) resulted in wide differences in the solid-state reactivity. To understand the reason for these differences, we analyzed the crystal structures of *myo*-inositol orthoester derivatives **A2.33**, **A2.43**, **A2.49**, **A2.51**, **A2.53** and **A2.33·43**.

As explained in the earlier section (see Figure A1.3), pertaining to the solid-state transesterification reaction of the dibenzoate **A2.33**, we first looked for the relative orientation of the reactive C4(6)- hydroxyl group (Nu) and the C6(4)- acyl carbonyl group (El) in terms of distance (d) and the angle (x) between them (Figure A2.1). The corresponding distance and the angle conducive for the reaction being about 3.2 Å and 80-120°[31] (see Figure A1.4). El…Nu interactions have earlier been observed in crystals of simple organic compounds[31,44-47] as well as in macromolecules.[48,49]

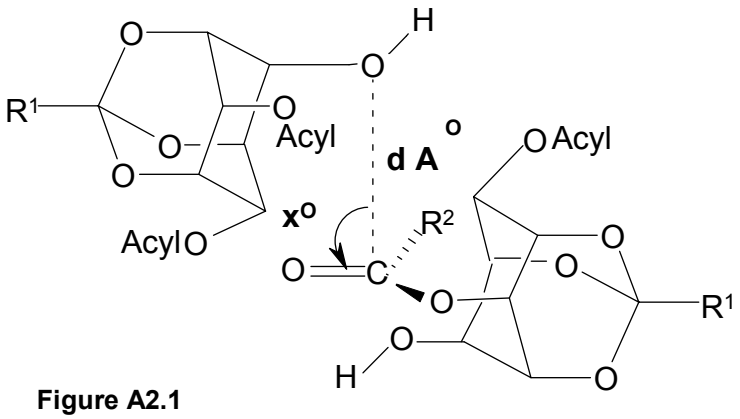

Figure A2.1

In crystals of **A2.33, A2.43** and **A2.53**, the molecules assemble to form a helix around the crystallographic two-fold screw axis (Figures 8A, 8B and 8C respectively), while in crystals of **A2.33·43** such a molecular association is around a non-crystallographic axis (Figure 8D). The successive molecules along the helix are linked by O-H…O hydrogen bonding; the OH group at the C4(6)- position donates its H atom to the carbonyl oxygen O8 of the C2-O-benzoyl group. This hydrogen bonding is not seen in case of other compounds and they don't form helix along any of the crystallographic axes (Figures A2.2-A2.7). Comparison of these crystal structures showed that the crystals of **A2.33**, **A2.43**, **A2.53** and **A2.33·43** have El – Nu geometry (see Table A2.1) conducive for the addition of the C4(6)-hydroxyl group to the C6(4)- ester carbonyl group, while in crystals of other derivatives such a geometry deviates from these parameters (Figures A2.2-A2.7). From Table A2.1 and / or figures A2.2-A2.7 it can be seen the compounds **A2.25**, **A2.27**, **A2.41**, **A2.49**, **A2.50** and **A2.51** do not fulfill both of these 'pre-organization' requirements – El…Nu distance and angle, for the transesterification reaction. This may be the reason for the poor-reactivity of these compounds (except **A2.49**) under solid-state transesterification conditions. Although the angle is good for **A2.L37** (105.47º) the distance (5.976 Å) is longer, which prevents the approach of the

nucleophile to the carbonyl group and thus no reaction was observed. Crystal structure of **A2.L37** is reported in the literature[13] and we have obtained the required El…Nu distance and angle from the reported data.

Table A2.1. Geometry of the reacting groups. Atom numbers refer to the packing diagrams (Figures A2.2- A2.9)

Comp. nos.	Distance (Å) / Angle (°)			
	C8…O4	∠O4…C8-O7	∠C4-O4…C8	∠H4A-O4…C8
A2.33	3.226[a]; 3.249 [b]	88.1[a]; 89.9[b]	117.6[a]; 113.1[b]	113.1[a]; 110.0[b]
A2.L37	5.976[c]	105.47[c]	127.31[c]	26.29[c]
A2.43	3.299[d]	84.01[d]	97.20[d]	105.8[d]
A2.49	4.362[e]; 6.566[f]	54.94[e]; 105.63[f]	149.13[e]; 96.72[f]	77.92[e]; 130.79[f]
A2.51	5.945[g]	86.63[g]	112.16[g]	123.49[g]
A2.53	3.533[d]	70.21[d]	97.65[d]	112.68[d]
A2.33·43	3.170[h]; 3.155[i]	85.9[h]; 88.4[i]	117.6[j]; 116.1[i]	107.9[j]; 119.8[i]

[a] 1-x, -½+y, ½-z; [b] 2-x, ½+y, ½-z; [c] -1+x, y, -1+z; [d] 3/2 –x, -½+y, ½-z; [e] ½-x, ½+y, z; [f] 1-x, -y, 1-z; [g] 3/2-x, -1/2+y, ½-z; [h] x, y, z benzoyl transfer at **I A2.33** → **A2.43**; [i] x, 1+y, z benzoyl transfer at **II A2.43** → **A2.33**; [j] ½-x, -1/2+y, -1/2+z.

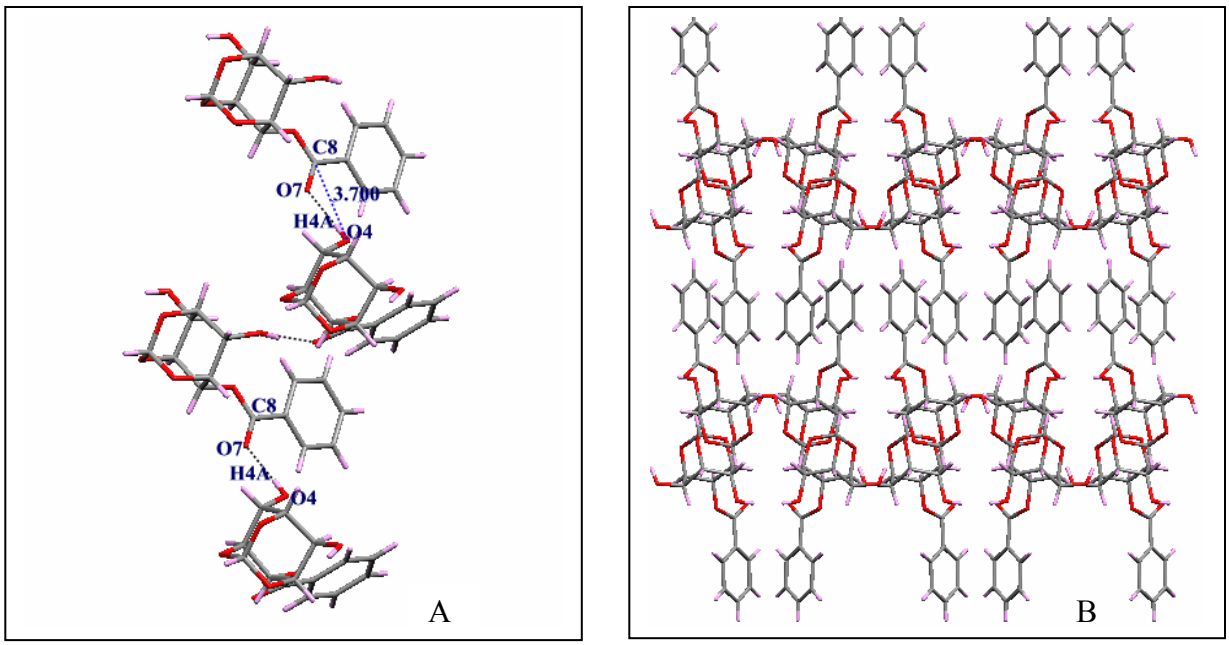

Figure A2.2. (A) O-H….O and El….Nu interactions and (B) packing of molecules viewed down the a- axis in crystals of A2.**25**.

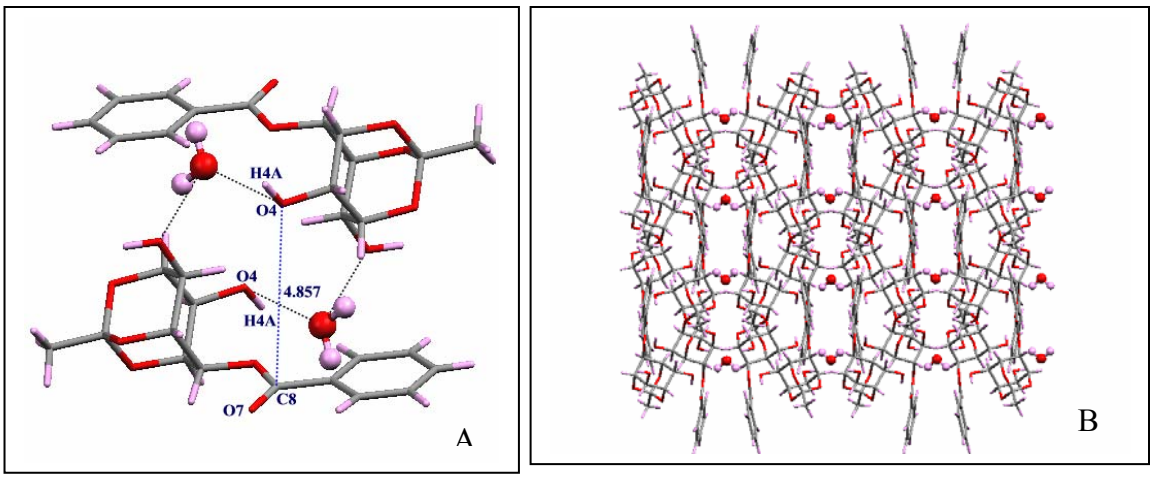

Figure A2.3. (A) El….Nu interactions and (B) packing of molecules viewed down the c-axis in crystals of **A2.27**.

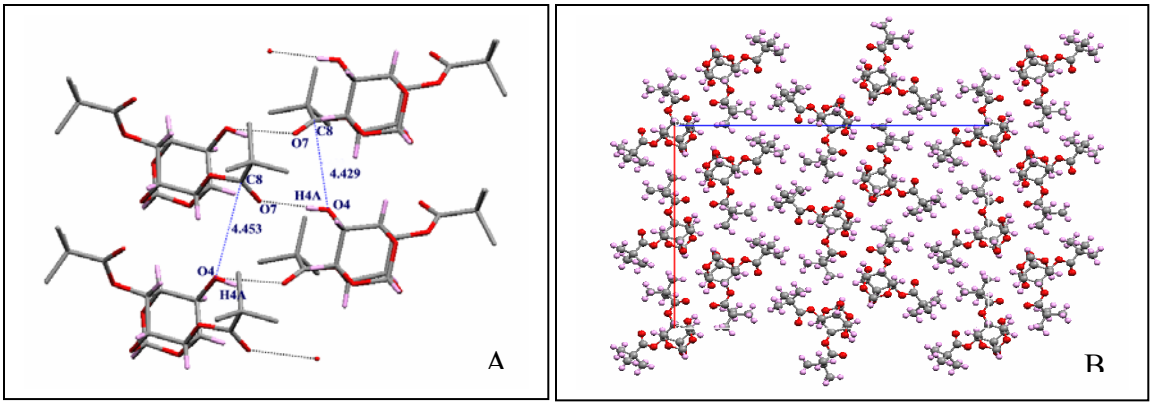

Figure A2.4. (A) O-H….O and El….Nu interactions and (B) packing of molecules viewed down the a- axis in crystals of **A2.41**.

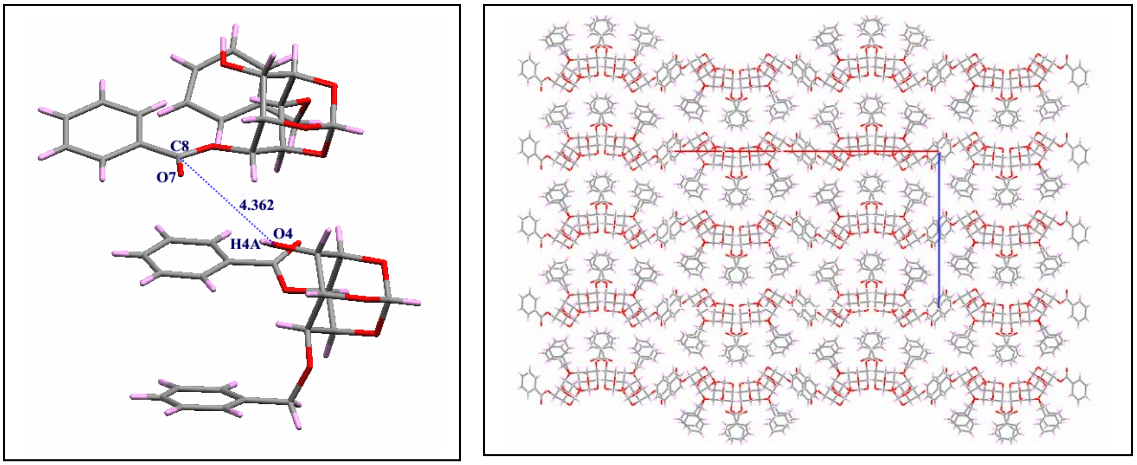

Figure A2.5. (A) El….Nu interactions and (B) packing of molecules viewed down the b-axis in crystals of A2.**49**.

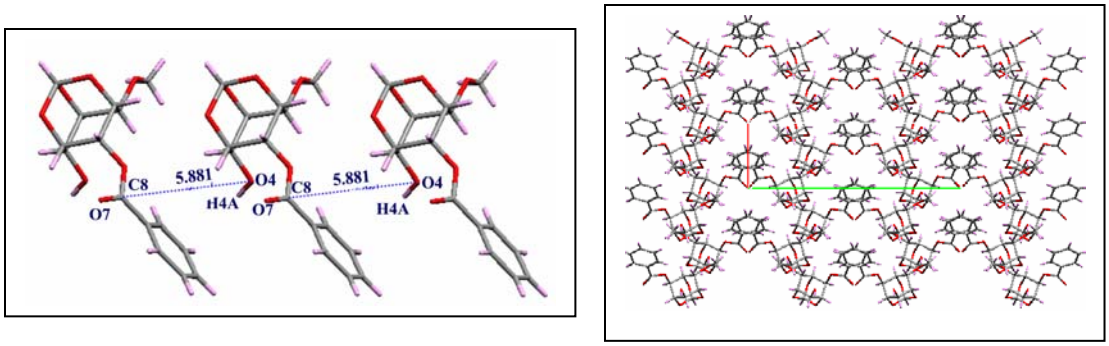

Figure A2.6. (A) El….Nu interactions and (B) packing of molecules viewed down the a-axis in crystals of **A2.50**.

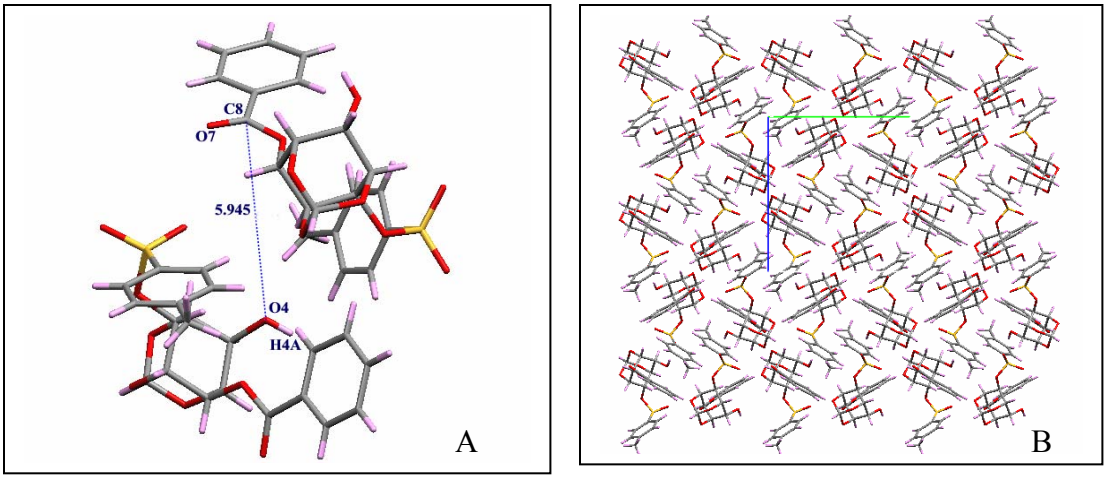

Figure A2.7. (A) El….Nu interactions and (B) packing of molecules viewed down the a-axis in crystals of **A2.51**.

Although, **A2.49** reacted to give a good yield of the corresponding transeterification products **A2.70** and **A2.47** (Scheme A2.19), examination of its crystal structure (Figure A2.5) revealed that neither El….Nu distance (4.362 Å) nor the angle of approach (54.94º) is conducive for intermolecular transesterification. The reactivity of **A2.49** in the molten state was found to be same as its reactivity in the solid-state. Therefore, it is thought that the reaction could be non-topochemical[50] benzoyl transfer,

which might start at some defects in crystals of **A2.49**. However, to understand the reactivity of **A2.49** completely, further study is required.

Although the arrangement of molecules in the crystals of **A2.33**, **A2.43**, **A2.53** and **A2.33·43** and their transesterification reactivity in solutions and in melt were comparable (see previous section), the transesterification reactivity in the solid-state were different. Hence the difference in the solid-state transesterification reactivity of **A2.33**, **A2.43**, **A2.53** and **A2.33·43** were thought to be an outcome of the packing of molecules in their crystals. Therefore, crystal structure analysis of the diesters **A2.33, A2.43, A2.53** and **A2.33·43** were carried out with a greater detail to understand the differences in their solid-state reactivities.

Thermal analysis of crystals of **A2.33**, **A2.43**, **A2.53** and **A2.33·43** (see pages 180-183) showed that these crystals did not undergo any phase transition upon heating. X-ray powder diffraction showed that mixing and grinding of the diesters **A2.33**, **A2.43**, **A2.52** and **A2.33·43** with sodium carbonate also did not result in any new crystalline phase (see pages 175-179). The crystal structure of **A2.33** re-determined at higher temperature (60 °C) did not show any significant increase of the anisotropies of the reactive functional groups (benzoyl and hydroxyl).

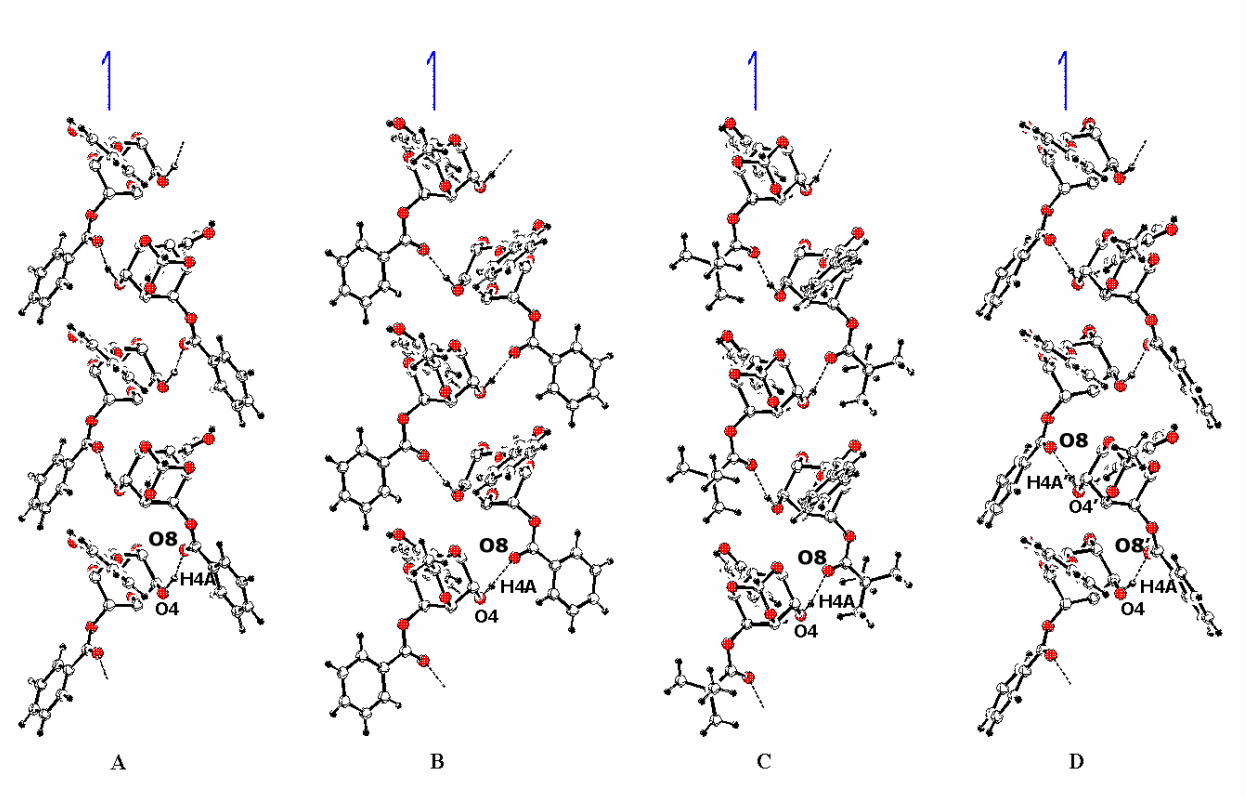

Figure A2.8. Helical self-assembly via O-H…O hydrogen bonding in crystals of (A) **A2.33**, (B) **A2.43**, (C) **A2.53** and (D) **A2.33·43** along 2_1 axis having a similar pitch value.

It was observed that all these structures belong to the monoclinic space groups with a strikingly similar unique axis b (~ 10 Å, Figure A2.8). It is noteworthy that O…O distances (Table A2.2) are somewhat longer in the more reactive crystals of **A2.33** and **A2.33·43** (ranging from 2.816(5) – 2.871(7) Å) as compared to the less reactive compounds **A2.43** and **A2.53** (2.775(2) – 2.782(2) Å); angles D-H…A (D= donor atom, C4(6)- hydroxyl oxygen in this case and A= acceptor, C6(4)- carbonyl carbon of the ester group here) do not show any marked differences. The carbonyl oxygen O7 of the reactive C6(4)-O-benzoyl group does not take part in any O-H…O type of hydrogen bonding. The helical assembly across two-fold via O-H…O bonding appears to be a consistent feature

in the organization of these molecules. The asymmetric unit of **A2.33·43** consists of one molecule each **A2.33** and **A2.43**, which repeats along the b-axis to create a *pseudo* two-fold screw axis, therefore the crystal space group is pseudo C2/c. The space group C2/c embodies a twofold axis and a twofold screw axis alternating along the a-axis. As the two-fold screw axis is not a true symmetry element in crystals of the complex **A2.33·43**, the crystals belong to space group Cc.

Table A2.2. Hydrogen bonding parameters.[a] Atom numbers refer to Figure A2.8.

	D-H…A	H…A (Å)	D…A (Å)	D-H…A (°)
A2.33	O(4)-H(4A)...O(8)[b] O(4')-H(4A')...O(8')[c]	1.94 1.91	2.871(7) 2.853(7)	158 166
A2.43	O(4)-H(4A)...O(8)[d]	1.93(3)	2.775(2)	175(2)
A2.53	O(4)-H(4A)...O(8)[e]	1.98	2.782(2)	164.7
A2.33·43	O(4)-H(4A)...O(8')[f] O(4')-H(4A')...O(8)[g]	2.06 2.00	2.848(5) 2.816(5)	160.9 172.2

[a] values for **A2.33** from reference 31; [b] 1-x, -½ +y, ½-z; [c] 2-x, ½+y, ½-z for the second independent molecule; [d] 3/2-x, -½+y, ½-z; [e] 3/2-x, -½+y, ½-z; [f] x, y, z; [g] x, 1+y, z.

The helical self-assemblies in crystals of **A2.33**, **A2.43**, **A2.53** and **A2.33·43** bring the reactive C6(4)-O-benzoyl group (El) and the C4(6)-hydroxyl group (Nu) along the helix in a varying degrees of 'pre-organized' geometries (Figure A2.9 and Table A2.1). The El...Nu geometries are quite comparable in **A2.33**, **A2.43** and **A2.33·43** showing favorable El…Nu interactions. In **A2.33·43** there are two types of El … Nu interactions; one between the C6-O-benzoyl group of **A2.33** and the C4'-hydroxyl group of **A2.43** (benzoyl transfer at **I**) and the other between the C6'-O-benzoyl group of **A2.43** and the C4-hydroxyl group of **A2.33** (benzoyl transfer at **II**, also see Scheme A2.17). However,

El…Nu geometry in **A2.53** deviates from these; the distance is somewhat longer (3.533 Å) and the angle O4…C8-O7 is 70.2º (much less than that found in reactive crystals of **A2.33**). The low reaction efficiency of **A2.53** compared to **A2.33** and **A2.33·43** can perhaps be rationalized on the basis of El…Nu geometry but not the lesser reactivity of **A2.43** (Table A2.1). The explanation to this was sought in terms of other interactions made by the reactive groups in the crystal lattice (see below).

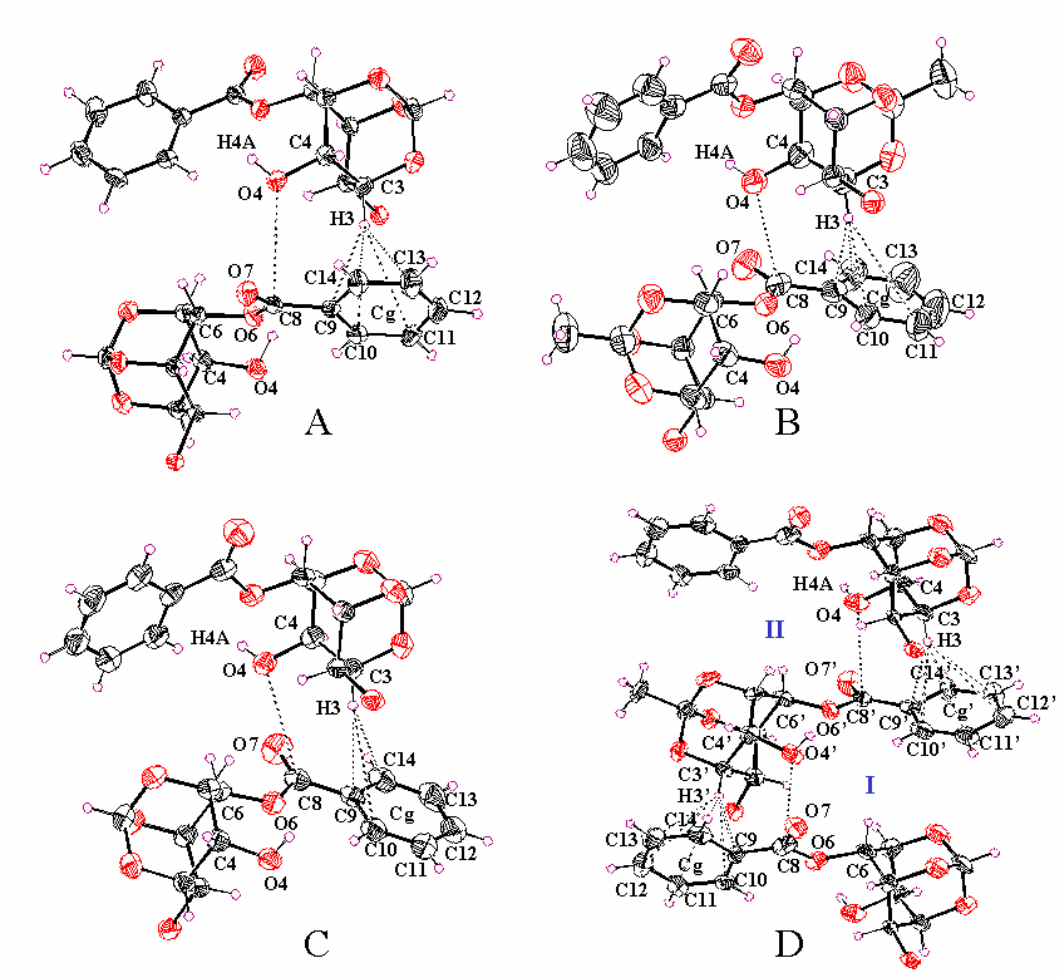

Figure A2.9. Relative orientation of the reacting molecules in crystals of (A) **A2.33**, (B) **A2.43**, (C) **A2.53** and (D) **A2.33·43** showing El...Nu and C-H…π interactions. The 2-*O*-benzoyl group is omitted for clarity.

Although the gross organization of the molecules in crystals of **A2.33**, **A2.43**, **A2.53** and **A2.33·43** is similar (Figure A2.8), significant differences are noticeable in the O-C bond lengths, C-H…O and C-H…π contacts.[51-54] The O-C bond length distribution showed significant trend in accordance with acyl transfer reactivities. The O6-C8 bond of the axial benzoyl group, which gets cleaved during the reaction, is consistently longer (1.360 – 1.361 Å) in the reactive crystals of **A2.33** and **A2.33·43** than the chemically equivalent O2-C15 bond (1.333 – 1.327 Å) of the equatorial benzoyl group. The difference in the corresponding axial and equatorial O-C bond lengths in **A2.43** and **A2.53** is not very significant (axial and the equatorial O-C bond lengths for **A2.43** are 1.333 Å and 1.316 Å and those for **A2.53** are 1.344 Å and 1.340 Å respectively).

Table A2.3. C-H…π interactions between non-reacting molecules

	X-H…Cg	H…Cg (Å)	X-H…Cg(°)	X…Cg (Å)
A2.33	C4-H4… Cg1'[a]	2.9254	145.89	3.818(4)
	C4'-H4'… Cg1[b]	2.8457	149.11	3.751(4)
	C18'-H18'…Cg2[c]	3.3391	127.82	4.051(5)
	C19-H19… Cg2'[c]	3.1932	135.51	3.992(5)
	C19'-H19' …Cg2[c]	3.2255	132.07	3.988(5)
A2.43	C19-H19… Cg2[d]	2.8050	160.66	3.6907
	C13-H13… Cg1[e]	2.7834	163.59	3.7189
A2.53	C19-H19B… Cg1[f]	3.2139	157.43	4.1169
A2.33·43	C4'-H4'… Cg1'[g]	3.0071	156.70	3.9264
	C4-H4… Cg1[h]	3.0149	154.79	3.9238
	C19-H19 …Cg2'[i]	3.1699	145.21	3.9693
	C19'-H19' …Cg2[j]	3.2540	143.59	4.0404

Cg1 and Cg2: geometric centers of phenyl rings C16-C21 and C9-C14 respectively. Cg1' and Cg2': geometric centers of phenyl rings C16'-C21' and C9'-C14' respectively. [a] 1-x, -1/2+y, 1/2-z; [b] 2-x, 1/2+y, 1/2-z; [c] x, y, z; [d] 1-x, 1-y, -z; [e] -1/2+x, 1/2-y, 1/2+z; [f] 1-x, 1-y, -z; [g] x, 1-y, 1/2+z; [h] x, -y, -1/2+z; [i] x, -1+y, z; [j] x, 1+y, z.

The lability of the O-C bond in crystals of **A2.33** and **A2.33·43** could be due to stronger El…Nu interactions. The geometry of C-H…π contacts made by the C3- H3 of the inositol ring with the phenyl ring of the C6(4)-O-benzoyl group from the next molecule along the helix varies considerably (Figure A2.9). The geometry of C-H…π contact in **A2.33** is significantly better than in **A2.43** and **A2.53**. It is interesting to note a significant improvement in overall C-H…π contacts along the helix in the molecular complex **A2.33·43** (Figure A2.9D) as compared to the crystals of **A2.43** alone (Table A2.3).

There are also significant differences in the C-H…O[55] contacts (Table A2.4) made by the reactive groups in the crystals. The C6(4)-O-benzoyl group of one of the molecules in the asymmetric unit in **A2.33** makes two C-H…O contacts along the helix whereas this benzoyl group is held by only a single rather weak C-H…O interaction in **A2.43** and **A2.53**, which are not along the helix. In **A2.33·43**, this benzoate makes short C-H…O contacts but are somewhat compromised on angles along the helix. The only similarity in all the four crystal structures is C1-H1…O7 contacts made by the carbonyl oxygen O7 of the axial benzoate. Thus intermolecular C-H…π and C-H…O contacts made by the reactive groups concerted with the El…Nu 'pre-organization' correlate well with the reaction efficiencies observed in crystals. Another notable feature that separates reactive crystals from the less reactive ones is the packing of the helices. Helices in **A2.33** and **A2.33·43** are packed much more discretely providing a well guided 'reaction tunnel' throughout the crystal as compared to those in **A2.43** and **A2.53** (Figure A2.10). Further, the helices in the former two crystals are held together by more inter-helical C-H…O and C-H…π interactions as compared to the latter two.

Table A2.4. Intermolecular C-H…O Interactions

	D-H…A	H…A (Å)	D…A (Å)	D-H…A (°)
A2.33	C(1)-H(1)...O(7')[a]	2.68	3.619(5)	150.3
	C(1')-H(1')...O(7)[b]	2.74	3.646(6)	148.09
	C(13)-H(13)...O(5)[c]	2.69	3.419(6)	127.6
	C(13')-H(13')...O(5')[d]	2.86	3.561(5)	125.2
	C(7)-H(7)...O(5)[e]	2.68	3.525(4)	141.4
	C(7')-H(7')...O(3')[f]	2.56	3.309(6)	128.5
	C(14')-H(14')...O(2)[b]	2.51	3.484(5)	155
	C(14)-H(14)...O(2')[a]	2.57	3.514(5)	153
	C(18')-H(18')...O(1)[g]	2.61	3.515(5)	145.8
	C(21)-H(21)...O(7)[b]	2.62	3.302(5)	122.2
	C(21')-H(21')…O(7')[a]	2.63	3.320 (6)	125.0
A2.43	C(1)-H(1)...O(7)[e]	2.925(16)	3.602(2)	131.0(11)
	C(22)-H(22A)...O(5)[h]	3.13(4)	3.967(5)	158(3)
	C(21)-H(21)...O(1)[b]	2.82(3)	3.519(3)	135(2)
	C(13)-H(13)...O(3)[i]	2.73(4)	3.413(4)	132(3)
	C(17)-H(17)...O(7)[e]	2.588(19)	3.448(3)	148.2(13)
A2.53	C(1)-H(1)...O(7)[j]	2.48	3.328(2)	144.9
	C(17)-H(17B)...O(3)[k]	2.79	3.387(3)	121.3
	C(13)-H(13)...O(5)[l]	2.74	3.647(3)	164.5
	C(5)-H(5)...O(8)[m]	2.69	3.364(2)	126.5
A2.33·43	C(1')-H(1')...O(7)[n]	2.48	3.396(6)	155.5
	C(1)-H(1)...O(7')[o]	2.47	3.382(6)	155.5
	C(11)-H(11)...O(5')[a]	2.83	3.337(7)	115.8
	C(11')-H(11')...O(5)[p]	2.70	3.293(7)	122.2
	C(13')-H(13')...O(3')[q]	2.77	3.417(6)	127.9
	C(13)-H(13)...O(3)[r]	2.86	3.459(7)	123.4
	C(14)-H(14)...O(2')[o]	2.74	3.648(6)	165.1
	C(14')-H(14')...O(2)[n]	2.78	3.662(7)	158.8

[a] x, -1+y, z; [b] x, 1+y, z; [c] 1-x, 1/2+y, 1/2-z; [d] 2-x, -1/2+y, 1/2-z; [e] 1-x, -y, -z; [f] 2-x, 2-y, 1-z; [g] x, 1/2-y, 1/2+z; [h] 2-x, -y, -z; [i] -1/2+x, 1/2-y, 1/2+z; [j] 3/2-x, -1/2+y, 1/2-z; [k] 2-x, 1-y, 1-z ; [l] 1-x, 2-y, 1-z; [m] 1+x, y, z; [n] x, 1-y, -1/2+z; [o] x, 1-y, 1/2+z; [p] x, y, z; [q] -1/2+x, 3/2-y, -1/2+z; [r] ½+x, 1/2-y, 1/2+z.

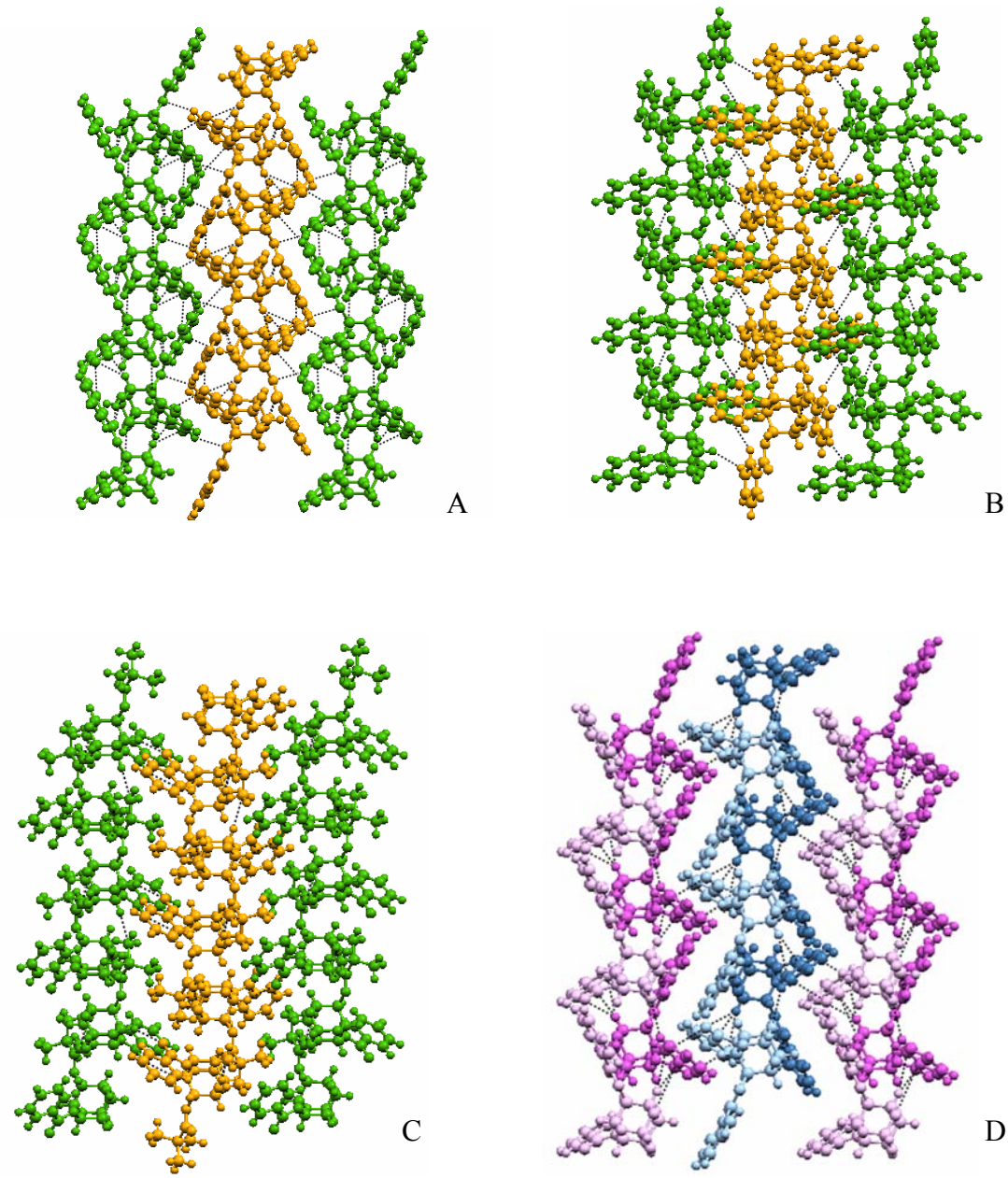

Figure A2.10. Packing of helices in crystals of (A) **A2.33**, (B) **A2.43**, (C) **A2.53** and (D) **A2.33·43**. Discrete helices are seen in reactive crystals of (A) **A2.33** and (D) **A2.33·43**, whereas such well defined channels are not noticeable in less reactive (B) **A2.43** and (C) **A2.53**. The color scheme is used to distinguish the neighboring helices in A, B and C; molecules of **A2.33** (light pink or light blue) and **A2.43** (dark pink or dark blue) make a single hybrid helix seen in D. Dotted lines in all the figures indicate C-H…O or C-H…π contacts.

A comparison of the crystal structures of **A2.33**, **A2.43**, **A2.53** and **A2.33·43** shows (Figure A2.8) that self-assembly around two-fold axis in **A2.33**, **A2.43** and **A2.32·43** results in moderate to excellent (as observed in crystals of **A2.33**) juxtaposition of the reactive groups. But, the favorable geometry of the reactants alone does not seem to completely explain the facility of these transesterification reactions (Schemes A2.14-A2.22). The reaction efficiencies can be explained if variation in O-C bond lengths, geometry of C-H…π and C-H…O contacts that the reactive benzoyl group makes with the neighboring molecules are taken into account. The clean reactions in **A2.33** and **A2.33·43** and not so very clean reactions with the emergence of other side products in **A2.43** and **A2.53** suggest the involvement of weak intermolecular interactions during the reaction in crystals. The facile reaction in hybrid crystals of **A2.33·43** supports this postulate. The significance of weak intermolecular interactions such as C-H… π and C-H…O is recognized in solid state topochemical polymerization, in solid-to-solid transformations,[56-60] and also have been suggested to play a significant role in the stability of peptides,[61] proteins[62] and in the conformation of small organic molecules.[51, 63-67] However, to completely establish the effect of weak interactions on the efficiency of the reactions in crystals discussed here, further examples and theoretical calculations are necessary.

A2.3.2. Proposed mechanism of acyl transfer in the solid state in crystals of A2.33 and A2.33·43:

Usually chemical reactions in crystals lead to the distortion of the crystal lattice due to appearance of products, only exceptions to this being single crystal to single crystal transformations.[68-77] Distortion of the crystal structure is usually high enough to

cause a collapse which result in rather low conversion to the product due to loss of topochemical control. However, if the reaction proceeds in a domino fashion along an axis in the crystal of the reactant, higher conversion and better yield of the products can be expected. The examples of **A2.33** and **A2.33·43** having very good facility of the heterogeneous transesterification that proceeds to greater than 90% completion (revealed by the disappearance of the starting material) can be categorized in the above class, with reaction proceeding along the helix (schematic representation is shown in Scheme A2.25).

It is likely that the base (Na_2CO_3) initiates the reaction at one end of the helix by aiding deprotonation of the C4(6)- hydroxyl group, which enables the oxygen to attack the C6(4)- benzoyl carbonyl carbon group of the neighboring diester molecule along the helix (**A2.80**). Acyl group transfer along the helix then generates a molecule of the triester and the corresponding diol oxyanion (**A2.81**). The latter functions as a base and deprotonates the hydroxyl group of its neighboring diester within the helix (**A2.82**). The oxyanion of the diester so generated functions as a nucleophile for the attack on C6(4)-benzoyl carbonyl group of the next molecule to generate another molecule of tribenzoate and the diol anion (**A2.83**). Thus in a domino fashion, these two steps lead to the generation of two transesterification products resulting in the destruction of the helix and eventually of the crystal, as the reaction proceeds. The facility of the reaction and the higher yield of the products in the case of **A2.33** and **A2.33·43** correlate well with the intra and inter helical interactions. In the absence of these lattice interactions, the progress of the reaction along the helix is not likely to proceed in a domino fashion and the group transfer can terminate prematurely, lowering the yield and facility of

transesterification. The formation of other products and incomplete consumption of the starting material observed for the other *myo*-inositol orthoester derivatives can thus be rationalized.

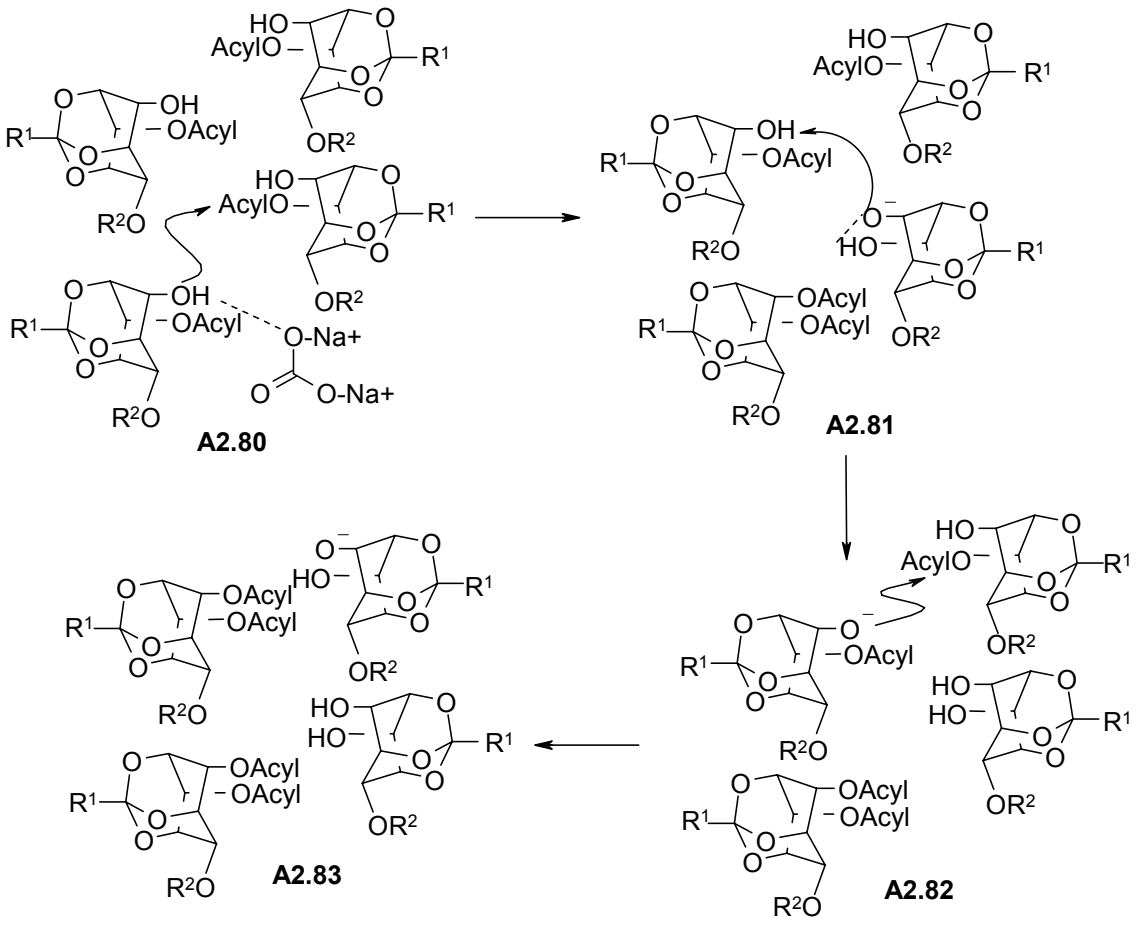

Scheme A2.25.

A2.3.3. Crystal structure analysis of *scyllo*-inositol 1,3,5-orthoformate derivatives A2.57, A2.63 and A2.64

Crystal structure of the *scyllo*-inositol orthoformate derivatives, **A2.57**, **A2.63** and **A2.64** were analyzed for parameters discussed for *myo*-inositol derivatives previously. The electrophile-nucleophile 'preorganization' parameters in the crystals of these compounds are presented in the Table A2.5 (also see Figures A2.11-A2.13).

Table A2.5. Geometry of the reacting groups in crystals of **A2.57**, **A2.63** and **A2.64**. Atom numbers refer to Figures A2.11-A2.13.

Comp. nos.	Distance (Å) / Angle (°)			
	C8…O4	∠O4…C8-O7	∠C4-O4…C8	∠H4A-O4…C8
A2.57	4.324[a]; 5.160 [b]; 5.774[c]	57.8[a]; 144.8[b]; 79.1[c]	81.9[a]; 99.6[b]; 104.0[c]	128.9[a] (102.1[a]); 164.1[b] (49.5[b]); 79.1[c] (49.2[c])
A2.63	3.046[d]	107.4[d]	127.8[d]	121.5[d]
A2.64	> 8			

[a] 1+x, y, z; [b] 1-x, 1-y, -z; [c] -x, 1-y, -z; [d] 2-x, -y, 2-z.
figures within parentheses are for ∠H4B-O4…C8.

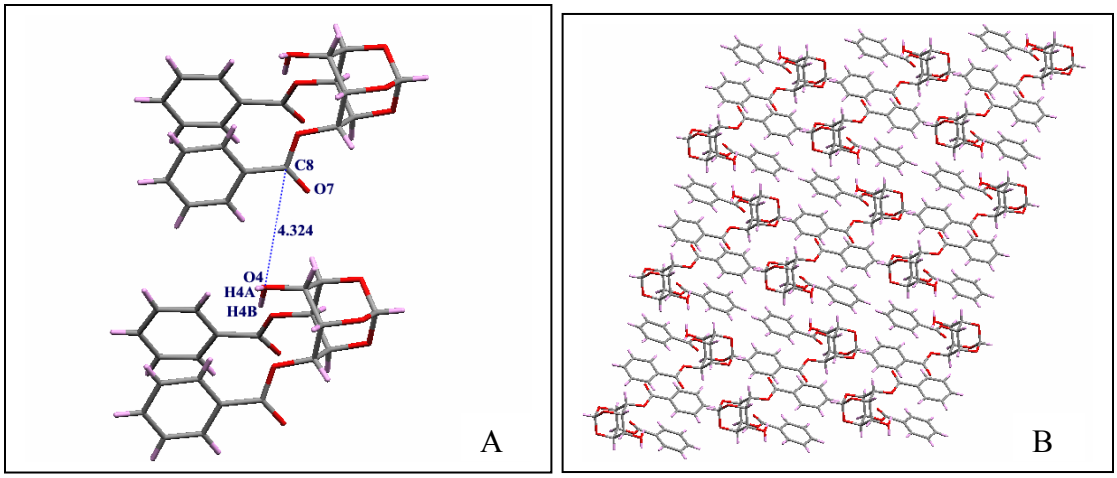

Figure A2.11. (A) El….Nu interactions and (B) packing of molecules viewed down the a- axis in crystals of **A2.57**.

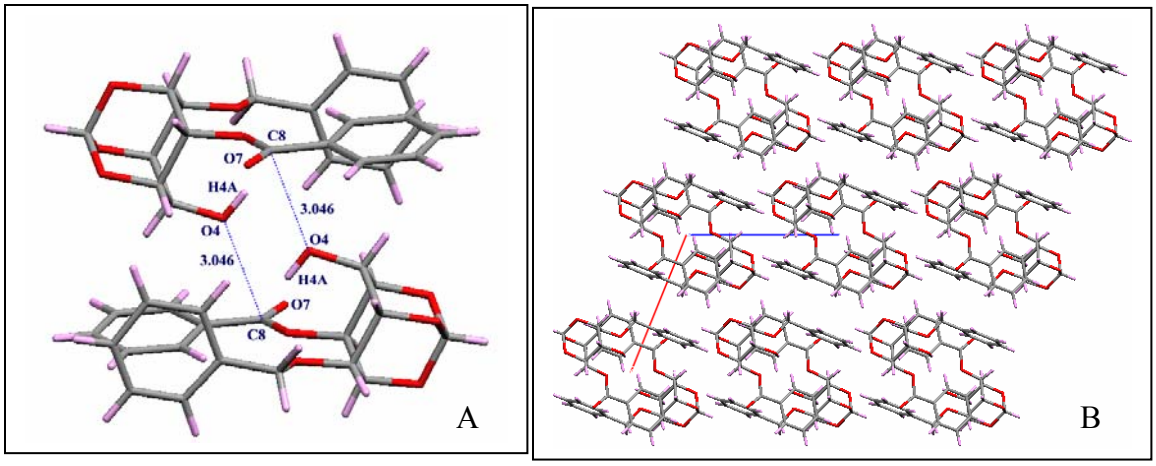

Figure A2.12. (A) El….Nu interactions and (B) packing of molecules viewed down the b- axis in crystals of **A2.63**.

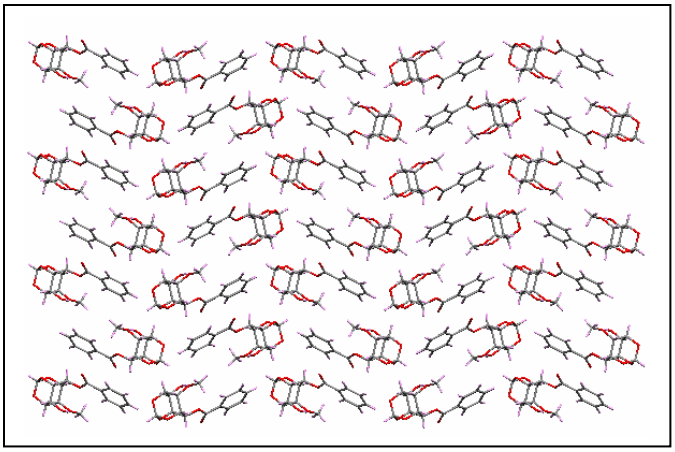

Figure A2.13. Packing of molecules viewed down the a- axis in crystals of **A2.64**.

The El…Nu distance and angles in Table A2.5 for crystals of **A2.57** and **A2.64** suggest that the benzoyl transfer reaction in these crystals may not be conducive. But in crystals of **A2.63** both the El…Nu distance and the angles appear to be good enough to allow intermolecular benzoyl transfer between neighboring molecules. Besides good El…Nu geometry, crystals of **A2.63** also have favorable C-H…..π contacts (Figure A2.14 and Table A2.6) as observed for *myo*-inositol based esters **A2.33** and **A2.33·43**. However, **A2.63** was unreactive in the solid state. A comparison of the crystal structures of **A2.33**, **A2.33·43** and **A2.63** reveals that arrangement of molecules in crystals of **A2.63** is not helical to allow a domino type of reaction (Scheme A2.25). Thus non-reactivity of **A2.63** in the solid-state raises a question whether the helix formation in the reactant crystal could be one of the necessary conditions for the intermolecular solid-state transesterification to proceed with observable yields? Hence it is possible that absence of helical arrangement of molecules (or any other packing that allows a domino type of reaction) could hinder the progress of the reaction in crystals of **A2.63**. Another curious observation in Figure A2.14 is that, if migration of both the benzoyl groups in the pair of

reacting molecules occurs with facility, then the product will be indistinguishable from the reactant! Hence, further work is essential to answer these questions clearly.

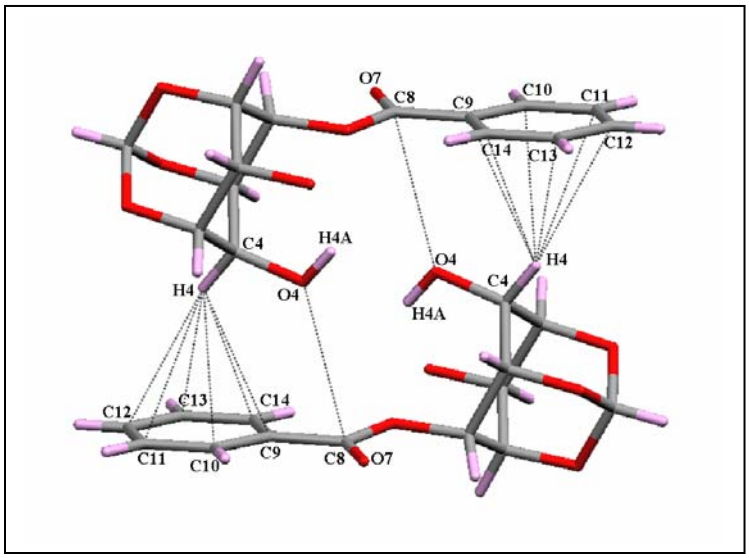

Figure A2.14. El…Nu and C-H…π interactions in **A2.63**; benzyl group is not shown for clarity.

Table A2.6. C-H…π interactions in **A2.63**.

	X-H…Cg	H…Cg (Å)	X-H…Cg(°)	X…Cg (Å)
A2.63	C4-H4… Cg5[a]	2.6977	141.31	3.516(4)
	C10-H10… Cg6[b]	2.9653	142.82	3.748(7)
	C21-H21…Cg5[c]	3.1459	164.82	4.050(9)

Cg5 and Cg6: geometric centers of phenyl rings C9-C14 and C16-C21 respectively.
[a] 2-x, -y, 2-z; [b] 1+x, y, z; [c] 2-x, 1-y, 2-z.

In case of the dibenzoate **A2.57**, the situation is opposite to that of **A2.63**. It was experimentally observed that the transesterification of **A2.57** proceeded with reasonably good yield of the tribenzoate **A2.75**, one of the products expected from the intermolecular migration of one of the benzoyl groups in **A2.57**. However, the other expected product (the diol **A2.84**, Scheme A2.26) arising out of intermolecular benzoyl transfer between two molecules of **A2.57** was not formed. The other isolated product was the triol **A2.56**,

which could arise by transesterification of the monobenzoate **A2.84** (generated by the initial transesterification of **A2.57**). Furthermore, the maximum yield of the tribenzoate **A2.75** expected from the intermolecular benzoyl group transfer in **A2.57** is 50%, the other product being the monobenzoate **A2.84** (maximum yield 50%). The formation of more than 50% of the tribenzoate **A2.75** in this reaction implies the occurrence of reactions other than the transesterification of **A2.57** in which **A2.75** is formed. All these observations point to the occurrence of more than one parallel benzoyl group transfers during the solid-state reaction of **A2.57**. Hence further work is essential to understand the observed reactivity of **A2.57** and correlate it with crystal structures. At present, it is clear that the experimental observations cannot be rationalized based on the crystal structure of **A2.57** alone.

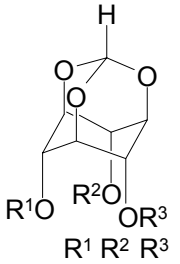

	R^1	R^2	R^3
A2.56	H	H	H
A2.57	Bz	Bz	H
A2.75	Bz	Bz	Bz
A2.84	Bz	H	H

A2.57 $\xrightarrow{a}$ **A2.75** + **A2.84**

A2.84 $\xrightarrow{a}$ **A2.75** + **A2.56**

A2.57 + **A2.84** $\xrightarrow{a}$ **A2.75** + **A2.56**

Scheme 26. a) Na_2CO_3 (8 eq), 160 ^oC, 48 h.

A2.4. Conclusions.

We have carried out a systematic investigation of the transesterification reaction of cyclitol derivatives, with special focus on *myo*-inositol 1,3,5-orthoester derivatives in the solid state and correlated the observed reaction efficiencies of some of the derivatives with the intermolecular interactions in their crystals. A comparison of the observed reactivity pattern and the crystal structures of inositol derivatives investigated suggest that the conditions necessary for the progress of clean tansesterification reaction in the

solid state are: (a) preorganization of the electrophile (C=O) and the nucleophile (OH) with good geometry; (b) good intermolecular interactions (such as CH…O, CH…pi, etc.) between the reacting molecules that hold them in position for the reaction; (c) assembly of molecules in their crystal which allow a domino type of reaction. The solid-state reactions described here belong to the class of group transfer reactions in crystals, which are rarely encountered. The fact that the less reactive **A2.43** could be co-crystallized[39-42] with the more reactive **A2.33**, producing an overall reactive lattice opens up avenues for enhancing solid-state reactivities by molecular complexation.[78]

A2.5. Experimental section

General methods: All the deuterated solvents, *myo*-inositol, 1*R*-(+)-camphoric acid, sodium hydride, calcium hydride, 1-naphthoic acid, triethylorthoformate and benzyl bromide were obtained from Aldrich Chemical Company, USA and were used as received. Benzoyl chloride, benzylamine, thionyl chloride, acetic anhydride, DMF, pyridine, THF, chloroform, dichloromethane, diethyl ether, triethylamine, *p*-toluene sulfonic acid, sodium bicarbonate, anhydrous sodium sulfate and sodium chloride were obtained from SD Fine Chemicals, India. All the solvents used, benzoyl chloride and *p*-toluene sulfonic acid were purified according to literature procedures.[79] Silica gels for column chromatography (60-120 mesh and 230-400 mesh) were obtained from Spectrochem India Ltd. Light petroleum refers to the 60-80º C boiling fraction of petroleum ether. 'Usual work-up' implies dilution of the reaction mixture with a solvent (ethyl acetate, chloroform or dichloromethane), washing of the organic layer with water, saturated sodium bicarbonate solution followed by brine, drying over anhydrous sodium sulfate and evaporation of the solvent under reduced pressure. Analytical TLC was performed on E-Merck pre-coated 60 F_{254} aluminum plates and the spots were rendered to visible either by shining UV light or by charring the plates after spraying chromic acid (ninhydrin solution for amines). Column chromatographic separations were carried out with light petroleum-ethyl acetate mixtures, unless otherwise mentioned. Preparative TLC were carried out on Merck pre-coated 60 F_{254} glass plates and the spots were rendered to visible by shining UV light. The fractions were isolated by scratching the plates and extraction with suitable solvents. The compounds **A2.23**,[32] **A2.24**,[32] **A2.25**,[30] **A2.27**,[30] **A2.29**,[30,35] **A2.33**,[12] **A2.34**,[32] **A2.D**36,[34] **A2.L36**,[34] **A2.D37**,[13] **A2.L37**,[13]

A2.38,[25] **A2.44**,[37] **A2.45**,[37] **A2.47**,[37] **A2.52**[30,36] and 1*S*-(-)-camphanoyl chloride[80] were prepared as reported earlier. 1-Naphthoyl chloride was prepared by refluxing 1-naphthoic acid with thionyl chloride. Synthesis of **A2.56**, **A2.58**, **A2.60** and **A2.62** are described in the Experimental section of Part B, Section 2 of this thesis. All the compounds previously reported in the literature were characterized by comparison of their melting point, optical rotation and ^{1}H NMR spectra with those of authentic samples.

IR spectra were recorded as film for liquid compounds, nujol mull or in solution (conc. 1μM) for solids on a Shimadzu FTIR-8400 spectrophotometer. NMR spectra were recorded either on Bruker ACF 200 (200 MHz for ^{1}H) or MSL 300 (300 MHz for ^{1}H) or DRX 500 (500 MHz for ^{1}H) spectrometers. Chemical shifts (δ) reported are referred to internal tetramethylsilane. Microanalytical data were obtained using a Carlo-Erba CHNS-0 EA 1108 Elemental analyzer. All the melting points reported are uncorrected and were recorded using a Büchi B-540 electro-thermal melting point apparatus. Specific rotations were determined using a Bellingham ADP220 polarimeter (accuracy to ±1°) or a JASCO P-1030 polarimeter (accuracy to ±0.1°).

Single crystal X-ray analysis: For single crystal X-ray diffraction analysis, good quality crystals were selected using Leica Polarizing microscope. X-ray intensity data were collected on a Bruker SMART APEX CCD diffractometer with graphite monochromatized (Mo K_α= 0.71073 Å) radiation at room temperature. All the data were corrected for Lorentzian, polarization and absorption effects using Bruker's SAINT and SADABS programs. SHELX-97[81] was used for structure solution and full matrix least squares refinement on F^2. Hydrogen atoms were included in the refinement as per the riding model. Crystal data and details of data collection, structure solution and

refinements, ORTEP[82] plots and packing diagrams for individual compounds are given in the appendix.

Thermal analysis: TG/DTA and DSC thermographs were recorded by using Seiko DTA/TG 320 and DSC 220C thermal analyzers. Thermographs of the individual compounds are given in the appendix.

X-ray powder diffraction: X-ray powder diffraction patterns were recorded by using a Philips PW1830 powder X-ray diffractometer. The X-ray powder diffraction patterns for the individual compounds are given in the appendix.

Racemic 2,4-di-*O*-benzoyl-*myo*-inositol (A2.9): The racemic dibenzoate **A2.33** (0.398 g, 1.00 mmol) was treated with a mixture of trifluoroacetic acid (0.8 mL) and water (0.2 mL) at room temperature for 1 h. Removal of solvents under reduced pressure followed by co-evaporation with toluene gave racemic **A2.9** (0.380 g, 98%) as a white solid.

Data for A2.9: **mp** 204 ^{o}C. lit.[24] mp 198-201 ^{o}C.

Racemic 2-*O*-benzoyl-4-*O*-benzyl-*myo*-inositol 1,3,5-orthoformate (A2.35): A solution of benzoyl chloride (0.27 g, 1.9 mmol) in dry pyridine (3 mL) was added dropwise to a solution of racemic 4-*O*-benzyl-*myo*-inositol 1,3,5-orthoformate[83] (0.50 g, 1.79 mmol) in dry pyridine (3 mL) and the mixture was stirred at room temperature for 12 h. Solvents were evaporated under reduced pressure and the mixture was worked up as usual using chloroform to obtain a gum. Purification of the gum by flash chromatography gave the benzoate **A2.35** (0.57 g, 83%) as a gum which became a solid on storing at 0 ^{o}C for 24 h.

Data for A2.35: **mp** 100 ^{o}C. lit.[33] mp 100 ^{o}C.

2,4,6-tri-*O*-benzoyl-*myo*-inositol (A2.39): The tribenzoate **A2.34** (0.502 g, 1.00 mmol) was treated with a mixture of trifluoroacetic acid (1.2 mL) and water (0.3 mL) at room

temperature for 1 h. Removal of solvents under reduced pressure followed by co-evaporation with toluene gave **A2.39** (0.470 g, 95%) as a white solid.

Data for A2.39: **mp** 196-198 ^{o}C. lit.[84] mp 200-2003 ^{o}C.

Racemic 2,4-di-*O*-pivaloyl-*myo*-inositol 1,3,5-orthoformate (A2.41): To a stirred cooled solution of the triol **A2.23** (0.570 g, 3 mmol) in dry pyridine (5 mL) a solution of pivaloyl chloride (0.76 g, 6.3 mmol) in dry pyridine (3 mL) was added dropwise and stirring continued for 12 h. Pyridine was evaporated under reduced pressure and usual work up (with chloroform) of the residue gave a gum. The products were separated by column chromatography to obtain the racemic dipivalate **A2.41** (0.69 g, 64%) and the known diol **A2.52**[30, 36] (0.232g, 28%) as white solids.

Data for A2.41: **mp** 121-122 ^{o}C.

IR (Nujol)ν = 1712, 1726, 3468 cm^{-1}.

^{1}H NMR ($CDCl_3$, 200 MHz): δ1.24 (s, 9H), 1.28 (s, 9H), 2.70-2.74 (d, *J* 7.3 Hz, 1H), 4.24-4.35 (m, 2H), 4.41-4.49 (m, 1H), 4.57-4.67 (m, 1H), 5.16-5.23 (m, 1H), 5.49-5.60 (m, 2H).

^{13}C NMR ($CDCl_3$, 50.3 MHz): δ 26.9, 38.8, 62.7, 67.2, 68.1, 68.4, 69.1, 71.7, 102.7, 176.8, 178.2.

Elemental analysis calcd for $C_{17}H_{26}O_8$; C 56.97%, H 7.31% found C 56.86%, H 7.79%.

The structure of **A2.41** was confirmed by X-ray crystallography (see page 115).

Racemic 2,4-di-*O*-[1-naphthoyl]-*myo*-inositol 1,3,5-orthoformate (A2.42): To a stirred cooled solution of the triol **A2.23** (0.608 g, 3.2 mmol) in dry pyridine (5 mL) a solution of naphthoyl chloride (1.278 g, 6.7 mmol) in dry pyridine (5 mL) was added dropwise and stirring continued for 12 h. Pyridine was evaporated under reduced pressure and

usual work up of the residue gave a gum. The products were separated by column chromatography to isolate the racemic dinaphthoate **A2.42** (0.897 g, 60%) and 2-*O*-[1-naphthoyl]-*myo*-inositol 1,3,5-orthoformate (0.281 g, 26%) as a white solids.

Data for A2.42: **mp** 206-207 ^{o}C.

IR ($CHCl_3$)ν = 1713, 3452 cm^{-1}.

^{1}H NMR ($CDCl_3$, 200 MHz): δ 2.52-2.68 (d, 1H, *J* 5.1 Hz, D_2O exchangeable), 4.61 (s, 1H), 4.76 (s, 3H), 5.73 (s, 1H), 5.81 (s, 1H), 5.98 (s, 1H), 7.42-7.73 (m, 6H), 7.82-7.93 (d, *J* 7.7 Hz, 2H), 8.01-8.10 (d, *J* 8.0 Hz, 2H), 8.26-8.36 (d, *J* 7.6 Hz, 1H), 8.36-8.44 (d, *J* 7.1 Hz, 1H), 8.90-9.03 (d, *J* 8.5 Hz, 2H).

^{13}C NMR (DMSO-D_6, 50.3 MHz): δ64.4, 66.2, 68.6, 68.8, 69.2, 71.6, 102.4, 124.9, 125.0, 125.3, 125.8, 126.6, 128.1, 128.2, 128.9, 130.5, 130.6, 130.8, 131.1, 133.5, 133.9, 134.1, 165.6, 166.4.

Elemental analysis calcd for $C_{29}H_{22}O_8$: C, 69.88%; H, 4.45% found C, 69.52%; H, 4.31%.

Data for 2-*O*-[1-naphthoyl]-*myo*-inositol 1,3,5-orthoformate: mp 135-136 ^{o}C.

IR ($CHCl_3$)ν = 1711, 3421 cm^{-1}.

^{1}H NMR ($CDCl_3$, 200 MHz): 1.70-2.50 (br s, 1H, D_2O exchangeable), 3.35-4.11 (br, s, 1H, D_2O exchangeable), δ4.31-4.48 (m, 1H), 4.49-4.64 (m, 2H), 4.64-4.79 (m, 2H), 5.61 (s, 1H), 5.62-5.73 (m, 1H), 7.40-7.72 (m, 3H), 7.82-7.94 (d, *J* 7.4 Hz, 1H), 8.02 -8.11 (d, *J* 8.2 Hz, 1H), 8.32-8.42 (d, *J* 7.0 Hz, 1H), 8.88-9.02 (d, *J* 8.6 Hz, 1H).

^{13}C NMR ($CDCl_3$, 50.3 MHz): 63.8, 68.1, 68.6, 71.9, 102.5, 124.5, 125.4, 126.0, 126.3, 128.1, 128.7, 131.2, 131.3, 133.8, 134.2, 167.6.

Elemental analysis calcd for $C_{18}H_{16}O_7$: C, 62.79%; H, 4.68%; found C, 62.37%, H, 4.67%.

The structure of this compound was also established by X-ray crystallography (see page 120).

Racemic 2,4-di-*O*-benzoyl-*myo*-inositol 1,3,5-orthoacetate (A2.43): *myo*-Inositol (**A2.40**, 5.400 g, 30.00 mmol) was allowed to react with triethylorthoacetate (7.342 g, 45.26 mmol) in the presence of *p*-toluenesulfonic acid (0.500 g, 2.91 mmol) at 100 ^{o}C in dry DMF (50 mL) for 4 h. The reaction mixture was then cooled to room temperature, triethylamine (2 mL) was added and the solvents were evaporated under reduced pressure to obtain a gum. The gum obtained was dissolved in dry pyridine (15 mL) and cooled in ice bath. Benzoyl chloride (9.083 g, 64.65 mmol) was added and the solution was stirred at room temperature for 12 h. Usual work-up (with chloroform) of the reaction mixture followed by isolation of the products by flash chromatography gave the racemic dibenzoate **A2.43** (7.590 g, 61%) and the known tribenzoate **A2.68**[32] (3.54 g, 22%) as white solids.

Data for A2.43: **mp** 164-165 ^{o}C.

IR (Nujol) ν = 1703, 1724, 3469 cm^{-1}.

^{1}H NMR ($CDCl_3$, 500 MHz): δ 1.56 (s, 3H), 2.60-2.61 (d, *J* 5.1 Hz, 1H, D_2O exchangeable), 4.47-4.50 (m, 1H), 4.53-4.57 (m, 1H), 4.58-4.62 (m, 1H), 4.66-4.70 (m, 1H), 5.60-5.62 (t, *J* 1.6 Hz, 1H), 5.77-5.81 (m, 1H), 7.43-7.49 (m, 4H), 7.56-7.62 (m, 2H), 8.03-8.06 (m, 2H), 8.13-8.16 (m, 2H).

^{13}C NMR ($CDCl_3$, 50.3 MHz): δ 24.1, 63.0, 67.2, 68.7, 70.4, 72.4, 108.9, 128.4, 128.5, 129.1, 129.9, 133.5, 165.3, 166.3.

Elemental analysis calcd for $C_{22}H_{20}O_8$; C 64.08%, H 4.89%; found C 63.70%, H 4.99%.

The structure of **A2.43** was confirmed by X-ray crystallography (see page 124).

Crystals of 1:1 molecular complex of racemic 2,4-di-*O*-benzoyl-*myo*-inositol 1,3,5-orthoformate and racemic 2,4-di-*O*-benzoyl-*myo*-inositol 1,3,5-orthoacetate (A2.33·43): The dibenzoates **A2.33** (0.200 g, 0.50 mmol) and **A2.43** (0.200 g, 0.49 mmol) were dissolved in chloroform (3 mL). Petroleum ether (bp 60-80 ^oC) was diffused in to this solution over a period of 7-10 days, to obtain crystals of the 1:1 molecular complex, **A2.33·43** (0.300 g, 75%).

Data for A2.33·43: mp 140 ^oC.

IR (Nujol)ν = 1706, 1722, 3461 cm^{-1}.

^{1}H NMR ($CDCl_3$, 200 MHz): δ 1.56 (s, 3H), 2.77-2.82 (d, *J* 6.0 Hz, 1H, D_2O exchangeable), 2.88-2.92 (d, *J* 4.0 Hz, 1H, D_2O exchangeable), 5.46-4.53 (m, 2H), 4.53-4.77 (m, 6H), 5.57-5.64 (m, 1H), 5.64-5.71 (m, 2H), 5.72-5.87 (m, 2H), 7.30-7.71 (m, 12H), 7.98-8.23 (m, 8H).

Elemental analysis calcd for $C_{43}H_{38}O_{16}$; C 63.70%, H 4.72%; found C 63.62%, H 4.64%.

The structure of **A2.33·43** was confirmed by X-ray crystallography (see page 126).

2-*O*-methyl-4,6-di-*O*-tosyl-*myo*-inositol 1,3,5-orthoformate (A2.46): Sodium hydride (0.42 g, 17.5 mmol) was suspended in dry DMF (10 mL) and the mixture was stirred for 5 min. 4,6-Di-*O*-tosyl-*myo*-inositol 1,3,5-orthoformate, (**A2.44**, 5.53 g, 11.1 mmol) and methyl iodide (3.15 g, 22.18 mmol) were added and the mixture stirred for another 5 min. The reaction was quenched by the addition of ice and the solvents evaporated under

reduced pressure. Usual work up of the solid obtained with dichloromethane gave the ditosyalte **A2.46** (5.68 g, 100%) as a white solid.

Data for A2.46: **mp** 138-140 ^{o}C.

^{1}H NMR ($CDCl_3$, 200 MHz): δ 2.46 (s, 6H), 3.40 (s, 3H), 3.57-3.65 (m, 1H), 4.12-4.22 (m, 1H), 4.25-4.35 (m, 2H), 5.08-5.11 (t, *J*= 3.9, 2H), 5.42-5.43 (d, *J* 1.0 Hz, 1H), 7.35-7.40 (d, *J* 8.3 Hz, 4H), 7.80-7.85 (d, *J* 8.8 Hz, 4H).

^{13}C NMR ($CDCl_3$, 50.3 MHz): δ 21.5, 56.8, 67.1, 67.4, 68.5, 71.6, 102.5, 127.8, 130.0, 132.4, 145.7.

Elemental analysis calcd for $C_{22}H_{24}O_{10}S_2$; C 51.55%, H 4.72%, found C 51.76%, H 4.95%.

2-*O*-methyl-*myo*-inositol 1,3,5-orthoformate (A2.48): The ditosyalte **A2.46** (4.8 g, 9.4 mmol) was dissolved in a mixture of dry methanol (90 mL) and dry THF (30 mL). Magnesium turnings (3.40 g, 139.7 mmol) were added and the mixture was stirred at room temperature for 3 h. The reaction mixture was adsorbed on silica gel (230-400 mesh) and purified by flash chromatography to obtain the diol **A2.48** (1.80 g, 94%) as a white solid.

Data for A2.48: **mp** 173-175 ^{o}C.

IR (Nujol) ν = 3323 cm^{-1}.

^{1}H NMR (DMSO-D_6, 200 MHz): δ 3.35 (s, 3H), 3.65-3.70 (m, 1H), 4.00-4.10 (m, 1H), 4.10-4.20 (m, 2H), 4.25-4.40 (m, 2H), 5.44 (s, 1H), 5.49-5.52 (d, *J* 6.0 Hz, 2H, D2O exchangeable).

^{13}C NMR (DMSO-D_6, 50.3 MHz): δ 56.0, 67.5, 68.4, 69.7, 71.3, 102.1.

Elemental analysis calcd for $C_8H_{12}O_6$; C 47.06%, H 5.92%, found C 46.91%, H 5.90%.

The structure of **A2.48** was confirmed by X-ray crystallography (see pages 130 and 131).

Racemic 2-*O*-benzyl-4-*O*-benzoyl-*myo*-inositol 1,3,5-orthoformate (A2.49): A solution of benzoyl chloride (0.727 g, 5.17 mmol) in dry pyridine (5 mL) was added dropwise to a stirred cooled solution of the diol **A2.47** (1.41 g, 5.0 mmol) in dry pyridine (5 mL) and the reaction was continued for 12 h. Pyridine was evaporated under reduced pressure to obtain a gum. Usual work up of the gum with chloroform followed by purification by column chromatography gave the racemic benzoate **A2.49** (1.55 g, 80%) as a white solid.

Data for A2.49: **mp** 124-125 ^{o}C.

IR ($CHCl_3$) ν = 1724, 3345 cm^{-1}.

^{1}H NMR ($CDCl_3$, 500 MHz): δ 1.95-2.57 (br s, 1H, D_2O exchangeable), 4.02 (s, 1H), 4.32-4.37 (m, 1H), 4.39-4.44 (m, 1H), 4.46-4.52 (m, 1H), 4.60-4.65 (m, 1H), 4.72-4.81 (q, J_1 12.3 Hz, J_2 7.1 Hz, 2H), 5.60 (s, 1H), 5.69-5.75 (m, 1H), 7.21-7.32 (m, 3H), 7.35-7.45 (m, 4H), 7.57-7.62 (t, J 7.5 Hz, 1H), 7.80-7.84 (d, J 7.2 Hz, 2H).

^{13}C NMR ($CDCl_3$, 50.3 MHz): δ 66.0, 67.0, 68.4, 69.2, 71.0, 71.7, 102.7, 127.9, 128.1, 128.4, 129.4, 129.6, 133.4, 137.0, 164.9.

Elemental analysis calcd for $C_{21}H_{20}O_7$; C 65.62%, H 5.24%; found C 65.37%, H 5.45%.

The structure of **A2.49** was confirmed by X-ray crystallography (see page 134).

Racemic 2-*O*-methyl-4-*O*-benzoyl-*myo*-inositol 1,3,5-orthoformate (A2.50): To a stirred cooled (in ice bath) solution of the diol **A2.48** (1.20 g, 5.9 mmol), in dry pyridine (15 mL), benzoyl chloride (0.91 g, 6.5 mmol) was added and the mixture was stirred for 12 h. Pyridine was evaporated under reduced pressure and the gum obtained was worked up by usual procedure with chloroform. Purification by column chromatography gave the racemic benzoate **A2.50** (1.35 g, 75%) as a white solid.

Data for A2.50: **mp** 139 ^{o}C.

IR ($CHCl_3$) ν = 1724, 3394 cm^{-1}.

^{1}H NMR ($CDCl_3$, 200 MHz): δ 2.65-2.69(d, *J* 6.4 Hz, 1H, D_2O exchangeable), 3.55 (s, 3H), 3.82-3.87 (m, 1H), 4.37-4.44 (m, 1H), 4.47-4.56 (m, 2H), 4.63-4.73 (m, 1H), 5.57-5.58 (d, *J* 1.5 Hz, 1H), 5.75-5.82 (m, 1H), 7.41-7.53 (m, 2H), 7.56-7.66 (m, 1H), 7.96-8.04 (m, 2H).

^{13}C NMR ($CDCl_3$, 50.3 MHz): δ 56.7, 66.9, 68.6, 68.8, 69.0, 70.9, 102.7, 128.5, 129.1, 129.6, 133.5, 165.1, 179.1.

Elemental analysis calcd for $C_{15}H_{16}O_7$; C 58.44%, H 5.23% found C 58.20%, H 5.70%.

The structure of **A2.50** was confirmed by X-ray crystallography (see page 137).

Racemic 2-*O*-tosyl-4-*O*-benzoyl-*myo*-inositol 1,3,5-orthoformate (A2.51): Tosyl chloride (0.382 g, 2.0 mmol) was added to a solution of the orthoformate, **A2.23** (0.380 g, 2.0 mmol) in dry pyridine (5 mL) and the mixture was stirred for 12 h at room temperature. Benzoyl chloride (0.281 g, 2.0 mmol) was then added and stirring continued for another 12 h. Pyridine was evaporated under reduced pressure. Usual work up of the gum obtained followed by purification by column chromatography gave the racemic benzoate **A2.51** (0.584 g, 65%) as a white solid.

Data for A2.51: **mp** 142 ^{o}C.

IR ($CHCl_3$)ν = 1726 cm^{-1}.

^{1}H NMR ($CDCl_3$, 200 MHz): δ 2.36 (s, 3H), 2.77-2.80 (d, *J* 5.3 Hz, 1H, D_2O exchangeable), 4.12-4.25 (m, 1H), 4.33-4.45 (m, 1H), 4.45-4.55 (m, 1H), 4.60-4.75 (m, 1H), 5.03-5.13 (m, 1H), 5.56 (s, 1H), 5.60-5.71 (m, 1H), 7.15-7.33 (m, 2H), 7.42-7.57 (m, 2H), 7.58-7.71 (m, 1H), 7.77-7.82 (d, *J* 8.3 Hz, 2H), 7.92-7.98 (d, *J* 8.3 Hz, 2H).

^{13}C NMR ($CDCl_3$, 125 MHz): δ 21.6, 67.3, 68.3, 69.4, 69.5, 72.1, 102.7, 127.8, 128.7, 129.8, 130.0, 133.8, 145.4, 164.7.

Elemental analysis calcd for $C_{21}H_{20}O_9S$; C 56.25%, H 4.50%, found C 55.85%; H 4.56%.

The structure of **A2.51** was confirmed by X-ray crystallography (see page 140).

Racemic 2-*O*-pivaloyl-4-*O*-benzoyl-*myo*-inositol 1,3,5-orthoformate (A2.53): A solution of pivaloyl chloride (0.390 g, 3.24 mmol) in dry pyridine (3 mL) was added to a stirred, cooled (in ice bath) solution of *myo*-inositol 1,3,5-orthoformate (0.570 g, 3.00 mmol) in dry pyridine (5 mL) and the reaction mixture was allowed to come to room temperature. After 12 h pyridine was evaporated under reduced pressure, the white solid obtained was dissolved in chloroform, washed respectively with water, saturated sodium bicarbonate solution and brine and then dried over anhydrous sodium sulfate. The solid obtained from the organic layer on evaporation of the solvent under reduced pressure was crystallized from a mixture of chloroform and petroleum ether to obtain 2-*O*-pivaloyl-*myo*-inositol 1,3,5-orthoformate, **A2.52** (0.520 g, 63%). mp 159 ^{o}C. lit.[30,36] mp 159 ^{o}C.

To a stirred cooled solution (in ice bath) of **A2.52** (0.440 g, 1.61 mmol) in dry pyridine (6 mL), benzoyl chloride (0.240 g, 1.71 mmol) was added and the reaction mixture was allowed to come to room temperature. Stirring was continued for 12 h and pyridine was removed under reduced pressure to obtain a gum, which was worked up with chloroform as above. The mixture of products was chromatographed to obtain the unreacted starting material (0.110 g, 25%) and **A2.53** (0.43 g, 71%) as white solids.

Data for A2.53: **mp** 160-161 ^{o}C.

IR (Nujol)ν = 1707, 1732, 3448 cm^{-1}.

^{1}H NMR ($CDCl_3$, 200 MHz): δ 1.28 (s, 9H), 2.50-2.90 (br s, 1H, D_2O exchangeable), 4.29-4.38 (m, 1H), 4.40-4.49 (m, 1H), 4.54-4.63 (m, 1H), 4.64-4.75 (m, 1H), 5.35-5.43 (m, 1H), 5.60 (d, *J* 1.5 Hz, 1H), 5.75-5.85 (m, 1H), 7.39-7.53 (m, 2H), 7.54-7.65 (m, 1H), 7.95-8.10 (m, 2H).

^{13}C NMR ($CDCl_3$, 50.3 MHz): δ 26.9, 38.9, 63.0, 67.2, 68.3, 68.5, 69.4, 71.5, 102.8, 128.5, 128.9, 129.8, 133.6, 165.3, 178.5.

Elemental analysis calcd for $C_{19}H_{22}O_8$; C 60.31%, H 5.86%; found C 59.93%, H 5.69%.

The structure of **A2.53** was confirmed by X-ray crystallography (see page 143).

Racemic 2-*O*-benzoyl-4-*O*-pivaloyl-*myo*-inositol 1,3,5-orthoformate (A2.54): To a stirred cooled (in ice bath) solution of the diol **A2.29** (0.880 g, 2.99 mmol) in dry pyridine (6 mL) a solution of pivaloyl chloride (0.390 g, 3.24 mmol) in dry pyridine (4 mL) was added and the reaction mixture was allowed to come to room temperature. Stirring was continued for 12 h and pyridine was evaporated under reduced pressure to obtain a gum. Usual work up of this gum (with chloroform) followed by purification by column chromatography gave the racemic pivalate **A2.54** (0.784 g, 69%) as a white solid.

Data for A2.54: **mp** 121-122 ^oC.

IR ($CHCl_3$) ν = 1718, 3138-3595 cm^{-1}.

^{1}H NMR ($CDCl_3$, 200 MHz): δ 1.27 (s, 9H), 2.67-2.71 (d, *J* 7.4 Hz, 1H, D_2O exchangeable), 4.40-4.55 (m, 3H), 4.61-4.74 (m, 1H), 5.44-5.51 (m, 1H), 5.55-5.65 (m, 2H), 7.40-7.55 (m, 2H), 7.55-7.67 (m, 1H), 8.12-8.22 (m, 2H).

^{13}C NMR ($CDCl_3$, 50.3 MHz): δ 27.0, 38.8, 63.6, 67.4, 68.1, 68.4, 69.3, 71.9, 102.8, 128.4, 129.4, 129.9, 133.4, 166.2, 176.8.

Elemental analysis calcd for $C_{19}H_{22}O_8$; C 60.31%, H 5.86% found C 60.37%, H 6.08%.

Racemic 2-*O*-benzoyl-4-*O*-tosyl-*myo*-inositol 1,3,5-orthoformate (A2.55):. To a solution of the diol **A2.29** (0.294 g, 1.00 mmol) in dry pyridine (6 mL) tosyl chloride (0.200 g, 1.05 mmol) was added and the mixture was stirred at room temperature for 24 h. Pyridine was evaporated under reduced pressure and the gum obtained was worked up with chloroform by usual procedure. Purification by column chromatography gave the racemic tosylate **A2.55** (0.378 g, 84%) and unreacted **A2.29** (0.03g, 10%) as white solids.

Data for A2.55: **mp** 175 ^{o}C.

IR ($CHCl_3$) ν = 1722, 3488 cm^{-1}.

^{1}H NMR ($CDCl_3$, 200 MHz): δ 2.45 (s, 3H), 2.60-3.30 (br s, 1H, D_2O exchangeable), 4.28-4.36 (m, 1H), 4.41-4.49 (m, 2H), 4.62-4.71 (m, 1H), 5.18-5.27 (m, 1H), 5.46-5.51 (m, 1H), 5.54 (s, 1H), 7.34-7.44 (m, 2H), 7.44-7.54 (m, 2H), 7.54-7.66 (m, 1H), 7.84-7.92 (d, *J* 8.3 Hz, 2H), 8.09-8.16 (dd, *J* 7.3 Hz, 1.0 Hz, 2H).

^{13}C NMR ($CDCl_3$, 125 MHz) δ: 21.7, 62.8, 67.3, 69.0, 69.5, 71.4, 73.2, 102.7, 128.1, 128.5, 129.5, 130.0, 130.3, 132.4, 146.0, 165.8.

Elemental analysis calcd for $C_{21}H_{20}O_9S$; C 56.25%, H 4.50%, found C 55.92%, H 4.54%.

2,4-di-*O*-benzoyl-*scyllo*-inositol 1,3,5-orthoformate (A2.57): To a stirred solution of the orthoformate, **A2.56**[42] (0.190 g, 1.00 mmol) in dry pyridine (3 mL), DMAP (0.020 g) was added and the mixture was cooled to 0 ^{o}C in an ice bath. Benzoyl chloride (0.300 g, 2.14 mmol) was added and the stirring continued for 24 h. Pyridine was evaporated under reduced pressure and the gum obtained was worked up by usual procedure with dichloromethane. Purification of the product by column chromatography gave the dibenzoate **A2.57** (0.250 g, 62%) as a white solid.

Data for A2.57: **mp** 177-180 ^{o}C.

IR ($CHCl_3$) ν = 1731, 3436, 3552, 3587, cm^{-1}.

^{1}H NMR ($CDCl_3$, 300 MHz): δ 3.15-3.26 (d, *J* 12.5 Hz, 1H, D_2O exchangeable), 4.50-4.75 (m, 3H), 4.95-5.05 (m, 1H), 5.68 (s, 1H), 5.77-5.82 (m, 2H), 7.12-7.25 (t, *J* 7.7 Hz, 4H), 7.45-7.55 (t, *J* 7.3 Hz, 2H), 7.70-7.80 (d, *J* 8.1 Hz, 4H).

^{13}C NMR ($CDCl_3$, 75 MHz): δ 66.5, 67.1, 67.9, 69.1, 102.7, 128.6, 129.7, 133.6, 164.8.

Elemental analysis calcd for $C_{21}H_{18}O_8$; C 63.32%, H 4.55%; found C 63.50%, H 4.93%.

The structure of **A2.57** was confirmed by X-ray crystallography (see page 150).

2-*O*-benzyl-4,6-di-*O*-tosyl-*scyllo*-inositol 1,3,5-orthoformate (A2.59): To a solution of 2,4-di-*O*-tosyl-*scyllo*-inositol 1,3,5-orthoformate, (**A2.58**, 1.000 g, 2.00 mmol) in dry DMF (5 mL) was added benzyl bromide (0.342 g, 2.00 mmol) and stirred for 5 min and sodium hydride (0.050 g, 2.10 mmol) was added. Stirring was continued for additional 5 min and the reaction was quenched by the addition of ice. Evaporation of DMF under reduced pressure, work up with dichloromethane by usual procedure followed by crystallization of the product from a mixture of chloroform and light petroleum gave 2-*O*-benzyl-4,6-di-*O*-tosyl-*scyllo*-inositol 1,3,5-orthoformate, (**A2.59**, 1.150 g, 97%) as a white solid.

Data for A2.59: **mp** 147-149 ^{o}C.

^{1}H NMR ($CDCl_3$, 200 MHz): δ 2.43 (s, 6H), 4.21-4.33 (m, 1H), 4.33-4.40 (m, 1H), 4.41-4.48 (m, 2H), 4.53 (s, 2H), 5.18-5.23 (t, *J* 3.5 Hz, 2H), 5.47 (s, 1H), 7.12-7.30 (m, 9H), 7.65-7.75 (d, *J* 8.6 Hz, 4H).

^{13}C NMR ($CDCl_3$, 50.3 MHz): δ 21.6, 67.5, 67.9, 69.4, 71.2, 102.5, 127.3, 127.8, 128.1, 129.8, 132.9, 137.2, 145.0.

Elemental analysis calcd for $C_{28}H_{28}O_{10}S_2$; C 57.13%, H 4.79% found C 56.90%, H 4.76%.

2-*O*-benzyl-*scyllo*-inositol 1,3,5-orthoformate (A2.61): Sodium methoxide (0.562 g, 10.41 mmol) was added to a suspension of the ditosylate **A2.59** (0.588 g, 1.00 mmol) in dry methanol (10 mL) and the mixture was refluxed with stirring for 24 h. The reaction mixture was cooled to ambient temperature, ice was added and solvents were evaporated under reduced pressure. Usual work-up with dichloromethane followed by purification of the product by flash chromatography gave the diol **A2.61** (0.272 g, 97%) as a white solid.

Data for A2.61: **mp** 124-125 ^{o}C.

IR ($CHCl_3$) ν = 3153-3604 cm^{-1}.

^{1}H NMR ($CDCl_3$, 500 MHz): δ 3.29-3.35 (d, *J* 8.0 Hz, 2H, D_2O exchangeable), 4.36-4.39 (m, 1H), 4.39-4.43 (m, 1H), 4.44-4.49 (m, 2H), 4.49-4.54 (m, 2H), 4.71 (s, 2H), 5.48 (s, 1H), 7.31-7.41 (m, 5H).

^{13}C NMR ($CDCl_3$, 125 MHz): δ 67.1, 69.1, 70.6, 72.2, 73.2, 102.1, 128.0, 128.4, 128.7, 136.5.

Elemental analysis calcd for $C_{14}H_{16}O_6$; C 60.00%, H 5.75%; found C 59.84%, H 5.58%.

Racemic 2-*O*-benzyl-4-*O*-benzoyl-*scyllo*-inositol 1,3,5-orthoformate (A2.63): The diol **A2.61** (0.200 g, 0.71 mmol) was dissolved in dry pyridine, DMAP (0.020 g) and benzoyl chloride (0.120 g, 0.85 mmol) were added and the mixture stirred at room temperature for 12 h. Evaporation of pyridine under reduced pressure followed by usual work up (with dichloromethane) gave a gum, which on purification by column chromatography gave the racemic benzoate **A2.63** (0.204 g, 72 %) as a white solid.

Data for A2.63: **mp** 120 ^{o}C.

IR ($CHCl_3$) ν = 1726, 3525 cm^{-1}.

^{1}H NMR ($CDCl_3$, 500 MHz): δ 3.90-3.95 (d, *J* 12.4 Hz, 1H, D_2O exchangeable), 4.43-4.50 (m, 2H), 4.52-4.57 (m, 2H), 4.58-4.68 (q, *J* 26.6 Hz, 11.2 Hz, 2H), 4.73-4.78 (m, 1H), 5.58 (s, 1H), 5.72-5.77 (m, 1H), 7.15-7.20 (m, 2H), 7.21-7.31 (m, 5H), 7.47-7.53 (m, 1H), 7.75-7.84 (dd, *J* 7.1 Hz, 1.6 Hz, 2H).

^{13}C NMR ($CDCl_3$, 125 MHz): δ 66.6, 67.4, 67.6, 68.3, 69.6, 72.7, 73.2, 102.4, 127.9, 128.4, 128.5, 128.6, 129.7, 133.4, 136.0, 165.2.

Elemental analysis calcd for $C_{21}H_{20}O_7$; C 65.62%, H 5.24% found; C 65.29%, H 5.11%.

The structure of **A2.63** was confirmed by X-ray crystallography (see page 157).

Racemic 2-*O*-methyl-4-*O*-benzoyl-*scyllo*-inositol 1,3,5-orthoformate (A2.64): the diol **A2.62** (0.131 g, 0.64 mmol) was dissolved in dry pyridine, DMAP (0.005 g) and benzoyl chloride (0.097 g, 0.69 mmol) were added and the mixture was stirred at room temperature for 6 h. Evaporation of pyridine under reduced pressure followed by usual work up (with dichloromethane) gave a gum, which on purification by column chromatography gave the racemic benzoate **A2.64** (0.140 g, 71%) as a white solid.

Data for A2.64: **mp** 128-129 ^oC.

IR ($CHCl_3$) ν = 1726, 3450-3579 cm^{-1}.

^{1}H NMR ($CDCl_3$, 500 MHz): δ 3.45 (s, 3H), 3.86-3.92 (d, *J* 11.9 Hz, 1H, D_2O exchangeable), 4.23-4.27 (m, 1H), 4.41-4.47 (m, 1H), 4.47-4.51 (m, 1H), 4.53-4.57 (m, 1H), 4.76-4.80 (m, 1H), 5.58 (s, 1H), 5.73-5.76 (m, 1H), 7.44-7.49 (m, 2H), 7.57-7.62 (m, 1H), 7.81-8.05 (m, 2H).

^{13}C NMR ($CDCl_3$, 125 MHz): δ 57.9, 66.5, 67.6, 68.2, 69.6, 75.1, 102.4, 128.6, 129.5, 133.5, 165.1.

Elemental analysis calcd for $C_{15}H_{16}O_7$; C 58.44%, H 5.23%; found C 58.44%, H 5.29%. The structure of **A2.64** was confirmed by X-ray crystallography (see page 160).

General procedure for the transesterification of *myo*-inositol esters in the solid-state: Crystals of the required *myo*-inositol derivative (0.025g to 0.500g) were ground together with sodium carbonate (8 eq) using a pestle and mortar and the mixture heated (1h to 192 h) below the mp of the inositol derivative, in an atmosphere of nitrogen in a hard glass tube. The solid obtained after heating was cooled to ambient temperature, extracted with chloroform followed by methanol; the combined organic extract was evaporated under reduced pressure and the products were separated by column chromatography.

General procedure for the transesterification of *myo*-inositol esters in solution: Crystals of the required *myo*-inositol derivative (0.100 g) and dry triethylamine (10 eq) were dissolved in dry acetonitrile (2 mL) and stirred at ambient temperature (reflux for **A2.41**) under nitrogen atmosphere for 144 h. Acetonitrile and triethylamine were evaporated under reduced pressure and the products were separated by column chromatography over silica gel.

General procedure for the transesterification of *myo*-inositol esters in the melt: Crystals of the required *myo*-inositol derivative (0.100g to 0.200g) were melted in a hard glass tube in an atmosphere of nitrogen and heated with sodium carbonate (8 eq) for 36 h. The solid obtained after cooling to ambient temperature, was extracted with chloroform followed by methanol; the combined organic extracts were evaporated under reduced pressure and the products were separated by chromatography.

Transesterification of racemic 2,4-di-*O*-benzoyl-*myo*-inositol (A2.9) in the solid-state:

The racemic dibenzoate **A2.9** (0.100 g, 0.26 mmol) and sodium carbonate (0.106 g, 1.00 mmol) were ground together and heated at 140 ^{o}C for 1 h. Analysis of the reaction mixture by TLC indicated the presence of several products. No attempt was made to separate and characterize these products.

Transesterification of racemic 4-*O*-benzoyl-*myo*-inositol 1,3,5-orthoformate (A2.25) in the solid-state: The racemic benzoate **A2.25** (0.300 g, 1.02 mmol) and sodium carbonate (0.848 g, 8.00 mmol) were ground together and heated at 120 ^{o}C in an atmosphere of nitrogen for 72 h. Isolation of the products as mentioned in the general procedure gave tribenzoate **A2.34**[32] (0.123 g, 24%), dibenzoate **A2.33**[12] (0.007, 1%; characterized by comparing TLC with authentic sample and ^{1}H NMR spectrum) and **A2.66**[30, 36] (0.007 g, 1%; characterized by comparing TLC with authentic sample and ^{1}H NMR spectrum), diol **A2.29**[35] (0.007g, 2%; characterized by comparing TLC with authentic sample and ^{1}H NMR spectrum), the triol **A2.23**[32] (0.110 g, 56%) and benzoic acid, **A2.65** (0.032 g, 25%) as white solids.

Transesterification of racemic 4-*O*-benzoyl-*myo*-inositol 1,3,5-orthoacetate (A2.27) in the solid-state: The racemic benzoate **A2.27** (0.308 g, 1.00 mmol) and sodium carbonate (0.848 g, 8.00 mmol) were ground together and heated at 120 ^{o}C in an atmosphere of nitrogen for 168 h. Isolation of the products as mentioned in the general method gave benzoic acid (**A2.65**, 0.060 g, 49%) and the triol **A2.24** (0.141 g, 69%) as white solids.

Data for A2.24: **mp** 185-186 ^{o}C. lit.[32] mp 185-187 ^{o}C.

Data for A2.65: **mp**120 ^{o}C; lit.[85] mp 122 ^{o}C.

Transesterification of racemic 2,4-di-*O*-benzoyl-*myo*-inositol 1,3,5-orthoformate (A2.33) (a) in the solid-state: The reaction was carried out as in reference 31 to obtain the tribenzoate **A2.34**[32] (0.06 g, 47%) and the diol **A2.29**[30, 35] (0.036 g, 49%).

(b) In solution: The reaction was carried out as in reference 31 to obtain the tribenzoate **A2.34** (0.040 g, 32%) and the diol **A2.29** (0.023 g, 31%) along with unreacted **A2.33** (0.036 g, 36%) as white solids.

(c) In melt: A molten sample of racemic dibenzoate **A2.33** (0.200g, 0.50 mmol) was heated with sodium carbonate (0.424 g, 4.00 mmol) for 36 h. The reaction was worked up as mentioned in the general procedure to obtain tribenzoate **A2.34**[32] (0.040 g, 16%), dibenzoate **A2.66**[30, 36] (0.018 g, 9%), diol **A2.29**[35] (0.022 g, 15%), axial benzoate **A2.25**[30] (0.019 g, 13%), and unreacted **A2.33** (0.045 g, 23%). Continuation of the reaction for longer period of time resulted in charring of the reaction mixture.

Transesterification of racemic 2-*O*-benzoyl-4-*O*-benzyl-*myo*-inositol 1,3,5-orthoformate (A2.35) in the solid-state: The racemic benzoate **A2.35** (0.025 g, 0.065 mmol) and sodium carbonate (0.055 g, 0.52 mmol) were ground together and heated at 90 ^{o}C for 60 h. No reaction was observed.

Transesterification of 1D-2-*O*-benzoyl-4-*O*-[(-)-*ω*-camphanoyl]-*myo*-inositol 1,3,5-orthoformate (A2.D36) in the solid-state: The camphanoate **A2.D36** (0.200 g, 0.42 mmol) and sodium carbonate (0.360 g, 3.39 mmol) were ground together and heated at 140 ^{o}C for 36 h. Analysis of the reaction mixture by TLC indicated the presence at least six products. No attempt was made to separate and characterize these products. No reaction was observed when the reaction was carried out at 110 ^{o}C for 60 h.

Transesterification of 1L-2-*O*-benzoyl-4-*O*-[(-)-*ω*-camphanoyl]-*myo*-inositol 1,3,5-orthoformate (A2.L36) in the solid-state: The camphanoate **A2.L36** (0.025 g, 0.053 mmol) and sodium carbonate (0.045 g, 0.42 mmol) were ground together and heated at 140 ^{o}C for 36 h. Analysis of the reaction mixture by TLC indicated the presence at least six products. No attempt was made to separate and characterize these products. No reaction was observed when the reaction was carried out at 110 ^{o}C for 60 h.

Transesterification of 1D-2,4-di-*O*-[(-)-*ω*-camphanoyl]-*myo*-inositol 1,3,5-orthoformate (A2.D37) (a) in the solid-state: The dicamphanoate **A2.D37** (0.025 g, 0.05 mmol) and sodium carbonate (0.039 g, 0.37 mmol) were ground together and heated at 170 ^{o}C for 48 h. No reaction was observed.

(b) In solution: **Procedure A:** A solution of the dicamphanoate **A2.D37** (0.100 g, 0.18 mmol) and triethylamine (0.218 g, 2.15 mmol) in acetonitrile (5 mL) was stirred at ambient temperature for 48 h. No reaction was observed.

Procedure B: To a solution of the dicamphanoate **A2.D37** (0.100 g, 0.18 mmol) in DMF (3 mL), sodium hydride (0.005 g, 0.21 mmol) was added and the mixture stirred at ambient temperature for 48 h. No reaction was observed.

Transesterification of 1L-2,4-di-*O*-[(-)-*ω*-camphanoyl]-*myo*-inositol 1,3,5 orthoformate (A2.L37) (a) in the solid-state: The dicamphanoate **A2.L37** (0.025 g, 0.05 mmol) and sodium carbonate (0.039 g, 0.37 mmol) were ground together and heated at 170 ^{o}C for 48 h. No reaction was observed.

(b) In solution: **Procedure A:** A solution of the dicamphanoate **A2.L37** (0.100 g, 0.18 mmol) and triethylamine (0.218 g, 2.15 mmol) in acetonitrile (5 mL) was stirred at ambient temperature for 48 h. No reaction was observed.

Procedure B: To a solution of the dicamphanoate **A2.L37** (0.100 g, 0.18 mmol) in DMF (3 mL), sodium hydride (0.005 g, 0.21 mmol) was added and the mixture stirred at room temperature for 48 h. No reaction was observed.

Transesterification of racemic 1,2-*O*-isopropylidine-3,6-di-*O*-benzoyl-*myo*-inositol (A2.38) in the solid-state: Racemic **A2.38** (0.107 g, 0.25 mmol) and sodium carbonate (0.212 g, 2.00 mmol) were ground together and heated at 120 ^{o}C for 1 h. Analysis of the reaction mixture by TLC indicated the presence of several products. No attempt was made to separate and characterize these products.

Transesterification of 2,4,6-tri-*O*-benzoyl-*myo*-inositol (A2.39) in the solid-state: The tribenzoate **A2.39** (0.100 g, 0.20 mmol) and sodium carbonate (0.065 g, 0.61 mmol) were ground together and heated at 120 ^{o}C for 1 h. Analysis of the reaction mixture by TLC indicated the presence of several products. No attempt was made to separate and characterize these products.

Transesterification of racemic 2,4-di-*O*-pivaloyl-*myo*-inositol 1,3,5-orthoformate (A2.41) (a) in the solid-state: The racemic dipivalate **A2.41** (0.200 g, 0.56 mmol) and sodium carbonate (0.483 g, 4.56 mmol) were ground together and heated at 125 ^{o}C in an atmosphere of nitrogen for 192 h. Isolation of the products as mentioned in the general procedure gave 2,4,6-tri-*O*-pivaloyl-*myo*-inositol 1,3,5-orthoformate, (**A2.67**, 0.056 g, 22%) and the known diol **A2.52**[30, 36] (0.092 g, 60%) as white solids.

Data for **A2.67**: **mp** 148-150 ^{o}C.

IR ($CHCl_3$) ν = 1735 cm^{-1}.

^{1}H NMR ($CDCl_3$, 200 MHz): δ 1.24 (s, 9H), 1.28 (s, 18H), 4.21-4.28 (m, 2H), 4.44-4.56 (m, 1H), 4.97-5.02 (m, 1H), 5.56-5.65 (m, 3H).

^{13}C NMR ($CDCl_3$, 1250 MHz): δ 27.0, 38.9, 62.5, 67.5, 68.1, 68.3, 69.1, 71.8, 102.8, 176.5, 178.1.

Elemental analysis calcd for $C_{22}H_{34}O_9$; C 59.99%, H 7.78%; found C 59.84%, H 7.81%.

(b) In solution: The racemic dipivalate **A2.41** (0.100 g, 0.28 mmol) and triethylamine (0.283 g, 2.80 mmol) were dissolved in dry acetonitrile (2 mL) and the mixture was refluxed under nitrogen atmosphere for 144 hours. Work up and isolation of the products as mentioned in the general procedure gave the tripivalate **A2.67** (0.024 g, 19%) and the known diol **A2.52**[30, 36] (0.014 g, 18%) along with unreacted **A2.41** (0.056 g, 56%) as white solids.

Transesterification of racemic 2,4-di-*O*-[1-naphthoyl]-*myo*-inositol 1,3,5-orthoformate (A2.42) in the solid-state: The dinaphthoate **A2.42** (0.025 g, 0.05 mmol) and sodium carbonate (0.042 g, 0.40 mmol) were ground together and heated at 170 ^{o}C for 72 h. No reaction was observed.

Transesterification of racemic 2,4-di-*O*-benzoyl-*myo*-inositol 1,3,5-orthoacetate (A2.43) (a) in the solid-state: The racemic dibenzoate **A2.43** (0.500 g, 1.25 mmol) and sodium carbonate (1.060 g, 10.0 mmol) were ground together and heated at 140 ^{o}C in an atmosphere of nitrogen for 168 h. Isolation of the products as mentioned in the general procedure gave the tribenzoate **A2.68**[32] (0.125 g, 19%), the diol **A2.31** (0.080 g, 21%); the dibenzoate **A2.69** (0.040 g, 8%), the racemic axial benzoate **A2.27**[30, 36] (0.060g, 16%,) and unreacted **A2.43** (0.070g, 14%).

Data for A2.69: **mp** 160-162 ^{o}C.

IR ($CHCl_3$) ν = 1728, 3186-3569 cm^{-1}.

^{1}H NMR ($CDCl_3$, 500 MHz): δ 1.57 (s, 3H), 3.15-3.19 (d, *J* 11.9 Hz, 1H, D_2O exchangeable), 4.20-4.24 (d, *J* 11.1 Hz, 1H), 4.43-4.46 (m, 2H), 4.84-4.88 (m, 1H), 5.74-5.78 (t, *J* 4.0 Hz, 2H), 7.15-7.20 (m, 4H), 7.44-7.49 (m, 2H), 7.78-7.81 (dd, *J* 7.2 Hz, 1.1 Hz, 4H).

^{13}C NMR ($CDCl_3$, 50.3 MHz): δ 24.2, 60.7, 66.8, 68.6, 72.5, 109.7, 128.3, 128.9, 129.8, 133.4, 165.2.

Elemental analysis calcd for $C_{22}H_{20}O_8$; C 64.08%, H 4.89%; found C 64.12%, H 5.33%.

The structure of **A2.69** was confirmed by X-ray crystallography (see page 165).

(b) In solution: The racemic dibenzoate **A2.43** (0.100 g, 0.24 mmol) and triethylamine (0.240g, 2.37 mmol) were dissolved in dry acetonitrile (2 mL) and the mixture was stirred at ambient temperature under nitrogen atmosphere for 144 hours. Isolation of the products as described in the general procedure gave the tribenzoate **A2.68** (0.038 g, 30%) and the diol **A2.31** (0.022 g, 29%) along with unreacted **A2.43** (0.036 g, 36%).

(c) In melt: A molten sample of the racemic dibenzoate **A2.43** (0.200g, 0.50 mmol) and sodium carbonate (0.424 g, 4.00 mmol) were heated at 180 °C for 36 h in a hard glass tube under nitrogen. TLC of the reaction suggested the formation of 4-5 products; no attempt was made to isolate these products.

Transesterification in 1:1 molecular crystals of racemic 2,4-di-*O*-benzoyl-*myo*-inositol 1,3,5-orthoformate and racemic 2,4-di-*O*-benzyol-*myo*-inositol 1,3,5-orthoacetate (A2.33·43) (a) in the solid-state: Crystals of the molecular complex **A2.33·43** (0.100 g, 0.12 mmol) and sodium carbonate (0.210 g, 1.97 mmol) were ground together and heated at 120 ^oC for 168 h. The reaction mixture was worked up as mentioned in the general procedure and a mixture of tribenzoates **A2.34** and **A2.68**

(0.052 g, 41%) as well as a mixture of the diols **A2.29** and **A2.31** (0.026 g, 35%) were isolated by column chromatography. Analysis of these mixtures by ^{1}H NMR spectroscopy showed that **A2.34** and **A2.68** (see page 166) were formed in the ratio 2.03:1.00 (67:33) while the mixture of **A2.29** and **A2.31** (see page 166) were formed in the ratio 1.00:1.88 (35:65). Other minor products formed in this reaction were not isolated.

Data for the mixture of A2.34 and A2.68:

^{1}H NMR ($CDCl_3$, 500 MHz): δ 1.62 (s, 3H), 4.66-4.74 (m, 4H), 4.90-4.95 (m, 1H), 4.95-5.03 (m, 1H), 5.63-5.68 (m, 1H), 5.69-5.74 (m, 1H), 5.74-5.77 (d, *J* 1 Hz, 1H), 5.79-5.84 (m, 1H), 5.84-5.90 (m, 3H), 7.14-7.24 (m, 8H), 7.43-7.53 (m, 8H), 7.58-7.65 (m, 2H), 7.83-7.90 (m, 8H), 8.14-8.20 (m, 4H).

Data for the isolated mixture of A2.29 and A2.31:

^{1}H NMR (CD_3OD & $CDCl_3$, 500 MHz): δ 1.45 (s, 3H), 4.09-4.14 (m, 2H), 4.14-4.16 (m, 1H), 4.16-4.20 (m, 1H), 4.20-4.23 (m, 1H), 4.36-4.41 (m, 2H), 4.43-4.47 (t, *J* 3.7 Hz, 2H), 4.47-4.50 (t, *J* 3.7 Hz, 2H), 5.41-5.43 (d, *J* 1 Hz, 1H), 5.54-5.56 (m, 1H), 7.47-7.53 (t, *J* 7.8 Hz, 2H), 7.59-7.65 (m, 1H), 8.10-8.16 (m, 2H).

(b) In solution: The 1: 1 molecular complex **A2.33·43**, (0.100 g, 0.24 mmol) and triethylamine (0.240 g, 2.37 mmol) were dissolved in dry acetonitrile (2 mL) and the mixture was stirred at ambient temperature under nitrogen atmosphere for 144 hours. Reaction was worked up as mentioned in the general procedure to obtain mixture of the tribenzoates **A2.34** and **A2.68** (0.040 g, 32%; **A2.34** : **A2.68** = 55 : 45, by ^{1}H NMR spectroscopy, see page 167) and the diols **A2.29** and **A2.31** (0.021 g, 28%; **A2.29** :

A2.31 = 56 : 44, by ^{1}H NMR spectroscopy, see pages 167 and 168) along with unreacted **A2.33·43** (0.033 g, 33%) as white solids.

(c) In melt: A molten sample of 1:1 molecular complex **A2.33·43** (0.100 g, 0.12 mmol) and sodium carbonate (0.210 g, 1.97 mmol) was heated in a hard glass tube under nitrogen at 180 °C for 36 h. TLC of the reaction mixture indicated the formation of about 8-10 products and the presence of unreacted starting material. No attempt was made to isolate the products.

Transesterification of racemic 2-*O*-benzyl-4-*O*-benzoyl-*myo*-inositol 1,3,5-orthoformate (A2.49) (a) in the solid state: The racemic benzoate **A2.49** (0.100 g, 0.26 mmol) and sodium carbonate (0.220 g, 2.08 mmol) were ground together and heated at 100 ^{o}C for 192 h. Work up and isolation of products as mentioned in the general method gave 2-*O*-benzyl-4,6-di-*O*-benzoyl-*myo*-inositol 1,3,5-orthoformate, (**A2.70**, 0.053 g, 41%) and the known diol **A2.47**[37] (0.033 g, 45%) as white solids.

Data for A2.70: **mp** 180 ^{o}C.

IR (Nujol)ν = 1726 cm^{-1}.

^{1}H NMR ($CDCl_3$, 200 MHz): δ 4.00-4.05 (m, 1H), 4.45-4.55 (m, 2H), 4.82 (s, 2H), 4.85-4.95 (m, 1H), 5.65-5.77 (m, 3H), 7.05-7.22 (t, *J* 7.8 Hz, 4H), 7.22-7.35 (m, 3H), 7.35-7.43 (m, 2H), 7.43-7.54 (m, 2H), 7.54-7.65 (m, 4H).

^{13}C NMR ($CDCl_3$, 50.3 MHz): δ 65.1, 67.0, 68.5, 69.2, 70.9, 103.3, 128.2, 128.5, 129.6, 133.4, 137.0, 164.9.

Elemental analysis calcd for $C_{28}H_{24}O_8$; C 68.85%, H 4.95%; found C 69.15%, H 5.34%.

The structure of **A2.69** was confirmed by X-ray crystallography (see page 170).

(b) In melt: The racemic benzoate **A2.49** (0.100 g, 0.26 mmol) was heated to 140 ^{o}C (melt). Sodium carbonate (0.220 g, 2.10 mmol) was added to this melt and mixed thoroughly and the mixture was heated under nitrogen atmosphere for 192 hours (8 days). The solid obtain after cooling the reaction mixture to ambient temperature was worked up as mentioned in the general procedure to isolate the dibenzoate **A2.70** (0.052 g, 41%) and the known diol **A2.47**[37] (0.031 g, 42%) as white solids.

Transesterification of racemic 2-*O*-methyl-4-*O*-benzoyl-*myo*-inositol 1,3,5-orthoformate (A2.50) (a) in the solid-state: The racemic benzoate **A2.50** (0.200 g, 0.65 mmol) and sodium carbonate (0.550 g, 5.19 mmol) were ground together and heated at 125 ^{o}C for 144 h. Work up and isolation of products as mentioned in the general method gave **A2.71** (0.041 g, 15%), the diol **A2.48** (0.073 g, 55%) and benzoic acid, (**A2.65**, 0.02 g, 25%) as white solids.

Data for A2.71: **mp** 178-180 ^{o}C.

IR ($CHCl_3$) ν = 1726 cm^{-1}.

^{1}H NMR ($CDCl_3$, 200 MHz): δ 3.61 (s, 3H), 3.83-3.93 (m, 1H), 4.57-4.71 (m, 2H), 4.86-5.00 (m, 1H), 5.69 (s, 1H), 5.76-5.85 (t, *J* 3.6 Hz, 2H), 7.11-7.28 (m, 4H), 7.41-7.51 (m, 2H), 7.73-7.93 (m, 4H).

^{13}C NMR ($CDCl_3$, 50.3 MHz): δ 57.0, 67.1, 68.5, 68.7, 69.6, 103.4, 128.4, 129.8, 133.5, 165.1.

Elemental analysis calcd for $C_{22}H_{20}O_8$; C 64.08%, H 4.89%; found C 64.17%, H 5.15%.

(b) In melt: The racemic benzoate **A2.50** (0.115 g, 0.37 mmol) was heated to 160 ^{o}C (melt). Sodium carbonate (0.314 g, 2.96 mmol) was added to this melt and mixed

thoroughly and the mixture was heated under nitrogen atmosphere for 12 h. This led to extensive charring and neither products nor the starting material could be isolated.

Transesterification of racemic 2-*O*-tosyl-4-*O*-benzoyl-*myo*-inositol 1,3,5-orthoformate (A2.51) in the solid-state: The racemic benzoate **A2.51** (0.200 g, 0.44 mmol) and sodium carbonate (0.379 g, 3.58mmol) were ground together and heated at 100 ^{o}C for 192 h. The reaction mixture turned black on heating. Work up and isolation of products as mentioned in the general procedure gave 2-*O*-tosyl-4,6-di-*O*-benzoyl-*myo*-inositol 1,3,5-orthoformate (**A2.72**, 0.042 g, 17%), 2-*O*-tosyl-*myo*-inositol 1,3,5-orthoformate[37] (**A2.73**, 0.016 g, 10%) and unreacted **A2.51** (0.006g, 3%).

Data for **A2.72**: **mp** 210 ^{o}C.

IR ($CHCl_3$) ν = 1718 cm^{-1}.

^{1}H NMR ($CDCl_3$, 200 MHz): δ 2.34 (s, 3H), 4.37-4.47 (m, 2H), 4.83-4.93 (m, 1H), 5.01-5.09 (m, 1H), 5.61-5.67 (m, 1H), 5.67-5.77 (m, 2H), 7.11-7.30 (m, 6H), 7.44-7.59 (m, 2H), 7.67-7.86 (m, 6H).

^{13}C NMR ($CDCl_3$, 50.3 MHz): δ 21.6, 66.7, 68.4, 69.4, 69.5, 103.1, 127.8, 128.5, 129.8, 130.1, 133.2, 133.7, 145.5, 164.7.

Elemental analysis calcd for $C_{28}H_{24}O_{10}S$; C 60.86%, H 4.38%; found C 61.26%, H 4.10%.

Data for A2.73: **mp** 116-117 ^{o}C; lit.[37] mp 117-119 ^{o}C.

Transesterification of racemic 2-*O*-pivaloyl-4-*O*-benzoyl-*myo*-inositol 1,3,5-orthoformate (A2.53) (a) in the solid-state: The racemic diester **A2.53** (0.100 g, 0.26 mmol) and sodium carbonate (0.220 g, 2.08 mmol) were ground together and heated at 140 ^{o}C for 168 h. The reaction mixture was worked up as mentioned in the general

procedure and 2-*O*-pivaloyl-4,6-di-*O*-benzoyl-*myo*-inositol 1,3,5-orthoformate, (**A2.74**, 0.018 g, 14%) was isolated by preparative TLC. Other products (about 8) formed in this reaction were not isolated.

Data for A2.74: **mp** 193-195 ^{o}C;

IR ($CHCl_3$) ν = 1726 cm^{-1}.

^{1}H NMR ($CDCl_3$, 500 MHz): δ 1.31 (s, 9H), 4.50-4.53 (m, 2H), 4.92-4.95 (m, 1H), 5.41-5.43 (m, 1H), 5.68-5.70 (d, *J* 1.2 Hz, 1H), 5.79-5.82 (t, *J* 3.8 Hz, 2H), 7.16-7.21 (m, 4H), 7.45-7.50 (m, 2H), 7.82-7.86 (dd, *J* 7.1 Hz, 1.2 Hz, 4H).

^{13}C NMR ($CDCl_3$, 75 MHz): δ 27.0, 39.0, 63.0, 67.0, 68.4, 69.3, 103.3, 128.3, 128.6, 129.8, 133.4, 165.1, 178.2.

Elemental analysis calcd for $C_{26}H_{26}O_9$; C 64.72%, H 5.43%; found C 64.63%, H 5.12%.

(b) In solution: The racemic diester **A2.53** (0.100 g, 0.26 mmol) and triethylamine (0.261 g, 2.58 mmol) were dissolved in dry acetonitrile (2 mL) and the mixture was stirred at ambient temperature under nitrogen atmosphere for 144 hours. Isolation of the products as mentioned in the general procedure gave the triester **A2.74** (0.030 g, 23%) and the diol **A2.52** (0.018 g, 25%) along with unreacted **A2.53** (0.046 g, 46%).

Transesterification of racemic 2-*O*-benzoyl-4-*O*-pivaloyl-*myo*-inositol 1,3,5-orthoformate (A2.54) in the solid-state: The racemic diester **A2.54** (0.100 g, 0.26 mmol) and sodium carbonate (0.220 g, 2.08 mmol) were ground together and heated at 100 ^{o}C for 72 h. No attempt was made to separate and characterize the products obtained (at least six as indicated by TLC). No reaction was observed (by TLC) at 90 ^{o}C (48 h).

Transesterification of racemic 2-*O*-benzoyl-4-*O*-tosyl-*myo*-inositol 1,3,5-orthoformate (A2.55) in the solid-state: The racecmic benzoate **A2.55** (0.100 g, 0.22

mmol) and sodium carbonate (0.187 g, 1.76 mmol) were ground together and heated at 145 ^{o}C for 36 h. No attempt was made to separate and characterize the products obtained (at least eight as indicated by TLC). No reaction was observed (by TLC) at 130 ^{o}C (48 h).

Transesterification of 2,4-di-*O*-benzoyl-*scyllo*-inositol 1,3,5-orthoformate (A2.57) in the solid-state: The dibenzoate **A2.57** (0.10 g, 0.25 mmol) and sodium carbonate (0.212 g, 2.0 mmol) were ground together and heated at 160 ^{o}C in an atmosphere of nitrogen for 48 h. Isolation of the products as mentioned in the general method gave 2,4,6-tri-*O*-benzoyl-*scyllo*-inositol 1,3,5-orthoformate[29] (**A2.75**, 0.087 g, 69%) and the triol **A2.56**[42] (0.008 g, 17%).

Data for A2.75: **mp** 251-253 ^{o}C. lit.[29] mp 248-250 ^{o}C.

Transesterification of racemic 2-*O*-benzyl-4-*O*-benzoyl-*scyllo*-inositol 1,3,5-orthoformate (A2.63) in the solid-state: The racemic benzoate **A2.63** (0.02 g, 0.053 mmol) and sodium carbonate (0.045 g, 0.43 mmol) were ground together and heated at 115 ^{o}C in an atmosphere of nitrogen for 48 h. No reaction was observed.

Transesterification of racemic 2-*O*-methyl-4-*O*-benzoyl-*scyllo*-inositol 1,3,5-orthoformate (A2.64) in the solid-state: The racemic benzoate **A2.64** (0.035 g, 0.114 mmol) and sodium carbonate (0.097 g, 0.92 mmol) were ground together and heated at 125 ^{o}C in an atmosphere of nitrogen for 48 h. No reaction was observed.

A2.6. References

1. Bruzik, K. S. Ed.; *Phosphoinositides: Chemistry, Biochemistry and Biomedical Applications*, ACS Symposium Series 718., American Chemical Society, Washington D.C. USA, 1999.
2. McConville, M. J.; Menon, A. K. *Mol. Membr. Biol.*, **2000**, *17*, 1.
3. Low, M. G. *Mol. Biol. Intell. Unit 7 (GPI-Anchored Membrane Proteins and Carbohydrates)*, **1999**, 1014.
4. Thomas, J. R.; Dwek, R. A.; Rademacher, T. W. *Biochem.*, **1990**, *29*, 5413.
5. Qiao, L.; Nan, F.; Kunkel, Gallegos, A.; Powis, G.; Kozikowski, A. P. *J. Med. Chem.*, **1998**, *41*, 3303.
6. Sureshan, K. M.; Shashidhar, M. S.; Praveen, T.; Das, T. *Chem. Rev.*, **2003**, *103*, 4477.
7. Watanabe, Y.; Shinohara, T.; Fujimoto, T.; Ozaki, S. *Chem. Pharm. Bull.*, **1990**, *38*, 562.
8. Salamończyk, G. M.; Pietrusiewicz, K. M. *Tetrahedron Lett.*, **1996**, *32*, 4031.
9. Shashidhar, M. S.; Volwerk, J. J.; Griffith, O. H.; Keana, J. F. W. *Chem. Phys. Lipids*, **1991**, *60*, 101.
10. Bruzik, K. S.; Kubiak, R. J. *Tetrahedron Lett.*, **1995**, *36*, 2415.
11. Flores-Mosquera, M.; Martin-Lomas, N.; Chiara, J. L. *Tetrahedron Lett.*, **1998**, *39*, 5085.
12. Banerjee, T.; Shashidhar, M. S. *Tetrahedron Lett.*, **1994**, *35*, 8053.
13. Potter, B. V. L; Riley, A. M.; Mahon, M. F. *Angew. Chem. Int. Ed. Engl.*, **1997**, *36*, 1472.

14. Garrett, S. W.; Liu, C.; Riley, A. M.; Potter, B. V. L. *J. Chem. Soc., Perkin Trans. 1*, **1998**, 1367.

15. Mills, S. J.; Riley, A. M.; Liu, C.; Mahon, M. F.; Potter, B. V. L. *Chem. Eur. J.*, **2003**, *9*, 6207.

16. Praveen, T.; Das, T.; Sureshan, K. M.; Shashidhar, M. S.; Samanta, U.; Pal, D.; Chakrabarti, P. *J. Chem. Soc., Perkin Trans. 2*, **2002**, 358.

17. Kim, T-H.; Holmes, A. B.; Andrew, B. *J. Chem. Soc., Perkin Trans. 1*, **2001**, 2524.

18. Brannigan, J. A.; Dodson, G.; Duggleby, H, J.; Moody, P. C. E.; Smith, J. L.; Tomchick, D. R.; Murzin, A. G. *Nature* (London), **1995**, *378*, 416.

19. Voet, D.; Voet, J. G. *Biomolecules*, *Mechanisms of Enzyme Action and Metabolism, Biochemistry,* Vol 1, Wiley, New York, 2003.

20. Patai, S. *The Chemistry of Functional Groups. The Chemistry of Carboxylic Acids and Esters,* (Ed.: Patai, S), Wiley, New York, **1969**, p. 1155.

21. Angyal, S. J.; Melrose, J. H *J. Chem. Soc.*, **1965**, 6494.

22. Angyal, S. J.; Merlose, G. J. H. *J. Chem. Soc.*, **1965**, 6501.

23. Shvets, V. I. *Russ. Chem. Rev.*, **1974**, *34*, 488.

24. Meek, J. L.; Davidson, F.; Hobbs, F. W. Jr. *J. Am. Chem. Soc.*, **1988**, *110*, 2317.

25. Chung, S-K.; Chang, Y-T. *J. Chem. Soc. Chem. Commun.*, **1995**, 11.

26. Chung, S-K.; Chang, Y-T.; Ryu, Y. *Pure and Appl. Chem.*, **1996**, *68*, 931.

27. Chung, S-K.; Chang, Y-T. *Korean J. Med. Chem.*, **1996**, *6*, 162.

28. Chung, S-K.; Kwon, Y-U.; Shin, J-H.; Chang, Y-T.; Lee. C.; Shin, B.G.; Kim, K-C.; Kim, M-J. *J. Org. Chem.*, **2002**, *67*, 5626.

29. Chung, S-K.; Kwon, Y-U.; Chang, Y-T.; Shon, K-H.; Shin, J-H.; Park, K-H.; Hong, B-J.; Chung, I-H. *Bioorg. Med. Chem.*, **1999**, *7*, 2577.

30. Sureshan K, M.; Shashidhar, M. S. *Tetrahedron Lett.*, **2000**, *41*, 4185.

31. Praveen, T.; Samanta, U.; Das, T., Shashidhar, M. S.; Chakrabarti, P. *J. Am. Chem. Soc.*, **1998**, *120*, 3842.

32. Praveen, T.; Shashidhar, M. S. *Carbohydr. Res.*, **2001**, *330*, 409.

33. Das, T.; Praveen, T.; Shashidhar, M. S. *Carbohydr. Res.*, **1998**, *313*, 55.

34. Chung, S-K.; Chang, Y-T.; Lee, E. J.; Kown, Y-U. *Korean J. Med. Chem.*, **1998**, *8*, 18.

35. Das, T.; Shashidhar, M. S. *Carbohydr. Res.*, **1998**, *308*, 165.

36. Sureshan, K. M., Ph.D. thesis; University of Pune, Pune-2002.

37. Sureshan, K. M.; Shashidhar, M. S.; Praveen, T.; Gonnade, R. G.; Bhadbhade, M. M. *Cabohydr. Res.*, **2002**, *337*, 2399.

38. Boese, R.; Clark, T.; Gavezzotti, A. *Helv. Chim. Acta*, **2003**, *86*, 1085.

39. Boese, R.; Kirchner, M. T.; Billups, W. E.; Norman, L. R. *Angew. Chem. Int. Ed. Engl.*, **2003**, *42*, 1961.

40. Thalladi, V. R.; Smolka, T.; Gehrke, A.; Boese, R.; Sustmann, R. *New J. Chem.*, **2000**, *24*, 143.

41. Zyss, J.; Ledoux-Rak, I;. Weiss, H-C.; Bläeser, D.; Boese, R.; Thallapally, P. K.; Thalladi, V. R.; Desiraju, G. R. *Chem. Mater.*, **2003**, *15*, 3063.

42. Lee, H. W.; Kishi, Y. *J. Org. Chem.*, **1985**, *50*, 4402.

43. Chung, S-K.; Chang, Y-T.; Whang, D.; Kim, K. *Carbohydr. Res.*, **1996**, *295*, 1.

44. Bürgi, H. B.; Dunitz, J. D.; Shefter, E. *J. Am. Chem. Soc.*, **1973**, *95*, 5065.

45. Bürgi, H. B.; Dunitz, J. D.; Shefter, E. *Acta Crystallogr.*, **1974**, *B30*, 1517.

46. Bürgi, H. B.; Lehn, J. M.; Wipff, G. J. *J. Am. Chem. Soc.*, **1974**, *96*, 1956.

47. Bürgi, H. B.; Dunitz, J. D. *Acc. Chem. Res*., **1983**, *16*, 153.

48. Marquart, M.; Walter, J.; Deisenhofer, J.; Bode, W.; Huber, R. *Acta Crystallogr.,* **1983**, *B39*, 480.

49. Chakrabarti, P.; Pal, D. *Protein Sci.*, **1997**, *6*, 851.

50. Venugopalan, P.; Venkatesan, K.; Klausen, J.; Novotny-Bregger, E.; Leumann, C.; Eschenmoser, A.; Dunitz, J. D. *Helv*. *Chim*. *Acta*, **1991**, *74*, 662.

51. Nishio, M.; Hirota, M.; Umezawa, Y. *The CH/π Interaction: Evidence, Nature and Consequences,* Wiley-VCH, New York, 1998.

52. Yamakawa, M.; Yamada, I.; Noyori, R. *Angew. Chem. Int. Ed. Engl*., **2001**, *40*, 2818.

53. Nishio, M. *Cryst. Engg. Comm*., **2004**, *6*, 130.

54. Boese, R.; Clark, T.; Gavezzotti, A. *Helv. Chim. Acta*, **2003**, *86*, 1085-1100.

55. Desiraju, G. R.; Steiner, T. *The Weak Hydrogen Bond in Structural Chemistry and Biology*, Oxford University Press Inc., New York, 1999.

56. Obata, T.; Shimo, T.; Yasutake, M.; Shinmyozu, T.; Kawaminami, M.; Yoshida, R.; Somekawa, K. *Tetrahedron*, **2001***, 57*, 1531.

57. Matsumoto, A.; Tanaka, T.; Tsubouchi, T.; Tashiro, K.; Saragai, S.; Nakamoto, S. *J. Am. Chem. Soc*., **2002**, *124*, 8891.

58. Matsumoto, A.; Sada, K.; Tashiro, K.; Miyata, M.; Tsubouchi, T.; Tanaka, T.; Odani, T.; Nagahama, S.; Tanaka, T.; Inoue, K.; Saragai, S.; Nakamoto, S. *Angew. Chem. Int. Ed. Engl.*, **2002**, *41*, 2502.

59. Nagahama, S.; Inoue, K.; Sada, K.; Miyata, M.; Matsumoto, A. *Cryst. Growth Des.*, **2003**, *3*, 247.

60. Fujimoto, D.; Tamura, R.; Lepp, Z.; Takashashi, H.; Ushio, T. *Cryst. Growth Des.*, **2003**, *3*, 973.

61. Tatko, C. D.; Waters, M. L. *J. Am. Chem. Soc.*, **2004**, *126*, 2028.

62. Brandl, M.; Weiss, M. S.; Jabs, A.; Suhnel, J.; Hilgenfeld, R. *J. Mol. Biol.*, **2001**, *307*, 357.

63. Umezawa, Y.; Tsuboyama, S.; Honda, K.; Uzawa, J. Nishio, M. *Bull. Chem. Soc. Jpn*., **1998**, *71*, 1207.

64. Umezawa, Y.; Tsuboyama, S.; Takahashi, H.; Uzawa, J.; Nishio, M. *Tetrahedron*, **1999**, *55*, 10047.

65. Corey, E. J.; Rhode, J. J.; Fischer, A.; Azimioara, M. D. *Tetrahedron Lett.*, **1997**, *38*, 33.

66. Corey, E. J.; Rohde, J. J. *Tetrahedron Lett.*, **1997**, *38*, 37.

67. Washington, I.; Houk, K. N. *Angew. Chem. Int. Ed. Engl.*, **2001**, *40*, 4485.

68. Sukenik, C. N.; Bonapace, J. A. P.; Mandel, N. S.; Lau, P-Y.; Wood, G.; Bergman, R. G. *J. Am. Chem. Soc.*, **1977**, *99*, 851.

69. Tang, C. P.; Chang, H. C.; Popovitz-Biro, R.; Frolow, F.; Lahav, M.; Leiserowitz, L.; McMullan, R. K. *J. Am. Chem. Soc.*, **1985**, *107*, 4058.

70. Jones, W.; Thomas, J. M. *Proc. Ind. Natl. Sci. Acad. Part A*, **1986**, *52*, 363.

71. Chang, H. C.; Popovitz-Biro, R.; Lahav, M.; Leiserowitz, L. *J. Am. Chem. Soc*., **1987**, *109*, 3883.

72. Weisinger-Lewin, Y.; Vaida, M.; Popovitz-Biro, R.; Chang, H. C.; Manning, F.; Frolow, F.; Lahav, M.; Leiserowitz, L. *Tetrahedron*, **1987**, *43*, 1449.

73. Sarma, J. A. R. P.; Duntiz, J. D. *Acta Crystallogr.*, **1990**, *B46*, 780.

74. Vyas, K.; Manohar, H.; Venkatesan, K. *J. Phys. Chem.*, **1990**, *94*, 6069.

75. Enkelmann, V.; Wegner, G.; Novak, K.; Wagener, K. B. *J. Am. Chem. Soc*., **1993**, *115*, 10390.

76. Dunitz, J. D. *Acta Crystallogr.*, **1995**, *B51*, 619.

77. Kaftory M. in *Organic Solid State Reaction*, (Ed.: F. Toda), Kluwar Academic Publishers, UK, 2002, p. 47.

78. Kim, J. H.; Hubig, S. M.; Lindeman, S. V.; Kochi, J. K. *J. Am. Chem. Soc*., **2001**, *123*, 87.

79. Perrin, D. D.; Armarego, L. F. *Purification of Laboratory Chemicals*, Pergamon Press, Oxford, UK, 1992.

80. Gerlach, H.; Kappes, D.; Boeckman, R. K. Jr.; Maw, G. N. *Org. Synth.*, **1993**, *71*, 48.

81. SHELX-97, Sheldrick, G. M. SHELX97, Program for crystal structure solution and refinement, University of Göttingen, Germany, 1997.

82. Burnett, M. N.; Johnson, C. K. ORTEP III, report ORNL- 6895, Oak Ridge National Laboratory, Tennesse, U.S.A., 1996.

83. Billington, D. C.; Baker, R.; Kulagowski, J. J.; Mawer, I. M.; Vacca, J. P.; deSolmes, S. J.; Huff, J. R. *J. Chem. Soc., Perkin Trans. 1*, **1989**, 1423.

84. Chung, S-K.; Chang, Y-T.; Sohn, K-H. *Korean J. Med. Chem*., **1994**, *4*, 57.

85. *Merck Index*, *12*, 1122.

A2.7. Appendix

Appendix index Page No

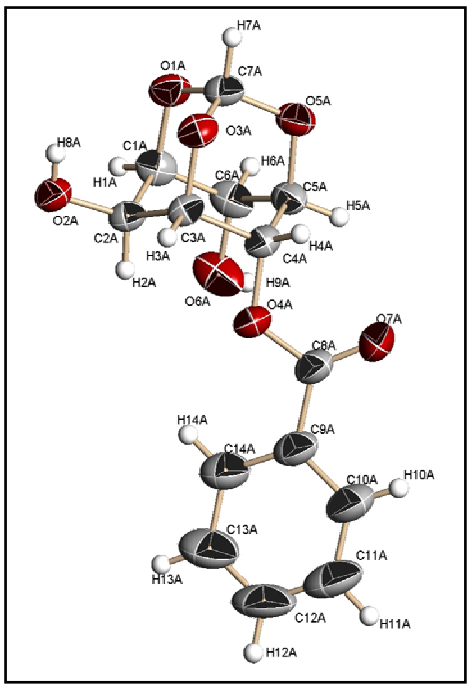

ORTEP of **A2.25**

Crystal data table of **A2.25**

Identification code	**A2.25** (crystallized from chloroform-light petroleum mixture)
Empirical formula	$C_{14}H_{14}O_7$
Formula weight	294.25
Temperature	566(2) K
Wavelength	0.71073Å
Crystal system, space group	Monoclinic, $P2_1/c$
Unit cell dimensions	a = 13.386(2)Å; α = 90º b = 10.4850(15)Å; β = 103.952(2)º c = 10.0238(15)Å; γ = 90º
Volume	1365.4(3) $Å^3$
Z, Calculated density	4, 1.431 Mg/m^3
Absorption coefficient	0.116 mm^{-1}
F(000)	616
Crystal size	0.31 × 0.17 × 0.06 mm
θ range for data collection	2.50 to 24.99º
Limiting indices	-14<=h<=15; -12<=k<=6; -11<=l<=11.
Reflections collected / unique	6617 / 2390 [R(int) = 0.0874]
Completeness to θ = 24.99	99.5%
Max. and min. transmission	0.9933 and 0.9647
Refinement method	Full-matrix least-squares on F^2
Data / restraints / parameters	2390 / 0 / 193
Goodness-of-fit on F^2	1.080
Final R indices [I>2σ (I)]	R1 = 0.0607, wR2 = 0.1728
R indices (all data)	R1 = 0.0676, wR2 = 0.1828
Extinction coefficient	0.050(9)
Largest diff. peak and hole (ρ_{max} & ρ_{min})	0.330 and -0.314 e. $Å^{-3}$

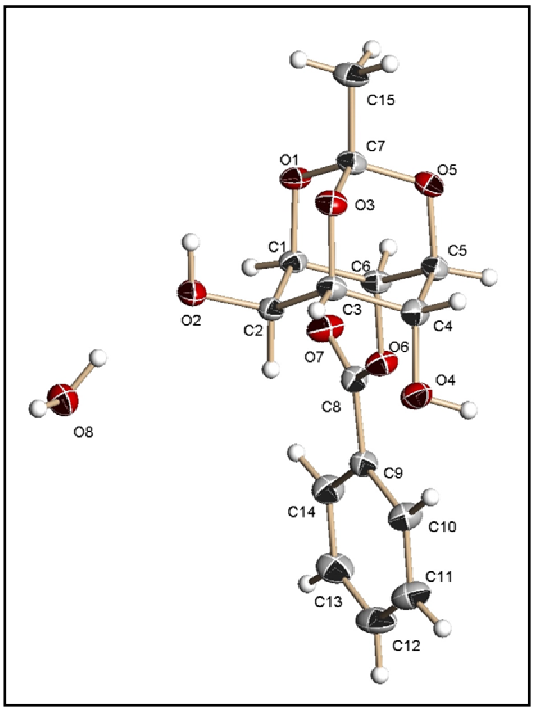

ORTEP of **A2.27**

Crystal data table of **A2.27**

Identification code	**A2.27** (crystallized from chloroform-light petroleum mixture)
Empirical formula	$C_{15}H_{17}O_{7.50}$
Formula weight	317.29
Temperature	568(2) K
Wavelength	0.71073Å
Crystal system, space group	Monoclinic, C2/c
Unit cell dimensions	a = 17.710(4) Å; α = 90° b = 11.774(2) Å; β = 120.339(3)° c = 16.174(3) Å; γ = 90°
Volume	2910.6(10) $Å^3$
Z, Calculated density	8, 1.448 Mg/m^3
Absorption coefficient	0.117 mm^{-1}
F(000)	1336
Crystal size	0.89 × 0.38 × 0.34 mm
θ range for data collection	2.18 to 25.00°
Limiting indices	-21<=h<=12; -13<=k<=14; -19<=l<=19.
Reflections collected / unique	6948 / 2549 [R(int) = 0.0485]
Completeness to θ = 25.00	99.4%
Max. and min. transmission	0.9608 and 0.9031
Refinement method	Full-matrix least-squares on F^2
Data / restraints / parameters	2549 / 0 / 273
Goodness-of-fit on F^2	1.037
Final R indices [I>2σ (I)]	R1 = 0.0498, wR2 = 0.1311
R indices (all data)	R1 = 0.0585, wR2 = 0.1412
Extinction coefficient	0.0011(5)
Largest diff. peak and hole (ρ_{max} & ρ_{min})	0.276 and -0.276 $e.Å^{-3}$

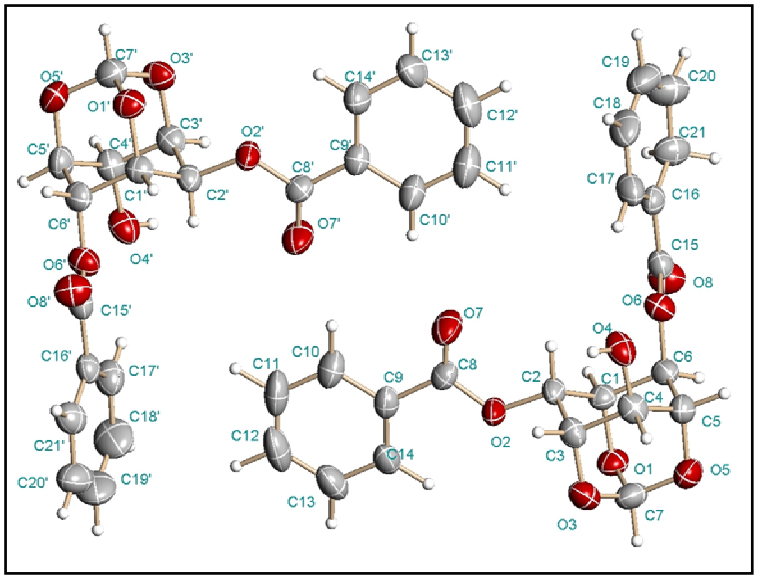

ORTEP of **A2.33**

Crystal data table of **A2.33** (at 60 ºC)

Identification code	**A2.33** (crystallized from chloroform-light petroleum mixture)
Empirical formula	$C_{21}H_{18}O_8$
Formula weight	398.35
Temperature	333(2) K
Wavelength	0.71073 Å
Crystal system, space group	Monoclinic, $P2_1/c$
Unit cell dimensions	a = 16.934(3) Å; α = 90º b = 9.886(2) Å; β = 90.60(3)º c = 22.723(5) Å; γ = 90º
Volume	3803.8(13) $Å^3$
Z, Calculated density	8, 1.391 Mg/m^3
Absorption coefficient	0.108 mm^{-1}
F(000)	1664
Crystal size	0.51 × 0.35 × 0.11 mm
θ range for data collection	1.20 to 25.00º
Limiting indices	-20<=h<=20; -9<=k<=11; -16<=l<=26
Reflections collected / unique	9490 / 5380 [R(int) = 0.0639]
Completeness to θ = 25.00	80.3 %
Max. and min. transmission	0.9882 and 0.9471
Refinement method	Full-matrix least-squares on F^2
Data / restraints / parameters	5380 / 0 / 525
Goodness-of-fit on F^2	0.998
Final R indices [I>2σ (I)]	R1 = 0.0975, wR2 = 0.2670
R indices (all data)	R1 = 0.1793, wR2 = 0.3520
Largest diff. peak and hole (ρ_{max} & ρ_{min})	0.360 and -0.352 e. $Å^{-3}$

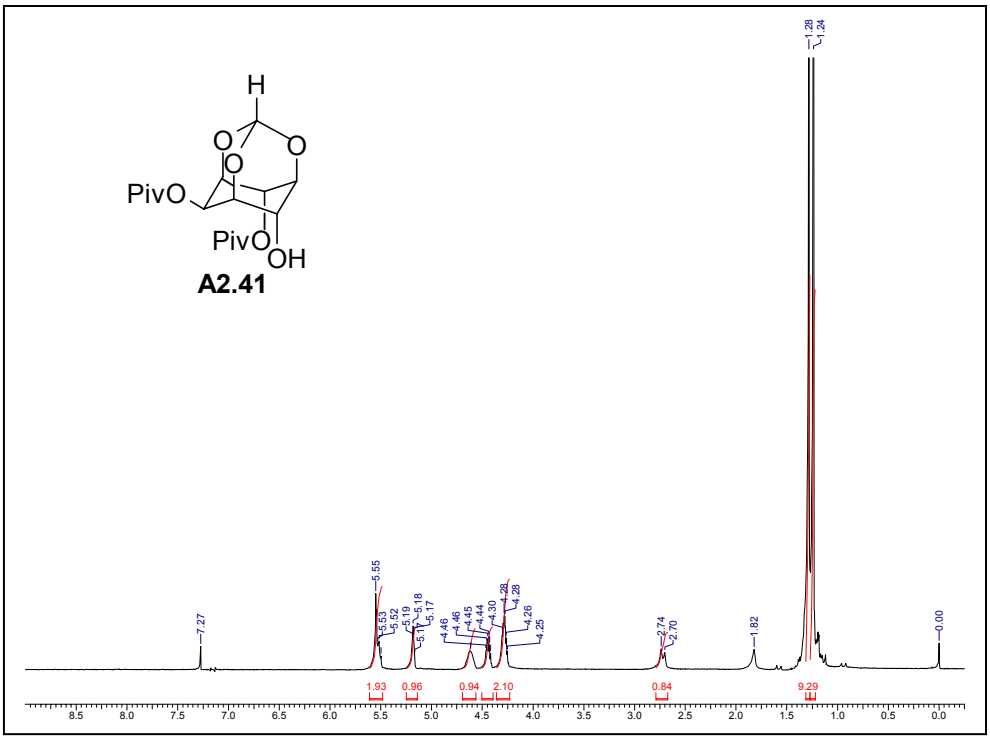
H
O
O
O
O
PivO
PivO
OH
A2.41

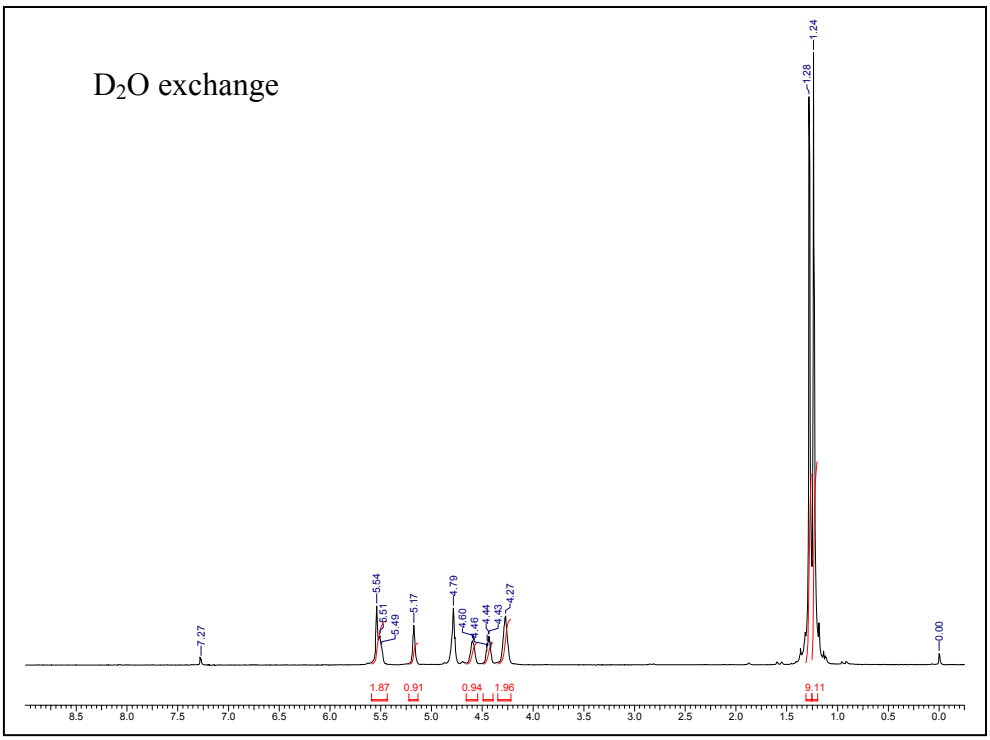
D2O exchange

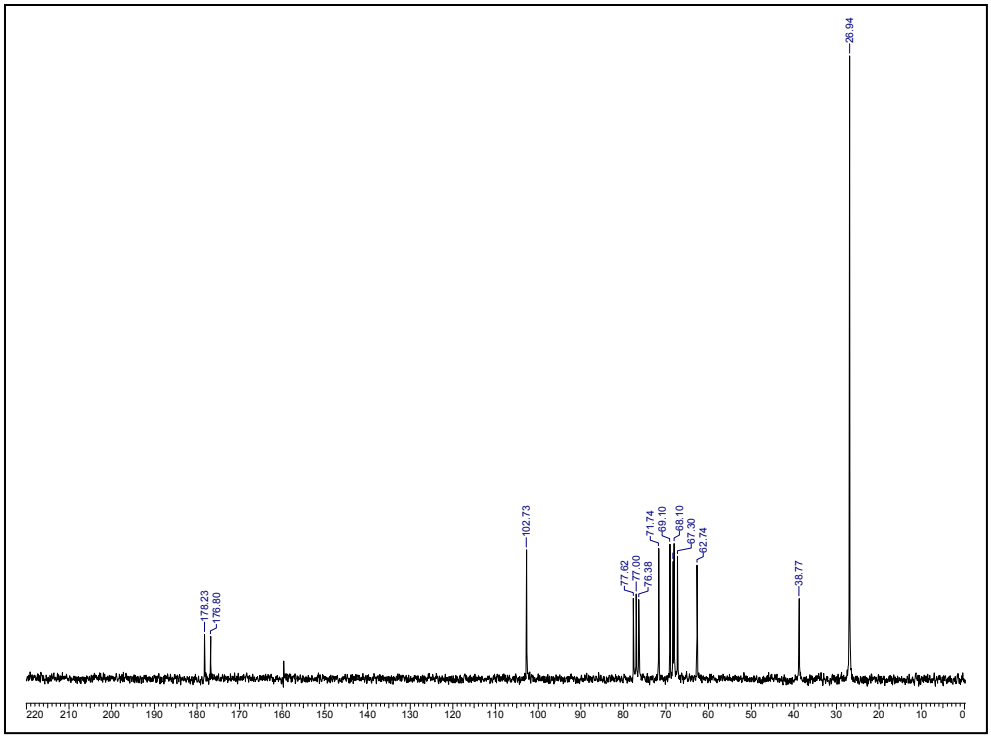
26.94
102.73
71.74
69.10
68.10
67.30
62.74
77.62
77.00
76.38
38.77
178.23
176.80
220 210 200 190 180 170 160 150 140 130 120 110 100 90 80 70 60 50 40 30 20 10 0

DEPT

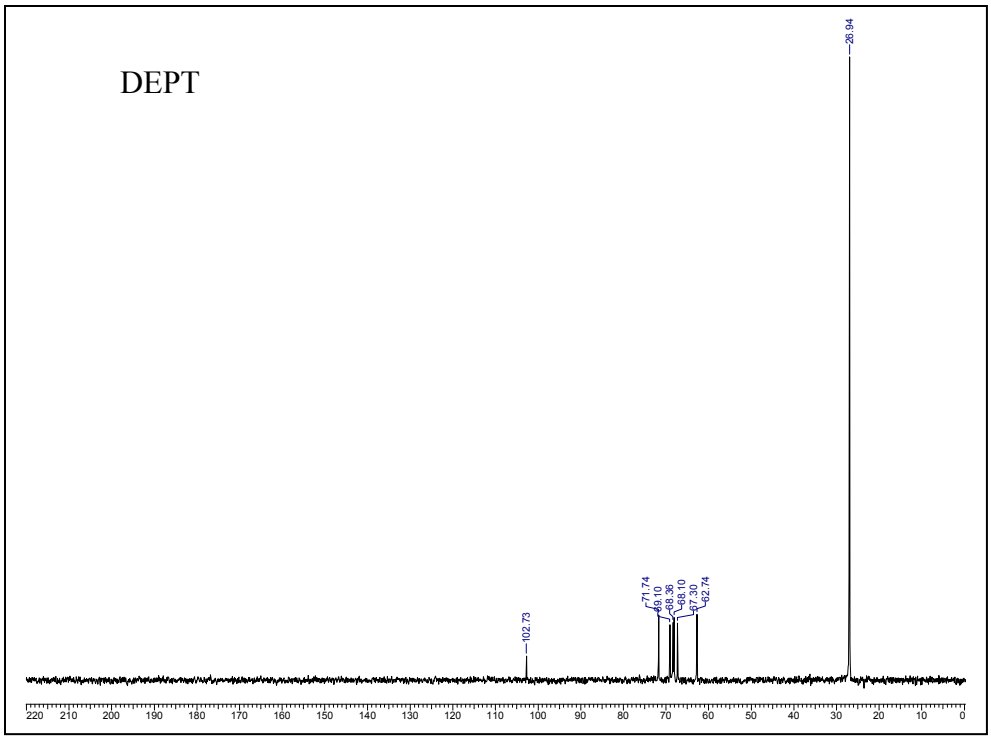
26.94
71.74
69.10
68.36
68.10
67.30
62.74
102.73
220 210 200 190 180 170 160 150 140 130 120 110 100 90 80 70 60 50 40 30 20 10 0

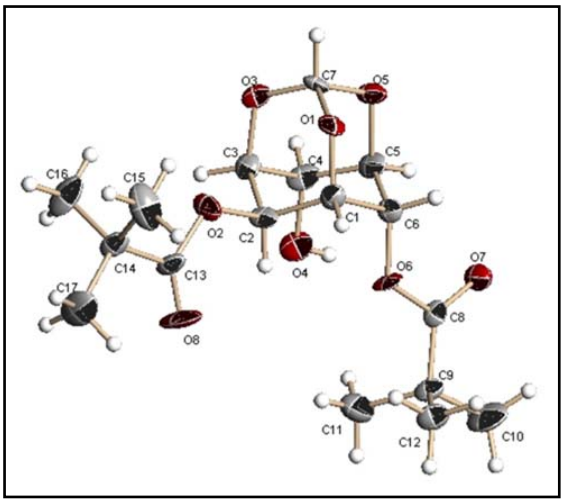

ORTEP of **A2.41**

Crystal data table of **A2.41**

Identification code	**A2.41** (crystallized from chloroform-light petroleum mixture)
Empirical formula	$C_{17}H_{26}O_8$
Formula weight	358.38
Temperature	293(2) K
Wavelength	0.71073 Å
Crystal system, space group	Orthorhombic, *P*na2$_1$
Unit cell dimensions	a = 21.733(8) Å; α = 90° b = 6.049(2) Å; β = 90° c = 28.624(11) Å; γ = 90°
Volume	3763(2) Å^3
Z, Calculated density	8, 1.265 Mg/m^3
Absorption coefficient	0.100 mm^{-1}
F(000)	1536
Crystal size	0.88 × 0.09 × 0.08 mm
θ range for data collection	1.42 to 25.00°
Limiting indices	-24<=h<=25; -7<=k<=5; -34<=l<=32.
Reflections collected / unique	17137 / 6117 [R(int) = 0.0983]
Completeness to θ = 25.00	99.6 %
Max. and min. transmission	0.9918 and 0.9173
Refinement method	Full-matrix least-squares on F^2
Data / restraints / parameters	6117 / 1 / 465
Goodness-of-fit on F^2	1.056
Final R indices [I>2σ (I)]	R1 = 0.0927, wR2 = 0.2021
R indices (all data)	R1 = 0.1553, wR2 = 0.2373
Largest diff. peak and hole (ρ_{max} & ρ_{min})	0.502 and -0.300 e. Å^{-3}

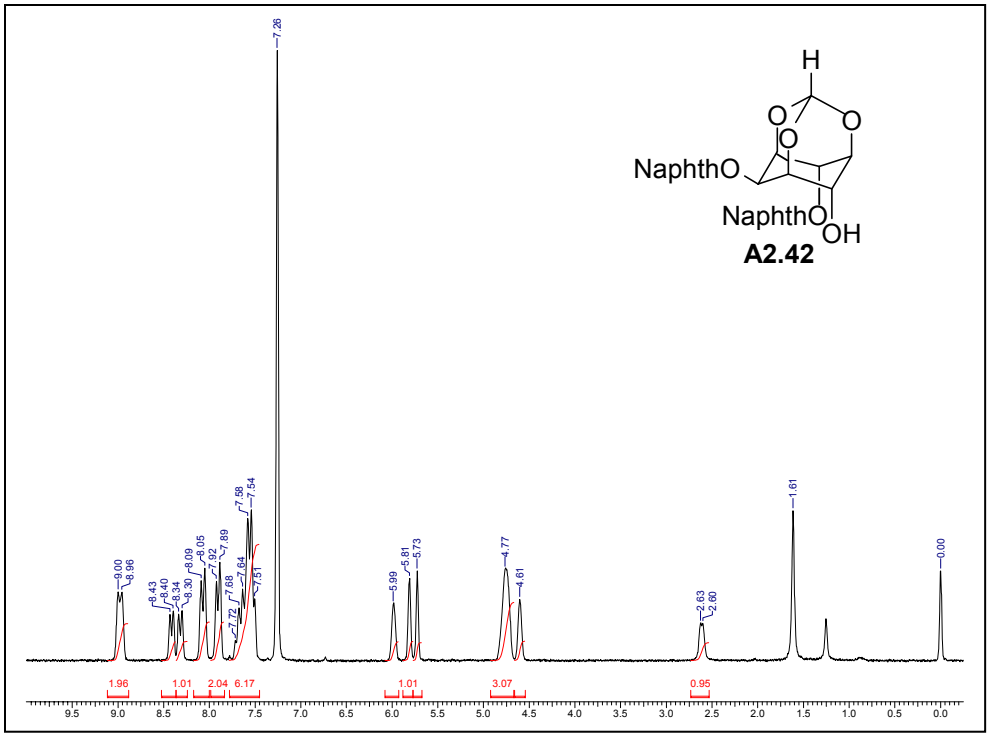
H
O
O
O
NaphthO
NaphthO
OH
A2.42

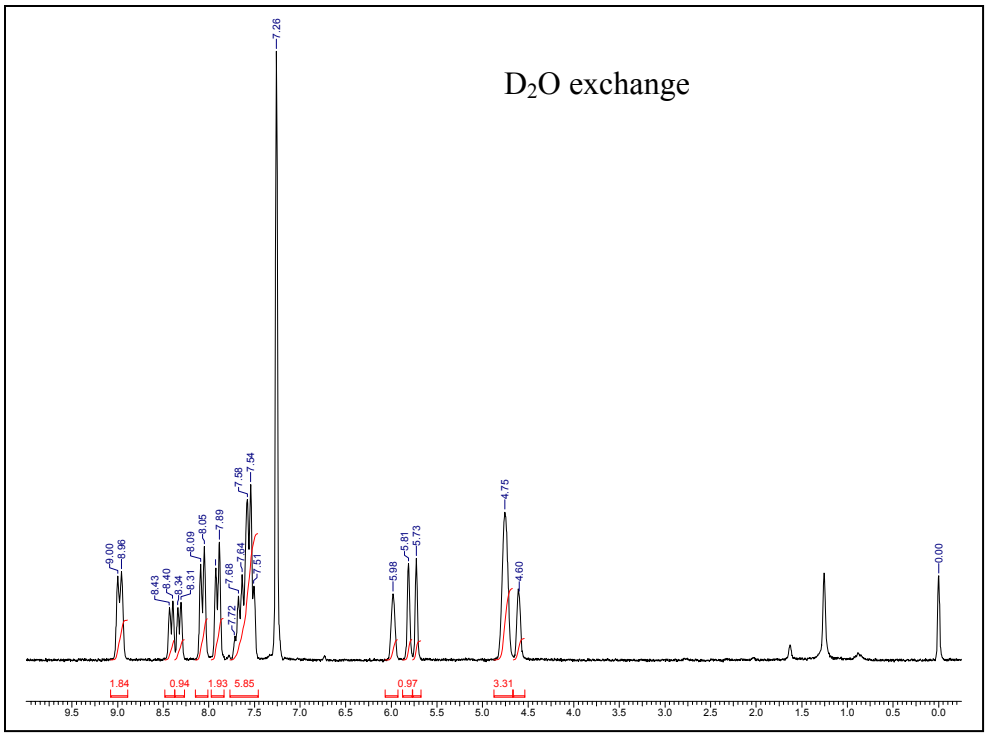
D2O exchange

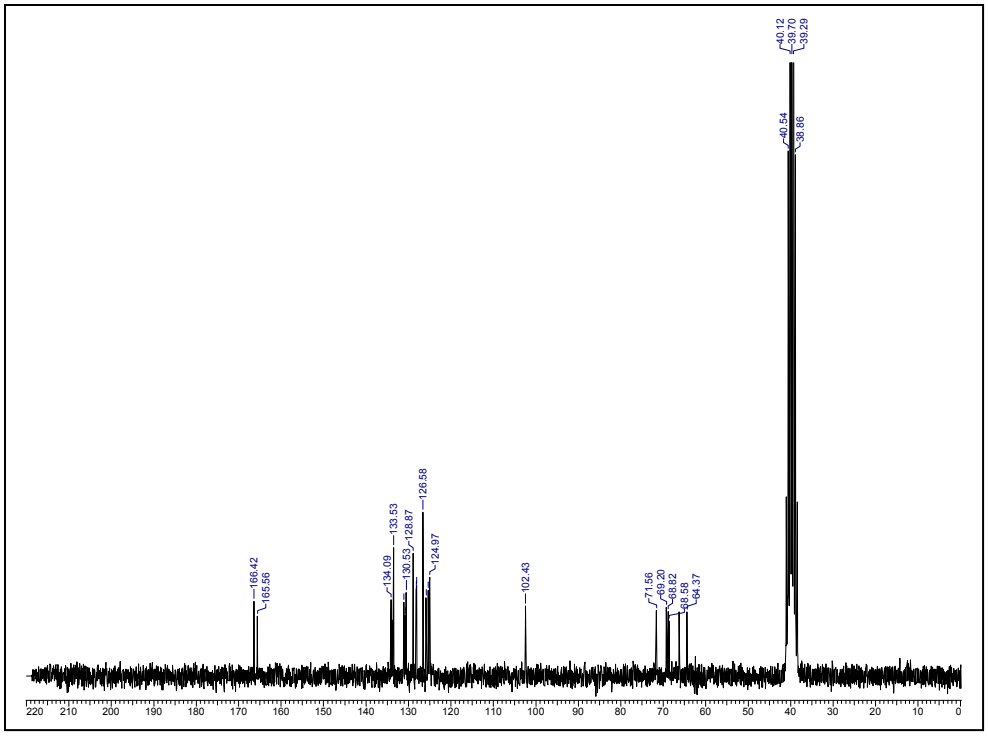
40.12
39.70
39.29
40.54
38.86
166.42
165.56
134.09
133.53
130.53
128.87
126.58
124.97
102.43
71.56
69.20
68.82
68.58
64.37
220 210 200 190 180 170 160 150 140 130 120 110 100 90 80 70 60 50 40 30 20 10 0

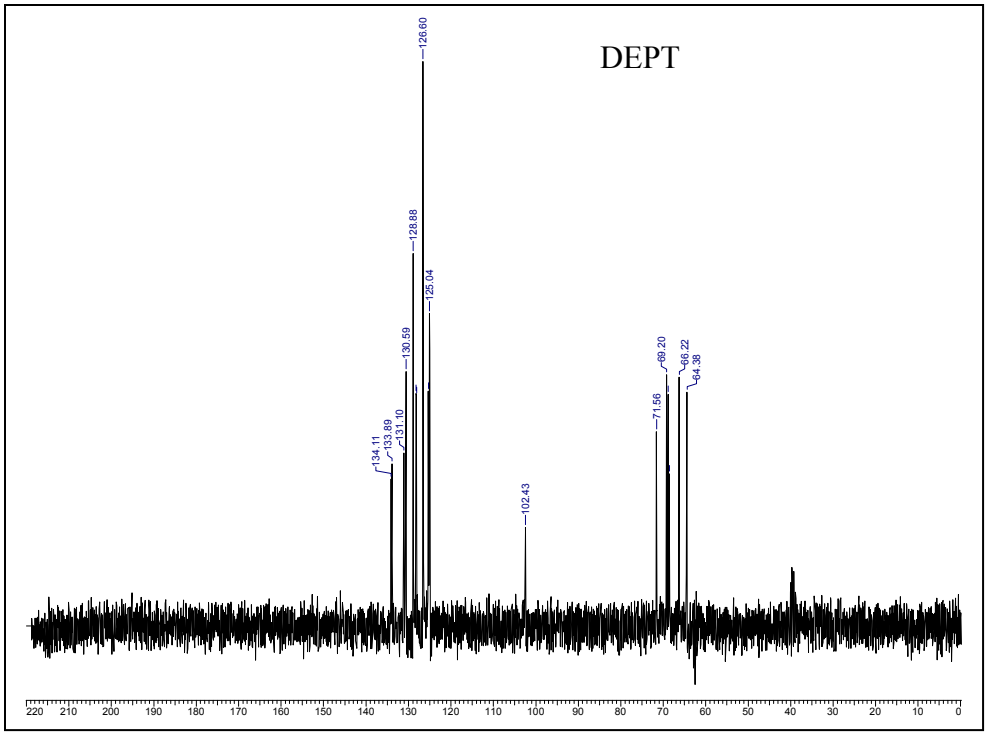
DEPT
126.60
128.88
125.04
130.59
134.11
133.89
131.10
102.43
71.56
69.20
66.22
64.38
220 210 200 190 180 170 160 150 140 130 120 110 100 90 80 70 60 50 40 30 20 10 0

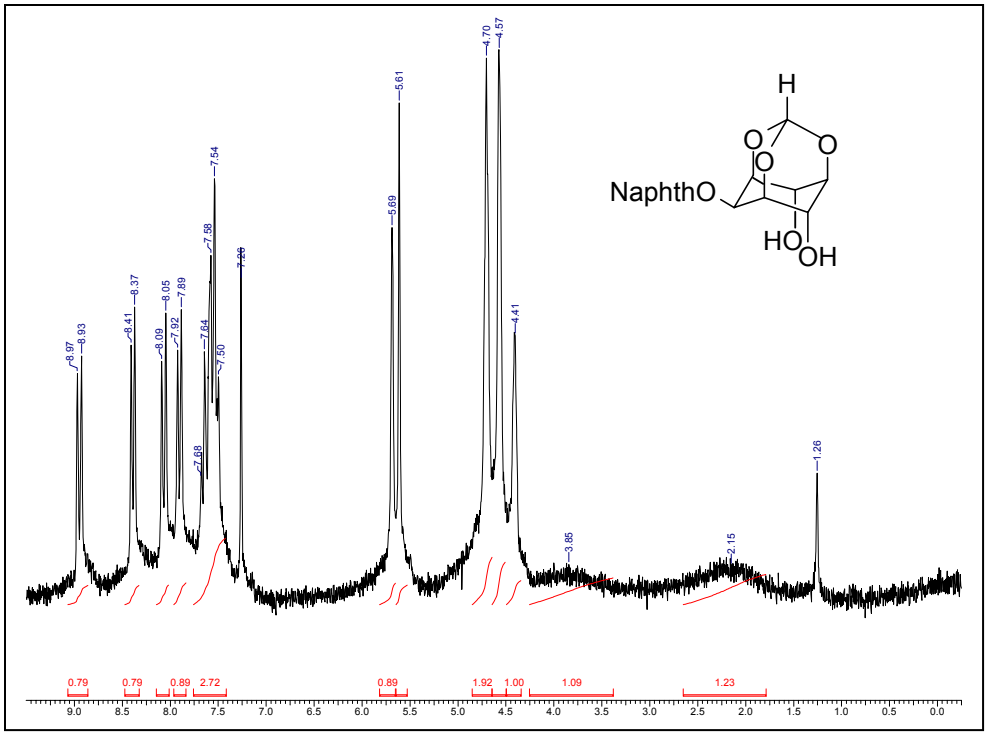
H
O
O
O
NaphthO
HO
OH
8.97
8.93
8.41
8.37
8.09
8.05
7.92
7.89
7.68
7.64
7.54
7.50
5.69
5.61
4.70
4.57
4.41
3.85
2.15
1.26
0.79
0.79
0.89
2.72
0.89
1.92
1.00
1.09
1.23

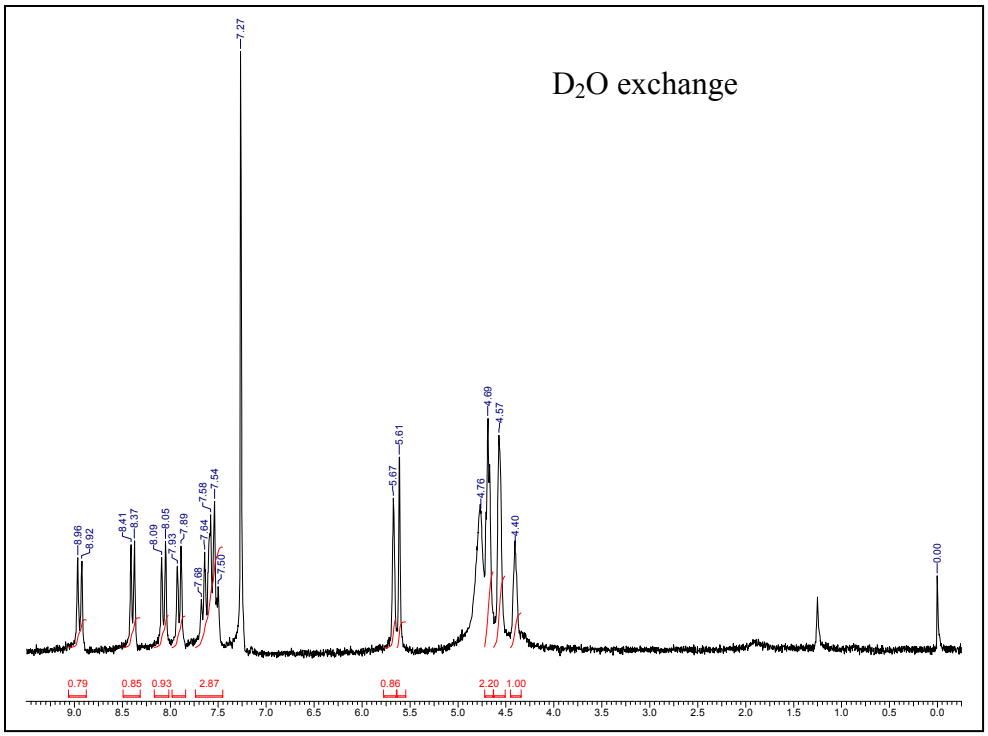
D2O exchange
7.27
8.96
8.92
8.41
8.37
8.09
8.05
7.83
7.89
7.68
7.64
7.58
7.54
7.50
5.67
5.61
4.69
4.57
4.76
4.40
0.00
0.79
0.85
0.93
2.87
0.86
2.20
1.00

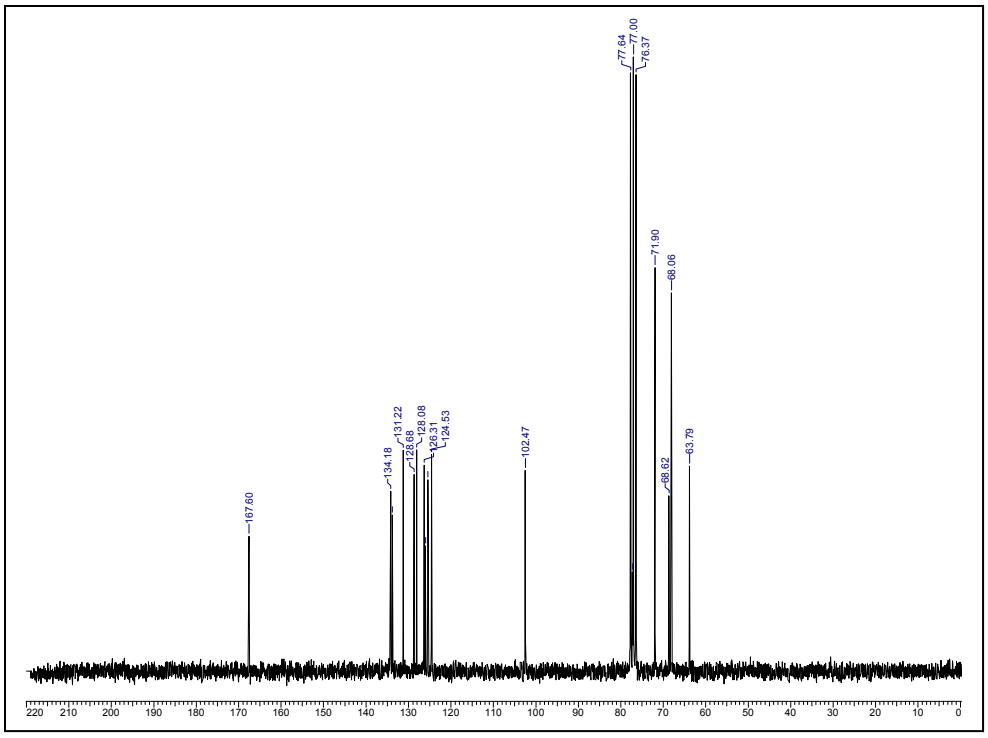
77.64
77.00
76.37
71.90
68.06
131.22
128.68
128.08
126.31
124.53
134.18
102.47
68.62
63.79
167.60
220 210 200 190 180 170 160 150 140 130 120 110 100 90 80 70 60 50 40 30 20 10 0

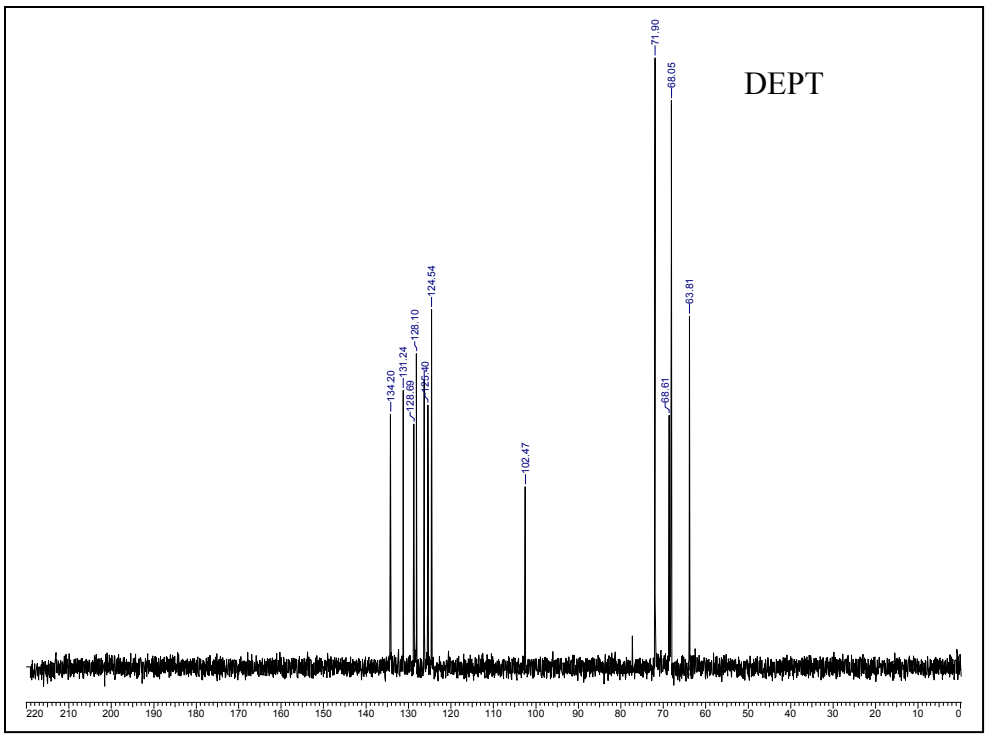
DEPT
71.90
68.05
124.54
63.81
128.10
131.24
134.20
128.69
125.40
68.61
102.47
220 210 200 190 180 170 160 150 140 130 120 110 100 90 80 70 60 50 40 30 20 10 0

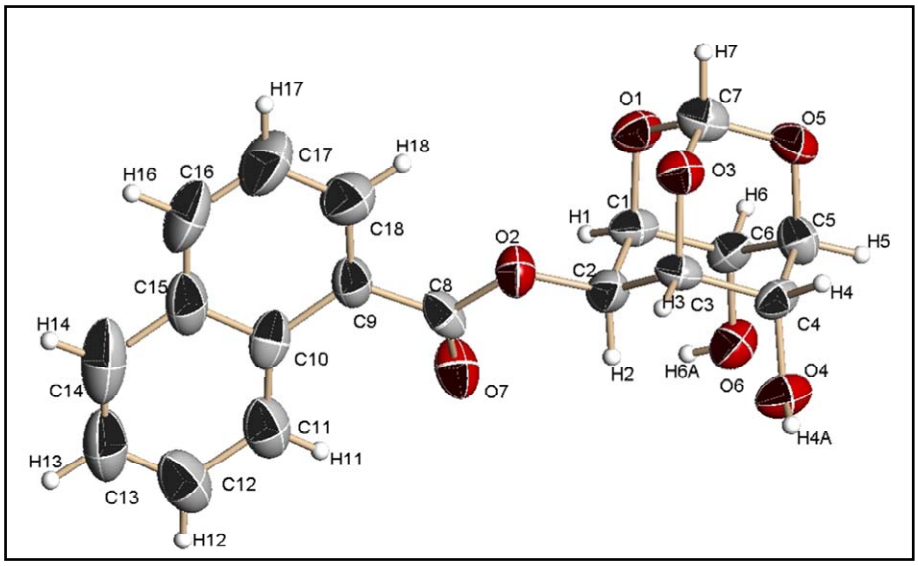

ORTEP of 2-*O*-[1-naphthoyl]-*myo*-inositol 1,3,5-orthoformate

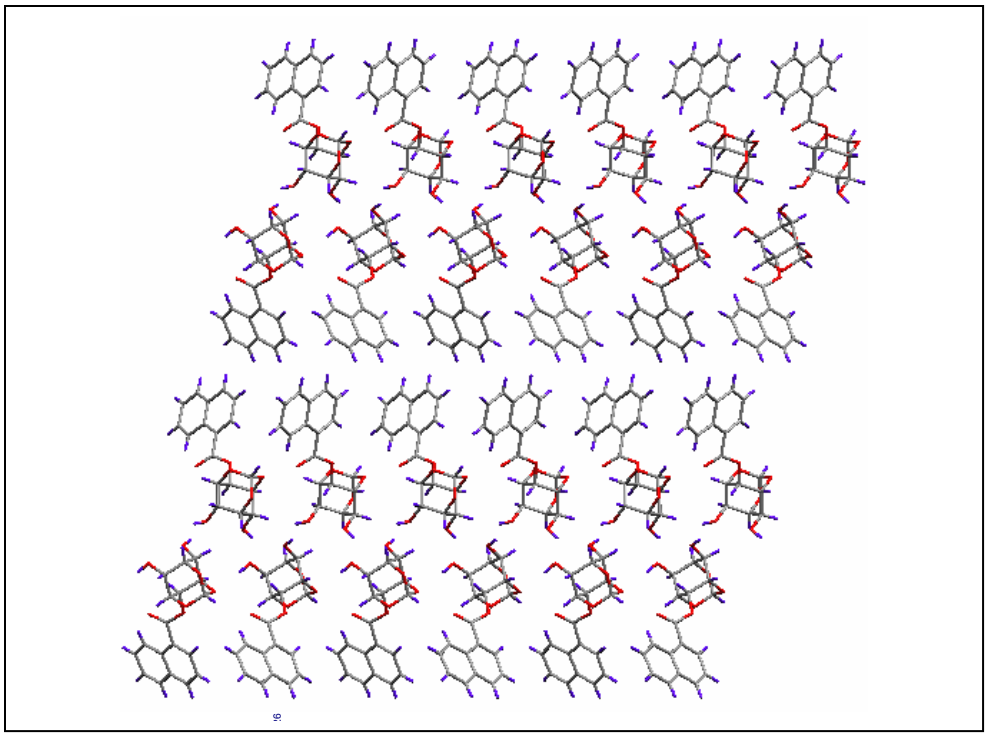

Packing of 2-*O*-[1-naphthoyl]-*myo*-inositol 1,3,5-orthoformate down the b-axis

Crystal data table of 2-*O*-[1-naphthoyl]-*myo*-inositol 1,3,5-orthoformate

Identification code	2-*O*-[1-naphthoyl]-*myo*-inositol 1,3,5-orthoformate (crystallized from chloroform-light petroleum mixture)
Empirical formula	$C_{18}H_{16}O_7$
Formula weight	344.31
Temperature	566(2) K
Wavelength	0.71073 Å
Crystal system, space group	Moniclinic, Cc
Unit cell dimensions	a = 43.06(6) Å; α = 90° b = 5.976(7) Å; β = 104.65(4)° c = 12.642(17) Å; γ = 90°
Volume	3147(7) $Å^3$
Z, Calculated density	8, 1.453 Mg/m^3
Absorption coefficient	0.113 mm^{-1}
F(000)	1440
Crystal size	0.56 x 0.12 x 0.03 mm
θ range for data collection	2.93 to 25.00°
Limiting indices	-50<=h<=50; -7<=k<=4; -15<=l<=10.
Reflections collected / unique	7098 / 4610 [R(int) = 0.0880]
Completeness to θ = 25.00	98.6 %
Max. and min. transmission	0.9966 and 0.9394
Refinement method	Full-matrix least-squares on F^2
Data / restraints / parameters	4610 / 2 / 455
Goodness-of-fit on F^2	1.008
Final R indices [I>2σ (I)]	R1 = 0.0716, wR2 = 0.1342
R indices (all data)	R1 = 0.1289, wR2 = 0.1587
Largest diff. peak and hole (ρ_{max} & ρ_{min})	0.228 and -0.204 e. $Å^{-3}$

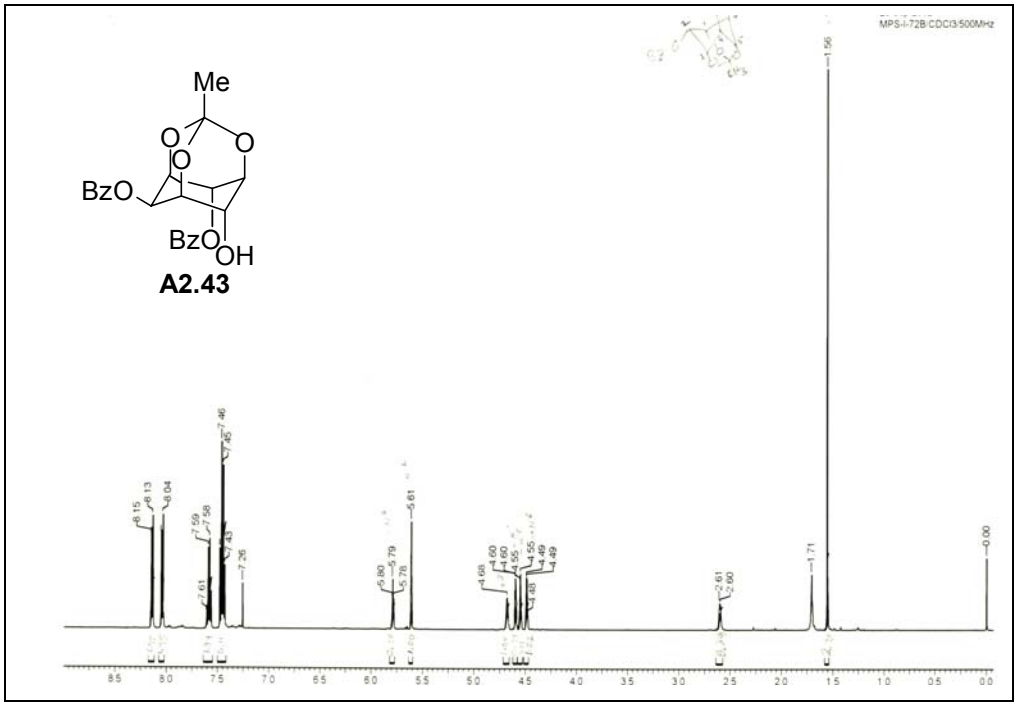
Me
O
O
O
BzO
BzO
OH
A2.43

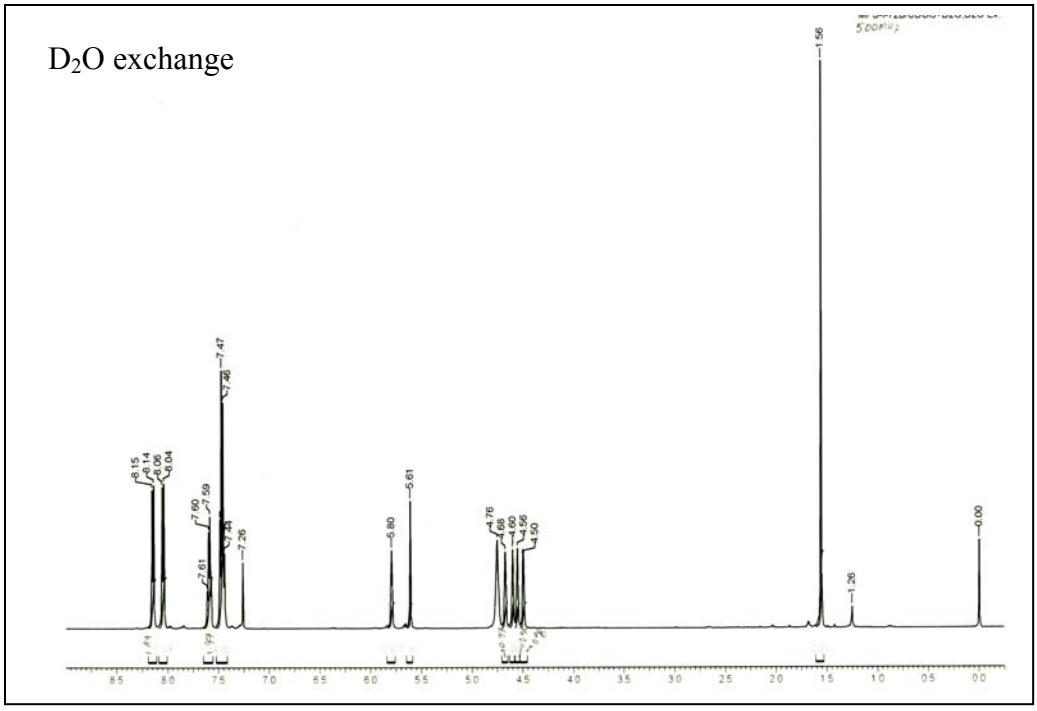
D2O exchange

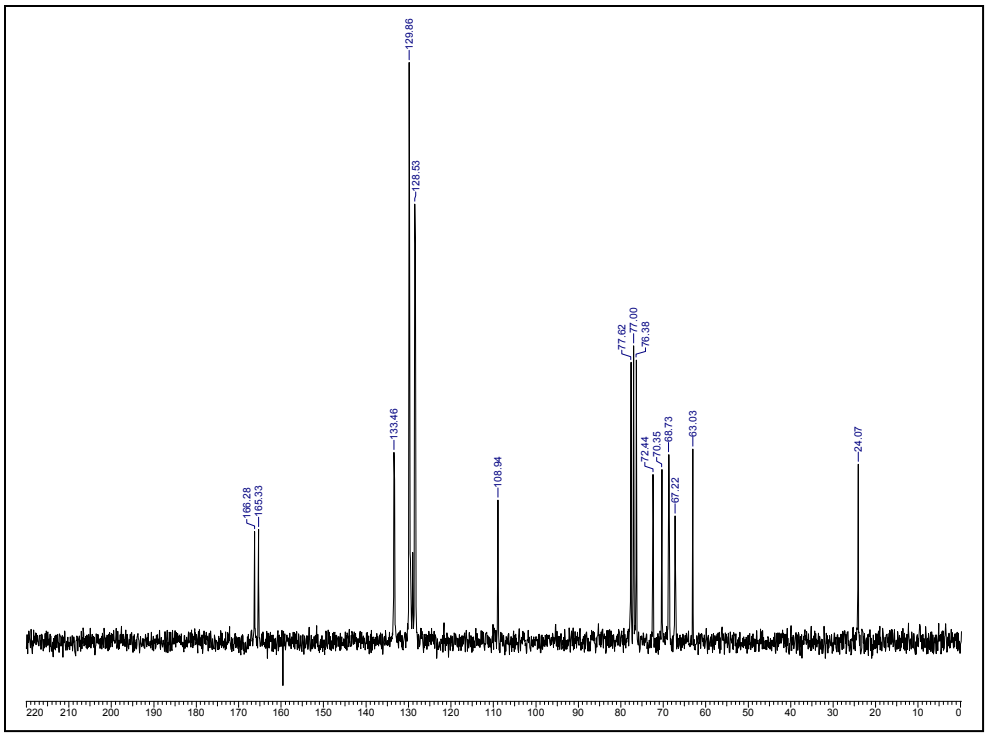
129.86
128.53
77.62
77.00
76.38
133.46
72.44
70.35
68.73
63.03
24.07
108.94
67.22
166.28
165.33
220 210 200 190 180 170 160 150 140 130 120 110 100 90 80 70 60 50 40 30 20 10 0

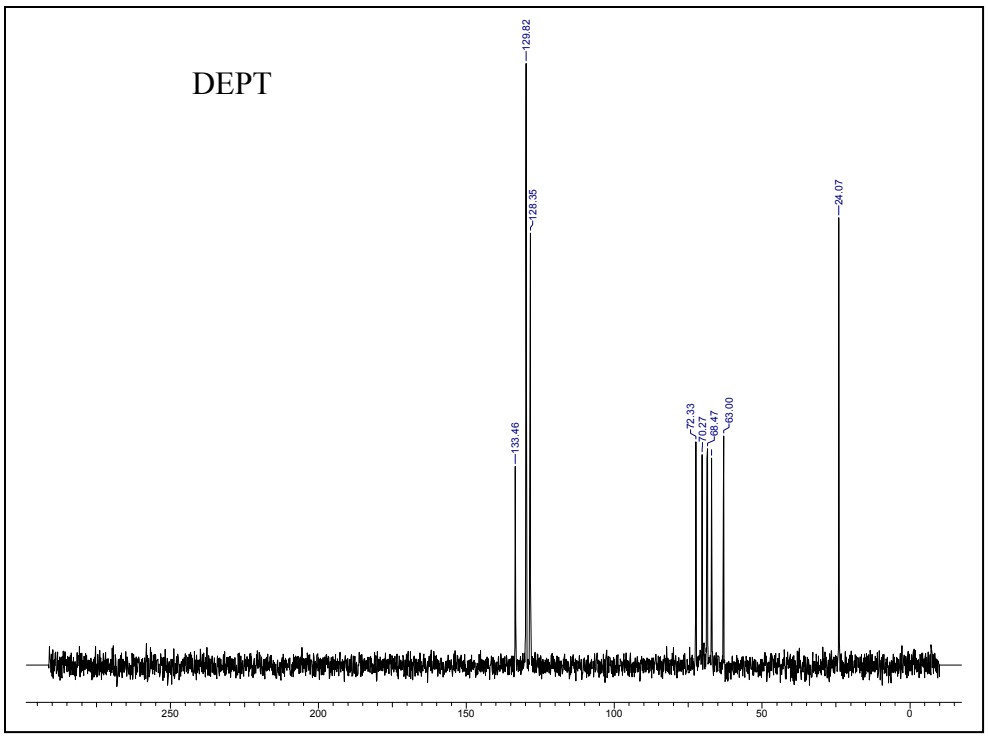
DEPT
129.82
128.35
24.07
133.46
72.33
70.27
68.47
63.00
250 200 150 100 50 0

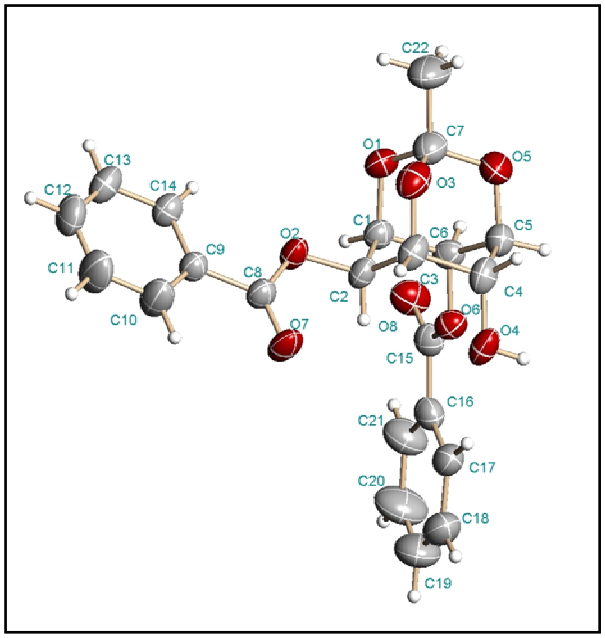

ORTEP of **A2.43**

Crystal data table of **A2.43**

Identification code	**A2.43** (crystallized from chloroform-light petroleum mixture)
Empirical formula	$C_{22}H_{20}O_8$
Formula weight	412.38
Temperature	293(2) K
Wavelength	0.71073 Å
Crystal system, space group	Monoclinic, $P2_1/n$
Unit cell dimensions	a = 13.592(6) Å; α = 90º b = 9.677(4) Å; β = 97.762(7)º c = 15.298(6) Å; γ = 90º
Volume	1993.7(14) $Å^3$
Z, Calculated density	4, 1.374 Mg/m^3
Absorption coefficient	0.105 mm^{-1}
F(000)	864
Crystal size	0.75 ×0.50 × 0.17 mm
θ range for data collection	2.15 to 25.00º
Limiting indices	-10<=h<=16; -11<=k<=11; -18<=l<=18
Reflections collected / unique	9736 / 3513 [R(int) = 0.0472]
Completeness to θ = 25.00	99.8 %
Max. and min. transmission	0.9820 and 0.9250
Refinement method	Full-matrix least-squares on F^2
Data / restraints / parameters	3513 / 0 / 352
Goodness-of-fit on F^2	1.046
Final R indices [I>2σ (I)]	R1 = 0.0457, wR2 = 0.1229
R indices (all data)	R1 = 0.0562, wR2 = 0.1320
Extinction coefficient	0.012(2)
Largest diff. peak and hole (ρ_{max} & ρ_{min})	0.175 and -0.166 e. $Å^{-3}$

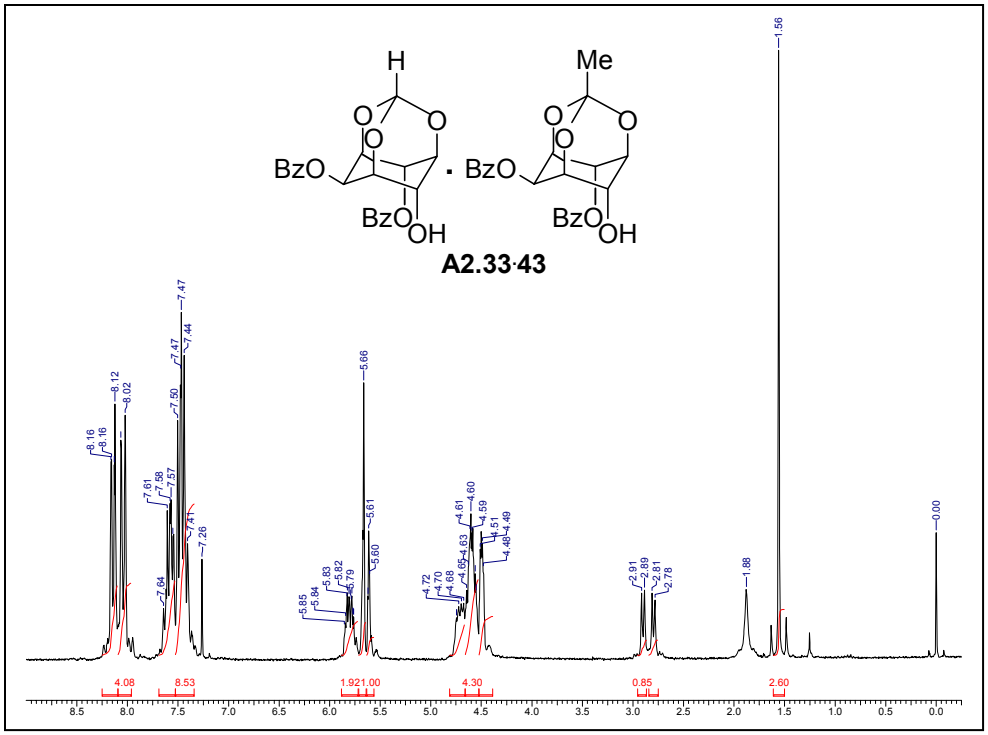
H
Me
BzO
BzO
OH
BzO
BzO
OH
A2.33·43

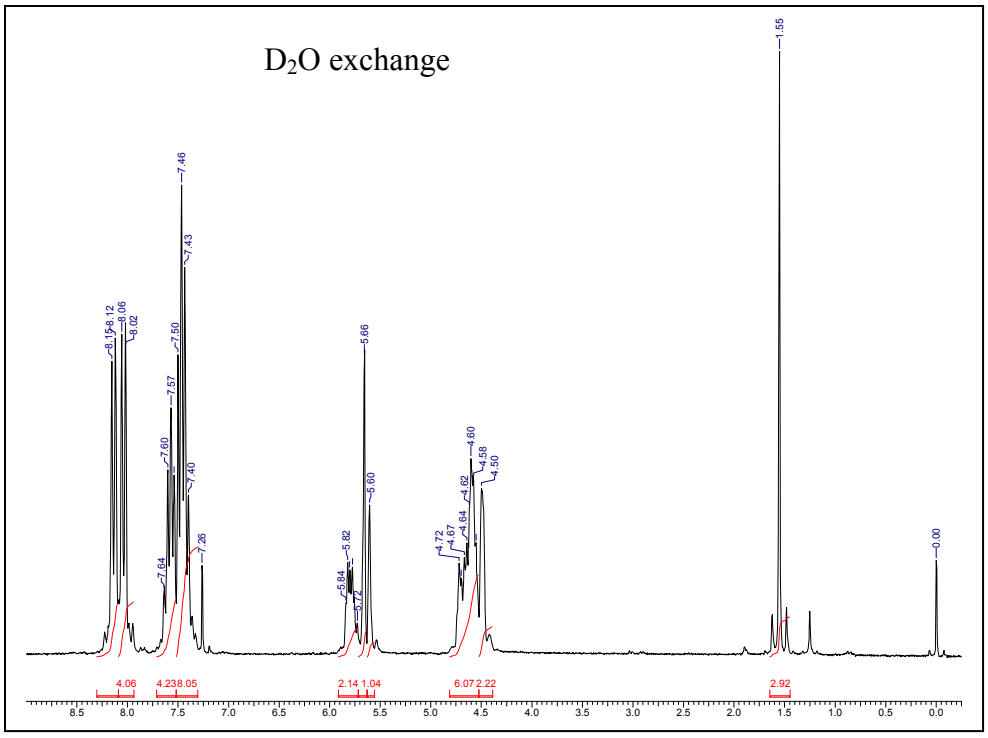
D2O exchange

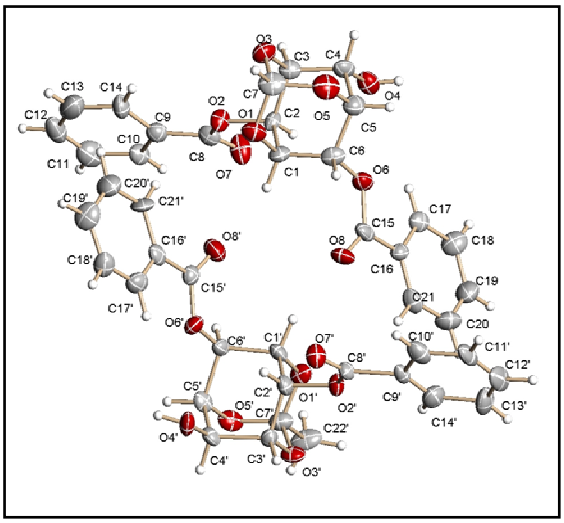

ORTEP of **A2.33·43**

Crystal data table of **A2.33·43**

Identification code	**A2. 33·43**
Empirical formula	$C_{43}H_{38}O_{16}$
Formula weight	810.73
Temperature	293(2) K
Wavelength	0.71073 Å
Crystal system, space group	Monoclinic, *Cc*
Unit cell dimensions	a = 27.291(9) Å; α = 90º b = 9.483(3) Å; β = 116.944(5)º c = 16.880(5) Å; γ = 90º
Volume	3894(2) $Å^3$
Z, Calculated density	4, 1.383 Mg/m^3
Absorption coefficient	0.107 mm^{-1}
F(000)	1696
Crystal size	0.58 × 0.24 × 0.18 mm
θ range for data collections	1.67 to 25.00º
Limiting indices	-32<=h<=32; -11<=k<=11; -20<=l<=20.
Reflections collected / unique	17787 / 6835 [R(int) = 0.0305]
Completeness to θ = 25.00	99.9 %
Max. and min. transmission	0.9807 and 0.9407
Refinement method	Full-matrix least-squares on F^2
Data / restraints / parameters	6835 / 2 / 535
Goodness-of-fit on F^2	1.059
Final R indices [I>2σ (I)]	R1 = 0.0506, wR2 = 0.1191
R indices (all data)	R1 = 0.0670, wR2 = 0.1292
Absolute structure parameter	0.9(13)
Largest diff. peak and hole (ρ_{max} & ρ_{min})	0.357 and -0.180 e. $Å^{-3}$

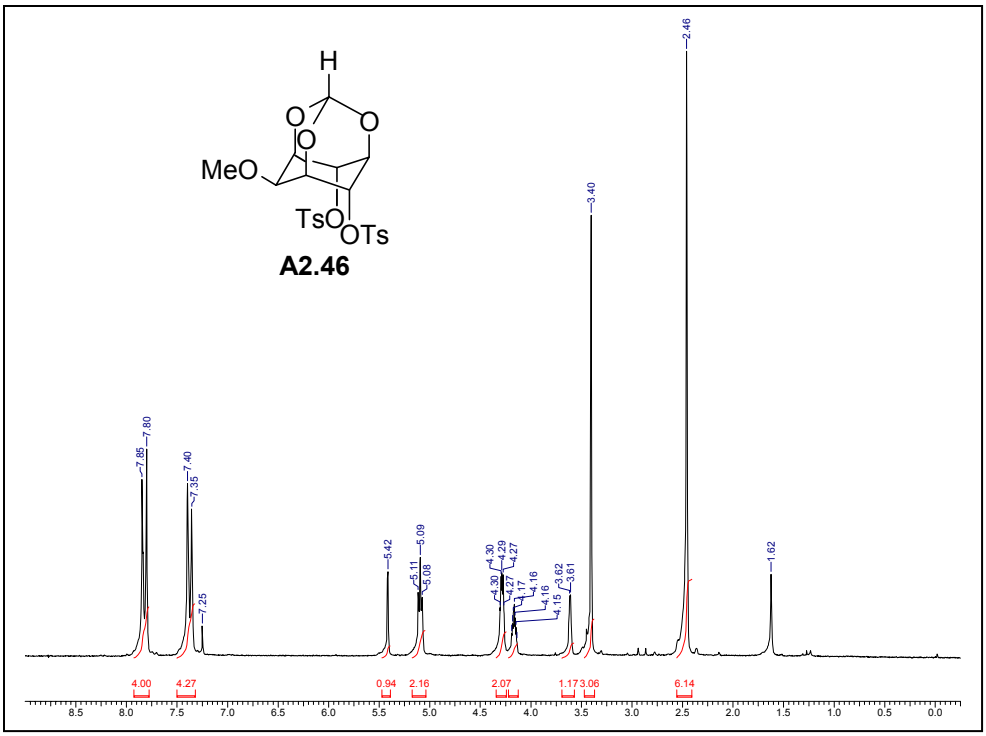
H
O
O
O
MeO
TsO
OTs
A2.46
2.46
3.40
1.62
7.80
7.85
7.40
7.35
7.25
5.42
5.11
5.09
5.08
4.30
4.29
4.27
4.17
4.16
4.15
3.62
3.61
4.00
4.27
0.94
2.16
2.07
1.17
3.06
6.14

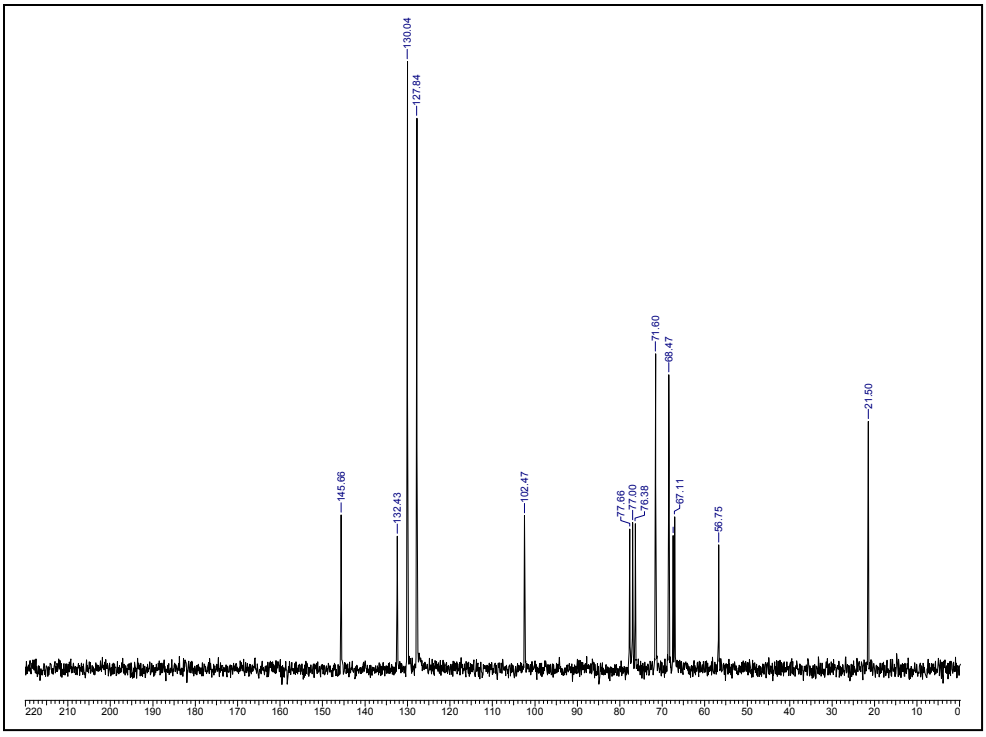
130.04
127.84
145.66
132.43
102.47
77.66
77.00
76.38
71.60
68.47
67.11
56.75
21.50

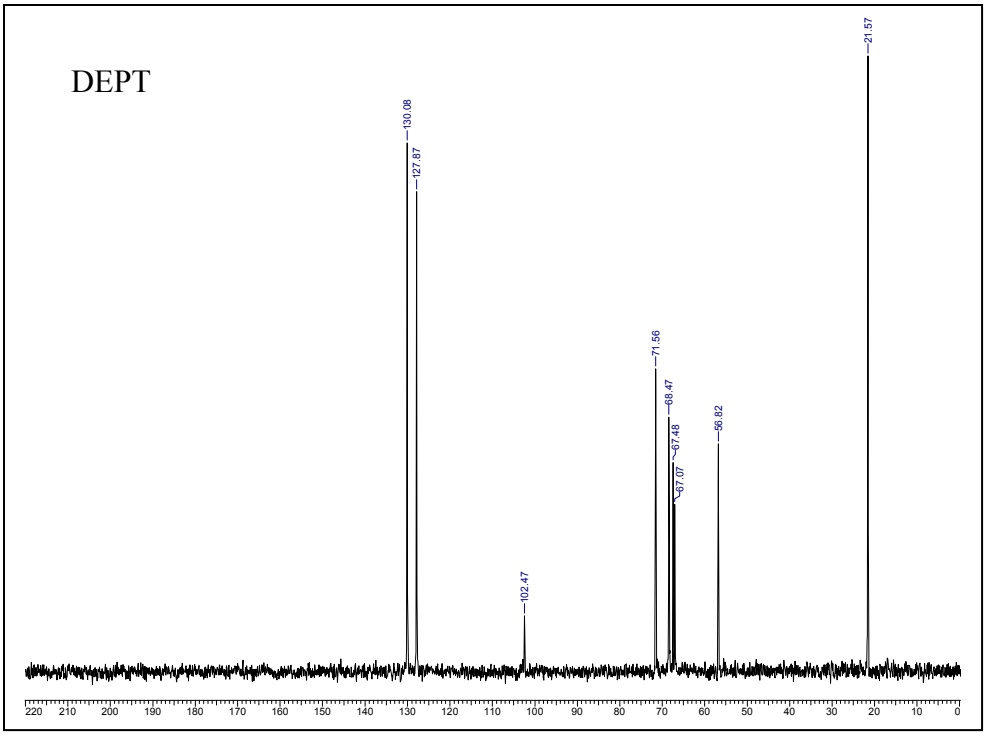
DEPT
130.08
127.87
102.47
71.56
68.47
67.48
67.07
56.82
21.57
220 210 200 190 180 170 160 150 140 130 120 110 100 90 80 70 60 50 40 30 20 10 0

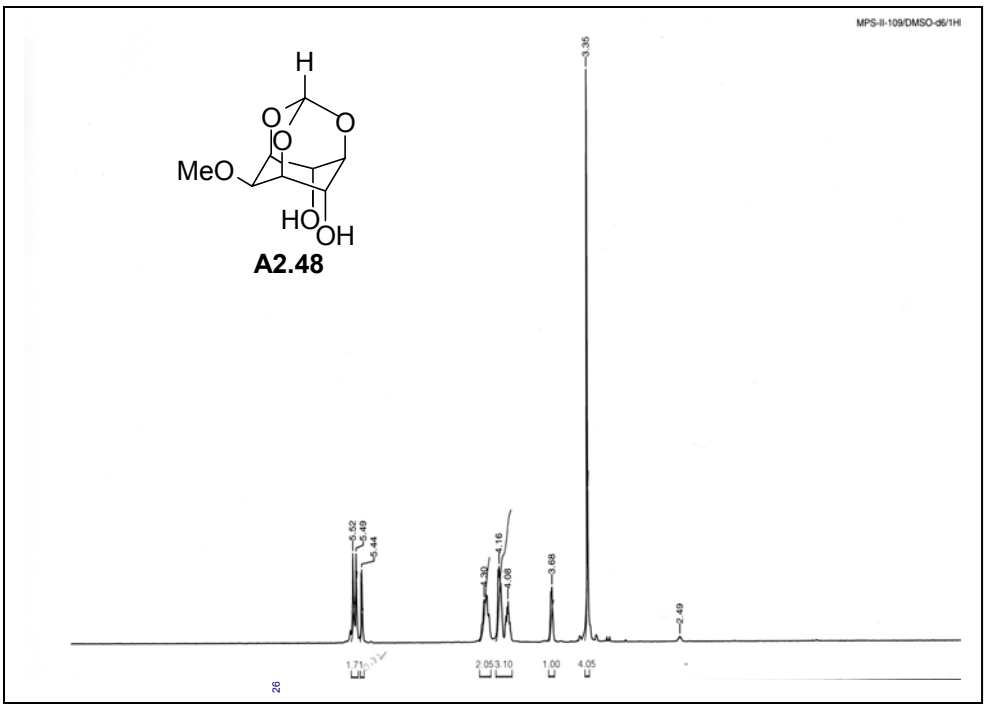
MPS-II-109/DMSO-d6/1H
H
O
O
O
MeO
HO
OH
A2.48
3.35
5.52
5.49
5.44
4.30
4.16
4.08
3.68
2.49
1.71
2.05
3.10
1.00
4.05
26

D_2O exchange

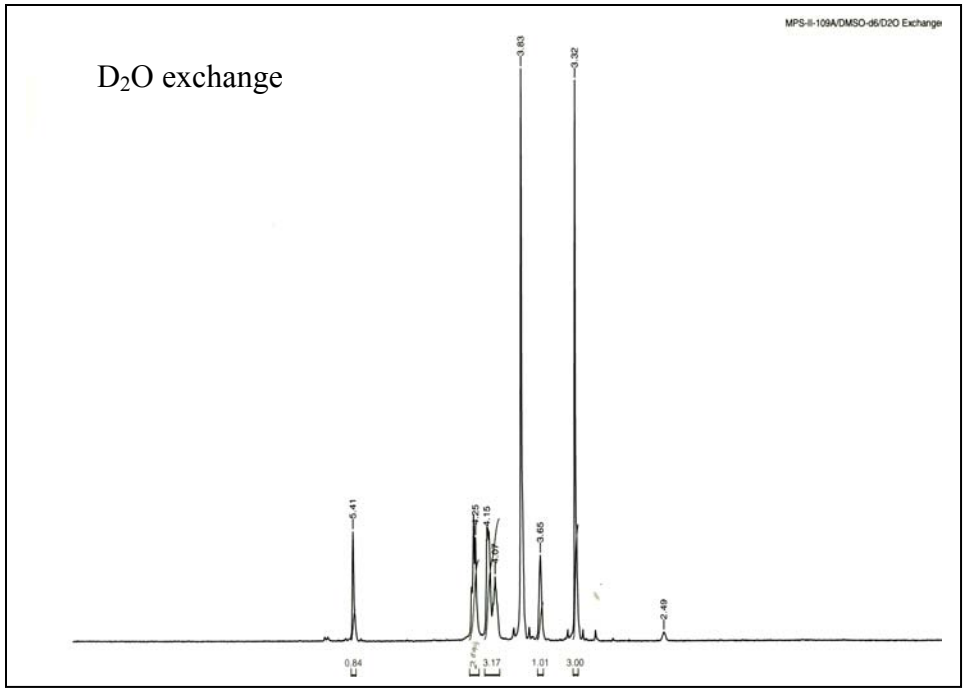

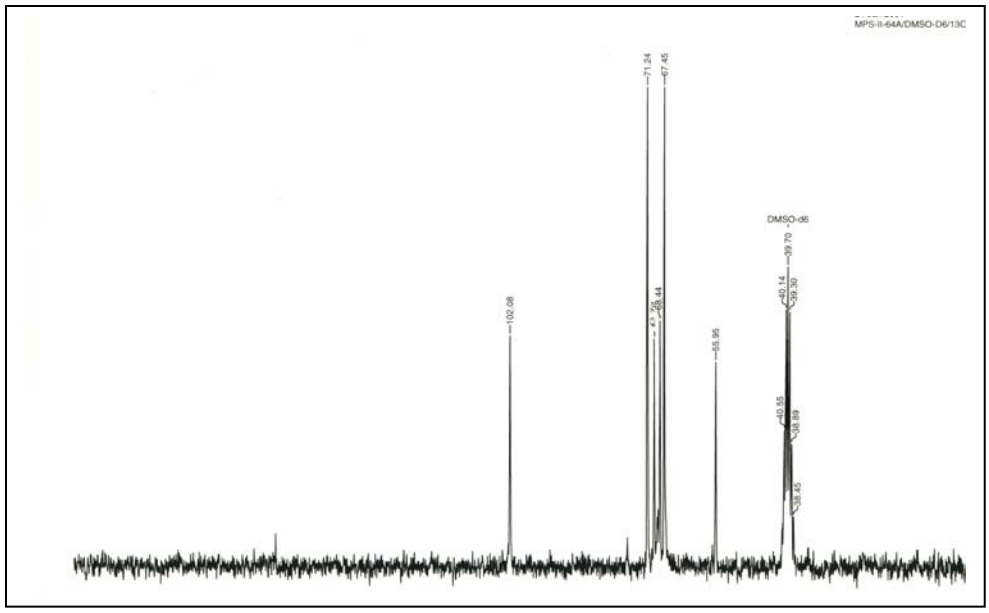

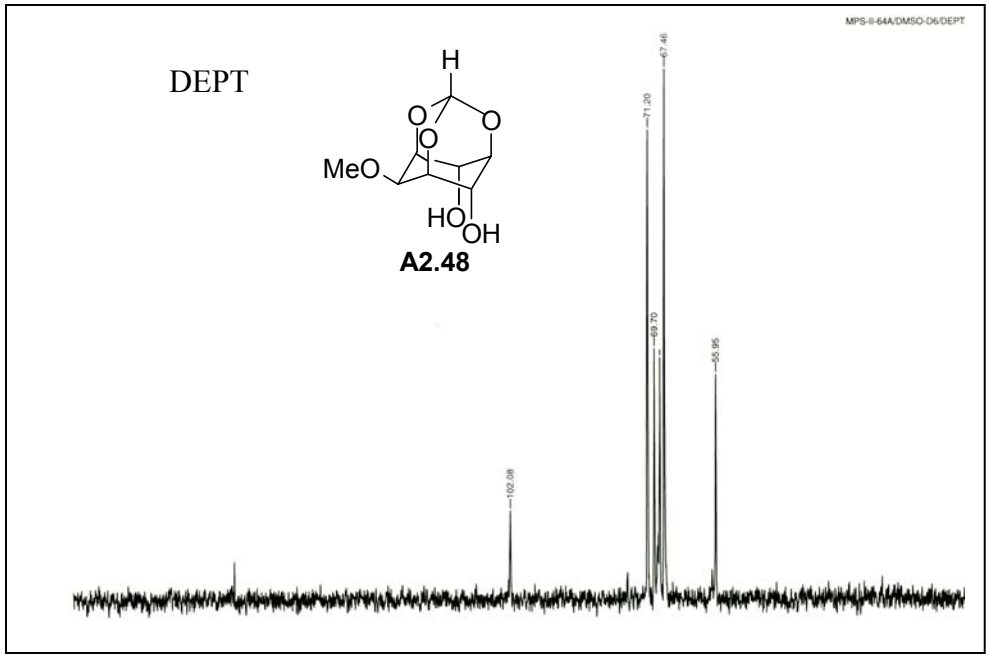

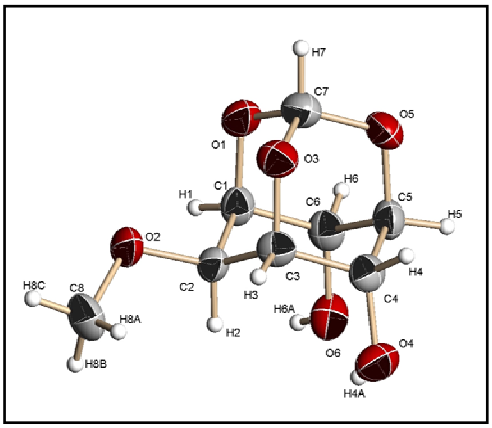

ORTEP of **A2.48**

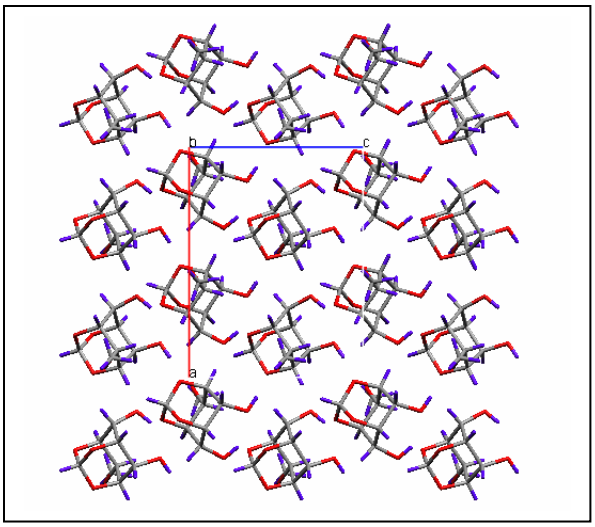

Packing of **A2.48** down the b-axis

Crystal data tabe of **A2.48**

Identification code	**A2.48** (crystallized from chloroform-light petroleum mixture)
Empirical formula	$C_8H_{12}O_6$
Formula weight	204.18
Temperature	566(2) K
Wavelength	0.71073 Å
Crystal system, space group	Orthorhombic, $Pna2_1$
Unit cell dimensions	a = 11.5659(14) Å; α = 90º b = 8.4668(10) Å; β = 90º c = 8.7249(11) Å; γ = 90º
Volume	854.4(18) $Å^3$
Z, Calculated density	4, 1.587 Mg/m^3
Absorption coefficient	0.138 mm^{-1}
F(000)	432
Crystal size	0.71 × 0.15 × 0.09 mm
θ range for data collection	2.98 to 24.99º
Limiting indices	-13<=h<=11; -10<=k<=7; -9<=l<=10
Reflections collected / unique	4020 / 1475 [R(int) = 0.0194]
Completeness to θ = 25.00	100 %
Max. and min. transmission	0.9881 and 0.9087
Refinement method	Full-matrix least-squares on F^2
Data / restraints / parameters	1475 / 1 / 175
Goodness-of-fit on F^2	1.077
Final R indices [I>2σ (I)]	R1 = 0.0266, wR2 = 0.0628
R indices (all data)	R1 = 0.0296, wR2 = 0.0641
Largest diff. peak and hole (ρ_{max} & ρ_{min})	0.114 and -0.155 e. $Å^{-3}$

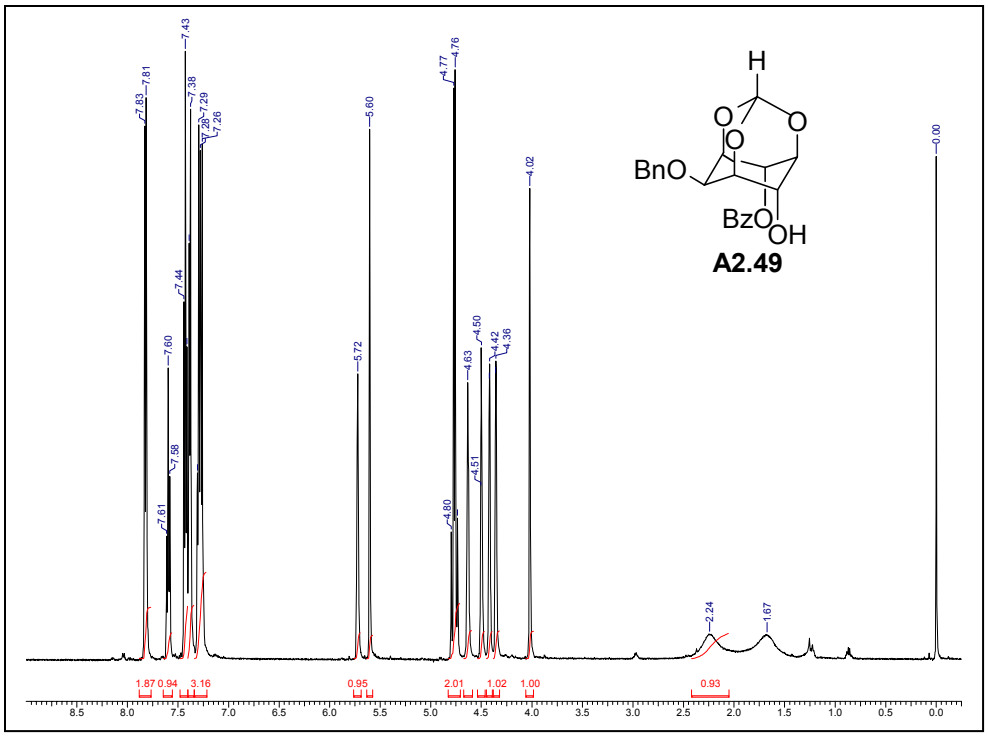
H
O
O
O
BnO
BzO
OH
A2.49

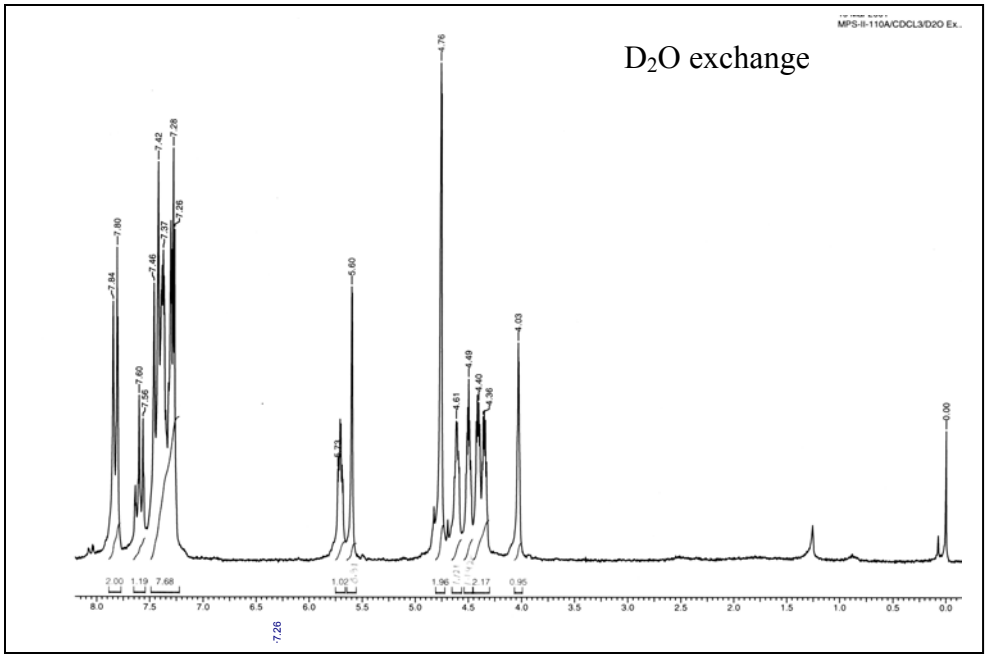
D2O exchange

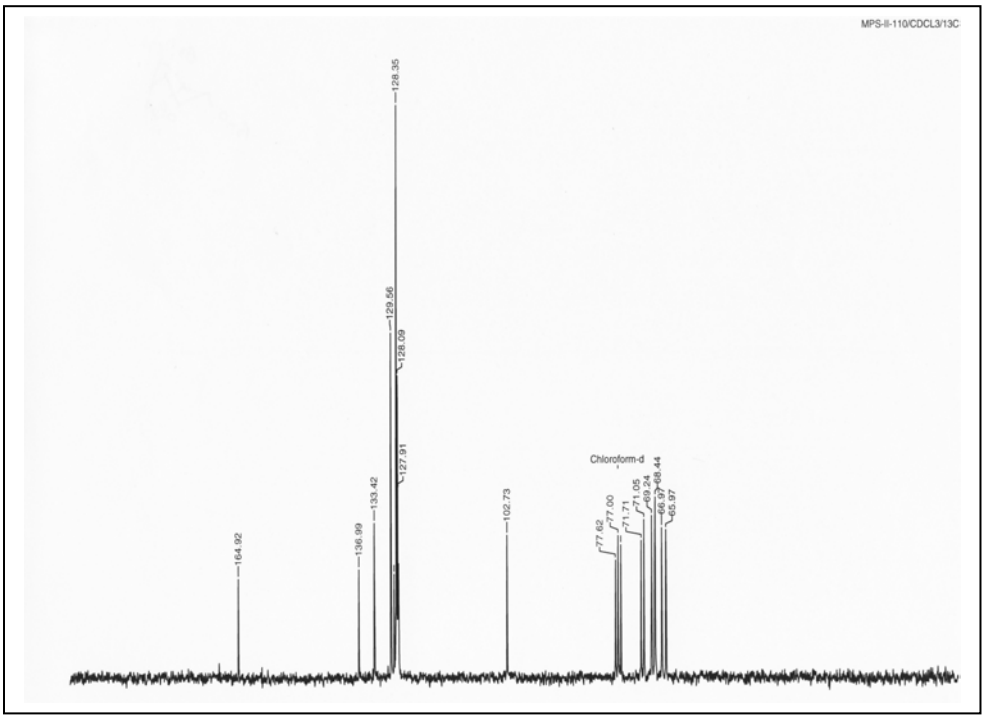
MPS-II-110/CDCL3/13C
128.35
129.56
128.09
127.91
164.92
136.99
133.42
102.73
Chloroform-d
77.62
77.00
71.71
71.05
69.24
68.44
66.97
65.97

DEPT

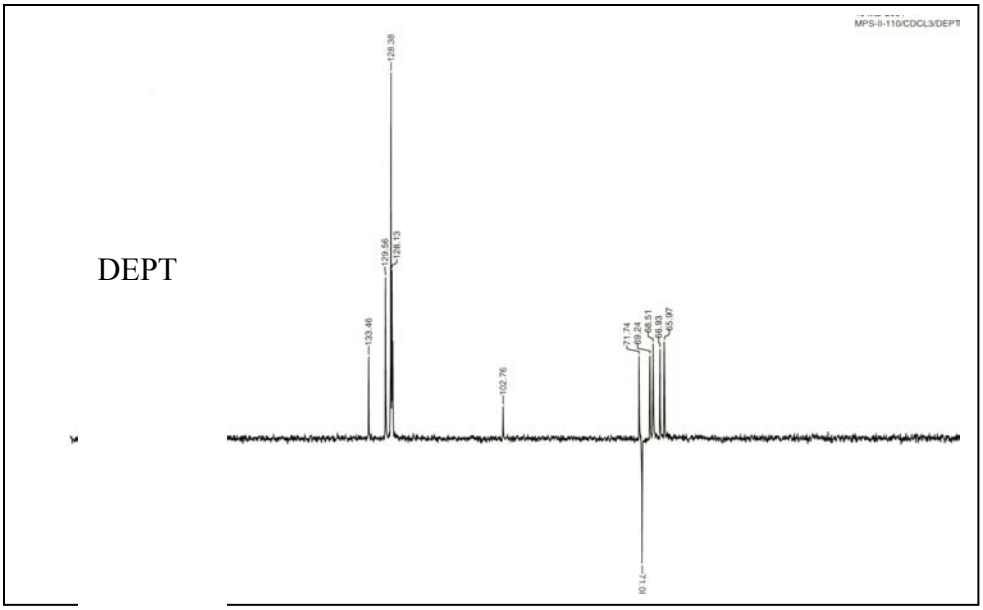
MPS-II-110/CDCL3/DEPT
128.38
129.56
128.13
133.46
102.76
71.74
69.24
68.51
66.89
65.97

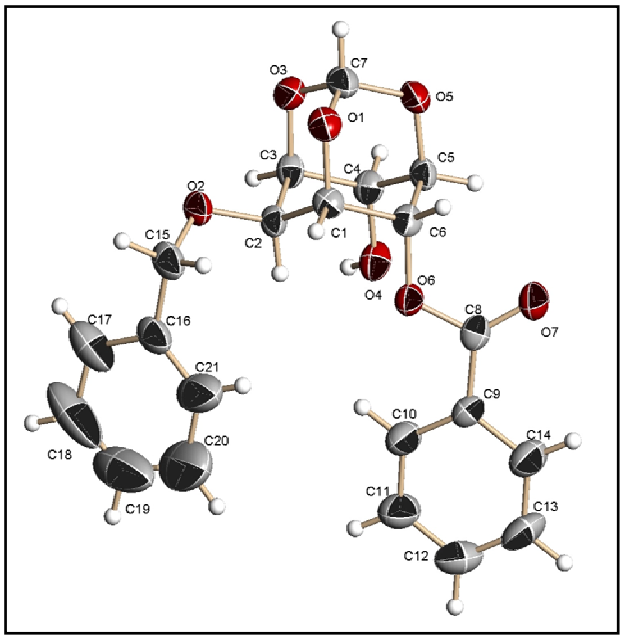

ORTEP of **A2.49**

Crystal data table of **A2.49**

Identification code	**A2.49** (crystallized from chloroform-light petroleum mixture)
Empirical formula	$C_{21}H_{20}O_7$
Formula weight	384.37
Temperature	293(2) K
Wavelength	0.71073 Å
Crystal system, space group	Orthorhombic, Pbcn
Unit cell dimensions	a = 35.833(10) Å; α = 90º b = 10.023(3) Å; β = 90º c = 20.763(6) Å; γ = 90º
Volume	7457(4) $Å^3$
Z, Calculated density	16, 1.369 Mg/m^3
Absorption coefficient	0.103 mm^{-1}
F(000)	3232
Crystal size	0.38 × 0.12 × 0.07 mm
θ range for data collection	1.96 to 25.00º
Limiting indices	-41<=h<=42; -11<=k<=11; -24<=l<=17
Reflections collected / unique	35389 / 6564 [R(int) = 0.0653]
Completeness to θ = 25.00	99.9 %
Max. and min. transmission	0.9928 and 0.9617
Refinement method	Full-matrix least-squares on F^2
Data / restraints / parameters	6564 / 0 / 507
Goodness-of-fit on F^2	1.162
Final R indices [I>2σ (I)]	R1 = 0.0892, wR2 = 0.1561
R indices (all data)	R1 = 0.1425, wR2 = 0.1761
Largest diff. peak and hole (ρ_{max} & ρ_{min})	0.257 and -0.240 e. $Å^{-3}$

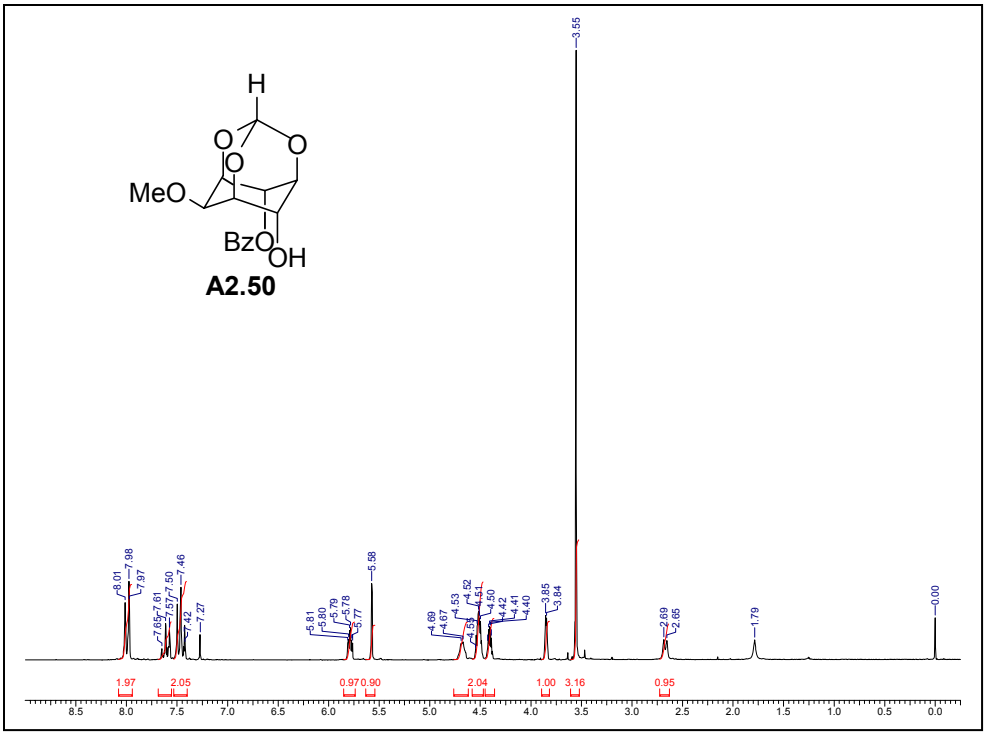
H
O
O
O
MeO
BzO
OH
A2.50

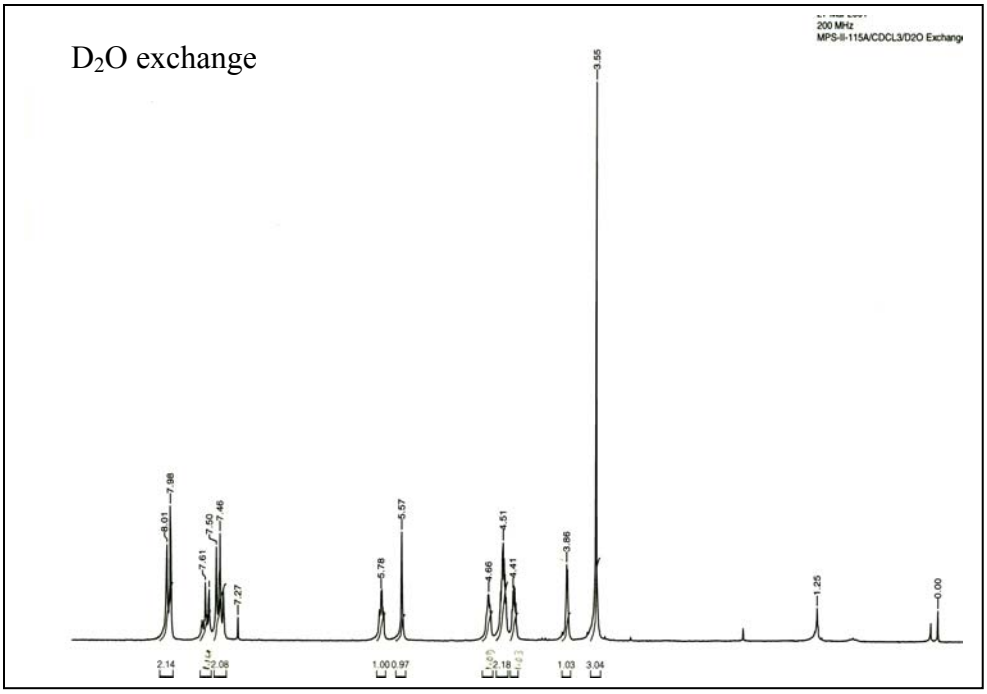
D2O exchange

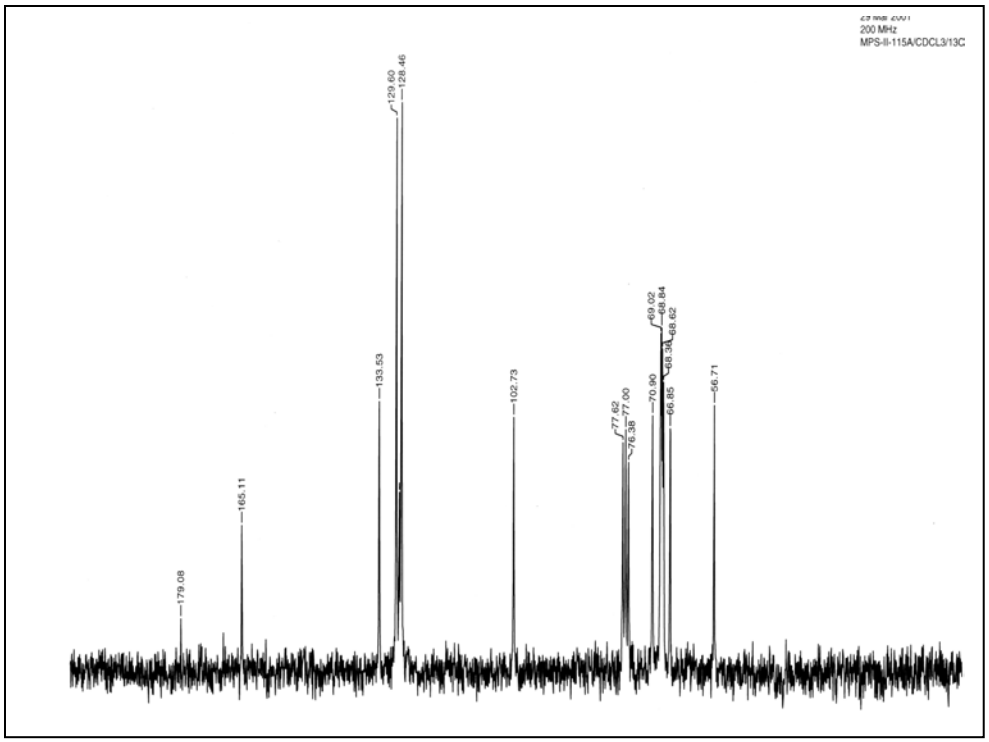
200 MHz
MPS-II-115A/CDCL3/13C
179.08
165.11
133.53
129.60
128.46
102.73
77.62
77.00
76.38
70.90
69.02
68.84
68.62
68.39
66.85
56.71

DEPT

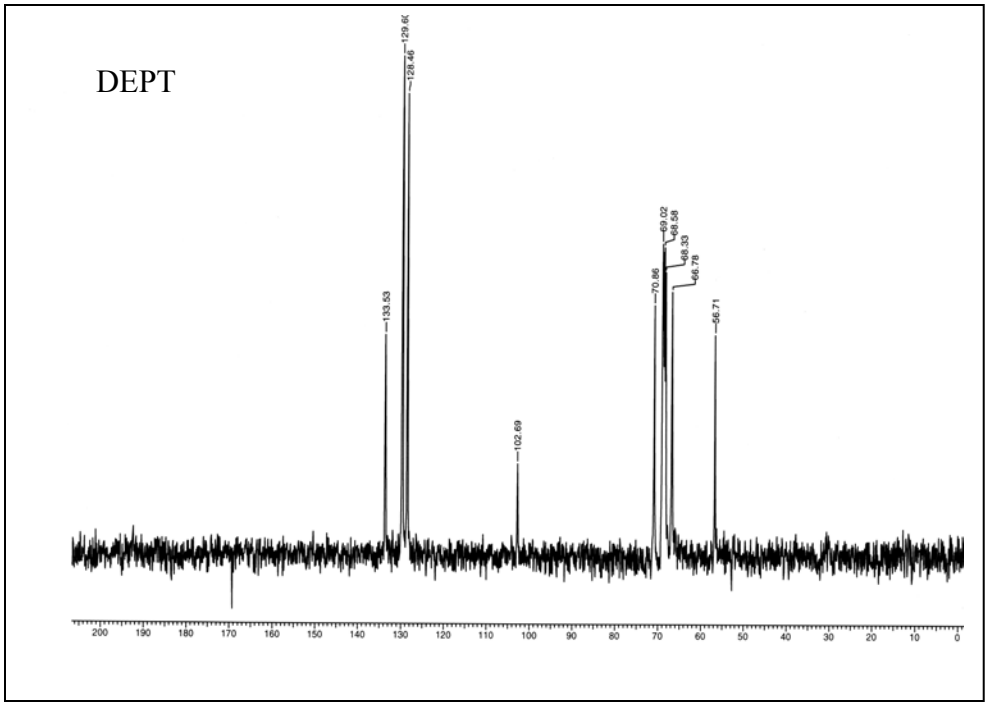
129.6
128.46
133.53
102.69
70.86
69.02
68.84
68.39
68.33
66.78
56.71
200 190 180 170 160 150 140 130 120 110 100 90 80 70 60 50 40 30 20 10 0

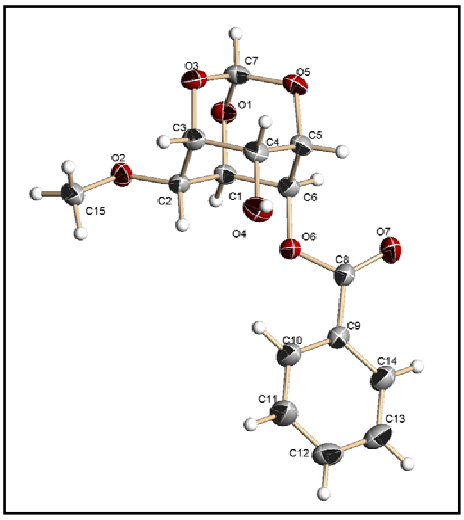

ORTEP of **A2.50**

Crystal data table of **A2.50**

Identification code	**A2.50** (crystallized from chloroform-light petroleum mixture)
Empirical formula	$C_{15}H_{16}O_7$
Formula weight	308.28
Temperature	293(2) K
Wavelength	0.71073 Å
Crystal system, space group	Monoclinic, Cc
Unit cell dimensions	a = 6.2355(16) Å; α = 90° b = 20.290(5) Å; β = 95.533(4)° c = 11.294(3) Å; γ = 90°
Volume	1422.3(6) $Å^3$
Z, Calculated density	4, 1.440 Mg/m^3
Absorption coefficient	0.115 mm^{-1}
F(000)	648
Crystal size	0.67 × 0.12 × 0.09 mm
θ range for data collection	2.01 to 24.99°
Limiting indices	-7<=h<=7; -24<=k<=23; -13<=l<=9.
Reflections collected / unique	3491 / 1871 [R(int) = 0.0242]
Completeness to θ = 24.99	99.3 %
Max. and min. transmission	0.9892 and 0.9263
Refinement method	Full-matrix least-squares on F^2
Data / restraints / parameters	1871 / 2 / 202
Goodness-of-fit on F^2	1.067
Final R indices [I>2σ (I)]	R1 = 0.0354, wR2 = 0.0886
R indices (all data)	R1 = 0.0374, wR2 = 0.0903
Absolute structure parameter	-0.2(11)
Extinction coefficient	0.0004(12)
Largest diff. peak and hole (ρ_{max} & ρ_{min})	0.152 and -0.157 e. $Å^{-3}$

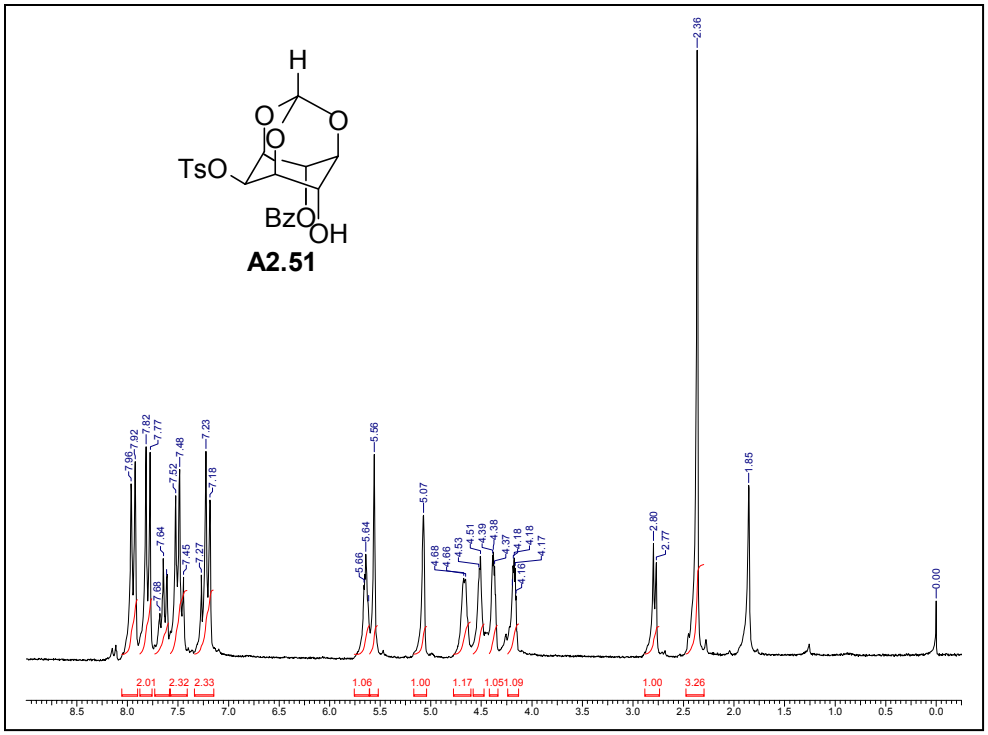
H
O
O
O
TsO
BzO
OH
A2.51
2.36
7.96
7.92
7.82
7.77
7.48
7.52
7.23
7.18
7.64
7.45
7.27
7.69
5.66
5.64
5.56
5.07
4.68
4.66
4.53
4.51
4.39
4.38
4.37
4.18
4.17
4.16
2.80
2.77
1.85
0.00
2.01
2.32
2.33
1.06
1.00
1.17
1.05
1.09
1.00
3.26

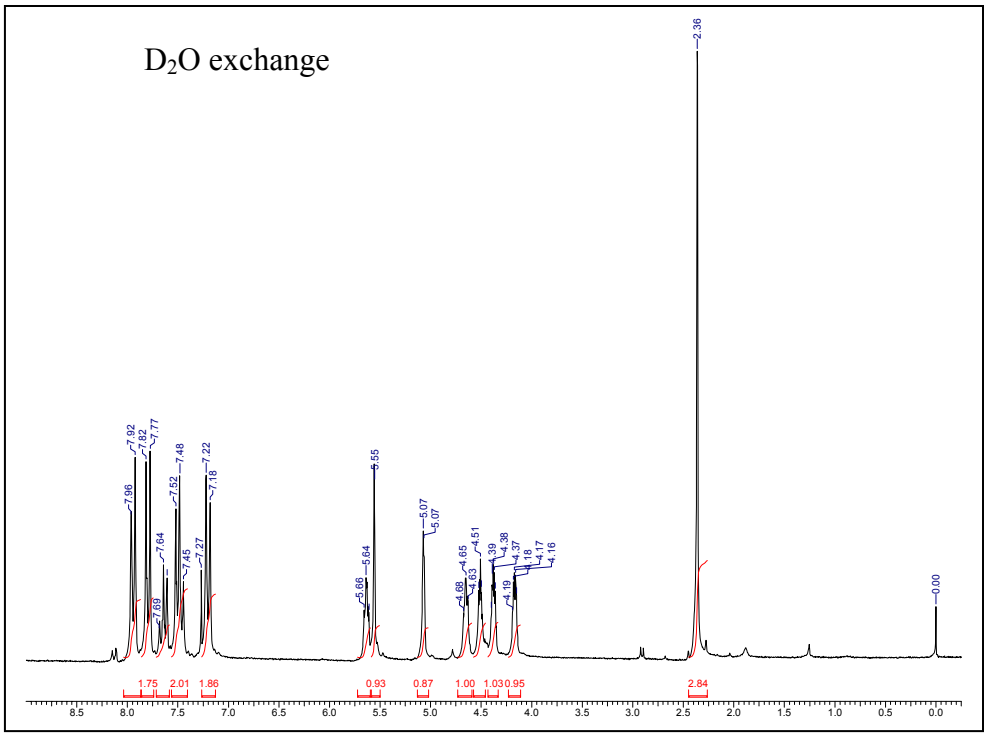
D2O exchange
2.36
7.92
7.82
7.77
7.48
7.52
7.22
7.18
7.96
7.64
7.45
7.27
7.69
5.66
5.64
5.55
5.07
5.07
4.68
4.65
4.53
4.51
4.39
4.38
4.37
4.19
4.18
4.17
4.16
0.00
1.75
2.01
1.86
0.93
0.87
1.00
1.03
0.95
2.84

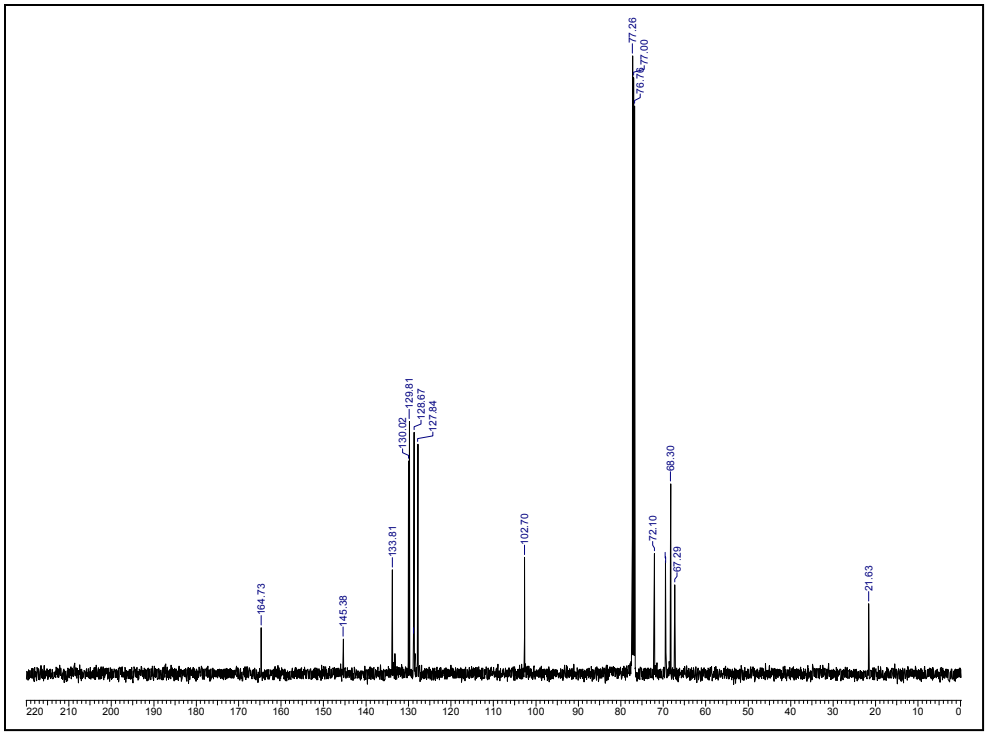
77.26
77.00
76.74
130.02
129.81
128.67
127.84
68.30
133.81
102.70
72.10
67.29
164.73
145.38
21.63
220 210 200 190 180 170 160 150 140 130 120 110 100 90 80 70 60 50 40 30 20 10 0

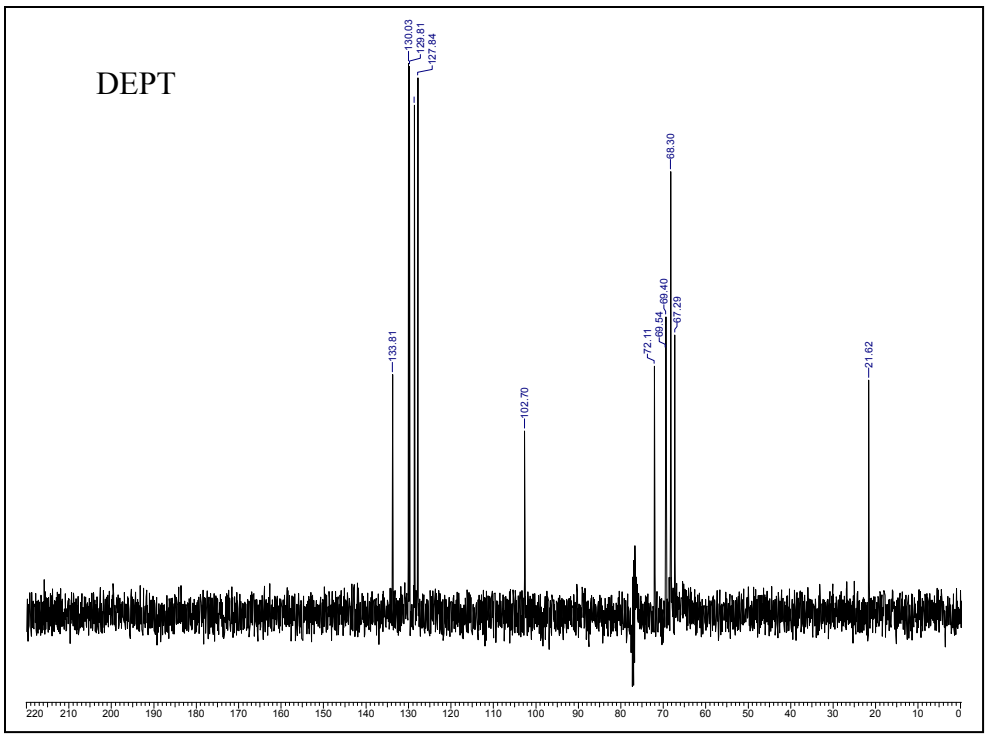
DEPT
130.03
129.81
127.84
68.30
69.40
69.54
67.29
72.11
133.81
102.70
21.62
220 210 200 190 180 170 160 150 140 130 120 110 100 90 80 70 60 50 40 30 20 10 0

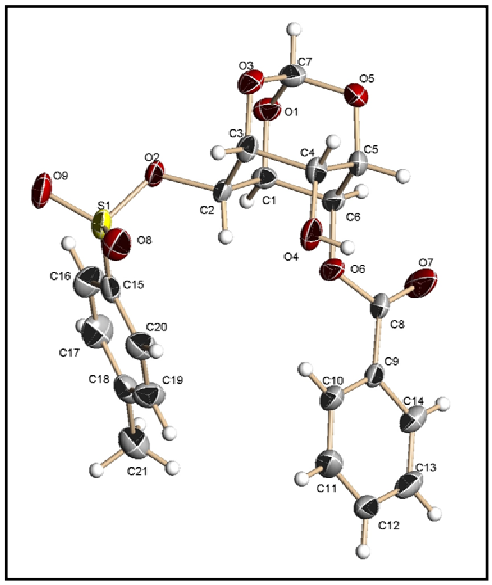

ORTEP of **A2.51**

Crystal data table of **A2.51**

Identification code	**A2.51** (crystallized from chloroform-light petroleum mixture)
Empirical formula	$C_{21}H_{20}O_9S$
Formula weight	448.43
Temperature	293(2) K
Wavelength	0.71073 Å
Crystal system, space group	Monoclinic, $P2_1/n$
Unit cell dimensions	a = 11.626(5) Å; α = 90° b = 12.534(5) Å; β = 95.573(7)° c = 13.719(6) Å; γ = 90°
Volume	1989.6(15) $Å^3$
Z, Calculated density	4, 1.497 Kg/m^3
Absorption coefficient	0.217 mm^{-1}
F(000)	936
Crystal size	0.57 × 0.50 × 0.06 mm
θ range for data collection	2.19 to 25.00°
Limiting indices	-13<=h<=13; -14<=k<=13; -13<=l<=16
Reflections collected / unique	9462 / 3484 [R(int) = 0.0351]
Completeness to θ = 25.00	99.6 %
Max. and min. transmission	0.9869 and 0.8855
Refinement method	Full-matrix least-squares on F^2
Data / restraints / parameters	3484 / 0 / 282
Goodness-of-fit on F^2	1.034
Final R indices [I>2σ(I)]	R1 = 0.0554, wR2 = 0.1230
R indices (all data)	R1 = 0.0849, wR2 = 0.1352
Largest diff. peak and hole (ρ_{max} & ρ_{min})	0.358 and -0.221 e. $Å^{-3}$

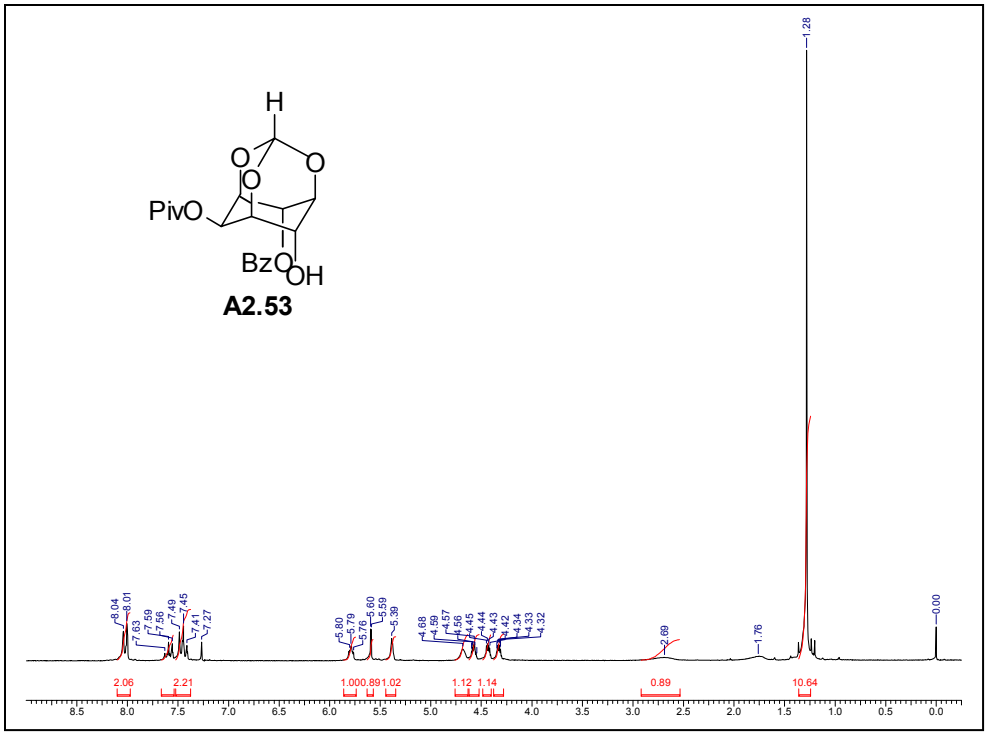
H
O
O
O
PivO
BzO
OH
A2.53

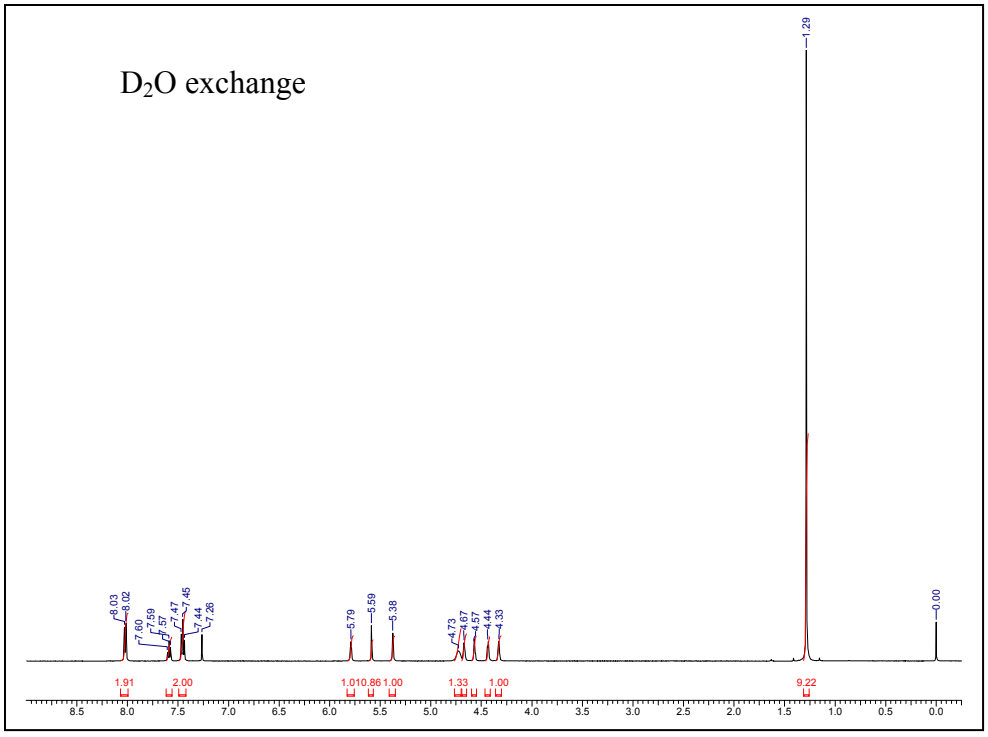
D2O exchange

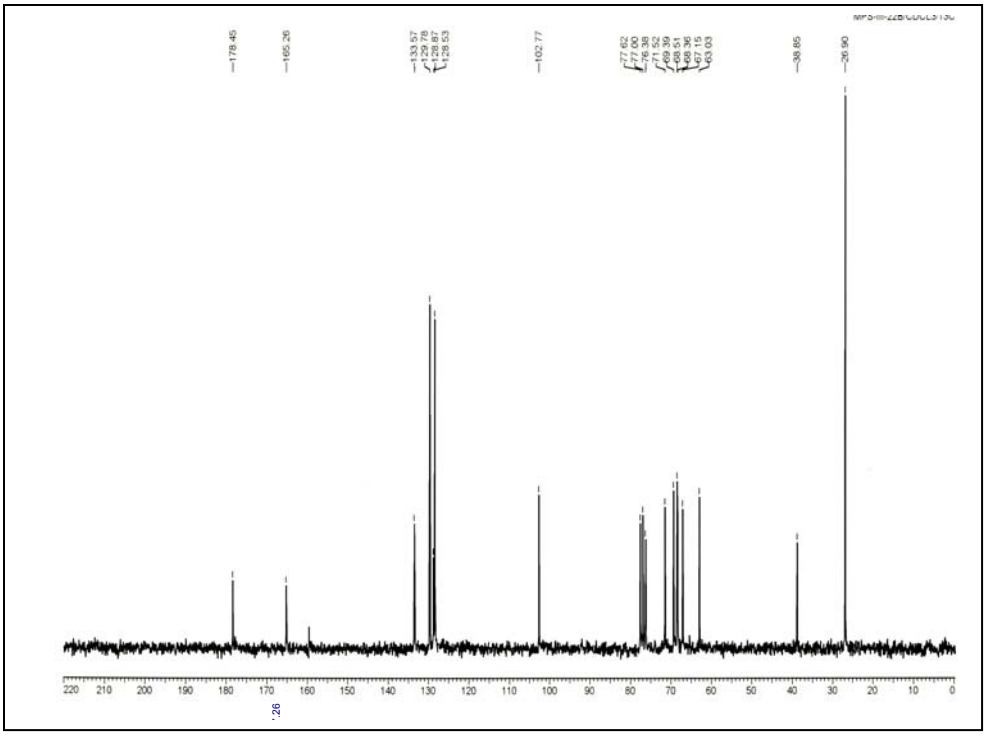
178.45
165.26
133.57
129.78
128.87
128.53
102.77
77.62
77.00
76.38
71.52
69.39
68.51
68.36
67.15
63.03
38.85
26.90

DEPT

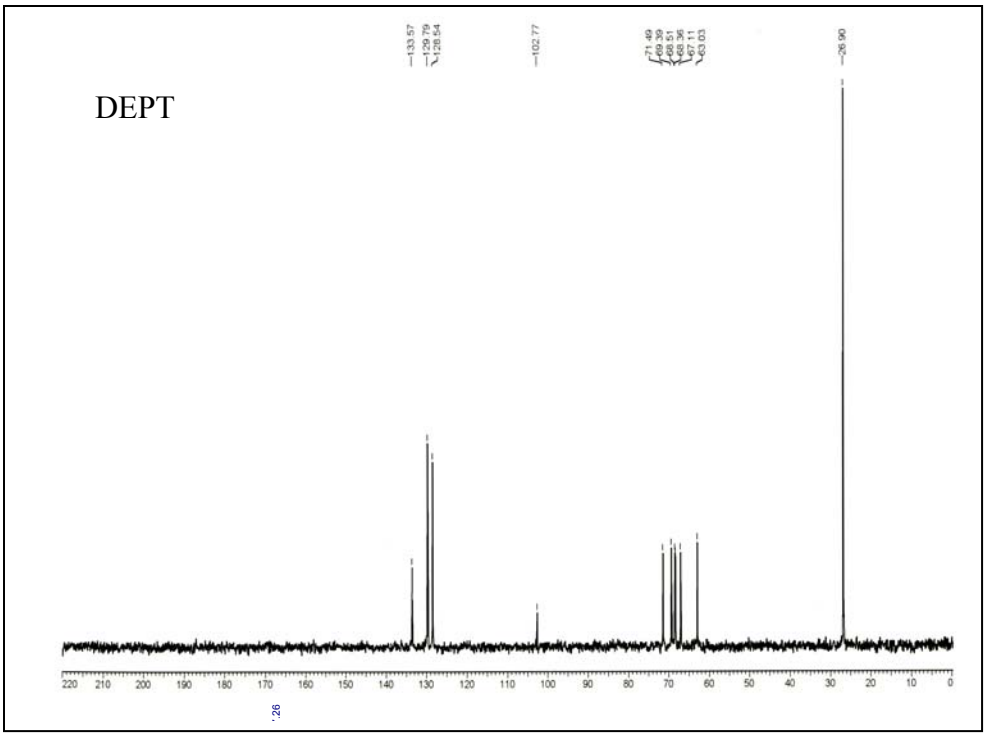
133.57
129.79
128.54
102.77
71.49
69.39
68.51
68.36
67.11
63.03
26.90

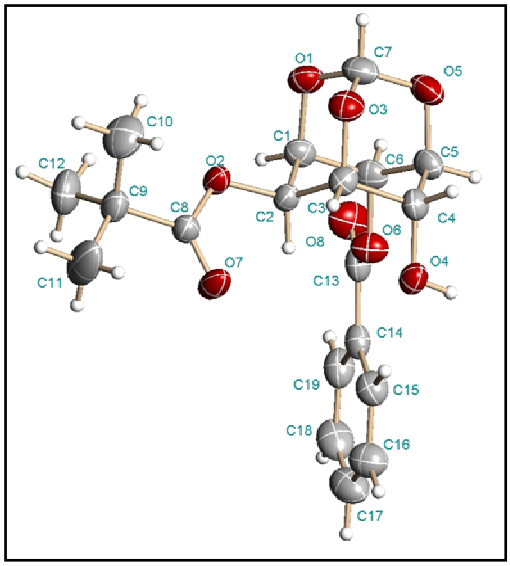

ORTEP of **A2.53**

Crystal data table of **A2.53**

Identification code	**A2.53** (crystallized from chloroform-light petroleum mixture)
Empirical formula	$C_{19}H_{22}O_8$
Formula weight	378.37
Temperature	293(2) K
Wavelength	0.71073 Å
Crystal system, space group	Monoclinic, $P2_1/n$
Unit cell dimensions	a = 11.4581(13) Å; α = 90º b = 10.1522(11) Å; β = 104.731(2)º c = 16.7158(18) Å; γ = 90º
Volume	1880.5(4) $Å^3$
Z, Calculated density	4, 1.336 Mg/m^3
Absorption coefficient	0.105 mm^{-1}
F(000)	800
Crystal size	0.51 × 0.50 × 0.49 mm
θ range for data collection	2.52 to 25.00º
Limiting indices	-13<=h<=13; -11<=k<=12; -19<=l<=19
Reflections collected / unique	11323 / 3292 [R(int) = 0.0218]
Completeness to θ = 25.00	99.3 %
Max. and min. transmission	0.9502 and 0.9481
Refinement method	Full-matrix least-squares on F^2
Data / restraints / parameters	3292 / 0 / 249
Goodness-of-fit on F^2	1.057
Final R indices [I>2σ (I)]	R1 = 0.0522, wR2 = 0.1416
R indices (all data)	R1 = 0.0566, wR2 = 0.1473
Extinction coefficient	0.039(4)
Largest diff. peak and hole (ρ_{max} & ρ_{min})	0.312 and -0.235 e. $Å^{-3}$

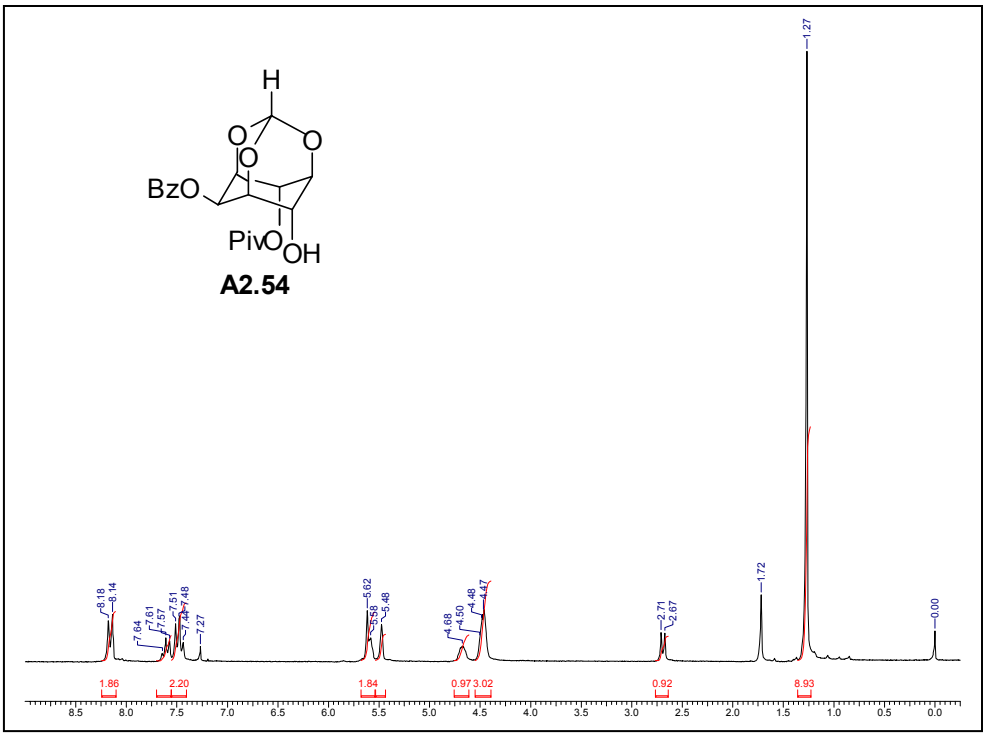
H
O
O
O
BzO
PivO
OH
A2.54
1.27
8.18
8.14
7.64
7.61
7.57
7.51
7.48
7.27
5.62
5.59
5.48
4.68
4.50
4.48
4.47
2.71
2.67
1.72
0.00
1.86
2.20
1.84
0.97
3.02
0.92
8.93

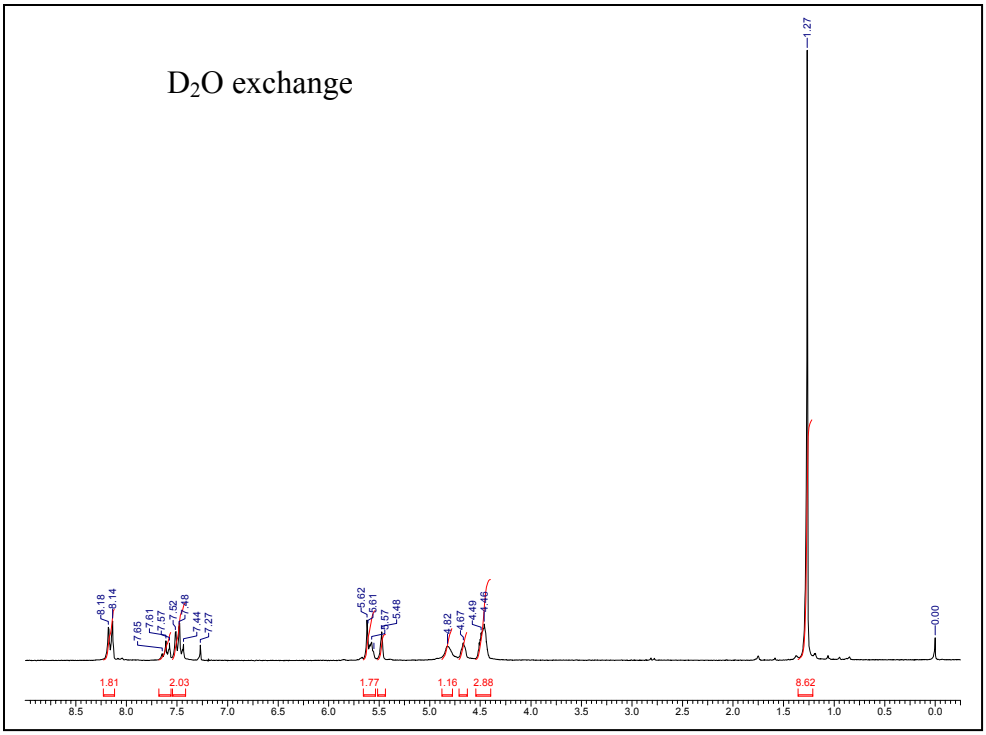
D2O exchange
1.27
8.18
8.14
7.65
7.61
7.57
7.52
7.48
7.44
7.27
5.62
5.61
5.57
5.48
4.62
4.57
4.49
4.46
0.00
1.81
2.03
1.77
1.16
2.88
8.62

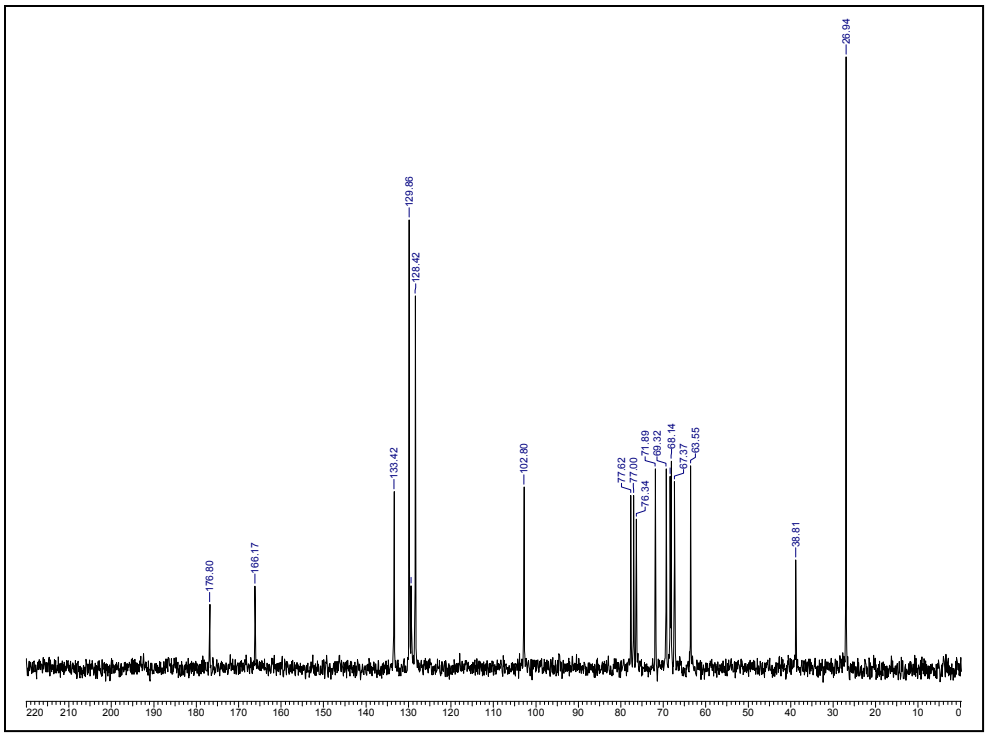
26.94
129.86
128.42
133.42
102.80
77.62
77.00
76.34
71.89
69.32
68.14
67.37
63.55
38.81
176.80
166.17
220 210 200 190 180 170 160 150 140 130 120 110 100 90 80 70 60 50 40 30 20 10 0

DEPT

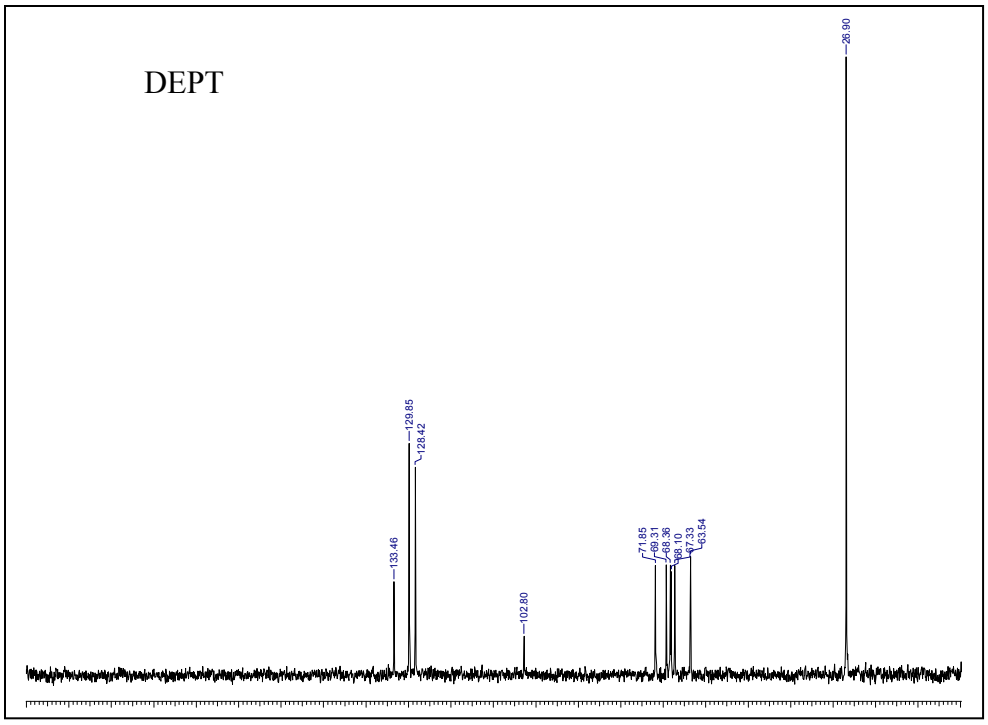
26.90
129.85
128.42
133.46
102.80
71.85
69.31
68.38
68.10
67.33
63.54

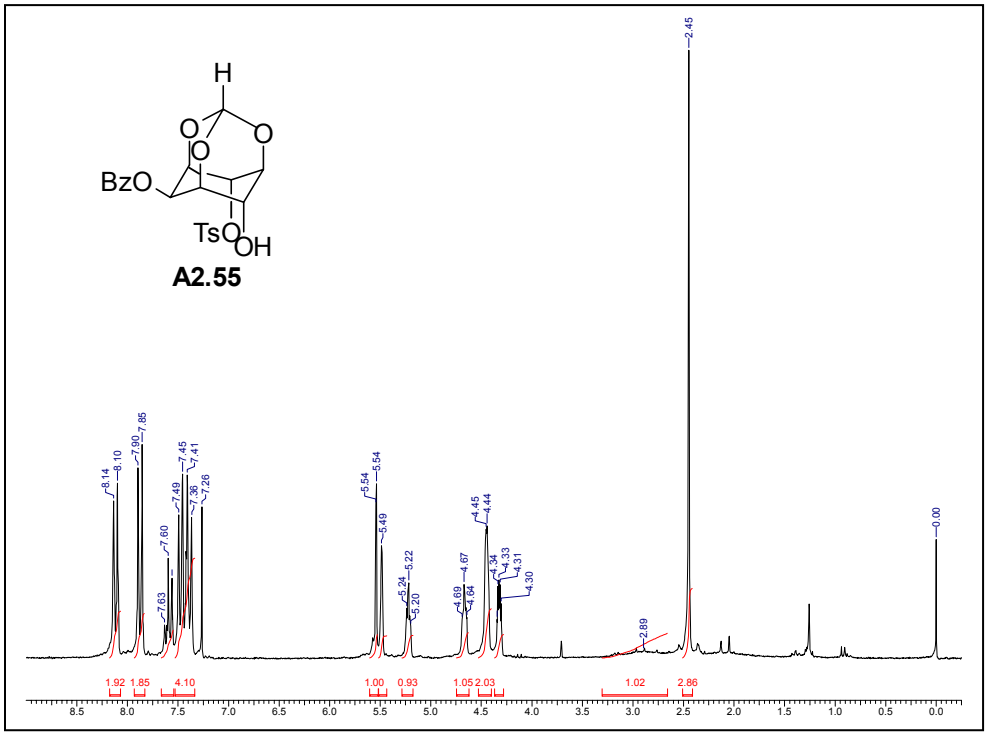
H
O
O
O
BzO
TsO
OH
A2.55
8.14
8.10
7.90
7.85
7.63
7.60
7.49
7.45
7.41
7.36
7.26
5.54
5.49
5.24
5.22
5.20
4.69
4.67
4.64
4.45
4.44
4.34
4.33
4.31
4.30
2.89
2.45
0.00
1.92 1.85 4.10 1.00 0.93 1.05 2.03 1.02 2.86

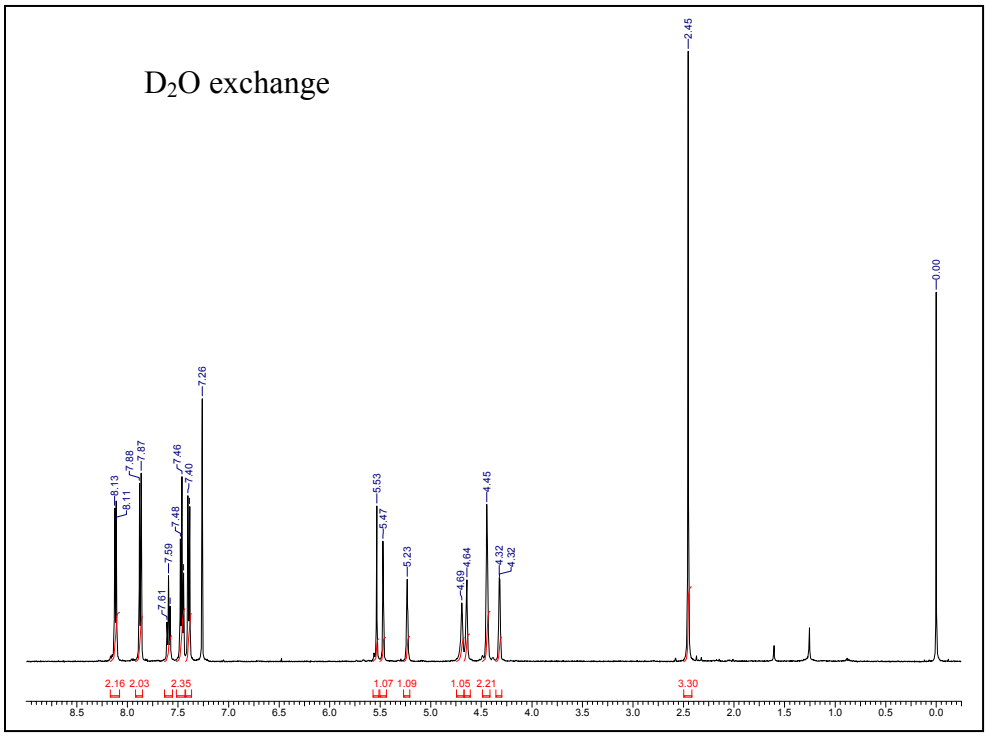
D2O exchange
8.13
8.11
7.88
7.87
7.61
7.59
7.48
7.46
7.40
7.26
5.53
5.47
5.23
4.69
4.64
4.45
4.32
4.30
2.45
0.00
2.16 2.03 2.35 1.07 1.09 1.05 2.21 3.30

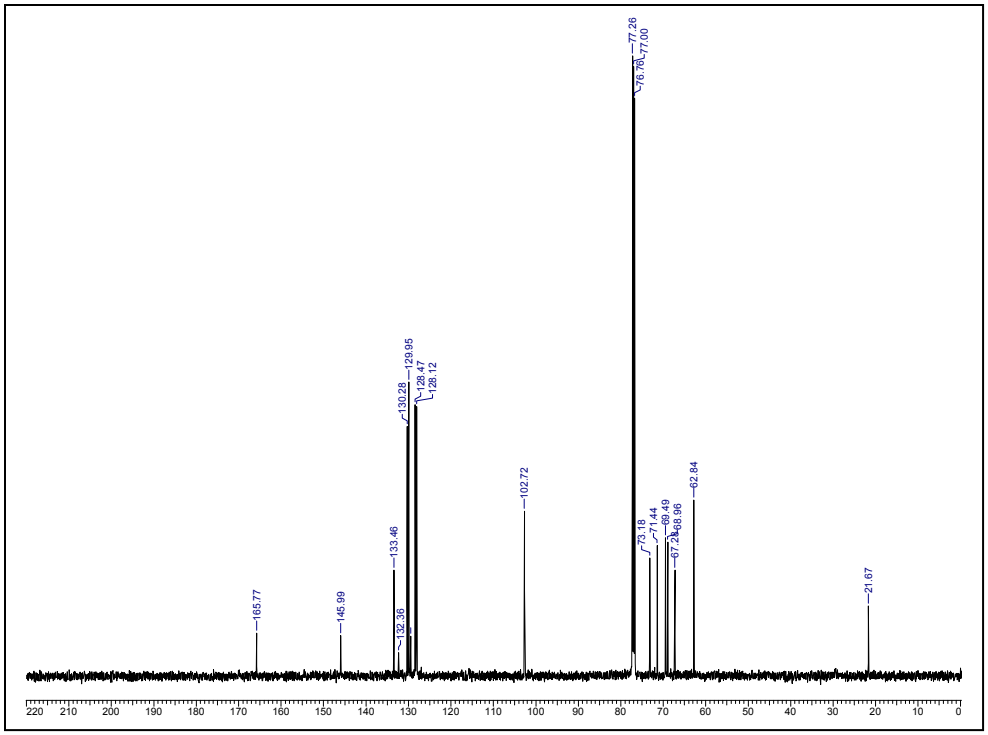
77.26
77.00
76.76
130.28
129.95
128.47
128.12
102.72
73.18
71.44
69.49
68.96
67.24
62.84
133.46
165.77
145.99
132.36
21.67
220 210 200 190 180 170 160 150 140 130 120 110 100 90 80 70 60 50 40 30 20 10 0

DEPT

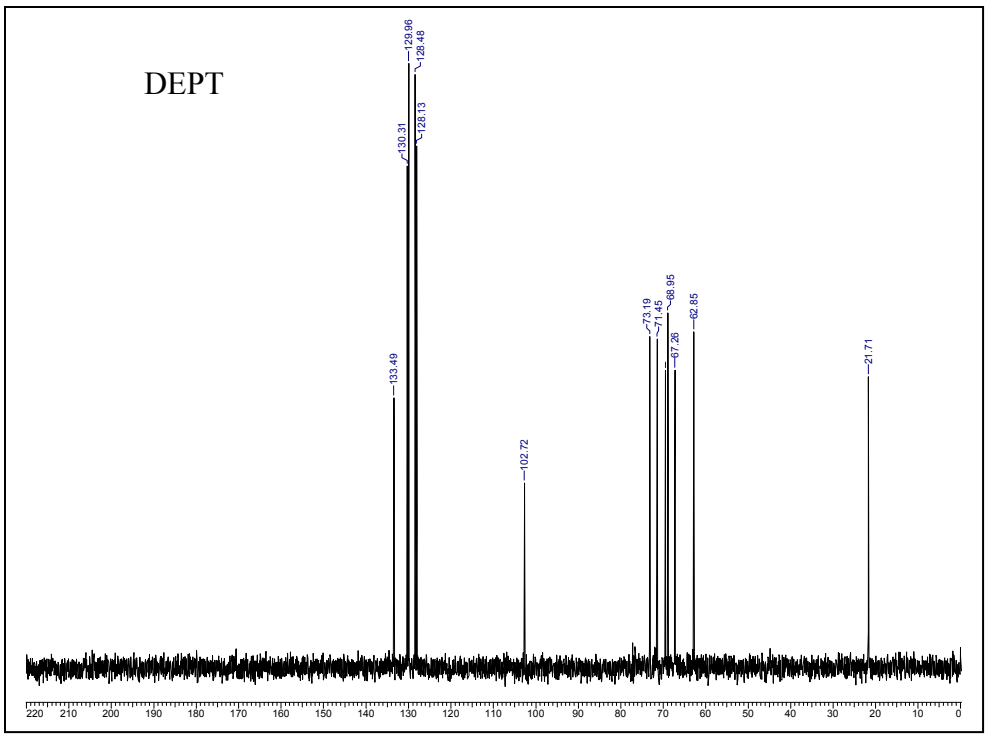
129.96
128.48
130.31
128.13
73.19
71.45
68.95
67.26
62.85
133.49
102.72
21.71
220 210 200 190 180 170 160 150 140 130 120 110 100 90 80 70 60 50 40 30 20 10 0

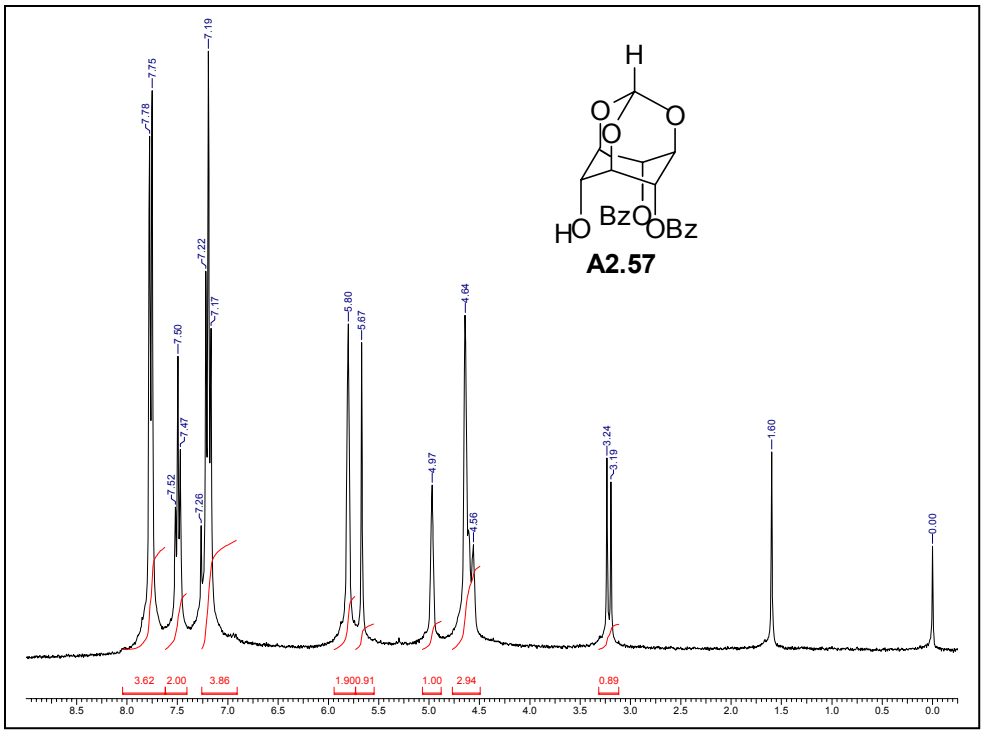
H
O
O
O
HO
BzO
OBz
A2.57
7.78
7.75
7.19
7.50
7.47
7.52
7.26
7.22
7.17
5.80
5.67
4.64
4.97
4.56
3.24
3.19
1.60
0.00
3.62
2.00
3.86
1.90
0.91
1.00
2.94
0.89

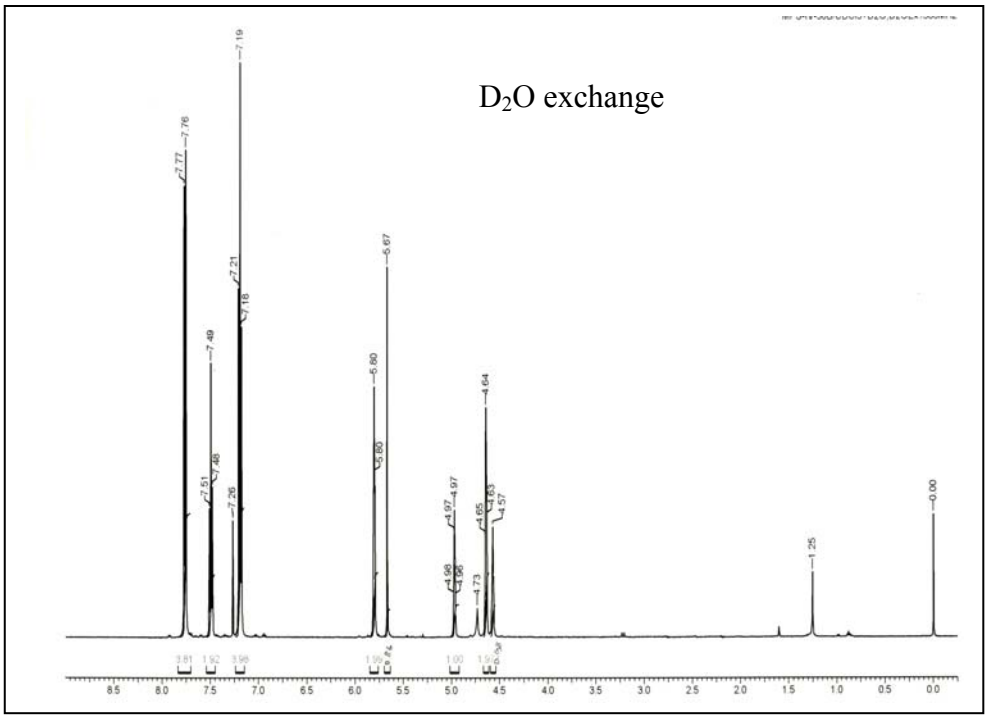
D2O exchange
7.77
7.76
7.19
7.49
7.51
7.48
7.26
7.21
7.18
5.80
5.67
4.97
4.65
4.64
4.57
4.73
1.25
0.00

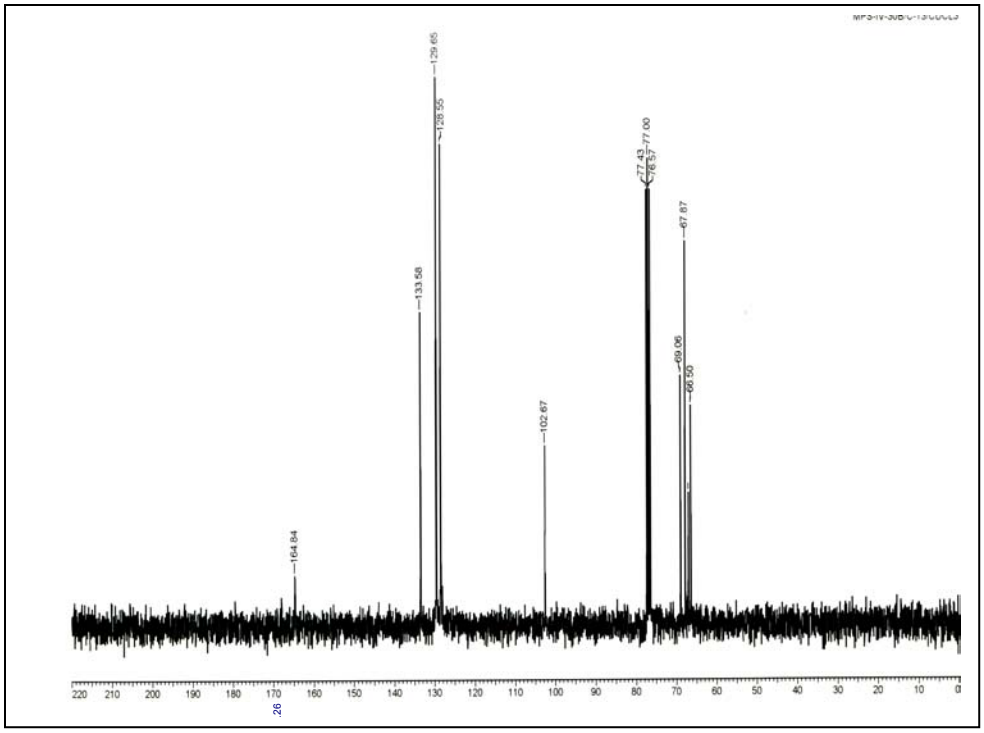
129.65
128.55
77.43
77.00
76.57
67.87
133.58
69.06
66.50
102.67
164.84
220 210 200 190 180 170 160 150 140 130 120 110 100 90 80 70 60 50 40 30 20 10
26

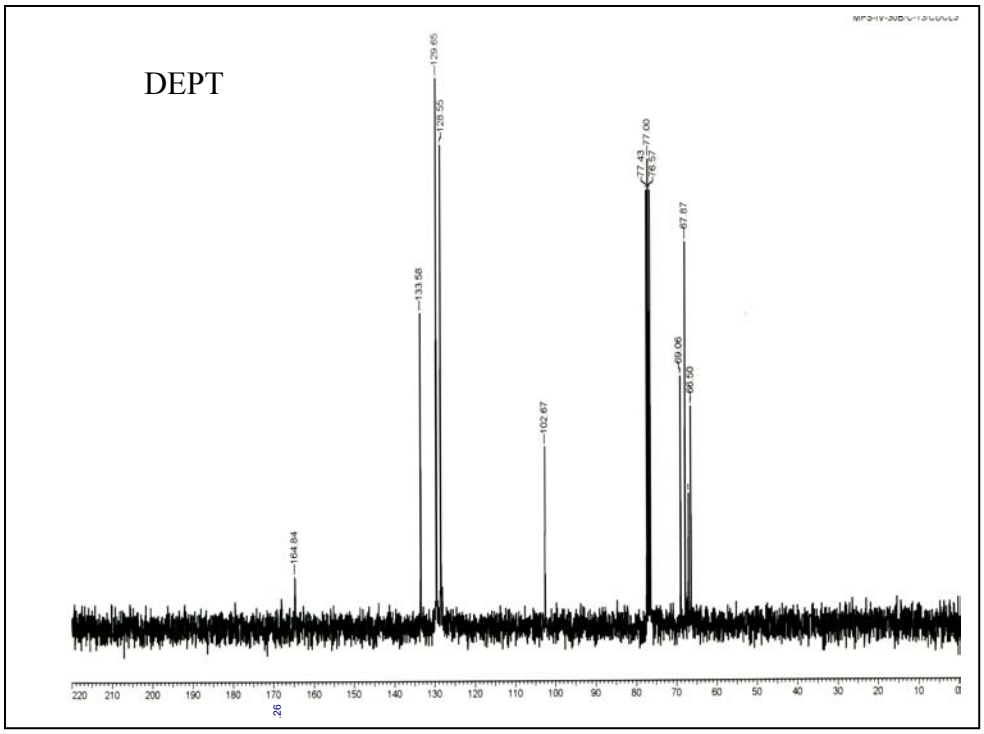
DEPT
129.65
128.55
77.43
77.00
76.57
67.87
133.58
69.06
66.50
102.67
164.84
220 210 200 190 180 170 160 150 140 130 120 110 100 90 80 70 60 50 40 30 20 10
26

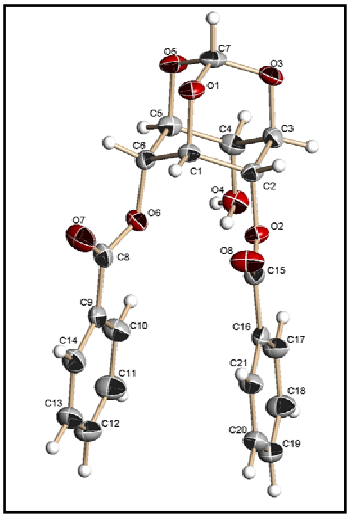

ORTEP of **A2.57**

Crystal data table of **A2.57**

Identification code	**A2.57** (crystallized from chloroform-light petroleum mixture)
Empirical formula	$C_{21}H_{18}O_8$
Formula weight	398.35
Temperature	293(2) K
Wavelength	0.71073 Å
Crystal system, space group	Triclinic, P-1
Unit cell dimensions	a = 8.298(5) Å; α = 110.135(9)º b = 10.346(6) Å; β = 92.066(10)º c = 11.825(7) Å; γ = 105.150(9)º
Volume	911.1(9) $Å^3$
Z, Calculated density	2, 1.452 Mg/m^3
Absorption coefficient	0.113 mm^{-1}
F(000)	416
Crystal size	0.68 × 0.14 × 0.04 mm
θ range for data collection	1.85 to 25.00º
Limiting indices	-9<=h<=9; -12<=k<=12; -14<=l<=14.
Reflections collected / unique	6517 / 3170 [R(int) = 0.0324]
Completeness to θ = 25.00	98.9 %
Max. and min. transmission	0.9951 and 0.9270
Refinement method	Full-matrix least-squares on F^2
Data / restraints / parameters	3170 / 0 / 338
Goodness-of-fit on F^2	1.188
Final R indices [I>2σ (I)]	R1 = 0.0691, wR2 = 0.1439
R indices (all data)	R1 = 0.1000, wR2 = 0.1571
Largest diff. peak and hole (ρ_{max} & ρ_{min})	0.244 and -0.203 e. $Å^{-3}$

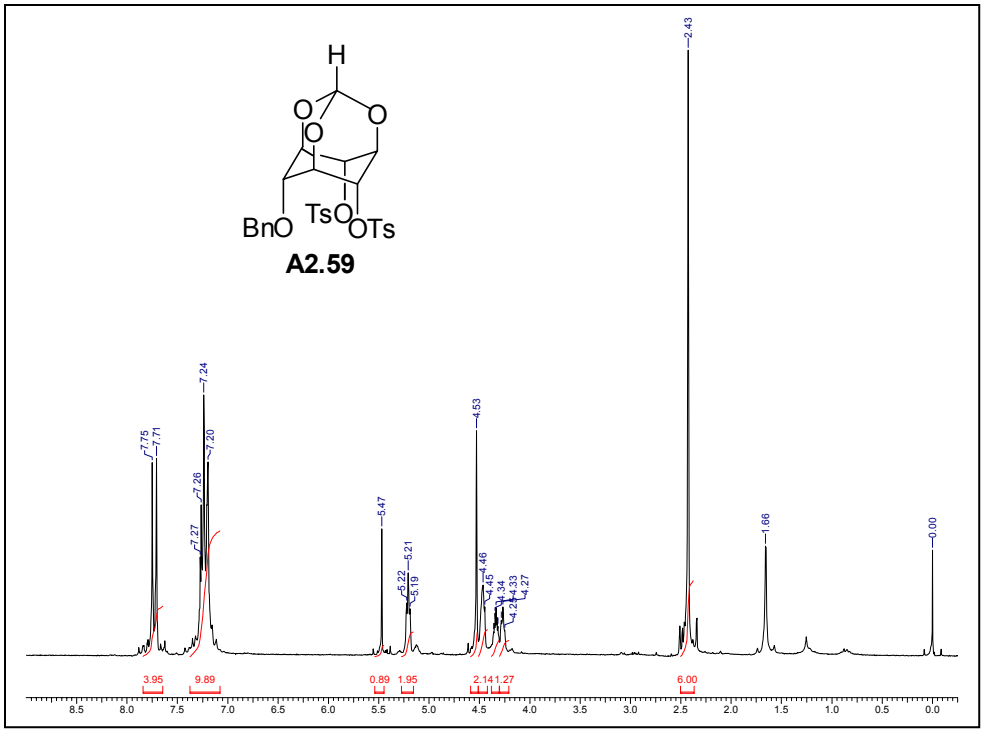
H
O
O
O
O
BnO
TsO
OTs
A2.59
2.43
7.75
7.71
7.24
7.20
7.28
7.27
5.47
5.21
5.22
5.19
4.53
4.46
4.45
4.44
4.43
4.27
1.66
0.00
3.95
9.89
0.89
1.95
2.14
1.27
6.00

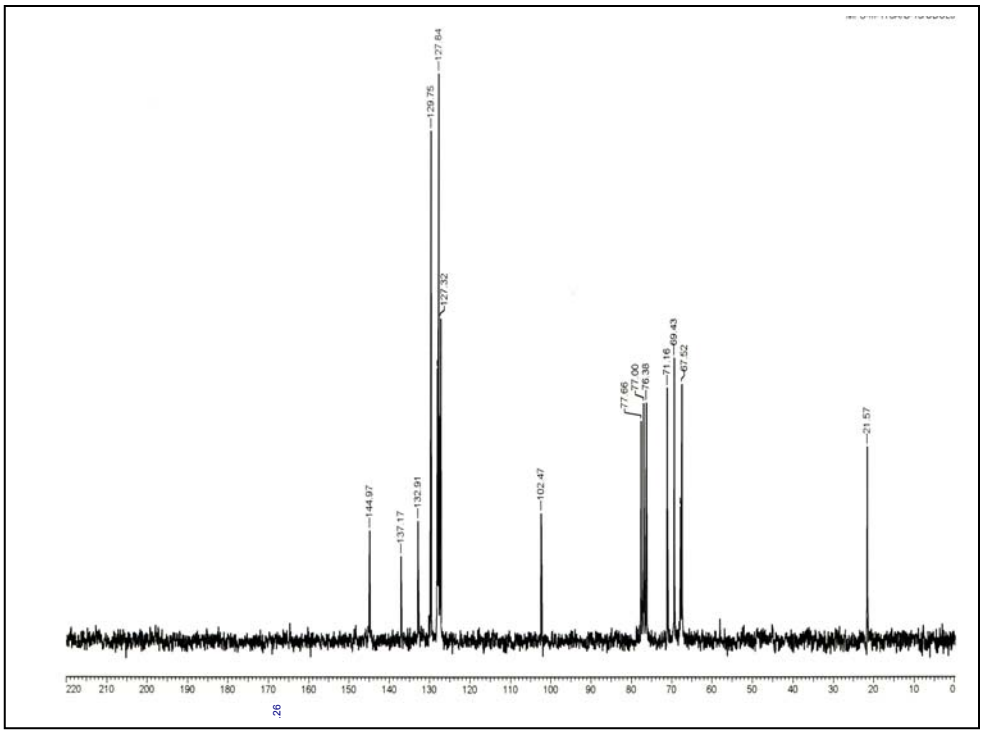
127.84
129.75
127.32
144.97
137.17
132.91
102.47
77.66
77.00
76.38
71.16
69.43
67.52
21.57

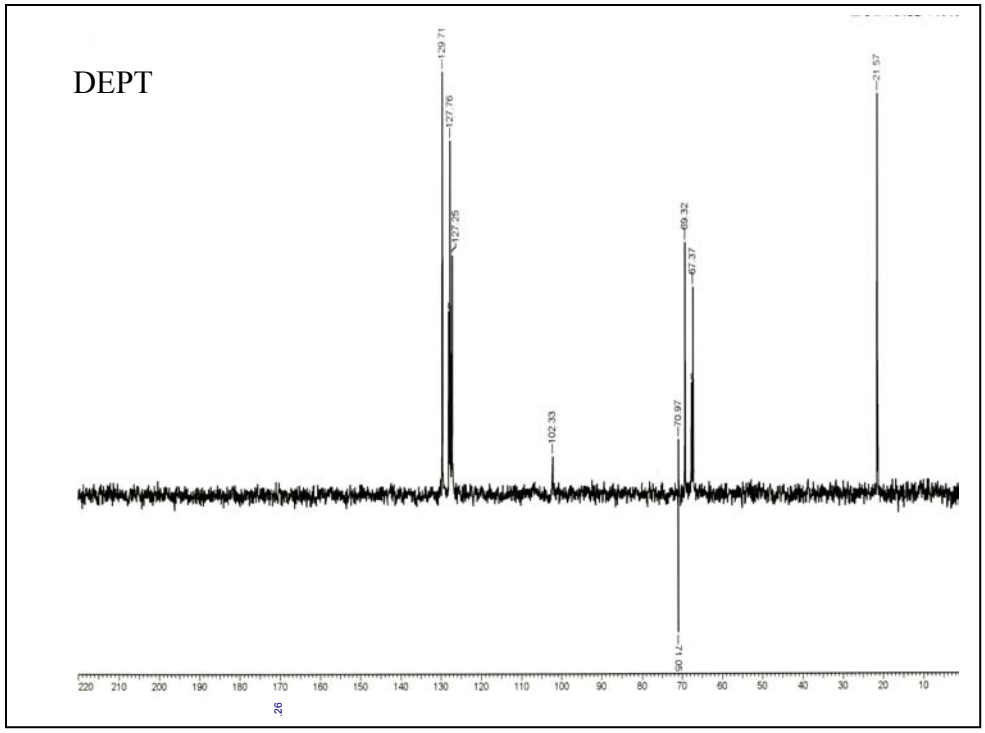
DEPT
129.71
127.76
127.25
102.33
70.97
69.32
67.37
21.57
90.17

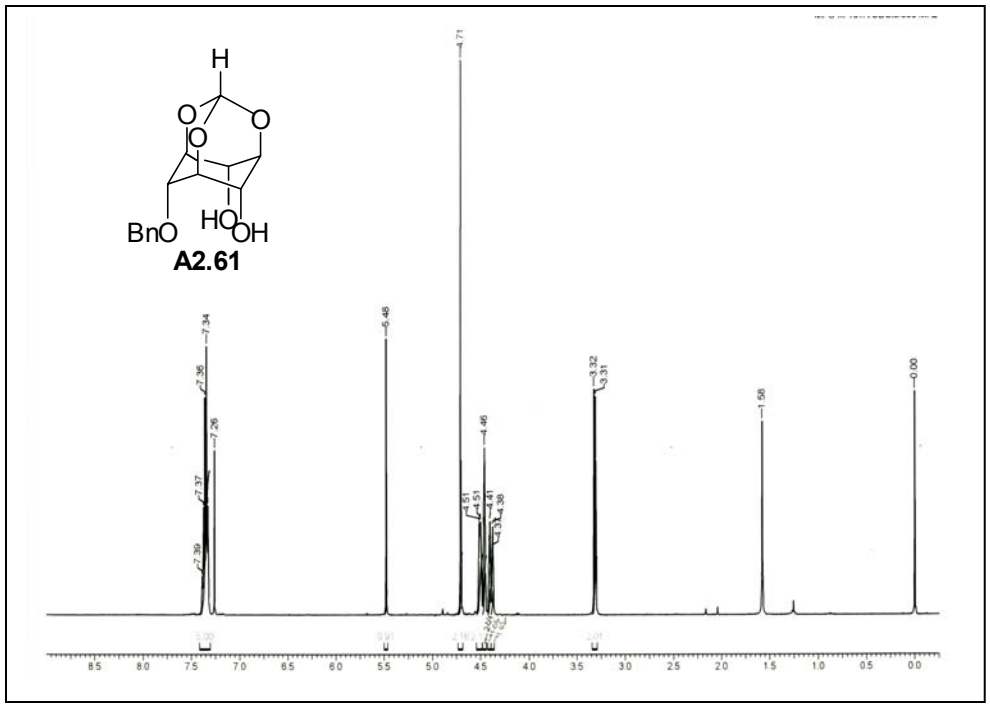
H
O
O
O
BnO
HO
OH
A2.61
7.34
7.36
7.37
7.39
7.26
6.48
4.71
4.46
4.51
4.45
4.41
4.38
3.32
3.31
1.58
0.00

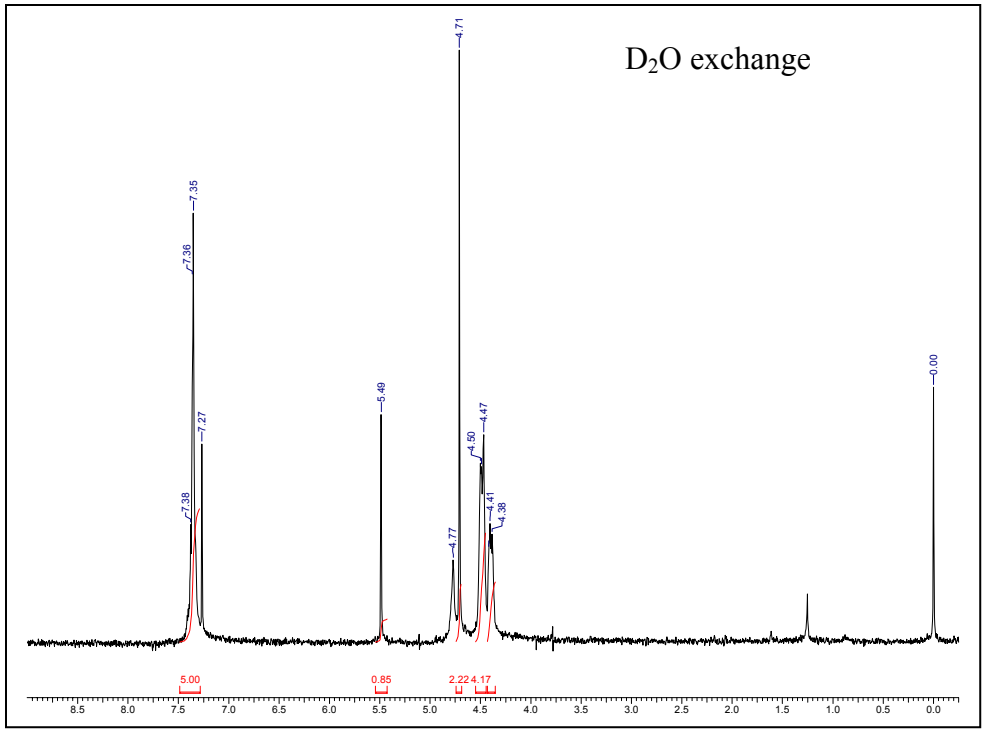
D2O exchange
4.71
7.35
7.36
5.49
7.27
0.00
7.38
4.50
4.47
4.41
4.38
4.17
5.00
0.85
2.22
4.17

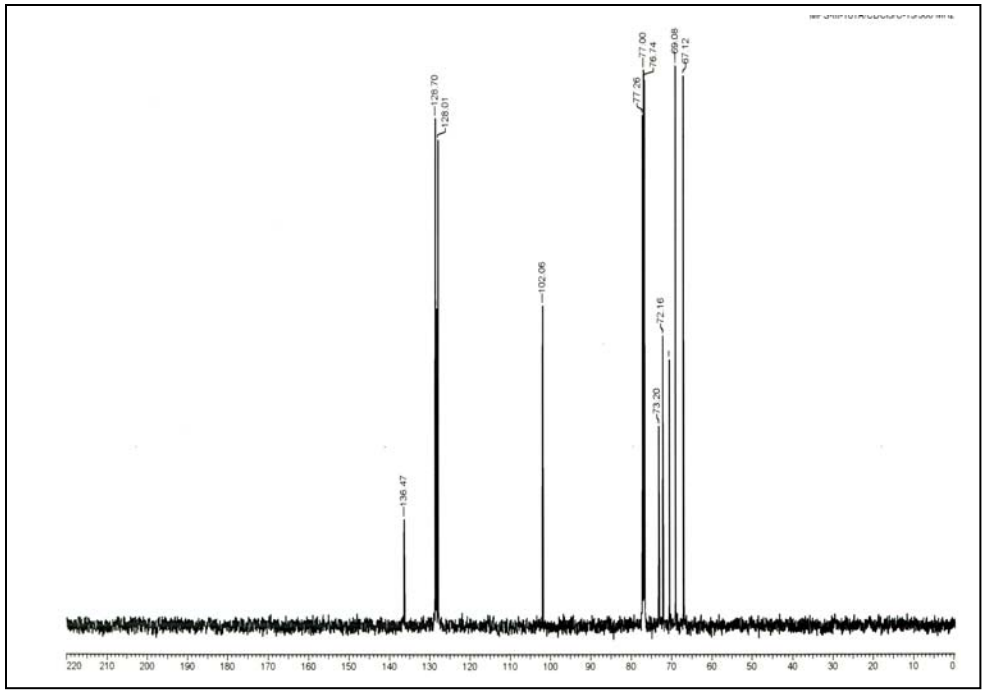
77.00
76.74
69.08
67.12
77.26
129.70
128.01
102.06
72.16
73.20
136.47

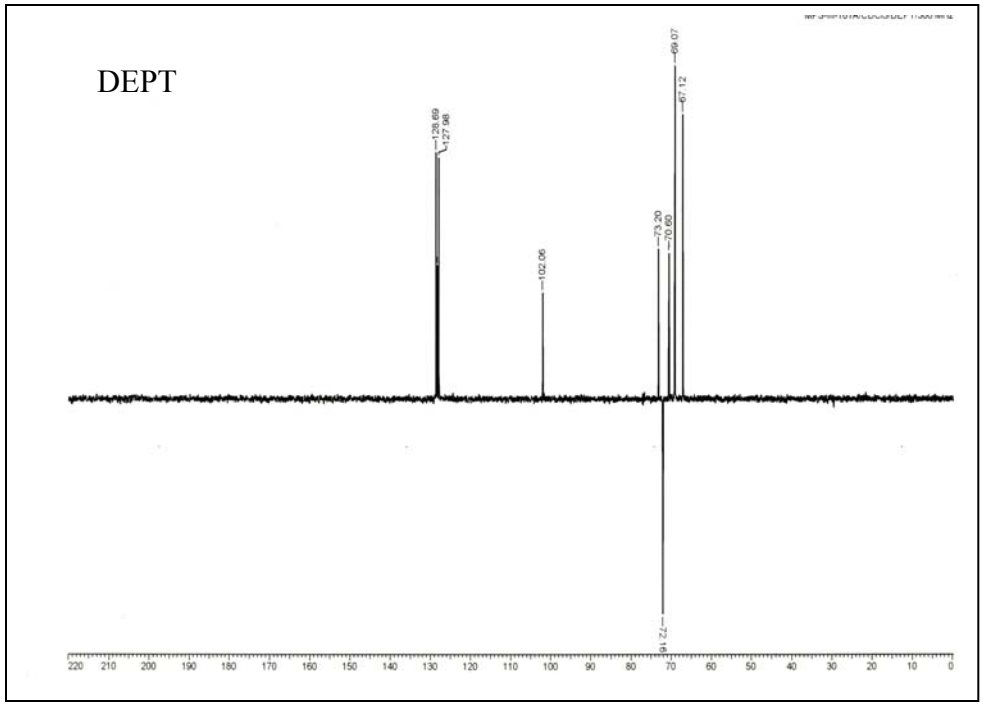
DEPT
128.69
127.98
102.06
73.20
70.60
69.07
61.12
91.21
220 210 200 190 180 170 160 150 140 130 120 110 100 90 80 70 60 50 40 30 20 10 0

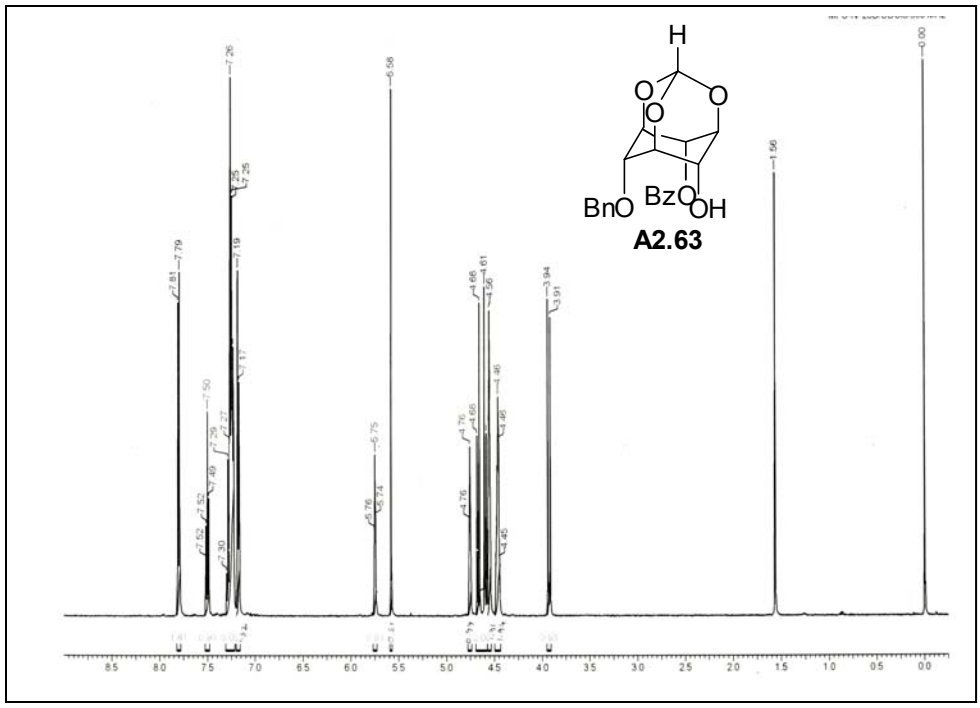
H
O
O
O
BnO
BzO
OH
A2.63
8.5 8.0 7.5 7.0 6.5 6.0 5.5 5.0 4.5 4.0 3.5 3.0 2.5 2.0 1.5 1.0 0.5 0.0

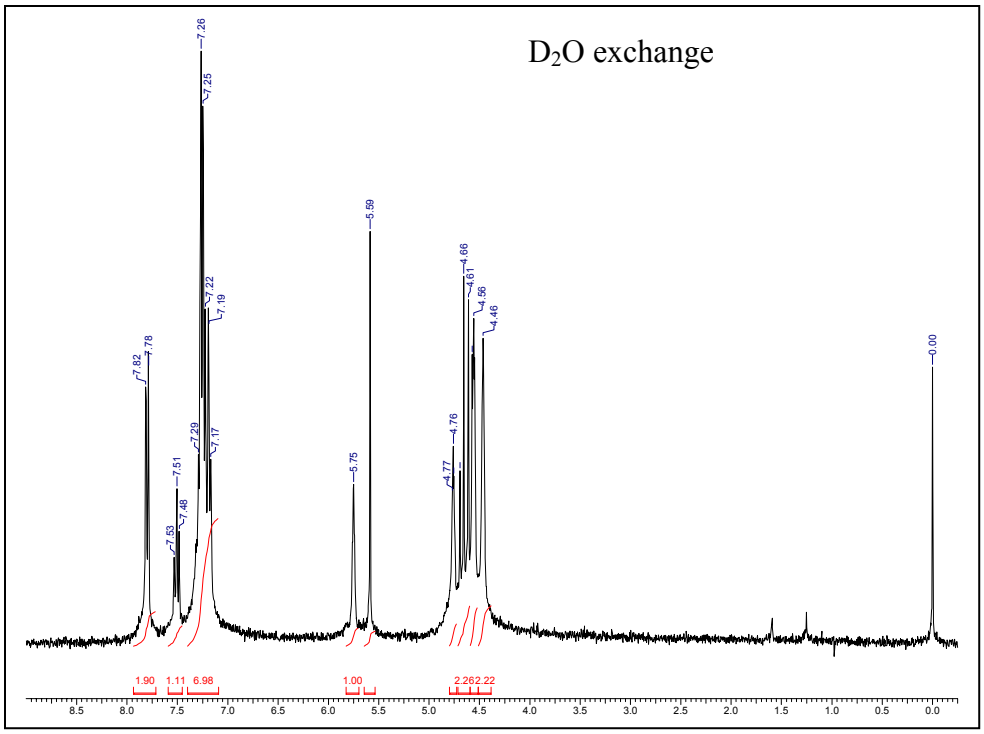
D2O exchange
7.82
7.78
7.53
7.51
7.49
7.29
7.26
7.25
7.22
7.19
7.17
5.75
5.59
4.77
4.76
4.66
4.61
4.56
4.46
0.00
1.90
1.11
6.98
1.00
2.26
2.22

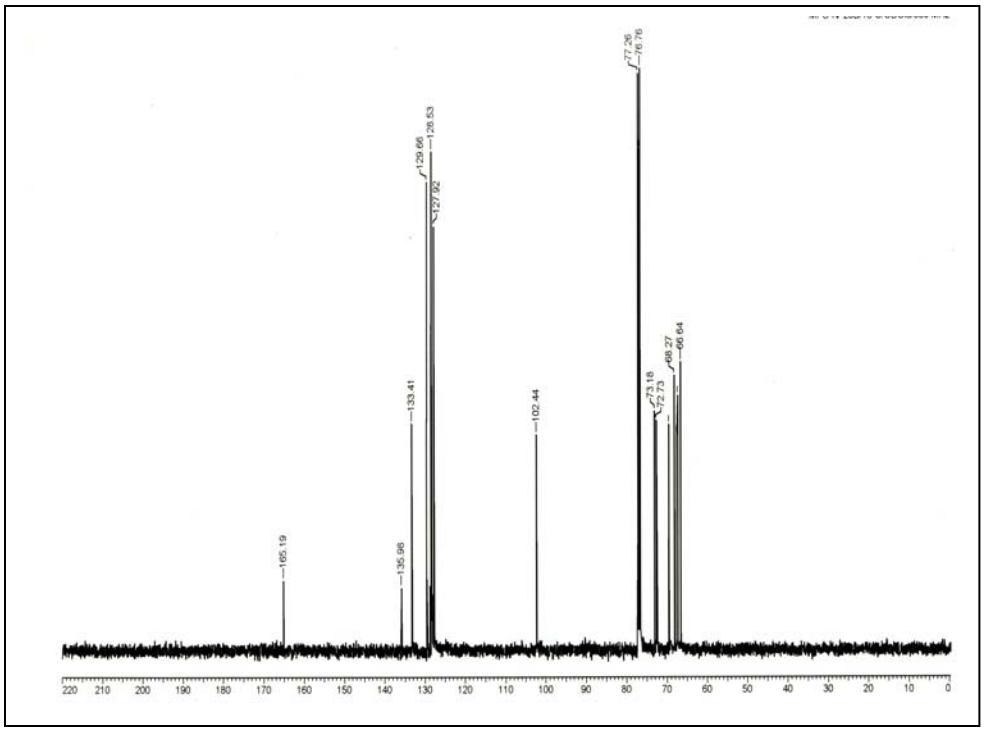
165.19
135.98
133.41
129.66
128.53
127.92
102.44
77.26
76.76
73.18
72.73
68.27
66.64

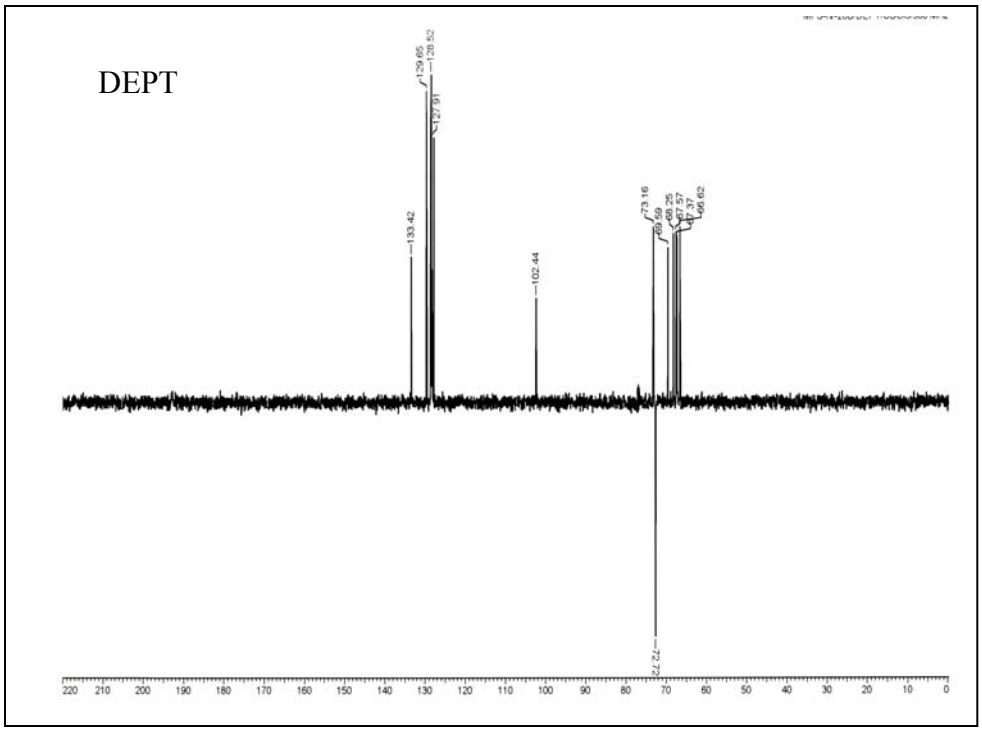
DEPT
129.65
128.52
127.91
133.42
102.44
73.16
69.59
69.25
67.37
67.17
66.62
72.72
220 210 200 190 180 170 160 150 140 130 120 110 100 90 80 70 60 50 40 30 20 10 0

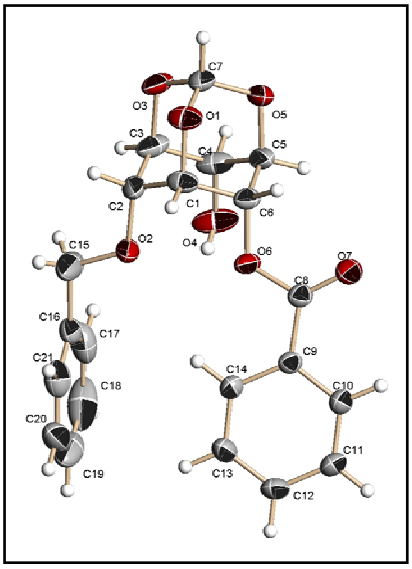

ORTEP of **A2.63**

Crystal data table of **A2.63**

Identification code	**A2.63** (crystallized from chloroform-light petroleum mixture)
Empirical formula	$C_{21}H_{20}O_7$
Formula weight	384.37
Temperature	293(2) K
Wavelength	0.71073 Å
Crystal system, space group	Triclinic, P-1
Unit cell dimensions	a = 9.817(5) Å; α = 108.038(8)º b = 10.291(5) Å; β = 107.271(8)º c = 10.492(5) Å; γ = 100.141(8)º
Volume	919.5(8) $Å^3$
Z, Calculated density	2, 1.388 Mg/m^3
Absorption coefficient	0.105 mm^{-1}
F(000)	404
Crystal size	0.57 × 0.55 × 0.08 mm
θ range for data collection	2.18 to 25.00º
Limiting indices	-11<=h<=11; -12<=k<=12; -12<=l<=12.
Reflections collected / unique	8752 / 3230 [R(int) = 0.0222]
Completeness to θ = 25.00	99.6 %
Max. and min. transmission	0.9920 and 0.9422
Refinement method	Full-matrix least-squares on F^2
Data / restraints / parameters	3230 / 0 / 254
Goodness-of-fit on F^2	1.040
Final R indices [I>2σ(I)]	R1 = 0.0590, wR2 = 0.1568
R indices (all data)	R1 = 0.0692, wR2 = 0.1670
Largest diff. peak and hole (ρ_{max} & ρ_{min})	0.275 and -0.311 e. $Å^{-3}$

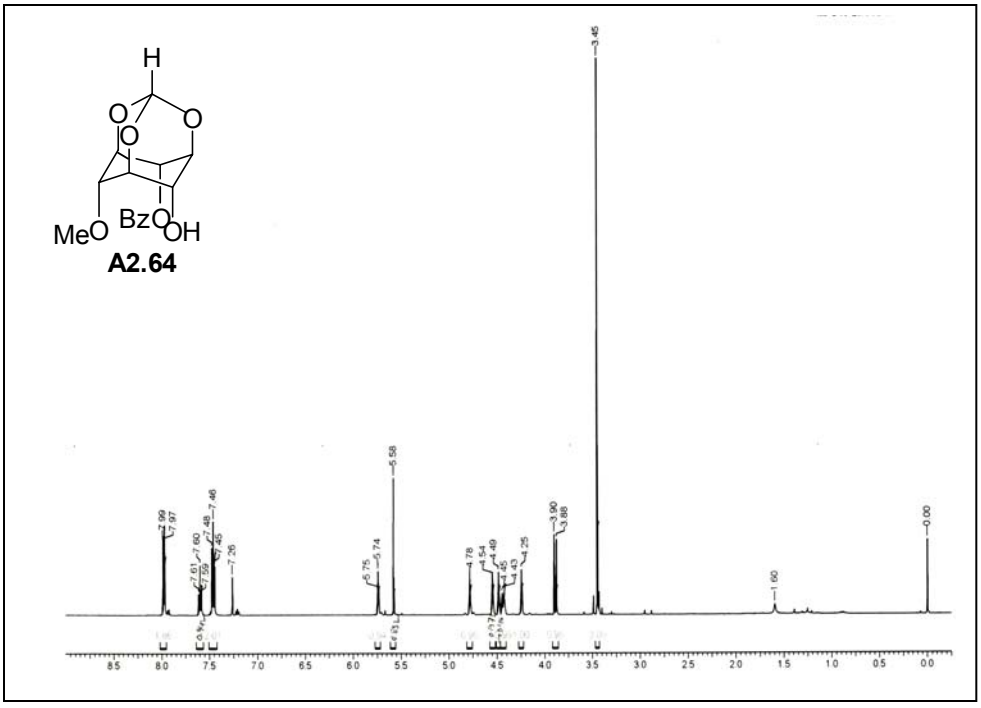
H
O
O
O
O
MeO
BzO
OH
A2.64

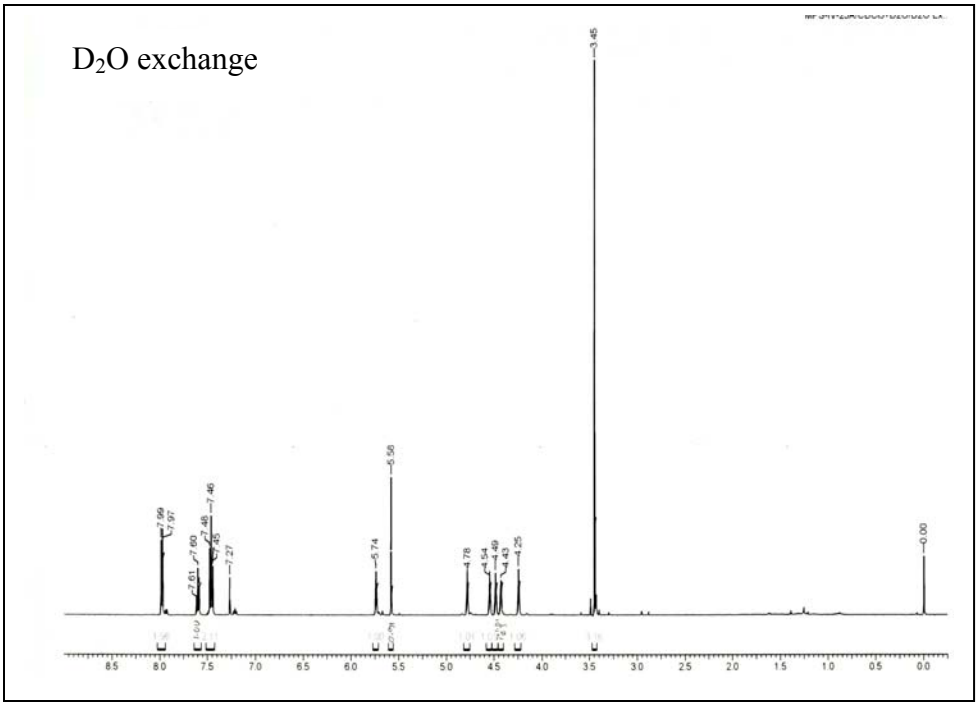
D2O exchange

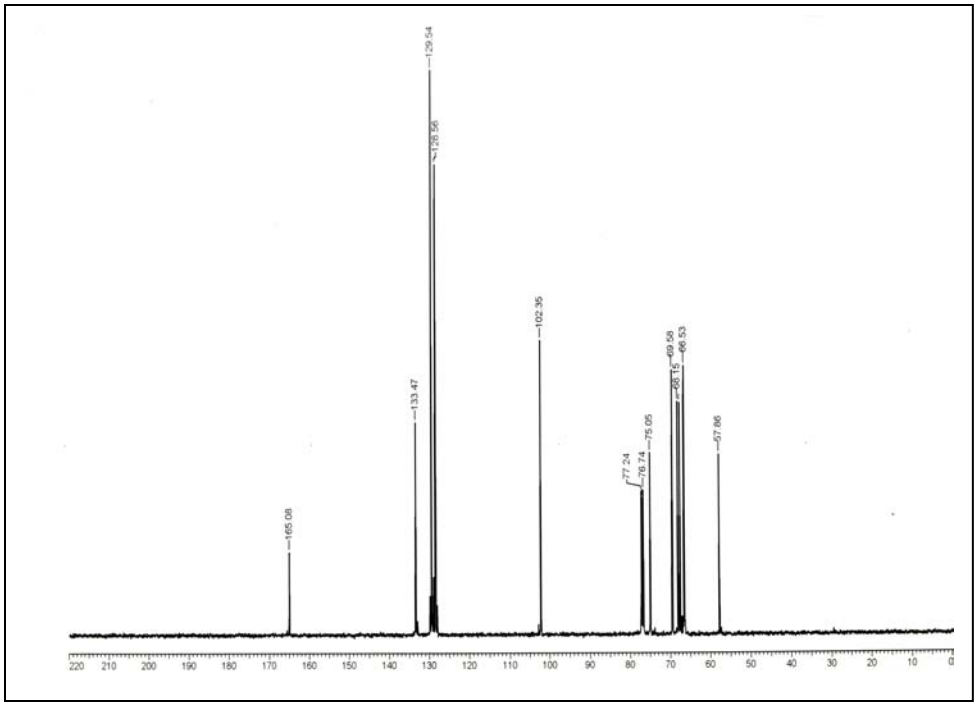
129.94
128.56
102.35
133.47
69.58
66.53
65.15
75.05
77.24
76.74
165.08
57.86
220 210 200 190 180 170 160 150 140 130 120 110 100 90 80 70 60 50 40 30 20 10 0

DEPT

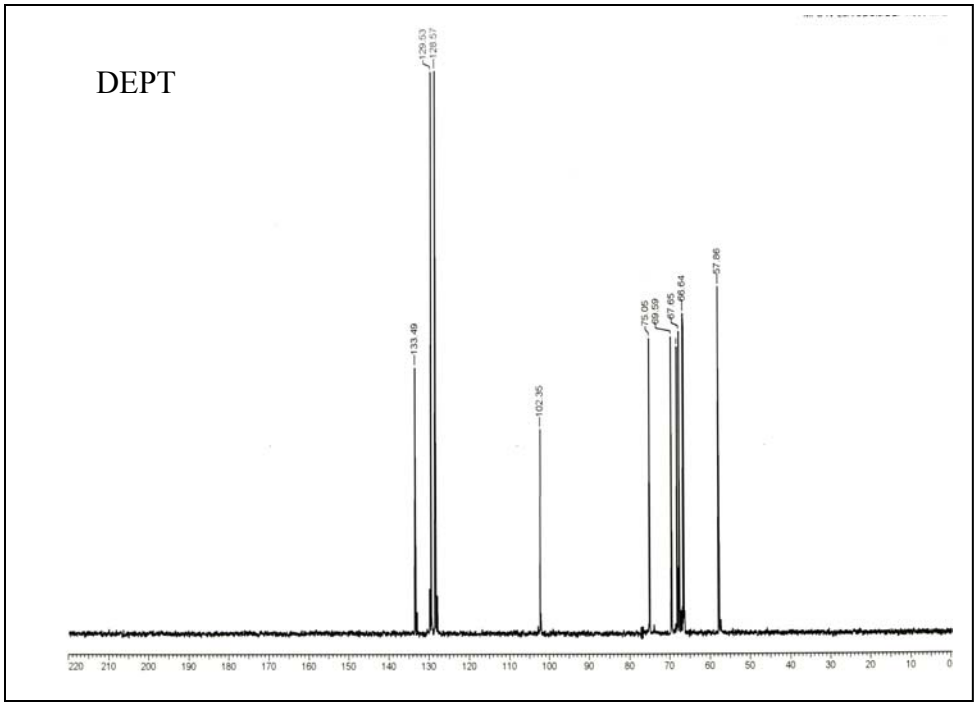
129.53
128.57
133.49
102.35
75.05
69.59
67.65
66.64
57.86
220 210 200 190 180 170 160 150 140 130 120 110 100 90 80 70 60 50 40 30 20 10 0

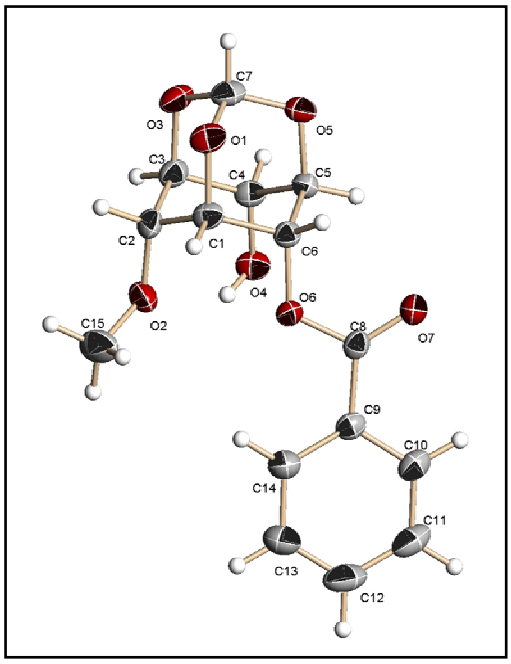

ORTEP of **A2.64**

Crystal data table of **A2.64**

Identification code	**A2.64** (crystallized from chloroform-light petroleum mixture)
Empirical formula	$C_{15}H_{16}O_7$
Formula weight	308.28
Temperature	293(2) K
Wavelength	0.71073 Å
Crystal system, space group	Monoclinic, $P2_1/n$
Unit cell dimensions	a = 6.4656(15) Å; α = 90º b = 21.597(5) Å; β = 91.478(4)º c = 10.124(2) Å; γ = 90º
Volume	1413.3(6) $Å^3$
Z, Calculated density	4, 1.449 Mg/m^3
Absorption coefficient	0.116 mm^{-1}
F(000)	648
Crystal size	0.69 × 0.20 × 0.14 mm
θ range for data collection	1.89 to 24.99º
Limiting indices	-7<=h<=6; -25<=k<=25; -12<=l<=11.
Reflections collected / unique	6939 / 2484 [R(int) = 0.0210]
Completeness to θ = 24.99	99.8 %
Max. and min. transmission	0.9834 and 0.9239
Refinement method	Full-matrix least-squares on F^2
Data / restraints / parameters	2484 / 0 / 201
Goodness-of-fit on F^2	1.077
Final R indices [I>2σ(I)]	R1 = 0.0469, wR2 = 0.1151
R indices (all data)	R1 = 0.0565, wR2 = 0.1213
Largest diff. peak and hole (ρ_{max} & ρ_{min})	0.300 and -0.158 e. $Å^{-3}$

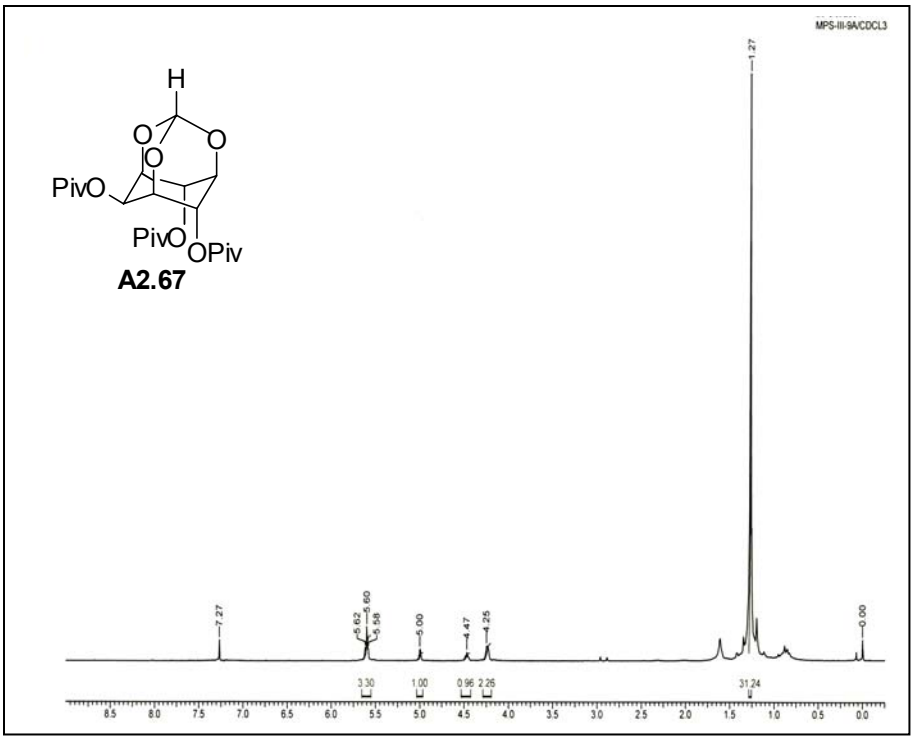
MPS-III-9A/CDCL3
H
O
O
O
PivO
PivO
OPiv
A2.67
1.27
7.27
5.62
5.60
5.58
5.00
4.47
4.25
0.00
3.30
1.00
0.96
2.26
31.24

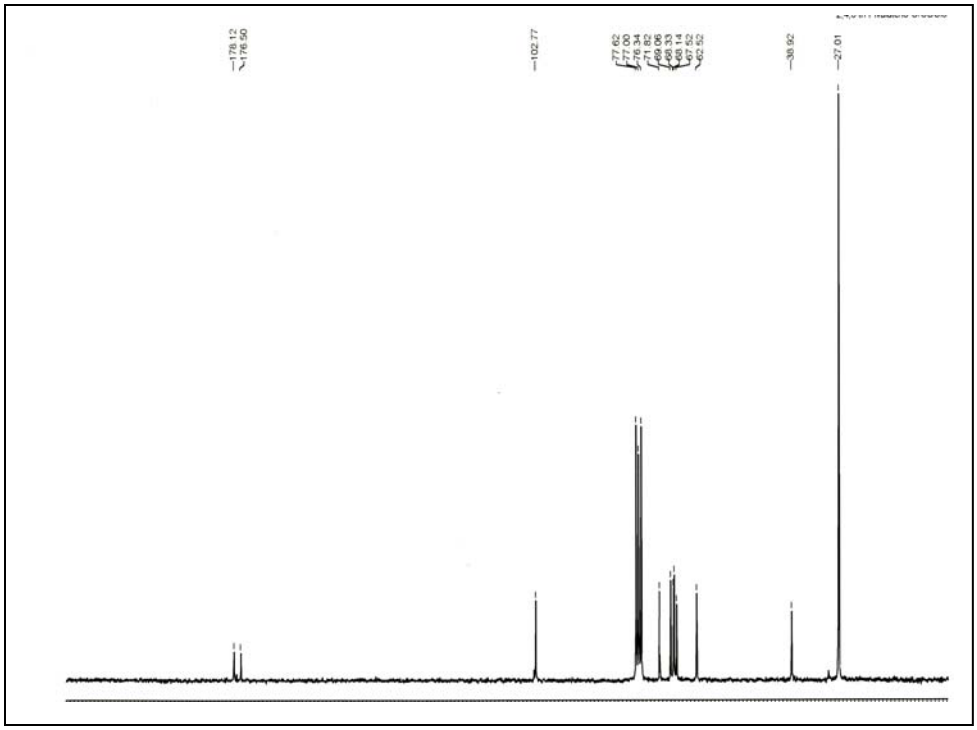
178.12
176.50
102.77
77.62
77.00
76.34
71.82
69.06
68.33
68.14
67.52
62.52
38.92
27.01

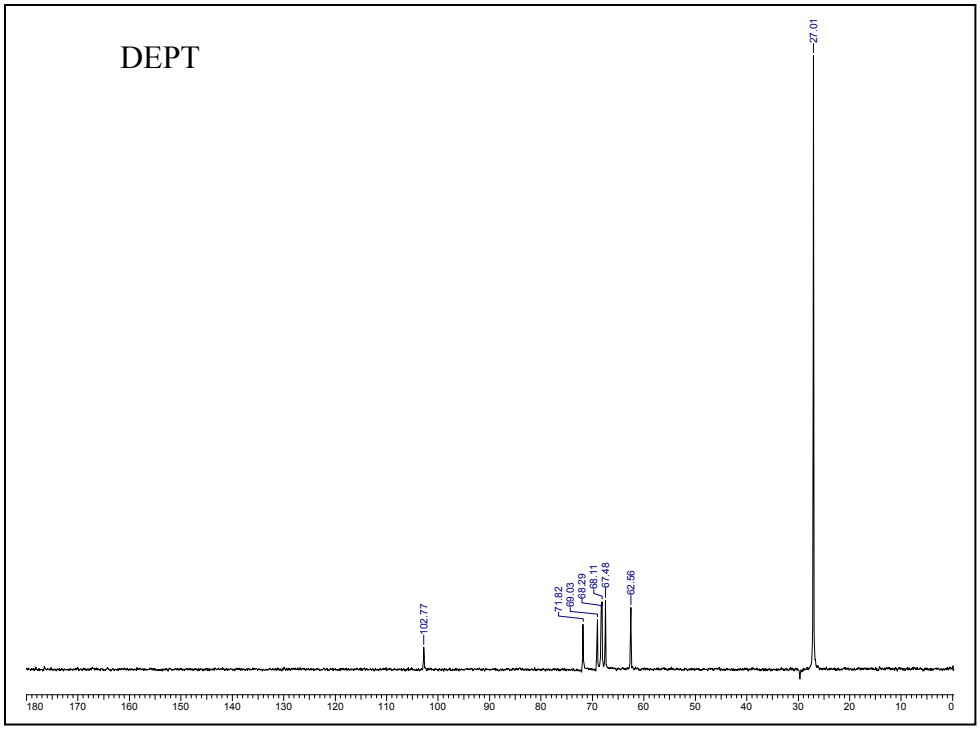
DEPT
27.01
102.77
71.82
69.03
68.29
68.11
67.48
62.56
180
170
160
150
140
130
120
110
100
90
80
70
60
50
40
30
20
10
0

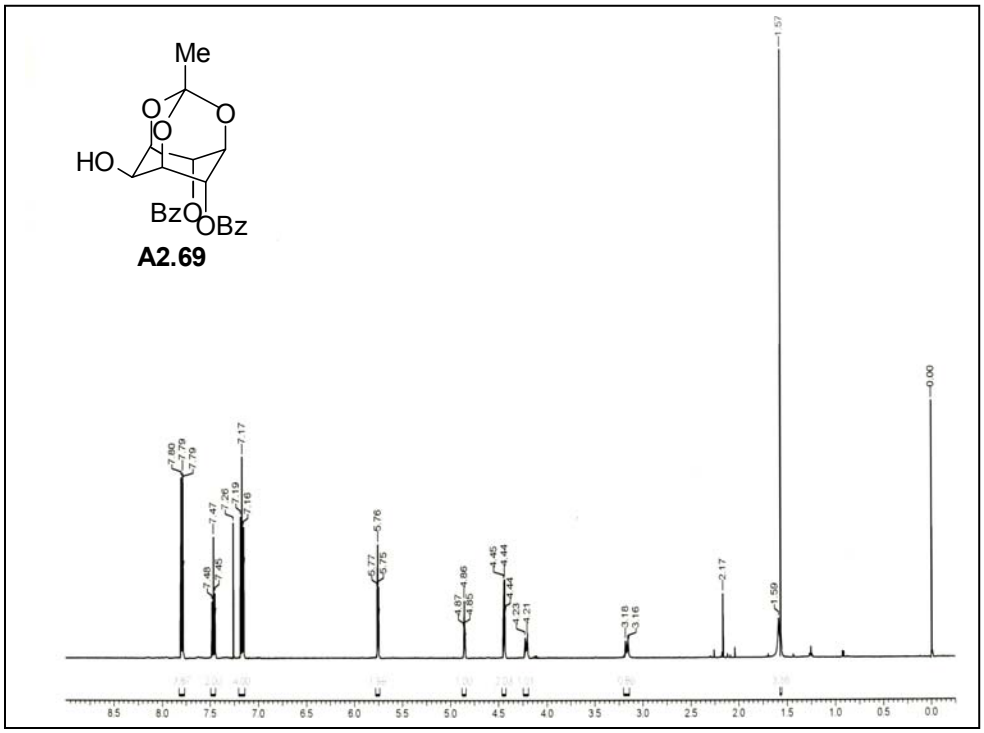
Me
O
O
O
HO
BzO
OBz
A2.69

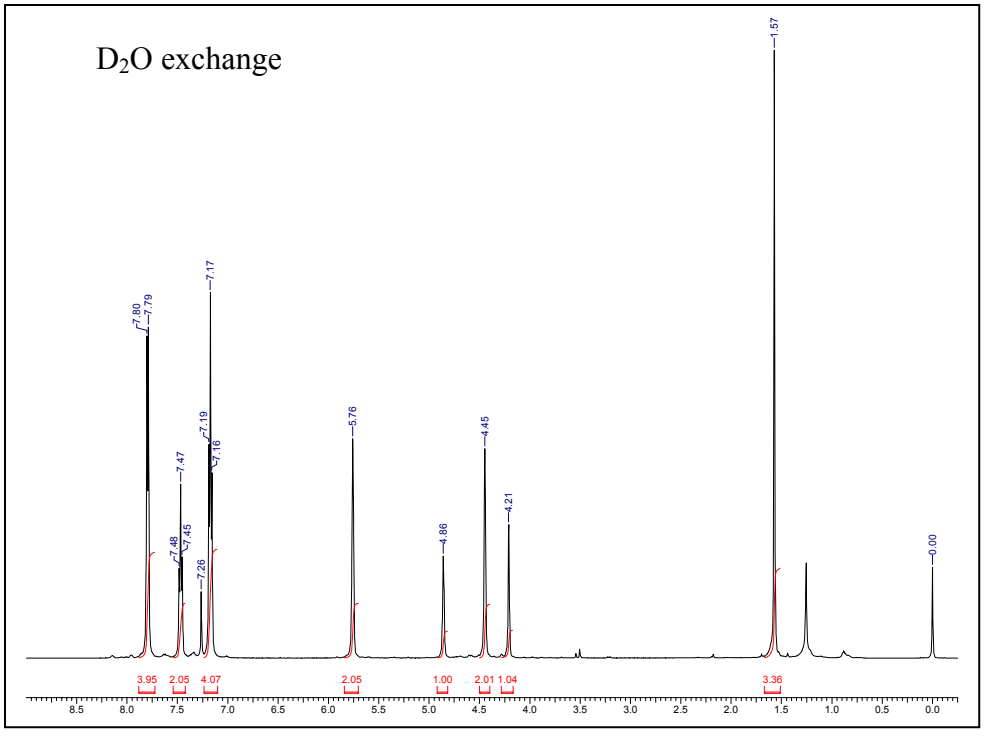
D2O exchange

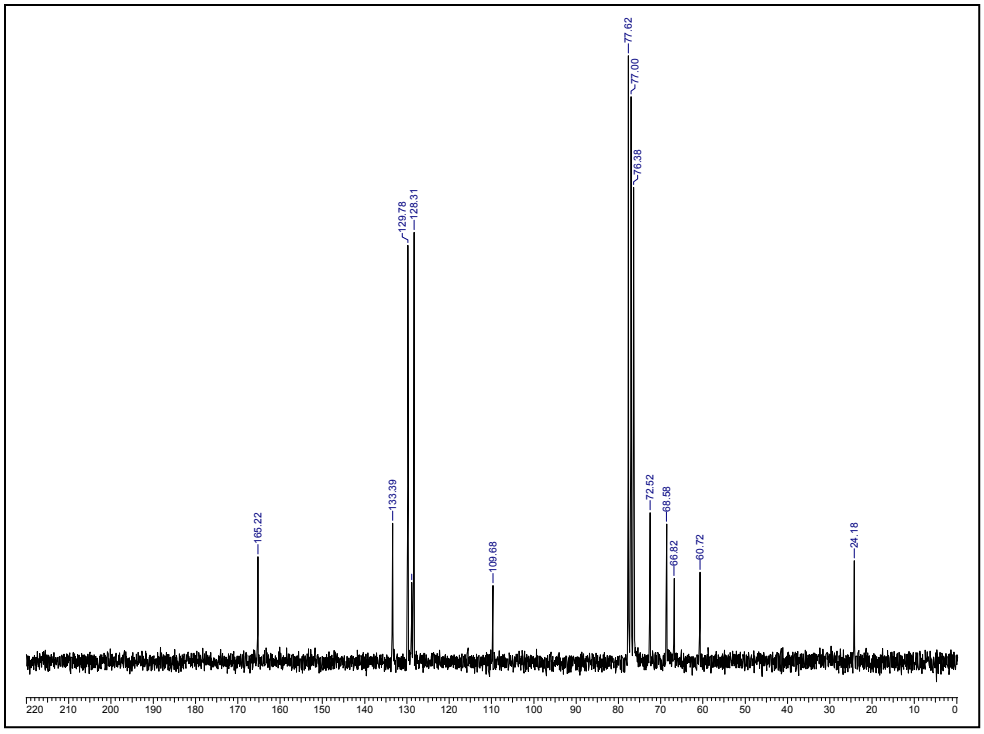
77.62
77.00
76.38
129.78
128.31
165.22
133.39
109.68
72.52
68.58
66.82
60.72
24.18

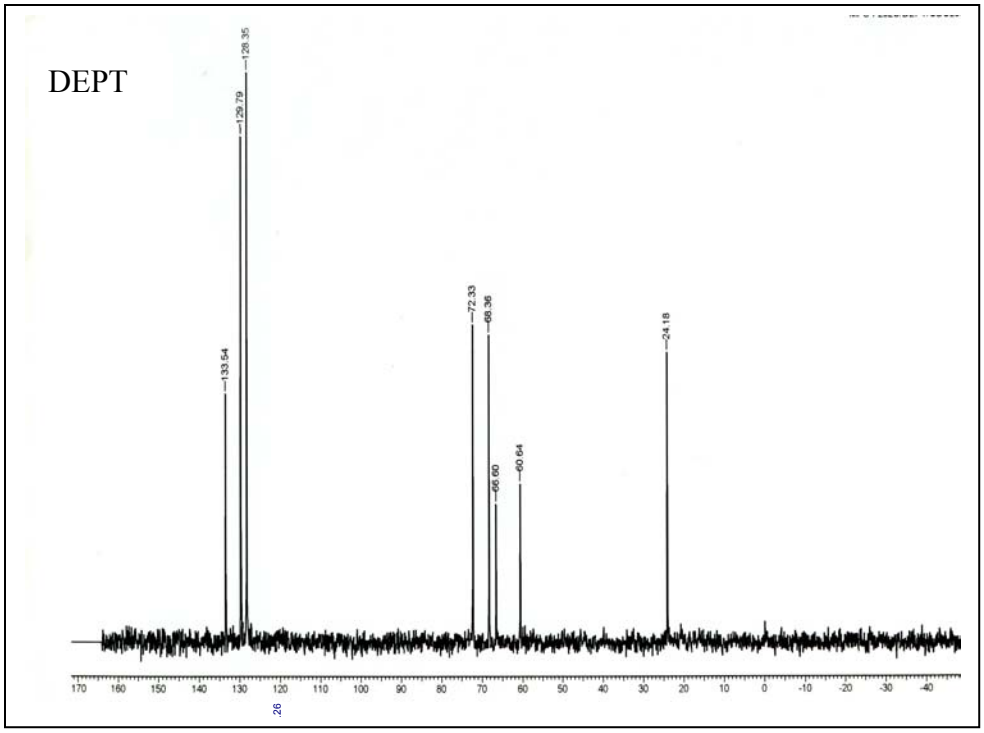
DEPT
129.35
129.79
133.54
72.33
68.36
65.60
60.64
24.18

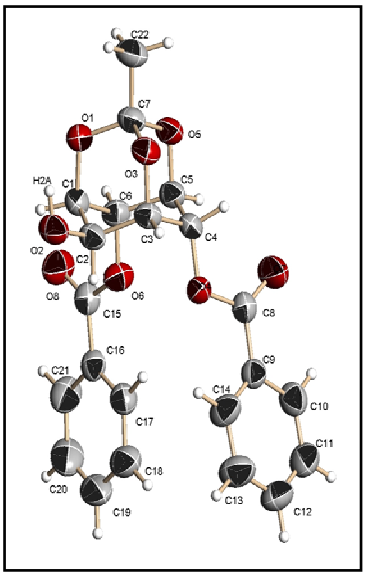

ORTEP of **A2.69**

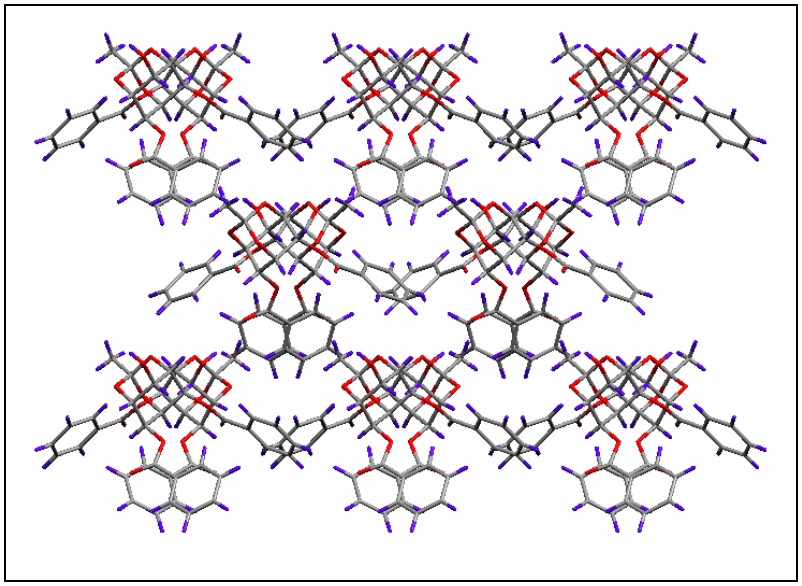

Packing of **A2.69** down the a axis

Crystal data table of **A2.69**

Identification code	**A2.69** (crystallized from chloroform-light petroleum mixture)
Empirical formula	$C_{22}H_{20}O_8$
Formula weight	412.38
Temperature	566(2) K
Wavelength	0.71073 Å
Crystal system, space group	Orthorhombic, $Pna2_1$
Unit cell dimensions	a = 11.646(3) Å; α = 90º b = 11.101(2) Å; β = 90º c = 14.949(3) Å; γ = 90º
Volume	1932.7(7) $Å^3$
Z, Calculated density	4, 1.417 Mg/m^3
Absorption coefficient	0.119 mm^{-1}
F(000)	864
Crystal size	0.65 × 0.13 × 0.13 mm
θ range for data collection	2.53 to 25.00º
Limiting indices	-13<=h<=13; -10<=k<=13; -17<=l<=17.
Reflections collected / unique	9116 / 3374 [R(int) = 0.0220]
Completeness to θ = 24.99	99.8 %
Max. and min. transmission	0.9860 and 0.9323
Refinement method	Full-matrix least-squares on F^2
Data / restraints / parameters	3374 / 1 / 351
Goodness-of-fit on F^2	1.059
Final R indices [I>2σ(I)]	R1 = 0.0297, wR2 = 0.0631
R indices (all data)	R1 = 0.0353, wR2 = 0.0653
Largest diff. peak and hole (ρ_{max} & ρ_{min})	0.094 and -0.131 e. $Å^{-3}$

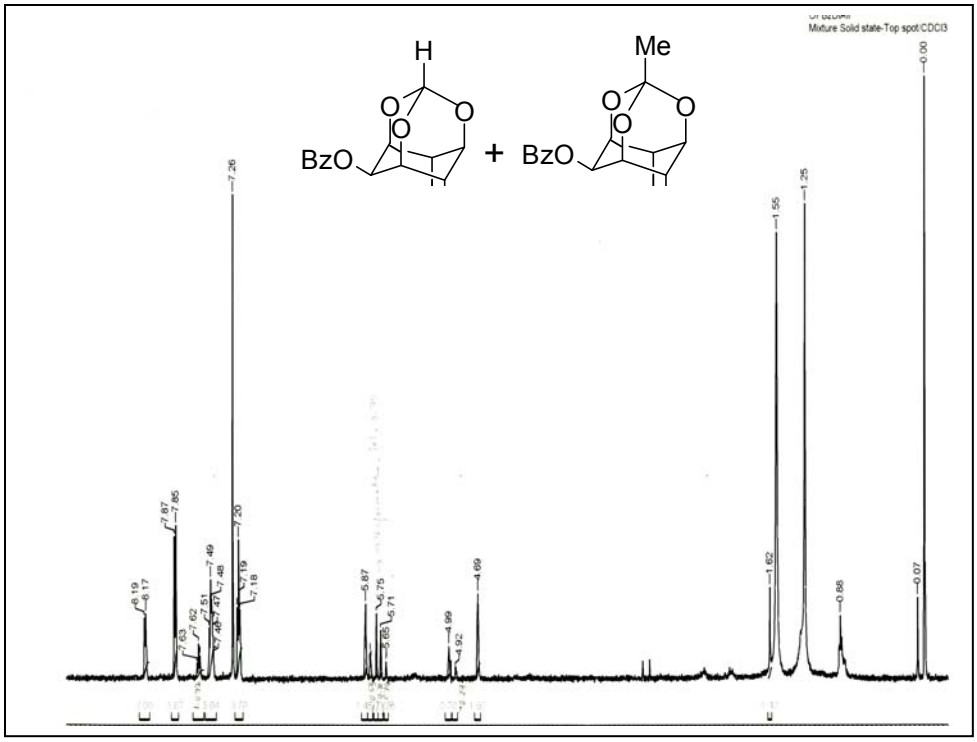
Mixture Solid state-Top spot/CDCl3
H
Me
BzO
BzO
+

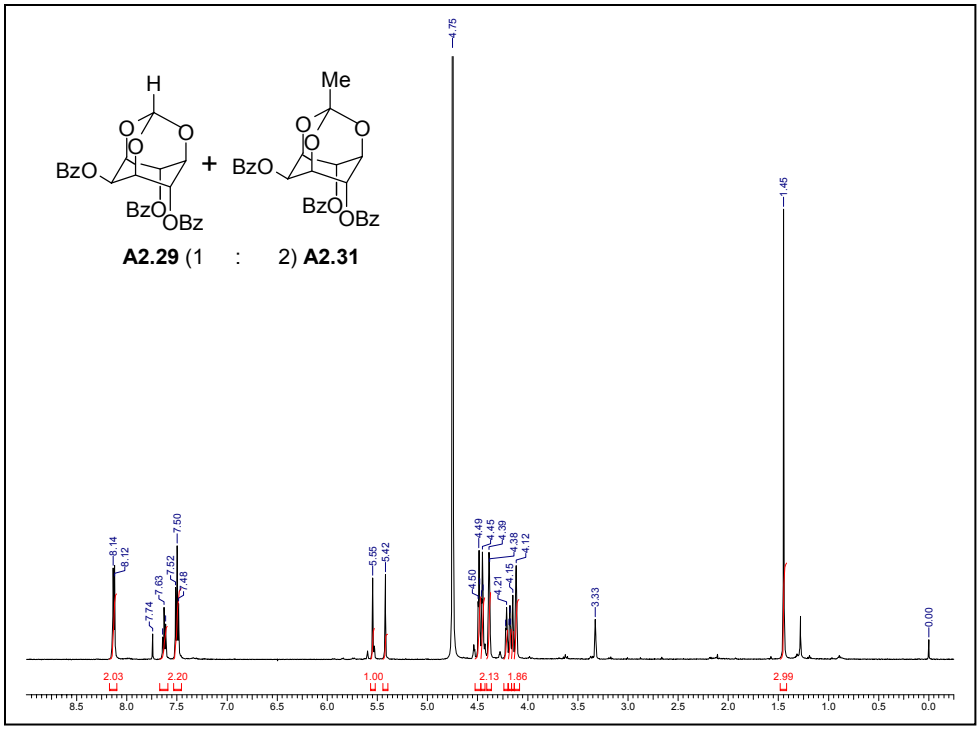
H
Me
BzO
BzO
OBz
BzO
BzO
OBz
+
A2.29 (1 : 2) A2.31

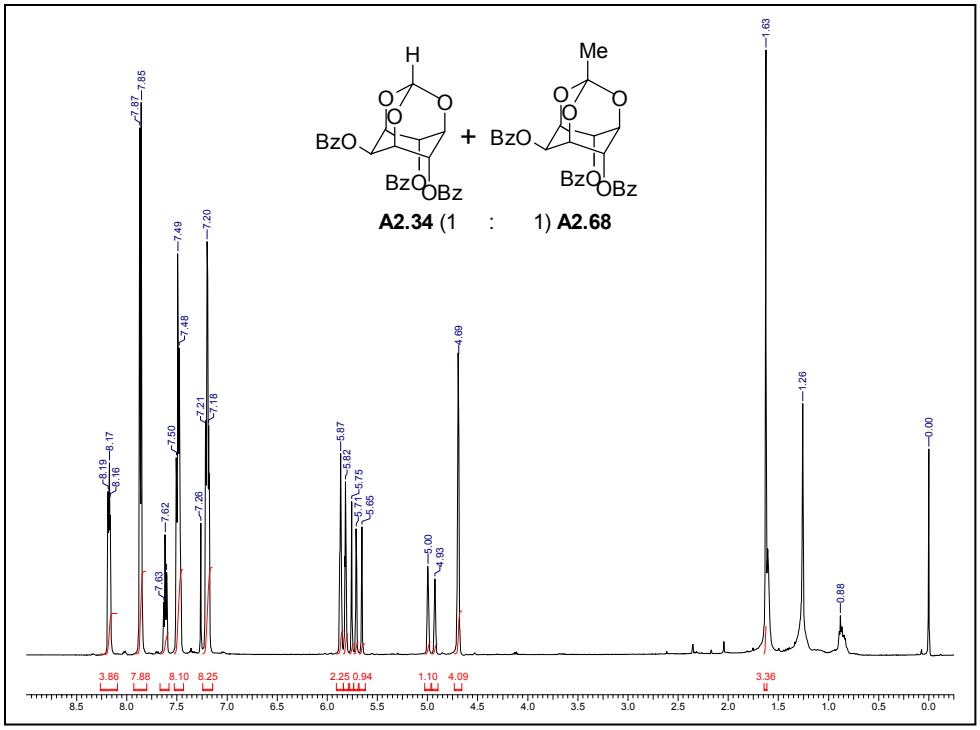
H
Me
BzO
OBz
A2.34 (1 : 1) A2.68

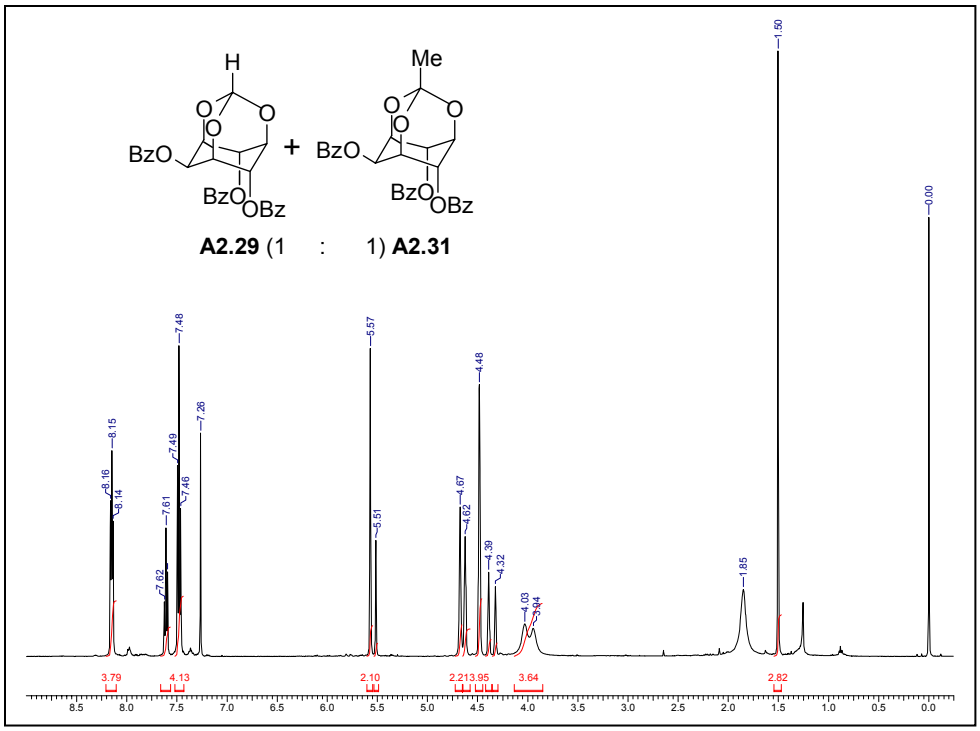
H
Me
BzO
OBz
A2.29 (1 : 1) A2.31

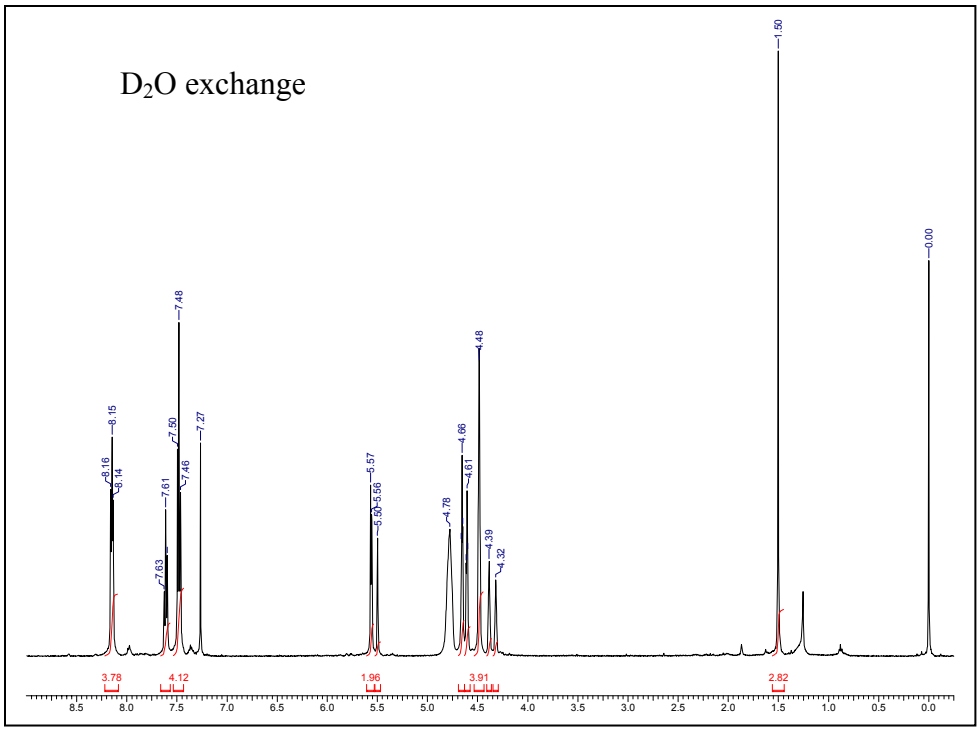
D2O exchange
8.16
8.15
8.14
7.63
7.61
7.50
7.48
7.46
7.27
5.57
5.56
5.50
4.78
4.66
4.61
4.48
4.39
4.32
1.50
0.00
3.78
4.12
1.96
3.91
2.82

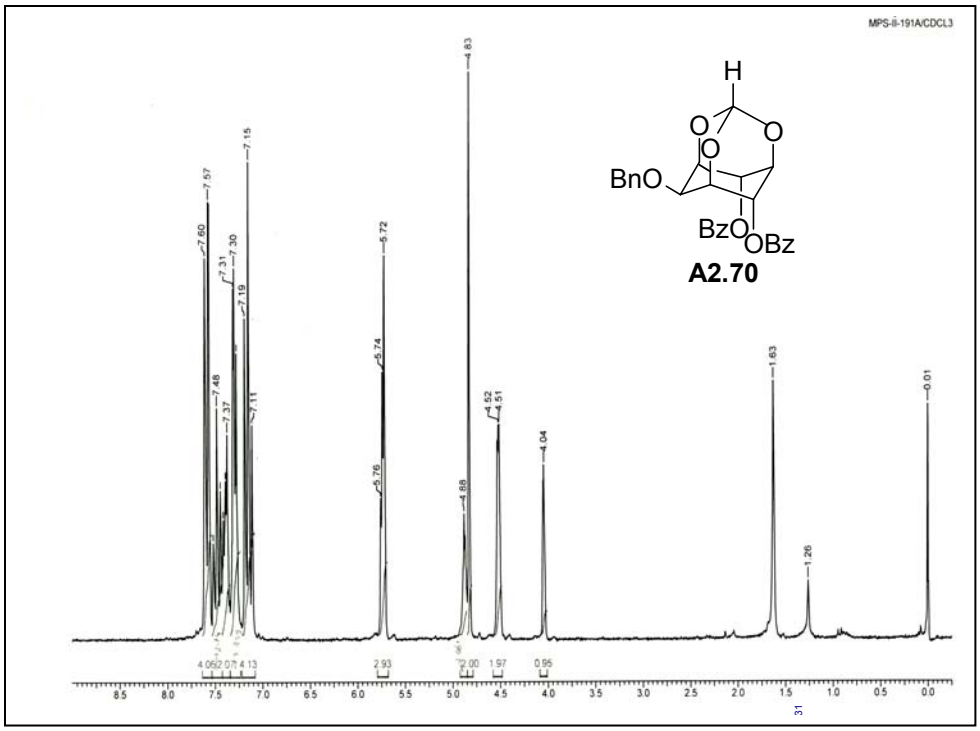
MPS-II-191A/CDCL3
H
O
O
O
BnO
BzO
OBz
A2.70
7.57
7.60
7.31
7.30
7.19
7.15
7.48
7.37
7.11
5.72
5.74
5.76
4.83
4.88
4.52
4.51
4.04
1.63
1.26
0.01

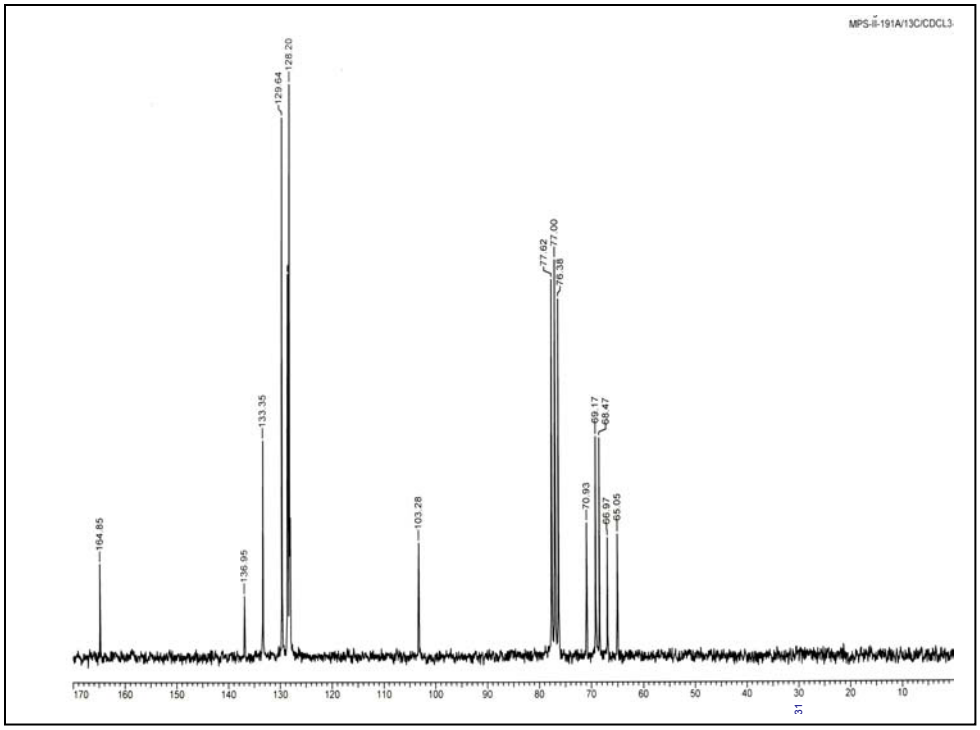
MPS-II-191A/13C/CDCL3
164.85
136.95
133.35
129.64
128.20
103.28
77.62
77.00
76.38
70.93
69.17
68.47
66.97
65.05

DEPT

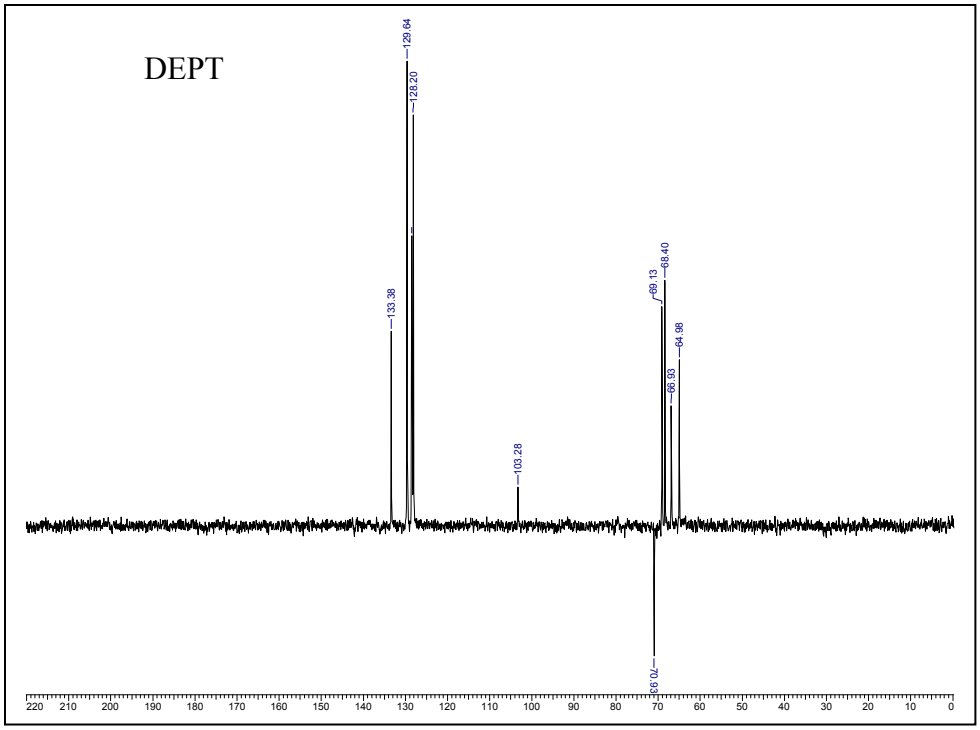
129.64
128.20
133.38
103.28
69.13
68.40
64.98
66.93
70.93

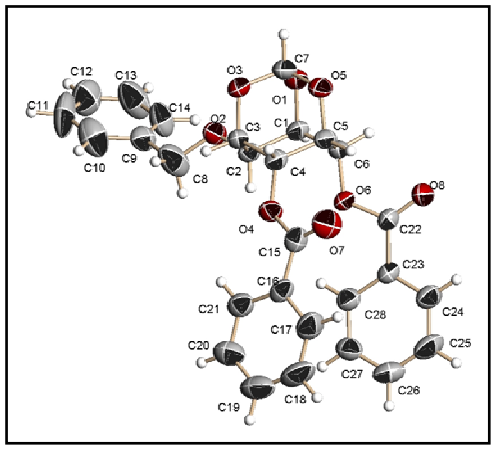

ORTEP of **A2.70**

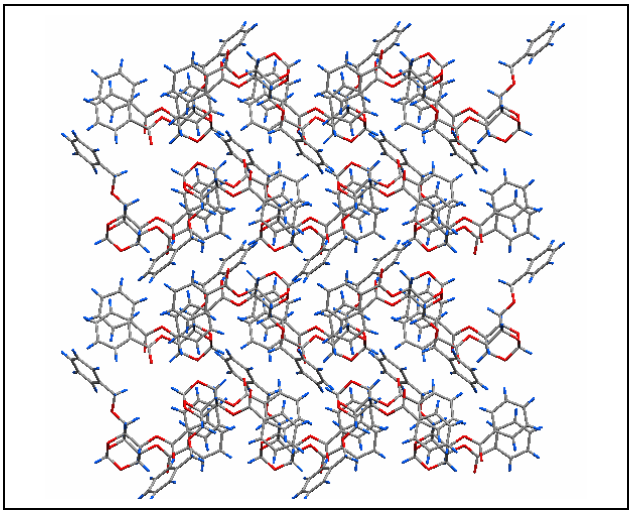

Packing of **A2.70** down the c axis

Crystal data table of **A2.70**

Identification code	**A2.70** (crystallized from chloroform-light petroleum mixture)
Empirical formula	$C_{28}H_{24}O_8$
Formula weight	488.27
Temperature	569(2) K
Wavelength	0.71073 Å
Crystal system, space group	Monoclinic, $P2_1/n$
Unit cell dimensions	a = 11.313(12) Å; α = 90º b = 16.051(17) Å; β = 92.29(2)º c = 12.964(14) Å; γ = 90º
Volume	2352(4) $Å^3$
Z, Calculated density	4, 1.379 Mg/m^3
Absorption coefficient	0.102 mm^{-1}
F(000)	1024
Crystal size	0.54 × 0.14 × 0.07 mm
θ range for data collection	2.02 to 25.00º
Limiting indices	-13<=h<=6; -18<=k<=19; -15<=l<=15.
Reflections collected / unique	11379 / 4127 [R(int) = 0.0353]
Completeness to θ = 24.99	99.6 %
Max. and min. transmission	0.9934 and 0.9475
Refinement method	Full-matrix least-squares on F^2
Data / restraints / parameters	4127 / 0 / 325
Goodness-of-fit on F^2	1.071
Final R indices [I>2σ(I)]	R1 = 0.0592, wR2 = 0.1282
R indices (all data)	R1 = 0.0958, wR2 = 0.1440
Largest diff. peak and hole (ρ_{max} & ρ_{min})	0.537 and -0.243 e. $Å^{-3}$

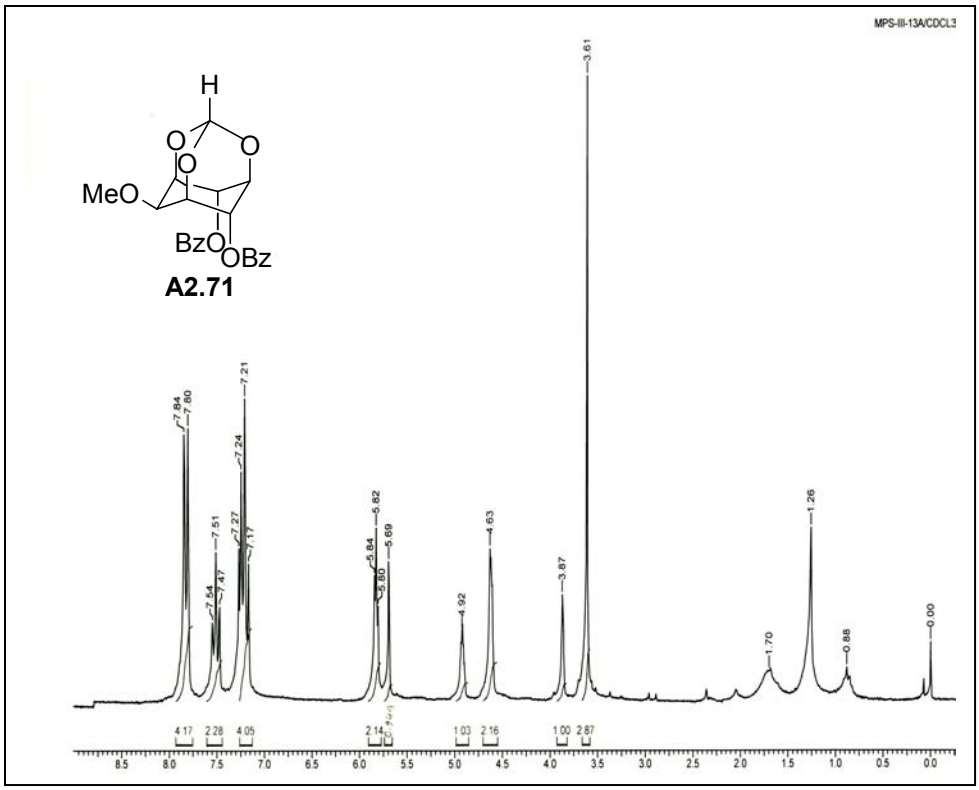
MPS-III-13A/CDCL3
H
O
O
O
O
MeO
BzO
OBz
A2.71
7.84
7.80
7.51
7.47
7.54
7.24
7.27
7.17
7.21
5.84
5.82
5.80
5.69
4.92
4.63
3.87
3.61
1.70
1.26
0.88
0.00
4.17
2.28
4.05
2.14
1.03
2.16
1.00
2.87

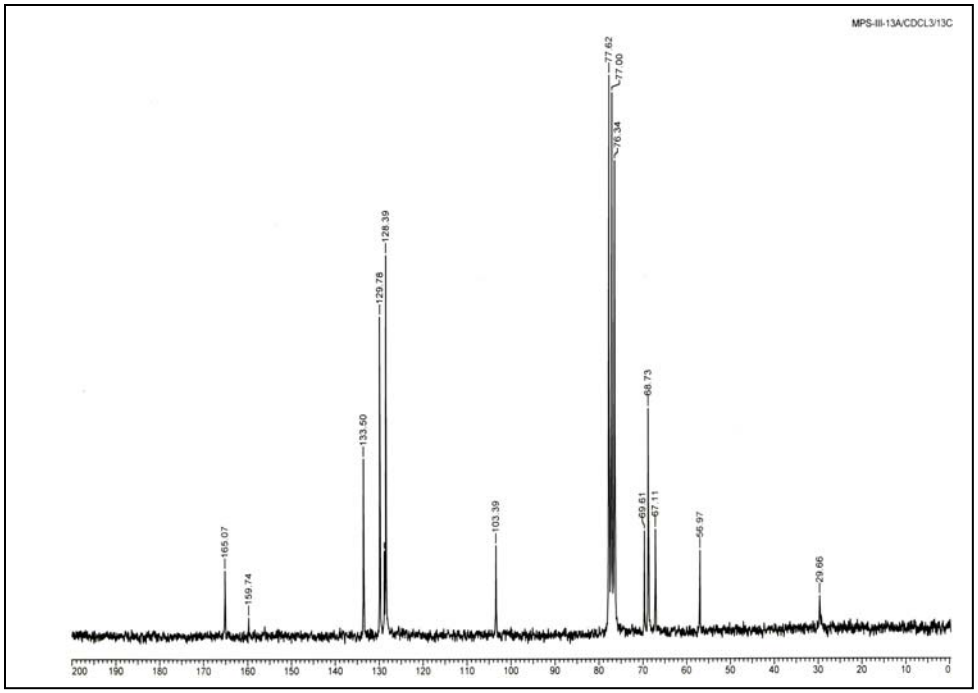
MPS-III-13A/CDCL3/13C
77.62
77.00
76.34
128.39
129.78
133.50
165.07
159.74
103.39
69.73
69.61
67.11
56.97
29.66

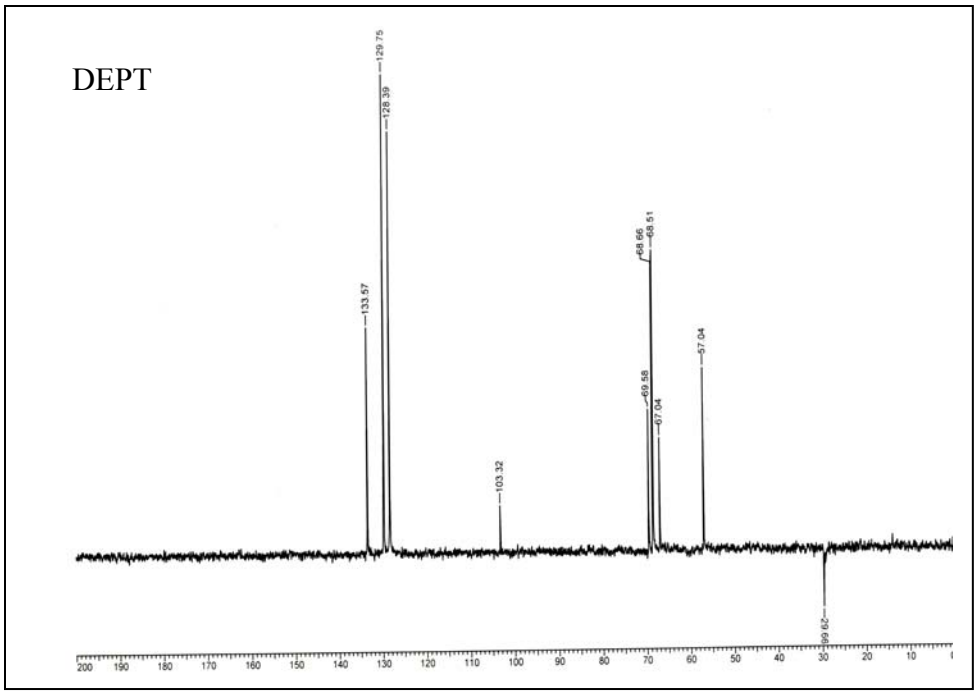
DEPT
129.75
128.39
133.57
103.32
68.66
68.51
69.58
67.04
57.04
39.62

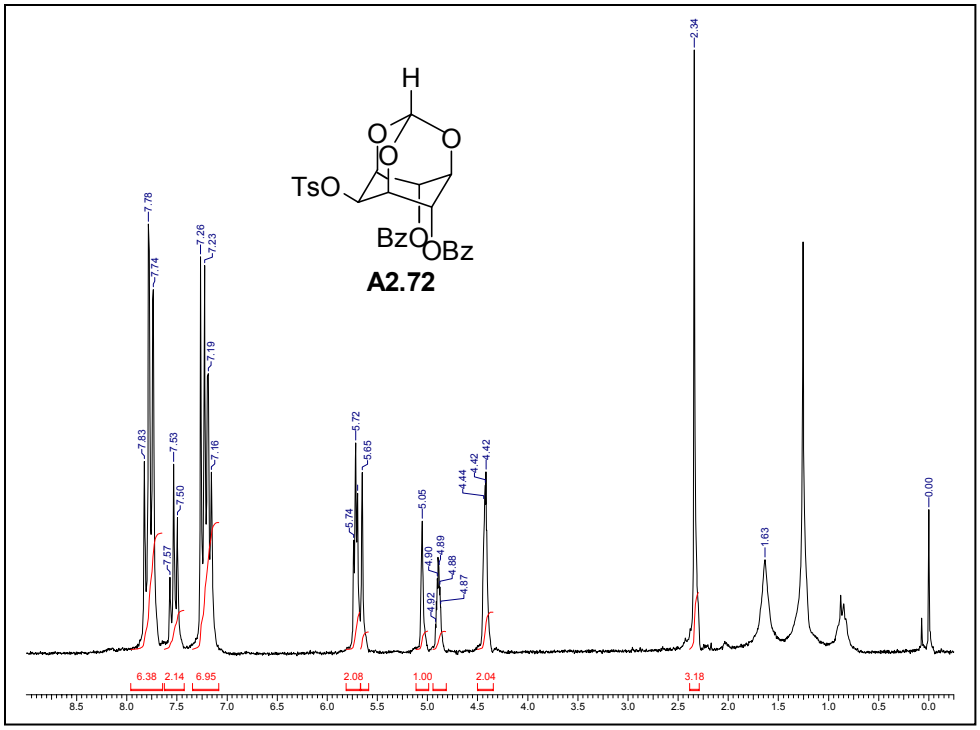
H
O
O
O
TsO
BzO
OBz
A2.72
2.34
7.78
7.74
7.26
7.23
7.19
7.83
7.53
7.50
7.16
7.57
5.72
5.65
5.74
5.05
4.90
4.89
4.88
4.87
4.92
4.44
4.42
4.42
1.63
0.00
6.38
2.14
6.95
2.08
1.00
2.04
3.18

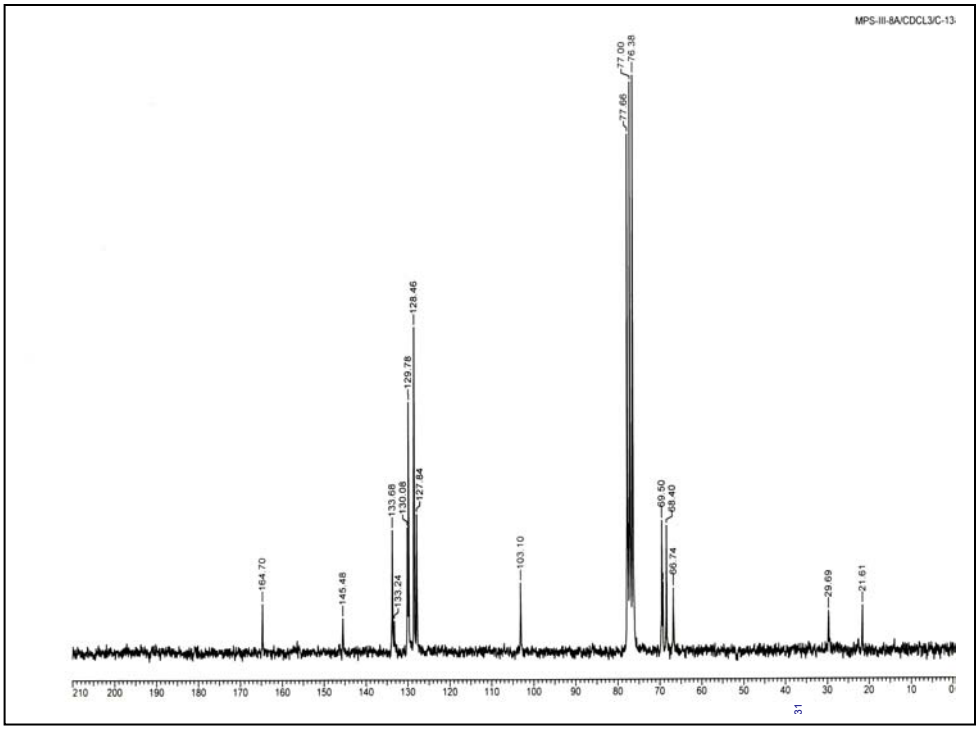
MPS-III-8A/CDCL3/C-13-
77.09
76.38
77.66
128.46
129.76
133.68
130.08
127.84
69.50
68.40
164.70
145.48
133.24
103.10
66.74
29.69
21.61
31

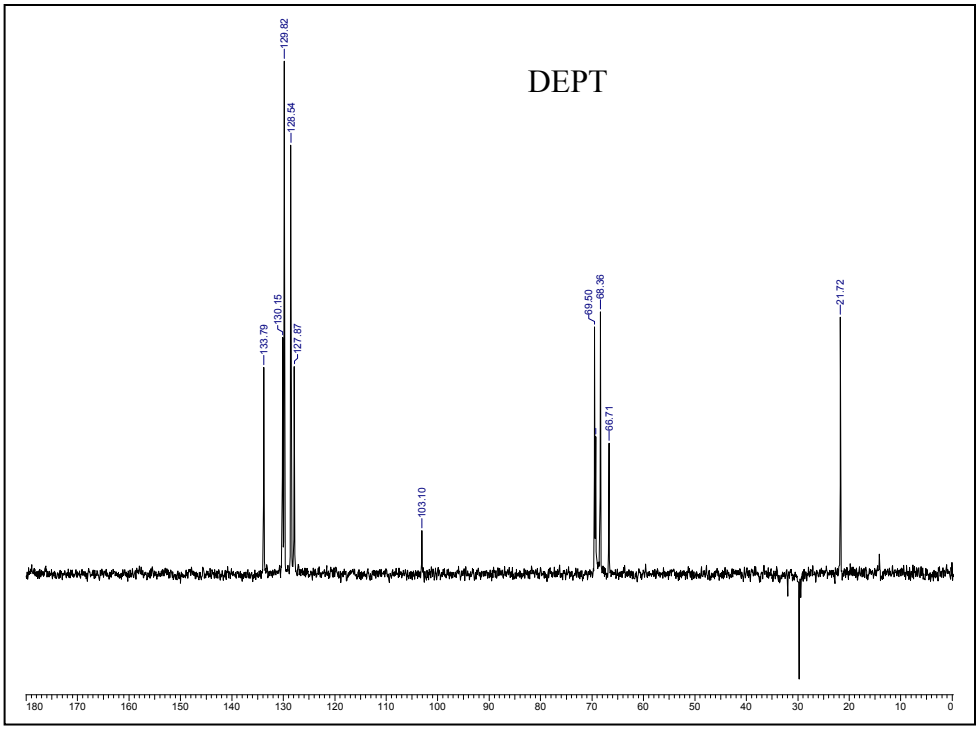
DEPT
129.82
128.54
133.79
130.15
127.87
69.50
68.36
66.71
103.10
21.72

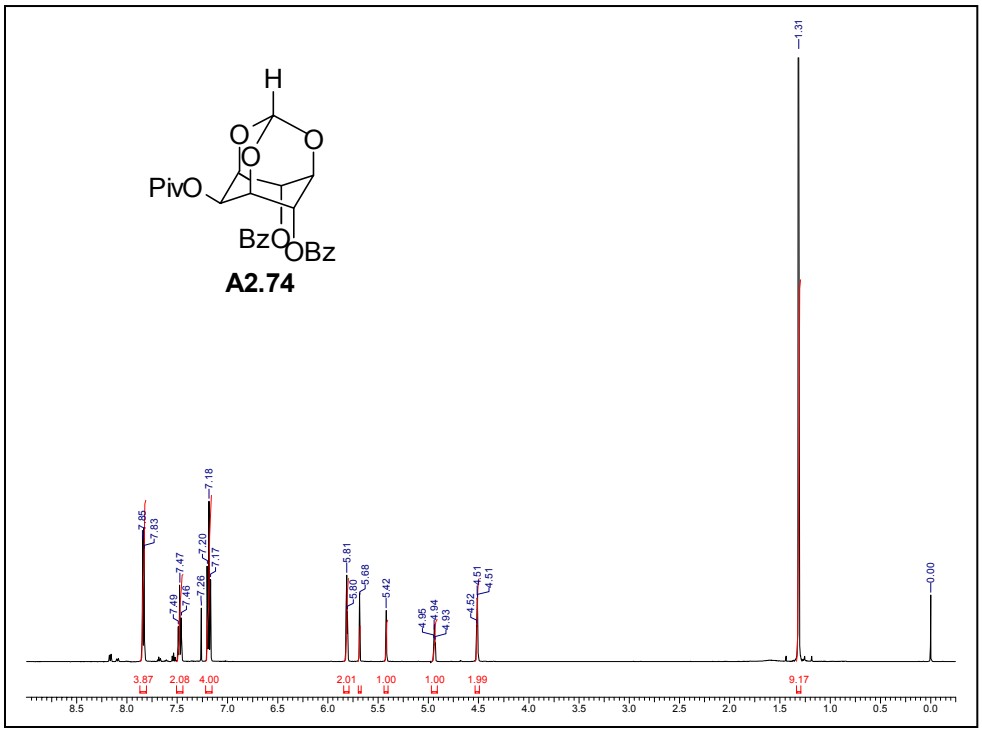
H
O
O
O
PivO
BzO
OBz
A2.74
1.31
7.86
7.83
7.47
7.46
7.40
7.26
7.20
7.18
7.17
5.81
5.80
5.68
5.42
4.95
4.94
4.93
4.52
4.51
4.51
0.00
3.87
2.08
4.00
2.01
1.00
1.00
1.99
9.17

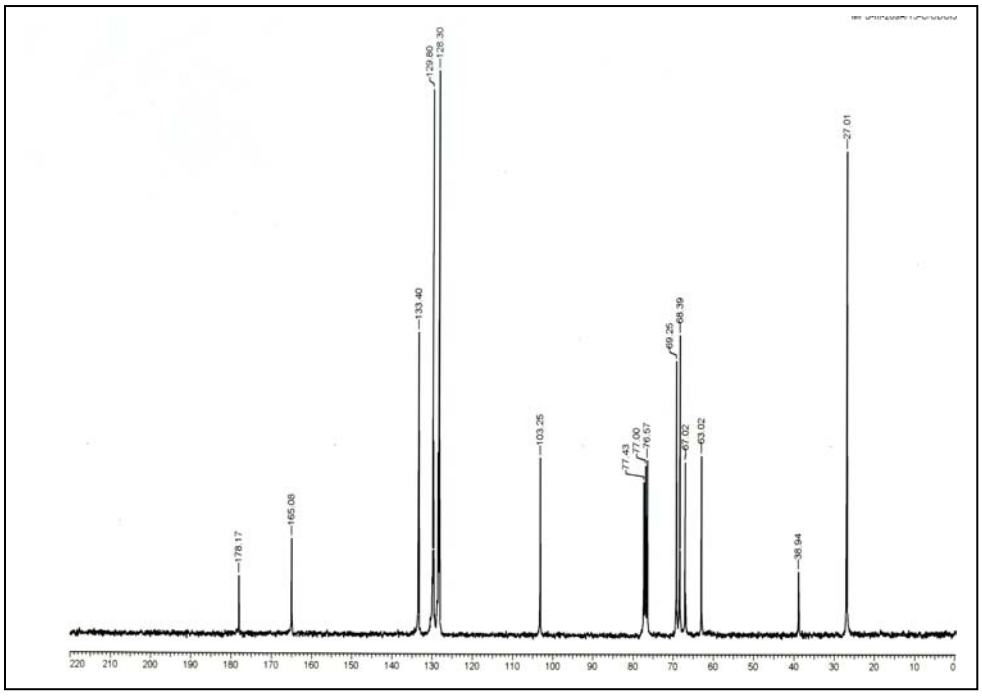
178.17
165.06
133.40
129.80
128.30
103.25
77.43
77.00
76.57
69.25
68.39
67.02
63.02
38.94
27.01

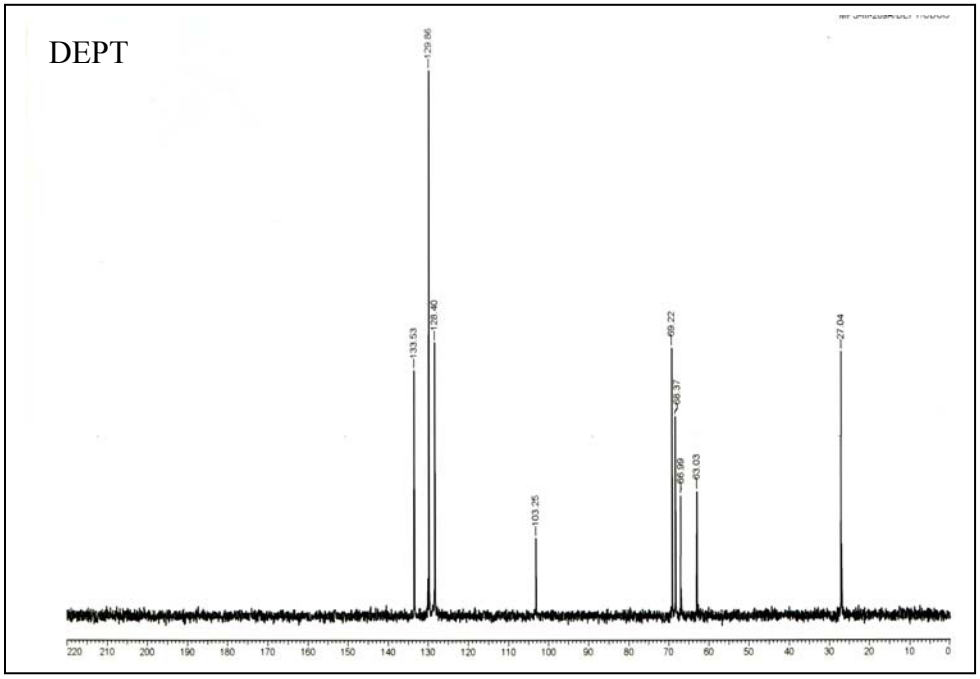

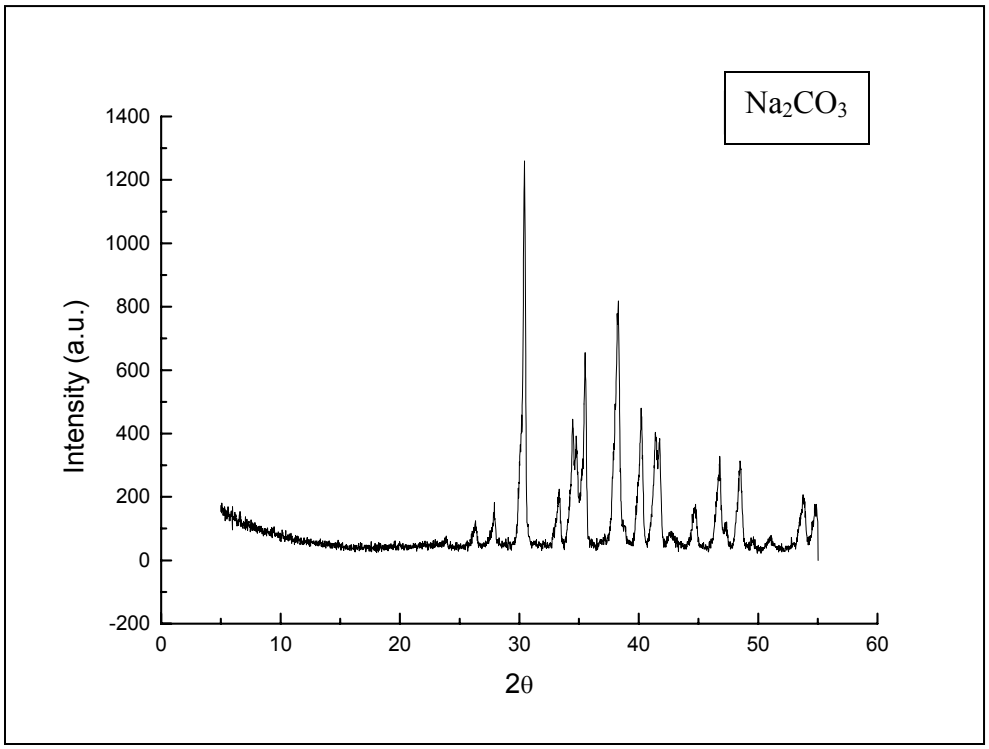

X-ray powder diffraction data for Na_2CO_3.

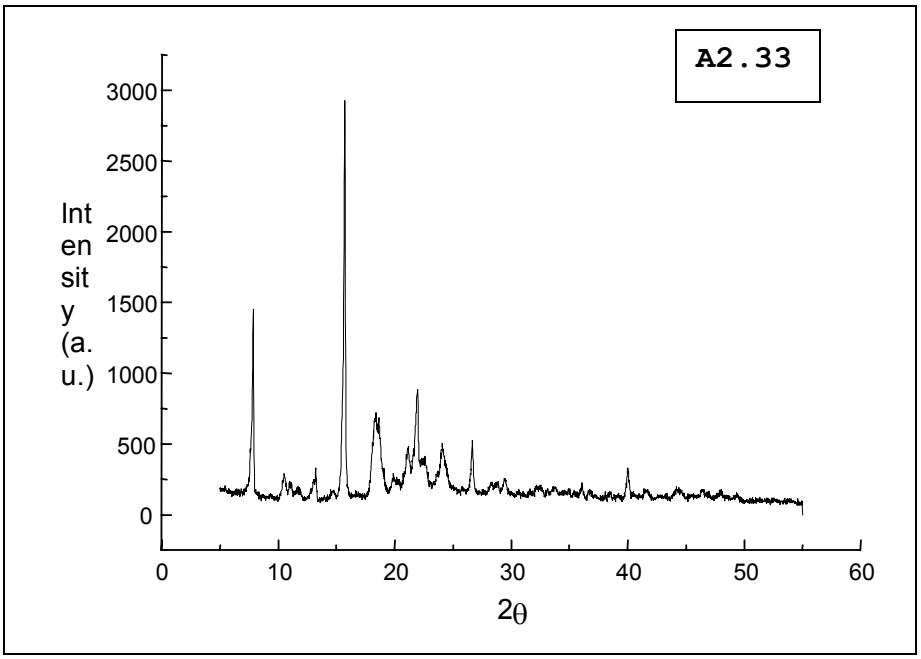

X-ray powder diffraction data for **A2.33.**

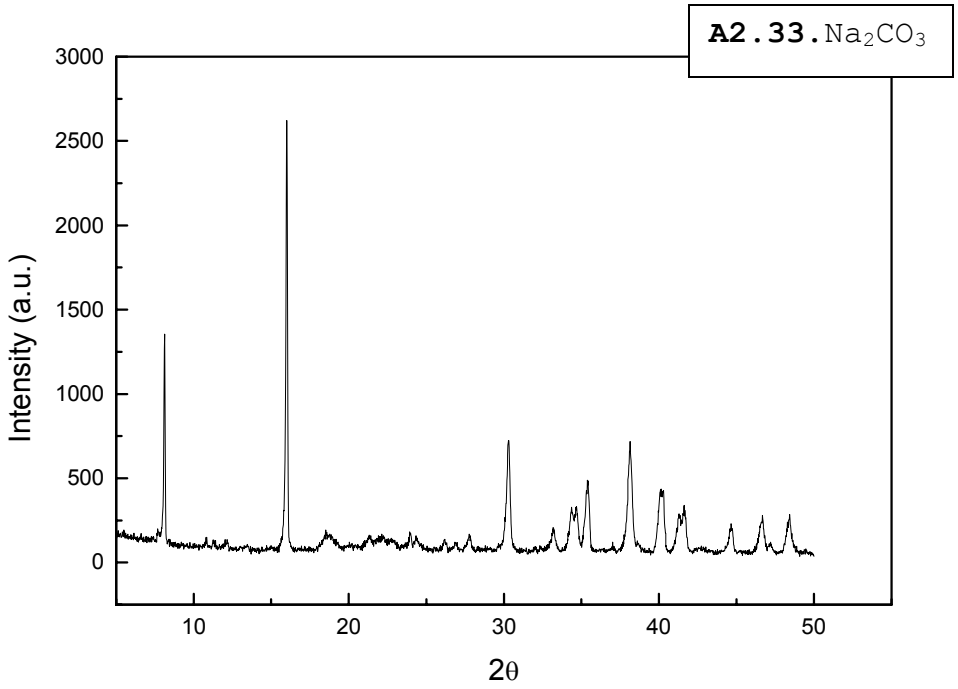

X-ray powder diffraction data for **A2.33.**Na_2CO_3.

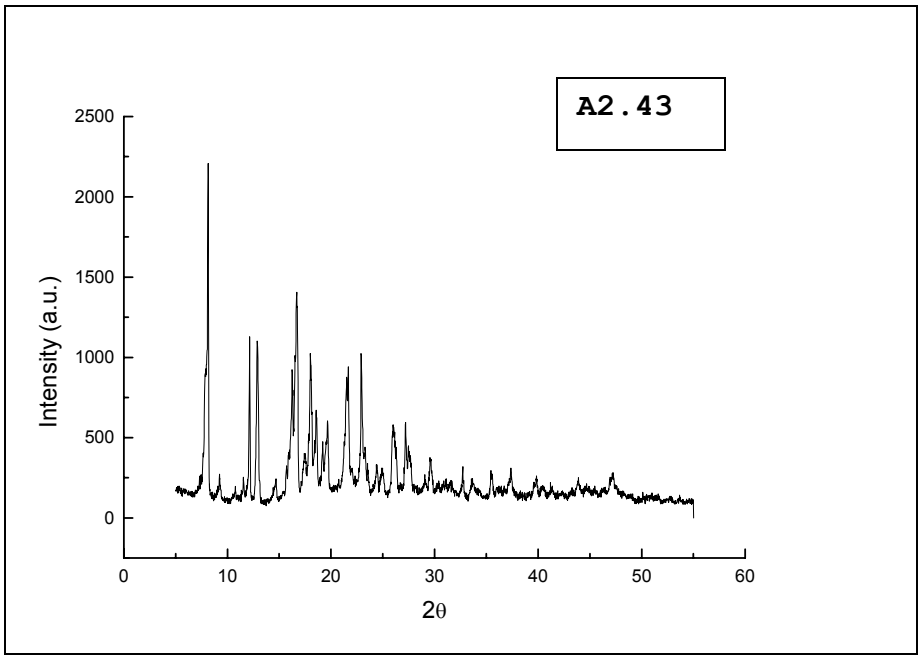

X-ray powder diffraction data for **A2.43.**

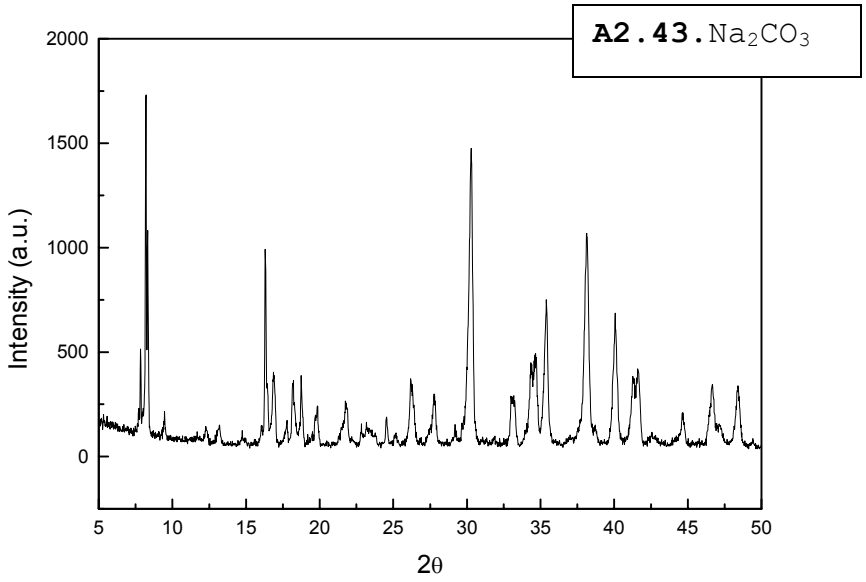

X-ray powder diffraction data for **A2.43.**Na_2CO_3.

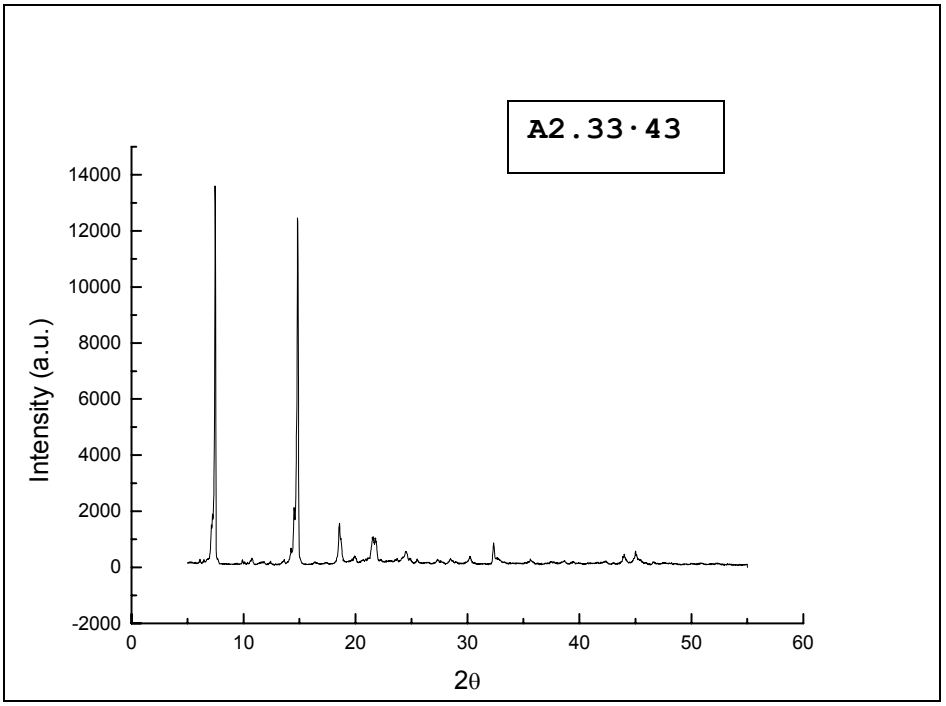

X-ray powder diffraction data for **A2.33·43.**

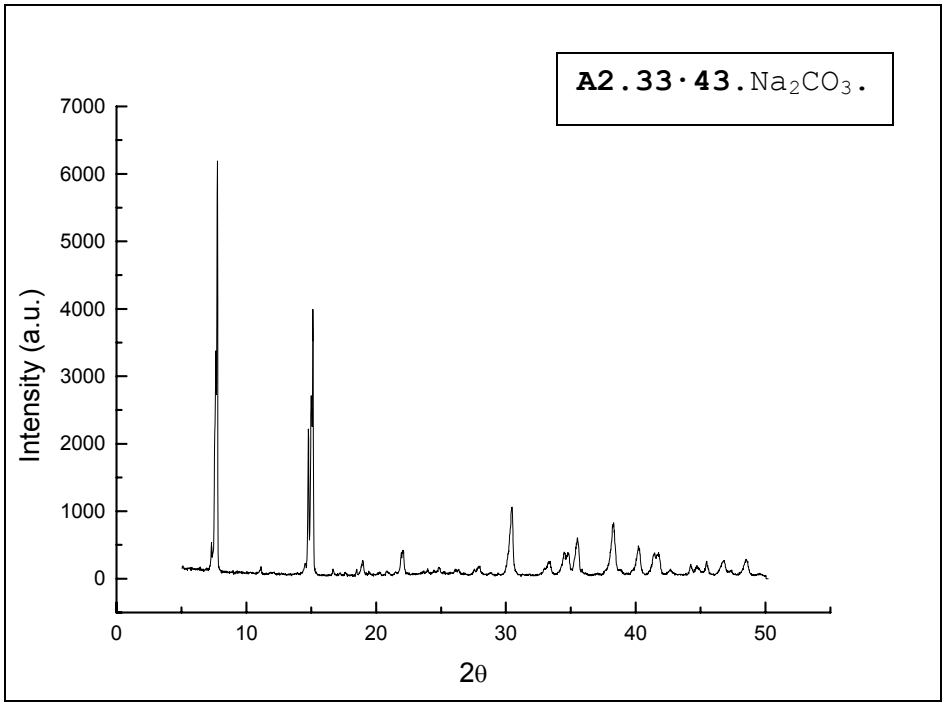

X-ray powder diffraction data for **A2.33·43.**Na_2CO_3.

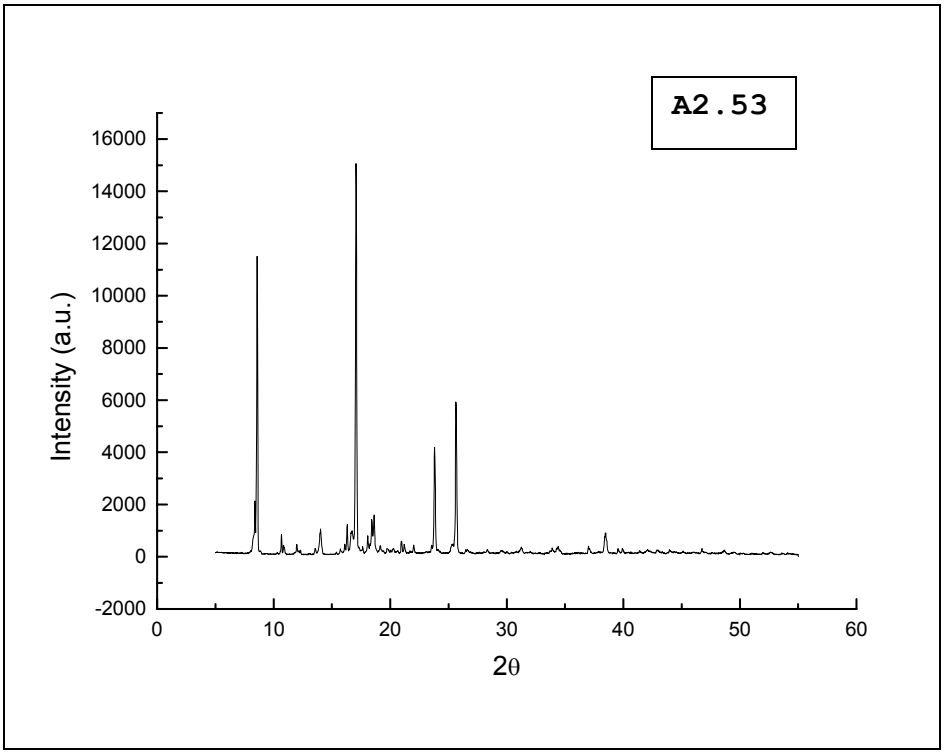

X-ray powder diffraction data for **A2.53.**

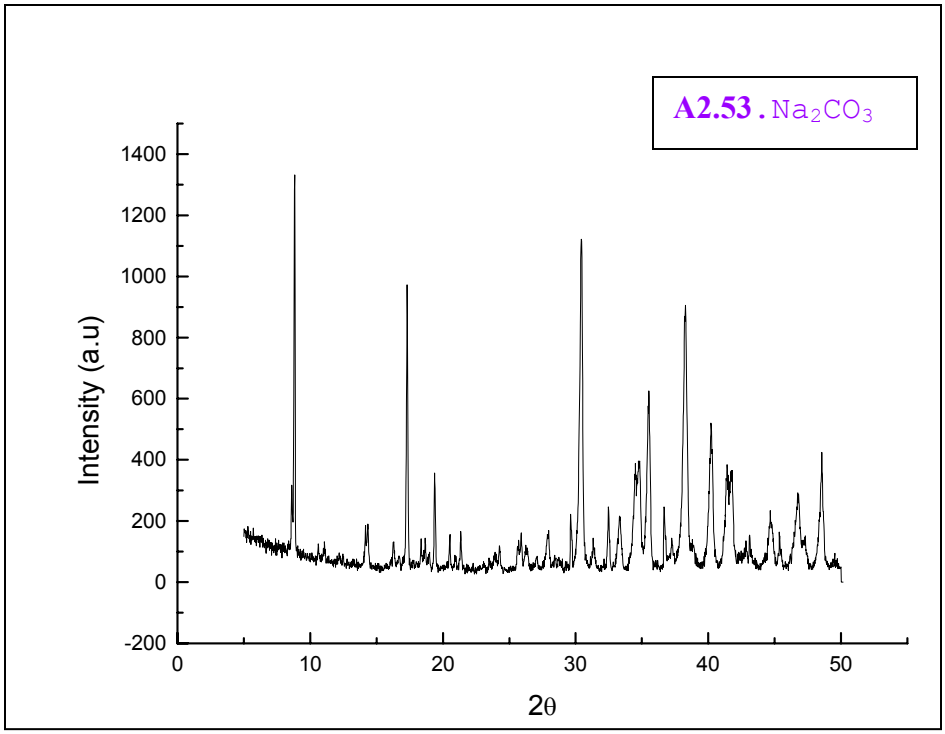

X-ray powder diffraction data for **A2.53.** Na_2CO_3.

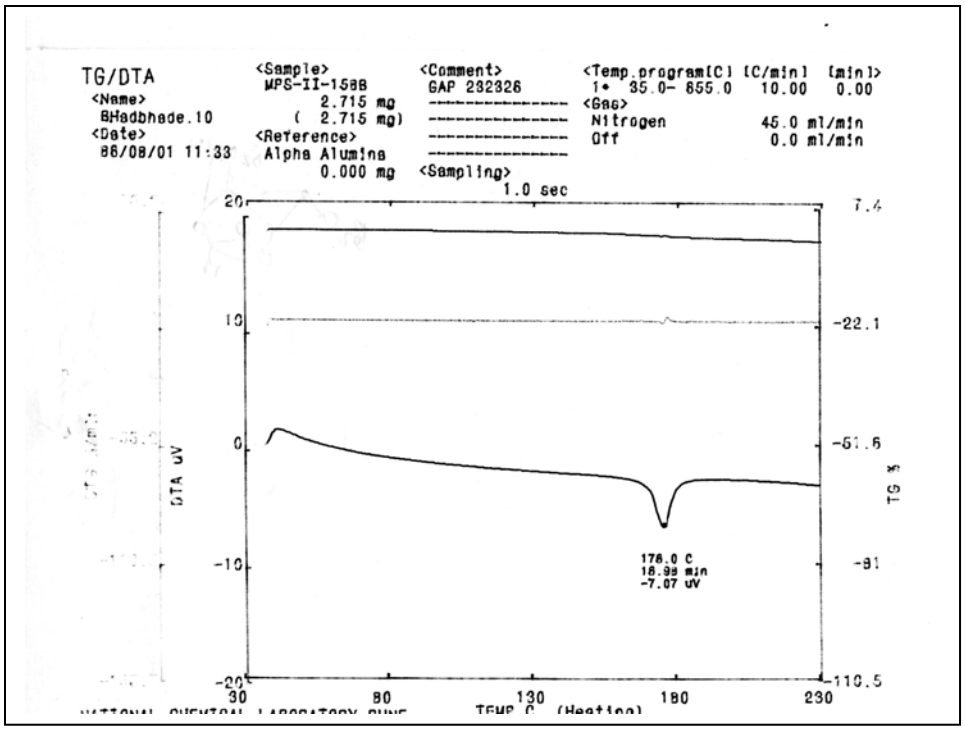

TG / DTA of **A2.33**

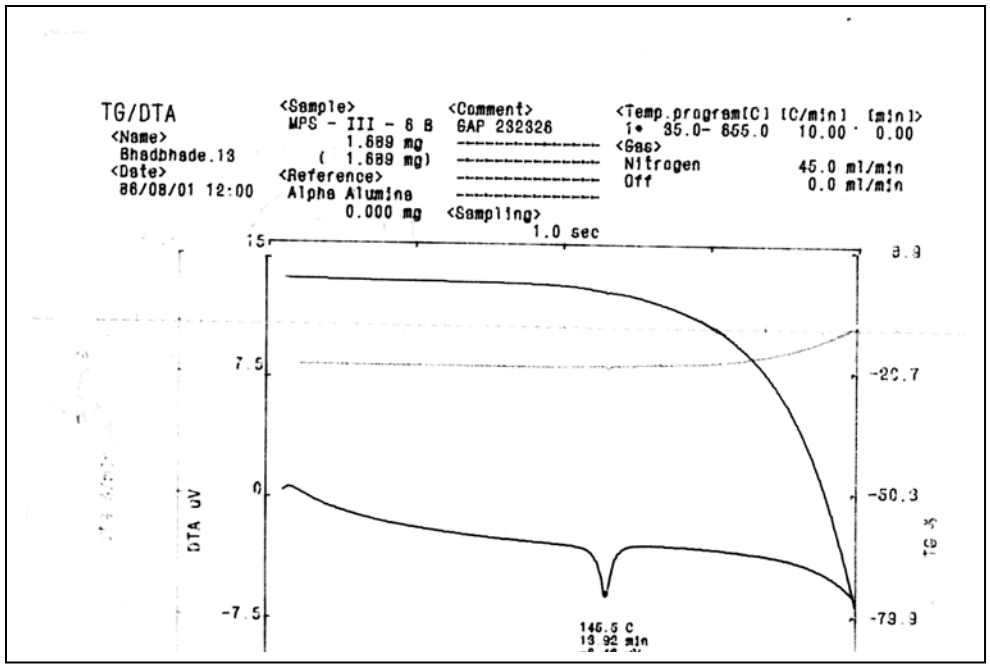

TG / DTA of **A2.41**

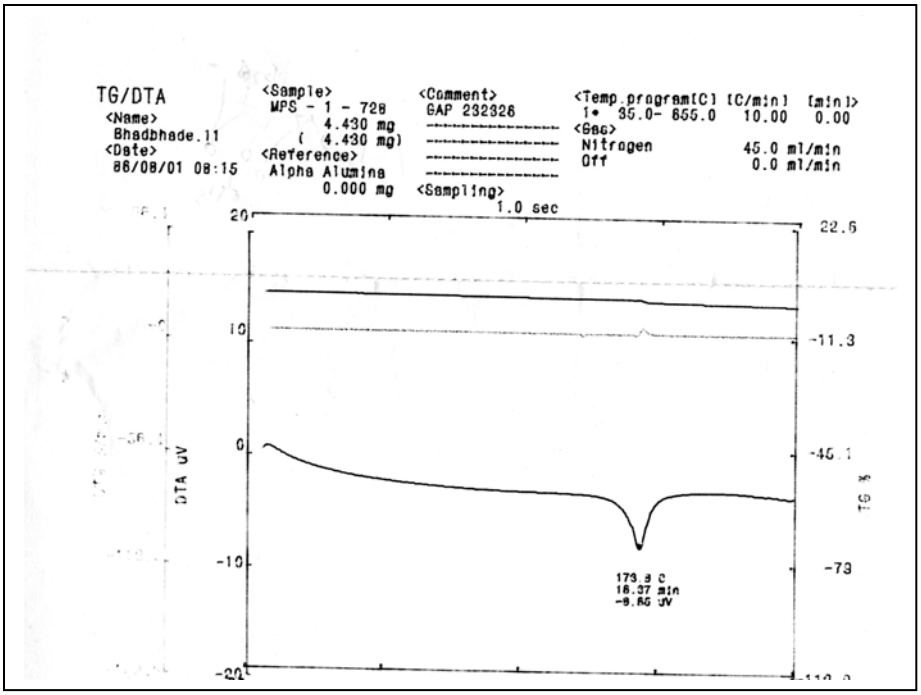

TG / DTA of **A2.43**

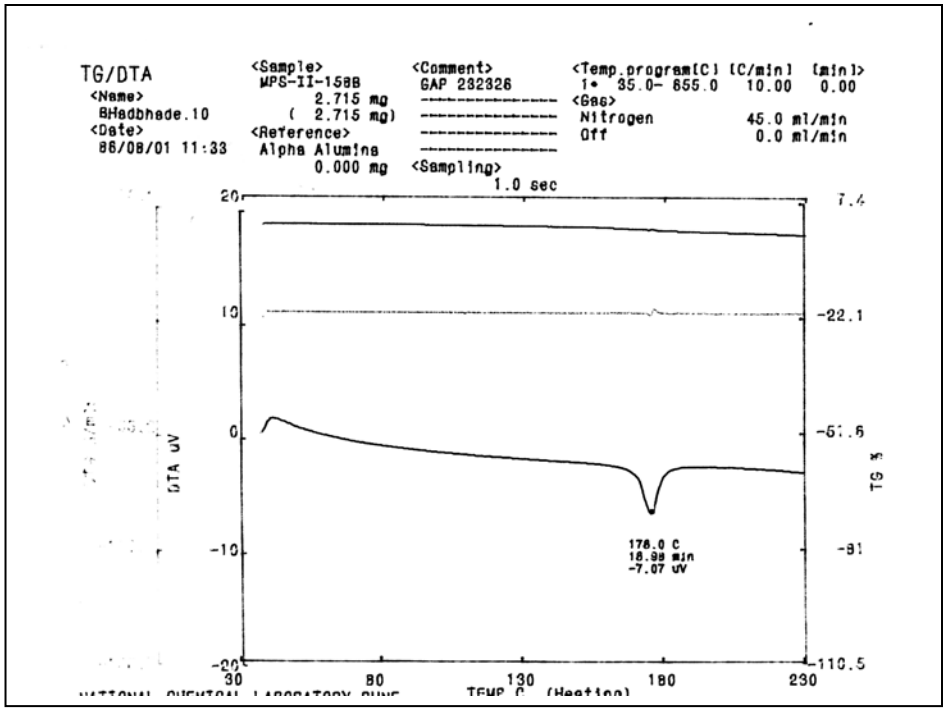

TG / DTA of **A2.33·43**

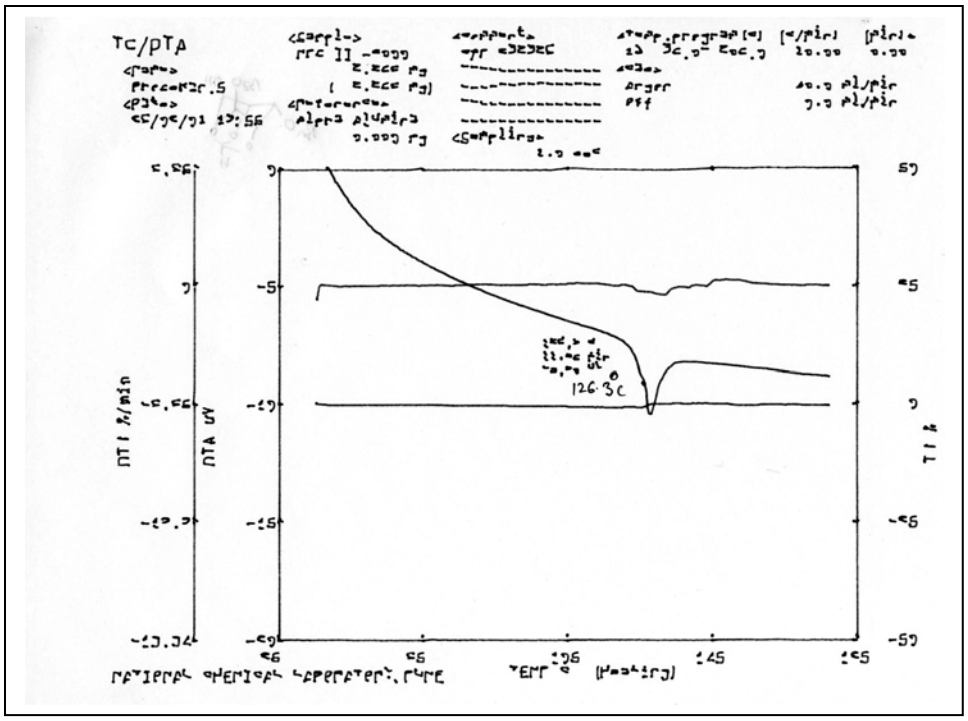

TG / DTA of **A2.49**

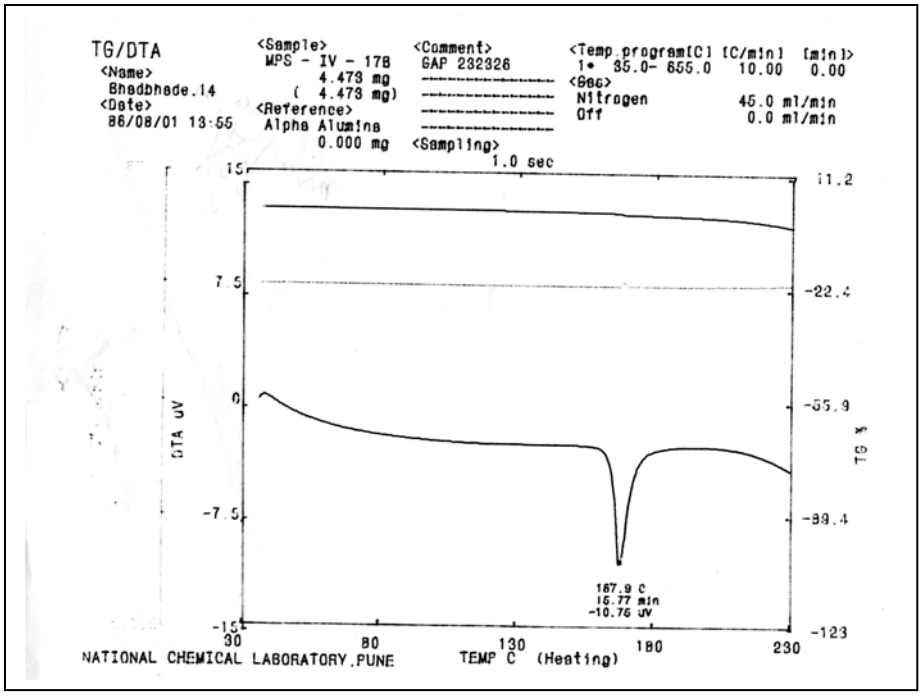

TG / DTA of **A2.53**

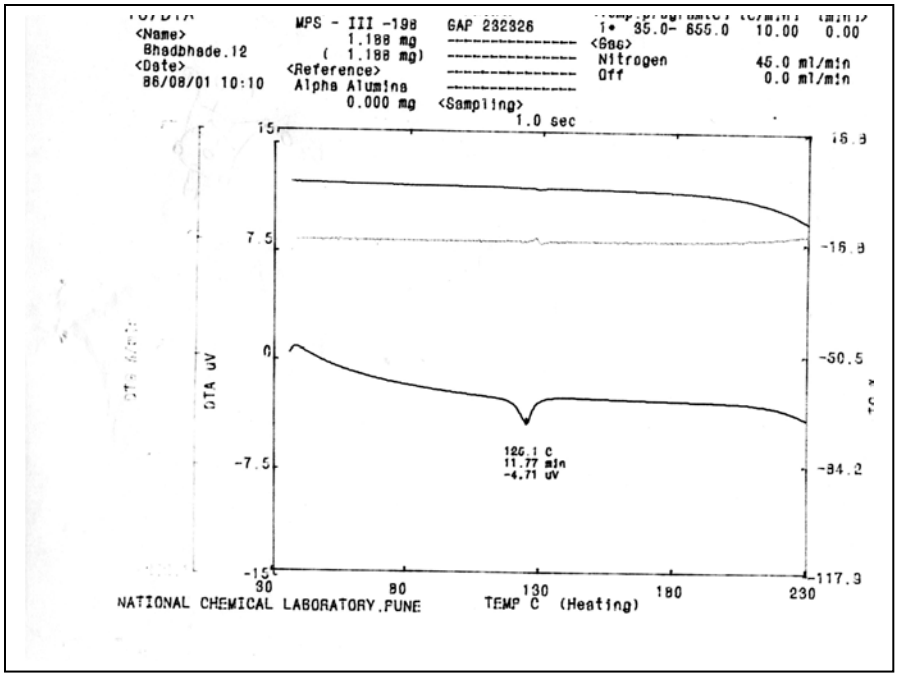

TG / DTA of **A2.54**

Part B

Use of sulfonate protecting groups for the synthesis of cyclitol derivatives

Section 1

Sulfonate groups as hydroxyl protecting groups: A Review

B1.1. Introduction

When a chemical transformation has to be carried out selectively at one site in a multifunctional molecule, other reactive sites are temporarily blocked with protecting groups. Protection – deprotection methods for various organic functional groups have been, and are being developed for this purpose.[1,2] A protecting group is expected to fulfill the following requirements: (a) the reagent used for the protection of a particular functional group should react selectively with the desired functional group, to give a good isolated yield of the protected substrate; (b) the protecting group must be stable to future project reactions; (c) the protecting group should allow the regeneration of the original functional group with ease; (d) deprotection conditions as required in (c) above, should not affect other functional groups present in the molecule; (e) the protecting group should have a minimum of additional functionality to avoid further sites of reaction; (f) preferably, the protecting group should form a derivative, without generation of new stereogenic centers.

Hydroxyl groups are one of the most commonly encountered functional groups in the compounds of biological and synthetic interest, including nucleosides, carbohydrates, steroids, alkaloids,[3] macrolides[4] etc (examples in Chart B1.1).

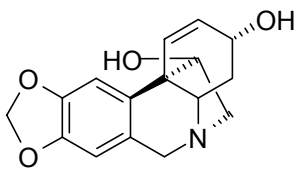

B1.1 (+)-Bulbispermine

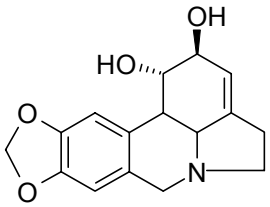

B1.2 (-)-Lyconine

Alkaloids from *Crinum Yemense*

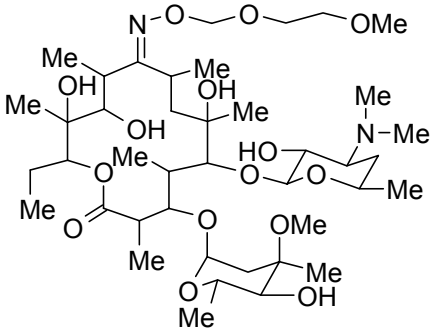

B1.3 Roxithromycin

Macrolide antibiotic in Honey

Chart B1.1

In polyfunctional molecules, selective protection becomes an issue that has been addressed by the development of a number of new methods. Alcoholic and phenolic hydroxyl groups are usually protected as their ethers, silyl ethers, esters, carbonates, boronates and phosphinate derivatives. Simultaneous protection of two hydroxyl groups as acetals, silyl ethers and orthoesters are also routinely encountered in the literature.[1,2,5,6] There are some reports in the literature on the use of sulfonates for the protection of hydroxyl groups. However, sulfonates are not frequently used as protecting groups because of the difficulties associated with their deprotection. Sulfonates, being good leaving groups, could undergo nucleophilic substitution or elimination under the conditions used for their deprotection. This could also result in either racemization or inversion at the carbon center bearing the sulfonate group. Although the general methods of introduction and removal of sulfonate protecting groups have been discussed in several books and monographs[1,2] their utility in particular cases has not been highlighted.

Although ethers and carboxylic acid esters are the most frequently used groups for the protection of hydroxyl groups, the yield and selectivity of etherification and esterification reactions vary. Moreover, carboxylic acid esters suffer from the additional drawback of migration in polyhydroxy compounds.[7-13] Also, it is desirable to have orthogonal protecting groups for the protection of hydroxyl groups in polyhydroxy compounds. At times it has been observed that sulfonylation of a polyol can be carried out with different selectivity than that observed for esterification.[14,15] In the present section of this thesis the literature available on the use of sulfonates as hydroxyl protecting groups during synthesis will be reviewed. A survey of the literature shows that among sulfonates, tosylates (toluene 4-sulfonate) and mesylates (methanesulfonate) are

the most widely used protecting groups, although occasionally other sulfonates such as benzenesulfonate, benzylsulfonate, 2-(4-nitrophenyl)ethylsulfonate etc. have also been used. For convenience, results from the literature are categorized under three heads: (i) tosyl group for protection; (ii) mesyl group for protection; (iii) other sulfonyl groups for protection. Reports on sulfonylation and desulfonylation of simple alcohols and phenols under special conditions have also been included, although many such reports have so far not found applications in synthesis.

B1.2. Use of tosyl group for protection

Instances on the use of tosyl group for protection are mostly encountered in the literature related to carbohydrates. Tosylation of alcohols is usually carried out by the reaction of an alcohol with tosyl chloride in the presence of a base such as pyridine,[16,17] potassium carbonate[18] or triethylamine and catalytic amount of trimethylamine hydrochloride[19] in an organic solvent (such as acetone, acetonitrile, dichloromethane, toluene, 1,2-dichloroethane, benzotrifluoride). N-tosyl imidazole and methyl triflate (by *in situ* formation of N-tosyl-N-methyl-imidizolium triflate) in THF[20] has also been efficiently used for the tosylation of alcohols. Recently solvent free synthesis of aryl tosylates by the reaction of phenols with tosyl chloride in the presence of potassium carbonate under microware radiation has been reported.[21]

The selective protection of primary hydroxyl group in the presence of secondary hydroxyl group is an important requirement in many organic syntheses. Acylation, sulfonylation and silylation of a mixture of 1-octanol and 2-octanol (Scheme B1.1) in dichloromethane different bases were compared (Scheme B1.1).[22] The results revealed

that the primary hydroxyl group could be preferentially tosylated in the presence of sterically hindered bases (Table B1.1).

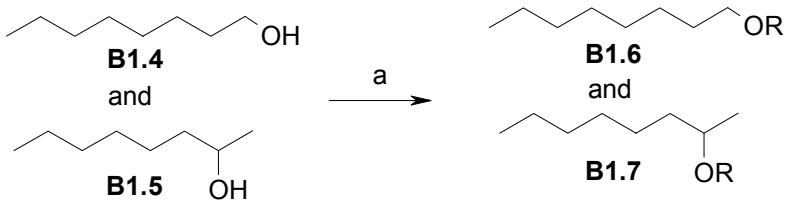

Scheme B1.1. a) RCl (0.5 eq), base (1 eq), DCM, -78-25 ^{o}C, 3-24 h.

Table B1.1. Observed selectivity during the sulfonylation of a mixture of **B1.4** and **B1.5**

Entry	RCl	Pyridine	Collidine	*i*-Pr_2EtN	PMP
1	TsCl	87[a] (81.3)[b]	47[a] (97.4)[b]	10[a] (97.8)[b]	
2	MsCl	64[a] (82.4)[c]	75[a] (91.2)[c]	94[a] (94.6)[c]	>99[a] (94.9)[b]

[a] Isolated yield (%) of **B1.6** + **B1.7**;
[b] yield (%) of **B1.6** by ^{1}H NMR spectroscopy;
[c] yield (%) of **B1.6** by HPLC analysis.

Tejima and co-workers exploited the selectivity observed during the tosylation of 1,6-anhydro-4',6'-*O*-benzylidene-β-lactose (**B1.8**)[23] and 1,6-anhydro-4',6'-*O*-benzylidene-β-maltose (**B1.13**)[24] for the synthesis of carbohydrate derivatives of biological importance. From the selectivity observed on tosylation of **B1.8** it was concluded that the reactivity of the secondary hydroxyl groups in **B1.8** followed the order 2> 3'> 3> 2'.[23] Similarly tosylation of **B1.13** suggested the order of relative reactivity of its secondary hydroxyl to be 2'> 2, 3'> 3.[24]

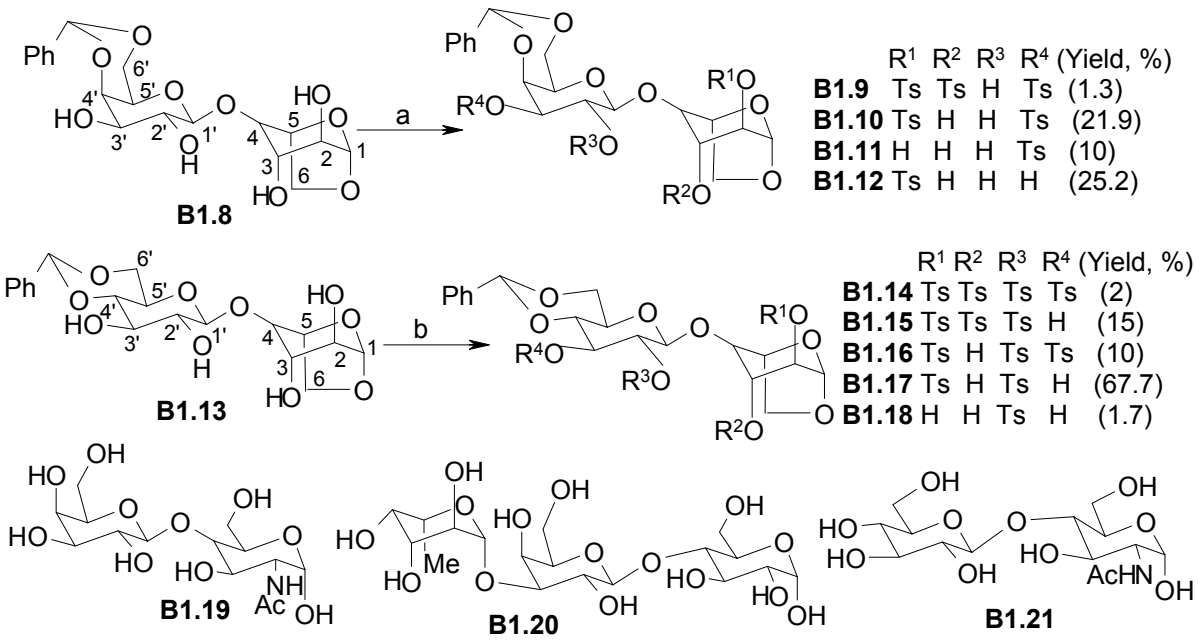

Scheme B1.2. a) TsCl (2.2 eq), Pyr, 0 ^{o}C-rt; b) TsCl (4.2 eq), Pyr, 0 ^{o}C-rt.

Tosylates **B1.10**-**B1.12** and **B1.17** were utilized for the synthesis of, N-acetyllactosamine derivative **B1.19**,[25,26] β-D-glucopyranose derivative **B1.20**[27] and α-D-glucopyranose **B1.21**,[28] which are the constituents of human milk.[24,29] In most of these synthetic schemes tosylates were deprotected by treatment with sodium amalgam in methanol.

Tsuda and co-workers studied the selectivity of tosylation of hydroxyl groups (using dibutyltinoxide) of glycosides, furanose derivatives, and their partially protected derivatives (Scheme B1.3).[30] The selectivity of tosylation observed was explained on the basis of the structure and stability of the dibutyltin acetal formed in the first step of the reaction. Kong and Grindley also studied the regioselectivity of tosylation reactions of dialkylstannylene acetal derivatives of furanosides under different tosylation conditions (temperature and solvent).[31]

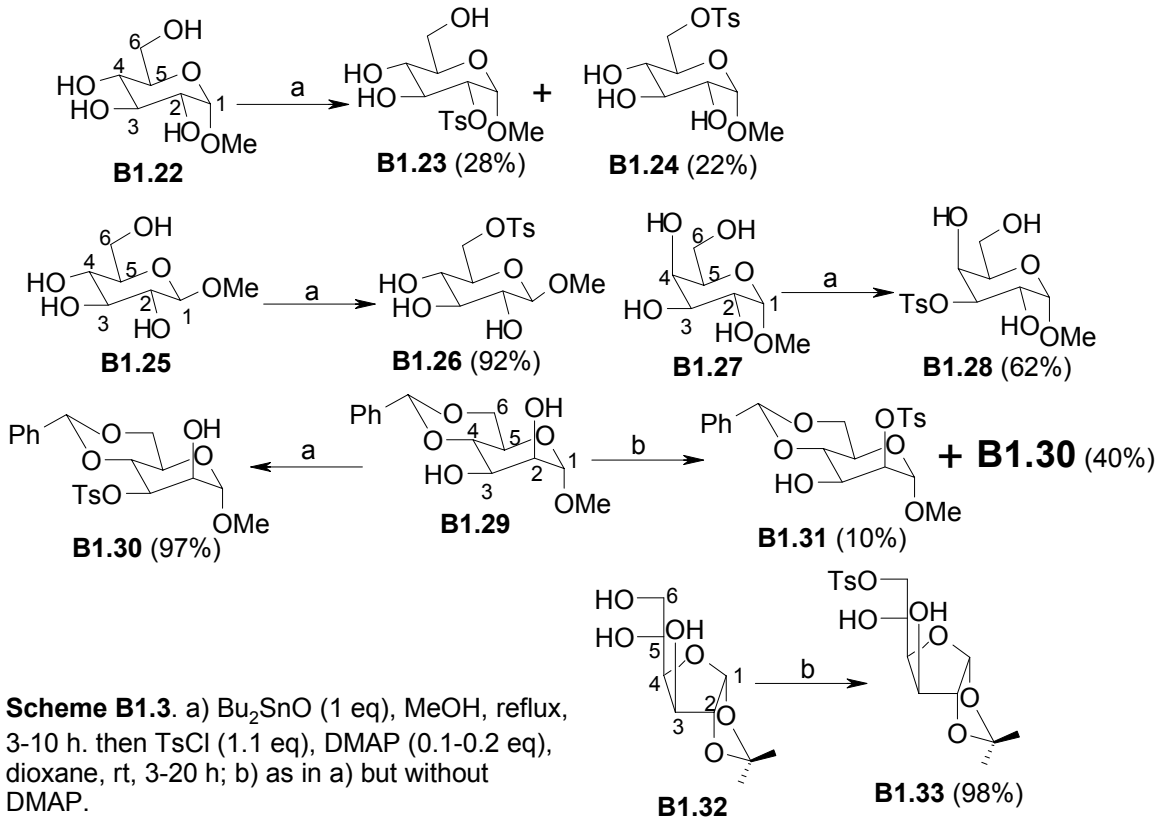

Scheme B1.3. a) Bu_2SnO (1 eq), MeOH, reflux, 3-10 h. then TsCl (1.1 eq), DMAP (0.1-0.2 eq), dioxane, rt, 3-20 h; b) as in a) but without DMAP.

Over the years, many methods such as hydrolysis,[25,27,32] solvolysis, hydride reduction,[33] reduction with metals (and alcohol or ammonia)[34,35] and electrochemical reduction[36,37] have been used for the deprotection of tosylates. Efficient deprotection was mostly achieved by the reductive cleavage of the S-O bond.[34,38-40] One of the oldest methods is the cleavage of tosylates by hydrogenolysis in the presence of Raney nickel.[41] Although hydrogenolysis of alkyl tosylates in ethanol gave the corresponding alcohol, aryl tosylates gave the corresponding hydrocarbon. The main limitation of this method is the requirement of large excess of Raney nickel. Low valent titanium (LVT) reagents cleave N- and O- tosylates; among the many LVT reagents investigated, $TiCl_3$-Li-THF was found to be most effective.[42] Cleavage of tosylates was also reported to occur by microwave irradiation in the presence of potassium fluoride-alumina in dry media.[43]

Many aromatic as well as aliphatic tosylates were cleaved with cerium chloride heptahydrate and sodium iodide in acetonitrile.[44] Tosylates of phenols can be cleaved using thiophenols (eg., PhSH, 4-Me-C_6H_4SH and 2-H_2N-C_6H_4SH) in the presence of catalytic amount of potassium carbonate in dipolar aprotic solvents (like DMPU, DMEU, NMP and DMF).[45] Alternately, the thiophenolate anion responsible for the cleavage of sulfonates could be generated *in situ* from diphenyl disulfide and sodium in NMP.[46] Nishida and co-workers also studied the hydrolysis of tosylates, under photo-sensitized conditions, by using a donor (DMN, DMNP, DABCO etc) and a co-reductant ($NaBH_4$, ascorbic acid, hydrazine hydrate etc).[47,48]

Tosyl derivatives of carbohydrates have been cleaved with sodium and liquid ammonia in THF at –80 °C to obtain the corresponding alcohol in good yield.[35] Reduction of tosylates with sodium and naphthalene also generated the corresponding alcohol.[38-40] This reaction was thought to follow either of the paths 'a' or 'b' (Scheme B1.4).

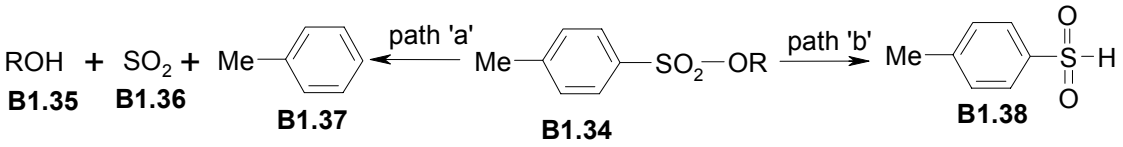

Scheme B1.4.

Reaction of tosylates with magnesium in methanol[34] also cleaves them efficiently. GC-MS analysis of the products obtained in this reaction showed formation of toluene, which suggested that the mechanism of cleavage might be similar to that with sodium and liquid ammonia (Scheme B1.4). Sulfonamides are reported to be stable towards Mg / methanol.[34]

Tosylates of cholesterol (**B1.39**) and cholestanol (**B1.43**) were cleaved by using potassium-dicyclohexyl-18-crown-6 in diglyme (Scheme B1.5).[49] Isolation of **B1.41** and **B1.42** from the reaction mixture suggested the occurrence of elimination of tosyl group and successive reduction of the conjugated diene during the reduction of **B1.39**.

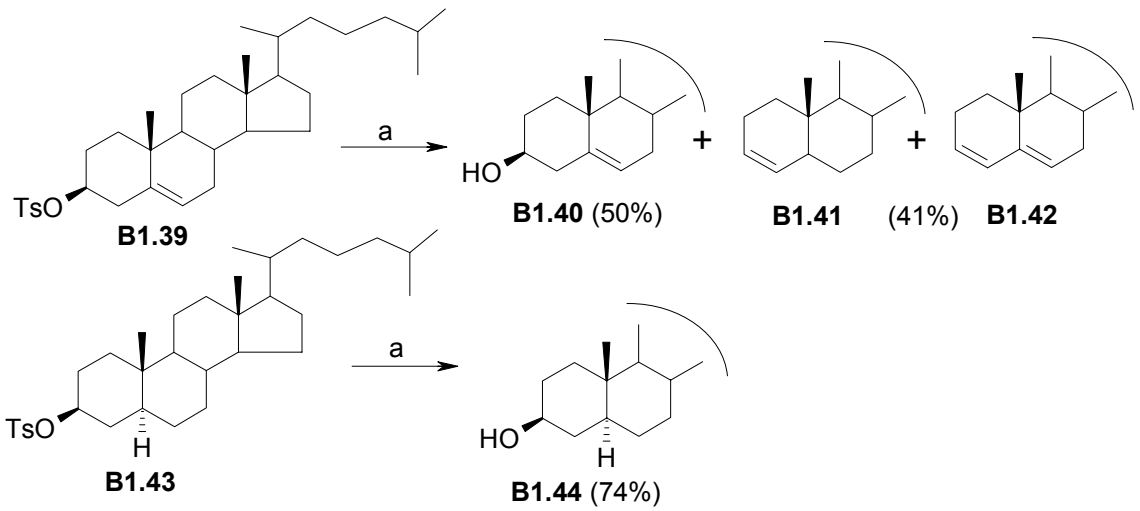

Scheme B1.5. a) K-dicyclohexyl-18-crown-6, diglyme, rt, 3 h.

Photolysis of tosylates in methanol in the presence of sodium methoxide,[50, 51] or triethyl amine[52,53] also regenerates the parent alcohol. Scheme B1.6 shows applications of this method of deprotection during the synthesis of a disaccharide, **B1.49**[53] and a fluorosugar, **B1.52.**[52]

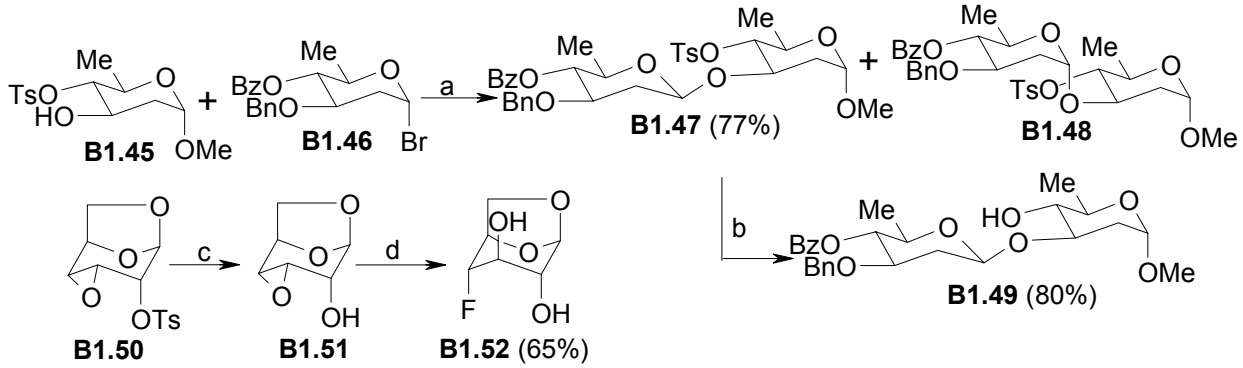

Scheme B1.6. a) $AgSiO_3$, toluene, rt, 12 h; b) Et_3N, MeOH, hν, 1h; c) NaOMe, MeOH, hν; d) KHF_2, ethylene glycol, reflux, 1 h.

Aryl tosylates can be cleaved by electrochemical reduction at mercury pool cathode[36] using tetraethyl ammonium bromide (TEAB) as supporting electrolyte in acetonitrile solution.[54] An application of this method for the synthesis of furo[2,3-*b*]benzofuran ring system (**B1.61**) of (+) and (-)-aflatoxins, is shown in Scheme B1.7. These aflatoxins are metabolites of the mold *Aspergillus flavus*, belonging to mycotoxin family.[37]

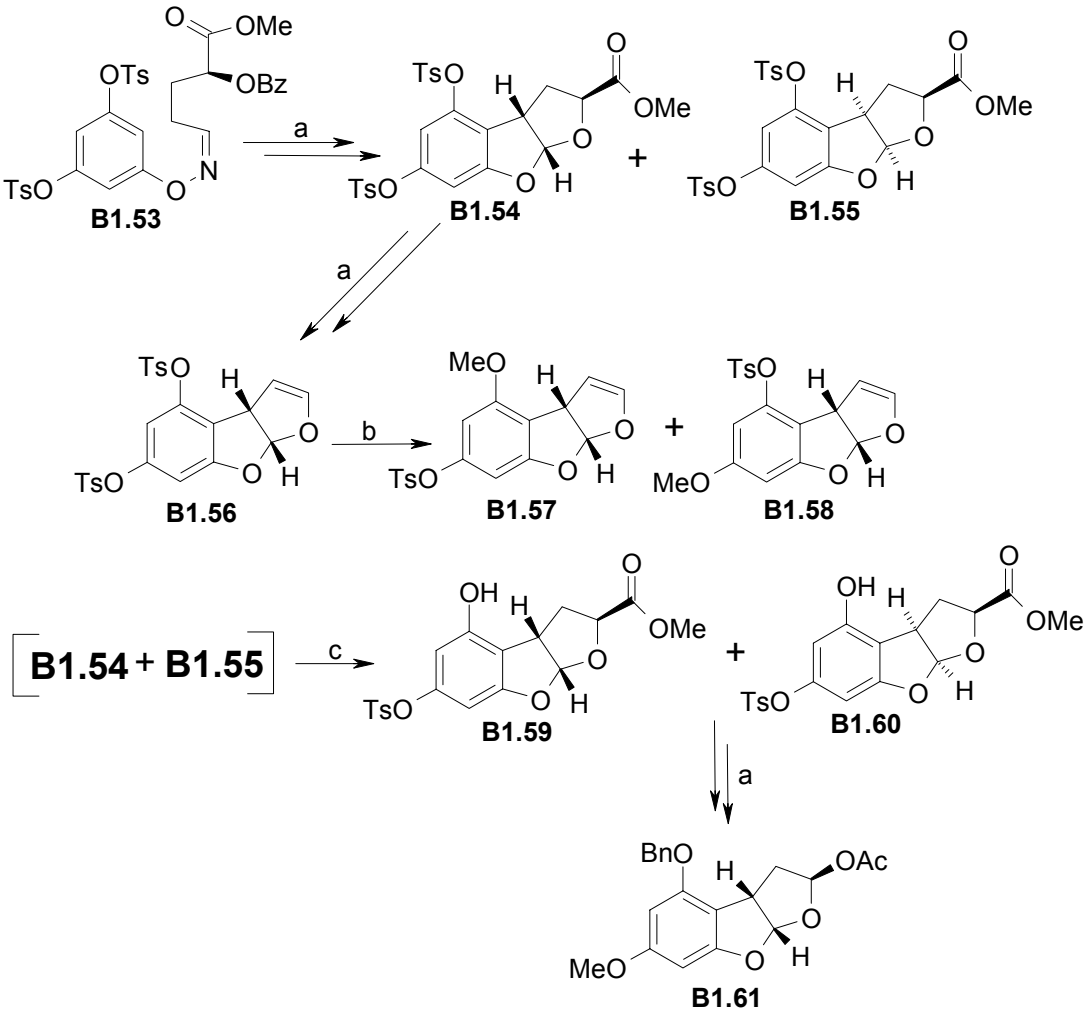

Scheme B1.7. a) as in reference 37; b) (i) -1.32 V, TEAB, MeCN, 12 h, (ii) MeI, K_2CO_3, DMF, 48 h (**B1.57** : **B1.58** = 89 : 11); c) -1.275 V, TEAB, MeCN, 20 h, 63%.

During the synthesis of kijidextrins and their protein conjugates, tosylate protected carbohydrates were used.[33] As an example the synthesis of kojibiose donor **B1.66** is shown in Scheme B1.8.

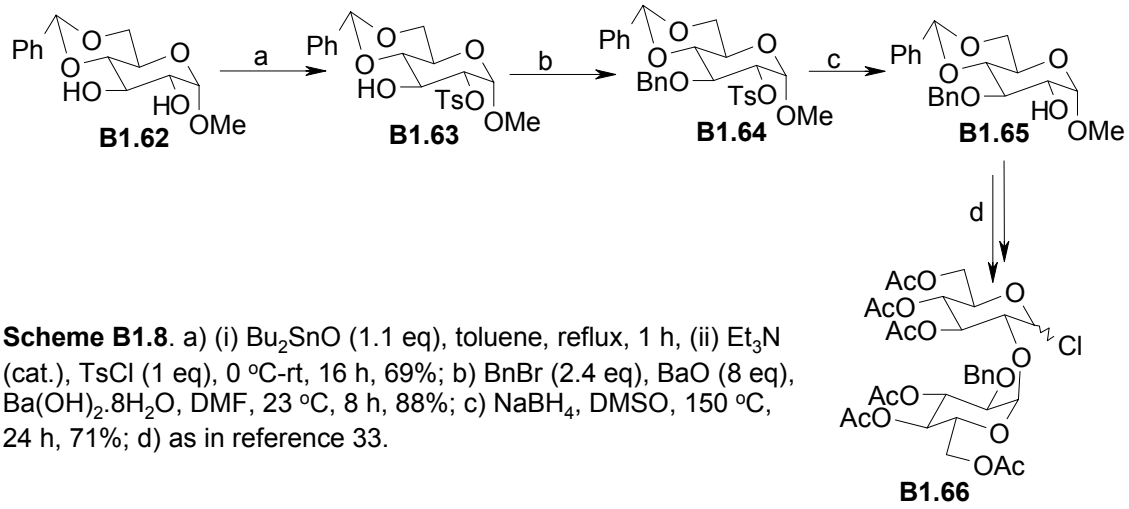

Scheme B1.8. a) (i) Bu_2SnO (1.1 eq), toluene, reflux, 1 h, (ii) Et_3N (cat.), TsCl (1 eq), 0 °C-rt, 16 h, 69%; b) BnBr (2.4 eq), BaO (8 eq), $Ba(OH)_2.8H_2O$, DMF, 23 °C, 8 h, 88%; c) $NaBH_4$, DMSO, 150 °C, 24 h, 71%; d) as in reference 33.

Selective sulfonylation of *myo*-inositol 1,3,5-orthoesters was reported from our laboratory (Scheme B1.9).[55,56] These tosyl protected inositol derivatives were used as key intermediates for the synthesis of *myo*-inositol-1,3,4.5-tetrakisphosphate precursors.[56] A comparison of the yields (Table B1.2) of D- and L-*myo*-inositol-1,3,4,5-tetrakisphosphate precursors, D- and L-2,4-di-*O*-benzyl-*myo*-inositol (**B1.D79**, **B1.L79**) obtained by using tosylate as protecting group[56] and by other methods reported in the literature[57-61] makes the advantage of using the tosylate as protecting group evident.

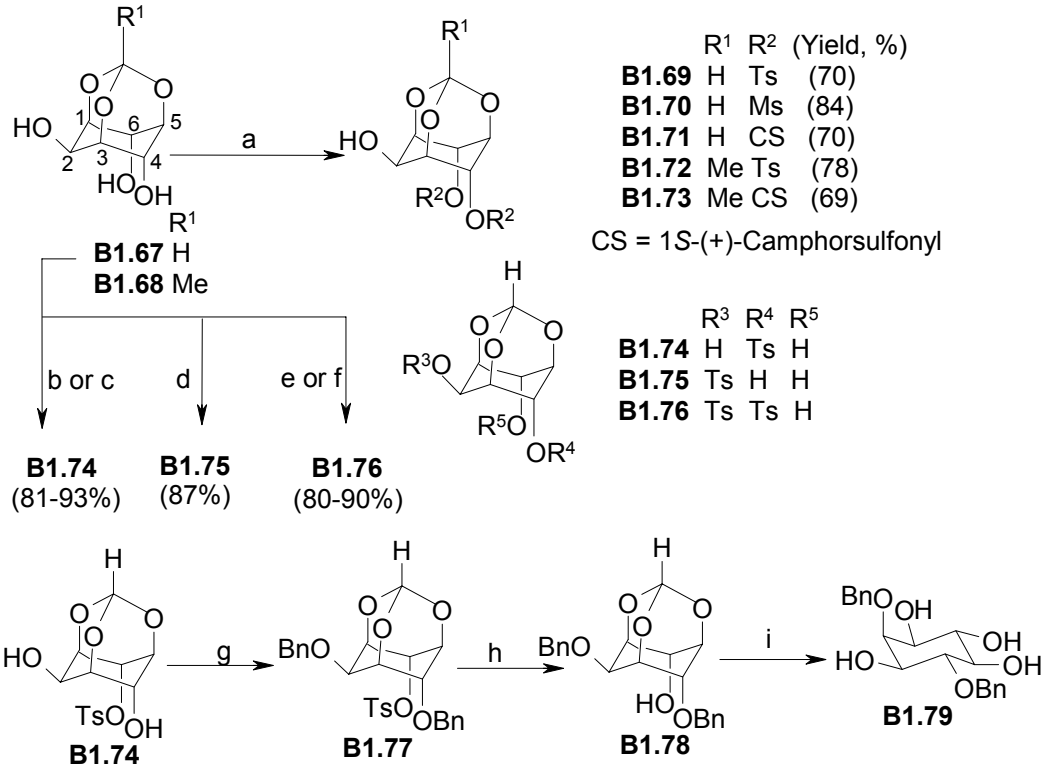

Scheme B1.9. a) R^2Cl (2.1 eq), NaH (2 eq) or *t*-BuOK (2 eq), DMF; b) TsCl (1 eq), NaH (1 eq), DMF, rt, 5 min; c) TsCl (1 eq), Et_3N, DMF, rt, 24 h; d) TsCl (1 eq), Pyr, 80 °C, 48 h; e) TsCl (2.2 eq), Pyr, 80 °C, 48 h; f) TsCl (2 eq), Et_3N, DMF, rt, 48 h; g) BnBr (2.2 eq), NaH (2.2 eq), DMF, rt, 5 min, 100%; h) NaOMe, MeOH, reflux, 12 h, 99%; i) TFA-H_2O (4 : 1), rt, 24 h, 99%.

Table B1.2.

Key intermediate	Yield (%)		Reference
	B1.D79	**B1.L79**	
myo-Inositol 1,3,5-orthoformate (**B1.67**)	27	27	57
myo-Inositol 1,3,5-orthoformate (**B1.67**)	12	13	58
myo-Inositol 1,3,5-orthoformate (**B1.67**)	15	14	58
1,2;4,5-di-*O*-cyclohexylidine-*myo*-inositol	3	NR	59
1,3,5-tri-*O*-benzoyl-*myo*-inositol	<8	NR	60
(-)-2,3;4,5-di-*O*-cyclohexylidine-*myo*-inositol	7	NR	61
myo-Inositol 1,3,5-orthoformate (**B1.67**)	37	39	56

NR= Not reported

B1.3. Use of mesyl group for protection

Mesylation of a hydroxyl group is generally carried out by the treatment of an alcohol or a phenol with mesyl chloride and a base such as pyridine,[62] triethylamine[63,64] triethylamine and catalytic amount of trimethylamine hydrochloride[19] or dibutyltinoxide.[65]

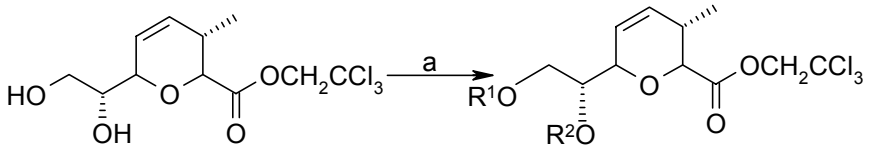

B1.80

B1.81 Ms H
B1.82 Ms Ms

Scheme B1.10. a) as in Table B1.3.

Table B1.3. Mesylation of **B1.80** (1 mmol) in DCM

Entry	Conc. (M)	Base[a]	MsCl (eq)	Tempr. (°C)	Time (h)	% yield	
						B1.81	**B1.82**
1	0.15	Et_3N[b]	1.4	-23~0	1.25	40	32
2	0.15	Et_3N[b]	1.1	-50	1.5	29	
3	0.05	Et_3N[c]	1.1	0~7	15.5	52	18
4	0.1	*i*-Pr_2NEt[b]	1.1	-78~0	3	47	14
5	0.06	Pyridine	1.1	5	48	56	11
6	0.06	Pyridine[b]	1.1	5	48	64	26
7	0.05	Pyridine[c]	1.1	0~7	15.5	47	8
8	0.06	Collidine	1.1	23	48	61	12
9	0.06	Collidine[c]	1.1	0~7	21	86	10
10	0.05	Collidine[c]	1.1	0~7	15.5	84	8
11	0.05	2,6-lutidine[c]	1.1	0~7	15.5	29	
12	0.05	2,6-di-*t*-butyl-4-methyl pyridine	1.1	0~7	15.5		

[a] 3 eq of base was used;
[b] a catalytic amount (5 mol%) of DMAP was used;
[c] 10 eq of base was used.

Mesylation of alcohols can be carried out in solvents like 1,2-dichloroethane, benzotrifluoride, acetone, acetonitrile, dichloromethane, toluene etc. O'Donnell and Burke investigated the mesylation of the vicinal diol **B1.80** (Scheme B1.10) systematically;[66] the observed selectivities are shown in Table B1.3. The results revealed that the primary hydroxyl group could be preferentially mesylated in the presence of sterically hindered bases, as observed for the tosylation of alcohols (Section B1.2).

Deprotection of mesylate has been effected by treatment with sodium methoxide in methanol,[67,68] potassium hydroxide in methanol,[69] sodium amalgam / propanol in diethyl ether,[70] LDA in THF[71] and methylmagnesium bromide in THF.[72] Methylmagnesium bromide can selectively cleave the mesylate in the presence of other functional groups, including tosylate.[72] Mesylates cannot be cleaved by photolysis or with sodium-naphthalene; in the latter procedure, the competing reaction, reduction of mesylate groups to the corresponding alkane becomes prominent.[39]

One of the early examples of the use of mesylate as a protecting group was during the synthesis of 6-substituted idofuranose derivatives (Scheme B1.11).[67]

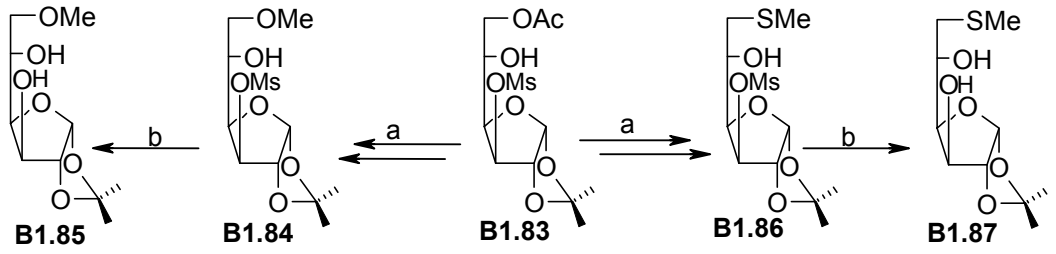

Scheme B1.11.a) as in reference 67; b) NaOMe, MeOH, reflux, 1.5-2 h.

Lantos and Loev used mesylate for the protection of a phenol **B1.88** during the synthesis of the alkaloid (±)-decinine (**B1.92**).[69] The stable crystalline mesylate derivative **B1.89**

was inert towards the Ullman coupling conditions during the synthesis of **B1.92**.

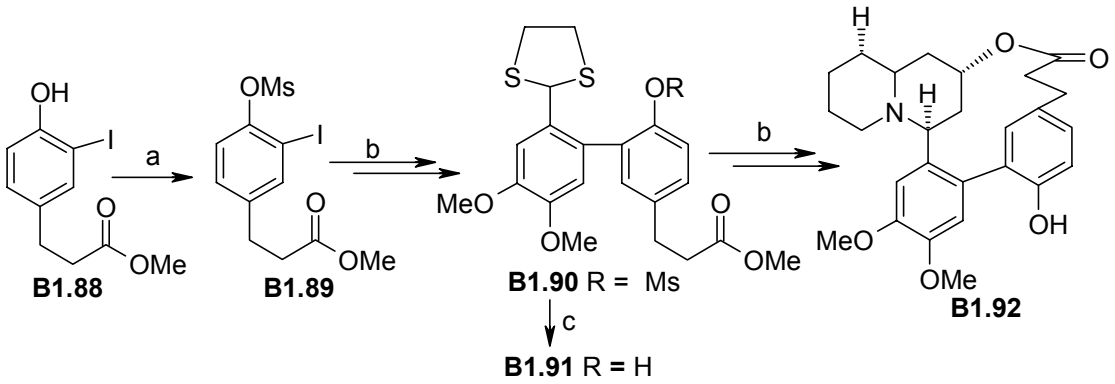

Scheme 1.12. a) MsCl, Pyr; b) as in reference 69; c) KOH, MeOH.

Mesylate was used for the protection of a hydroxyl group during the synthesis of β-D-mannopyranosides (Scheme B1.13). The deprotection was carried out by treatment with sodium and liquid ammonia.[73]

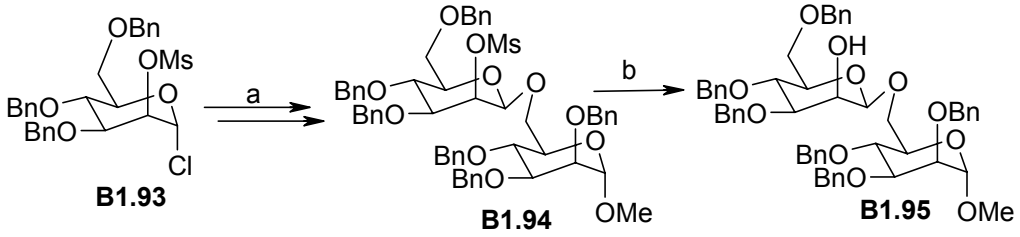

Scheme B1.13. a) as in reference 73; b) Na-NH_3, THF, rt, 45 min, 65%.

Hughes and Todhunter synthesized 1,6-epithio-hexofuranoses using the C-3 mesylated idofuranose derivative **B1.96**. The C3-hydroxyl group was later regenerated by treatment with sodium methoxide in methanol.[68]

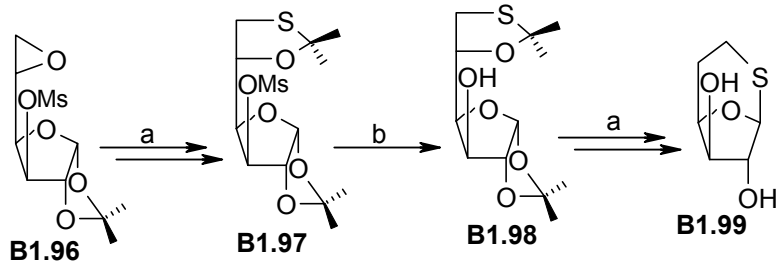

Scheme B1.14. a) as in reference 68; b) NaOMe, MeOH, reflux, 5 h, 72%.

Phosphatidyl-*myo*-inositol phosphates were synthesized by Kozikowski and co-workers by using mesylate protection for one of the hydroxyl groups of L-quebrachitol (**B1.100**), which was latter regenerated by reduction with lithium alluminium hydride in THF.[74]

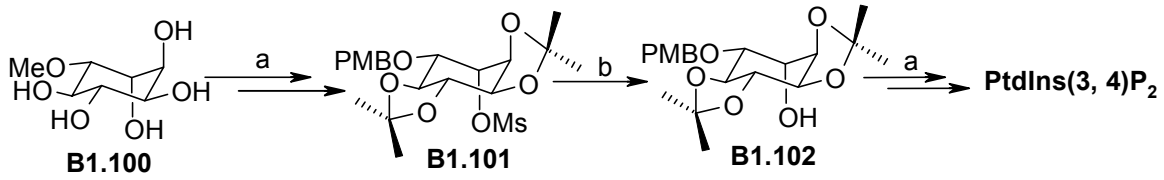

B1.100 **B1.101** **B1.102**

Scheme B1.15. a) as in reference 74; b) $LiAlH_4$ (3 eq), THF, 0 °C-rt, 2 h, 63%.

The hydroxyl group of guaiacol was protected as mesylate[75] to achieve electrophilic substitution at 5-position of the aromatic ring in **B1.103** (by deactivation of the phenolic functionality and thereby magnifying the *para* directing ability of the methoxy group) during the synthesis of 5-aminomethyl guaiacol and related compounds (Scheme B1.16). Later the mesyl group was hydrolyzed by refluxing with a 1:2 mixture of isopropanol and 5% aqueous potassium hydroxide solution.[75] Although authors could achieve the deactivation of the phenol moiety in **B1.103** towards electrophillic substitution by using other esters (acetate, trifluoroacetate, methyl carbamate) mesylate gave the best overall yield and showed stability under the other reaction conditions of the scheme.

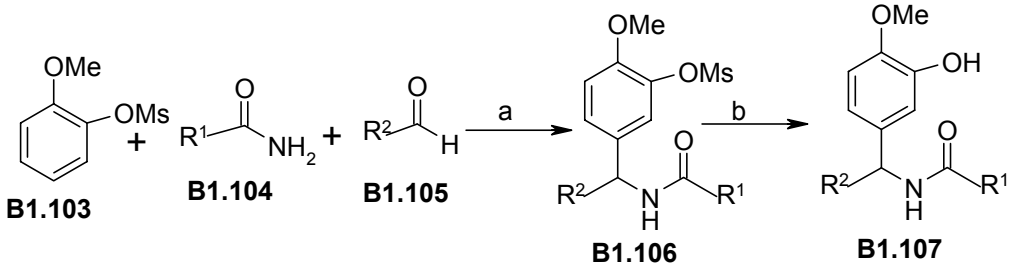

B1.103 **B1.104** **B1.105** **B1.106** **B1.107**

Scheme B1.16. a) AcOH-H_2SO_4 (3 : 2), 80 °C, 6 h, 90%; b) 5% aq KOH-*i*-PrOH (2 : 1), reflux, 6 h, 98%.

B1.4 Use of other sulfonyl groups for protection

Instances of hydroxyl group protection as the corresponding benzenesulfonate, benzylsulfonate, bromobenzenesulfonate, 2-(4-nitrophenyl)ethylsulfonate (Npes), 1*S*-(+)-

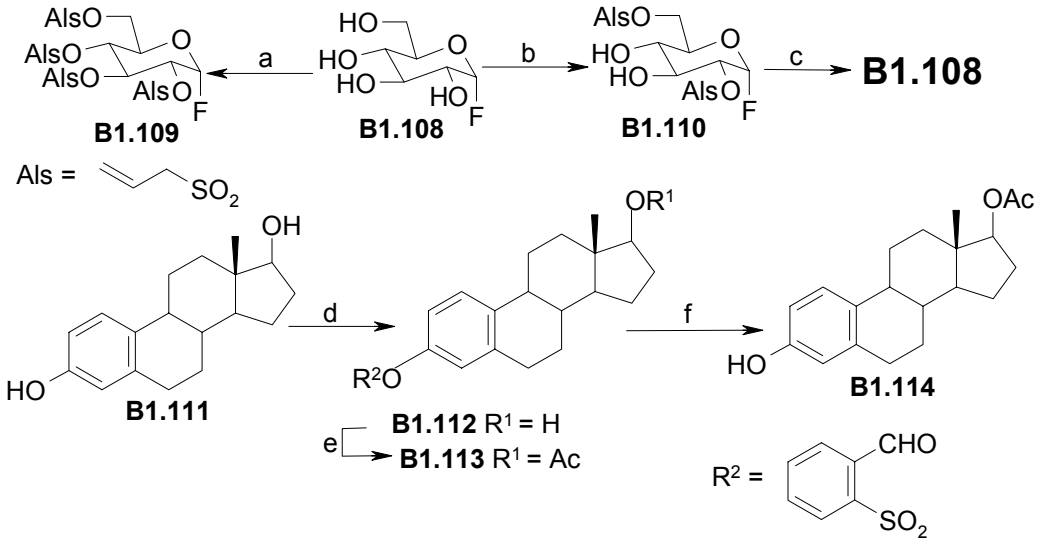

Scheme B1.17. a) AlsCl (4.8 eq), Pyr-DCM (1 : 1), -78 ^{o}C, 1 h; b) AlsCl (2.4 eq), Pyr-DCM (1 : 1), -78 ^{o}C, 1 h; c) $(Ph_3P)_4Pd$ (cat.), THF-morpholine-35% aq. formaldehyde (4 : 1 : 1), 2 h, rt, 85%; d) R^2Cl, Et_3N, Et_2O, rt, 4 h; e) AcCl, Et_3N, Et_2O; f) 0.05 M NaOH, aq acetone, 25 ^{o}C, 5 min.

10-camphorsulfonate have been reported. Methods of deprotection for most of these sulfonates are similar to those used for tosylates and mesylates.[38,39] Although there are reports on the ease of introduction and deprotection of allyl sulfonate,[76] and 2-formyl benzenesulfonate,[77] (Scheme B1.17) there is no literature on their use during synthesis.

Phenolic hydroxyl group was protected as benzene sulfonate for the synthesis of streptonigris (**B1.120**),[78] a metabolite of a few species of *Streptomyces* and *Actinomyces*. Benzene sulfonate protected aldehyde **B1.116** was used for condensation with **B1.115** and the sulfonate removed by methanolysis after the construction of the quinoline ring. (Scheme B1.18).

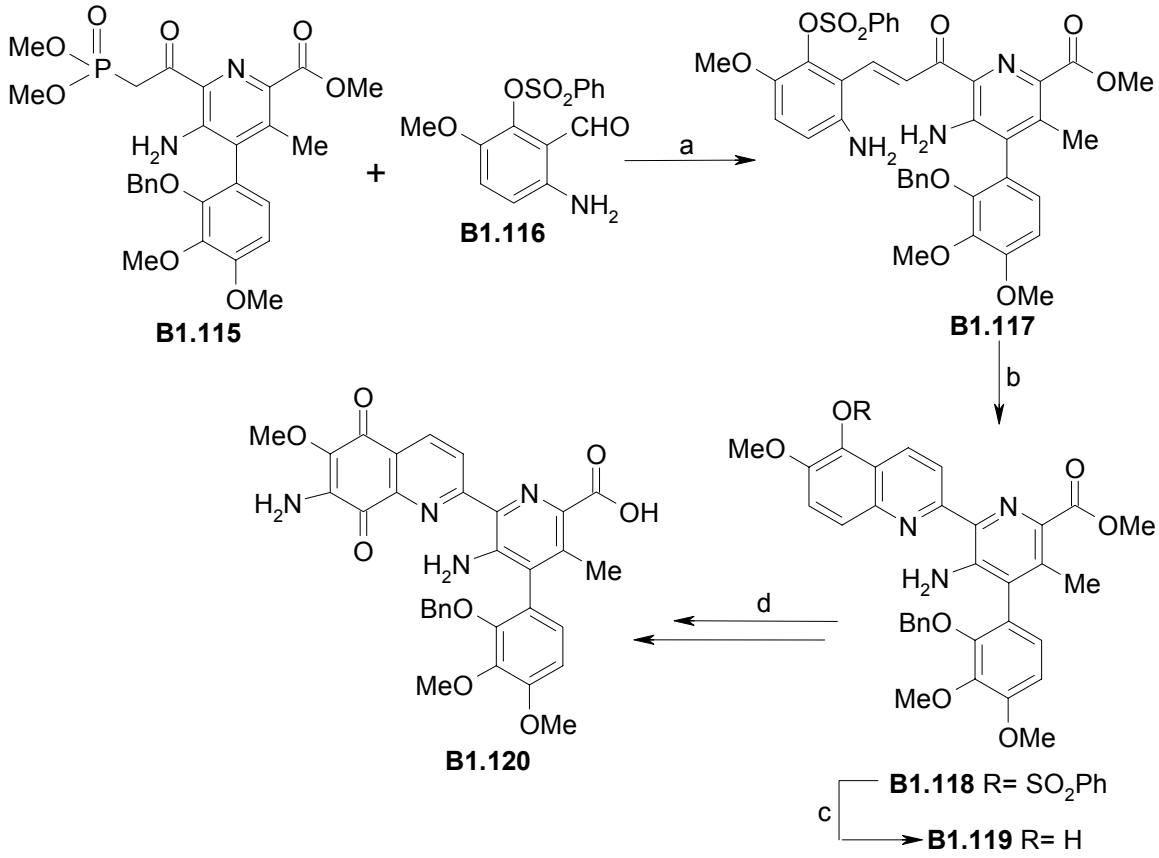

Scheme B1.18. a) KH, benzene, rt, 2 h, 65%; b) $NaHSO_3$, MeOH-H_2O, reflux, 2 h; c) NaOMe, MeOH, 40 °C, 40 min, 90%; d) as in reference 78.

The C-2 hydroxyl group of the mannose moiety was protected as the corresponding benzylsulfonate during the synthesis of methyl 3-*O*-(β-D-mannopyranosyl)-α-D-mannopyranoside (Scheme B1.19).[79]

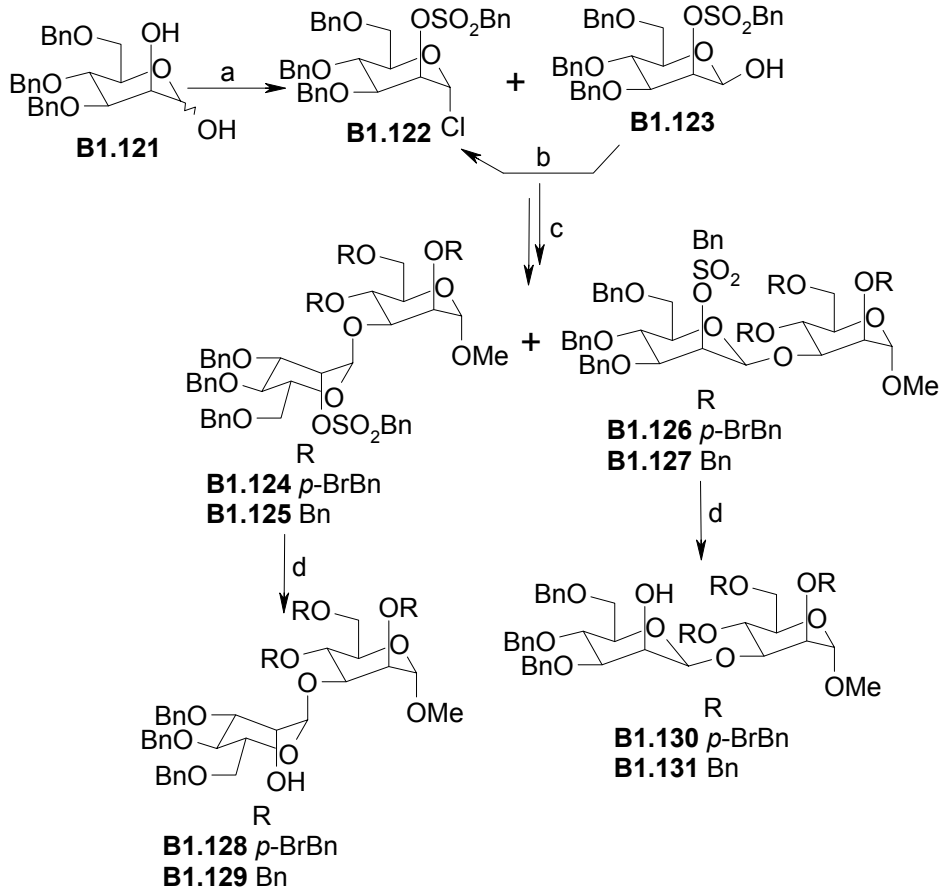

Scheme B1.19. a) $BnSO_2Cl$ (2.2 eq), 2,6-lutidine (2.5 eq), DCM, rt, 12 h, 72%; b) HCl, Et_2O, 0 °C, 12 h, 90%; c) as in reference 79; d) $NaNH_2$

Pfister and co-workers used 2-(4-nitrohphenyl)ethylsulfonate (Npes) group for the protection of hydroxyl group during synthesis of 2',5'-adenylate trimers.[80- 82] Npes group was cleaved by treatment with DBU in acetonitrile. One of the trimers synthesised (**B1.137**) is shown in Scheme B1.20.

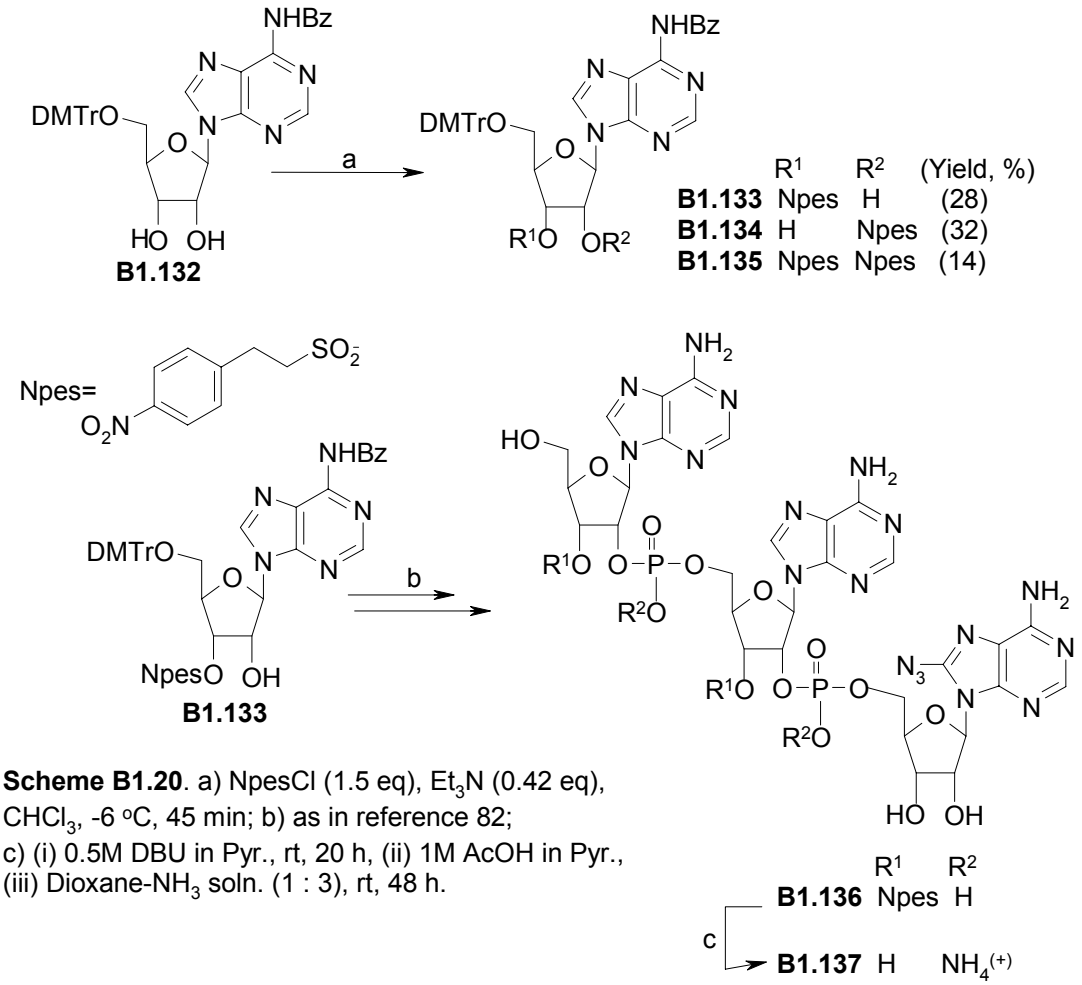

Scheme B1.20. a) NpesCl (1.5 eq), Et_3N (0.42 eq), $CHCl_3$, -6 °C, 45 min; b) as in reference 82; c) (i) 0.5M DBU in Pyr., rt, 20 h, (ii) 1M AcOH in Pyr., (iii) Dioxane-NH_3 soln. (1 : 3), rt, 48 h.

1*S*-(+)-10-camphorsulfonyl group being chiral and derived from a natural product has served as a protecting group as well as a resolving agent for *myo*-inositol derivatives (Scheme B1.21). Table B1.4 compares the yield of *myo*-inositol 1,3,4,5-tetrakisphosphate precursors[83] obtained by using camphorsulfonyl group for protection, with other methods reported in the literature.

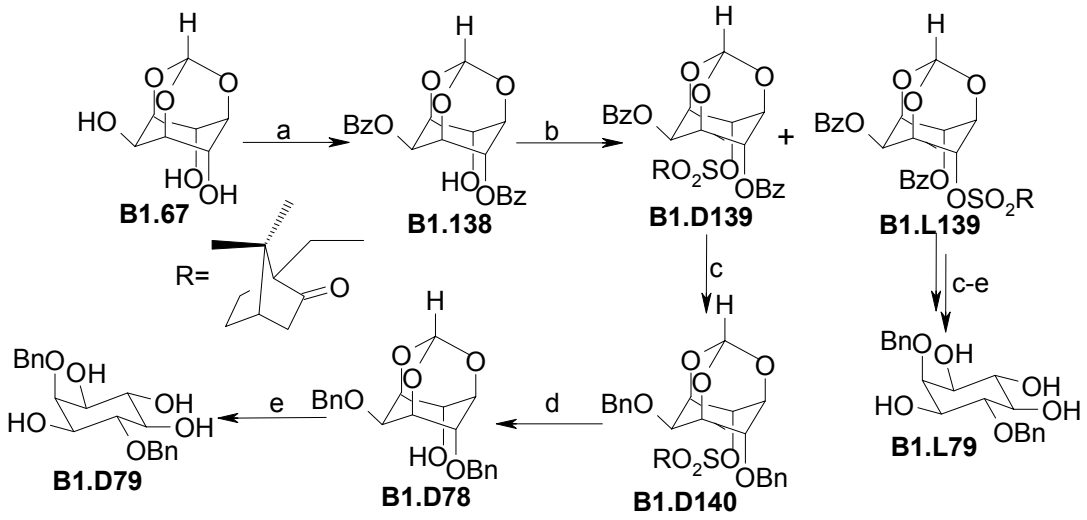

Scheme B1.21. a) BzCl (2 eq), Pyr., 0 ^{o}C-rt, overnight; b) RSO_2Cl, Pyr., rt, 24 h, 40% **B1.D139** & 45% **B1.L139**; c) BnBr, Ag_2O, DMF, 0 ^{o}C-rt, 80 h; d) NaOMe, MeOH, reflux, 24 h, 99%; e) aq. TFA, rt, 24 h, 99%.

Table B1.4.

Key intermediate	Yield (%)		Reference
	B1.L79	**B1.D79**	
myo-Inositol 1,3,5-orthoformate (**B1.67**)	27	27	57
myo-Inositol 1,3,5-orthoformate (**B1.67**)	12	13	58
myo-Inositol 1,3,5-orthoformate (**B1.67**)	15	14	58
1,2;4,5-di-*O*-cyclohexylidine-*myo*-inositol	3	NR	59
1,3,5-tri-*O*-benzoyl-*myo*-inositol	<8	NR	60
(-)-2,3;4,5-di-*O*-cyclohexylidine-*myo*-inositol	7	NR	61
myo-Inositol 1,3,5-orthoformate (**B1.67**)	28	28	83

NR- not reported

B1.5. Conclusions

A survey of the literature shows that sulfonyl groups can be efficiently used for the protection of hydroxyl groups in phenols and carbohydrates. However, the use of sulfonyl groups, for the protection of hydroxyl groups in other classes of organic compounds are rare. Perhaps the reasons for this tendency could be (a) the stability of the

tosyl derivatives obtained; (b) the selectivity observed during tosylation; (c) carbohydrates being polyols, require a number of different orthogonal hydroxyl protecting groups. In cyclitols, the use of sulfonates as protecting groups led to improved yields of the final products. We have extended the use of sulfonates as protecting group for the synthesis of other cyclitol derivatives, which are discussed in the subsequent section of this thesis.

B1.6. References

1. Greene, T. W.; Wuts, P. G. M. *Protective Groups in Organic Synthesis, Third Edition*, John Wiley, New York, 1999.
2. Kocieneski, P. J. *Protecting Groups*, Thieme, Stuttgart, Germany, 1994.
3. Abdel-Halim, O. B.; Morikawa, T.; Ando, S.; Matsuda, H.; Yoshikawa, M. *J. Nat. Prod*., **2004**, *67*, 1119.
4. Wang, J. *J. Agric. Food Chem*., **2004**, *52*, 171.
5. Ueki, M.; Sano, Y.; Sori, I.; Shinozaki, K.; Oyamada, H.; Ikeda, S. *Tetrahedron Lett*., **1986**, *27*, 4181.
6. Ueki. M.; Inazu, T.; *Bull. Chem. Soc. Jpn*., **1982**, *55*, 204.
7. Angyal, S. J.; Melrose, J. H *J. Chem. Soc*., **1965**, 6494.
8. Chung, S-K.; Chang, Y-T. *J. Chem. Soc. Chem. Commun.*, **1995**, 11.
9. Chung, S-K.; Chang, Y-T.; Ryu, Y. *Pure and Appl. Chem*., **1996**, *68*, 931.
10. Chung, S-K.; Chang, Y-T. *Korean J. Med. Chem*., **1996**, *6*, 162.
11. Chung, S-K.; Kwon, Y-U.; Chang, Y-T.; Shon, K-H.; Shin, J-H.; Park, K-H.; Hong, B-J.; Chung, I-H. *Bioorg. Med. Chem*., **1999**, *7*, 2577.
12. Sureshan, K. M.; Shashidhar, M. S. *Tetrahedron Lett*., **2000**, *41*, 4185.

13. Praveen, T. *Ph. D. Thesis*, University of Pune, Pune, 1999.
14. Tsuda, Y.; Nishimura, M.; Kobayashi, T.; Sato, Y.; Kanemitsu, K. *Chem. Pharm. Bull.*, **1991**, *39*, 2883.
15. Tsuda, Y.; Haque, M. E.; Yoshimoto, K. *Chem. Pharm. Bull.*, **1983**, *31*, 1612.
16. Fieser, L. F.; Fieser, M. *Reagents for Organic Synthesis, Vol. 1*, Wiley-Interscience, New York, 1967, p. 1179.
17. Kabalka, G. W.; Varma, M.; Varma, R. S. *J. Org. Chem.*, **1986**, *51*, 2386.
18. Wolform, M. L.; Koos, E. W.; Bhat, H. B. *J. Org. Chem.*, **1967**, *32*, 1058.
19. Yoshida, Y.; Sakakura, Y.; Aso, N.; Okada, S.; Tanabe, Y. *Tetrahedron*, **1999**, *55*, 2183.
20. Gerspacher, M.; Rapoport, H. *J. Org. Chem.*, **1991**, *56*, 3700.
21. Xu, L-w.; Xia, C-g. *Synth. Commun.*, **2004**, *34*, 1199.
22. Ishihara, K.; Kurihara, H.; Yamamoto, H. *J. Org. Chem.*, **1993**, *58*, 3791.
23. Takamura, T.; Tejima, S. *Chem. Pharm. Bull.*, **1978**, *26*, 1117.
24. Mori, M.; Tejima, S. *Chem. Pharm. Bull.*, **1981**, *29*, 71.
25. Takamura, T.; Chiba, T.; Tejima, S. *Chem. Pharm. Bull.*, **1979**, *27*, 721.
26. Bhavanandan, V. P.; Meyer, K. *J. Biol. Chem.*, **1967**, *242*, 4352.
27. Takamura, T.; Chiba, T.; Tejima, S.; *Chem. Pharm. Bull.*, **1981**, *29*, 1027.
28. Takamura, T.; Chiba, T.; Teima, S. *Chem. Pharm. Bull.*, **1981**, *29*, 1076.
29. Mori, M.; Tejima, S. *Chem. Pharm. Bull.*, **1981**, *29*, 421.
30. Tsuda, Y.; Nishimura, M.; Kobayashi, T.; Sato, Y.; Kanemitsu, K. *Chem. Pharm. Bull.*, **1991**, *39*, 2883.
31. Kong, X.; Grindley, T. B.; *Can. J. Chem.*, **1994**, *72*, 2396.

32. Kadowaw, J-i.; Sato, M.; Karasu, M.; Tagaya, H.; Chiba, K. *Angew. Chem. Int. Ed. Engl.*, **1998**, *37,* 2372.

33. Pozsgay, V.; Dubois, E. P.; Pannell, L. *J. Org. Chem.*, **1997**, *62*, 2832.

34. Sridhar, M.; Ashok Kumar, B.; Narender, R. *Tetrahedron Lett.*, **1998**, *39*, 2847.

35. Miljković, M. A.; Pešić, M.; Jokić, A.; Davidson, E. A. *Carbohydr. Res.*, **1970**, *15*, 162 and references theirin.

36. Roemmele, R. C.; Rapoport, H. *J. Org. Chem.*, **1988**, *53*, 2367.

37. Civitello, E. R.; Rapoport, H. *J. Org. Chem.*, **1994**, *59*, 3775.

38. Closson, W. D.; Wriede, P.; Bank, S. *J. Am. Chem. Soc.*, **1966**, *88*, 1581 and references cited therein.

39. Jarrell, H. C.; Ritchie, R. G. S.; Szarek, W. A.; Jones, J. K. N. *Can. J. Chem.*, **1973**, *15*, 1767.

40. Also see, Kovacks, J.; Ghatak, U. R. *J. Org. Chem.*, **1966**, *31*, 119.

41. Kenner, G. W.; Murray, M. A. *J. Chem. Soc.*, **1949**, S178.

42. Nayak, S. K. *Synthesis*, **2000**, 1575.

43. Sabitha, G.; Abraham, S.; Reddy, B. V. S.; Yadav, J. S. *Synlett*, **1999**, 1745.

44. Reddy, G. S.; Hari Mohan, G.; Iyenger, D. S.; *Synth. Commun.*, **2000**, *30*, 3829.

45. Chakraborti, A. K.; Nayak, M. K.; Sharma, L. *J. Org. Chem.*, **1999**, *64*, 8027.

46. Chakraborti, A. K.; Nayak, M. K.; Sharma. L. *J. Org. Chem.*, **2002**, *67*, 1776.

47. Nishida, A.; Hamada, T.; Yonemitsu, O. *J. Org. Chem.*, **1988**, *53*, 3387.

48. Nishida, A.; Hamada, T.; Yonemitsu, O. *Chem. Pharm. Bull.*, **1990**, *38*, 2977.

49. Ohsawa, T.; Takagaki, T.; Ikehara, F.; Takahashi, Y.; Oishi, T. *Chem. Pharm. Bull.*, **1982**, *30*, 3178.

50. Zen, S.; Tashima, S.; Kotō, S. *Bull. Chem. Soc. Jpn.*, **1968**, *41*, 3025.

51. Bradford, A. D.; Foster, A. B.; Westwood, J. H. *Carbohydr. Res.*, **1970**, *13*, 189.

52. Binkley, R. W.; Koholic, J. *J. Org. Chem.*, **1989**, *54*, 3577.

53. Masnovi, J.; Koholic, D. J.; Berki, R. J.; Binkley, R. W. *J. Am. Chem. Soc.*, **1987**, *109*, 2851.

54. Civitello, E. R.; Rapoport, H. *J. Org. Chem.*, **1992**, *57*, 834.

55. Sureshan, K. M.; Shashidhar, M. S. *Tetrahedron Lett.*, **2001**, *42*, 3037.

56. Sureshan, K. M.; Shashidhar, M. S.; Praveen, T.; Gonnade, R. G.; Bhadbhade, M. M. *Carbohydr. Res.*, **2002**, *337*, 2399.

57. Lauman, K.; Ghisalba, O. *Biosci. Biotechnol. Biochem.*, **1999**, *63*, 1374.

58. Baudin, G.; Glanzer, B. I.; Swaminathan, K. S.; Vasella, A. *Helv. Chim. Acta*, **1988**, *71*, 1367.

59. Ozaki, S.; Kondo, Y.; Nakahira, H.; Yamaoka, S.; Watanabe, Y. *Tetrahedron Lett.*, **1987**, *28*, 4692.

60. Watanabe, Y.; Oka, A.; Shimizu, Y.; Ozaki, S.; *Tetrahedron Lett.*, **1990**, *31*, 2613.

61. Gou, D-M.; Chen, C-S. *Tetrahedron Lett.*, **1992**, *33*, 721.

62. Fieser, L. F.; Fieser, M. *Reagents for Organic Synthesis, Vol. 1*, Wiley-Interscience, New York, 1967, p. 662.

63. Heusser, H.; Wuthier, H. *Helv. Chim. Acta*, **1947**, *30*, 1454.

64. Crossland, R. K.; Servis, K. L. *J. Org. Chem.*, **1970**, *35*, 3195.

65. Bredenkamp, M. W.; Holzapfel, C. W.; Swanepoel, A. D. *Tetrahedron Lett.*, **1990**, *31*, 2759.

66. O'Donnelll, C. J.; Burke, S. D. *J. Org. Chem.*, **1998**, *63*, 8614.

67. Hughes, N. A.; Tyson, P. D. *Carbohydr*. *Res*., **1977**, *57*, 317.

68. Hughes, N. A.; Todhunter, N. D. *Carbohydr*. *Res*., **2000**, *326*, 81.

69. Lantos, I.; Loev, B. *Tetrahedron Lett*., **1975**, *16*, 2011.

70. Webster, K. T.; Eby, R.; Schuerch, C. *Carbohydr*. *Res*., **1983**, *123*, 335.

71. Ritter, T.; Stanek, K.; Larrosa, I.; Carreira, E. M. *Org*. *Lett*., **2004**, *6*, 1513.

72. Cossy, J.; Ranaivosata, J-L.; Brllosta, V.; Wietzke, R. *Synth*. *Commun*., **1995**, *25*, 3109.

73. Srivastava, V. K.; Schuerch, C. *J*. *Org*. *Chem*., **1981**, *46*, 1121.

74. Qiao, L.; Hu, Y.; Nan, F.; Powis, G.; Kozikowski, A. P. *Org*. *Lett*., **2000**, *2*, 115.

75. Bensel, N.; Pevere, V.; Desmurs, J. R.; Wagner, A.; Mioskowski, C. *Tetrahedron Lett*., **2002**, *43*, 4281.

76. Brill, W. K. –D.; Kunz, H. *Synlett*, **1991**, 163.

77. Shashidhar, M. S.; Bhatt, M. V. *J*. *Chem*. *Soc*., *Chem*. *Commun*., **1987**, 654.

78. Basha, F. Z.; Hibino. S.; Kim, D.; Pye, W. E.; Wu, T-T.; Weinreb, S. M. *J*. *Am*. *Chem*.. *Soc*., **1980**, *102*, 3962.

79. Awad, L. F.; El Ashrey, E. S. H.; Schuerd, C. *Bull*. *Chem*. *Soc*. *Jpn*., **1986**, *59*, 1587.

80. Pfister, M.; Schirmeister, H.; Mohr, M.; Farkas, S.; Stengele, K-P.; Reiner, T.; Dunkel, M.; Gokhle, S.; Charubala, R.; Pfieiderer, W. *Helv*. *Chim*. *Acta*, **1995**, *78*, 1705.

81. Schirmister, H.; Pfleiderer, W. *Helv*. *Chim*. *Acta*, **1994**, *77*, 10.

82. Charubala, R.; Pfleiderer, W.; Sobol, R. W.; Li, S-W.; Suhadolinik, R. J. *Helv*. *Chim*. *Acta*, **1995**, *78*, 1075.

83. Sureshan, K. M.; Das, T.; Shashidhar, M. S.; Gonnade, R. G.; Bhadbhade, M. M. *Eur. J. Org. Chem.*, **2003**, 1035.

Section 2

Synthesis of cyclitol derivatives with the aid of *p*-toluenesulfonyl group for the protection of inositol hydroxyl groups

B2.1. Introduction

Selective protection and deprotection of various functional groups is an indispensable tool for the synthesis of complex organic molecules. Efficiency of protection and / or deprotection during the course of a synthesis could decide the overall yield of the desired product. Molecules having non-equivalent functional groups of the same kind (polyols, polyamines, polyacids etc.) pose challenges during their chemical manipulation as the difference in their reactivity is often subtle. A number of methods have been explored to achieve regioselective protection and deprotection of hydroxyl groups of inositols[1] and these have provided means for the synthesis of naturally occurring phosphoinositols and their analogs. Cyclitols, their derivatives and analogs have continued to attract the attention of chemists and biologists due to their involvement in various biological phenomena such as cellular signal transduction, calcium mobilization, insulin stimulation, exocytosis, cytoskeletal regulation, intracellular trafficking of vesicles and anchoring of certain proteins to cell membranes.[2-5] *myo*-Inositol has also been used as a starting material for the synthesis of natural products and their analogs.[6,7] *myo*-Inositol orthoesters have been used extensively for the synthesis of phosphoinositols and their derivatives.[1,8,9]

Methylated inositols are of particularly marked abundance in grains and forage legumes[10,11] and thus comprise a significant portion of the diet of animals grazing legumes, and humans relying on legume grains as protein source in their diet. *O*-methylated inositols (Chart B2.1) such as (+)-onoinitol (1D-4-O-methyl-*myo*-inositol, **B2.D1**), (+)-bornesitol (1D-3-O-methyl-*myo*-inositol, **B2.D2**), sequoyitol (5-O-methyl-*myo*-inositol, **B2.3**), (+)-pinitol (1D-3-O-methyl-*chiro*-inositol, **B2.D5**) (-)-quebrachitol

(1L-2-O-methyl-*chiro*-insoitol, **B2.L6**), are present in seeds of many plants, frequently in combination with one another; their glycosylated derivatives are abundant in seeds such as adzuki bean.[12] *O*-methyl-*scyllo*-inositol (**B2.4**) has been isolated from mung bean seeds.[13] Galactosyl cyclitols are thought to protect membranes and other cellular structures during seed desiccation or storage in the dry state.[14]

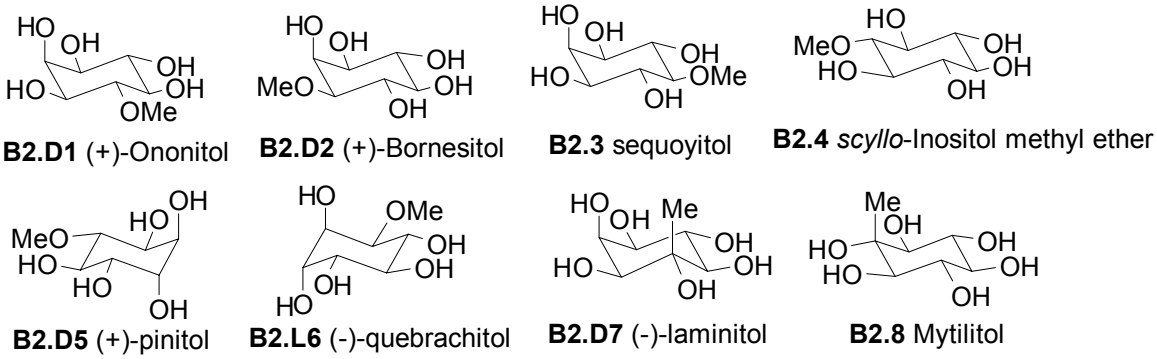

Chart B2.1

(-)- Laminitol (**B2.D7**) and mytilitol (**B2.8**), are C-methyl inositols having *myo*- and *scyllo*-type configuration respectively, occur in marine algae.[15,16] Epimerization of laminitol to mytilitol observed in *Chlorella fusca* suggests a biosynthetic path for mytilitol.[17] We have developed high yielding procedures (overall yield in parenthesis) for the synthesis of both (+)- & (-)-ononitol (32%), *scyllo*-inositol methyl ether (60%), mytilitol (48%), racemic laminitol (63%), (-)- & (+)- laminitol (30%) and *scyllo*-inositol (64%) from *myo*-inositol (**B2.9**).

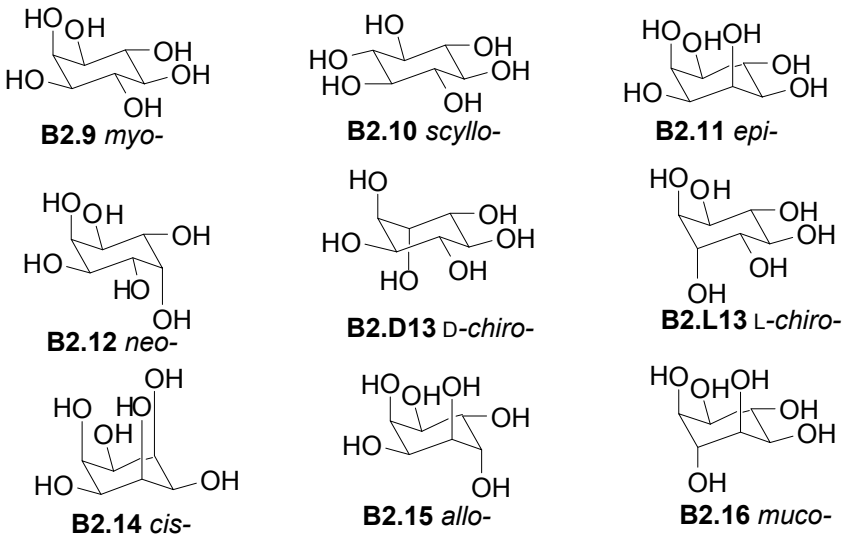

Chart B2.2

scyllo-Inositol (**B2.10**), the cyclitol having six equatorial hydroxyl groups, is found in many plants and animals[18,19] and also has been isolated from human brain[20-23] It has been suggested that certain human diseases are associated with *scyllo*-inositol depletion.[22] Among the nine isomers of inositols known (Chart B2.2), *myo*- isomer, having five equatorial and one axial hydroxyl group is the most abundant in nature and hence there have been efforts to convert *myo*-inositol to other isomers.[24-30] Isomeric inositols have also been synthesized from carbohydrates[31-34] as well as from benzene[35,36] and its derivatives.[37-41] Synthesis of isomeric inositols from other compounds such as *endo*- and *exo*-oxabicyclo-[2.2.1]-hept-5-ene-2,3-diols,[42] cyclohexene,[43] tetrahydroxyquinone[44] were also reported. Podeschwa and co-workers have synthesized isomeric inositols from *para*-benzoquinone.[45] A common-intermediate strategy for the synthesis of conduritols and inositols via β-hydroxy cyclohexenylsilanes is also reported.[46] In a recent report enantiopure cyclitols were synthesized from (±)-3-bromocyclohexene using (*S*, *S*)-hydrobenzoin and *S*-mandelic acid as chiral sources.[47]

There are few reports on the conversion of *myo*-inositol to *scyllo*-inositol[26-28] or its derivatives[24,25,48-50] in overall yields of 10-40%.

epi-Inositol (**B2.11**) having two axial and four equatorial hydroxyl groups is a member of the cyclitol family. Shaldubina and co-workers have shown that *epi*-inositol has the ability to modify the expression of the yeast *INO1* gene encoding the *myo*-inositol-3-phosphate synthatase.[51] *epi*-Inositol is thus biologically active in its ability to affect the regulation of the *myo*-inositol biosynthetic pathway. *epi*-Inositol has also been evaluated as a potential antidepresent drug that could interact with lithium and *myo*-inositol receptors in the brain.[52-55] *epi*-Inositol and racemic *epi*-inosose were tested for the inhibition activity towards phospatidylinositol-specific phospholypase C (PI-PLC) from *Bacillus cereus*, (IC_{50} for *epi*-inositol = 2 mM; IC_{50} for racemic *epi*-inosose = 3 mM).[56] Several synthetic routes for *epi*-inositol, starting from different starting materials like furan,[42] D-glucose,[34] D-galactose,[34,57] *myo*-inositol[24,25] and benzene[35] are known in the literature. Recently a chemoenzymatic route for the synthesis of *epi*-inositol, starting from bromobenzene was also reported.[58] Racemic *epi*-inositol 1,4,5-trisphosphate was been synthesized as an analog of D-Ins(1,4,5)P_3 and found to have lower receptor binding ability towards Ins(1,4,5)P_3 receptors.[59]

Free and conjugated amino- derivatives of *myo*-inositol are capable of inhibiting glycosidases and play an active role in antibiotic action.[60] Azido- and amino-*myo*-inositol derivatives selectively inhibit cell growth.[61] Aminocyclitols were also synthesized from conduritol derivatives.[62] Recently Watanabe and co-workers[63] reported the synthesis of amino and di-amino cyclitols with *chiro*- and *allo*-configuration by using regioselective sulfonylation and nucleophilic displacement of the sulfonate (triflate) as key steps. Other

aminocyclitols of biological interest have also been synthesized in the last decade.[64-76] However there are only a few syntheses of amino-*myo*-inositols reported in the literature till date. We have developed high yielding synthetic routes for the synthesis of both the enantiomers of 4-deoxy-4-amino *myo*-inositol (25% overall yield).

During the synthesis of all the cyclitol derivatives presented in this part of the thesis, tosyl group was used as a protecting group. Hydroxyl groups are seldom protected as their sulfonates due to problems (such as elimination, nucleophilic substitution etc.) associated with their deprotection (Scheme B2.1). Although there are many reports in the literature on the sulfonates (mesylates, tosylates) of cyclitols, most of them were used for further functionalization of the cyclitol moiety by nucleophilic substitution or deoxygenation.

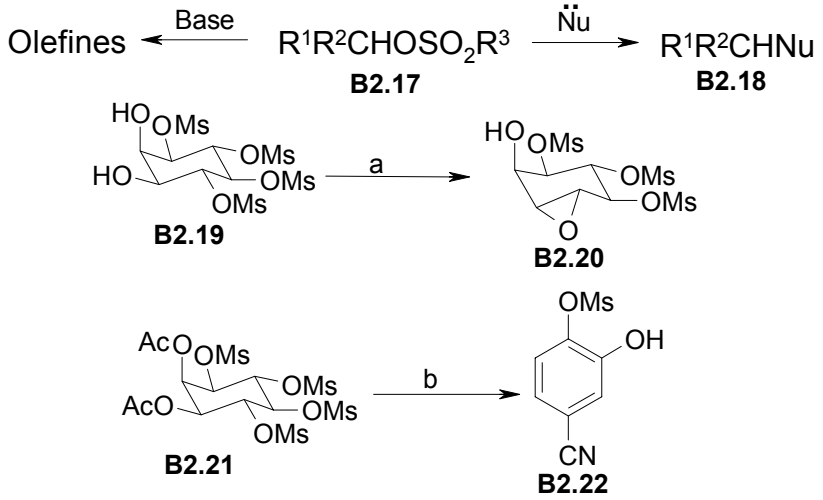

Scheme B2.1. a) NaOMe (1 eq), MeOH, reflux, 15 min, 91%;
b) KCN (4 eq), 2-methoxyethanol, 100 ^{o}C, 42%.

However, previous work in our laboratory[77] had shown that the three hydroxyl groups of *myo*-inositol orthoesters could be sulfonylated with very good regioselectivity (discussed in Section B1.2). Furthermore, the resulting sulfonates could be cleaved efficiently with

retention of configuration of the *myo*-inositol ring. This is mainly because these orthoesters are trioxaadamantanes.[77-79] The regioselectivity observed during sulfonylation and the efficient removal of the sulfonates to regenerate the parent alcohol was utilized to synthesize precursors of both D- and L-Ins(1,3,4,5)P_4.[77] In the present work, we have extended the use of sulfonate protection in *myo*-inositol orthoesters for the synthesis of ononitol, laminitol, *scyllo*-inositol and its methyl ether, mytilitol and D-4 and D-6-deoxy-amino-*myo*-inositol.

B2.2. Synthesis of cyclitol derivatives having the *myo*-configuration

B2.2.1. Synthesis of (+)- and (-)- Ononitol

B2.2.1.1. Known methods of synthesis

The known methods of synthesis of racemic[80] as well as enantiomeric ononitols[81, 82] are shown in Scheme B2.2. Epimerization of pinitol in acetic acid also results in the formation of ononitol as one of the products (identified by gas chromatography).[83] Hence this method is not suitable for the preparation of ononitol. Racemic ononitol was synthesized from *myo*-inositol (**B2.9**) via the dibenzoate **B2.24**.[80] The dibenzoate was methylated under controlled conditions to obtain the methyl ether **B2.25** which on deprotection gave racemic ononitol (**B2.1**) in 47% overall yield. Pietrusiewicz and Salamończyk synthesized of (+) and (-)- ononitol from *myo*- inositol.[82] They obtained the tripivalate **B2.D27**[84] from *myo*-inositol in 31% overall yield in two steps. This tripivalte on methylation and deprotection gave D-ononitol (**B2.D1**). L-Ononitol (**B2.L1**) was obtained in a similar fashion starting from **B2.L27**.[84]

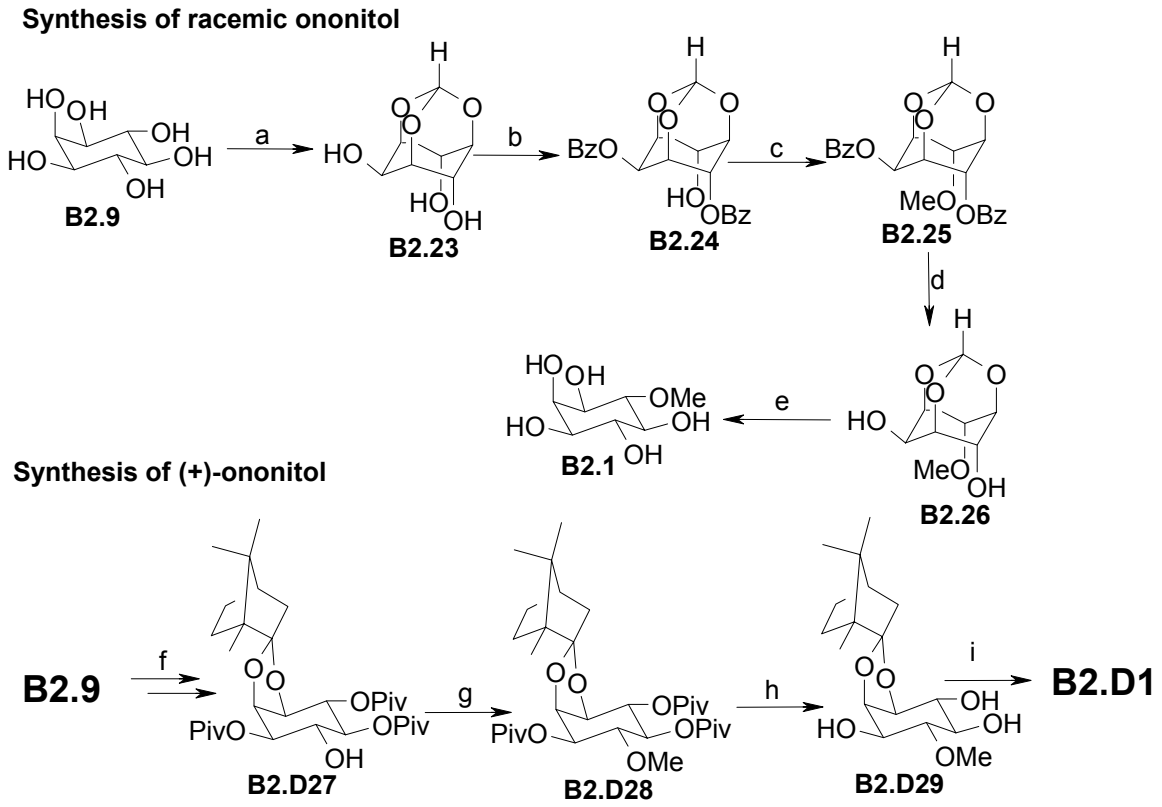

Scheme B2.2. a) $(EtO)_3CH$ (1. 5eq), TsOH, DMF, 100 ^oC, 2 h; b) BzCl (2 eq), Pyr, 0 ^oC -rt, overnight, 60%.; c) MeI (1 eq), Ag_2O (5 eq), DMF, 0 ^oC-rt, 2 h, 80%; d) *i*-$BuNH_2$, MeOH, rt, 19 h; e) TsOH, MeOH, rt, 24 h, 98%; f) as in reference 84, 31%; g) MeI (4 eq), Ag_2O, (2 eq), DMF, 4 ^oC, 16 h, 90%.; h) NaOH (10 eq), MeOH-H_2O (10 : 1), rt, 36 h, 90%; i) 80% aq AcOH, 100 ^oC, 1 h, 92%.

B2.2.1.2. Present work

Synthetic routes for (+)- and (-)-ononitols (**B2.D1** & **B2.L1**) are shown in Schemes B2.3 and Scheme B2.4 respectively. The synthesis started with ditosylation of the triol **B2.23** in the presence of pyridine or triethyl amine to obtain the racemic ditosylate **B2.30**.[77] The racemic ditosylate was resolved by converting it to diastereomeric 1*S*-(-)-camphanoate esters, **B2.31** and **B2.dia31**. These diastereomeric esters could be separated by column chromatography. The absolute configurations of these diastereomers were established by X-ray crystallography. The enantiomer **B2.L30** was obtained by aminolysis of the camphanoate **B2.31** with isobutyl amine. Methylation

of **B2.L30** with methyl iodide and sodium hydride in DMF gave the methyl ether **B2.L32** in 95% yield. Methanolysis of the tosylates in **B2.L32** with sodium methoxide in methanol gave 1D-ononitol orthoformate (**B2.D26**). Acid hydrolysis of **B2.D26** with trifluoroacetic acid in water gave D-ononitol (**B2.D1**), which was characterized by comparing its melting point, ^{1}H NMR and specific rotation with those reported in the literature.[82]

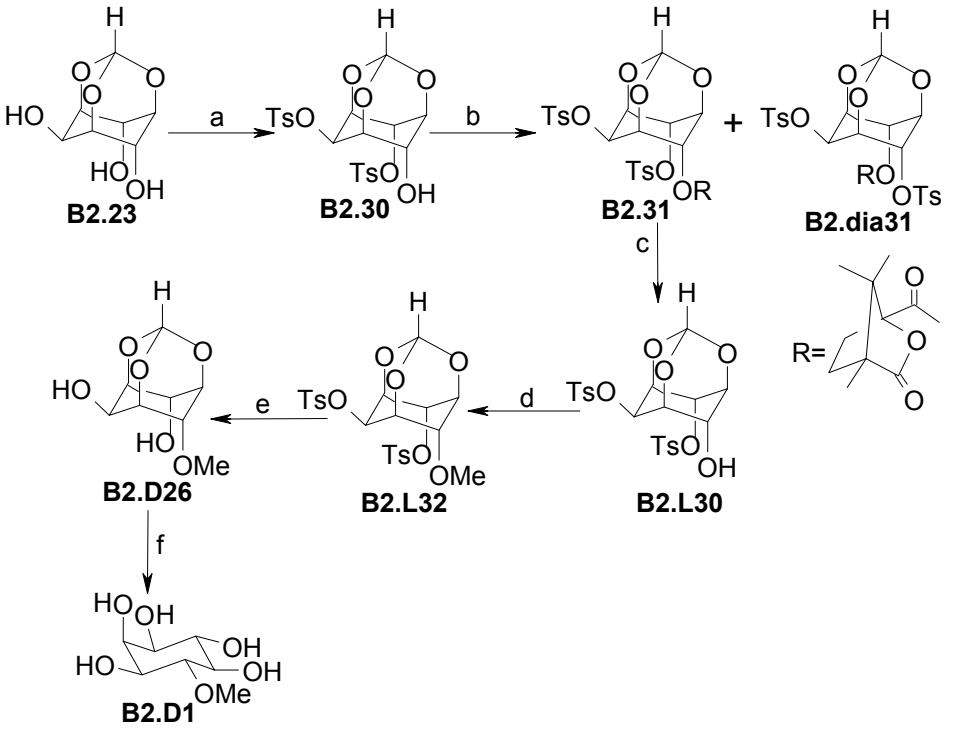

Scheme B2.3. a) TsCl (2.1 eq), Pyr, 80-100 °C, 48 h, 90%; b) RCl (1.5 eq), DMAP, Pyr, 80-100 °C, 12 h, 97%; (**B2.31**, 43% ; **B2.dia31**, 44%); c) *i*-BuNH$_2$, MeOH, reflux, 12 h, 96%; d) MeI (1.2 eq), NaH (1.1 eq), DMF, rt, 5 min, 95%; e) NaOMe, MeOH, reflux, 12 h, 99%; f) TFA-H$_2$O (4:1), rt, 1 h, 100%.

Same sequence of reactions, as described above for the synthesis of D-ononitol (**B2.D1**), on **B2.dia31** gave L-ononitol (**B2.L1**) in 32% overall yield from *myo*-inositol (Scheme B2.4).

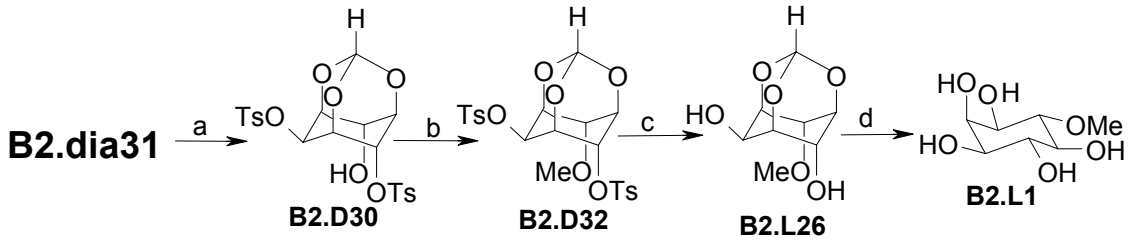

Scheme B2.4. a) *i*-$BuNH_2$, MeOH, reflux, 12 h, 97%; b) MeI (1.2 eq), NaH (1.1 eq), DMF, rt, 5 min, 95%; c) NaOMe, MeOH, reflux, 12 h, 99%; d) TFA-H_2O (4:1), rt, 1 h, 98%.

Table B2.1 shows a comparison of the yields obtained in the present work with those reported in the literature.

Table B2.1. Comparision of the yields of (+)- and (-)- ononitol obtained (from *myo*-inositol) with literature methods.

Number of steps	Overall yield (%) of ononitol			Reference
	(±)	(+)	(-)	
4	47	NR	NR	80
5	NR	17	18	82
9	NR	32	32	Present work

NR- Not reported

B2.2.1.3. Polymorphism of inositol derivatives encountered during the synthesis of ononitol

The triol **B2.23** showed polymorphism on crystallization from different solvents (Figure B2.1 A and B). The crystal structure of **B2.23** was reported in the literature (Figure B2.1B),[85] which belonged to monoclinic space group $P2_1/c$. Although the solvent of crystallization was not mentioned earlier by the authors,[85] we could successfully obtain the same crystal form when crystallized from nitromethane. We obtained a new polymorph of **B2.23**, when crystallized from ethyl acetate column fraction, which belongs to orthorhombic space group, $Pna2_1$ (Figure B2.1A). The conformational

freedom of three hydroxyl groups in **B2.23** and their ability to form vsrious intermolecular and intramolecular H-bonding contacts was responsible for the appearance of different polymorphic modifications.

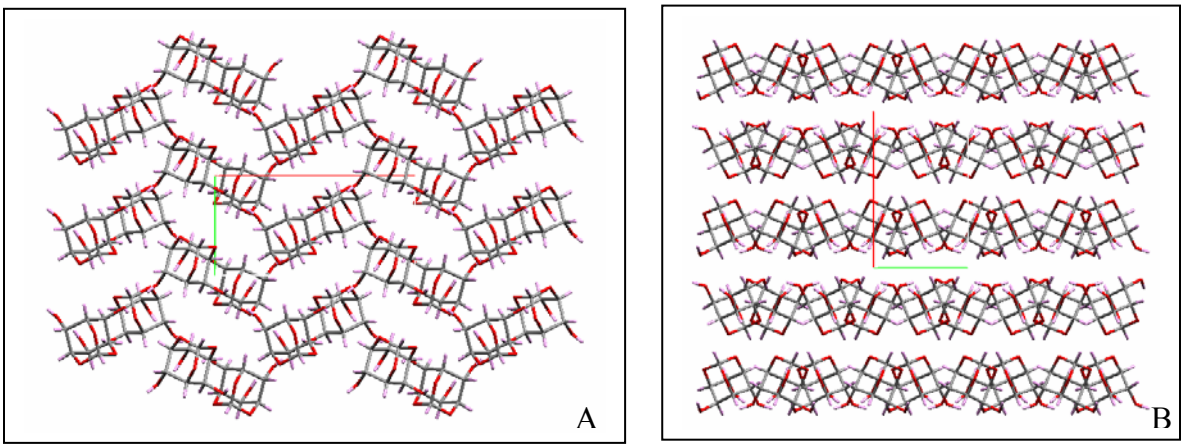

Figure B2.1. Packing of molecules in crystals of **B2.23** (view down the c-axis) obtained (A) from ethyl acetate, (B) crystals for which structure was reported in the literature.[85]

B2.2.2. Synthesis of (-)- and (+)-Laminitol

B2.2.2.1. Known methods of synthesis

Posternak established the absolute configuration of laminitol[86] and reported its first synthesis.[87,88] Posternak and Falbriard synthesized racemic laminitol (**B2.7**)[87,88] starting form the pentaacetate **B2.33**, and (-)-laminitol (**B2.D7**)[87,88] from the optically active cyclohexane derivative **B2.D36** (Scheme B2.5). Both **B2.D36** and **B2.33** were obtained from *myo*-inositol.

Synthesis of racemic laminitol

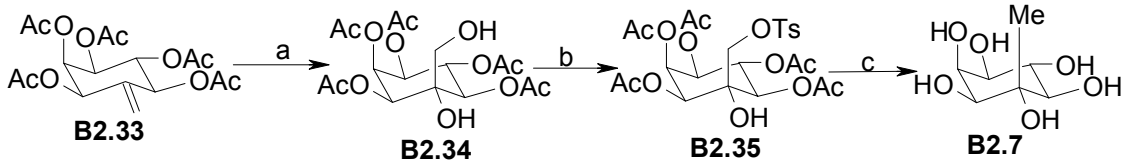

Synthesis of (-)-laminitol

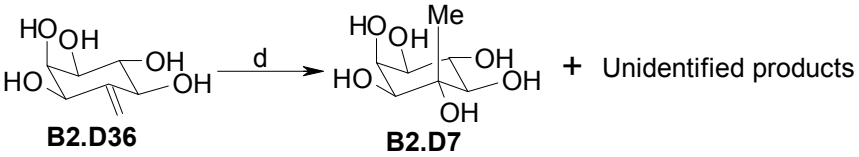

Scheme B2.5. a) OsO_4, Pyr-benzene, dark, rt, 24 h, 100%; b) TsCl, Pyr; c) (i) $LiAlH_4$, THF, 90 °C, 4 h., (ii) Doex 50 (H^+); d) (i) 0.04M HOBr, rt, 1,5 h, (ii) Amberlite IR-4B, (ii) H_2 / Raney Ni, 100-125 atm, rt, 48 h.

Gigg synthesized racemic laminitol derivative **B2.42**[30] (Scheme B2.6) starting from racemic 1,2-*O*-isopropylidine-3,4,5-tri-*O*-benzyl-*myo*-inositol (**B2.37**).[30]

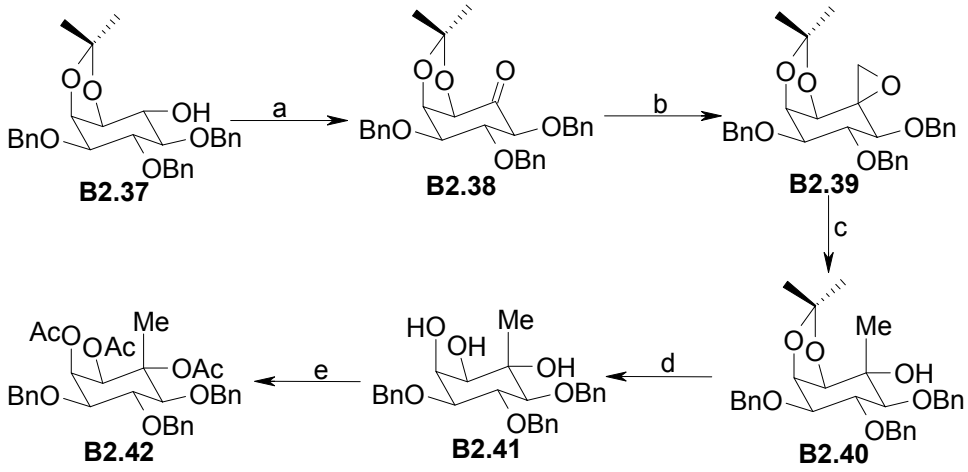

Scheme B2.6. a) DMSO, Pyr-SO_3, Et_3N, 20 °C, 30 min, 80%; b) DCM, Et_2O, MeOH (trace), 20 °C, overnight, 59%; c) $LiAlH_4$, Et_2O, rt, 30 min, 71%; d) 1M HCl-MeOH (1 : 9), reflux, 30 min; e) Ac_2O, DMAP, Et_3N, DCM, rt, 18 h.

Carless and Oak's synthesis of (-)-laminitol (Scheme B2.7) started with the *cis*-diol **B2.43** which was obtained by the oxidation of toluene with *Pseudomonas putida*.[89] In this synthesis the conversion of **B2.44** to **B2.45** was low yielding and the epoxide opening in **B2.47** gave **B2.48** as a side product, along with (-)-laminitol (**B2.D7**).

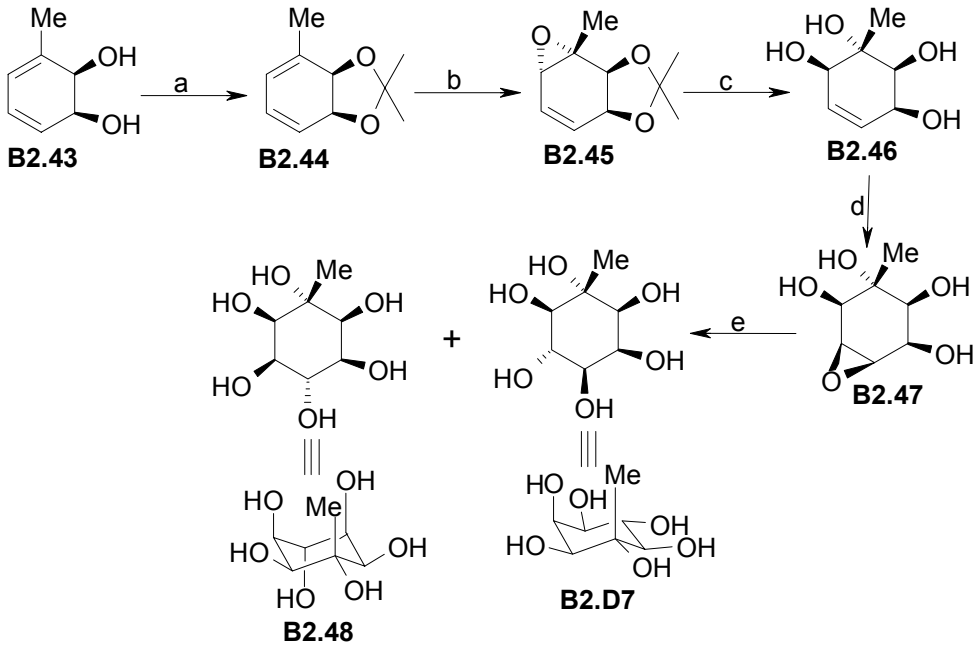

Scheme B2.7. a) 2,2-dimethoxypropane, TsOH, 65%; b) *m*-CPBA, DCM, Na_2CO_3, 0 °C, 12 h, 47%; c) TsOH, THF-H_2O (5 : 1), 20 °C, 6 d, 78%; d) *m*-CPBA, DCM, 10 d, 73%; e) TFA-H_2O, reflux, 4 h, 35% **B2.D7** and 55% **B2.48**.

Sato and co-workers reported the synthesis of (-)-laminitol using D-glucose (**B2.49**) as the starting material (Scheme B2.8).[90] This method of synthesis of (-)-laminitol involved large number of synthetic transformations including the Ferrier cyclization[91,92] and some of the steps gave mixture of isomeric cyclitols. There is no report in the literature on the synthesis of the unnatural isomer, (+)-laminitol, till date.

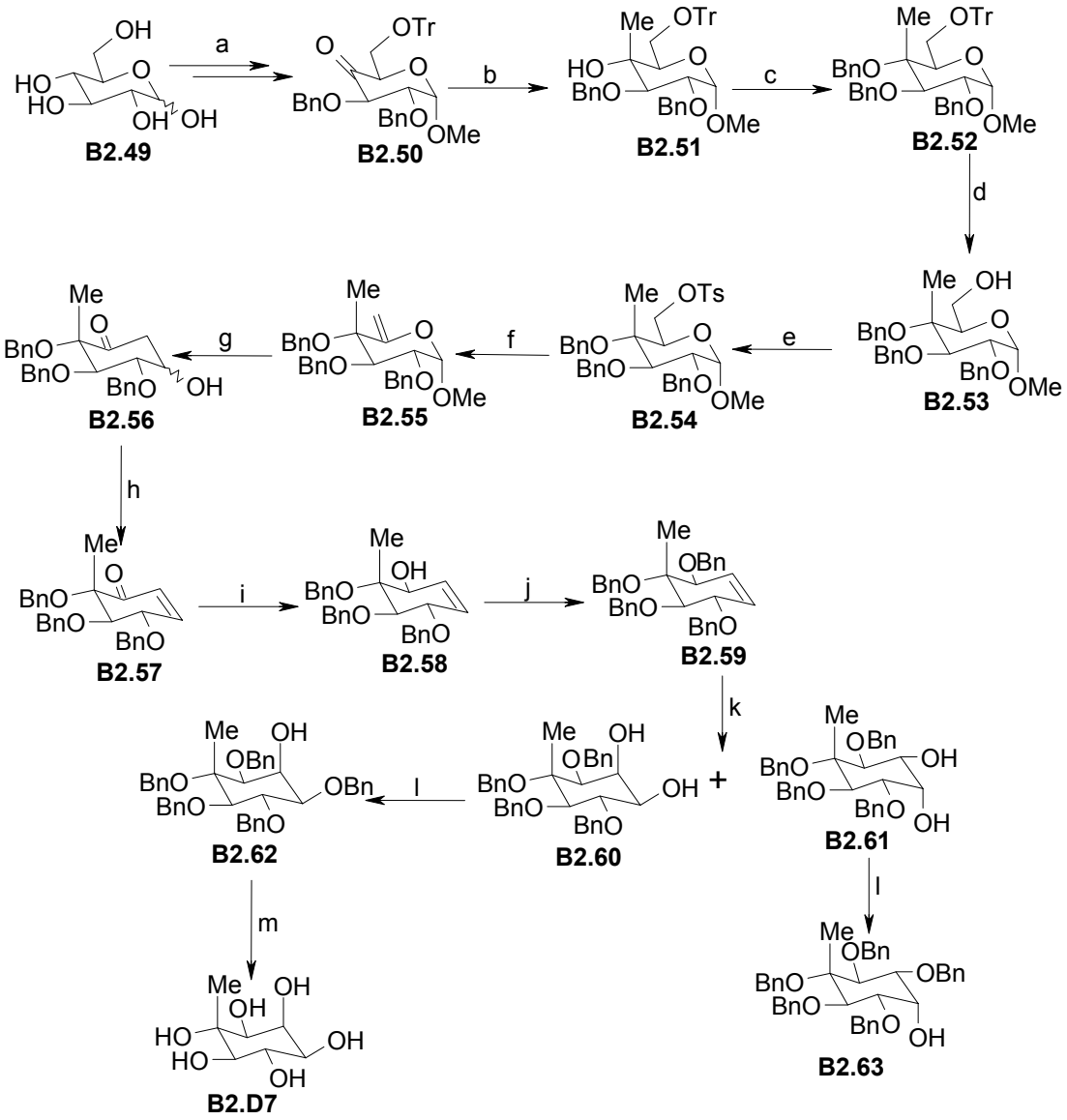

Scheme B2.8. a) 6 steps, 28%; b) MeLi, Et_2O, -78 °C, 72%; c) BnBr (7.4 eq), NaH (6.6 eq), DMF, rt, 30 min, 78%; d) 70% AcOH, 70 °C, 100%; e) TsCl (1.5 eq), Pyr, rt, 3 h, 99%; f) NaI (7.5 eq), Bu_4NI (0.73 eq), 4Å MS then DBU (7.5 eq), DMSO, 120 °C, 12 h, 61%; g) $HgCl_2$ (4.3 eq), acetone-H_2O (2 : 5), 80 °C, 3 h, 72% (α : β = 1 : 2); h) Ac_2O, Pyr, rt, 12 h, 94%; i) $NaBH_4$ (1. 8eq), $CeCl_3.7H_2O$ (1.5 eq), DCM-EtOH (1 : 2), -78 °C, 5 h, 91%; j) BnBr (3.1 eq), NaH (3.0 eq), DMF, rt, 30 min, 100%; k) OsO_4, NMO (1.5 eq), *t*-BuOH-H_2O (4 : 1), rt, 24 h, 84% (**B2.60** : **B2.61** = 3 : 5); l) Bu_2SnO (1. 5 eq), toluene, reflux, 2 h then BnBr (10 eq), DMF, 80 °C, 3 h, 92% **B2.62** & 74% **B2.63**; m) H_2, 10% Pd / C, rt,100%.

B2.2.2.2. Present work

We initially attempted to execute the synthesis of racemic laminitol from the racemic ditosylate **B2.30** (Scheme B2.9). Oxidation of **B2.30** by Swern's method[93,94] as well as by DMSO and acetic anhydride[95-97] gave a mixture of the ketone **B2.64** and the *gem* diol **B2.65**, in which **B2.65** was the major constituent.

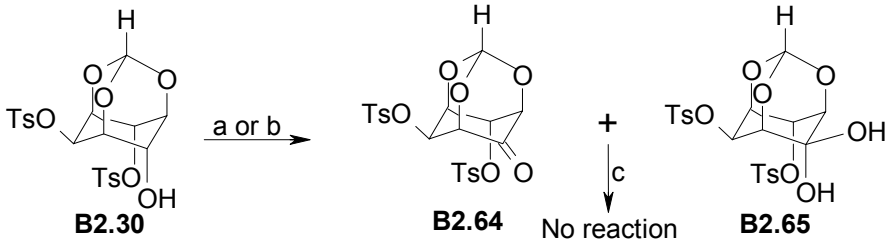

B2.30 **B2.64** **B2.65**

Scheme B2.9. a) DMSO (3 eq), $(COCl)_2$ (1.5 eq), DCM, -78 ^oC, 1 h then Et_3N (5 eq), rt, 3 h, 82%; b) DMSO-Ac_2O, 40 h, 94%; c) MeMgI, Et_2O, 0 ^oC-rt, 24 h.

The IR spectrum of the oxidation product of **B2.30** did not show any peak characteristic of the carbonyl group, but showed peaks between 3250 and 3525 cm^{-1}, characteristic of hydroxyl groups. The ^{13}C NMR spectrum did not show any peak for carbonyl carbon but showed a peak at δ 89.2, characteristic of a quaternary carbon, bearing two hydroxyl groups (*gem* diol). Elemental analysis of this product however matched for the ketone **B2.64**. We attempted to convert the diol **B2.65** to the ketone **B2.64** by azeotropic distillation with dry benzene or dry toluene. Unfortunately, all these efforts failed to yield **B2.64**. Grignard reaction on a mixture of **B2.64** and **B2.65** with methylmagnesium iodide in diethyl ether also failed. (Scheme B2.9). Therefore we synthesized racemic laminitol from unsymmetrical dibenzyl ether **B2.68** (Scheme B2.10).

The racemic dibenzyl ether **B2.68** was prepared from the racemic tosylate **B2.66** (Scheme B2.10) as reported earlier.[77] Oxidation of racemic **B2.68** by Swern's method

gave the corresponding ketone **B2.69** in high yield. Although this oxidation could be affected by DMSO-acetic anhydride as well, the yield was low (72%) in comparision to Swern's method. The IR spectrum of the product obtained by oxidation of **B2.68** showed peaks characteristic of carbonyl group (1765 cm^{-1}) as well as those due to hydroxyl groups (3180-3630 cm^{-1}). The ^{1}H NMR spectrum also showed peaks characteristic of both ketone **B2.69** and the corresponding *gem* diol **B2.70**, but the ketone **B2.69** was the major constitutent. Two peaks corresponding to the orthoformate proton were observed at δ 5.45 and at δ 5.69 suggesting the presence of ketone and the *gem* diol. ^{13}C NMR spectrum however showed a signal at δ102.1 corresponding to the orthoformate carbon and at δ 198.5 for the carbonyl carbon. Absence of a signal corresponding to the carbon carrying the *gem* diol and the absence of two signals for the orthoformate carbon (in contrast to the presence of two signals in the ^{1}H NMR spectrum) suggests that oxidation

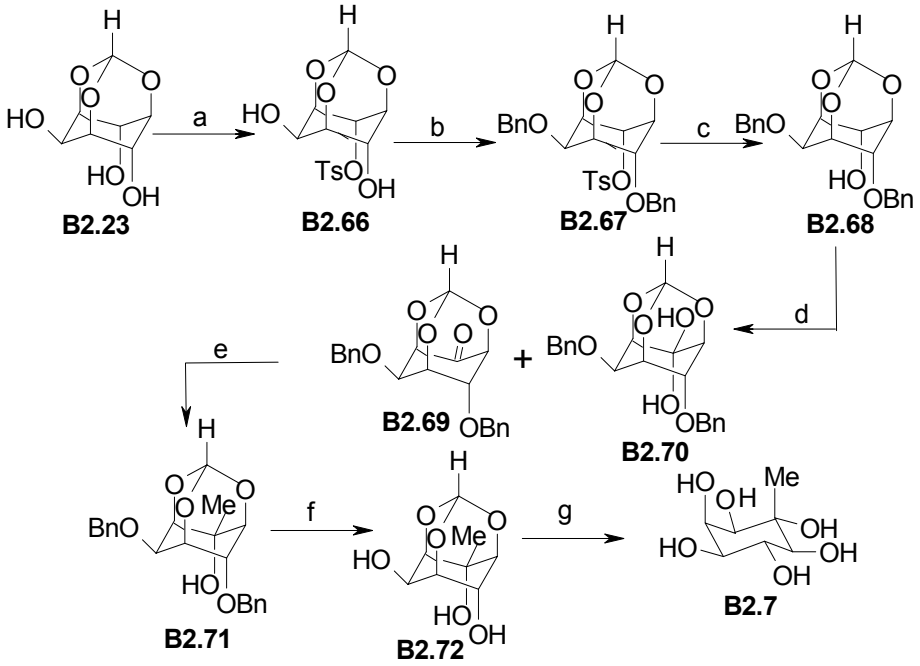

Scheme B2.10. a) TsCl (1 eq), NaH (1 eq), DMF, rt, 5 min, 95%; b) BnBr (2.1 eq), NaH (2.4 eq), DMF, rt, 5 min, 99%; c) NaOMe, MeOH, reflux, 12 h, 99%; d) DMSO (2 eq), $(COCl)_2$ (1.1 eq), DCM, -78 ^{o}C, 1 h then Et_3N (5 eq), rt, 3 h, 92%; e) MeMgI (5 eq), Et_2O, 0 ^{o}C-rt, 30 min, 88%; f) $Pd(OH)_2$, H_2/ 30 psi, MeOH, 6 h, rt, 98%; g) TFA : H_2O (4 : 1), rt, 1 h, 98%.

product of **B2.68** consists mostly of the ketone **B2.69**.

Grignard reaction of this ketone-diol mixture, **B2.69** + **B2.70,** with methyl magnesium iodide in diethyl ether gave racemic **B2.71**. Removal of the benzyl groups in racemic **B2.71** by hydrogenolysis gave racemic **B2.72**. The structure of racemic **B2.72** was confirmed by X-ray crystallography. Acid hydrolysis of the racemic **B2.72** gave the known racemic laminitol **B2.7**.[87, 88]

After the successful synthesis of racemic laminitol **B2.7**, both D- and L-laminitol (**B2.D7** and **B2.L7**) were synthesized from enantiomeric dibezyl ethers **B2.L68** and **B2.D68** respectively (Schemes B2.11 and B2.12). For this purpose, the racemic dibenzyl ether **B2.68** was resolved as its diastereomeric 1*S*-(-)-camphanoate esters according to procedure previously developed in our laboratory (Scheme B2.11).[77]

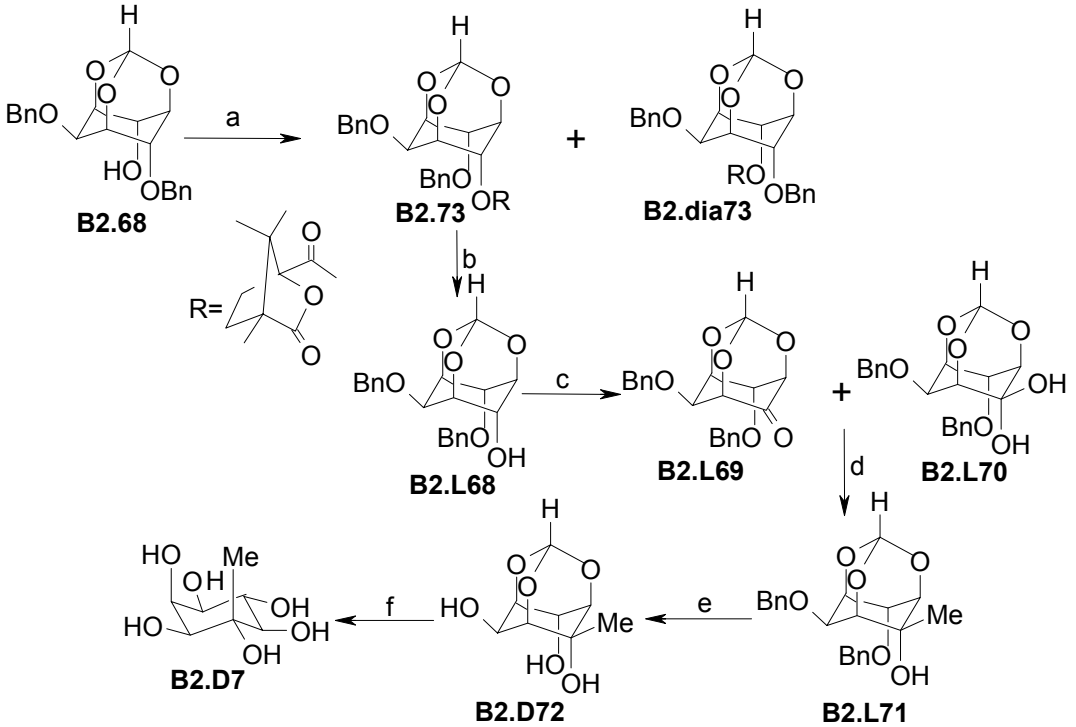

Scheme B2.11. a) RCl (1.2 eq), Pyr, rt, overnight, 46% **B2.73** and 47% **B2.dia73**; b) NaOMe, MeOH, rt, 6 h, 100%; c) DMSO (2 eq), $(COCl)_2$ (1.1 eq), DCM, -78 °C, 1 h then Et_3N (5 eq), rt, 3 h, 95%; d) MeMgI (5 eq), Et_2O, 0 °C-rt, 30 min, 89%; e) $Pd(OH)_2$, H_2/ 30 psi, MeOH, 6 h, rt, 98%; f) TFA : H_2O (4 : 1), rt, 1 h, 95%.

B2.L68 and **B2.D68** were obtained by the removal of camphanoates from **B2.73** and **B2.dia73** by treatment with sodium methoxide in methanol. The naturally occurring D-laminitol (**B2.D7**) was synthesized from the dibenzyl ether **B2.L68** by following the same reaction sequence that was used for the synthesis racemic laminitol.

L-Laminitol (**B2.L7**) was synthesized (Scheme B2.12) from enantiomeric dibenzyl ether **B2.D68** by following the same reaction sequence used for the synthesis racemic laminitol. Spectral data for the enantiomeric laminitols were identical with those of racemic laminitol. The specific rotations for the two enantiomers were same but had opposite signs. The yields obtained in the present method are compared with literature methods in Table B2.2.

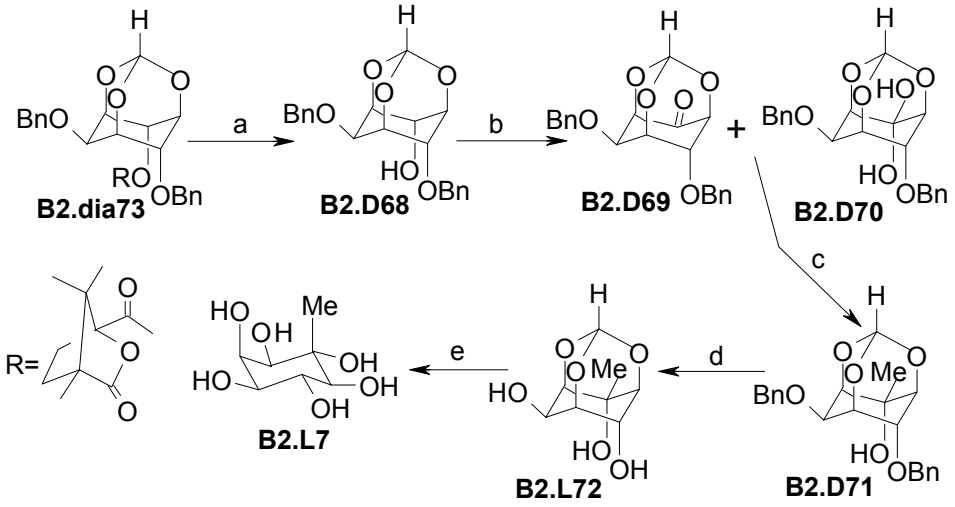

Scheme B2.12. a) NaOMe, MeOH, rt, 6 h, 97%; b) DMSO (2 eq), $(COCl)_2$ (1.1 eq), DCM, -78 °C, 1 h then Et_3N (5 eq), rt, 3 h, 95%; c) MeMgI (5 eq), Et_2O, 0 °C-rt, 30 min, 88%; d) $Pd(OH)_2$, H_2/ 30 psi, MeOH, 6 h, rt, 98%; e) TFA : H_2O (4 : 1), rt, 1 h, 98%.

Table B2.2. A comparision of the yield of racemic, (-)- and (+)- laminitol obtained by the present method with the literature methods.

Starting material	Steps	Overall yield (%) of laminitol			Reference
		(±)	(-)	(+)	
myo-Inositol		<15	NR	NR	98
myo-Inositol		< 30%	NR	NR	30
Toluene	6	NR	<8	NR	89
D-Glucose	18	NR	3	NR	90
myo-Inositol	12	63	30	30	Present work

NR – Not reported

B2.2.2.3. Polymorphism of inositol derivatives encountered during the synthesis of laminitol

Racemic laminitol orthoformate (**B2.72**) gave polymorphic crystals on crystallization from methanol and hot ethyl acetate (for the crystal packing see Figure B2.2 A and B). On crystallization from nitromethane, **B2.72** gave both the polymorphic forms obtained separately by crystallization from methanol and hot ethyl acetate.

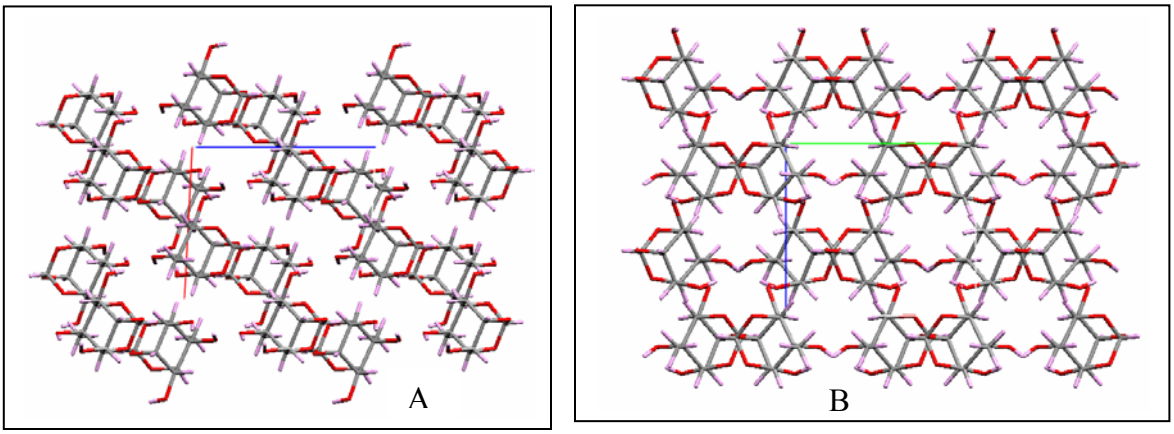

Figure B2.2. Packing of molecules in crystals of **B2.72** (view down the b-axis) from (A) hot ethyl acetate and (B) methanol.

Polymorphic structures arose due to the conformational freedom of the three-hydroxyl groups in **B2.72** and the variation in intermolecular and intramolecular H-bonding contacts. These polymorphs have only differences in the O-H group orientations as seen from the Figure B2.2.

B2.2.3. Syntheses of D- and L-4-deoxy-4-amino-*myo*-inositol derivatives

B2.2.3.1. Known methods of synthesis

Earlier synthetic efforts starting from *myo*-inositol were based on the introduction of nitrogen in the carbocyclic ring by nucleophilic substitution (double inversion) of a specific hydroxyl group. Ballereau and co-workers synthesized the aminoinositol derivative **B2.83** as a precursor for the preparation of the amino analog of Ins(1,4,5)P_3 (Scheme B2.13).[59]

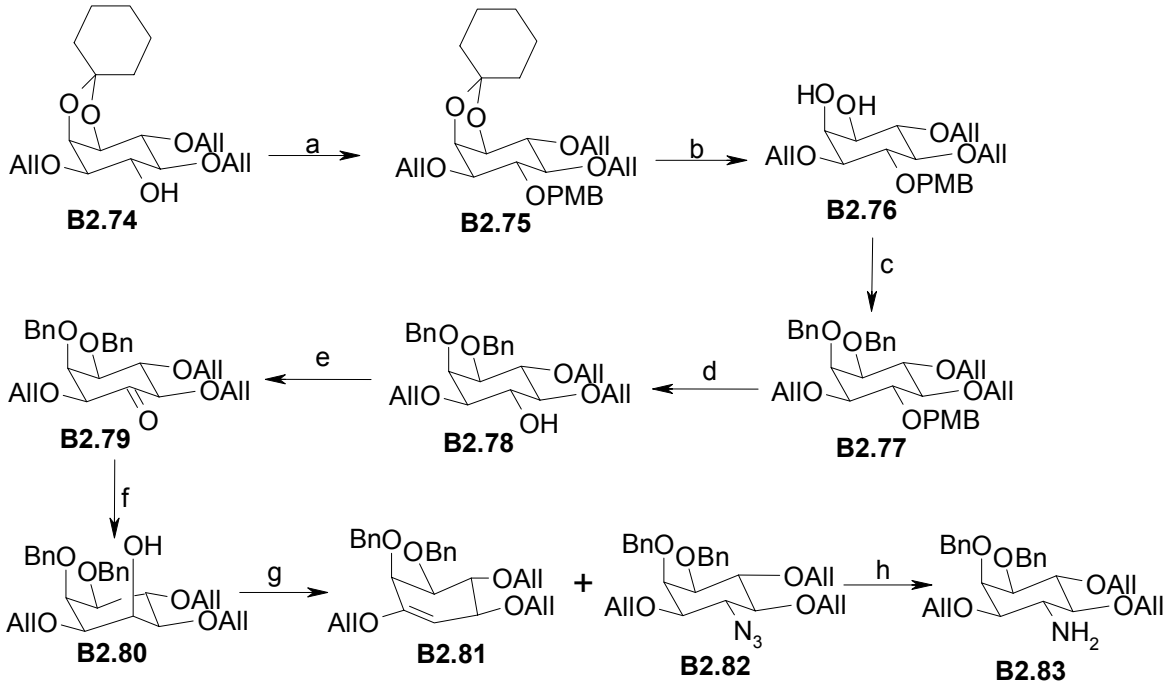

Scheme B2.13. a) PMB-Cl (2 eq), NaH (2.5 eq), DMF, 0 °C-rt, overnight, 100%; b) TFA-H_2O (3 : 1), THF-MeOH (1 : 10), reflux, 2 h, 84%; c) BnBr (5 eq), NaH (6 eq), DMF, 0 °C-rt, overnight, 96%; d) MeOH-3N HCl (2 : 1), THF, reflux, 25 h, 96%; e) $(COCl)_2$ (5 eq), DMSO (6.3 eq), DCM, -78 °C, 40 min, then Et_3N (20 eq), rt, 20 min; f) $NaBH_4$ (5 eq), EtOH, 0 °C, rt, 1 h, 73%; g) (i) Tf_2O (2.2 eq), Pyr-DCM, 0 °C, 2 h, (ii) NaN_3 (5 eq), DMF, 0 °C-rt, overnight, 27% **B2.81** & 59% **B2.82**; h) $SnCl_2$ (2 eq), thiophenol (8 eq), Et_3N (6 eq), MeCN, 1 h.

Sanfilippo and co-workers synthesized acetate salt of optically active 6-deoxy-6-amino-*myo*-inositol from 1,2-di-acetyl-conduritol E (**B2.84**) (Scheme B2.14).[62]

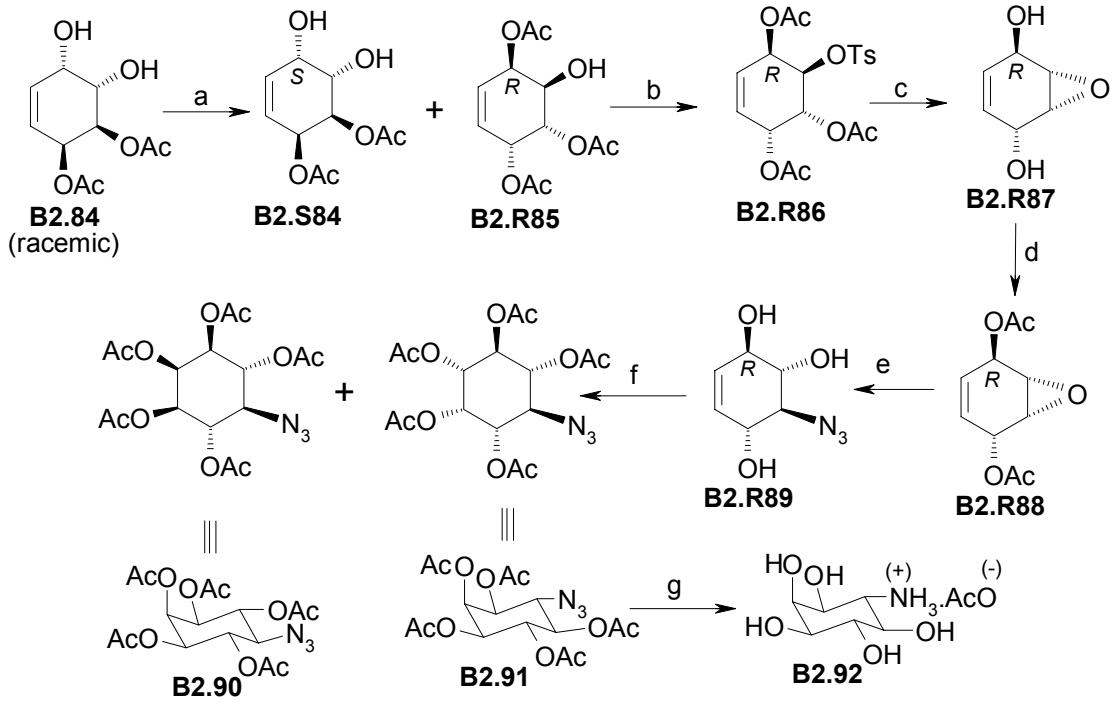

Scheme B2.14. a) Lipozyme IM, Vinyl acetate, *t*-BME, 40 °C; b) TsCl (1.2 eq), Pyr-DCM, 35 °C, overnight, 94%; c) aq. KOH, MeOH, rt, 25 h; d) Ac_2O, Pyr, rt, overnight, 84%; e) (i) NaN_3 (3 eq), NH_4Cl (3 eq), DMF, (ii) MeOH-NH_4OH (9 : 1), 78%; f) (i) NMO (1.1 eq), OsO_4 (cat.), H_2O-Acetone (1 : 4), rt, 96 h, (ii) Ac_2O, Pyr, 34% **B2.90** & 42% **B2.91**; g) (i) H_2, Pd / C, EtOH, 78%; (ii) MeOH-NH_4OH (9 : 1), 98%.

Podeschwa and co-workers[99] synthesized both 4- and 6-deoxy-6-amino-*myo*-inositols and their phosphate derivatives along with other azido- and amino- *myo*-inositol derivatives starting from *para*-benzoquinone. Podeschwa's synthesis of 6-deoxy-6-amino-*myo*-inositol (1L-4-deoxy-4-amino-*myo*-inositol, **B2.L104**)[99] is shown in Scheme B2.15.

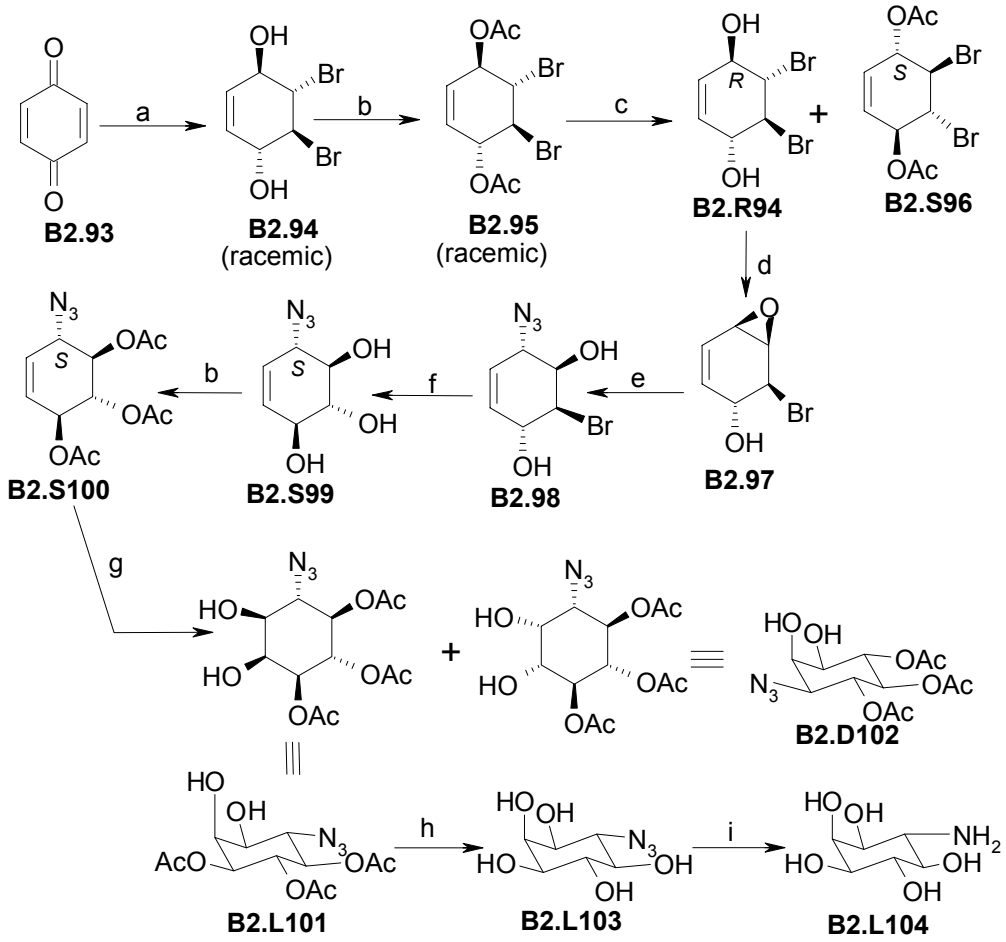

Scheme B2.15. a) (i) Br_2, $CHCl_3$, 0 °C-rt, 3 h ,98%, (ii) $NaBH_4$, Et_2O, -20 °C- rt, 2 h, 88%; b) Ac_2O, Pyr, rt, 12 h, 68% **B2.95** & 96% **B2.S100** c) PPL, phosphate buffer (pH = 7.0), Et_2O, rt, 4 d, 38% **B2.R94** & 38% **B2.S96** (ee >99%); d) LiOH (2.2 eq), Et_2O-MeOH (2 : 1), 0 °C, 2 h, 99%; e) NaN_3 (4 eq), NH_4Cl (4 eq), DME-H_2O-EtOH, 0 °C, 3 h, 90%; f) (i) LiOH (2.2 eq), Et_2O-MeOH (2 : 1), 0 °C- 10 °C, 2 h, (ii) TsOH, H_2O, rt, 2 d, 47%; g) $RuCl_3$ (0.07 eq), $NaIO_4$ (1.5 eq), MeCN-H_2O, rt, 8 min, 91% (50% **B2.L101** & 40% **B2.D102**); h) NaOMe, MeOH, rt, 12 h, 99%; i) H_2, Pd / C, MeOH, rt, overnight, 99%.

B2.2.3.2. Present work

Reductive amination of ketones for the preparation of amines is a well-known reaction in the literature.[100-105] Therefore we planned the synthesis of aminoinositol by the reductive amination of the ketone **B2.69** (Scheme B2.16). Racemic **B2.69** was reacted with benzyl amine in methanol and the resulting imine was reduced with sodium

cyanoborohydride to obtain the racemic amine **B2.105**. Cleavage of the orthoformate moiety and the benzyl groups in **B2.105** were achieved in one step by hydrogenolysis (with Pearlman's catalyst at 60 psi) in a 1 : 1 mixture of methanol and TFA. Exhaustive acetylation of the product gave the racemic hexaacetate **B2.106** in 50% overall yield. The structure of **B2.107** was confirmed by X-ray crystallography.

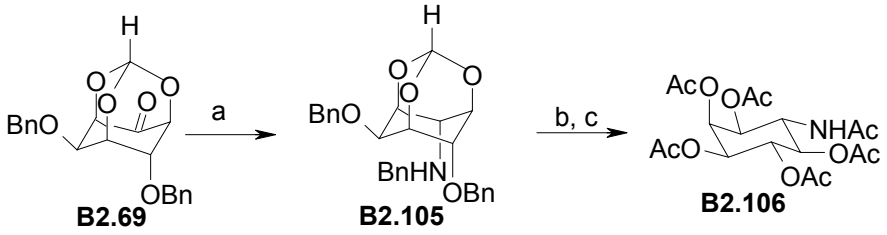

Scheme B2.16. a) $BnNH_2$ (3 eq), MeOH, 50 °C, 3 h followed by $NaBH_3CN$ (3 eq), rt, 1 h 90%; b) $Pd(OH)_2$, TFA-MeOH (1 : 1), H_2 / 60 psi, 8 h; c) Ac_2O, Pyr., DMAP, rt, 12 h, 81% in two steps.

We tried to isolate the racemic 4-deoxy-4-amino-*myo*-inositol 1,3,5-orthoformate (prior to acetylation), but the debenzylation did not go to completion even on using 1 : 1 (by weight) of Pearlman's catalyst in the absence of an acid. This could be due to poisoning of the catalyst by the inosamine produced. Aminocyclitols are known to inhibit Pd / C catalyzed and $Pd(OH)_2$ / C catalyzed hydrogenolysis of benzyl ethers.[106] We could obtain the intermediate, 4-deoxy-4-amino-*myo*-inositol 1,3,5-orthoformate (characterized as tri acetate) by hydrogenolysis of **B2.105** in acetic acid but the isolated yield was very low.

The enantiomeric hexaacetate derivatives **B2.D106** and **B2.L106** were prepared from the enantiomeric dibenzyl ether ketones **B2.D69** and **B2.L69** (Scheme B2.17) following the same reaction sequences (as in Scheme B2.16) in 25% overall yields. These hexaacetate derivatives exhibited spectral data similar to the racemic hexaacetate **B2.106** and had the same specific rotation with opposite signs.

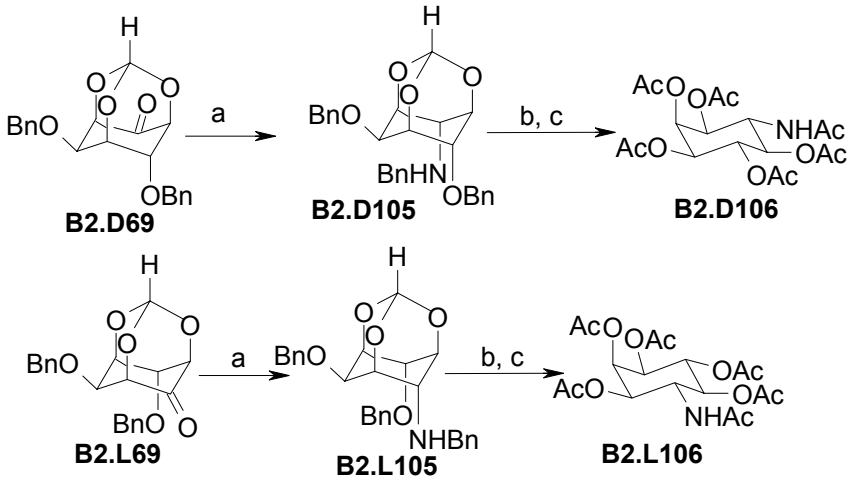

Scheme B2.17. a) $BnNH_2$ (3 eq), MeOH, 50 °C, 3 h followed by $NaBH_3CN$ (3 eq), rt, 1 h 89%; b) $Pd(OH)_2$, TFA-MeOH (1 : 1), H_2 / 60 psi, 8 h; c) Ac_2O, Pyr., DMAP, rt, 12 h, 81% **B2.D106** and 82% **B2.L106** in two steps.

B2.3. Synthesis of cyclitol derivatives with *scyllo*-configuration

B2.3.1. Synthesis of *scyllo*-inositol

B2.3.1.1. Known methods of synthesis

myo-Inositol is the most abundant cyclitol in nature and also most well studied. While methylated derivatives of D- and L-*chiro*-inositols occur in nature to a lesser extent, other isomeric cyclitols (*scyllo*-, D-*chiro*-, L-*chiro*- and *neo*-) have only been detected in minute amounts from natural sources and other known isomers (*epi*-, *cis*-, *allo*-, *muco*-) do not occur in nature at all. Hence there are attempts to convert *myo*-inositol to other isomeric inositols.

There are few reports on the conversion of *myo*-inositol (**B2.9**) to *scyllo*-inositol (**B2.10**).[26-28] Posternak obtained *scyllo*-inositol by the reduction of *scyllo*-inosose (**B2.107**), which was obtained by the oxidation of *myo*-inositol with *acetobacter suboxydans*.[26,27] Husson and co-workers obtained *scyllo*-inositol in 20-30% yield (estimated by NMR spectroscopy) by refluxing *myo*-inositol with Raney nickel in distilled water.[28] Both of these methods gave mixture of *myo*- and *scyllo*- inositols.

Posternak's synthesis

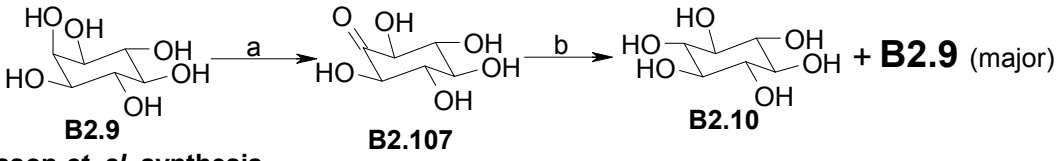

Husson *et. al*. synthesis

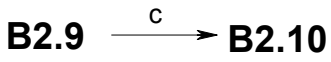

Scheme B2.18. a) *Acetobacter suboxydens*; b) H_2 / PtO_2, neutral aq. solution; c) Raney Ni, H_2O, pH = 10, reflux, 24 h, 20-30%.

scyllo-Inositol was also synthesized from D-glucose derivative **B2.108**[33,34] by using Ferrier transformation[91,92] reaction as the key reaction to convert the pyranose ring to the carbocyclic ring (Scheme B2.19).

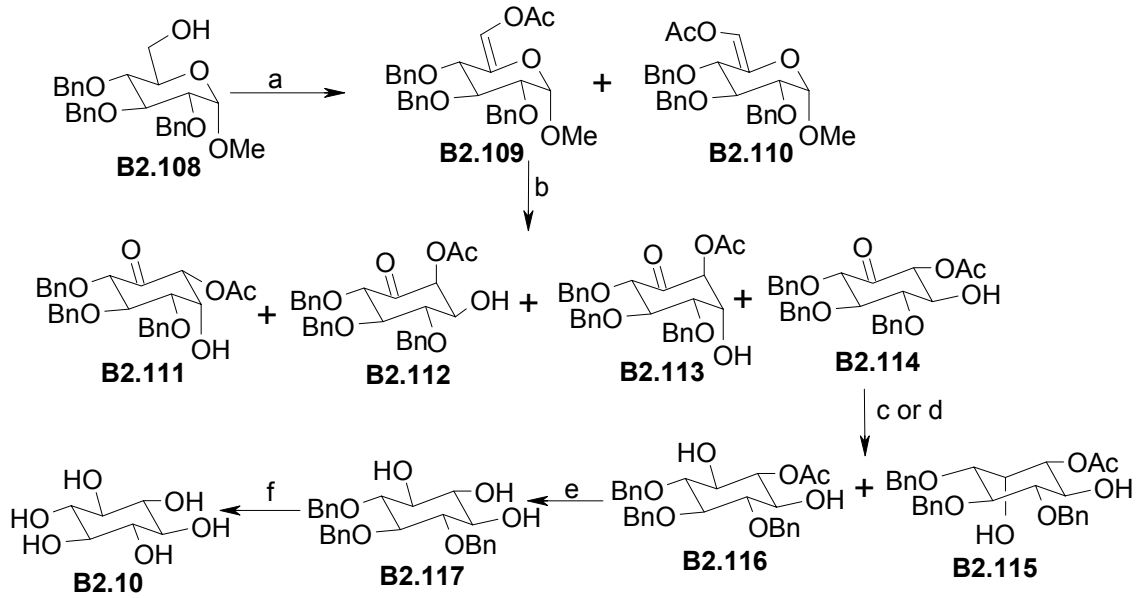

Scheme B2.19. a) (i) TFA (0.5 eq), Pyr (1 eq), DCC (3eq), DMSO-benzene (1 : 1), rt, 1 d (ii) Ac_2O (4 eq), Et_3N (4 eq), DMAP (0.1 eq), 1,2-dichloroethane, reflux, 3 h, 83% (**B2.109** : **B2.110** = 92 : 8); b) $PdCl_2$ (0.05 eq), dioxane-H_2O (4 : 1), 60 ^oC, 3 h, 74.2% (**B2.111** : **B2.112** : **B2.113** : **B2.114** = 49 : 24 : 17 : 10); c) $Me_4NBH(OAc)_3$ (5 eq), MeCN-AcOH, rt, 24 h, 37% (**B2.115** : **B2.116** = 78 : 22); d) $NaBH_4$ (1.5 eq), MeOH, 0 ^oC, 30 min, 86% (**B2.115** : **B2.116** = 22 : 78). e) 10 N NaOH, MeOH, rt, 12 h; f) H_2 / $Pd(OH)_2$-C, rt, 24 h, 100%.

The Ferrier cyclization step gave mixture of four products and the yield of the intermediate **B2.114**, required for the synthesis of *scyllo*-inositol was only 7.5%.

Reduction of **B2.114** gave mixture of both *myo*- and *scyllo*- isomers. Therefore this method is not very convenient for the synthesis of *scyllo*-inositol.

Podeschwa and co-workers[45] synthesized *scyllo*-inositol from the diacetate **B2.96** (Scheme B2.20) which was obtained from *para*-benzoquinone (Scheme 2.15).

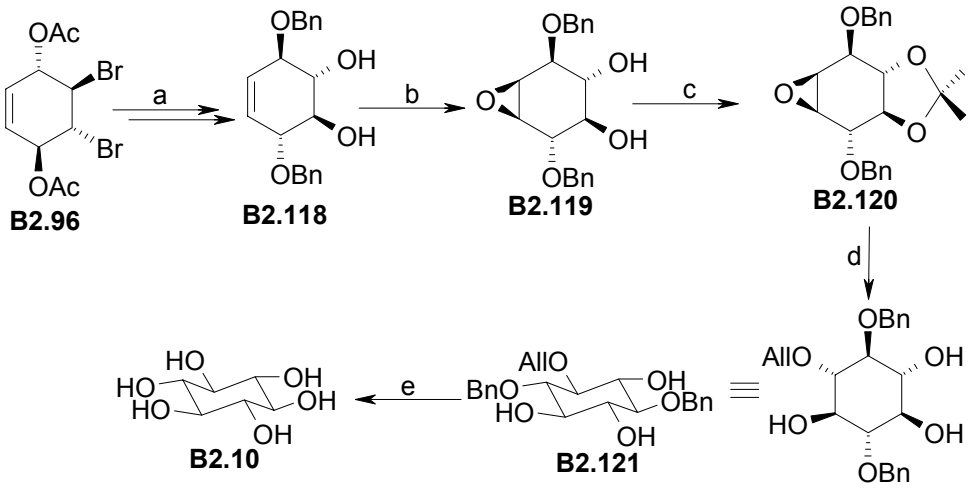

Scheme B2.20. a) as in reference 45; b) $(CF_3CO_2)_2$-H_2O_2 (1 : 1), DCM, 0 °C, 30 min, reflux, 2 h and rt, 3 h, 71%; c) 2,2-dimethoxypropane, PPTS, acetone, rt, 16 h, 96%; d) (i) NaOAll, AllOH, 90 °C, 24 h, (ii) 4M HCl, 60%; e) (i) Pd / C, MeOH, reflux, 6 h, (ii) 2M HCl, 80 °C, (iii) H_2, Pd / C, rt, 12 h, 85%.

There are several other reports on the synthesis of of *scyllo*-inositol derivatives from *myo*-inositol, in overall yields of 10-40%.[24, 25, 48-50, 107] Roemer and co-workers, during the synthesis of *scyllo*-Ins(1,2,3,4)P_4, synthesized the *scyllo*-inositol derivative **B1.125** by sequential oxidation – reduction of **B2.123**.[48] The *scyllo*-inositol derivative **B2.125** was purified by preparative HPLC. Similarly, during the synthesis of *scyllo*-Ins(1,2,3)P_3, Lampe and co-workers converted the *myo*-triflate derivative **B2.128** to the *scyllo*-inositol derivative **B2.129** by nucleophilic substitution.[49] The key intermediate **B2.127** for this synthesis was obtained from *myo*-inositol in very low yield (16%). Chung and co workers prepared the *scyllo*-inositol derivative **B2.126** by Mitsunobu reaction[108-110] on racemic **B2.122**. The *scyllo*-inositol derivative **B2.126** was used as a precursor for

the synthesis of *scyllo*-inositol phosphate derivatives.[107] The key steps used for the conversion of *myo*-isomers to *scyllo*-isomers in the reports metinoned above are shown in Scheme B2.21.

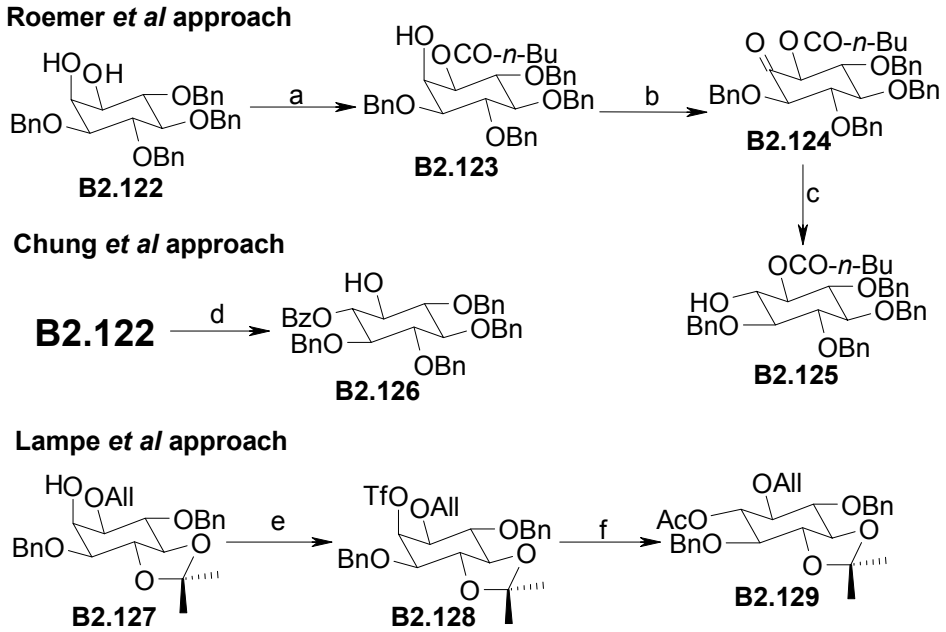

Scheme B2.21. a) (*n*-Bu-CO)$_2$O (1 eq), Pyr., rt, 24 h, 78%; b) DMSO, Ac_2O, rt, 15 h, 81%; c) $NaBH_4$ (1.1 eq), *i*-PrOH, 50 ^oC, 30 min, 73%; d) PPh_3 (1.1 eq), DEAD (1.2 eq), BzOH (1.1 eq), 3Å MS, benzene, 80 ^oC, 4 h, 72%; e) Tf_2O (1.8 eq), Pyr.-DCM (1 : 5), -78 ^oC-rt, 2 h, 100%; f) CsOAc (1.5 eq), DMF, rt, 2 h, 91%.

Chung and Kwon synthesized *scyllo*-inositol derivative **B2.134** from the *myo*-inositol derivative **B2.130**[24] via the intermediacy of the conduritol derivative **B2.131** (Scheme B2.22). The epoxide opening in **B2.133** gave mixture of *scyllo*- and *chiro*-isomers and the *scyllo*- isomer was the minor product.

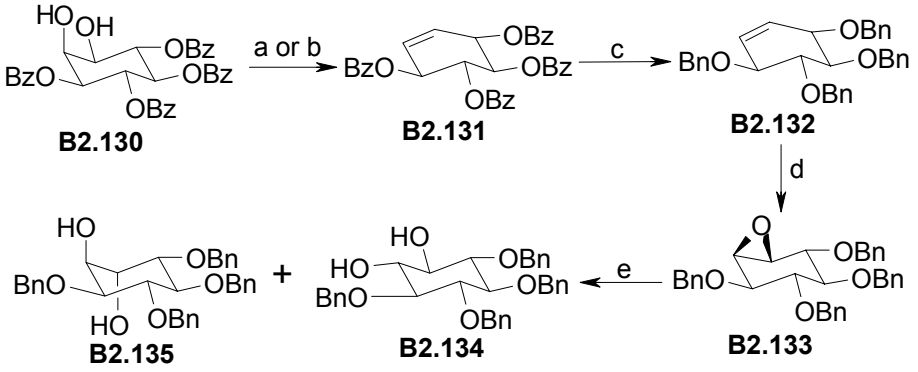

Scheme B2.22. a) (i) $ClPPh_2$ (2.2 eq), Imidazole (6 eq), I_2 (2 eq), toluene, reflux, (ii) Zn, 85%; b) PPh_3 (2.2 eq), Imidazole (6 eq), I_2 (2 eq), toluene, reflux, 79%; c) (i) NaOMe, MeOH, reflux, (ii) BnBr, NaH, DMF, rt, 91%; d) I_2, Ag_2O, aq.dioxane, 90 ^oC, 91%; e) TFA (or H_2SO_4), aq.THF, 50 ^oC, 15.5% **B2.134** and 67% **B2.135**.

Same authors also synthesized optically active *scyllo*-inositol derivatives **B2.142**

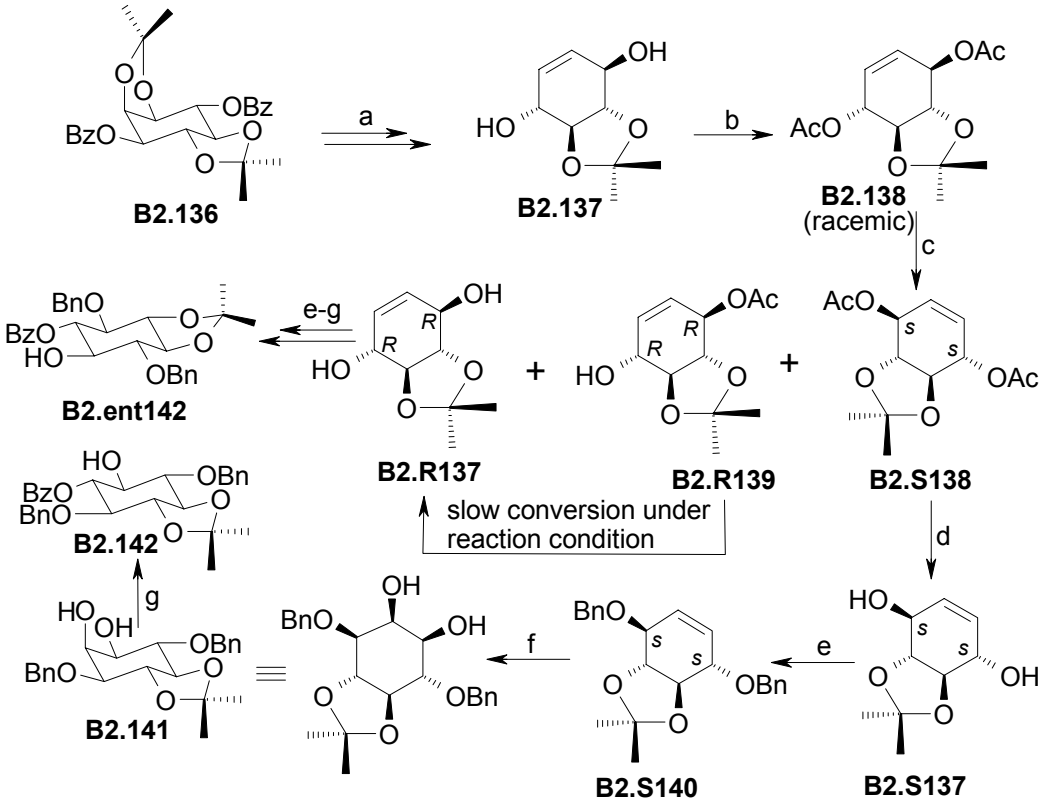

Scheme B2.23. a) as in reference 25; b) Ac_2O, Pyr., 0 ^oC-rt, overnight, 99%; c) Novozyme 435, *t*-Bu_2O, *n*-BuOH, 45 ^oC 49% **B2.S138** (98% ee); d) NaOMe, MeOH, rt, 100%; e) BnBr (4 eq), NaH (5 eq), DMF, rt, overnight, 96%; f) NMO (4.5 eq), OsO_4, Acetone-H_2O (8 : 1), rt, 12 h, 95%; g) Ph_3P (1.8 eq), BzOH (1.8 eq), DEAD (1.8 eq), toluene, 80 ^oC, overnight, 79%.

and **B2.ent142** by enzymatic resolution of partially protected conduritol derivative **B2.138** (Scheme B2.23).[25]

Lee and Kishi used *myo*-inositol 1,3,5-orthoformate (**B2.23**) as the starting material for the synthesis of *scyllo*-inositol monoorthoformate (Scheme B2.24);[50] the latter was used for the synthesis of enterobactin analogs.[111] The shortcomings of this method were: (a) poor yield during silylation of the triol **B2.23**; (b) isolation of **B2.148** by preparative TLC; (c) inconsistent results during hydrogenolysis of the benzyl groups in **B2.148**;[112, 113] (d) poor overall yield of *scyllo*-inositol 1,3,5-orthoformate (**B2.149**).

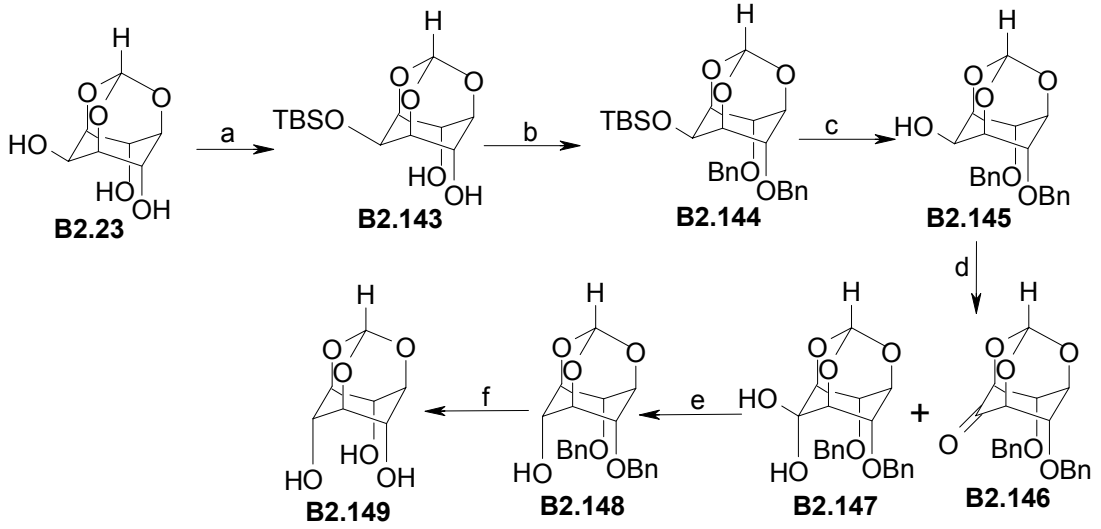

Scheme B2.24. a) TBS-Cl (1.2 eq), imidazole (2.5 eq), DMF, 0 ^{o}C-rt, 20 h, 48%; b) BnBr (3 eq), NaH (3 eq), DMF, rt, 24 h, 93%; c) TBAF (3 eq), THF, 30 min; d)$(COCl)_2$ (2 eq), DMSO (4 eq), -78 ^{o}C, 1 h, Et_3N (10 eq), rt, e) $NaBH_4$ (2.5 eq), MeOH-THF (4 : 1), 20 min, 87%; f) H_2, Pearlman's catalyst, THF, 50 psi, rt, 3 h, 94%.

B2.3.1.2. Present work

Our scheme of synthesis for *scyllo*-inositol (**B2.10**) was similar to that of Lee and Kishi.[50] *myo*-Inositol orthoformate was benzoylated[114] as reported earlier to obtain the diol **B2.150**. Tosylation of the diol in pyridine with tosyl chloride gave the symmetric

ditosylate **B2.151** (Scheme B2.25). Aminolysis of the benzoate in **B2.152** with isobutylamine in methanol gave the corresponding known alcohol **B2.152**.[77] These two steps could be performed in a single pot without isolating the benzoate **B2.151**. Tosylation of the triol **B2.23** with tosyl chloride in the presence of excess of sodium hydride is known to give the symmetric ditosylate **B2.152** (upto 1 mmol scale).[77] However, unfortunately our attempts to scale-up this reaction were not successful due to formation of isomeric tosylates.[77] Attempts to oxidize **B2.152** with PCC and PDC failed while oxidation with DMSO and acetic anhydride,[95-97] gave **B2.153** in 38% yield. Formation of thio compounds under DMSO-acetic anhydride oxidation condition is known in the literature.[95]

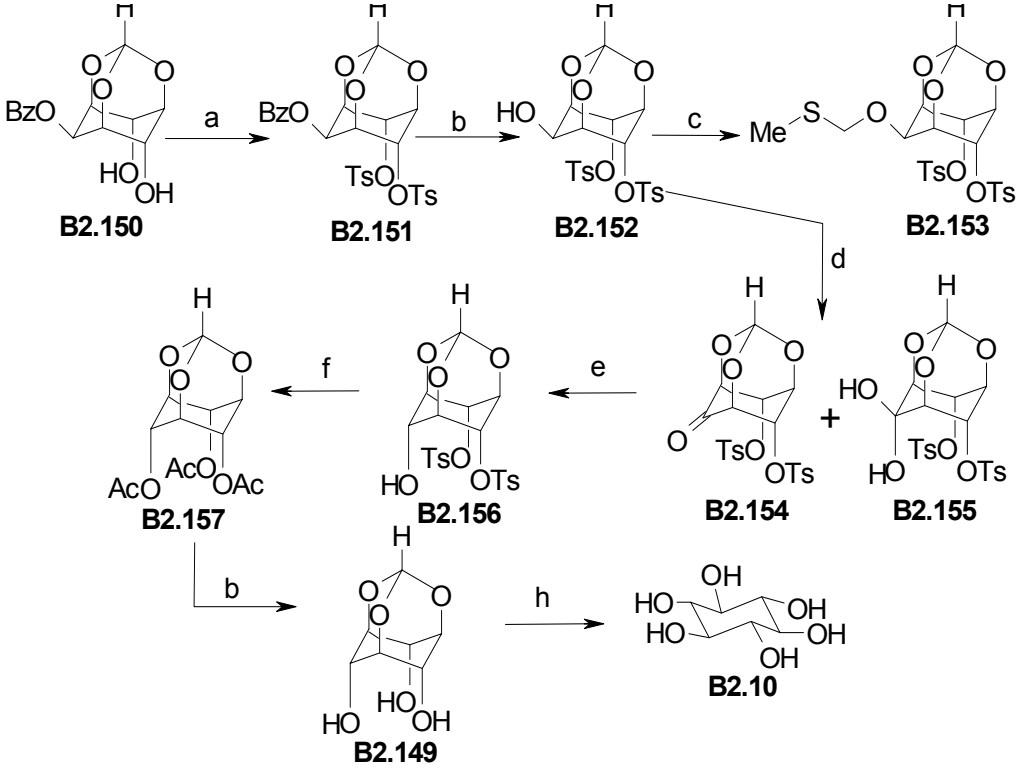

Scheme B2.25. a) TsCl (3 eq), Pyr, 80-100 ^{o}C, 12 h, b) *i*-BuNH$_2$, MeOH, reflux, 12 h, 95% for **B2.152** and 92% for **B2.149**; c) DMSO-Ac$_2$O, rt, 7 d, 35%; d) DMSO (2 eq), (COCl)$_2$ (1.1 eq), DCM, -78 ^{o}C, 1 h then Et$_3$N (5 eq), rt, 3 h, 100%; e) NaBH$_4$ (3 eq), MeOH-THF (4 : 1), 30 min, rt, 99%; f) (i) NaOMe, MeOH, reflux, 12 h (ii) Ac$_2$O, Pyr, rt, 12 h, 96%; h) TFA-H$_2$O (4 : 1), rt, 1 h, 100%.

Oxidation of **B2.152** was successful under Swern's oxidation[93,94] condition. IR spectrum of the product of oxidation of **B2.152** showed peaks characteristic of carbonyl group (1774 cm^{-1}) and hydroxyl group (3180-3641 cm^{-1}), suggesting the presence of ketone **B2.154** and the corresponding *gem* diol **B2.155**. Absence of prominent peaks corresponding to the *gem* diol in the ^{13}C NMR spectrum suggested that the amount of the *gem* diol present in the mixture was low. Reduction of the ketone **B2.154** with sodium borohydride in a mixture of tetrahydrofuran and methanol gave the *scyllo*-inositol derivative **B2.156**. Methanolysis of the tosylates in **B2.156** with sodium methoxide in methanol followed by acetylation gave the known triacetate **B2.157**[59] in good yield. We initially attempted to isolate the triol **B2.149** directly by column chromatography, but the yield was poor (25%). This could be due the ability of **B2.149** to bind with the metal ions present in silica gel. *syn*-1.3.5-cyclohexanetriols are known to form complexes with metal ions.[115-118] Aminolysis of the acetates in **B2.157** with isobutylamine gave the known *scyllo*-orthoester **B2.149**.[50] Hydrolysis of the orthoformate in **B2.149** with aqueous trifluoroacetic acid gave the known *scyllo*-inositol (**B2.10**)[28,33,34,45] in 64% overall yield from *myo*-inositol. The method of synthesis of *scyllo*-inositol and its orthoformate described here does not involve chromatographic purification of the product in any of the steps and hence has the potential for scaling upto larger amounts. Literature reports[50] suggest that synthesis of mono orthoformate of *scyllo*-inositol was not feasible from *scyllo*-inositol and hence this synthesis of *scyllo*-inositol shown in Scheme B2.25 also provides an excellent route to *scyllo*-inositol monoorthoformate (**B2.149**). Table

B2.3 compares the yield of *scyllo*-inositol or its derivatives obtained in the present work with those reported in the literature.

Table B2.3. Comparision of the yield of *scyllo*-inositol obtained by the present method with the literature methods.

Starting material	Number of steps	Yield (%)*	Reference
myo-Inositol	1	20-30%	28
D-Glucose	5	<7	34
para-Benzoquinone	12	6	45
myo-Inositol	6	21 (**B2.125**)	48
myo-Inositol	5	46 (**B2.126**)	107
myo-Inositol	9	15 (**B2.129**)	49
myo-Inositol	9	<10 (**B2.134**)	24
myo-Inositol	12	3 (**B2.142** & **B2.ent142**)	25
myo-Inositol	7	28 (**B2.149**)	50
myo-Inositol	12	64	Present work

* Overall yield of *scyllo*-inositol or its derivative.

B2.3.1.3. Polymorphism of inositol derivatives encountered during the preparation of *scyllo*-inositol

Crystallization of the oxidation product of **B2.152** from dichloromethane and chloroform yielded crystals of the ketone **B2.154** in two different polymorphic forms. The crystal packing of both the polymorphic forms are shown in Figure B2.3. The polymorphic behavior of **B2.154** can be attributed to the conformational flexibility of the tosyl groups along the S-O bond that generates different patterns of intermolecular weak interactions (C-H…O interactions in this case).

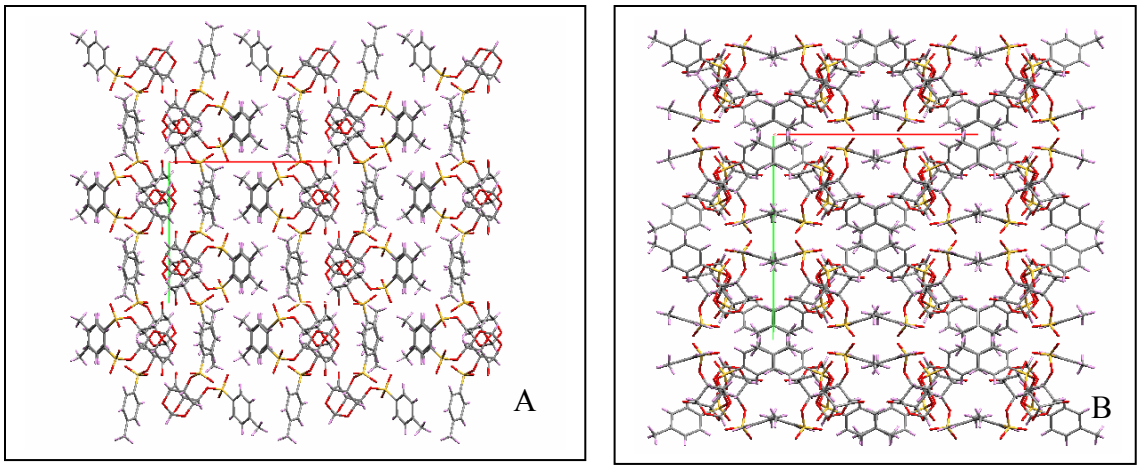

Figure B2.3. Packing of molecules in crystals of **B2.154** (view down the c-axis) (A) from dichloromethane and (B) from chloroform.

B2.3.2. Synthesis of *scyllo*-inositol methyl ether

Synthesis of *scyllo*-inositol methyl ether is not reported in the literature. We synthesized *scyllo*-inositol methyl ether (**B2.4**) from the symmetric ditosylate **B2.156** obtained during the preparation of *scyllo*-inositol (Scheme B2.25). The ditosylate **B2.156** was methylated with methyl iodide and sodium hydride in DMF.

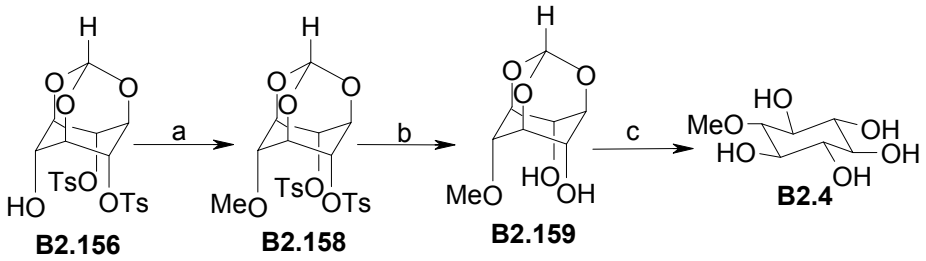

Scheme B2.26. a) MeI (1.3 eq), NaH (1.1 eq), DMF, rt, 5 min, 92%; b) NaOMe, MeOH, reflux, 8 h, 94% ; c) TFA-H_2O (4 : 1), rt, 1 h 96%.

Methanolysis of the tosylates in **B2.158** with sodium methoxide in methanol gave the orthoformate of **B2.159**. Acid hydrolysis of the orthoformate in **B2.159** with aqueous trifluoroacetic acid gave *scyllo*-inositol methyl ether (**B2.4**) in 63% overall yield from *myo*-inositol.

B2.3.3. Synthesis of mytilitol

B2.3.3.1. Known method of synthesis

The only report on the synthesis of mytilitol (**B2.8**) in the literature[90] is shown in Scheme B2.27. As mentioned earlier, compound **B2.63** was obtained during the synthesis of (-)-laminitol (Scheme B2.8) from D-glucose.

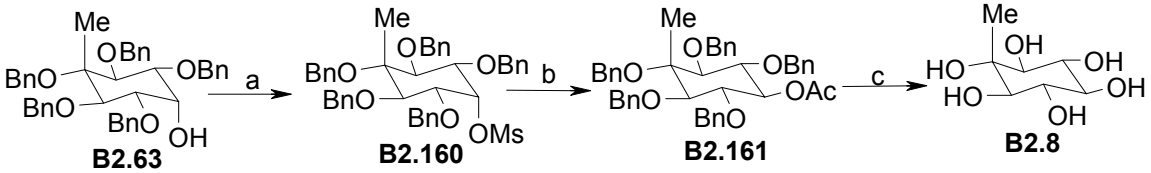

Scheme B2.27. a) MsCl (18 eq), Pyr, 0 °C, 24 h, 97%; b) CsOAc (10 eq), DMF, 80 °C, 12 h, 93%; c) (i) NaOMe, EtOH, rt, (ii) H_2, Pd / C, MeOH, 100%.

B2.3.3.2. Present work

We synthesized mytilitol (**B2.8**, Scheme B2.28) from the ketone **B2.154** (Scheme B2.25). Grignard reaction of the ketone **B2.154** with methylmagnesium iodide in a mixture of diethyl ether and THF gave the 2-*C*-methyl -*scyllo*-inositol derivative **B2.162**. Removal of the tosylates in **B2.162** by methanolysis with sodium methoxide in methanol,

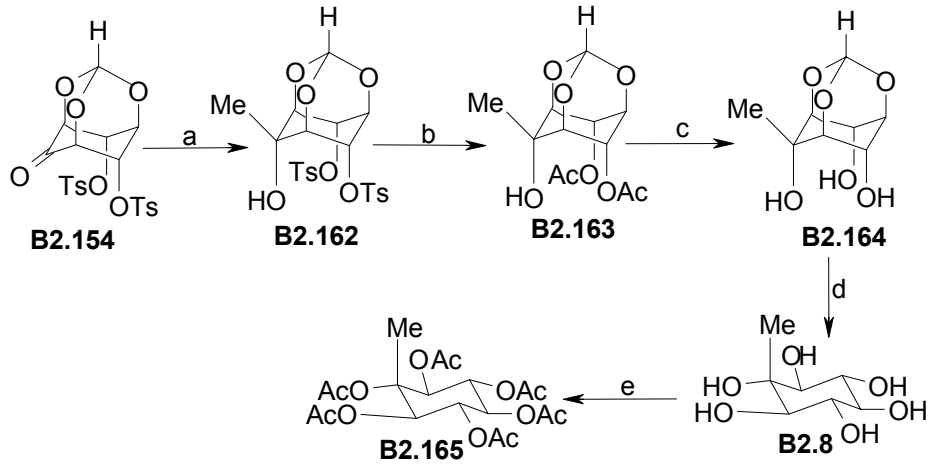

Scheme B2.28. a) MeMgI (5 eq), Et_2O-THF (3 : 1), 0°C-rt, 6 h, 74%; b) (i) NaOMe, MeOH, reflux, 8 h, (ii) Ac_2O, Pyr, 24 h, rt, 96%; c) *i*-$BuNH_2$, MeOH, reflux, 12 h, 94% d) TFA-H_2O (4 : 1), rt, 1 h, 100%; e) Ac_2O, Pyr, DMAP, rt, 24 h, 93%.

followed by acetylation gave the diacetate **B2.163**. The tertiary hydroxyl group in **B2.163** did not undergo acetylation under these experimental conditions. The structure of **B2.163** was confirmed by X-ray crystallography. Removal of the acetates in **B2.163** by aminolysis gave mytilitol orthoformate (**B2.164**). Acid hydrolysis of the orthoester in **B2.164** using aqueous trifluoroacetic acid gave mytilitol (**B2.8**) in 48% overall yield from *myo*-inositol. Mytilitol was characterized by converting it to the known hexaacetate **B2.165**.[90] Table B2.4 compares the yield of mytilitol obtained in the present work with other known methods in the literature.

Table B2.4. Comparision of the yield of mytilitol obtained by the present method with the literature methods.

Starting material	Number of steps	Overall yield (%)	Reference
D-Glucose	21	3	90
myo-Inositol	12	48	Present work

B2.4. Attempted synthesis of *epi*-inositol

B2.4.1. Known methods of synthesis

epi-Inositol was first obtained as one of the products of hydrogenation of hexahydroxy benzene in 6% yield.[41] Several synthetic routes for *epi*-inositol, starting from furan,[42] D-glucose,[33,34] D-galactose,[33,34,57] *myo*-inositol,[24, 25, 30] *para* benzoquinone,[45] benzene[119] and its derivatives[58] are reported in the literature.

Kowarski and Seral[42] synthesized *epi*-inositol from the bicyclic carbonate **B2.170** (Scheme B2.29) which was obtained as one of the products of the Diels-Alder addition[120-123] of vinyl carbonate to furan. The Diels-Alder reaction gave a mixture of both *endo*- and *exo*- products and most of the other synthetic steps were low yielding.

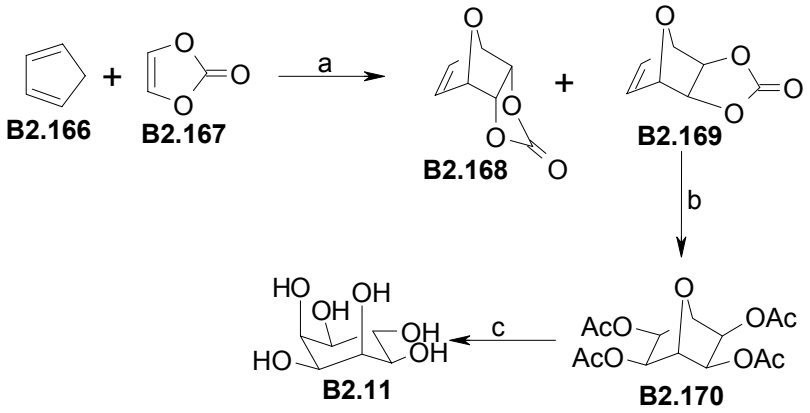

Scheme B2.29. a) (i) Sealed ampule, mixing in dry ice bath, (ii) 120 ^{o}C, 12 h, 21% (**B2.168** : **B2.169** = 4.5 : 1); b) (i) OsO_4, Pyr-EtOAc, rt, 24 h, (ii) Na_2SO_3, H_2O-EtOH, reflux, 7 h, (iii) 5% NaOH (w / v), rt, 1 h, (iv) Ac_2O, Pyr., rt, 24 h, 6.6%; c) 80% aq. AcOH, H_2SO_4 (cat.), reflux, 14 h.

Synthesis of *epi*-inositol by Takahashi and co-workers[34] from glucose and galactose are shown in Scheme B2.30. Both these routes involve the hydride reduction of inosose derivatives **B2.111** and **B2.178** which generate mixture of isomeric inositols, *myo*- and *epi*- in the former (**B2.171** and **B2.172**) while *epi*- and *muco*- in the latter (**B2.181** and **B2.182**).

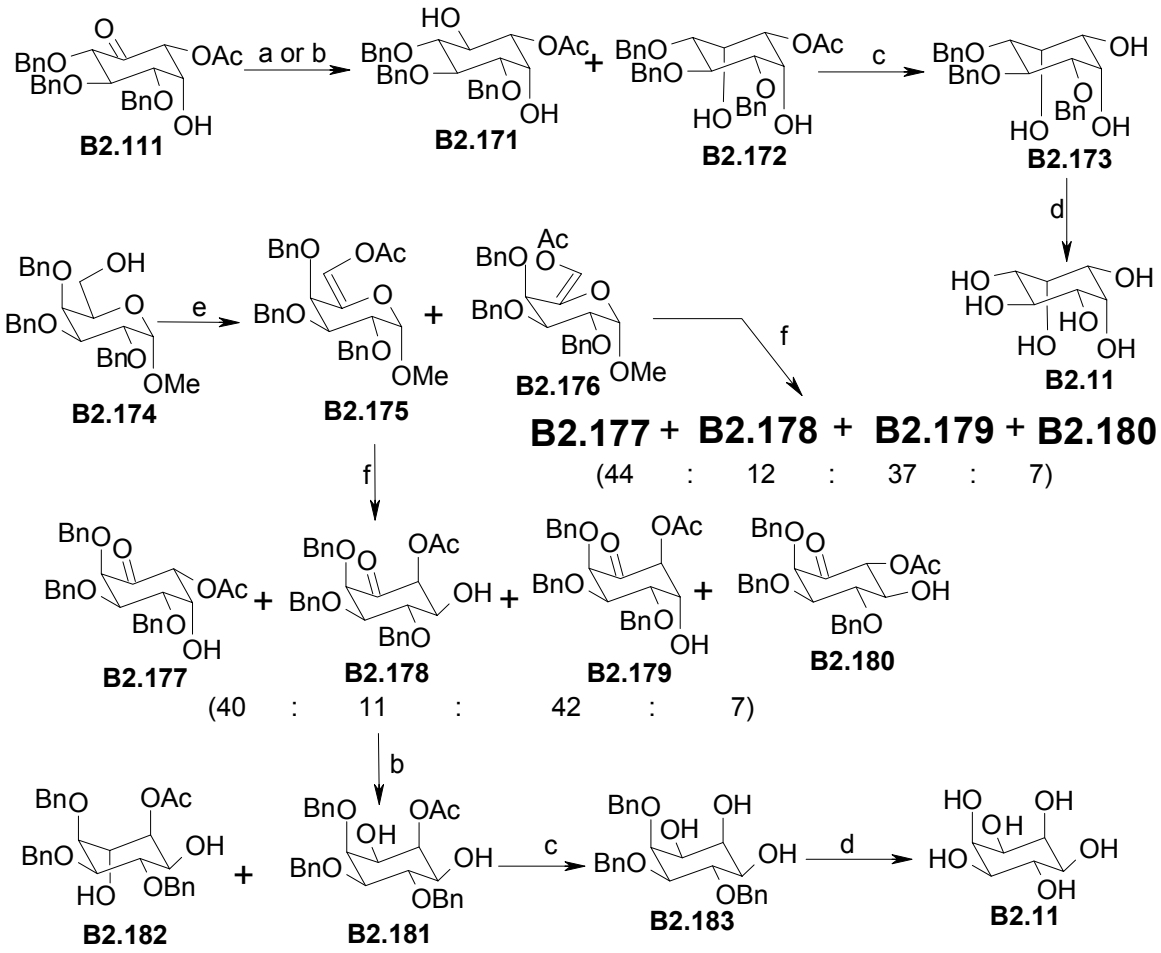

Scheme B2.30. a) $Me_4NBH(OAc)_3$ (5 eq), MeCN-AcOH, rt, 3 h, 94% (**B2.171** : **B2.172** = 99 : <1); b) $NaBH_4$ (1.5 eq), MeOH, 0 °C, 30 min, 97% for **B2.111** (**B2.171** : **B2.172** = <1 : 99) and 94% for **B2.178** (**B2.181** : **B2.182** = <1 : 99); c) 10 N NaOH, MeOH, rt, 12 h; d) H_2 / $Pd(OH)_2$-C, rt, 24 h, 73% for **B2.173** and 100% for **B2.183** e) (i) TFA (0.5 eq), Pyr (1 eq), DCC (3 eq), DMSO-benzene (1 : 1), rt, 1 d, (ii) Ac_2O (4 eq), Et_3N (4 eq), DMAP (0.1 eq), 1,2-dichloroethane, reflux, 3 h; f) $PdCl_2$ (0.05 eq), dioxane-H_2O (2 : 1), 60 °C, 3 h, 88% for **B2.175** and 15% for **B2.176**.

Pistará and co-workers[57] also synthesized *epi*-inositol from methyl-β-D-galactopyranoside (**B2.184**, Scheme B2.31).

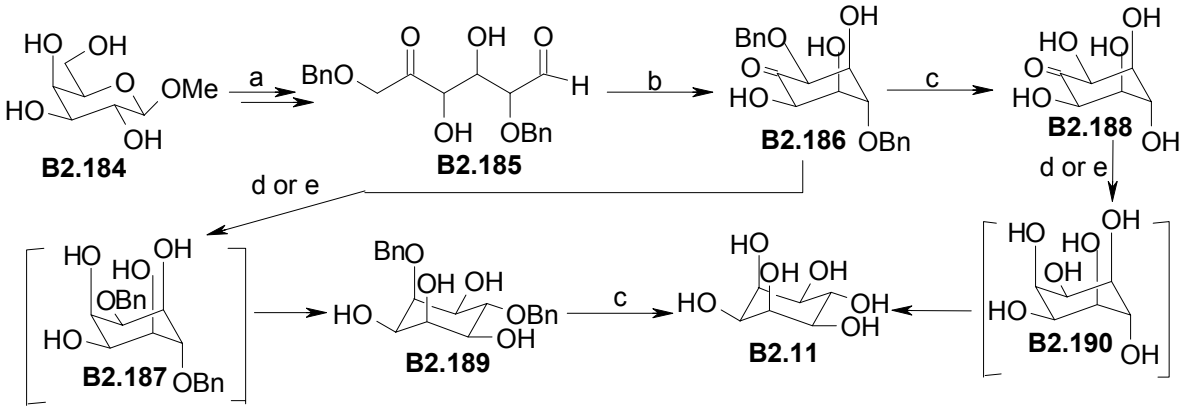

Scheme B2.31. a) as in reference 124; b) DBU, toluene, 60%; c) H_2, Pd / C, MeOH, 100%; d) H_2, Raney-Ni; e) $NaBH_4$, -78 ^oC, 90%.

Carless and co-workers[119] synthesized *epi*-inositol from *cis*-1,2-cyclohexadienediol (**B2.191**, Scheme B2.32), which was obtailed by microbial oxidation of benzene with *Pseudomonas Putida*.

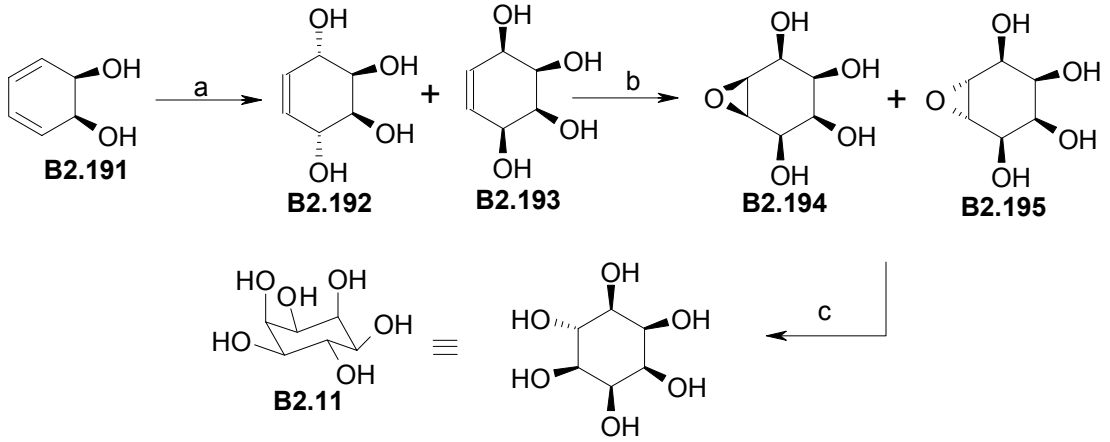

Scheme B2.32. a) (i) $^1O_2$, -70 ^oC, (ii) thiourea, MeOH-DCM, 12 h, 14% **B2.192** & 34% **B2.193**; b) AcOOH, AcOH, 39% **B2.194** & 15% **B2.195**; c) (i) $H_3O^{(+)}$, 80 ^oC, 90-100%, (ii) K_2CO_3, MeOH.

Gigg synthesized *epi*-inoistol[30] from racemic *epi*-inosose derivative **B2.38** (Scheme B2.33), the intermediate obtained during the synthesis of racemic laminitol derivative **B2.42** (Scheme B2.6).

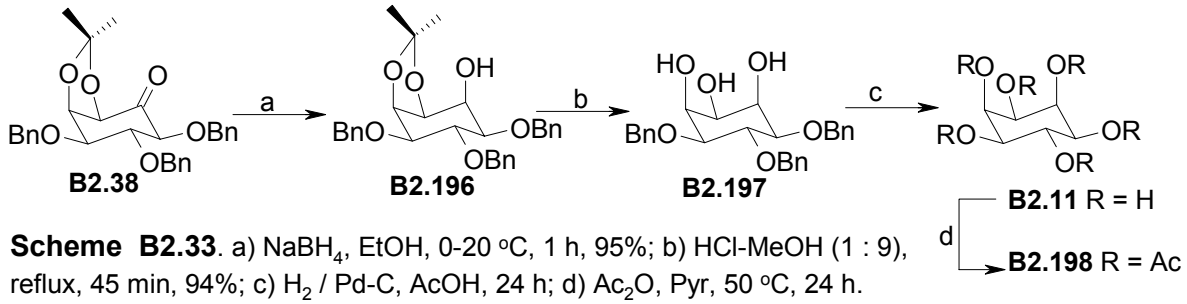

Scheme B2.33. a) $NaBH_4$, EtOH, 0-20 ^oC, 1 h, 95%; b) HCl-MeOH (1 : 9), reflux, 45 min, 94%; c) H_2 / Pd-C, AcOH, 24 h; d) Ac_2O, Pyr, 50 ^oC, 24 h.

Chung and Kwon synthesized[24] *epi*-inositol derivative **B2.203** from the di-*O*-isopropylidine derivative **B2.136** (Scheme B2.34). A mixture of isomeric inositol derivatives was obtained during the dihydroxylation of the double bond in **B2.200**.

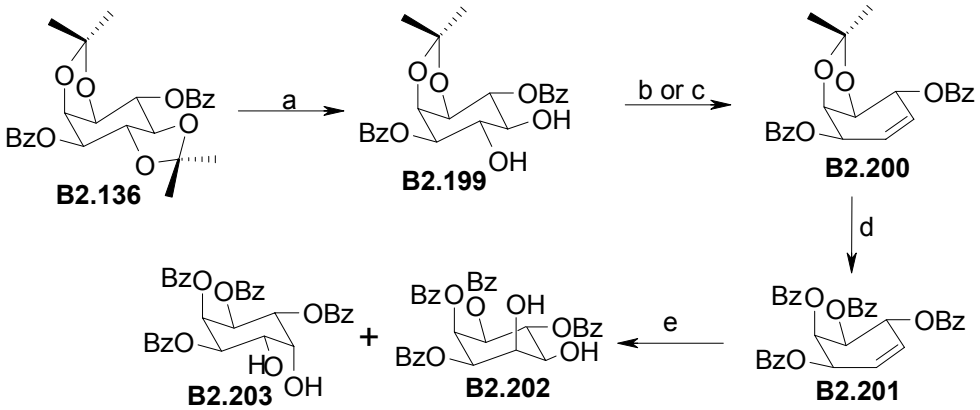

Scheme B2.34. a) AcCl (cat.), DCM-MeOH, 75%; b) (i) $ClPPh_2$ (2.2 eq), imidazole (6 eq), I_2 (2 eq), toluene, reflux, (ii) Zn, 50%; c) PPh_3 (2.2 eq), imidazole (6 eq), I_2 (2eq), toluene, reflux, 77%; d) (i) AcOH-H_2O (4 : 1), 100 ^oC, (ii) BzCl, Pyr, 91%; e) OsO_4, NMO, acetone-H_2O (8 : 1), 31% **B2.202** & 42% **B2.203**.

Same authors also synthesized[25] optically active *epi*-inositol derivatives **B2.207** and **B2.ent207** by the enzymatic resolution of the conduritol derivative **B2.205** (Scheme B2.35).

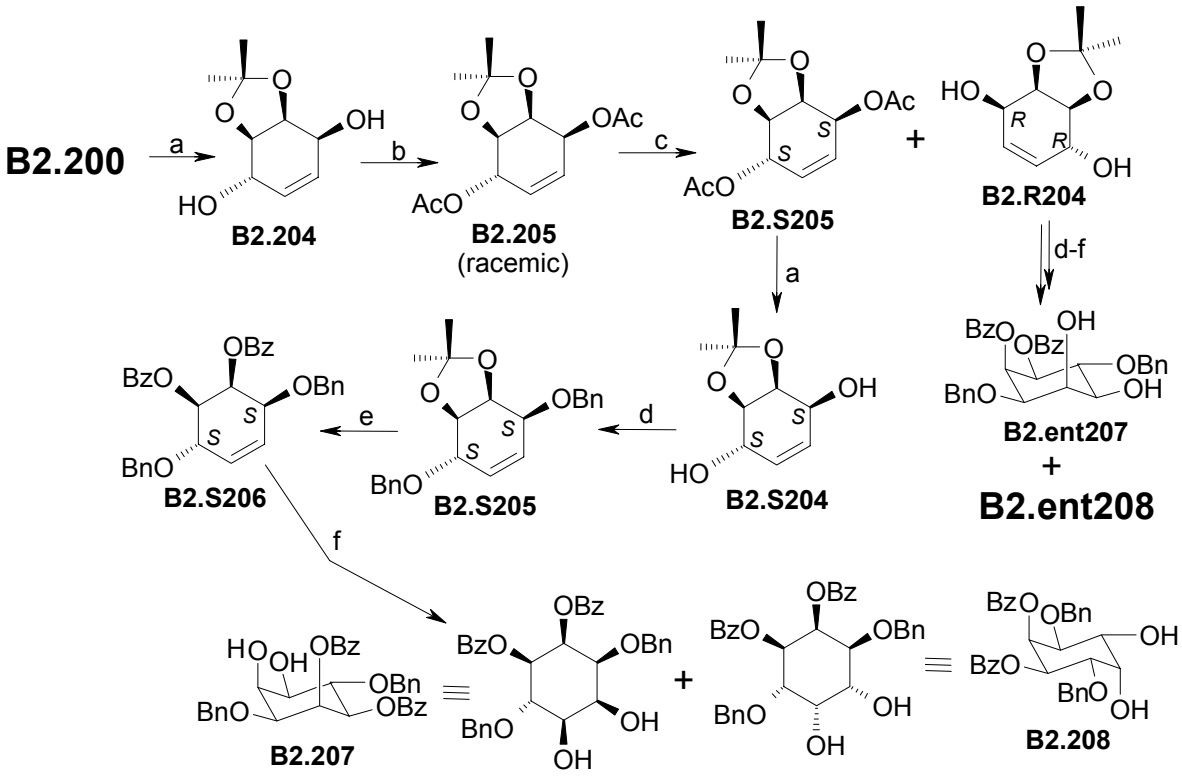

Scheme B2.35. a) NaOMe, MeOH, reflux, 3 h, 96%; b) Ac_2O, Pyr.; 0 ^oC-rt, overnight, 97%; c) *Candida Rugosa* lipase, 0.5 N Na_3PO_4 buffer (pH = 7.0), rt, 3 h, 49% **B2.S205** (95% ee), 48% **B2.R204** (95% ee); d) BnBr (4 eq), NaH (5 eq), DMF, 0 ^oC-rt, overnight, 99%; e) (i) AcOH-H_2O (4 : 1), 100 ^oC, 3 h, (ii) BzCl, Pyr., 0 ^oC-rt, overnight, 96%; f) NMO (4.5 eq), OsO_4(cat), acetone-H_2O (8 : 1), rt, 12 h, 39% **B2.207** and 45% **B2.208**.

In a recent report, chemoenzymatic synthesis of *epi*-inositol from bromobenzene in an overall yield of 40% was reported (Scheme B2.36).[58]

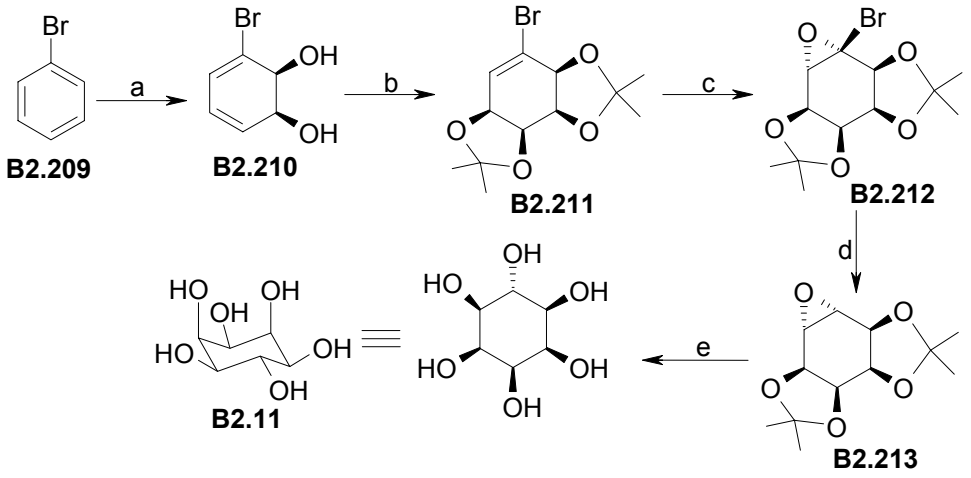

Scheme B2.36. a) toluene dioxygeneage; b) (i) OsO_4, NMO (1.5 eq), DCM, rt, overnight, (ii) 2,2-dimethoxy propane, TsOH (1.5 eq), acetone, rt, 45 min, 75%; c) *m*-CPBA (2 eq), DCM-$CHCl_3$ (1 : 1), reflux, 6 h, 70%; d) Bu_3SnH (1.4 eq), $(PhCO_2)_2$ (0.3 eq), THF, reflux, 4 h, 85%; e) Dowex IX8-200, H_2O, reflux, 24 h, 90%.

Podeschwa and co-workers[45] used *para* benzoquinone as the starting material for the synthesis of *epi*-inositol (Scheme B2.37). The key intermediate was the dibromide **B2.96** (Scheme B2.15), which was obtained from *para* benzoquinone in 22% yield in four steps.

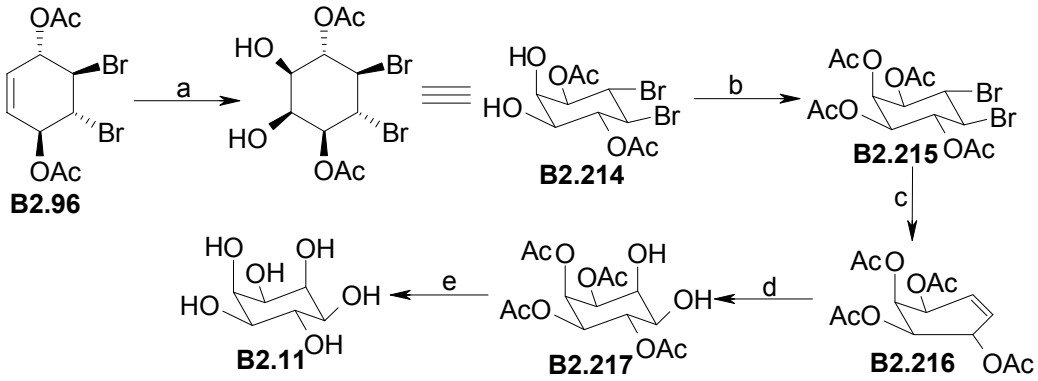

Scheme B2.37. a) $RuCl_3$ (0.06 eq), $NaIO_4$ (1.5 eq), MeCN-H_2O, rt, 10 min, 81% (80% de); b) Ac_2O, Pyr, rt, 12 h, 99%; c) Zn, AcOH, Et_2O, reflux, 12 h, 68%; d) $RuCl_3$ (0.1 eq), $NaIO_4$ (1.5 eq), MeCN-H_2O, rt, 10 min, 74% (80% de); e) NaOMe, MeOH, 4 ^oC-rt, 12 h, 99%.

B2.4.2. Present work

We first attempted the synthesis of *epi*-inositol (**B2.11**) from the ketone **B2.69** (Scheme B2.38). The ketone **B2.69** was subjected to acid hydrolysis in aqueous trifluoroacetic acid to obtain the *epi*-inosose derivative **B2.218**. Since **B2.218** was unstable, we attempted to prepare its tribenzoate derivative prior to reduction of the carbonyl group. But benzoylation of **B2.218** with benzoyl chloride in pyridine gave a mixture of products that could not be separated by flash chromatography. Hence we were unable to prepare *epi*-inositol from **B2.218**. One of the products, the enol-benzoate **B2.219** (yield 23%) could however be isolated by crystallization from dichloromethane - light petroleum mixture. Structure of **B2.219** was confirmed by X-ray crystallography. The enolization of *epi*-inosose in aqueous sodium and barium hydroxide solutions is known.[125]

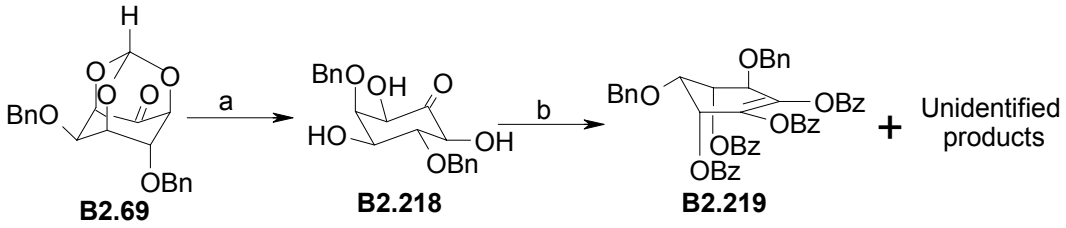

B2.69 **B2.218** **B2.219**

Scheme B2.38. a) TFA-H_2O (4:1), rt, 2-3 h, 94%; b) BzCl, pyr, rt, 12 h, 23%.

Next we attempted the synthesis of *epi*-inositol from the mixture of ketone **B2.64** and *gem* diol **B2.65** (Scheme B2.9). The *gem* diol was converted to its dimethyl ketal **B2.220** by methylation with methyl iodide and sodium hydride in DMF. Tosylate groups in **B2.220** were solvolyzed with sodium methoxide in methanol to obtain the orthoformate **B2.221**. Treatment of **B2.221** with aqueous trifluoroacetic acid gave the known *epi*-inosose **B2.222**.[125] We reduced **B2.222** with sodiumborohydride in methanol. The product obtained after the reduction of **B2.222** was acetylated with acetic anhydride

in pyridine at ambient temperature. TLC analysis of the product showed the presence of several products, separation of which was not attempted. Further work on the reduction of the inosose **B2.222** is under progress.

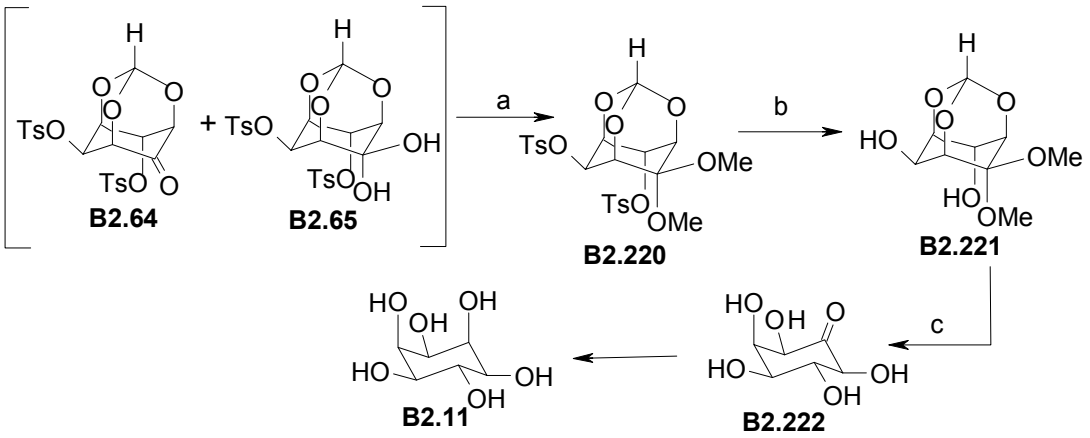

Scheme B2.39. a) MeI (3.0 eq), NaH (2.2 eq), DMF, rt, 5 min, 76%; b) NaOMe, MeOH, reflux, 12 h, 75%; c) TFA-H_2O (4:1), rt, 2-3 h, 99%.

It is of interest to compare the ease of hydration of the three inositol orthoformate derived ketones **B2.64**, **B2.69** and **B2.154** described in this work (Scheme B2.40), since the dibenzyl ether **B2.68** and the symmetric ditosylate **B2.152** gave the corresponding ketones **B2.69** and **B2.154** as major products, while the unsymmetric ditosylate **B2.30** gave the *gem* diol **B2.65** as the major product (as revealed by IR and NMR spectroscopy). The factors that could control the relative stability of a ketone and its *gem* diol (or the ease of hydration of a ketone) are electrophilicity of the carbonyl carbon (eg. α-fluoro ketones often exist as *gem* diols) and steric factors that could stabilize the ketone or the *gem* diol.

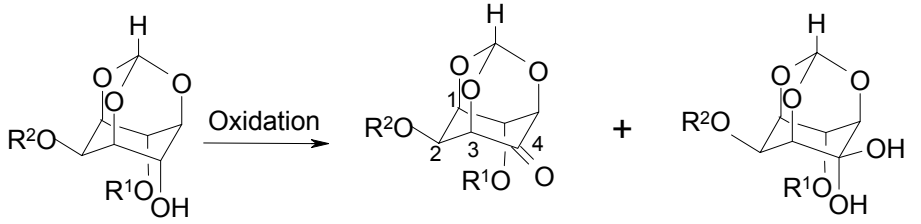

	R^1	R^2
B2.30	Ts	Ts
B2.68	Bn	Bn
B2.223	TBS	TBS
B2.224	Bn	TBS

B2.64
B2.69 (major)
B2.225 (major)
B2.227 (major)

B2.65 (major)
B2.70
B2.226
B2.228

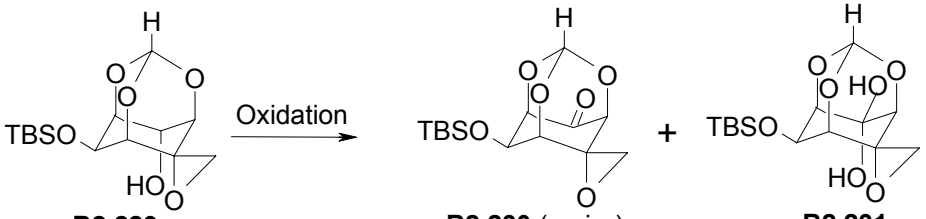

B2.229

B2.230 (major)

B2.231

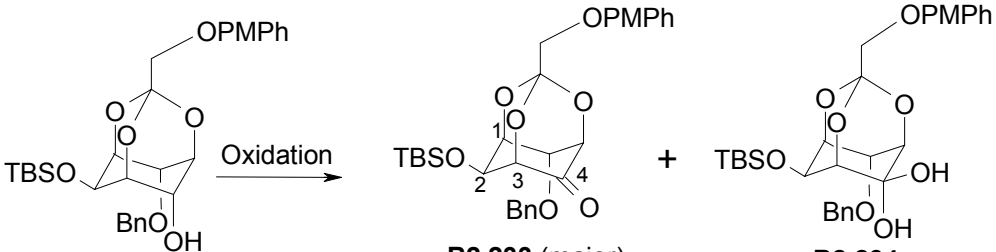

B2.232

B2.233 (major)

B2.234

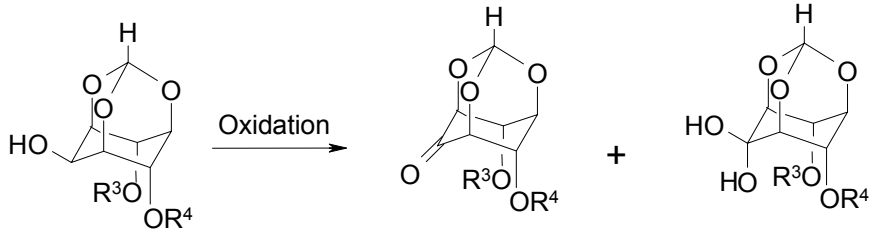

	R^3	R^4
B2.145	Bn	Bn
B2.152	Ts	Ts
B2.235	PMB	PMB
B2.236	Me	Bn

B2.146 (major)
B2.154 (major)
B2.237 (major)
B2.239

B2.147
B2.155
B2.238
B2.240

Scheme B2.40

Scheme B2.40 continued.

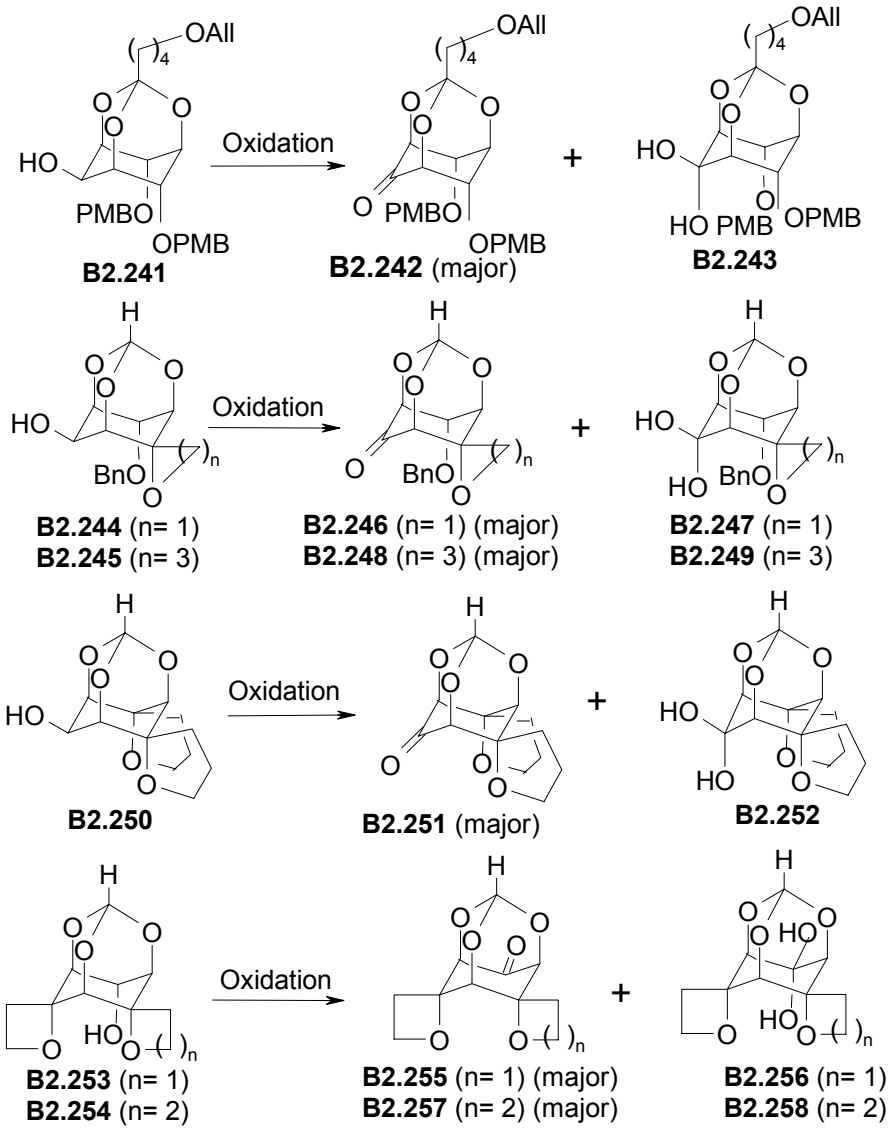

myo-Inositol 1,3,5-orthoester derived ketones and the corresponding gem diols resulting by their hydration, reported in the literature are shown in Scheme B2.40. All of them are trioxaadamantanes with very rigid molecular framework that is expected to make the introduction of a planar sp2 carbon difficult. Among the 4-keto derivatives **B2.64**, **B2.69**, **B2.225,**[126] **B2.227**,[127,128] **B2.230**[127,128] and **B2.233**[127,128] only the ditosylate **B2.64** gives the *gem* diol **B2.65** with ease. Most of the 2-keto derivatives (**B2.146**,[129] **B2.154**, **B2.237**,[130] **B2.242**,[131] **2.246**,[127,128] **B2.248**[127,128] and **B2.252**[128]) exist in the keto

from. Although the oxidation of the methyl ether **B2.236** is reported[73] we could not judge whether the ketone **B2.239** or the *gem* diol **B2.240** is the major constituent, from the published data. Thus majority of the *myo*-inositol orthoester derived ketones exist in the keto form. Perhaps the presence of two electron withdrawing tosylate groups in the inositol ring makes the ketone at the 4-position in **B2.64** more electrophilic and hence it undergoes hydration readily. The diol **B2.65** is quite stable since the steric strain is not much due to the presence of one tosylate and one hydrogen on 4,6-diaxial oxygen atoms. In the case of the 2-ketones **B2.146**, **B2.237** and **B2.239**, hydration of the ketone takes place to some extent. The ketone **B2.237** could be converted to the *gem*- diol **B2.238** in 76% yield by stirring with water in dioxane.[130] But hydration of **B2.154** was difficult. If the electron withdrawing nature of the tosylates solely decided the extent of hydration of the keto group, then the 2-ketone **B2.154** should have existed as the corresponding *gem* diol **B2.155**, since the tosylate groups are three bonds away from the carbonyl carbon as in the case of the isomeric 4-ketone **B2.64**. However, hydration of the 2-ketone **B2.154** would result in steric crowding due to the presence of three axial substituents (in the diol **B2.155**). Hence perhaps, the steric crowding drives the equilibrium back towards the 2-ketone **B2.154** in the symmetric ditosylate. Thus it appears that the relative stability of the ketone and the gem diol in these rigid trioxaadamantane systems depends on a balance between the electron withdrawing effect of the sulfonyl groups as well as 1,3-diaxial steric interactions (Scheme B2.41).

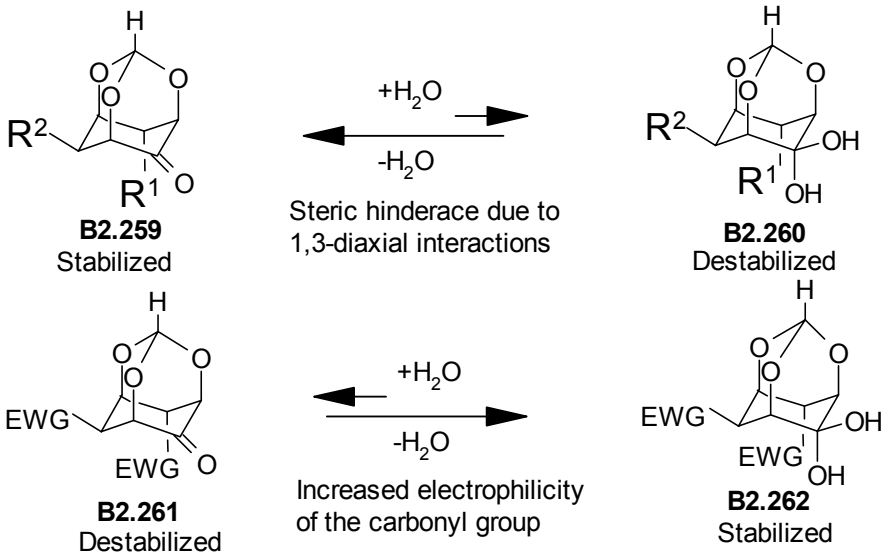

B2.259
Stabilized

B2.260
Destabilized

B2.261
Destabilized

B2.262
Stabilized

Scheme B2.41

B2.5. Conclusions

We have demonstrated that *myo*-inositol 1,3,5-orthoformate is a versatile intermediate for the synthesis of O- and C-alkylated cyclitol derivatives and that the sulfonate esters can be used efficiently for the protection of inositol orthoester hydroxyl groups. It is interesting to note that both O- and C-alkylation could be carried out efficiently in the presence of sulfonate moieties as the adamantane framework does not allow the tosylate groups to function as efficient leaving groups. As evident from the yields of the final products, this unusual protection of hydroxyl groups as their sulfonates resulted in more efficient synthesis of inositol derivatives. These synthetic sequences are perhaps one of the very few reports in the literature where tosylate groups have been used for the efficient protection of hydroxyl groups and the preparation of enantiomeric end products. Synthesis of isomeric inositols and aminocyclitol derivatives was also successfully carried out by using tosylate as protecting group for the protection of inositol hydroxyl groups and yields of the final products were found to be better than that obtained by earlier reported methods.

B2.6. Experimental section

General methods: General experimental methods are same as those described in section A2.5. Compounds **B2.30**,[77] **B2.66**,[77] **B2.67**,[77] **B2.68**,[77] **B2.D68**,[77] **B2.L68**,[77] **B2.73**,[77] **B2.dia73**[77] and were prepared as reported earlier.

L- & D-2,4-di-*O*-tosyl-6-*O*-[(-)-ω-camphanoyl]-*myo*-inositol 1,3,5-orthoformate (B2.31 and B2.dia31): Racemic **B2.30** (1.000g, 2.01 mmol), DMAP (0.050 g) and freshly prepared 1*S*-(-)-camphanoyl chloride (0.566 g, 2.61 mmol) were dissolved in dry pyridine (10 mL) and heated at 80 °C for 10 h. The reaction mixture was cooled to ambient temperature, pyridine was evaporated under reduced pressure and worked up with dichloromethane get a gum. Flash chromatography of the gum obtained gave **B2.31** (0.585 g, 43 %), **B2.dia31** (0.600 g, 44 %) and a mixture of **B2.31** and **B2.dia31** (0.135 g, 10 %).

Data for B2.dia31: **mp** 222-225 °C.

IR ($CHCl_3$)ν = 1776 cm^{-1}.

$[\alpha]_D^{26}$ = -7.7 (c 1, $CHCl_3$).

^{1}H NMR ($CDCl_3$, 500 MHz): δ 0.98 (s, 3H), 1.10 (s, 3H), 1.15 (s, 3H), 1.70-1.80 (m, 1H), 1.90-2.05 (m, 1H), 2.05-2.12 (m, 1H), 2.40-2.55 (m, 1H), 2.48 (s, 6H), 4.05-4.15 (m, 1H), 4.30-4.40 (m, 2H), 4.85-4.90 (m, 1H), 4.93-5.00 (m, 1H), 5.48 (d, *J* 5.0 Hz, 1H), 5.55-5.65 (m, 1H), 7.40-7.50 (m, 4H), 7.73 (d, *J* 10.0 Hz, 2H), 7.83 (d, *J* 10.0 Hz, 2H).

^{13}C NMR ($CDCl_3$, 125 MHz): δ 9.7, 16.7, 17.0, 21.8, 29.0, 30.5, 54.3, 54.9, 66.5, 67.7, 67.9, 69.1, 69.5, 72.0, 90.7, 102.6, 127.8, 128.1, 130.3, 130.5, 131.6, 133.0, 145.8, 146.4, 165.9, 177.5.

Elemental Analysis calcd for $C_{31}H_{34}O_{13}S_2$; C 54.86%, H 5.05%; found C 54.77%, H 4.84%.

Data for B2.31: **mp** 184-185 °C

IR ($CHCl_3$)ν = 1768, 1788 cm^{-1}.

$[\alpha]_D^{25}$ = -25.4 (c 1, $CHCl_3$).

^{1}H NMR ($CDCl_3$, 500 MHz): δ 0.95 (s, 3H), 1.07 (s, 3H), 1.15 (s, 3H), 1.65-1.73 (m, 1H), 1.90-2.05 (m, 2H), 2.40-2.45 (m, 1H), 2.45 (s, 3H), 2.48 (s, 3H), 4.03-4.07 (m, 1H), 4.20-4.23 (m, 1H), 4.48-4.52 (m, 1H), 4.74 (d, *J* 2.0 Hz, 1H), 5.05-5.10 (m, 1H), 5.45-5.48 (m, 1H), 5.50 (s, 1H), 7.39 (d, *J* 10.0 Hz, 2H), 7.43 (d, *J* 10.0 Hz, 2H), 7.78 (d, *J* 10.0 Hz, 2H), 7.83 (d, *J* 10.0 Hz, 2H).

^{13}C NMR ($CDCl_3$, 125 MHz): δ 9.7, 16.6, 21.6, 21.7, 28.8, 30.4, 54.4, 54.8, 66.6, 67.7, 68.0, 68.8, 69.5, 71.8, 90.5, 102.6, 128.0, 128.1, 130.3, 130.4, 131.9, 132.5, 145.7, 146.1, 166.1, 177.7.

Elemental Analysis calcd for $C_{31}H_{34}O_{13}S_2$; C 54.86%, H 5.05%; found C 55.04%, H 5.03%.

Configuration of both the diastereomers were confirmed by X-ray crystallography (see pages 301 and 304).

L-2,4-di-*O*-tosyl-*myo*-inositol 1,3,5-orthoformate (B2.L30): Isobutylamine (2 mL) and **B2.31** (0.400 g, 0.590 mmol) were dissolved in a mixture of methanol (10 mL) and dichloromethane (10 mL) and refluxed for 6 h. Removal of the solvents under reduced pressure, usual work-up with dichloromethane followed by column chromatography gave **B2.L30** (0.286 g, 96%) as a white solid.

Data for B2.L30: **mp** 112-114 °C.

IR ($CHCl_3$)ν = 3184-3659 cm^{-1}.

$[\alpha]_D^{29}$ = -9 (c 1, $CHCl_3$).

^{1}H NMR ($CDCl_3$, 300 MHz): δ 2.46 (s, 3H), 2.49 (s, 3H), 2.45-2.65 (broad s, 1H, D_2O exchangeable), 4.00-4.10 (m, 1H), 4.15-4.25 (m, 1H), 4.30-4.40 (m, 1H), 4.50-4.60 (m, 1H), 4.95-5.02 (m, 1H), 5.02-5.10 (m, 1H), 5.44 (d, *J* 1.4 Hz, 1H), 7.35 (d, *J* 8.0 Hz, 2H), 7.41 (d, *J* 8.1 Hz, 2H), 7.82 (t, *J* 8.8 Hz, 4H).

^{13}C NMR ($CDCl_3$, 50.3 MHz): δ 21.6, 66.6, 68.6, 69.6, 71.4, 72.9, 102.3, 127.8, 128.0, 130.1, 130.3, 131.9, 133.0, 145.5, 146.1.

Elemental Analysis calcd for $C_{21}H_{22}O_{10}S_2$; C 50.60%, H 4.45%; found C 50.37%, H 4.42%.

L-2,4-di-*O*-tosyl-6-*O*-methyl-*myo*-inositol 1,3,5-orthoformate (B2.L32): To a solution of methyl iodide (0.086 g, 0.606 mmol) and **B2.L30** (0.200 g, 0.402 mmol) in dry DMF (3 mL), was added sodium hydride (0.011 g, 0.458 mmol) and stirred for 5 min. Reaction was quenched with ice, DMF was evaporated under reduced pressure and the reaction mixture was worked-up with dichloromethane to obtain a gum. Purification of the gum by column chromatography gave **B2.L32** (0.195 g, 95%) as a gum.

Data for B2.L32:

$[\alpha]_D^{29}$ = -5 (c 1, $CHCl_3$)

^{1}H NMR ($CDCl_3$, 200 MHz): δ 2.47 (s, 3H), 2.48 (s, 3H), 3.38 (s, 3H), 3.90-4.00 (m, 1H), 4.03-4.14 (m, 1H), 4.20-4.30 (m, 1H), 4.37-4.45 (m, 1H), 4.85-4.94 (m, 1H), 4.95-5.07 (m, 1H), 5.44 (d, *J* 1.2 Hz, 1H), 7.36 (d, *J* 3.5 Hz, 2H), 7.39 (d, *J* 3.5 Hz, 2H), 7.78 (d, *J* 8.2 Hz, 2H), 7.85 (d, *J* 8.2 Hz, 2H).

^{13}C NMR ($CDCl_3$, 50.3 MHz): δ 21.5, 57.0, 66.6, 68.6, 69.4, 69.6, 72.3, 74.3, 77.2, 102.4, 127.7, 130.0, 132.2, 133.1, 145.3, 145.7.

Elemental Analysis calcd for $C_{22}H_{24}O_{10}S_2$; C 51.55%, H 4.72%; found C 51.79%, H 4.88%.

D-4-*O*-methyl-*myo*-inositol 1,3,5-orthoformate (D-Ononitol orthoformate, B2.D26): To a stirred solution of **B2.L32** (0.142 g, 0.277 mmol) in dry methanol (5 mL) was added sodium methoxide (0.151 g, 2.796 mmol) and the mixture refluxed for 12 h. The reaction was quenched with ice, methanol was evaporated under reduced pressure and the product was purified by flash chromatography to obtain **B2.D26** (0.056 g, 99%) as a white solid.

Data for B2.D26: **mp** 102-104 °C.

IR (nujol)ν = 3076-3472, 3523 cm $^{-1}$.

$[\alpha]_D^{20}$ = + 3.9 (c 1, EtOH).

^{1}H NMR (500 MHz, CD_3OD): δ 3.39 (s, 3H), 3.90-4.00 (m, 2H), 4.05-4.18 (m, 2H), 4.18-4.26 (m, 1H), 4.28-4.38 (m, 1H), 5.42 (s, 1H).

^{13}C NMR (CD_3OD, 125 MHz): δ 57.9, 61.2, 69.1, 69.8, 73.6, 76.1, 77.7, 104.3.

Elemental Analysis calcd for $C_8H_{12}O_6$; C 47.06%, H 5.92; found C 47.00, H 5.81%.

D-ononitol (B2.D1): The orthoformate **B2.D26** (0.040 g, 0.196 mmol) was stirred with a mixture of trifluoroacetic acid (0.9 mL) and distilled water (0.3 mL) for 1 h. Evaporation of solvents under reduced pressure followed by co-evaporation with toluene gave D-ononitol **B2.D1** (0.038 g, 100%) as a white solid.

Data for B2.D1: **mp.** 167-169 °C; lit.[82] Mp. 167-169 °C.

$[\alpha]_D^{25}$ = +5.2 (c 2.2, H_2O); lit.[82] $[\alpha]_D$= +5.5 (c 2.2, H_2O).

^{1}H NMR (D_2O, 200 MHz): δ 3.30-3.40 (m, 2H), 3.40-3.50 (m, 1H), 3.50-3.67 (m, 5H), 3.95-4.05 (m, 1H).

D-2,4-di-*O*-tosyl-*myo*-inositol 1,3,5-orthoformate (B2.D30): Reaction of **B2.dia31** (0.450 g, 0.663 mmol) with isobutylamine (3 mL) as for the synthesis of **B2.L30** gave **B2.D30** (0.320 g, 97%) as a white solid.

Data for B2.D30: **mp** 112-113 °C.

IR ($CHCl_3$)ν = 3340-3583 cm^{-1}.

$[\alpha]_D^{29}$ = +9 (c 1, $CHCl_3$).

^{1}H NMR ($CDCl_3$, 300 MHz): δ 2.46 (s, 3H), 2.49 (s, 3H), 2.45-2.65 (broad, 1H, D_2O exchangeable), 4.00-4.10 (m, 1H), 4.15-4.25 (m, 1H), 4.30-4.40 (m, 1H), 4.50-4.60 (m, 1H), 4.95-5.02 (m, 1H), 5.02-5.10 (m, 1H), 5.44 (d, *J* 1.4 Hz, 1H), 7.35 (d, *J* 8.0 Hz, 2H), 7.41 (d, *J* 8.1 Hz, 2H), 7.82 (t, *J* 8.8 Hz, 4H).

^{13}C NMR ($CDCl_3$, 50.3 MHz): δ 21.6, 66.6, 68.6, 69.6, 71.4, 72.9, 102.3, 127.8, 128.0, 130.1, 130.3, 131.9, 133.0, 145.5, 146.1.

Elemental Analysis calcd for $C_{21}H_{22}O_{10}S_2$; C 50.60%, H 4.45%; found C 50.66%, H 4.63%.

D-2,4-di-*O*-tosyl-6-*O*-methyl- *myo*-inositol 1,3,5-orthoformate (B2.D32): Methylation of **B2.D30** (0.310 g, 0.622 mmol) with methyl iodide (0.114 g, 0.803 mmol) as for the synthesis of **B2.L32** gave **B2.D32** (0.300 g, 95%) as a gum.

Data for B2.D32:

$[\alpha]_D^{27}$ = +5 (c 1, $CHCl_3$).

^{1}H NMR ($CDCl_3$, 200 MHz): δ 2.47 (s, 3H), 2.48 (s, 3H), 3.38 (s, 3H), 3.90-4.00 (m, 1H), 4.03-4.14 (m, 1H), 4.20-4.30 (m, 1H), 4.37-4.45 (m, 1H), 4.85-4.94 (m, 1H), 4.95-

5.07 (m, 1H), 5.44 (d, *J* 1.2 Hz, 1H), 7.36 (d, *J* 3.5 Hz, 2H), 7.39 (d, *J* 3.5 Hz, 2H), 7.78 (d, *J* 8.2 Hz, 2H), 7.85 (d, *J* 8.2 Hz, 2H).

^{13}C NMR ($CDCl_3$, 50.3 MHz): δ 21.5, 57.0, 66.6, 68.6, 69.4, 69.6, 72.3, 74.3, 102.4, 127.7, 130.0, 132.2, 133.1, 145.3, 145.7.

Elemental analysis calcd for $C_{22}H_{24}O_{10}S_2$; C 51.55%, H 4.72%; found C 51.79%, H 4.83%.

L-4-*O*-methyl-*myo*-inositol 1,3,5-orthoformate (L-Ononitol orthoformate, B2.L26): Methanolysis of **B2.D32** (0.250 g, 0.488 mmol) as for the synthesis of **B2.D26** gave **B2.L26** (0.099 g, 99%) as a white solid.

Data for B2.L26: **mp** 102-104 °C.

IR (nujol) ν = 3105-3475, 3523 cm $^{-1}$.

$[\alpha]_D^{20}$ = – 3.8 (c 1, EtOH);.

^{1}H NMR (200 MHz, CD_3OD): δ 3.39 (s, 3H), 3.90-4.00 (m, 2H), 4.05-4.18 (m, 2H), 4.18-4.26 (m, 1H), 4.28-4.38 (m, 1H), 5.36 (s, 1H).

^{13}C NMR (CD_3OD, 125 MHz): δ 57.9, 61.2, 69.1, 69.8, 73.6, 76.1, 77.7, 104.3.

Elemental analysis calcd for $C_8H_{12}O_6$; C 47.06%, H 5.92%: found C 47.15%, H 5.72%.

L–ononitol (B2.L1): Acid hydrolysis of **B2.L26** (0.060 g, 0.294 mmol) as for the synthesis of **B2.D1** gave L-ononitol (**B2.L1**, 0.056 g, 98%) as a white solid.

Data for B2.L1: **mp**. 167-169 °C; lit.[82] Mp. 168-169 °C.

$[\alpha]_D^{26}$ = -5.2 (c 2, H_2O); lit.[82] $[\alpha]_D$= -5.7 (c 2, H_2O).

^{1}H NMR (D_2O, 500 MHz): δ 3.35-3.45 (m, 2H), 3.50-3.55 (m, 1H), 3.60-3.70 (m, 5H), 4.05-4.10 (m, 1H).

Oxidation of racemic 2,4-di-*O*-tosyl-*myo*-inositol 1,3,5-orthoformate (B2.30): Method A: To a cooled (–78 ^{o}C) solution of oxalyl chloride (0.520 g, 4.127 mmol) in dry dichloromethane (4 mL) was added drop wise, a solution of dry dimethyl sulfoxide (0.627 g, 8.038 mmol) in dry dichloromethane (3 mL) and the reaction mixture stirred for 15 min. To this mixture was added (drop wise) a solution of racemic **B2.30** (1.000 g, 2.008 mmol) in dry dichloromethane (8 mL) and stirring was continued for 1 h. Dry triethylamine (1.234 g, 12.218 mmol) was then added and the reaction mixture was allowed to warm to room temperature slowly. The reaction was quenched by adding a few drops of water and the organic layer was separated, dried over anhydrous sodium sulfate and the solvent was evaporated under reduced pressure. Purification of the crude product by column chromatography gave a mixture of **B2.64** and the *gem* diol **B2.65** (0.850 g, 82%) as a white solid.

Data for B2.64+**B2.65**: **mp** 133-134 °C.

IR ($CHCl_3$)ν = 3421-3522 cm^{-1}.

^{1}H NMR see page 317.

^{13}C NMR ($CDCl_3$, 50.3 MHz): δ 21.7, 69.0, 69.1, 69.4, 69.8, 70.1, 71.0, 72.7, 74.7, 75.6, 89.2, 102.4, 102.6, 127.8, 128.0, 130.2, 130.3, 130.5, 131.9, 133.0, 145.6, 146.1.

Elemental analysis calcd for $C_{21}H_{22}O_{11}S_2$ - H_2O; C 50.80%, H 4.06%; found C 50.55%, H 3.84%.

Method B: Acetic anhydride (3 mL, 31.79 mmol) and dry DMSO (5 mL, 64.64 mmol) were mixed and stirred for 30 min. Solid racemic 2,4-di-*O*-tosyl-*myo*-inositol 1,3,5-orthoformate, **B2.30** (0.498 g, 1.00 mmol) was added to this mixture and stirring continued for 40 h. The reaction mixture was diluted with ethyl acetate (30 mL), washed

with saturated sodium bicarbonate solution (5 mL), followed by brine (3 × 5 mL). The organic layer was dried over anhydrous sodium sulfate and solvents evaporated under reduced pressure to obtain a gum. Purification of this gum by column chromatography gave a mixture of the ketone **B2.64** and the *gem* diol **B2.65** (0.481 g, 94%) as a white solid.

Data for B2.64+**B2.65**: **mp** 133-134 °C.

Oxidation of racemic 2,4-di-*O*-benzyl-*myo*-inositol 1,3,5-orthoformate (B2.68): To a cooled (–78 ^{o}C) solution of oxalyl chloride (0.303 g, 2.405 mmol) in dry dichloromethane (3 mL) was added drop wise, a solution of dry dimethylsulfoxide (0.341 g, 4.372 mmol) in dry dichloromethane (2 mL) and the reaction mixture stirred for 15 min. To this mixture was added (drop wise) a solution of the racemic dibenzyl ether **B2.68** (0.800 g, 2.162 mmol) in dry dichloromethane (5 mL) and stirring was continued for 1 h. Dry triethylamine (1.096 g, 10.851 mmol) was then added and the reaction mixture was allowed to warm to room temperature slowly. The reaction was quenched by the addition of a few drops of water and the organic layer was separated, dried over anhydrous sodium sulfate and the solvent was evaporated under reduced pressure. Purification of the product by column chromatography afforded a mixture of the racemic ketone **B2.69** and the corresponding *gem* diol **B2.70** (0.730 g, 92%) as a gum.

Data for B2.69+**B2.70**:

IR (neat)ν = 1765, 3180-3630 cm^{-1}.

^{1}H NMR ($CDCl_3$, 200 MHz): δ 3.76 (d, *J* 1.5 Hz, 1H), 4.30-4.38 (m, 2H), 4.38-4.46 (m, 1H), 4.46-4.65 (m, 3H), 4.69 (q, 12.7, 11.7 Hz, 2H), 5.67 (d, *J* 1.4 Hz, 1H), 7.12-7.25 (m, 2H), 7.26-7.52 (m, 8H).

^{13}C NMR ($CDCl_3$, 50.3 MHz): δ 69.6, 69.7, 70.5, 70.9, 71.0, 75.7, 75.9, 78.1, 102.1, 127.1, 127.2, 127.4, 127.6, 127.8, 135.6, 136.1, 198.5.

Elemental analysis calcd for $C_{21}H_{20}O_6$ + 0.5 H_2O C 66.83%, H 5.61%; found C 66.73%, H 5.68%.

2, 4-di-*O*-benzyl-6-*C*-methyl-*myo*-inositol 1,3,5-orthoformate (B2.71): To a stirred cooled (ice bath) solution of a mixture of the racemic ketone **B2.69** and the *gem* diol **B2.70** (0.150 g, 0.408 mmol) in dry diethyl ether (5 mL), a freshly prepared solution (1.0 M, 2.0 mL) of methylmagnesium iodide in diethylether was added and stirring continued and the reaction mixture was allowed to warm to ambient temperature (3-4 h) while stirring. The reaction mixture was then diluted with dichloromethane (10 mL) and washed with a saturated aqueous solution of ammonium chloride (3 mL). The aqueous layer was extracted with dichloromethane (3 × 5 mL), the combined organic layer was washed with brine (5 mL) and the solvent removed by evaporation under reduced pressure to obtain a gum. Purification of this gum by column chromatography afforded racemic **B2.71** (0.138 g, 88%) as a gum.

Data for B2.71:

IR ($CHCl_3$)ν = 3338-3595 cm^{-1}.

^{1}H NMR ($CDCl_3$, 200 MHz): δ 1.56 (s, 3H), 3.86-3.96 (m, 2H), 3.96-4.02 (m, 1H), 4.18-4.28 (m, 1H), 4.33 (s, 1H, D_2O exchangeable), 4.39 (t, *J* 3.9 Hz, 1H), 4.54 (q, J_1 4.9 Hz, J_2 10.8 Hz, 2H), 4.73 (q, J_1 15.6 Hz, J_2 12.3 Hz, 2H), 5.52 (d, *J* 1.0 Hz, 1H), 7.15-7.25 (m, 2H), 7.25-7.50 (m, 8H).

^{13}C NMR ($CDCl_3$, 50.3 MHz): δ 24.1, 67.3, 69.3, 69.7, 71.3, 71.9, 72.8, 74.8, 75.9, 102.6, 127.9, 128.4, 128.6, 128.7, 135.9, 137.7.

Racemic laminitol orthoformate (B2.72): Racemic **B2.71** (0.120 g, 0.313 mmol) was subjected to hydrogenolysis (30 psi) in the presence of Pearlman's catalyst (20% $Pd(OH)_2$ on carbon, 0.044 g) in methanol (5 mL) for 6 h. Removal of the catalyst by filtration followed by removal of the solvent under reduced pressure gave racemic **B2.72** (0.063 g, 98%) as a white solid. This compound was found to exhibit polymorphism on crystallization from MeOH (Figure B2.2 B) and hot ethyl acetate (Figure B2.2 A).

Data for B2.72: **mp**. 179-181 °C (crystals obtained from MeOH); 201-202 °C (crystals obtained from hot EtOAc).

IR (nujol)ν = 3011-3690 cm^{-1}.

^{1}H NMR (CD_3OD, 200 MHz): δ 1.44 (s, 3H), 3.63 (dd, J_1 1.9 Hz, J_2 2.0 Hz, 1H), 3.70-3.77 (m, 1H), 3.93-3.98 (m, 1H), 4.04-4.10 (m, 1H), 4.34 (t, *J* 3.9 Hz, 1H), 5.30 (d, *J* 1.5 Hz, 1H).

^{13}C NMR (CD_3OD, 50.3 MHz): δ 23.7, 61.1, 68.2, 70.2, 73.3, 74.1, 78.7, 102.8.

Elemental analysis calcd for $C_8H_{12}O_6$ C 47.06%, H 5.92%; found C 47.00%, H 6.30%. The structure of compound **B2.72** was confirmed by X-ray crystallography (see page 325).

Racemic laminitol (B2.7): Racemic **B2.72** (0.030 g, 0.147 mmol) was treated with a mixture of trifluoroacetic acid (0.8 mL) and water (0.2 mL) at room temperature for 1 h. Removal of trifluoroacetic acid and water under reduced pressure gave racemic laminitol (**B2.7**, 0.028 g, 98%) as a white solid.

Data for B2.7: **mp** 256-258 °C; lit.[98] mp. 262-268 °C.

^{1}H NMR (D_2O, 200 MHz): δ 1.20 (s, 3H), 3.13-3.28 (m, 1H), 3.41-3.54 (m, 3H), 3.93-4.07 (m, 1H).

Oxidation of L-2,4-di-*O*-benzyl-*myo*-inositol 1,3,5-orthoformate (B2.L68): Oxidation of **B2.L68** (0.370 g, 1.000 mmol) as for the oxidation of **B2.68** gave a the ketone **B2.L69** (0.350 g, 95%) containing a small amount of the corresponding *gem* diol **B2.L70** as a gum.

Data for B2.L69+B2.L70:

IR (neat)ν = 1765, 3175-3620 cm^{-1}.

$[\alpha]_D^{26}$ = -21.0 (c 1, $CHCl_3$).

^{1}H NMR ($CDCl_3$, 200 MHz): δ 3.76 (d, *J* 1.5 Hz, 1H), 4.30-4.38 (m, 2H), 4.38-4.46 (m, 1H), 4.46-4.65 (m, 3H), 4.69 (q, 12.7, 11.7 Hz, 2H), 5.67 (d, *J* 1.4 Hz, 1H), 7.12-7.25 (m, 2H), 7.26-7.52 (m, 8H).

^{13}C NMR ($CDCl_3$, 50.3 MHz): δ 69.7, 69.8, 70.5, 70.9, 71.0, 75.7, 76.0, 78.1, 102.1, 127.1, 127.2, 127.4, 127.7, 127.9, 135.6, 136.1, 198.6.

Elemental analysis calcd for $C_{21}H_{20}O_6$ + 0.6 H_2O C 66.52%, H 5.64%; found C 66.43%, H 5.63%.

L-2, 4-di-*O*-benzyl-6-*C*-methyl-*myo*-inositol 1,3,5-orthoformate (B2.L71): C-methylation of the mixture of the ketone **B2.69** and the *gem* diol **B2.L70** (0.100 g, 0.272 mmol) as for the synthesis of **B2.71** afforded **B2.L71** (0.093 g, 89%) as a gum.

IR ($CHCl_3$)ν = 3338-3541 cm^{-1}.

$[\alpha]_D^{26}$ = - 9 (c 1, $CHCl_3$).

^{1}H NMR ($CDCl_3$, 200 MHz): δ 1.56 (s, 3H), 3.86-3.96 (m, 2H), 3.96-4.02 (m, 1H), 4.18-4.28 (m, 1H), 4.33 (s, 1H, D_2O exchangeable), 4.39 (t, *J* 3.9 Hz, 1H), 4.54 (q, J_1 4.9 Hz, J_2 10.8 Hz, 2H), 4.73 (q, J_1 15.6 Hz, J_2 12.3 Hz, 2H), 5.52 (d, *J* 1.0 Hz, 1H), 7.15-7.25 (m, 2H), 7.25-7.50 (m, 8H).

^{13}C NMR ($CDCl_3$, 50.3 MHz): δ 24.0, 67.2, 69.1, 69.6, 71.1, 71.7, 72.6, 74.6, 75.8, 102.4, 127.7, 128.3, 128.6, 128.7, 135.7, 137.5.

D-laminitol orthoformate (B2.D72): Hydrogenolysis of **B2.L71** (0.080 g, 0.208 mmol) as for the hydrogenolysis of **B2.71** gave **B2.D72** (0.042 g, 98%) as a white solid.

Data for B2.D72: **mp** 178-181 °C.

IR (nujol)ν = 3011-3657 cm^{-1}.

$[\alpha]_D^{27}$ = - 3 (c 1, EtOH).

^{1}H NMR (CD_3OD, 200 MHz): δ 1.44 (s, 3H), 3.63 (dd, J_1 1.9 Hz, J_2 2.0 Hz, 1H), 3.70-3.77 (m, 1H), 3.93-3.98 (m, 1H), 4.04-4.10 (m, 1H), 4.34 (t, *J* 3.9 Hz, 1H), 5.30 (d, *J* 1.5 Hz, 1H).

^{13}C NMR (CD_3OD, 50.3 MHz): δ 23.7, 61.1, 68.2, 70.2, 73.3, 74.1, 78.7, 102.8.

Elemental analysis calcd for $C_8H_{12}O_6$ C 47.06%, H 5.92%; found C 47.25%, H 5.76%.

D-laminitol (B2.D7): Hydrolysis of the orthoformate **B2.D72** (0.030 g, 0.147 mmol) as for the synthesis of **B2.7** gave D-laminitol (**B2.D7**, 0.027 g, 95%) as a white solid.

Data for B2.D7: **mp** 257-259 °C; lit.[16] mp 260 °C.

$[\alpha]_D^{27}$ = -2.94 (c 1, H_2O); lit.[89] $[\alpha]_D$= -3° (c= 1, H_2O).

^{1}H NMR (D_2O, 200 MHz): δ 1.20 (s, 3H), 3.20-3.40 (m, 1H), 3.45-3.65 (m, 3H), 3.95-4.10 (m, 1H).

Oxidation of D-2,4-di-*O*-benzyl-*myo*-inositol 1,3,5-orthoformate (B2.D68): Oxidation of **B2.D68** (0.370 g, 1.000 mmol) as for the oxidation of **B2.68** gave the ketone **B2.D69** (0.350 g, 95%) containing a small amount of the corresponding *gem* diol **B2.D70**, as a gum.

IR (neat)ν = 1765, 3175-3624 cm^{-1}.

$[\alpha]_D^{26}$ = +21.17 (c 1, $CHCl_3$).

^{1}H NMR ($CDCl_3$, 200 MHz): δ 3.76 (d, *J* 1.5 Hz, 1H), 4.30-4.38 (m, 2H), 4.38-4.46 (m, 1H), 4.46-4.65 (m, 3H), 4.69 (q, 12.7, 11.7 Hz, 2H), 5.67 (d, *J* 1.4 Hz, 1H), 7.12-7.25 (m, 2H), 7.26-7.52 (m, 8H).

^{13}C NMR ($CDCl_3$, 50.3 MHz): δ 69.6, 69.7, 70.4, 70.8, 70.9, 75.7, 75.9, 78.0, 102.1, 127.0, 127.1, 127.3, 127.6, 127.8, 135.5, 136.1, 198.5.

Elemental analysis calcd for $C_{21}H_{20}O_6$ + 0.6 H_2O C 66.52%, H 5.64%; found C 66.37%, H 5.51%.

D-2, 4-di-*O*-benzyl-6-*C*-methyl-*myo*-inositol 1,3,5-orthoformate (B2.D71): C-methylation of a mixture of the ketone **B2.69** and the *gem* diol **B2.L70** (0.100 g, 0.272 mmol) as for the synthesis of **B2.71** afforded **B2.D71** (0.092 g, 88%) as a gum.

Data for B2.D71:

IR ($CHCl_3$)ν = 3339-3545 cm^{-1}.

$[\alpha]_D^{26}$ = + 9 (c 1, $CHCl_3$).

^{1}H NMR ($CDCl_3$, 200 MHz): δ 1.56 (s, 3H), 3.86-3.96 (m, 2H), 3.96-4.02 (m, 1H), 4.18-4.28 (m, 1H), 4.33 (s, 1H, D_2O exchangeable), 4.39 (t, *J* 3.9 Hz, 1H), 4.54 (q, J_1 4.9 Hz, J_2 10.8 Hz, 2H), 4.73 (q, J_1 15.6 Hz, J_2 12.3 Hz, 2H), 5.52 (d, *J* 1.0 Hz, 1H), 7.15-7.25 (m, 2H), 7.25-7.50 (m, 8H).

^{13}C NMR ($CDCl_3$, 50.3 MHz): δ 24.2, 67.3, 69.3, 69.8, 71.4, 71.8, 72.9, 74.7, 75.9, 102.6, 128.0, 128.5, 128.7, 128.8, 135.8, 137.6.

L-laminitol orthoformate (B2.L72): Hydrogenolysis of the dibenzyl ether **B2.D71** (0.080 g, 0.208 mmol) as for the synthesis of **B2.72** afforded **B2.L72** (0.041 g, 98%) as a white solid.

Data for B2.L72: **mp** 178-180 °C.

IR (nujol)ν = 3026-3651 cm^{-1}.

$[\alpha]_D^{25}$ = + 3 (c 1, EtOH).

^{1}H NMR (CD_3OD, 200 MHz): δ 1.44 (s, 3H), 3.63 (dd, J_1 1.9 Hz, J_2 2.0 Hz, 1H), 3.70-3.77 (m, 1H), 3.93-3.98 (m, 1H), 4.04-4.10 (m, 1H), 4.34 (t, *J* 3.9 Hz, 1H), 5.30 (d, *J* 1.5 Hz, 1H).

^{13}C NMR (CD_3OD, 50.3 MHz): δ 23.7, 61.1, 68.2, 70.2, 73.3, 74.1, 78.7, 102.8.

Elemental analysis calcd for $C_8H_{12}O_6$ C 47.06%, H 5.92%; found C 47.21%, H 5.86%.

L-laminitol (B2.L7): Hydrolysis of **B2.L72** (0.030 g, 0.147 mmol) as for the synthesis of **B2.7** gave L-laminitol (**B2.L7**, 0.028 g, 98%) as a white solid.

Data for B2.L7: **mp** 258-261 °C.

$[\alpha]_D^{27^oC}$= + 3.44 (c= 1, H_2O).

^{1}H NMR (D_2O, 200 MHz): δ 1.11 (s, 3H), 3.14-3.30 (m, 1H), 3.40-3.60 (m, 3H), 3.90-4.05 (m, 1H).

Racemic 2,4-di-*O*-benzyl-6-deoxy-6-(benzylamino)-*myo*-inositol 1,3,5-orthoformate (B2.105): Racemic **B2.69** (0.250 g, 0.68 mmol) was heated with benzyl amine (0.216 g, 2.02 mmol) in dry methanol (5 mL) at 50 ºC for 3 h at the end of which TLC indicated the absence of the inososе. The reaction mixture was cooled to room temperature, sodium cyanoborohydride (0.127 g, 2.02 mmol) was added and the mixture stirred for 30 min. Methanol was evaporated under reduced pressure, the gummy residue was dissolved in dichloromethane (20 mL) and washed with saturated ammonium chloride solution (10 mL). The aqueous layer was extracted with dichloromethane (3 × 20 mL); the combined organic layer was washed with brine (5 mL) and dried over anhydrous sodium sulfate.

Sodium sulfate was filtered off and the filtrate was evaporated under reduced pressure. Purification of the residue by flash chromatography gave racemic **B2.105** (0.280 g, 90%) as a gum.

Data for B2.105:

IR (neat)ν = 3248-3441 cm^{-1}.

^{1}H NMR ($CDCl_3$, 200 MHz): δ 3.58-3.66 (m, 1H), 3.66-3.79 (m, 2H), 3.79-3.85 (m, 1H), 3.85-3.95 (br s, 1H, D_2O exchangeable), 4.16-4.41 (m, 4H), 4.41-4.58 (q, J_1 5.9 Hz, J_2 11.3 Hz, 2H), 4.59-4.75 (q, J_2 3.1 Hz, J_2 12.2 Hz, 2H), 5.49-5.54 (d, J 1.2 Hz, 1H), 7.05-7.25 (m, 5H), 7.27-7.55 (m, 10H).

^{13}C NMR ($CDCl_3$, 50.3 MHz): δ 51.8, 57.0, 66.7, 68.2, 70.1, 71.3, 71.9, 72.3, 74.8, 103.2, 127.1, 127.7, 127.9, 128.0, 128.2, 128.5, 128.6, 136.7, 137.7, 139.9.

Elemental analysis calcd for $C_{28}H_{29}O_5N$; C 73.18%, H 6.36%, N 3.05%; found C 73.19%, H 6.45%, N 3.11%.

Racemic 1,2,3,4,5-penta-*O*-acetyl-6-deoxy-6-(acetylamino)-*myo*-inositol (B2.106): Racemic **B2.105** (0.100 g, 0.29 mmol) was hydrogenolyzed (at 60 psi) in the presence of Pearlman's catalyst (20% $Pd(OH)_2$ / carbon, 0.070 g) in a mixture of methanol (2 mL) and trifluoroacetic acid (2 mL) for 8 h. The catalyst was filtered off, solvent was evaporated under reduced pressure and the gum obtained was suspended in dry pyridine (2 mL) and stirred after the addition of acetic anhydride (0.5 mL) and DMAP (0.004 g, 10 mol%) for 12 h. Pyridine was then evaporated under reduced pressure. The solid obtained after co-evaporation of the residue with toluene was worked up as usual (with chloroform) to obtain a white solid. Crystallization of this solid from a mixture of

chloroform and light petroleum (bp 60-80 ºC) gave **B2.106** (0.076 g, 81%) as white crystals.

Data for B2.106: **mp** 236-237 ºC.

IR ($CHCl_3$)ν = 1678, 1753, 3144-3458 cm^{-1}.

^{1}H NMR ($CDCl_3$, 200 MHz): δ 1.91 (s, 3H), 2.00 (s, 3H), 2.03 (s, 6H), 2.05 (s, 3H), 2.23 (s, 3H), 4.62-4.80 (q, J_1 11.7 Hz, J_2 9.8 Hz, 1H), 4.95-5.18 (m, 3H), 5.45-5.63 (m, 2H), 5.65-5.75 (d, J 9.0 Hz, 1H, D_2O excheangeable).

^{13}C NMR ($CDCl_3$, 50.3 MHz): δ 20.4, 20.5, 20.7, 23.0, 49.7, 68.3, 68.9, 69.5, 71.4, 77.2, 169.5, 169.7, 170.0, 170.3, 171.0.

Elemental analysis calcd for $C_{18}H_{25}O_{11}N$; C 50.12%, H 5.84%, N 3.25%; found C 49.51%, H 5.89%, N 2.99.

The structure of compound **B2.106** was confirmed by X-ray crystallography (see page 343).

Racemic 2,4-di-*O*-acetyl-6-deoxy-6-(acetyl amino)-*myo*-inositol 1,3,5-orthoformate:

Racemic **B2.105** (0.100 g, 0.29 mmol) was hydrogenolyzed (at 60 psi) with Pearlman's catalyst (20% $Pd(OH)_2$ / C, 0.070g) in acetic acid (3 mL), for 18 h. The catalyst was filtered off and the filtrate concentrated under reduced pressure. The gummy residue obtained was dissolved in dry pyridine (2 mL)and stirred after the addition of acetic anhydride (0.6 mL) for 12 h. Pyridine was evaporated under reduced pressure and the residue on co-evaporation with toluene gave a gum. Usual work up of this gum with dichloromethane followed by flash chromatography gave racemic 2,4-di-*O*-acetyl-6-deoxy-6-(acetyl amino)-*myo*-inositol 1,3,5-orthofromate (0.40 g, 58 %) as a white solid.

Data for racemic 2,4-di-*O*-acetyl-6-deoxy-6-(acetylamino)-*myo*-inositol 1,3,5-orthofromate :

mp 174-176 ºC.

IR ($CHCl_3$)ν = 1741, 3130-3427 cm^{-1}.

^{1}H NMR ($CDCl_3$, 200 MHz): δ 2.03 (s, 3H), 2.20 (s, 3H), 2.22 (s, 3H), 4.25-4.33 (m, 2H), 4.33-4.40 (m, 1H), 5.01 (s, 1H), 5.03-5.10 (m, 1H), 5.61 (s, 1H), 5.64-5.73 (m, 1H), 6.12-6.25 (d, *J* 8.1 Hz, 1H, D_2O exchangeable).

^{13}C NMR ($CDCl_3$, 125 MHz): δ 20.8, 21.0, 23.4, 48.3, 62.9, 67.3, 68.4, 68.8, 70.0, 103.0, 167.7, 169.4, 170.7.

Elemental analysis calcd for $C_{13}H_{17}O_5N$: C 49.52%, H 5.43%, N 4.44%; found C 49.58%, H 5.44%, N 4.12%.

D-2,4-di-*O*-benzyl-6-deoxy-6-(benzylamino)-*myo*-inositol 1,3,5-orthoformate (B2.D105): Reductive amination of **B2.D69** (0.320 g, 0.87 mmol) with benzyl amine (0.284 g, 2.65 mmol) and sodium cyanoborohydride (0.164 g, 2.61 mmol) in dry methanol (5 mL) as for the synthesis of **B2.105** gave **B2.D105** (0.356 g, 89%) as a gum.

Data for B2.D105:

$[\alpha]_D^{24.5}$ = + 4.71 (c 1, $CHCl_3$).

IR (neat)ν = 3205-3501 cm^{-1}.

^{1}H NMR ($CDCl_3$, 200 MHz): δ 3.53-3.66 (m, 1H), 3.66-3.79 (m, 2H), 3.79-3.85 (m, 1H), 3.85-3.95 (br s, 1H, D_2O exchangeable), 4.15-4.40 (m, 4H), 4.40-4.58 (q, J_1 5.9 Hz, J_2 11.4 Hz, 2H), 4.58-4.75 (q, J_2 2.7 Hz, J_2 12.5 Hz, 2H), 5.52 (s, 1H), 7.01-7.23 (m, 5H), 7.26-7.56 (m, 10H).

^{13}C NMR ($CDCl_3$, 50.3 MHz): δ 51.8, 57.0, 66.7, 68.3, 70.0, 71.3, 72.0, 72.3, 74.9, 103.2, 127.1, 127.7, 127.9, 128.0, 128.2, 128.5, 128.6, 136.8, 137.7, 140.0.

Elemental analysis calcd for $C_{28}H_{29}O_5N$ + 1.0 H_2O; C 70.42%, H 6.54%, N 2.93%; found 70.05%, H 6.15%; 3.07%.

D-1,2,3,4,5-penta-*O*-acetyl-6-deoxy-6-(acetylamino)-*myo*-inositol (B2.D106): Hydrogenolysis of **B2.D105** (0.180 g, 0.39 mmol) with Pearlman's catalyst (20% $Pd(OH)_2$ over C, 0.137 g) in a mixture of methanol (2 mL) and trifluoroacetic acid (2 mL) followed by acetylation of the reaction mixture with acetic anhydride (1.1 mL) and DMAP (0.014 g) in dry pyridine (4 mL) as for the synthesis of **B2.105** gave **B2.D106** (0.090 g, 81%) as white crystals.

Data for B2.D106: **mp** 232-235 ºC.

$[\alpha]_D^{28.1}$ = + 6 (c 1, $CHCl_3$).

IR ($CHCl_3$)ν = 1680, 1753, 3248-3533 cm^{-1}.

^{1}H NMR ($CDCl_3$, 200 MHz): δ 1.90 (s, 3H), 1.98 (s, 3H), 2.01 (s, 6H), 2.04 (s, 3H), 2.21 (s, 3H), 4.62-4.81 (q, J_1 10.6 Hz, J_2 10.5 Hz, 1H), 4.95-5.16 (m, 3H), 5.46-5.67 (m, 2H), 5.81-5.94 (d, J 10.2 Hz, 1H, D_2O excheangeable).

^{13}C NMR ($CDCl_3$, 50.5 MHz): δ 20.4, 20.5, 20.7, 23.0, 49.7, 68.3, 68.9, 69.5, 71.4, 77.2, 169.5, 169.7, 170.0, 170.3, 171.0.

Elemental analysis calcd for $C_{18}H_{25}O_{11}N$; C 50.12%, H 5.84%, N 3.25%; found C 49.45%, H 6.11%, N 3.19.

L-2,4-di-*O*-benzyl-6-deoxy-6-(benzylamino)-*myo*-inositol 1,3,5-orthoformate (B2.L105): Reductive amination of **B2.L69** (0.270 g, 0.73 mmol) with benzylamine

(0.235 g, 2.19 mmol) and sodium cyanoborohydride (0.138 g, 2.19 mmol) in dry methanol (5 mL) as for the synthesis of **B2.105** gave **B2.L105** (0.300 g, 89%) as a gum.

Data for B2.L105:

$[\alpha]_D^{24.8}$ = - 4.95 (c 1, $CHCl_3$).

IR (neat)ν = 3207-3447 cm^{-1}.

^{1}H NMR ($CDCl_3$, 200 MHz): δ 3.56-3.66 (m, 1H), 3.66-3.79 (m, 2H), 3.79-3.85 (m, 1H), 3.85-3.95 (br s, 1H, D_2O exchangeable), 4.15-4.41 (m, 4H), 4.41-4.59 (q, J_1 5.9 Hz, J_2 11.7 Hz, 2H), 4.59-4.75 (q, J_2 3.1 Hz, J_2 12.1 Hz, 2H), 5.48-5.55 (d, J 1.2 Hz, 1H), 7.02-7.24 (m, 5H), 7.26-7.57 (m, 10H).

^{13}C NMR ($CDCl_3$, 50.3 MHz): δ 51.8, 57.0, 66.8, 68.3, 70.1, 71.3, 72.0, 72.3, 74.9, 103.2, 127.1, 127.7, 127.9, 128.0, 128.2, 128.5, 128.6, 136.8, 137.7, 140.0.

Elemental analysis calcd for $C_{28}H_{29}O_5N$ + 0.5 H_2O; C 71.78%, H 6.45%, N 2.99%; found C 72.00%, H 6.16%, N 3.06.

L-1,2,3,4,5-penta-*O*-acetyl-6-deoxy-6-(acetylamino)-*myo*-inositol (B2.L106): Hydrogenolysis of **B2.L105** (0.131 g, 0.29 mmol) with Pearlman's catalyst (20% $Pd(OH)_2$ over C, 0.100 g) in a mixture of methanol (2 mL) and trifluoroacetic acid (2 mL) followed by acetylation of the reaction mixture with acetic anhydride (0.9 mL) and DMAP (0.009 g) in dry pyridine (3 mL) gave **B2.L106** (0.139 g, 82%) as white crystals.

Data for B2.L106: **mp** 232-234 ºC.

$[\alpha]_D^{28.3}$ = - 6 (c 1, $CHCl_3$).

IR ($CHCl_3$)ν = 1680, 1753, 3247-3452 cm^{-1}.

^{1}H NMR ($CDCl_3$, 200 MHz): δ 1.90 (s, 3H), 1.97 (s, 3H), 2.00 (s, 6H), 2.04 (s, 3H), 2.20 (s, 3H), 4.62-4.81 (q, J_1 10.2 Hz, J_2 11.2 Hz, 1H), 4.92-5.22 (m, 3H), 5.43-5.68 (m, 2H), 5.93-6.22 (d, *J* 13.6 Hz, 1H, D_2O excheangeable).

^{13}C NMR ($CDCl_3$, 50.3 MHz): δ 20.4, 20.5, 20.7, 23.0, 49.7, 68.3, 68.9, 69.5, 71.4, 77.2, 169.5, 169.7, 170.0, 170.3, 171.0.

Elemental analysis calcd for $C_{18}H_{25}O_{11}N$; C 50.12%, H 5.84%, N 3.25%; found C 50.26%, H 5.67%, N 3.18%.

Attempted oxidation of 4,6-di-*O*-tosyl-*myo*-inositol 1,3,5-orthoformate (B2.152) with DMSO-acetic anhydride mixture (B2.152): A mixture of acetic anhydride (2.5 mL) and DMSO (5 mL) was stirred at ambient temperature under nitrogen atmosphere for 30 min. The ditosyalte **B2.152** (0.498 g, 1.00 mmol) was added to this solution and the reaction continued for 7 d. The reaction mixture was then diluted with ethyl acetate (10 mL), washed with saturated bicarbonate solution (5 mL) and water (5 mL) and worked up as usual to obtain a gum. Column chromatographic purification of the gum obtained gave **B2.153** (0.932 g, 35%), starting material, **B2.152** (0.215 g, 43%) and some other minor unidentified products.

Data for B2.153:

^{1}H NMR ($CDCl_3$, 200 MHz): δ 2.13 (s, 3H), 2.47 (s, 6H), 4.06-4.12 (m, 1H), 4.13-4.21 (m. 1H), 4.22-4.34 (m, 2H), 4.67 (s, 2H), 5.10-5.20 (t, *J* 3.9 Hz, 2H), 5.44-5.46 (d, *J* 1.5 Hz, 1H), 7.35-7.45 (d, *J* 8.3 Hz, 4H), 7.80-7.90 (d, *J* 8.3 Hz, 4H).

^{13}C NMR ($CDCl_3$, 50.3 MHz): δ 14.0, 21.7, 64.1, 67.2, 69.5, 71.7, 74.5, 102.6, 128.0, 130.2, 132.6, 145.8.

Oxidation of 4,6-di-*O*-tosyl-*myo*-inositol 1,3,5-orthoformate (B2.152): Oxidation of the ditosylate **B2.152** (1.500 g, 3.01 mmol) using oxalyl chloride (0.419 g, 3.30 mmol), dry dimethyl sulfoxide (0.473g, 6.05 mmol) and dry triethylamine (1.525 g, 15.07 mmol) in dry dichloromethane (25 mL) as for the oxidation of **B2.30** (method A) gave a mixture of the ketone **B2.154** (1.490 g, 100%) with small amount of the corresponding *gem* diol **B2.155** as a white solid.

Data for B2.154+**B2.155**: **mp** 142-144 ^{o}C;

IR ($CHCl_3$)ν = 1774 cm^{-1}.

^{1}H NMR ($CDCl_3$, 200 MHz): δ 2.47 (s, 6 H), 4.25-4.35 (m, 2 H), 4.50-4.60 (m, 1 H), 5.35-5.50 (m, 2 H), 5.64 (s, 1 H), 7.30-7.45 (d, 4 H, *J* 8 Hz), 7.80-7.95 (d, 4 H, *J* 8 Hz).

^{13}C NMR ($CDCl_3$, 50.3 MHz): δ 21.5, 67.7, 71.5, 72.5, 73.4, 76.3, 102.0, 127.8, 130.0, 132.0, 145.8, 195.0.

Elemental analysis calcd for $C_{21}H_{20}O_{10}S_2$; C 50.80%, H 4.06%; found C 50.76%, H 4.11%.

The structure of compound **B2.154** was confirmed by X-ray crystallography (see page 357 and 358).

2,4-di-*O*-tosyl-*scyllo*-inositol 1,3,5-orthoformate (B2.156): The crude ketone, **B2.154** (1.990 g, 4.01 mmol) was dissolved in a mixture of dry THF (10 mL) and dry methanol (40 mL) and reduced with sodium borhydride (0.452 g, 11.90 mmol) at room temperature for 30 min. Solvents were evaporated under reduced pressure and the residue was worked up as usual (with dichloromethane) to obtain the ditosylate **B2.156** (1.980 g, 99%) as a white solid.

Data for B2.156: **mp** 150-151 ^{o}C.

IR ($CHCl_3$)ν = 3394 cm^{-1}.

^{1}H NMR ($CDCl_3$, 200 MHz): δ 2.48 (s, 6H), 2.75-2.85 (d, 1H, *J* 12 Hz, D_2O exchangeable), 4.20-4.40 (m, 4H), 5.10-5.20 (m, 2H), 5.42 (s, 1H), 7.35-7.45 (d, 4H, *J* 9 Hz), 7.80-7.90 (d, 4H, *J* 9 Hz).

^{13}C NMR ($CDCl_3$, 50.3 MHz): δ 21.6, 65.7, 67.4, 68.7, 70.8, 101.9, 128.0, 130.1, 132.1, 145.9.

Elemental analysis calcd for $C_{21}H_{22}O_{10}S_2$; C 50.60%, H 4.45%; found C 50.48%, H 4.12%.

The structure of compound **B2.156** was confirmed by X-ray crystallography (see page 361).

2,4,6-tri-*O*-acetyl-*scyllo*-inositol 1,3,5-orthoformate (B2.157): The ditosylate **B2.156** (0.5 g, 1.00 mmol) was refluxed with NaOMe (0.324 g, 6.00 mmol) in dry methanol (10 mL) for 12 h. The solvents were evaporated and the solid obtained was treated with acetic anhydride (12 mL) in pyridine (20mL) at room temperature for 24 h. Evaporation of the solvents under reduced pressure followed by usual work-up with chloroform gave the triacetate **B2.157** (0.316 g, 100%) as a white solid.

Data for B2.157: **mp** 124-126 °C; lit.[50] mp 124-126 °C.

***scyllo*-Inositol 1,3,5 orthoformate (B2.149):** The triacetate **B2.157** (0.316 g, 1.00 mmol) was treated with isobutyl amine (1 mL) in methanol (3 mL) under reflux for 12 h. The solvents were evaporated and the gum obtained was washed with dichloromethane - light petroleum mixture (1:3) several times to obtain the triol **B2.149** (0.175g, 92%) as a white solid.

Data for B2.149: **mp** 322-326° C; lit.[50] mp 330° C (sealed tube).

^{1}H NMR (200 MHz, D_2O): δ 4.40-4.42 (m, 3 H), 4.49-4.51 (m, 3H), and 5.62 (s, 1H).[50]

***scyllo*-Inositol (B2.10):** Acid hydrolysis of the triol **B2.149** (0.100 g, 0.5 mmol) with trifluoroacetic acid (0.75 mL) and distilled water (0.25 mL) as for the synthesis of **B2.D1** gave *scyllo*-inositol (**B2.10**, 0.094 g, 100%) as a white solid.

Data for B2.10:

^{1}H NMR (200 MHz, D_2O): δ 3.25 (s).

2-*O*-methyl-4,6-di-*O*-tosyl-*scyllo*-inositol 1,3,5-orthoformate (B2.158): To a solution of the ditosylate **B2.156** (0.662 g, 1.329 mmol) in dry DMF (4 mL) was added methyl iodide (0.568 g, 4.002 mmol) and the mixture stirred for 5 min. Sodium hydride (0.041 g, 1.708 mmol) was added and stirring continued for additional 5 min. The reaction was quenched by the addition of ice. Evaporation of DMF under reduced pressure followed by work up with dichloromethane by usual procedure gave **B2.158** (0.627 g, 92%) as a white solid.

Data for B2.158: **mp** 149-150 ^oC.

^{1}H NMR ($CDCl_3$, 300 MHz): δ 2.46 (s, 6H), 3.35 (s, 3H), 4.03-4.11 (m, 1H), 4.15-4.24 (m, 1H), 4.43-4.52 (m, 2H), 5.06-5.24 (m, 2H), 5.45 (s, 1H), 7.37 (d, *J* 8.8 Hz, 4H), 7.85 (d, *J* 8.3 Hz, 4H).

^{13}C NMR ($CDCl_3$, 75 MHz): δ 21.5, 56.9, 67.2, 67.6, 69.6, 72.9, 102.4, 127.7, 129.8, 133.0, 145.0.

Elemental analysis calcd for $C_{22}H_{24}O_{10}S_2$; C 51.55%, H 4.72%; found C 51.78%, H 4.88%.

2-*O*-methyl-*scyllo*-inositol 1,3,5-orthoformate (B2.159): Sodium methoxide (0.475 g, 8.796 mmol) and the methyl ether **B2.158** (0.461 g, 0.900 mmol) were dissolved in dry

methanol (5 mL) and refluxed for 8 h. Evaporation of the solvent and purification of the product by flash chromatography gave the diol **B2.159** (0.172 g, 94%) as a white solid.

Data for B2.159: **mp** 128-129 ^{o}C.

IR ($CHCl_3$)ν = 3332-3469 cm^{-1}.

^{1}H NMR (D_2O, 300 MHz): δ 3.47 (s, 3H), 4.22-4.27 (m, 1H), 4.33-4.40 (m, 1H), 4.44-4.50 (m, 2H), 4.53-4.59 (m, 2H), 5.64 (s, 1H).

^{13}C NMR (D_2O, 125 MHz): δ 57.1, 65.6, 68.4, 69.9, 74.2, 101.3.

Elemental analysis calcd for $C_8H_{12}O_6$; C 47.06%, H 5.92%; found C 47.18%, H 6.23%. The structure of compound **B2.159** was confirmed by X-ray crystallography (see page 366).

***scyllo*-Inositol methyl ether (B2.4)):** The orthoformate **B2.159** (0.050 g, 0.245 mmol) was stirred with a mixture of trifluoroacetic acid (0.4 mL) and distilled water (0.1 mL) for 1h. Evaporation of solvents under reduced pressure followed by co-evaporation with toluene gave **B2.4** (0.047 g, 96%) as a white solid.

Data for B2.4: **mp** 248-249 ^{o}C, lit.[13] mp 243 ^{o}C.

IR (Nujol)ν = 3032-3630 cm^{-1}.

^{1}H NMR (D_2O, 200 MHz): δ 2.95-3.20 (m, 2H), 3.20-3.50 (m, 4H), 3.85 (s, 3H).

^{13}C NMR (D_2O, 50.3 MHz): δ 21.9, 34.9, 35.5, 45.4.

Elemental analysis calcd for $C_7H_{14}O_6$; C 43.30%, H 7.27%; found C 43.39%, H 7.26%.

2-*C*-methyl-4,6-di-*O*-tosyl-*scyllo*-inositol 1,3,5-orthoformate (B2.162): The ketone **B2.154** (0.750 g, 1.512 mmol) was allowed to react with a freshly prepared diethylether solution of methylmagnesium iodide (1M, 5.3 mL) in a mixture of dry diethylether (9

mL) and dry THF (3 mL) for 6 h as for the synthesis of **B2.71** to obtain **B2.162** (0.572 g, 74%) as a white solid.

Data for B2.162: **mp** 152-153 °C.

IR ($CHCl_3$)ν = 3078-3730 cm $^{-1}$.

^{1}H NMR ($CDCl_3$, 200 MHz): δ 1.46 (s, 3H), 2.48 (s, 6H), 3.22 (s, D_2O exchangeable, 1H), 3.80-3.95 (m, 2H), 4.25-4.35 (m, 1H), 5.17 (t, *J* 3.9 Hz, 2H), 5.39 (s, 1H), 7.40 (d, *J* 7.8 Hz, 4H), 7.85 (d, *J* 8.8 Hz, 4H).

^{13}C NMR ($CDCl_3$, 50.3 MHz): δ 21.5, 24.6, 67.2, 71.9, 72.7, 101.8, 128.0, 130.1, 132.4, 145.8.

Elemental analysis calcd for $C_{22}H_{24}O_{10}S_2$; C 51.55%, H 4.72%; found C 51.94%, H 4.85%.

2-*C*-methyl-4,6-di-*O*-acetyl-*scyllo*-inositol 1,3,5-orthoformate (B2.163): The ditosylate **B2.162** (0.400 g, 0.781 mmol) was suspended in dry methanol (5 mL) containing sodium methoxide (0.421 g, 7.796 mmol) and refluxed for 9 h. The reaction mixture was quenched with a few drops of 2% hydrochloric acid solution (to pH 5) and the solvent was evaporated under reduced pressure to obtain a solid. The solid obtained was suspended in dry pyridine (5 mL) containing acetic anhydride (3 mL) and the mixture was stirred at room temperature for 24 h. Usual work-up with dichloromethane followed by column chromatography gave the diacetate **B2.163** (0.217 g, 96 %) as a white solid.

Data for B2.163: **mp** 130-132 °C.

IR ($CHCl_3$)ν = 1745, 3560 cm $^{-1}$.

^{1}H NMR ($CDCl_3$, 200 MHz): δ 1.56 (s, 3H), 2.13 (s, 6H), 3.59 (d, *J* 0.9 Hz, 1H, D_2O exchangeable), 4.04-4.10 (m, 2H), 4.45-4.53 (m, 1H), 5.53 (s, 1H), 5.60 (t, *J* 4.0 Hz, 2H).

^{13}C NMR ($CDCl_3$, 50.3 MHz): δ 20.7, 24.6, 66.1, 67.8, 68.0, 72.4, 102.3, 168.3.

Elemental analysis calcd for $C_{12}H_{16}O_8$; C 50.00%, H 5.60%; found C, 50.15%, H, 5.44%.

The structure of compound **B2.163** was confirmed by X-ray crystallography (see page 373).

Mytilitol orthoformate (B2.164): Isobutylamine (2 mL) and **B2.163** (0.150 g, 0.521 mmol) were dissolved in methanol (5 mL) and refluxed for 6 h. The solvents were evaporated under reduced pressure to obtain a gum. The gum obtained was washed with hot light petroleum (60-80° C) several times followed by dichloromethane to obtain **B2.164** (0.101 g, 94%) as a white solid.

Data for B2.164: **mp** 199-201 °C.

IR (Nujol)ν = 3051-3524 cm $^{-1}$.

^{1}H NMR (CD_3OD, 200 MHz): δ 1.34 (s, 3H), 3.72 (q, J_1 2.5 Hz, J_2 1.9 Hz, 2H), 4.00-4.10 (m, 1H), 4.30 (t, *J* 3.9 Hz, 2H), 5.24 (s, 1H).

^{13}C NMR (CD_3OD, 50.3 MHz): δ 25.0, 68.4, 71.7, 75.4, 102.3.

Elemental analysis calcd for $C_8H_{12}O_6$; C 47.06%, H 5.92%; found C 47.52%, H 5.72%.

The structure of compound **B2.164** was confirmed by X-ray crystallography (see page 376).

Mytilitol (B2.8): The orthoformate **B2.164** (0.090 g, 0.441 mmol) was stirred with trifluoroacetic acid (1.6 mL) and distilled water (0.4 mL) for 1 h. Evaporation of the solvent followed by co-evaporation with toluene gave mytilitol (**B2.8**, 0.085 g, 100%) as a white solid.

Data for B2.8: **mp** 264-268 °C.

^{1}H NMR (D_2O, 200 MHz): δ 0.97 (s, 3H), 3.23 (s, 5H).

Mytilitol hexaacetate (B2.165): Mytilitol (**B2.8**, 0.030 g, 0.155 mmol), was stirred with acetic anhydride (0.5 mL) and DMAP (0.005 g) in dry pyridine (1 mL) at room temperature for 24 h. Evaporation of the solvents under reduced pressure followed by usual work-up with dichloromethane gave a gum. Purification of this gum by column chromatography gave the known hexaacetate **B2.165** (0.065g, 93%) as a white solid.

Data for B2.165: **mp** 179-180 °C; lit.[90] mp 181 °C.

Racemic 2,4-di-*O*-benzyl-*epi*-inosose (B2.218): Racemic **B2.69** (0.280 g, 0.76 mmol) was stirred with trifluoroacetic acid (0.8 mL) and water (0.2 mL) for 3 h. Evaporation of the solvent under reduced pressure followed by co-evaporation with toluene gave racemic ketone **B2.218** (0.256 g, 94%) as a colorless gum. The colorless gum turned red on storage for few hours and hence it appeared to be unstable.

Data for B2.218:

IR ($CHCl_3$)ν = 1736, 3120-3670 cm^{-1}.

^{1}H NMR ($CDCl_3$, 200 MHz): δ 2.35-2.65 (br s, 1H, D_2O exchangeable), 3.15-3.40 (br s, 1H, D_2O exchangeable), 3.40-3.60 (br s, 1H, D_2O exchangeable), 3.70-3.84 (t, *J* 9.3 Hz, 1H), 3.90-4.04 (dd, J_1 7.8 Hz, J_2 2.0 Hz, 1H), 4.17-4.27 (t, *J* 3.3 Hz, 1H), 4.27-4.45 (m, 2H), 4.65-4.90 (m, 3H), 5.03-5.15 (d, *J* 11.3 Hz, 1H), 7.10-7.28 (m, 3H), 7.28-7.50 (m, 7H).

^{13}C NMR ($CDCl_3$, 50.3 MHz): δ 70.8, 74.6, 75.1, 76.2, 80.0, 83.5, 127.3, 127.4, 127.7, 128.0, 128.1, 128.2, 137.8, 206.1.

Elemental analysis calcd for $C_{20}H_{22}O_6$; C 67.03%, H 6.19%; found C 66.30%, H 7.23% (this compound decomposes on storing for few hours).

Benzoylation of racemic 2,4-di-*O*-benzyl-*epi*-inosose (B2.218): The *epi*-inosose, **B2.218** (0.400 g, 1.09 mmol) was treated with benzoyl chloride (2.301 g, 16.38 mmol) in pyridine (5 mL) at ambient temperature for 24 h. TLC analysis showed the formation of several products. Evaporation of pyridine followed by usual work up with dichloromethane gave a gum containing a mixture of several products (by TLC). Crystallization from a mixture of dichloromethane and light petroleum (bp 60-80 °C), yielded racemic 1,2,3,5-tetra-*O*-benzoyl-4,6-di-*O*-benzyl-cyclohexene hexol, **B2.219** (0.200 g, 23%).

Data for B2.219: **mp** 181-182 °C.

IR ($CHCl_3$)ν = 1714, 1744 cm^{-1}.

^{1}H NMR ($CDCl_3$, 200 MHz): δ 4.55-4.65 (dd, J_1 2.9 Hz, J_2 2.0 Hz, 1H), 4.60-4.85 (m, 5 H), 5.73-5.83 (t, *J* 3.1 Hz, 1H), 6.54-6.60 (d, *J* 4.7 Hz, 1H), 6.98-7.13 (m, 3H), 7.13-7.19 (m, 3H), 7.19-7.23 (m, 2H), 7.23-7.28 (m, 3H), 7.28-7.33 (m, 2H), 7.33-7.40 (m, 4H), 7.40-7.48 (m, 3H), 7.48-7.65 (m, 3H), 7.82-7.92 (m, 3H), 7.92-8.00 (m, 2H), 8.17-8.23 (d, *J* 7.4 Hz, 2H).

^{13}C NMR ($CDCl_3$, 50.3 MHz): δ 66.1, 70.8, 71.8, 72.3, 72.7, 73.7, 127.8, 128.4, 130.1, 130.2, 133.0, 133.1, 133.6, 133.9, 137.1, 137.4, 138.8, 163.1, 163.3, 166.3.

Elemental analysis calcd for $C_{44}H_{38}O_6$; C 74.41%, H 4.94%; found C 74.18%, H 5.13%.

The structure of compound **B2.219** was confirmed by X-ray crystallography (page 382).

Racemic 2,4-di-*O*-tosyl-*epi*-inososse 1,3,5-orthoformate-dimethyl ketal (B2.220): The racemic ketone-*gem* diol mixture, **B2.64** + **B2.65** (0.400 g, 0.78 mmol) was treated with methyl iodide (0.332 g, 2.34 mmol) and sodium hydride (0.041g, 1.71 mmol) in dry DMF (5 mL) at room temperature for 5 minutes. The reaction was quenched with pieces of ice, the solvents evaporated under reduced pressure to obtain a solid. Usual work-up (with dichloromethane) of the solid obtained followed by purification by column chromatography gave the racemic dimethyl ketal **B2.220** (0.320 g, 76%) as a white solid.

Data for B2.220: **mp** 160-162 °C.

^{1}H NMR ($CDCl_3$, 200 MHz): δ 2.47 (s, 3H), 2.48 (s, 3H), 3.23 (s, 3H), 3.28 (s, 3H), 3.88-3.94 (m, 1H), 4.17-4.23 (m, 1H), 4.23-4.29 (m, 1H), 4.85-4.89 (m, 1H), 4.96-5.00 (t, *J* 4.0 Hz, 1H), 5.46 (s, 1H), 7.35-7.42 (q, J_1 3.6 Hz, J_2 4.2 Hz, 4H), 7.75-7.79 (d, *J* 8.3 Hz, 2H), 7.81-7.86 (d, *J* 8.3 Hz, 2H).

^{13}C NMR ($CDCl_3$, 50.3 MHz): δ 21.7, 48.1, 48.7, 69.1, 69.7, 69.9, 71.1, 93.8, 102.6, 127.9, 130.0, 130.3, 132.1, 133.2, 145.4, 146.0.

Elemental analysis calcd for $C_{23}H_{26}O_{11}S_2$; C 50.91%, H 4.84%; found C 51.12%, H 5.18%.

The structure of compound **B2.220** was confirmed by X-ray crystallography (see page 385).

Racemic *epi*-inososse 1,3,5-orthoformate-dimethyl ketal (B2.221): The racemic dimethyl ketal, **B2.220** (0.240 g, 0.44 mmol) was refluxed with sodium methoxide (0.238 g, 4.4 mmol) in dry methanol for 12 h. The reaction was quenched with pieces of ice, methanol was evaporated under reduced pressure and the residue was purified by flash chromatography to obtain the dimethyl ketal **B2.221** (0.077 g, 75 %) as a white solid.

Data for B2.221: **mp** 155-156 °C.

IR (Nujol)ν = 3209-3533 cm^{-1}.

^{1}H NMR ($CDCl_3$, 200 MHz): δ 3.25-3.35 (br s, 1H), 3.37 (s, 3H), 3.45 (s, 3H), 3.54-3.66 (d, *J* 10.6 Hz, 1H, D_2O exchangeable), 3.83-3.94 (m, 1H), 4.14-4.23 (m, 2H), 4.26-4.34 (m, 1H), 4.42-4.55 (m, 1H), 5.51 (d, *J* 1.3 Hz, 1H).

^{13}C NMR ($CDCl_3$, 50.3 MHz): δ 48.4, 49.0, 62.3, 66.1, 67.6, 73.7, 74.2, 95.9, 102.8.

Elemental analysis calcd for $C_9H_{14}O_7$; C 46.16%, H 6.03%; found C 46.19%, H 5.77%.

Racemic *epi*-inososе (B2.222): The dimethyl ketal **B2.221** (0.40 g, 0.17 mmol) was stirred with a mixture of trifluoroacetic acid (0.8 mL) and water (0.2 mL) at room temperature for 2 h. Evaporation of the solvents under reduced pressure followed by co-evaporation of the residue with toluene gave *epi*-inososе (**B2.222**, 0.030g, 99%) as a white solid.

Data for B2.222: **mp** 182-185 °C.

IR (Nujol)ν = 1726, 3078-3622 cm^{-1}.

^{1}H NMR (D_2O, 200 MHz): δ 3.66-3.81 (t, *J* 9.8 Hz, 1H), 3.95-4.05 (dd, J_1 7.5 Hz, J_2 2.3 Hz, 1H), 4.24-4.29 (t, *J* 3.5 Hz, 1H), 4.29-4.34 (d, *J* 1.6 Hz, 1H), 4.58-4.65 (dd, J_1 1.5 Hz, J_2 1.6 Hz, 1H).

B2.7. **References**

1. Sureshan, K. M.; Shashidhar, M. S.; Praveen, T.; Das, T. *Chem. Rev.*, **2003,** *103,* 4477.
2. *The Inositol Phosphates. Chemical Synthesis and Biological Significance*, Billington, D. C. VCH, New York, N.Y. 1993.
3. *Phosphoinositides: Chemistry, Biochemistry and Biomedical Applications*, Bruzik, K. S. Ed.; ACS Symposium Series 718. American Chemical Society, Washington D. C. USA, 1999.
4. Dalko, P. I.; Sinay, P. *Organic Synthesis Highlights V*, *1-14*. Edited by: Schmalz, H-G.; Wirth, T. Wiley-VCH Verlag GmbH & Co. KGaA: Weinheim, Germany. 2003.
5. Schedler, D. J. A.; Baker, D. C. *Carbohydr*. *Res*., **2004**, *339*, 1585.
6. Suzuki, T.; Suzuki, S. T.; Yamada, I.; Koashi, Y.; Yamada, K.; Chida, N. *J. Org. Chem.*, **2002**, *67,* 2874
7. Chida, N.; Ogawa, S. *Chem. Commun.*, **1997**, 807.
8. Sculimbrene, B. R.; Morgan, A. J.; Miller, S. J. *Chem. Commun*., **2003**, 1781
9. Shashidhar, M. S. *ARKIVOC*, **2002**, (VII), 63 and references cited therein.
10. Ford, C. W. *Phytochem*., **1982**, *21*, 1149.
11. Ford, C. W. *Phytochem*., **1984**, *23*, 1007.
12. Peterbauer, T.; Brereton, I.; Richter, A. *Carbohydr*. *Res*., **2003**, *338*, 2017 and references cited therein.
13. Ueno, Y.; Hasegawa, A.; Tsuchiya, T. *Carbohydr, Res.*, **1973**, *29*, 520.
14. Obendorf, R. L. *Seed Sci*. *Res*., **1997**, *7*, 63.

15. Lindberg, B.; Mcpherson, J. *Acta Chem*. *Scand*., **1954**, *8*, 1875.

16. Percival, E.; Young, M. *Carbohydr*. *Res*., **1974**, *32*, 195.

17. Wöber, G.; Hoffmann-Ostenhof, O. *Eur*. *J*. *Biochem*., **1970**, *17*, 393.

18. Narasimhan, B.; PliskaMatyshak, G.; Kinnard, R.; Carstensen, S.; Ritter, M. A.; vonWeymarn, L.; Murthi, P. P. N. *Plant Physiol*., **1997**, *113*, 1385.

19. Ichimura, K.; Kohata, K.; Yamaguchi, Y.; Douzono, M.; Ikeda, H.; Koketsu, M. *Biosci*. *Biotechnol*. *Biochem*., **2000**, *64*, 865.

20. Shapiro, J.; Belmaker, R. H.; Biegon, A.; Seker, A.; Agam, G. *J*. *Neural*. *Transm*., **2000**, *107*, 603.

21. McLaurin, J.; Golomb, R.; Jurewicz, A.; Antel, J. P.; Fraser, P. E. *J*. *Biol*. *Chem*., **2000**, *275*, 18495.

22. Lien, Y. H. H.; Michaelis, T.; Moats, R. A.; Ross, B. D. *Life Sci*., **1994**, *54*, 1507.

23. Strieleman, P. J.; Metzger, B. E. *Teratology*, **1993**, *48*, 267.

24. Chung, S-K.; Kown, Y. U. *Bioorg*. *Med*. *Chem*. *Lett*., **1999**, *9*, 2135.

25. Kwon, Y-U.; Lee, C.; Chung, S-K. *J. Org. Chem.*, **2002**, *67*, 3327.

26. Posternak, T. *Helv. Chim. Acta*, **1941**, *24*, 1045.

27. Posternak, T. *Chem*. *Abstr*., **1942**, *36*, 2256[8].

28. Husson, C.; Odier, L.; Vottéro, Ph. J. A. *Carbohydr. Res.*, **1998**, *307*, 163.

29. Tagliaferri, F.; Wang, S-N.; Berlin, W. K.; Outten, R. A.; Shen, T. Y. *Tetrahedron Lett*., **1990**, *31*,1105.

30. Gigg, J.; Gigg, R. *Carbohydr*. *Res*., **1997**, *299*,77.

31. Watanabe, Y.; Mitani, M.; Ozaki, S. *Chem*. *Lett*., **1987**, 123.

32. Chung, S-K.; Yu, S-H. *Bioorg*. *Med*. *Chem*. *Lett*., **1996**, *6*, 1461.

33. Takahashi, H.; Kittaka, H.; Ikegami, S. *Tetrahedron Lett*., **1998**, *39*, 9707.

34. Takahashi, H.; Kittaka, H.; Ikegami, S. *J. Org. Chem*., **2001**, *66*, 2705.

35. Carless, H. A. J.; Busia, K. *Tetrahedron Lett*., **1990**, *31*, 1617.

36. Motherwell, W. B.; Williams, A. S. *Angew. Chem. Int. Ed. Engl*., **1995**, *34*, 2031.

37. Brammer, L. E. Jr.; Hudlicky, T. *Tetrahedron Asymmetry*, **1998**, *9*, 2011.

38. Desjardins, M.; Brammer, L. E. Jr.; Hudlicky, T. *Carbohydr*. *Res*., **1997**, *304*, 39.

39. Hudlicky, T.; Mandel, M.; Rouden, J.; Lee, R. S.; Bachmann, B.; Dudding, T.; Yost, K. J.; Merola, J. S. *J. Chem*. *Soc*., *Perkin Trans*. *1*, **1994**, 1553.

40. *J. Chem*. *Soc*., *Perkin Trans*. *1*, **1993**, 741.

41. Anderson, R. C.; Wallis, E. S. *J. Am*. *Chem*. *Soc*., **1948**, *70*, 2931.

42. Kowarski, C. R.; Sarel, S. *J. Org*. *Chem*., **1973**, *38*, 117.

43. Kim, S. K.; Park, J. I.; Moon, H. K.; Yi, H. *Chem*. *Commun*., **1998**, 1945.

44. Angyal, S. J.; Odier, L.; Tate, M. E. *Carbohydr*. *Res*., **1995**, *266*, 143.

45. Podeschwa, M.; Plettenburg, O.; Brocke, J. v.; Block, O.; Adelt, S.; Altenbach, H-J. *Eur*. *J. Org*. *Chem*., **2003**, 1958.

46. Heo, J-N.; Holson, E. B.; Roush, W. R. *Org*. *Lett*., **2003**, *5*, 1697.

47. Lee, Y. J.; Lee, K.; Jung, S. I.; Jeon, H. B.; Kim, K. S. *Tetrahedron*, **2005**, *61*, 1987.

48. Roemer, S.; Stadler, C.; Rudolf, M. T.; Jastorff, B.; Schultz, C. *J. Chem. Soc. Perkin Trans 1*, **1996**, 1683.

49. Lampe, D.; Liu, C.; Mahon, M. F.; Potter, B. V. L. *J. Chem. Soc. Perkin Trans 1*, **1996**, 1717.

50. Lee, H. W.; Kishi, Y. *J. Org. Chem.*, **1985**, *50*, 4402.

51. Shaldubina, A.; Ju, S.; Vaden, D. L.; Ding, D.; Belmaker, R. H.; Greenberg, M. L. *Molecular Psychiatry*, **2002**, *7*, 174.

52. Williams, R. S.; Cheng, L.; Mudge, A. W.; Harwood, A. J. *Nature*, **2002**, *417*, 292.

53. Einat, H.; Shaldubina, A.; Belmaker, R. H. *Drug Develop*. *Res*. **2000**, *50*, 309-315.

54. Einat, H.; Elkabaz-Shwortz, Z.; Cohen, H.; Kofman, O.; Belmaker, R. H. *Int*. *J*. *Neuropsychopharmacology* **1998**, *1*, 31.

55. Belmaker, R. H.; Agam, G.; van Calker, D.; Richards, M. H.; Kofman, O. *Neuropsychopharmacology*, **1998**, *19*, 220.

56. Ryan, M.; Smith, M. P.; Vinod, T. K.; Lau, W. L.; Keana, J. F. W.; Griffith, O. H. *J*. *Med*. *Chem*., **1996**, *39*, 4366.

57. Pistará, V.; Barili, P. L.; Catelani, G.; Corsaro, A.; D'Andrea, F.; Fisichella, S. *Tetrahedron Lett*., **2000**, *41*, 3253.

58. Vitelio, C.; Bellomo, A.; Brovetto, M.; Seoane, G.; Gonzalez, D. *Carbohydr*. *Res*., **2004**, *339*, 1773.

59. Ballereau, S.; Guédat, P.; Poirier, S. N.; Guillemette, G.; Spiess, B.; Schlewer, G. *J*. *Med*. *Chem*., **1999**, *42*, 4824.

60. Legler, G. *Adv*. *Carbohydr*. *Chem*. *Biochem*., **1990**, *48*, 319.

61. Kozikowski, A. P.; Fauq, H.; Powis, G. *Curr*. *Med*. *Chem*., **1994**, *1*, 1.

62. Sanfilippo, C.; Patti, A.; Piattelli, M.; Nicolosi, G. *Tetrahedron Asymm*., **1998**, *9*, 2809.

63. Sureshan, K. M.; Ikeda, K.; Asano, N.; Watanabe, Y. *Tetrahedron Lett*., **2004**, *45*, 8367.

64. Beier, B.; Schuerrle K.; Werbitzky, O.; Piepersberg, W. *J. Chem. Soc*., *Perkin Trans. 1*, **1990**, 2255.

65. Ogawa, S.; Isaka, A. *Carbohydr. Res*., **1991**, *210*, 105.

66. Schuerrle, K.; Beier, B.; Werbitzky, O.; Piepersberg, W. *Carbohydr. Res*., **1991**, *212*, 321.

67. Vaerman, J. L.; Viche, H. G. *Tetrahedron Asymm*., **1990**, *1*, 403.

68. Marco-Castelles, J.; Martinez, L.; Martinez-Grau, A.; Poznelo, C.; Jimeno, M. L. *Tetrahedron Lett*., **1991**, *32*, 6437.

69. Peet, N. P.; Huber, E. W.; Farr, R. A. *Tetrahedron*, **1991**, *47*, 7537.

70. Angeland, R.; Landais, Y.; Schenk, K. *Tetrahedron Lett*., **1997**, *38*, 1407.

71. Acena, J. L.; Arjona, O.; Iradier, F.; Plumet, J. *Tetrahedron Lett*., **1996**, *37*, 105.

72. Arjona, O.; DeDies, A.; Plumet, J.; Saeg, B. *Tetrahedron Lett*., **1995**, *36*, 1319.

73. Krief, A.; Dumount, W.; Billen, D.; Letteson, J-J.; Lestrate, P.; Murphy, P. J.; Lacroix, D. *Tetrahedron Lett*., **2004**, *45*, 1461.

74. Azev, V. N.; D'Alarcao, M. *J. Org. Chem*., **2004**, *69*, 4839.

75. Yu, J.; Spencer, J. B. *Tetrahedron Lett*., **2001**, *42*, 4219.

76. Suzuki, T.; Suzuki, S. T.; Yamada, I.; Koashi, Y.; Yamada, K.; Chida, N. *J. Org. Chem*., **2002**, *67*, 2874.

77. Sureshan, K. M.; Shashidhar, M. S.; Praveen, T.; Gonnade, R. G.; Bhadbhade, M. M.; *Carbohydr. Res*., **2002**, *337*, 2399.

78. Bone, J. A.; Whiting, M. C. *J. Chem. Soc*., *Chem. Commun*., **1970**, 115.

79. Subramaniam, R.; Fort, R. C. Jr. *J. Org. Chem.*, **1984**, *49*, 2896.

80. Das, T.; Shashidhar, M. S. *Carbohydr. Res.*, **1998**, *308*, 165.

81. Krylova, V. N.; Lyutik, A. I.; Kobel'kova, N. N.; Shvets, V. I.; Evstigneeva, R. P. *Zh. Org. Khim.*, **1978**, *14*, 1858.

82. Pietrusiewicz, K. M.; Salamończyk, G. M. *Synth. Commun.*, **1995**, *25*, 1863.

83. Angyal, S. J.; Gorin, P. A. J.; Pitman, M. E. *J. Chem. Soc.*, **1965**, 1807.

84. Pietrusiewicz, K. M.; Salamończyk, G. M.; Bruzik, K. S.; Wieezorek, W. *Tetrahedron*, **1992**, *48*, 5523.

85. Uhlmann, P.; Vasella, A. *Helv. Chim. Acta*, **1992**, *75*, 1979.

86. Posternak, T.; Falbriard, J-G. *Helv. Chim. Acta*, **1960**, *43*, 2142.

87. Posternak, T.; Falbriard, J-G. *Helv. Chim. Acta*, **1961**, *44*, 2080.

88. Posternak, T.; Falbriard, J-G. *Chem. Abstr.*, **1962**, *57*, 2302g.

89. Carless, H. A. J.; Oak, O. Z. *Tetrahedron Lett.*, **1991**, *32*, 1671.

90. Sato, K-i.; Bokura, M.; Taniguchi, M. *Bull. Chem. Soc. Jpn.*, **1994**, *67*, 1633.

91. Ferrier, R. J. *J. Chem. Soc., Perkin Trans.*, **1979**, 1455.

92. Ferrier, R. J.; Middleton, S. *Chem. Rev.*, **1993**, *93*, 2779.

93. Mancuso, A. J.; Huang, S-L.; Swern, D. *J. Org. Chem.*, **1978**, *43*, 2480.

94. Mancuso, A. J.; Brownfain, D. S.; Swern, D. *J. Org. Chem.*, **1979**, *44*, 4148.

95. Albright, J. D.; Goldman, L. *J. Am. Chem. Soc.*, **1965**, *87*, 4214.

96. Albright, J. D.; Goldman, L. *J. Am. Chem. Soc.*, **1967**, *89*, 2416.

97. Epstein, W. W.; Sweat, F. W. *Chem. Rev.*, **1967**, *67*, 247.

98. Angyal, S. J.; Klavins, J. E.; Mills. J. A. *Aust. J. Chem.*, **1974**, *27*, 1075.

99. Podeschwa, M. A. L.; Plettenburg, O.; Altenbach, H-J. *Org*. *Biomol*. *Chem*., **2003**, *1*, 1919.

100. Freifelder, M. in *Practical Catalytic Hydrogenations*, Wiley Interscience, New York, 1971, Chapter 16.; p. 333.

101. Freifelder, M. *Catalytic Hydrogenation in Organic Synthesis: Procedures and Commentry* John Wiley and Sons, New York 1978, Chapter 10, p 90.

102. Hutchins, R. O.; Su, W-Y.; Sivakumar, R.; Cistane, F.; Stercho, Y. P. *J*. *Org*. *Chem*., **1983**, *48*, 3412.

103. Gribble, G. W.; Nutaitis, C. F. *Org*. *Prep*. *Proc*. *Int*., **1985**, *17*, 317.

104. Hutchin, R. O.; Natale, N. R. *Org*. *Prep*. *Proc*. *Int*., **1979**, *11*, 201.

105. Lane, C. F. *Synthesis*, **1975**, 135.

106. Bashir-Uddin, S. M.; Akhter, M.; Allemann, R. K. *Tetrahedron Lett*., **2004**, *45*, 1223.

107. Chung, S-K, *Bioorg*. *Med*. *Chem*., **1999**, *7*, 2577.

108. Mitsunobu, O.; Yamada, M.; Mukaiyama, T. *Bull*. *Chem*. *Soc*. *Jpn*., **1967**, *40*, 935.

109. Mitsunobu, O.; Yamada, M. *Bull*, *Chem*. *Soc*. *Jpn*., **1967**, *40*, 2380.

110. Mitsunobu, O. *Synthesis*, **1981**, 1.

111. Tse, B.; Kishi, Y. *J*. *Am*. *Chem*. *Soc*., **1993**, *115*, 7892.

112. Das, T.; Praveen, T.; Shashidhar, M. S. *Carbohydr*. *Res*., **1998**, *313*, 55.

113. Praveen, T.; Ph. D. Thesis, University of Pune, 1999.

114. Sureshan K, M.; Shashidhar, M. S. *Tetrahedron Lett*., **2000**, *41*, 4185.

115. Angyal, S. J.; *Adv*. *Carbohydr*. *Chem*. *Biochem*., **1989**, *47*, 1.

116. Hancock, R. D.; Hegetschweiler, K. *J. Chem. Soc., Dalton Trans.*, **1993**, 2137.

117. Angyal, S. J.; McHugh, D. J. *J. Chem. Soc.*, **1957**, 1423.

118. Angyal, S. J. *Carbohydr. Res.*, **2000**, *325*, 313.

119. Carless, H. A. J.; Busia, K.; Oak, O. Z. *Synlett*, **1993**, 672.

120. Diels, O.; Alder, K. *Ann.*, **1928**, *460*, 98.

121. Diels, O.; Alder, K. *Ann.*, **1929**, *470*, 62.

122. Diels, O.; Alder, K. *Ber.*, **1929**, *62*, 2081.

123. Diels, O.; Alder, K. *Ber.*, **1929**, *62*, 2087.

124. Barili, P. L.; Berti, G.; Catelani, G.; D'Andrea, F.; *Gazz. Chim. Ital.*, **1992**, *122*, 135.

125. Angyal, S. J.; Range, D. *Carbohydr. Res.*, **1979**, *76*, 121.

126. Craig, B. N.; Janssen, M. U.; Wickersham, B. M.; Rabb, D. M.; Chang, P. S.; O'Leary, D. J. *J. Org. Chem.*, **1996**, *61*, 9610.

127. Paquette, L. A.; Ra, C. S.; Gallucci, J. C.; Kang, H-J.; Ohmori, N.; Arrington, M. P.; David, W.; Brodbelt, J. S. *J. Org. Chem.*, **2001**, *66*, 8629.

128. Paquette, L. A.; Tae J. *J. Am. Chem. Soc.*, **2001**, *123*, 4974.

129. Wu, Y.; Zhou, C.; Roberts, M. F. *Biochem.*, **1997**, *36*, 356.

130. Riley, A. M.; Guédat, P.; Schlewer, G.; Spiess, B.; Potter, B. V. L. *J. Org. Chem.*, **1998**, *63*, 295.

131. Kim, T-H.; Holmes, A. B. *J. Chem. Soc., Perkin Trans. 1*, **2001**, 2524.

B2.8. Appendix

Appendix index Page No

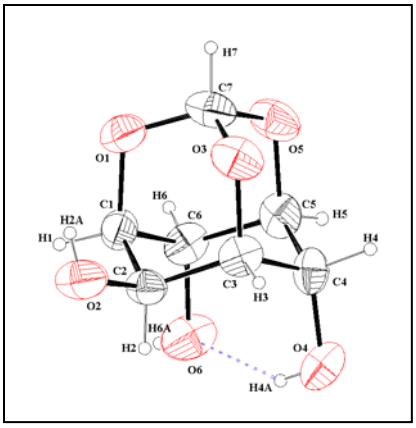

ORTEP of **B2.23**, crystallized from ethyl acetate.

Crystal data table of **B2.23**

Identification code	**B2.23** (crystallized from ethyl acetate)
Empirical Formula	$C_7H_{10}O_6$
Formula weight	190.15
Crystal form, colour	Plate, colourless
Crystal size (mm)	0.61 × 0.27 × 0.09
Wavelength	0.71073
Temperature (K)	293(2) K
Crystal system, space group	Orthorhombic, *P*na2$_1$
Unit cell Dimensions	a = 12.174(4) Å; α = 90° b = 6.155(2) Å; β = 90° c = 10.050(3) Å; γ = 90°
Volume	753.0(4) Å^3
Z , Calculated density	4, 1.677 Mg/m^3
F(000)	400
Absorption coefficient (μ)	0.150 mm^{-1}
Maximum and minimum transmission	0.9865 and 0.9140
Reflection collected / unique/ observed	4069 / 1636 / 1556
θ range for data collection	3.35-28.16
Limiting indices	-16⇐h⇒14; -8⇐k⇒6; -12⇐l⇒13
Goodness-of-fit on F^2	1.083
Final R indices [I >2σ(I)]	R1 = 0.0359, wR2 = 0.0906
R indices [all data]	R1 = 0.0379, wR2 = 0.0920
Data / restraints / parameters	1636 / 0 / 158
H-atom treatment	From difference Fourier map
Largest diff. Peak and hole (ρ_{max}, & ρ_{min})	0.201 & -0.235 eÅ^{-3}

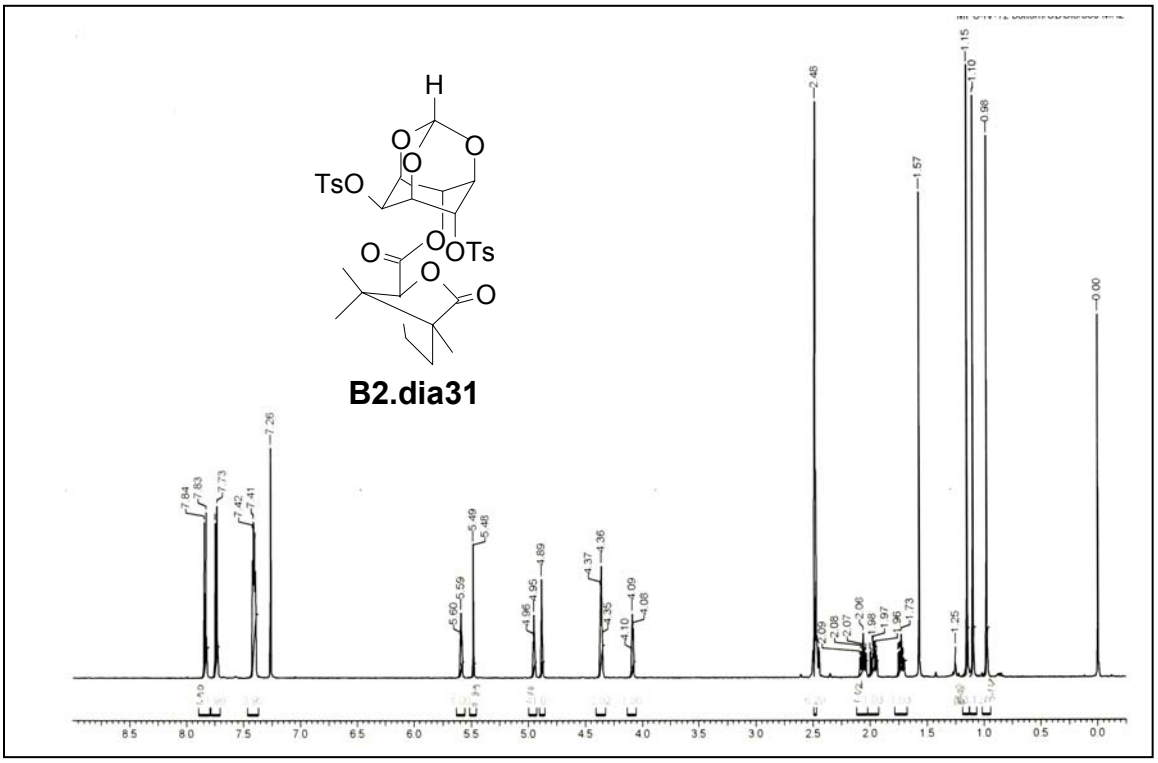
H
O
O
O
O
TsO
O
O
OTs
O
O
B2.dia31
7.84
7.83
7.73
7.42
7.41
7.26
5.60
5.59
5.49
5.48
4.96
4.95
4.89
4.37
4.36
4.35
4.10
4.09
4.08
2.48
2.09
2.08
2.07
2.06
1.98
1.97
1.96
1.73
1.57
1.25
1.15
1.10
0.98
0.00

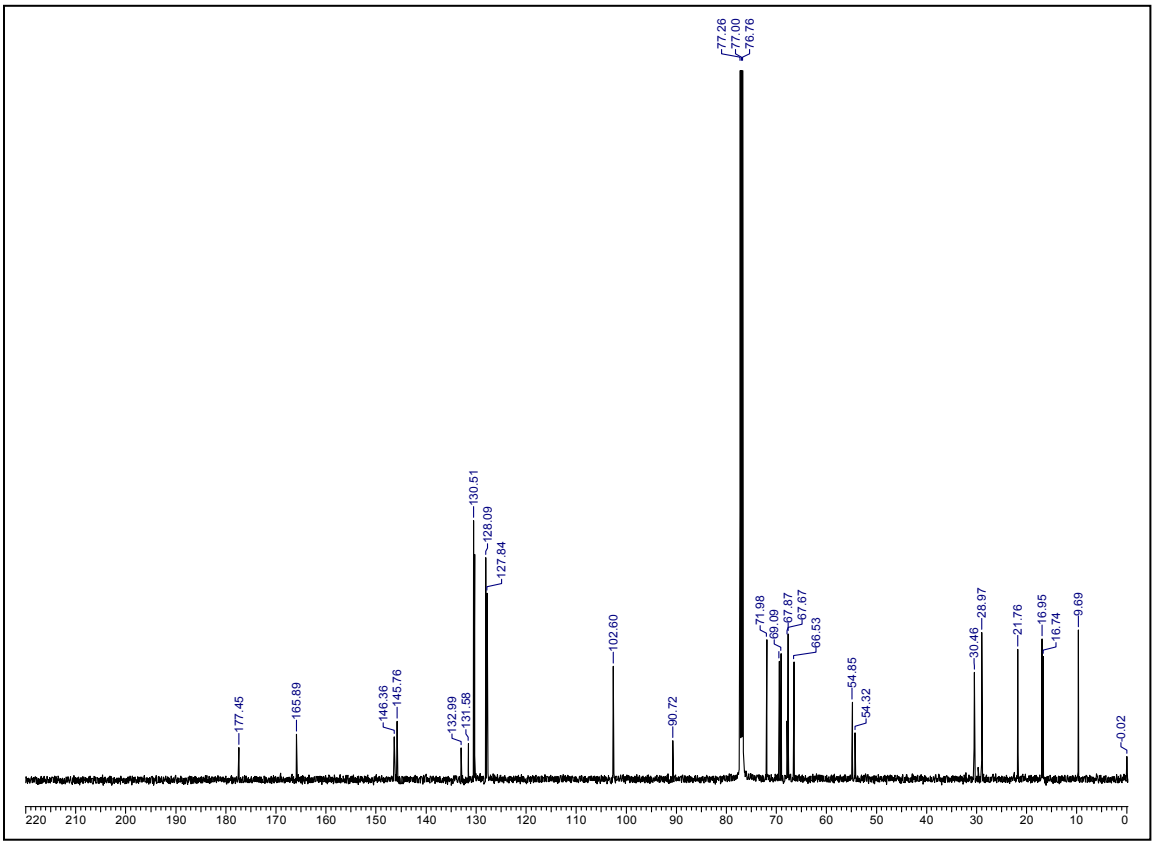
177.45
165.89
146.36
145.76
132.99
131.58
130.51
128.09
127.84
102.60
90.72
77.26
77.00
76.76
71.98
69.09
67.87
67.67
66.53
54.85
54.32
30.46
28.97
21.76
16.95
16.74
9.69
0.02

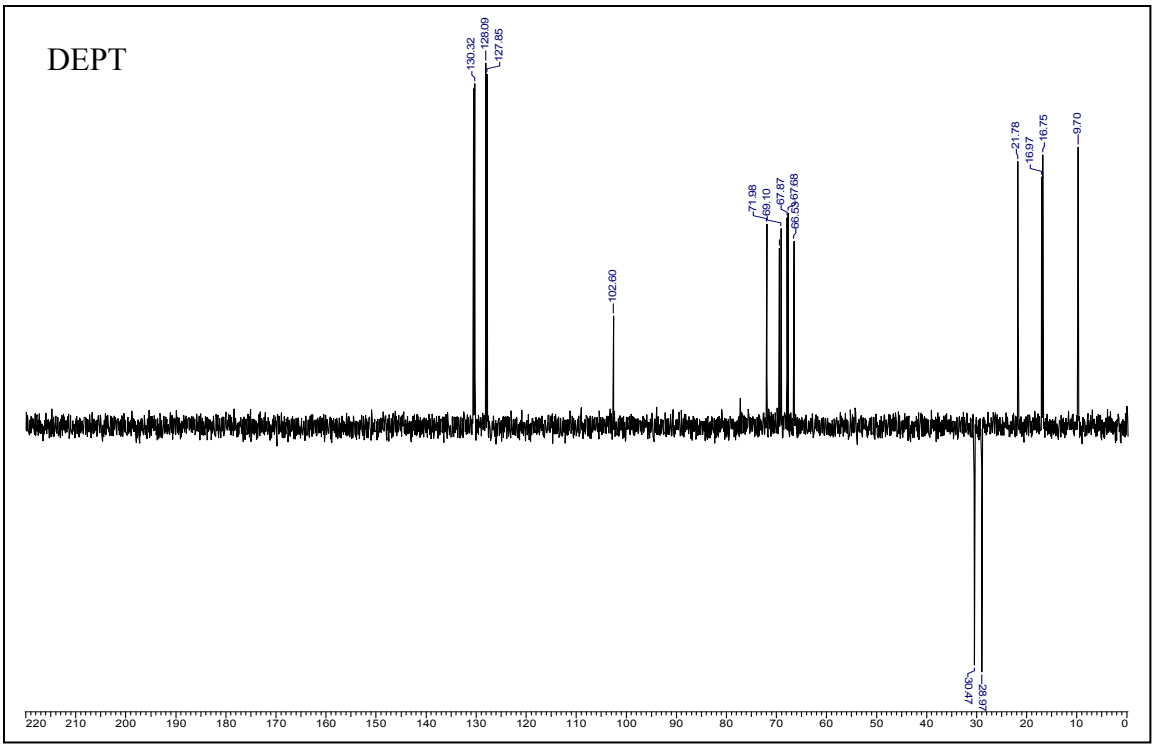
DEPT
130.32
128.09
127.85
102.60
71.98
69.10
67.87
66.53
67.68
21.78
16.97
16.75
9.70
30.47
28.97
220 210 200 190 180 170 160 150 140 130 120 110 100 90 80 70 60 50 40 30 20 10 0

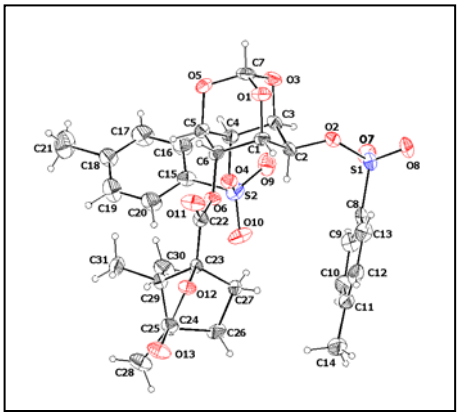

ORTEP of **B2.dia31**

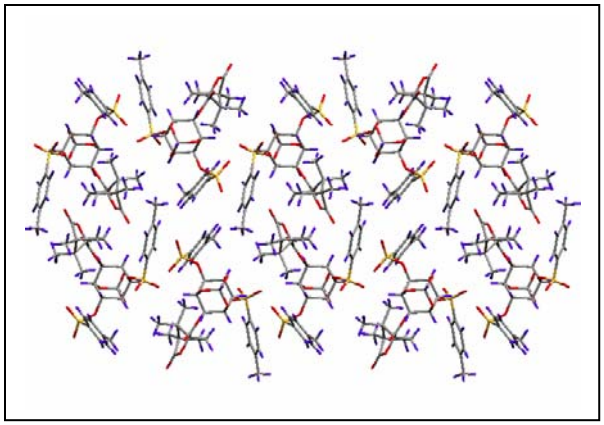

Packing of **B2.dia31** down a-axis

Crystal data table of **B2.dia31**

Identification code	**B2.dia31** (crystallized from chloroform-light petroleum mixture)
Empirical formula	$C_{31}H_{34}O_{13}S_2$
Formula weight	678.70
Temperature	293(2) K
Wavelength	0.71073 Å
Crystal system, space group	Orthorhombic, $P2_12_12_1$
Unit cell dimensions	a = 20.24(4) Å; α = 90° b = 17.98(4) Å; β = 90° c = 9.14(2) Å; γ = 90°
Volume	3326(12) $Å^3$
Z, Calculated density	4, 1.355 Mg/m^3
Absorption coefficient	0. 0.224 mm^{-1}
F(000)	1424
Crystal size	0.74 x 0.08 x 0.07 mm
θ range for data collection	1.51 to 25°
Limiting indices	-12⇒ h ⇒ 24; -21 ⇒ k ⇒ 21; -10 ⇒ l ⇒ 10.
Reflections collected / unique	16688 / 5836 [R(int) =]
Completeness to θ = 25°	99.9%
Max. and min. transmission	0.8517and 0.9843
Refinement method	Full-matrix least-squares on F^2
Data / restraints / parameters	5836 / 0 / 420
Goodness-of-fit on F^2	1.066
Final R indices [I>2σ (I)]	R1 = 0.0743, wR2 =0.1134
R indices (all data)	R1 = 0.1303, wR2 = 0.1289
Extinction coefficient	none
Largest diff. peak and hole (ρ_{max} & ρ_{min})	-0.161, 0.208 e. $Å^{-3}$

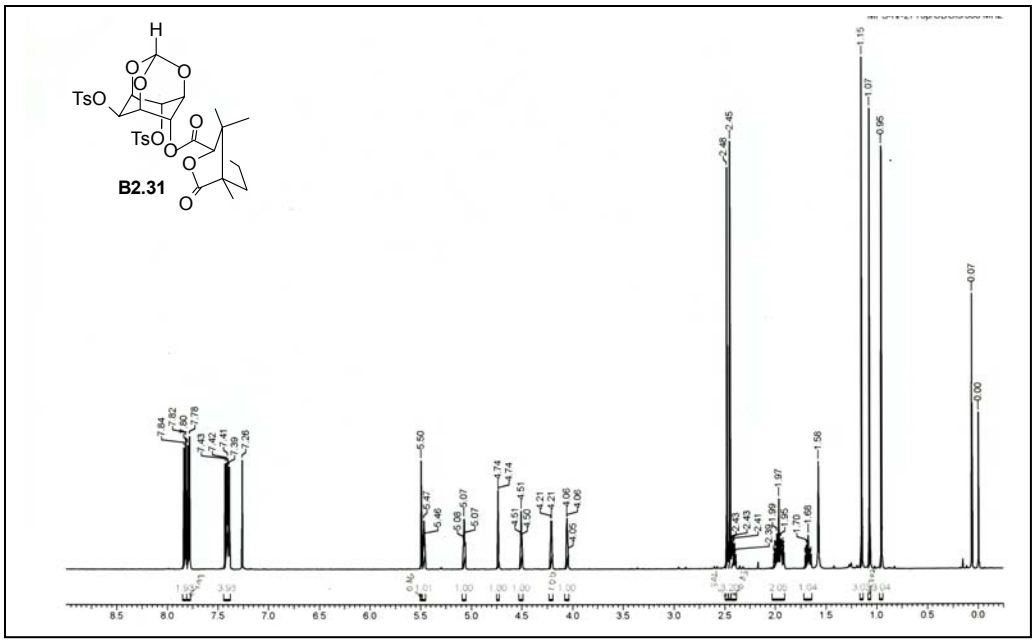
B2.31
TsO
TsO

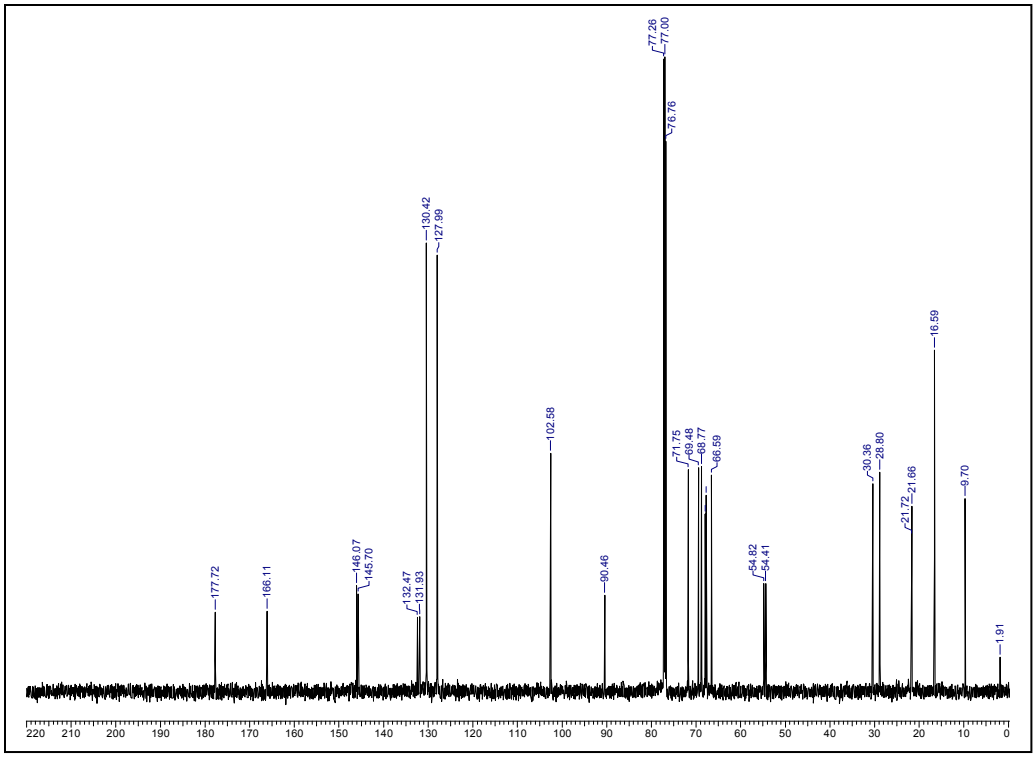

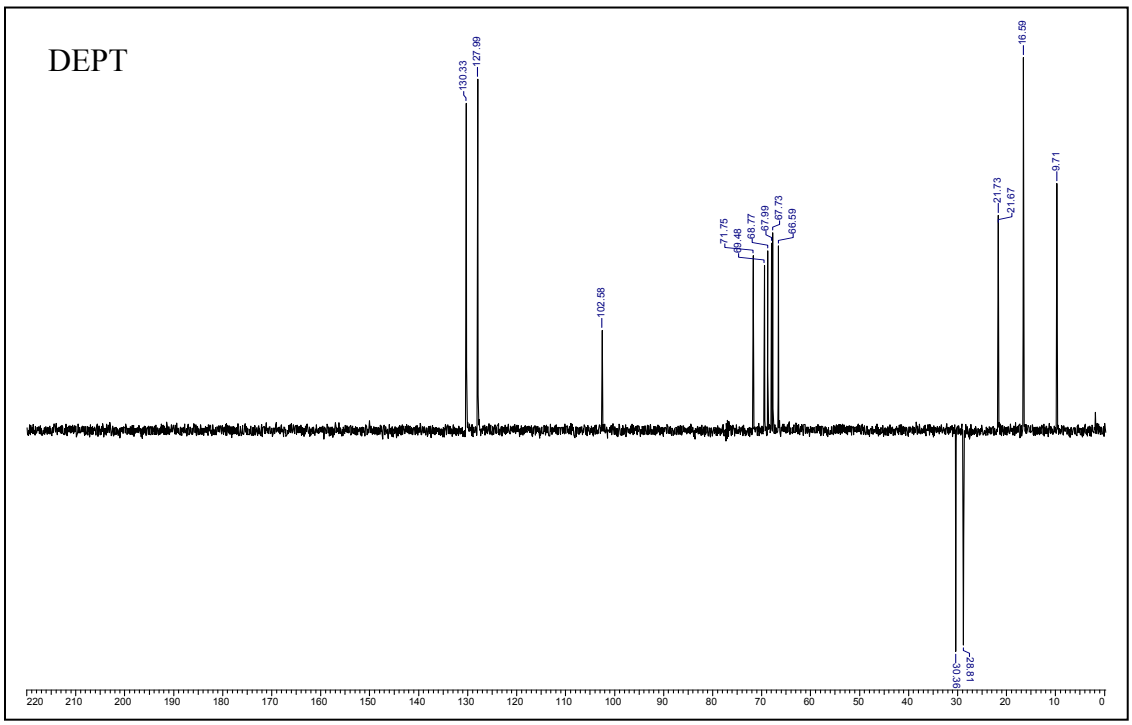
DEPT
130.33
127.99
102.58
71.75
69.48
68.77
67.99
67.73
66.59
30.36
28.81
21.73
21.67
16.59
9.71
220 210 200 190 180 170 160 150 140 130 120 110 100 90 80 70 60 50 40 30 20 10 0

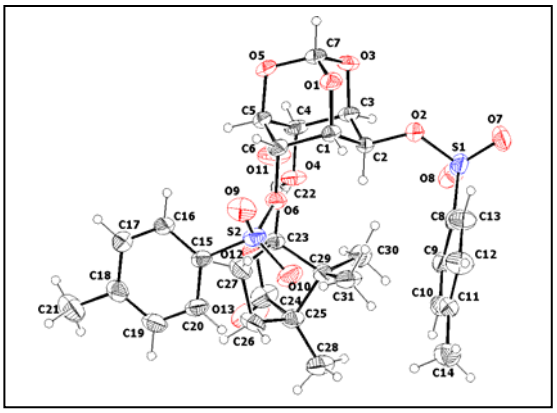

ORTEP of **B2.31**

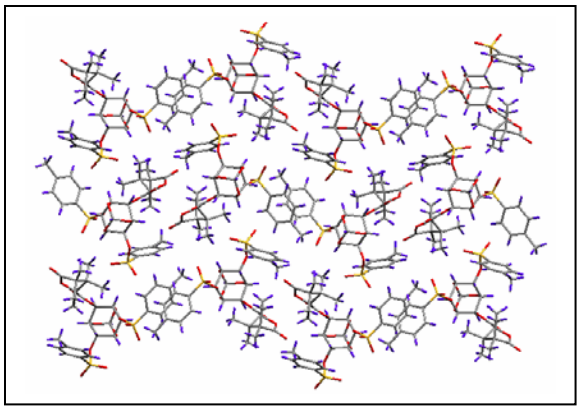

Packing of **B2.31** down a-axis

Crystal data table of **B2.31**

Identification code	**B2.31**(crystallized from chloroform-light petroleum mixture)
Empirical formula	$C_{31}H_{34}O_{13}S_2$
Formula weight	678.70
Temperature	293(2) K
Wavelength	0.71073 Å
Crystal system, space group	orthorhombic, $P2_12_12_1$
Unit cell dimensions	a = 9.057(4) Å; α = 90° b = 15.627(7) Å; β = 90° c = 22.226(10) Å; γ = 90°
Volume	3146(2) $Å^3$
Z, Calculated density	4, 1.433 Mg/m^3
Absorption coefficient	0. 0.237 mm^{-1}
F(000)	1424
Crystal size	0.71 x 0.14 x 0.08 mm
θ range for data collection	1.59 to 25°
Limiting indices	-10⇒ h ⇒ 10; -18⇒ k ⇒ 16; -26 ⇒ l ⇒ 24.
Reflections collected / unique	15869 / 5531
Completeness to θ = 25°	99.7%
Max. and min. transmission	0.8497 and 0.9824
Refinement method	Full-matrix least-squares on F^2
Data / restraints / parameters	5531 / 0 / 420
Goodness-of-fit on F^2	1.155
Final R indices [I>2σ (I)]	R1 = 0.0594, wR2 = 0.1106
R indices (all data)	R1 = 0.0755, wR2 = 0.1161
Extinction coefficient	none
Largest diff. peak and hole (ρ_{max} & ρ_{min})	-0.239, 0.213 e. $Å^{-3}$

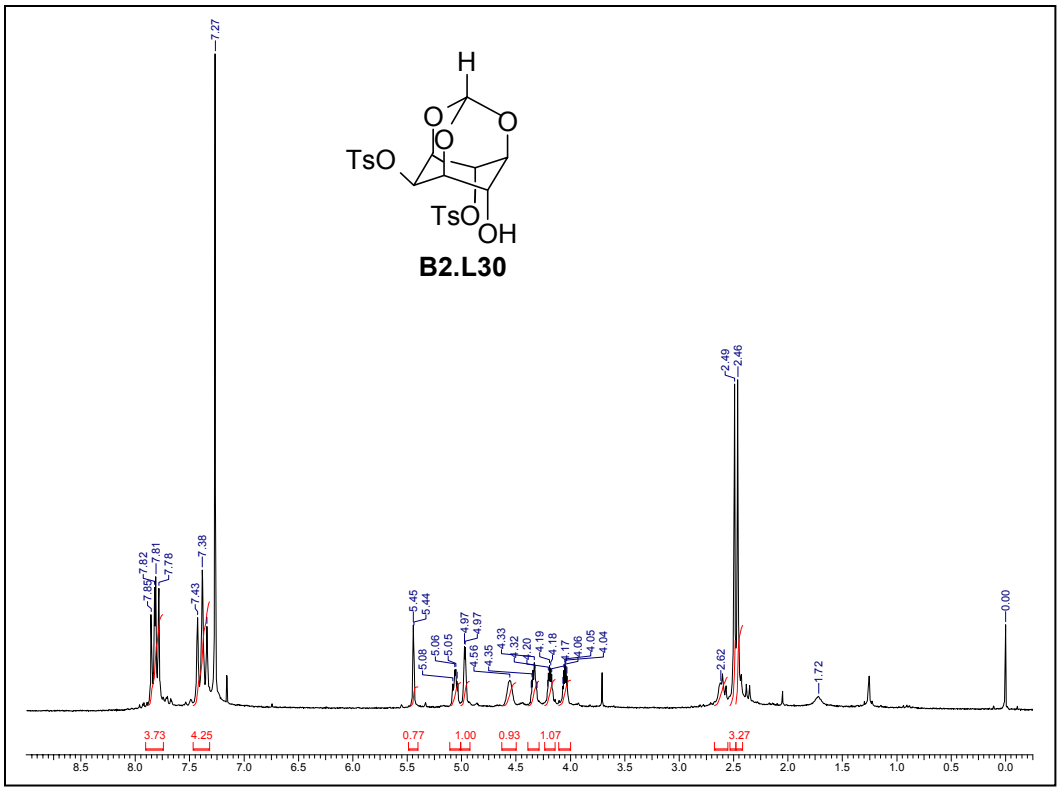
H
O
O
O
TsO
TsO
OH
B2.L30

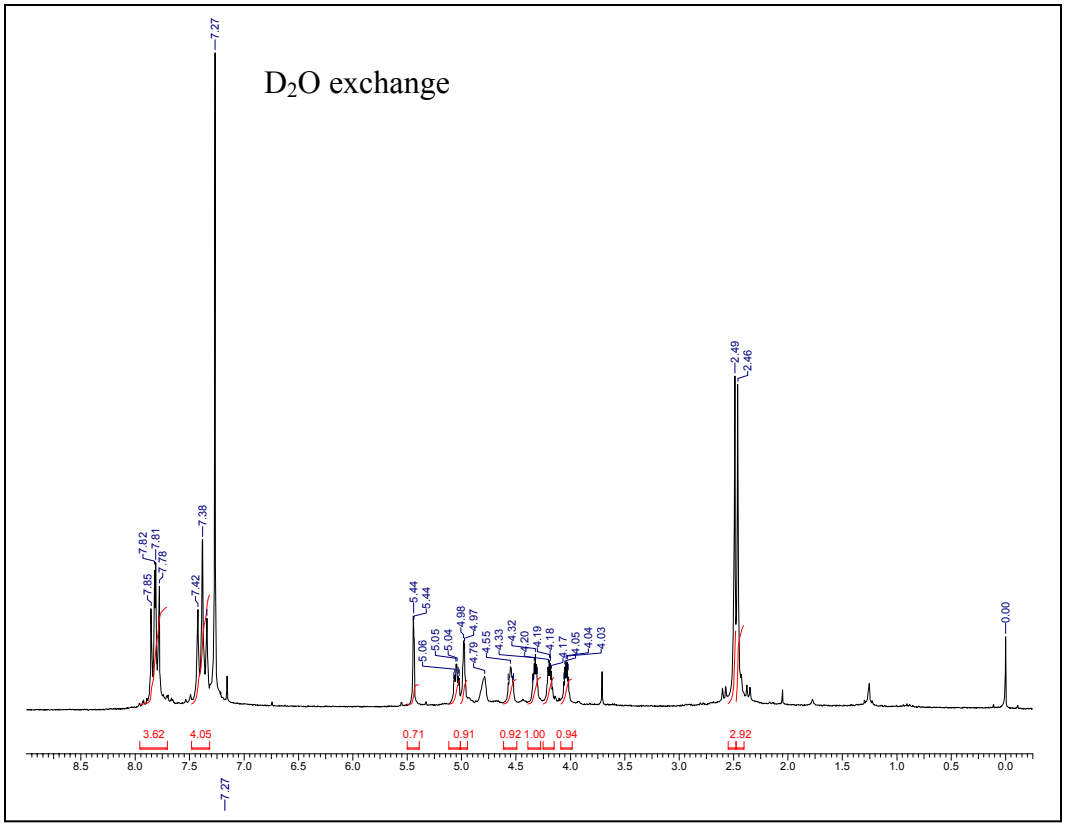
D2O exchange

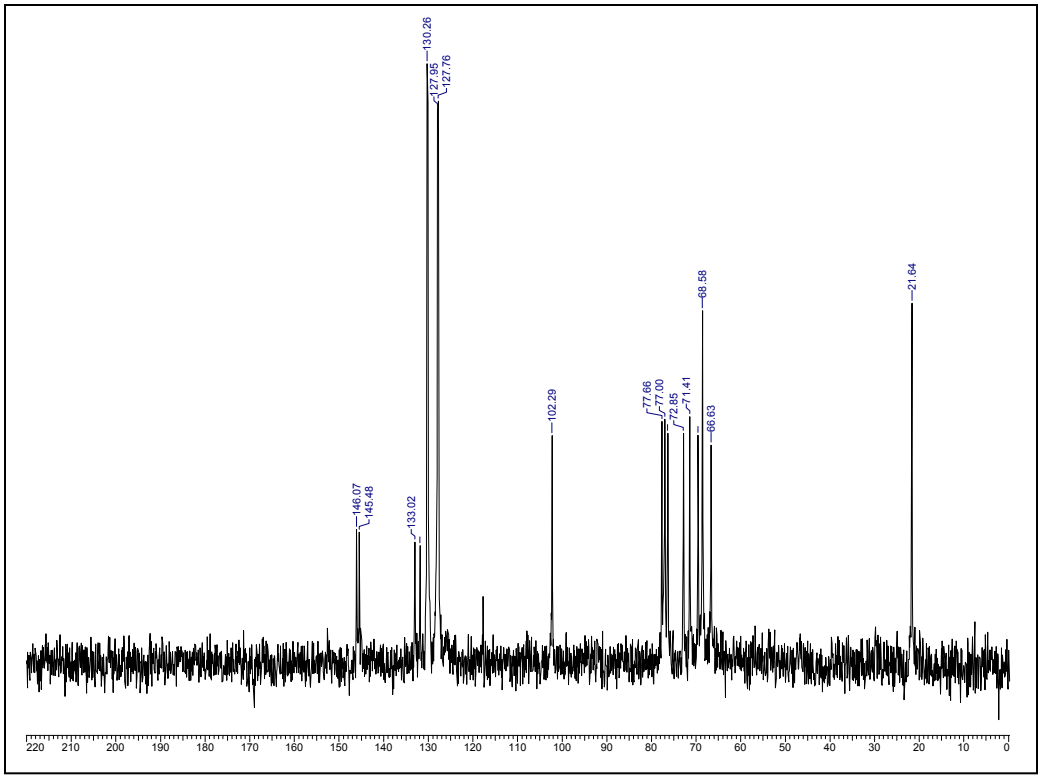
130.26
127.95
127.76
68.58
21.64
77.66
77.00
72.85
71.41
66.63
102.29
146.07
145.48
133.02
220 210 200 190 180 170 160 150 140 130 120 110 100 90 80 70 60 50 40 30 20 10 0

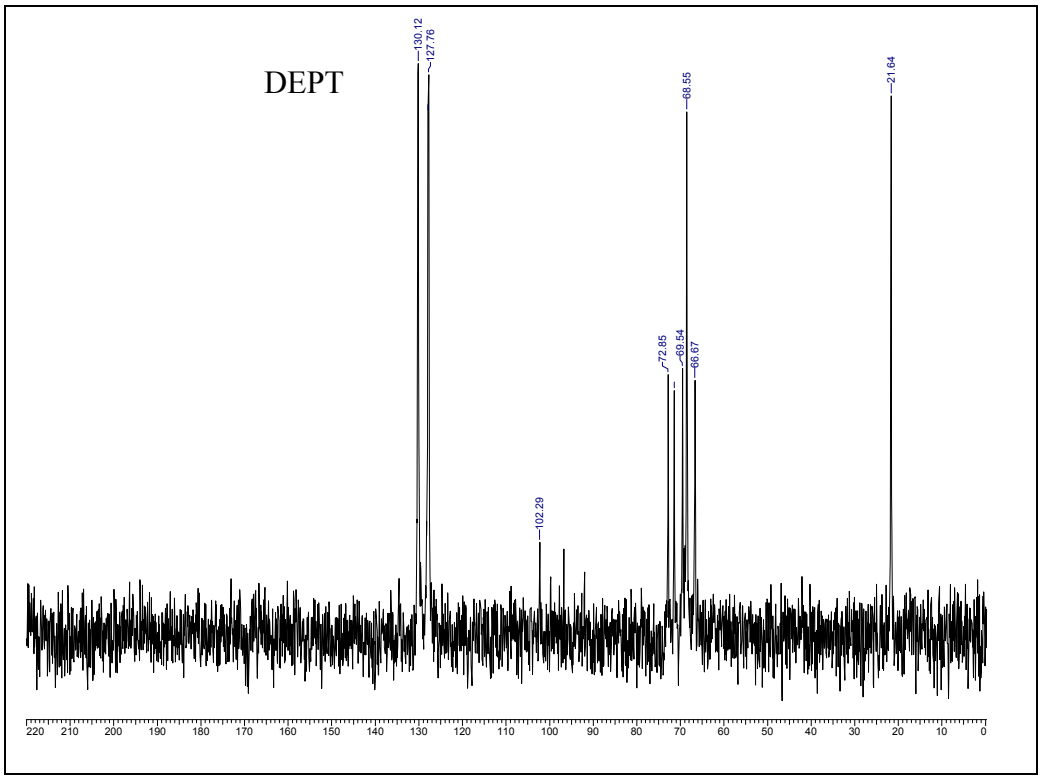
DEPT
130.12
127.76
68.55
21.64
72.85
69.54
66.67
102.29
220 210 200 190 180 170 160 150 140 130 120 110 100 90 80 70 60 50 40 30 20 10 0

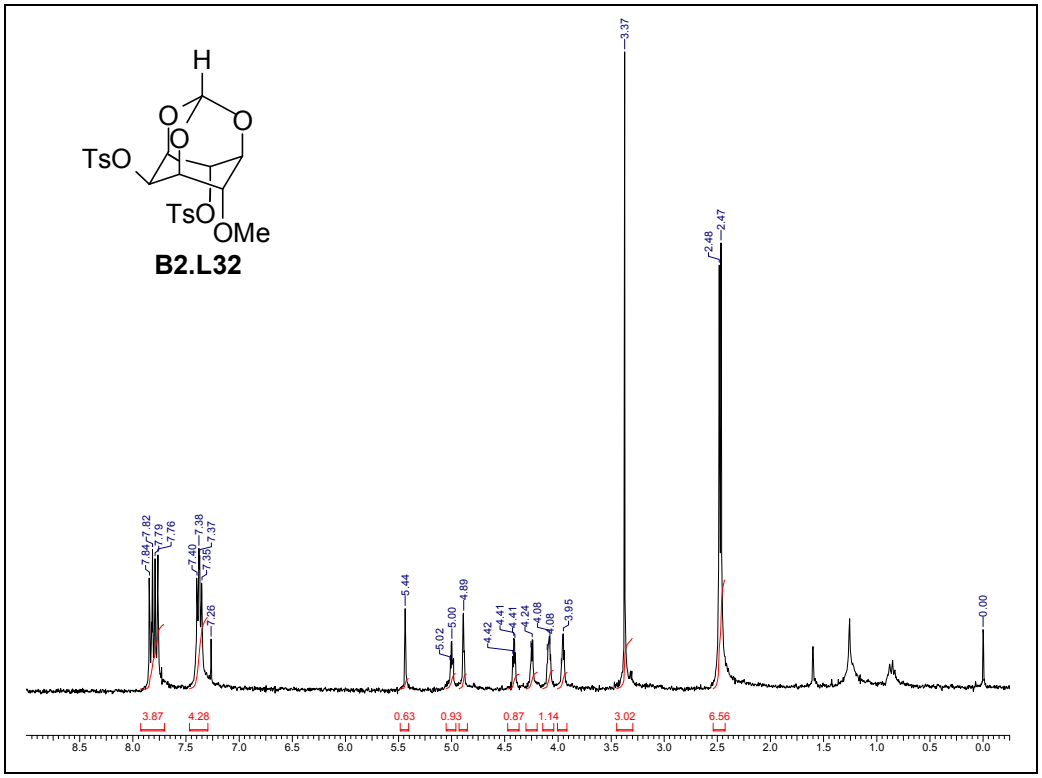
H
O
O
O
O
TsO
TsO
OMe
B2.L32
3.37
2.48
2.47
7.84
7.82
7.79
7.78
7.76
7.40
7.38
7.38
7.37
7.26
5.44
5.02
5.00
4.89
4.42
4.41
4.41
4.24
4.08
4.08
3.95
0.00
3.87
4.28
0.63
0.93
0.87
1.14
3.02
6.56

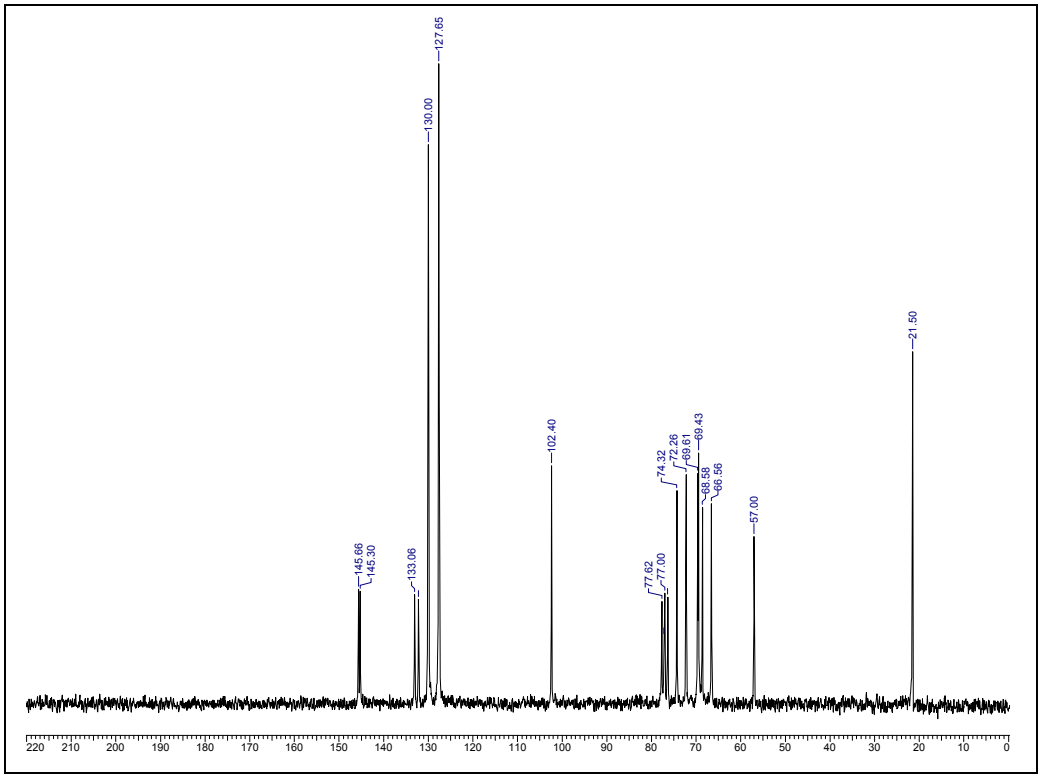
127.65
130.00
102.40
145.66
145.30
133.06
77.62
77.00
74.32
72.26
69.61
69.43
68.58
66.56
57.00
21.50

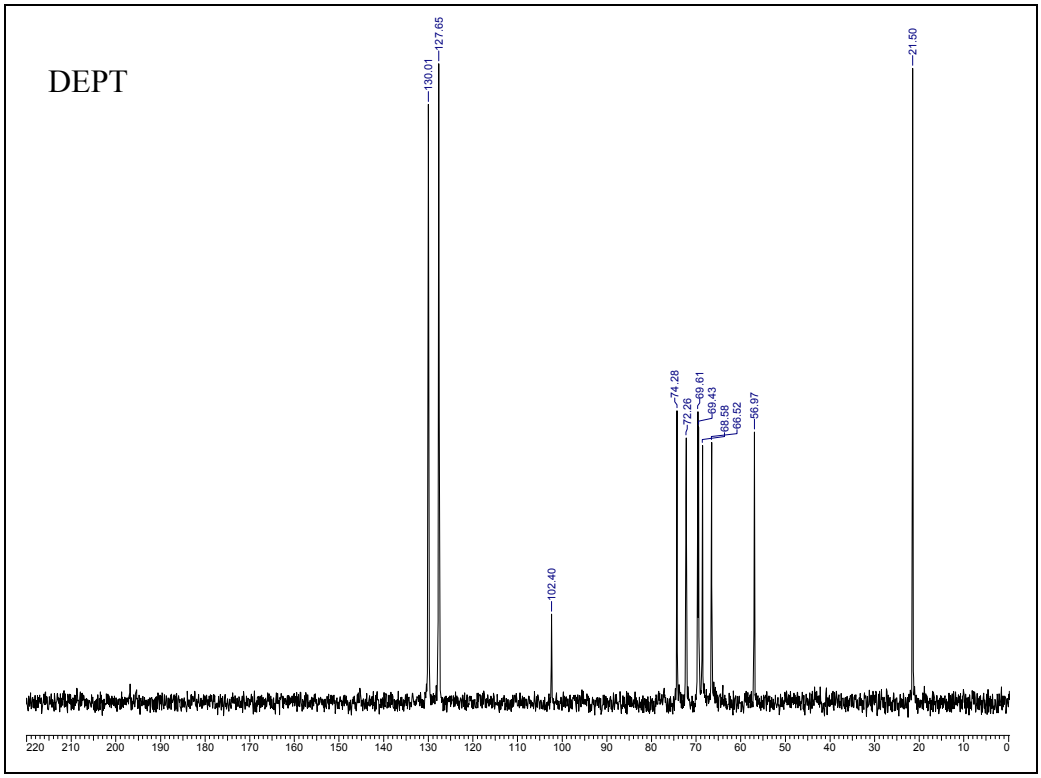
DEPT
130.01
127.65
21.50
74.28
72.26
69.61
69.43
68.58
66.52
56.97
102.40
220 210 200 190 180 170 160 150 140 130 120 110 100 90 80 70 60 50 40 30 20 10 0

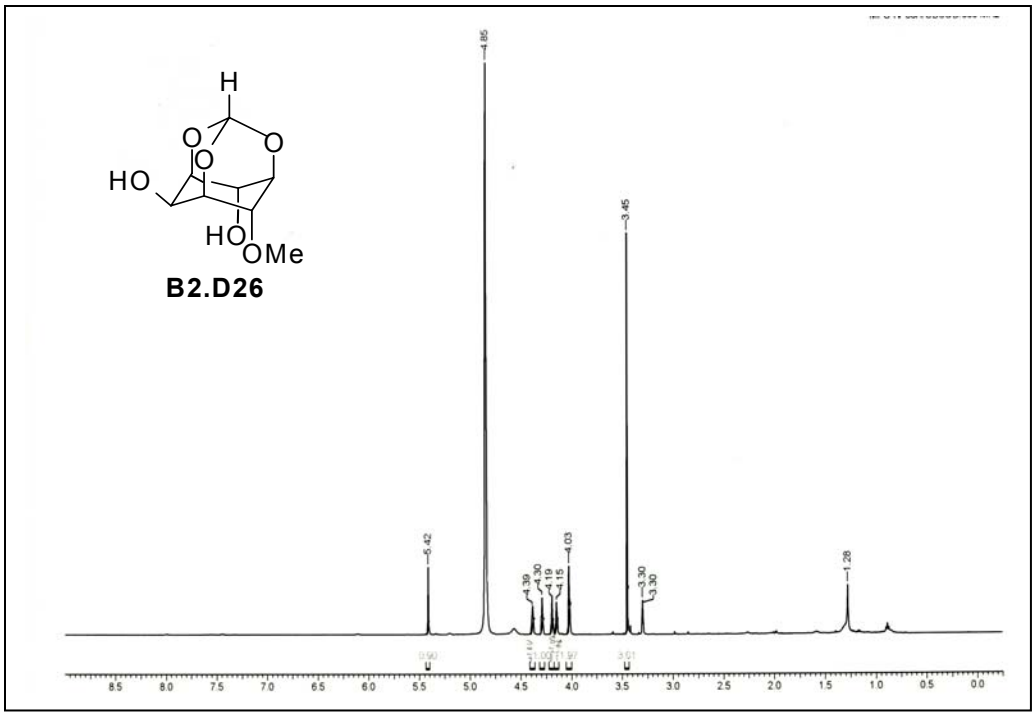
H
O
O
O
HO
HO
OMe
B2.D26
4.85
3.45
5.42
4.39
4.30
4.19
4.15
4.03
3.30
3.30
1.28
8.5 8.0 7.5 7.0 6.5 6.0 5.5 5.0 4.5 4.0 3.5 3.0 2.5 2.0 1.5 1.0 0.5 0.0

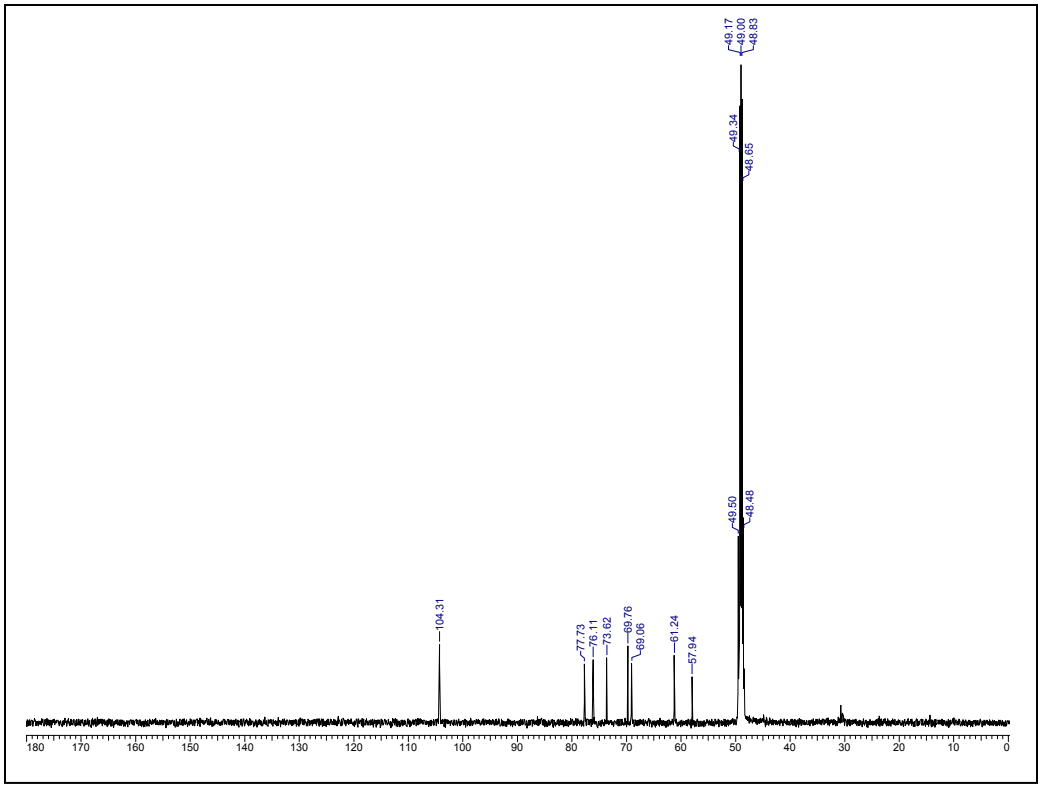
49.17
49.00
48.83
49.34
48.65
49.50
48.48
104.31
77.73
76.11
73.62
69.76
69.06
61.24
57.94
180 170 160 150 140 130 120 110 100 90 80 70 60 50 40 30 20 10 0

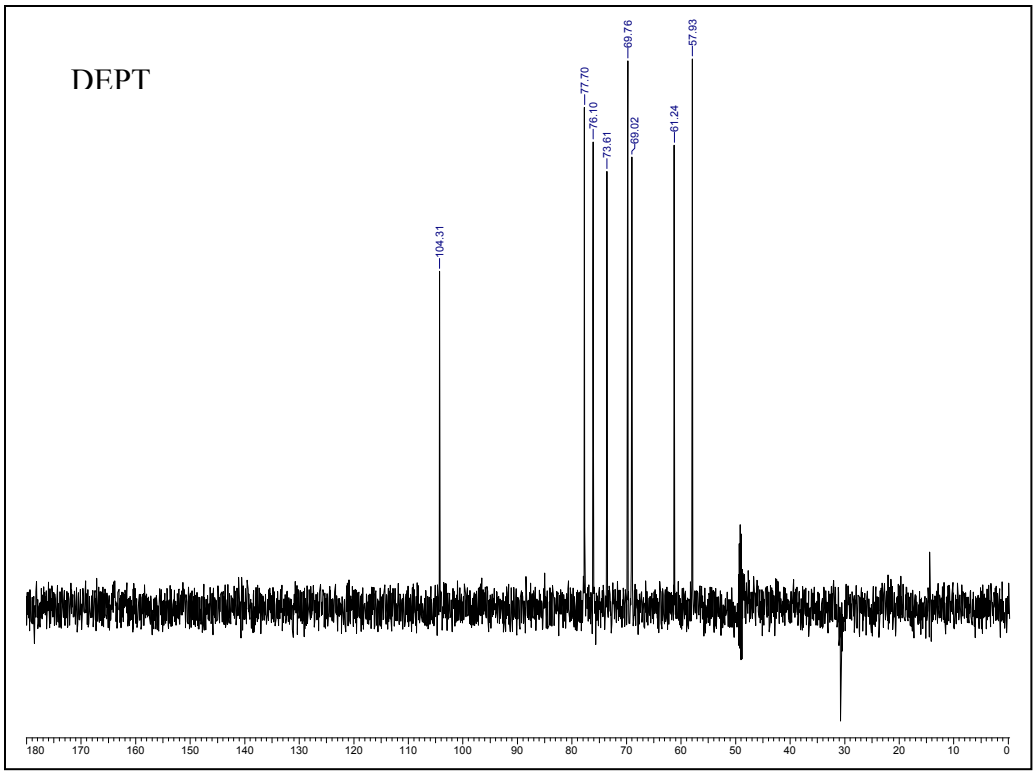
DEPT
104.31
77.70
76.10
73.61
69.76
69.02
61.24
57.93
180 170 160 150 140 130 120 110 100 90 80 70 60 50 40 30 20 10 0

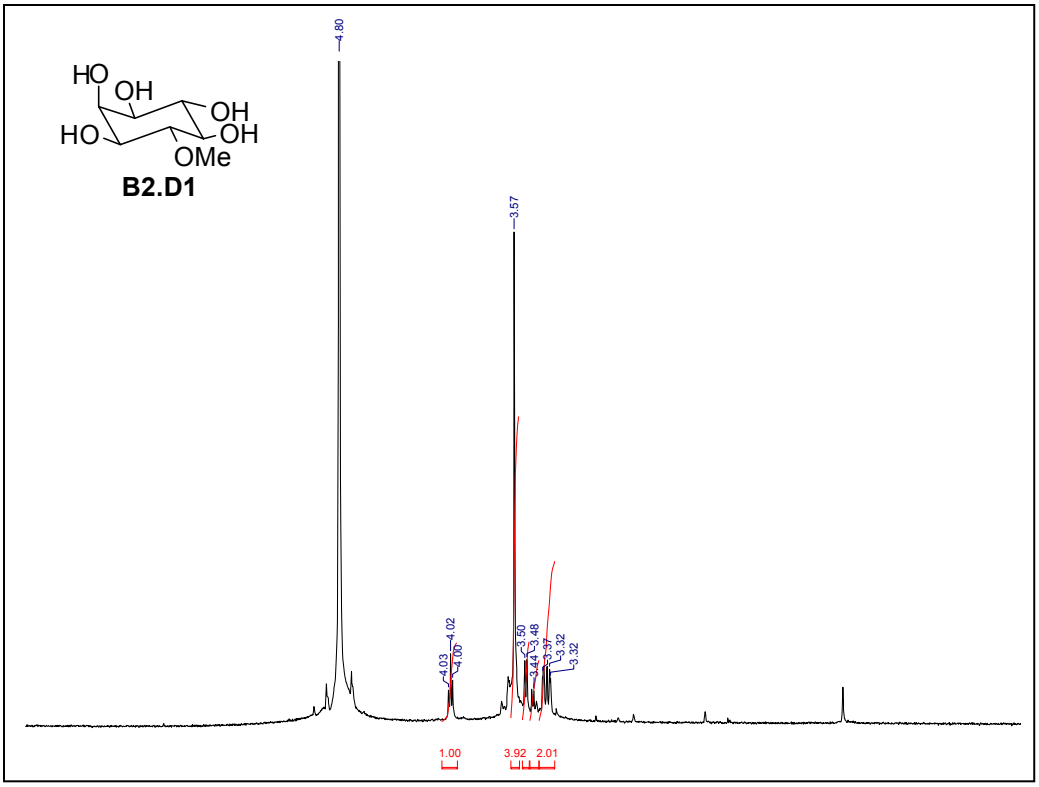
HO
OH
OH
HO
OH
OMe
B2.D1
4.80
3.57
4.03
4.02
4.00
3.50
3.48
3.37
3.34
3.32
3.32
1.00
3.92
2.01

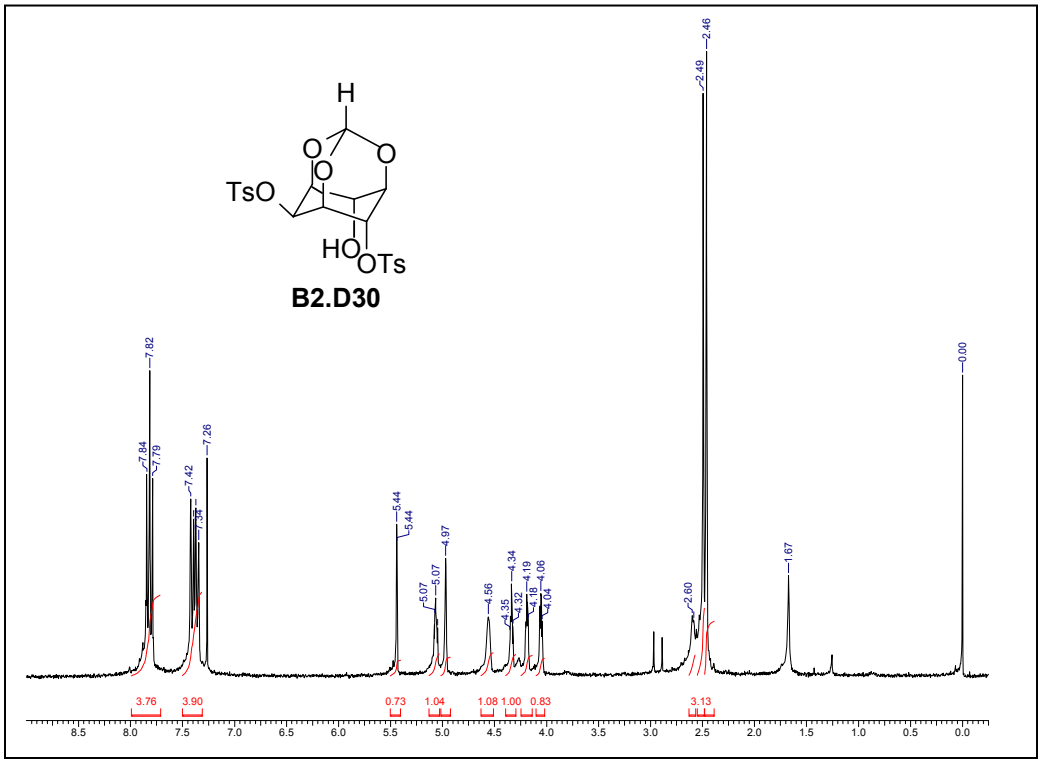
H
O
O
O
TsO
HO
OTs
B2.D30
7.82
7.84
7.79
7.42
7.26
5.44
5.44
5.07
5.07
4.97
4.56
4.35
4.34
4.32
4.19
4.18
4.06
4.04
2.60
2.49
2.46
1.67
0.00
3.76
3.90
0.73
1.04
1.08
1.00
0.83
3.13

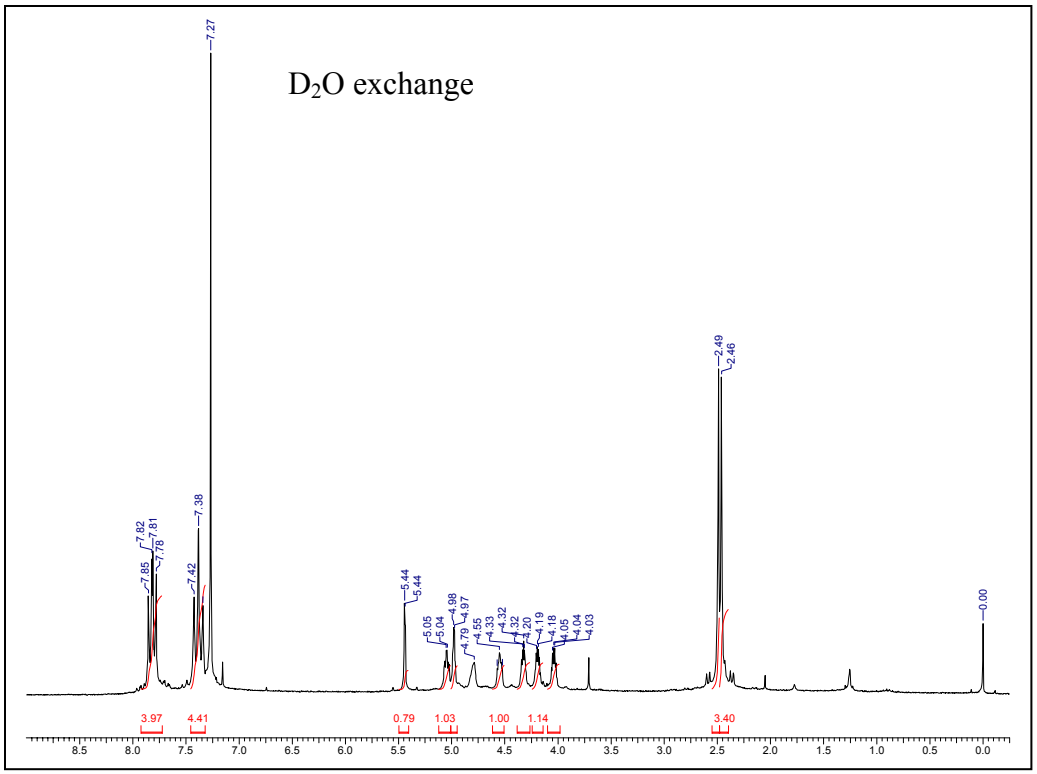
D2O exchange
7.27
7.82
7.81
7.78
7.85
7.42
7.38
5.44
5.44
5.05
5.04
4.98
4.97
4.79
4.55
4.33
4.32
4.20
4.19
4.18
4.05
4.04
4.03
2.49
2.46
0.00
3.97
4.41
0.79
1.03
1.00
1.14
3.40

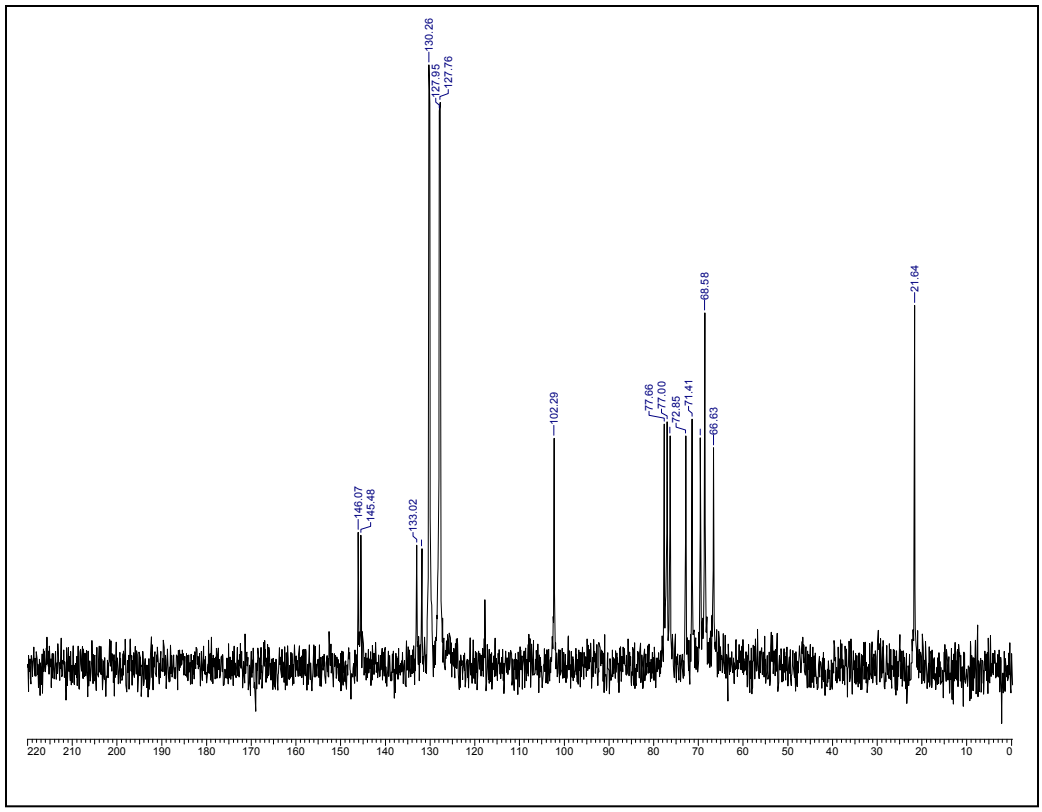
130.26
127.95
127.76
146.07
145.48
133.02
102.29
77.66
77.00
72.85
71.41
68.58
66.63
21.64
220 210 200 190 180 170 160 150 140 130 120 110 100 90 80 70 60 50 40 30 20 10 0

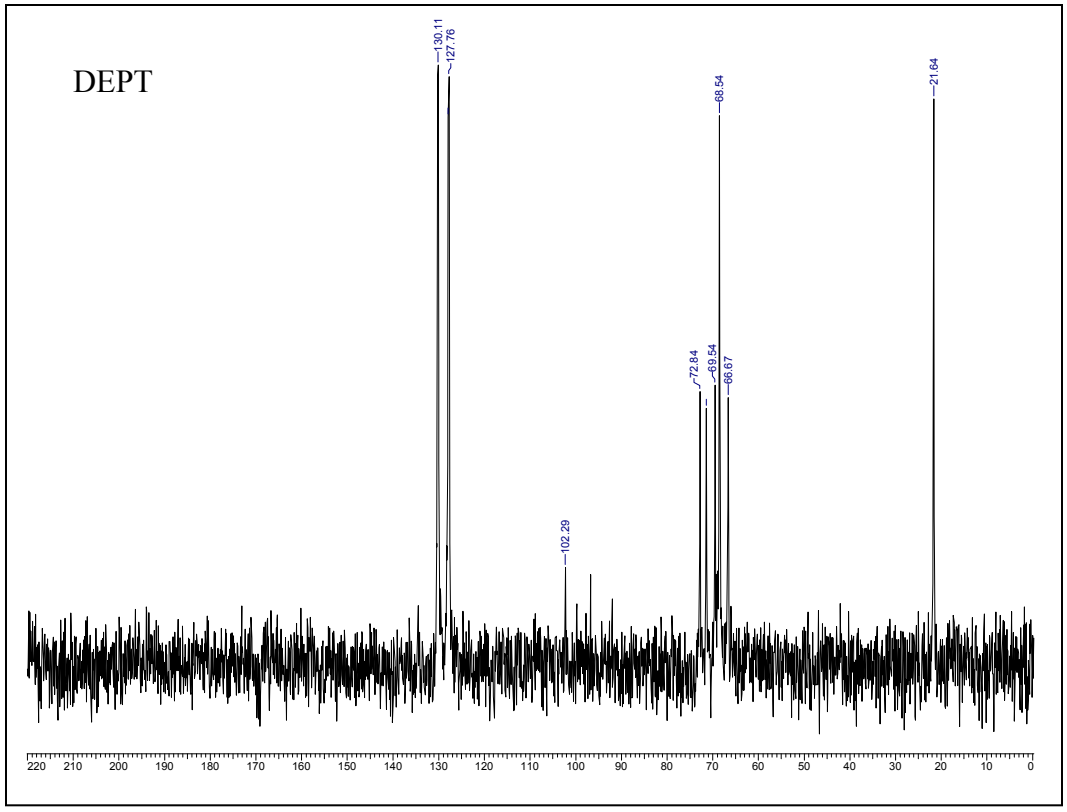
DEPT
130.11
127.76
68.54
21.64
72.84
69.54
66.67
102.29
220 210 200 190 180 170 160 150 140 130 120 110 100 90 80 70 60 50 40 30 20 10 0

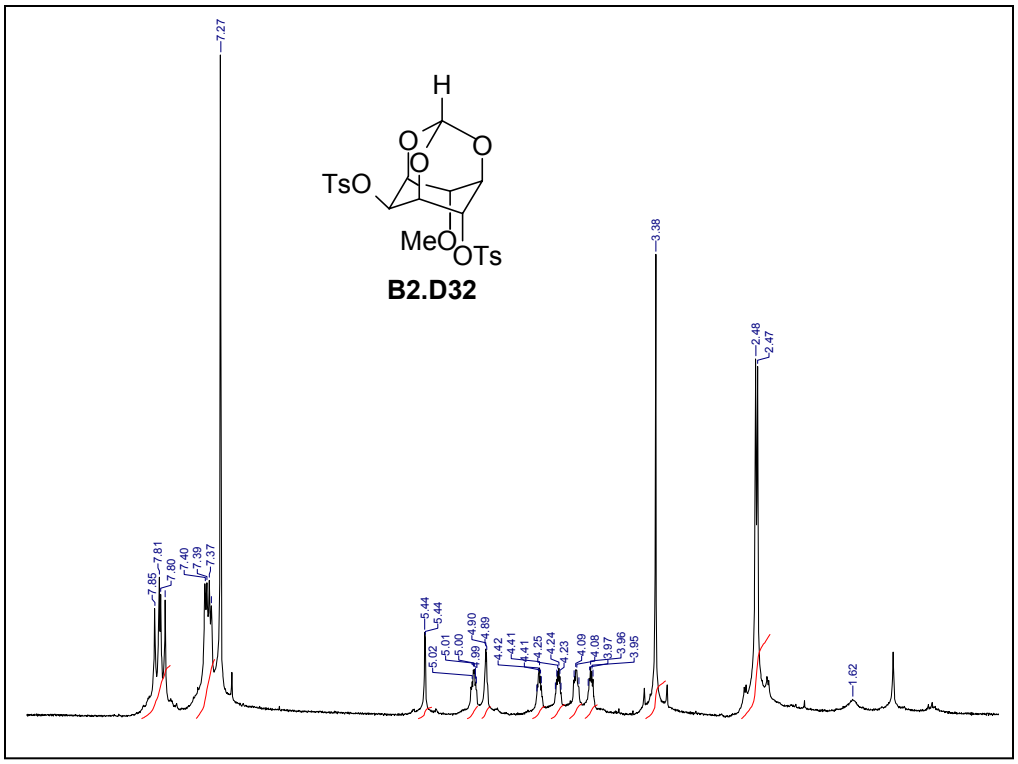
H
O
O
O
O
TsO
MeO
OTs
B2.D32
7.27
7.85
7.81
7.80
7.40
7.39
7.37
5.44
5.44
5.02
5.01
5.00
4.99
4.90
4.89
4.42
4.41
4.41
4.25
4.24
4.23
4.09
4.08
3.97
3.96
3.95
3.38
2.48
2.47
1.62

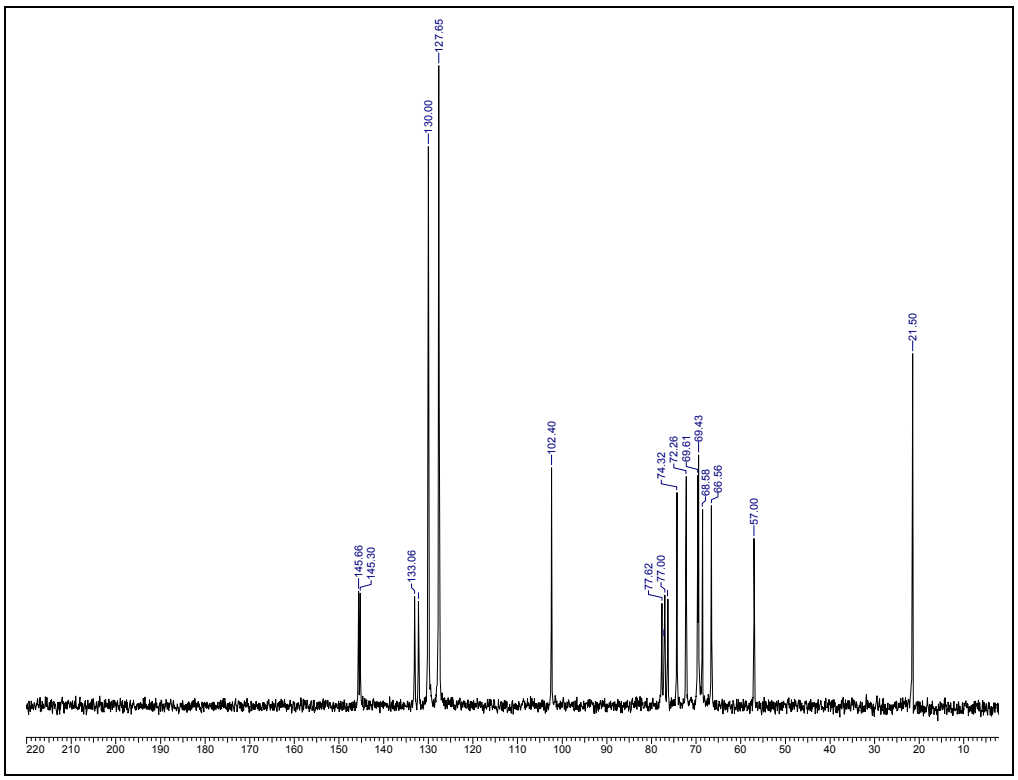
127.65
130.00
145.66
145.30
133.06
102.40
77.62
77.00
74.32
72.26
69.61
69.43
68.58
66.56
57.00
21.50
220 210 200 190 180 170 160 150 140 130 120 110 100 90 80 70 60 50 40 30 20 10

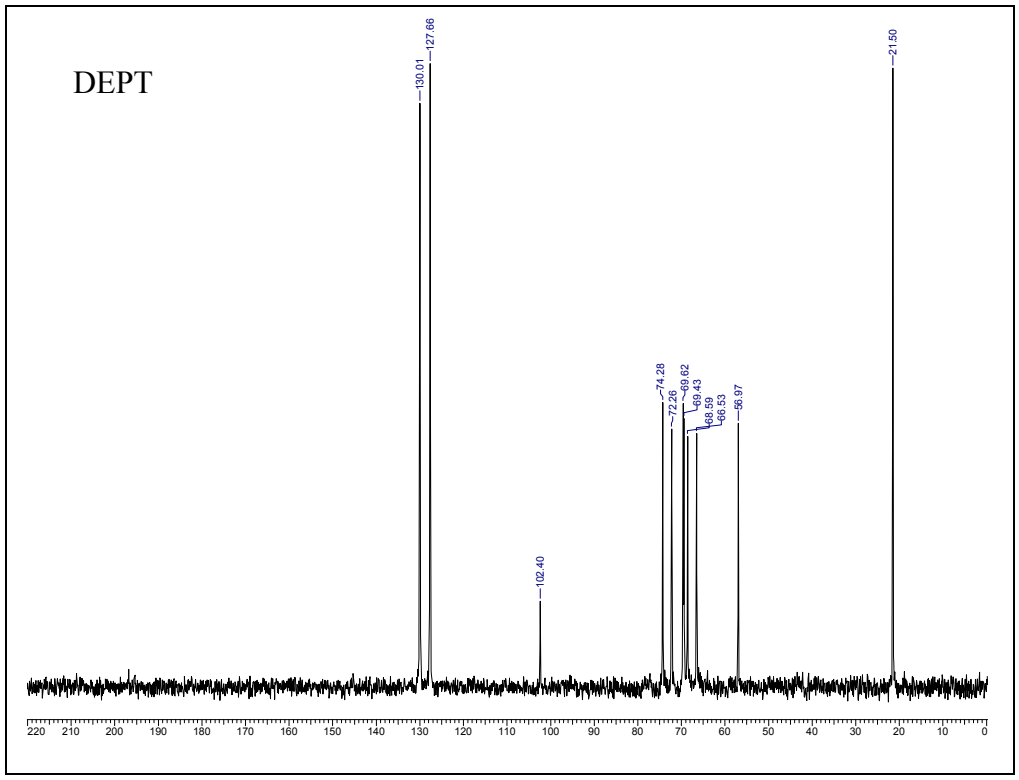
DEPT
130.01
127.66
21.50
74.28
72.26
69.62
69.43
68.59
66.53
56.97
102.40
220 210 200 190 180 170 160 150 140 130 120 110 100 90 80 70 60 50 40 30 20 10 0

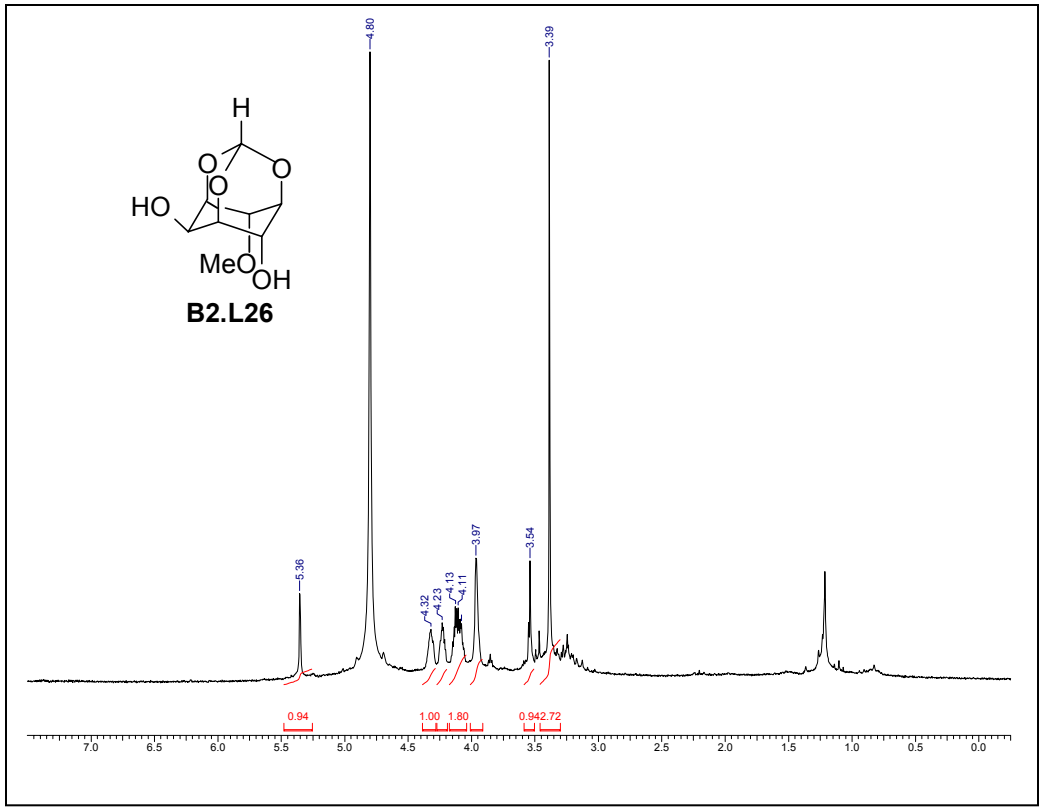
H
O
O
O
HO
MeO
OH
B2.L26
4.80
3.39
5.36
4.32
4.23
4.13
4.11
3.97
3.54
0.94
1.00
1.80
0.94
2.72
7.0 6.5 6.0 5.5 5.0 4.5 4.0 3.5 3.0 2.5 2.0 1.5 1.0 0.5 0.0

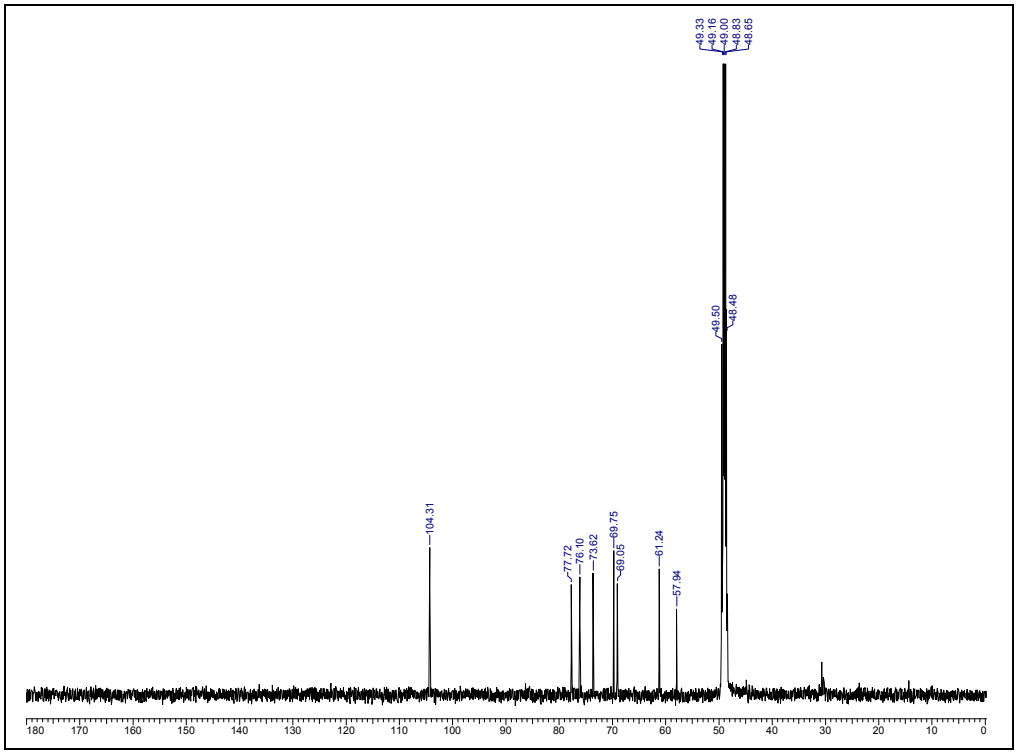
49.33
49.16
49.00
48.83
48.65
49.50
48.48
104.31
77.72
76.10
73.62
69.75
69.05
61.24
57.94
180 170 160 150 140 130 120 110 100 90 80 70 60 50 40 30 20 10 0

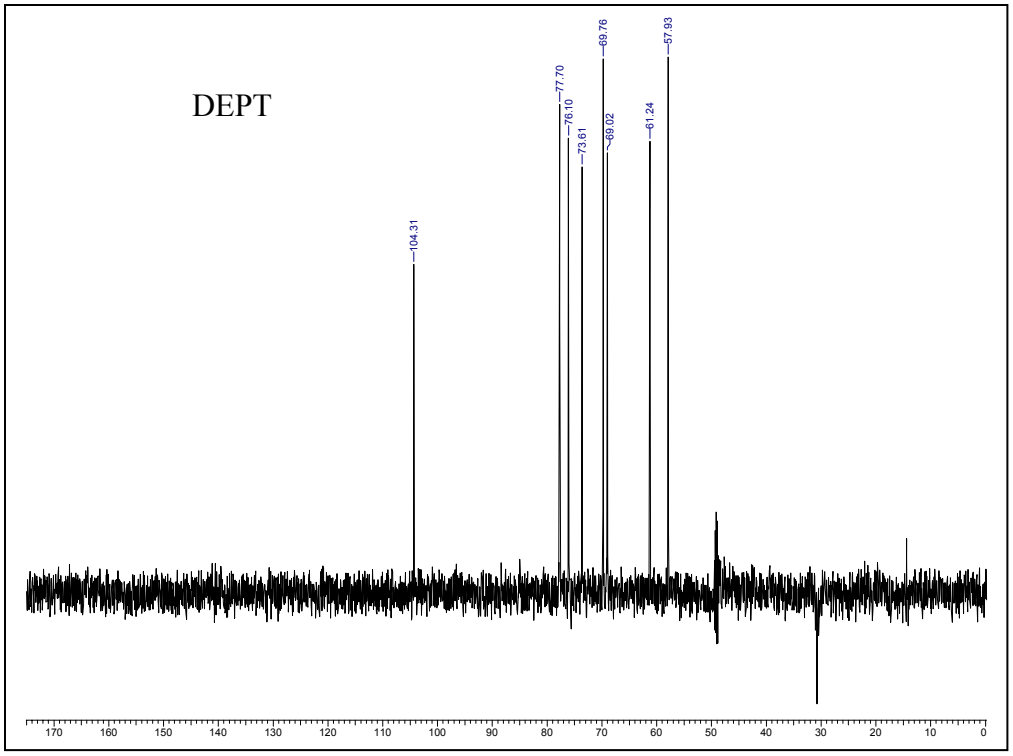
DEPT
69.76
57.93
77.70
76.10
73.61
69.02
61.24
104.31
170 160 150 140 130 120 110 100 90 80 70 60 50 40 30 20 10 0

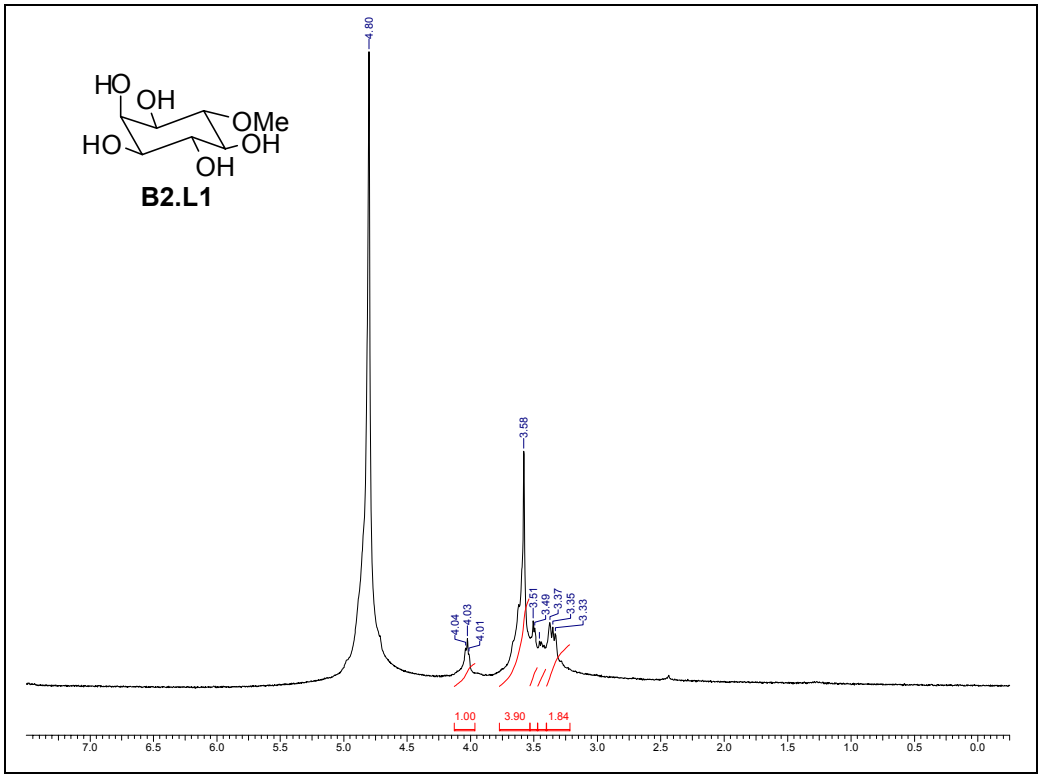
HO
OH
OMe
HO
OH
OH
B2.L1
4.80
3.58
4.04
4.03
4.01
3.51
3.49
3.37
3.35
3.33
1.00
3.90
1.84
7.0
6.5
6.0
5.5
5.0
4.5
4.0
3.5
3.0
2.5
2.0
1.5
1.0
0.5
0.0

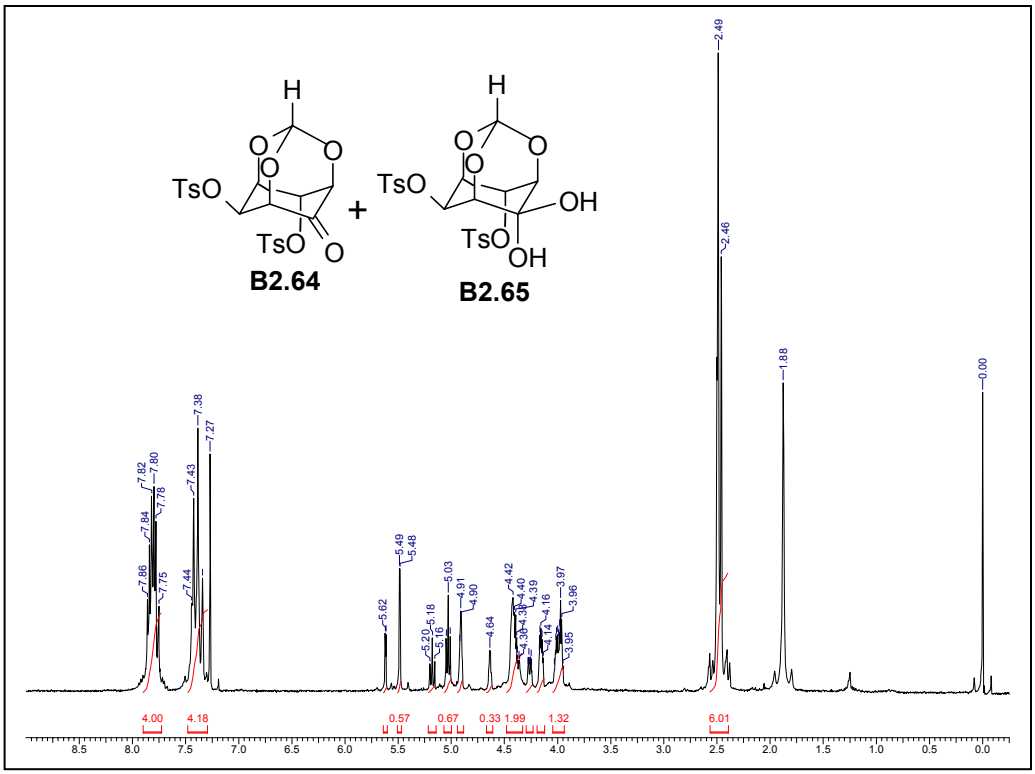
H
O
O
O
TsO
TsO
O
B2.64
+
H
O
O
O
TsO
OH
TsO
OH
B2.65
2.49
2.46
1.88
0.00
7.82
7.80
7.78
7.84
7.86
7.75
7.44
7.43
7.38
7.27
5.49
5.48
5.62
5.20
5.18
5.16
5.03
4.91
4.90
4.64
4.42
4.40
4.39
4.38
4.16
4.14
3.97
3.96
3.95
4.00
4.18
0.57
0.67
0.33
1.99
1.32
6.01

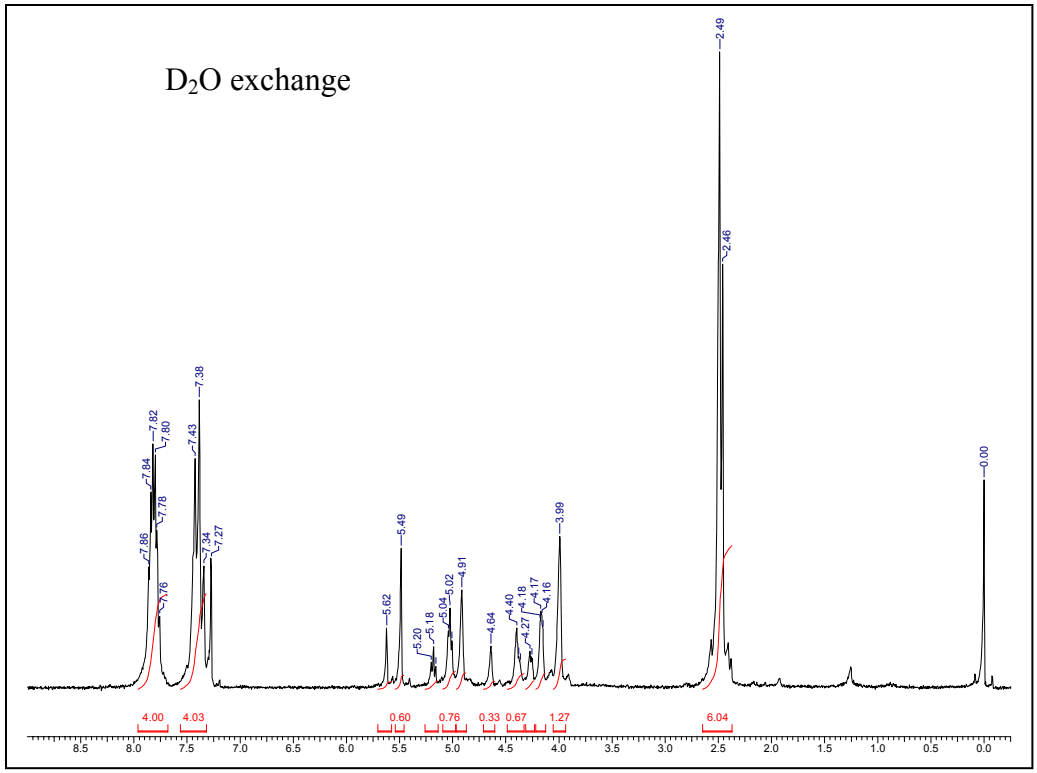
D2O exchange
2.49
2.46
0.00
7.82
7.80
7.84
7.78
7.86
7.76
7.43
7.38
7.34
7.27
5.49
5.62
5.20
5.18
5.04
5.02
4.91
4.64
4.40
4.27
4.18
4.17
4.16
3.99
4.00
4.03
0.60
0.76
0.33
0.67
1.27
6.04

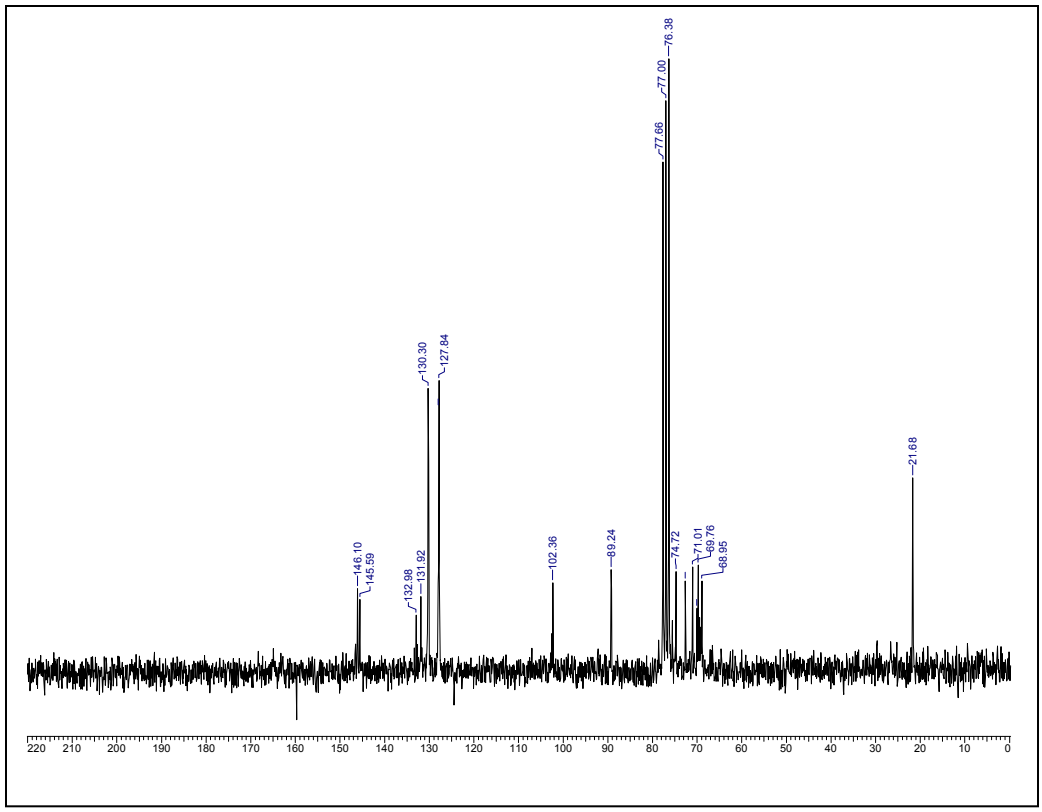
76.38
77.00
77.66
130.30
127.84
21.68
146.10
145.59
132.98
131.92
102.36
89.24
74.72
71.01
69.76
68.95
220 210 200 190 180 170 160 150 140 130 120 110 100 90 80 70 60 50 40 30 20 10 0

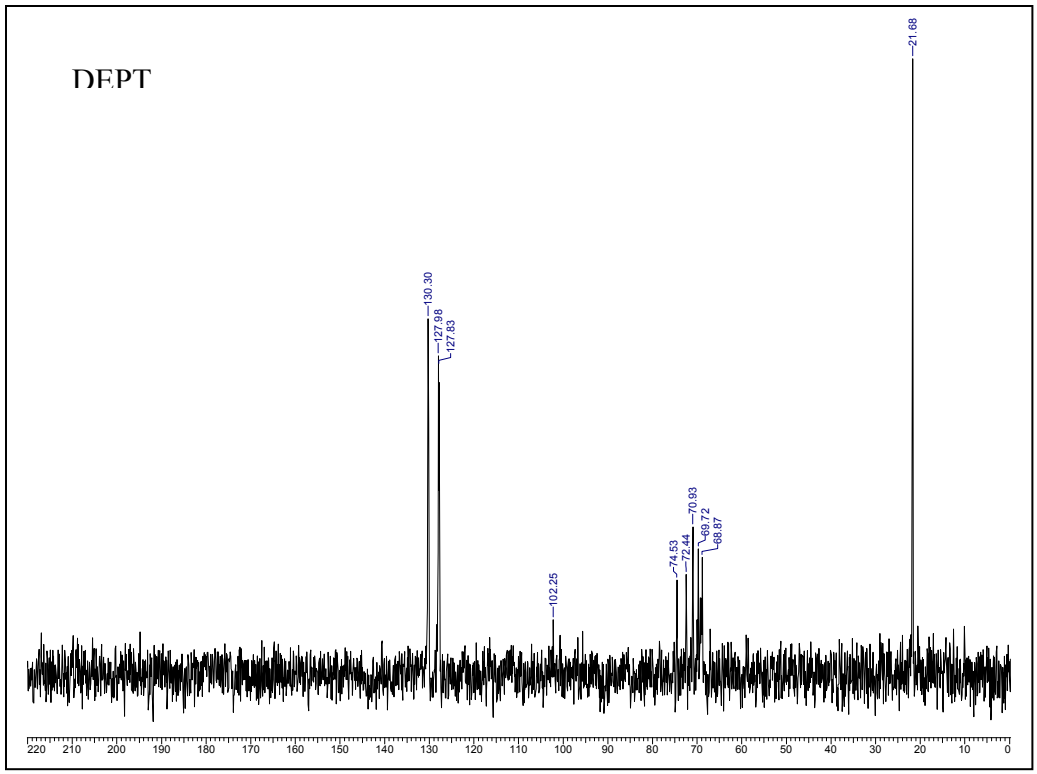
DEPT
21.68
130.30
127.98
127.83
102.25
74.53
72.44
70.93
69.72
68.87
220 210 200 190 180 170 160 150 140 130 120 110 100 90 80 70 60 50 40 30 20 10 0

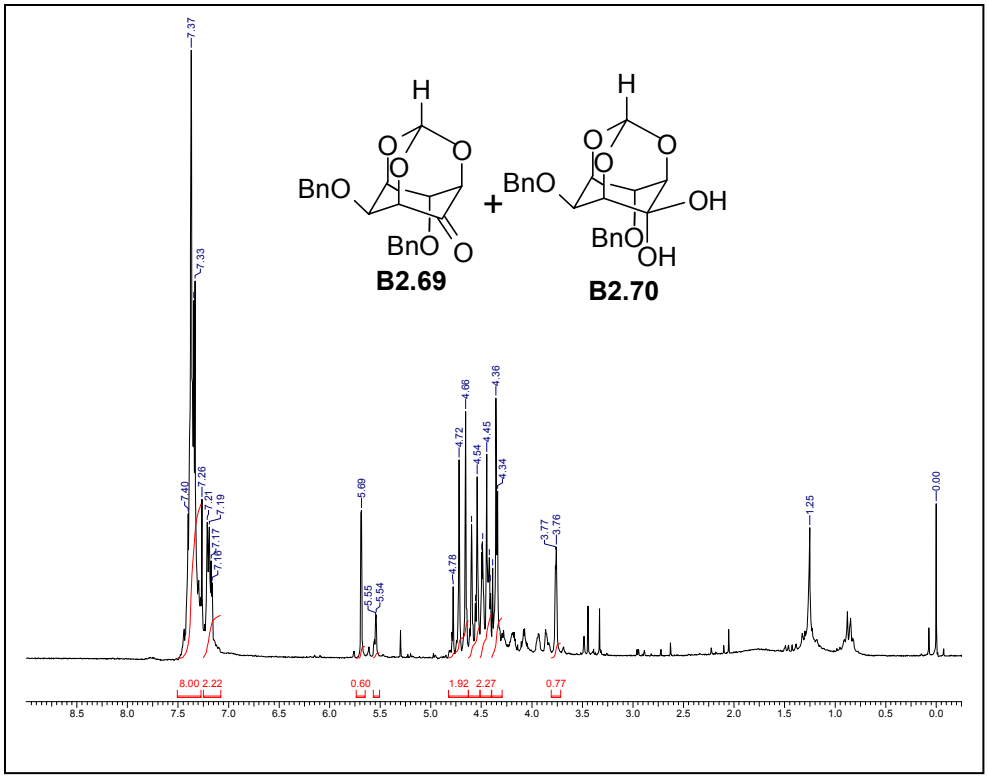
H
O
O
O
BnO
BnO
O
B2.69
+
H
O
O
O
BnO
OH
BnO
OH
B2.70
7.37
7.33
7.40
7.26
7.21
7.19
7.17
7.16
5.69
5.55
5.54
4.78
4.72
4.66
4.54
4.45
4.36
4.34
3.77
3.76
1.25
0.00
8.00
2.22
0.60
1.92
2.27
0.77

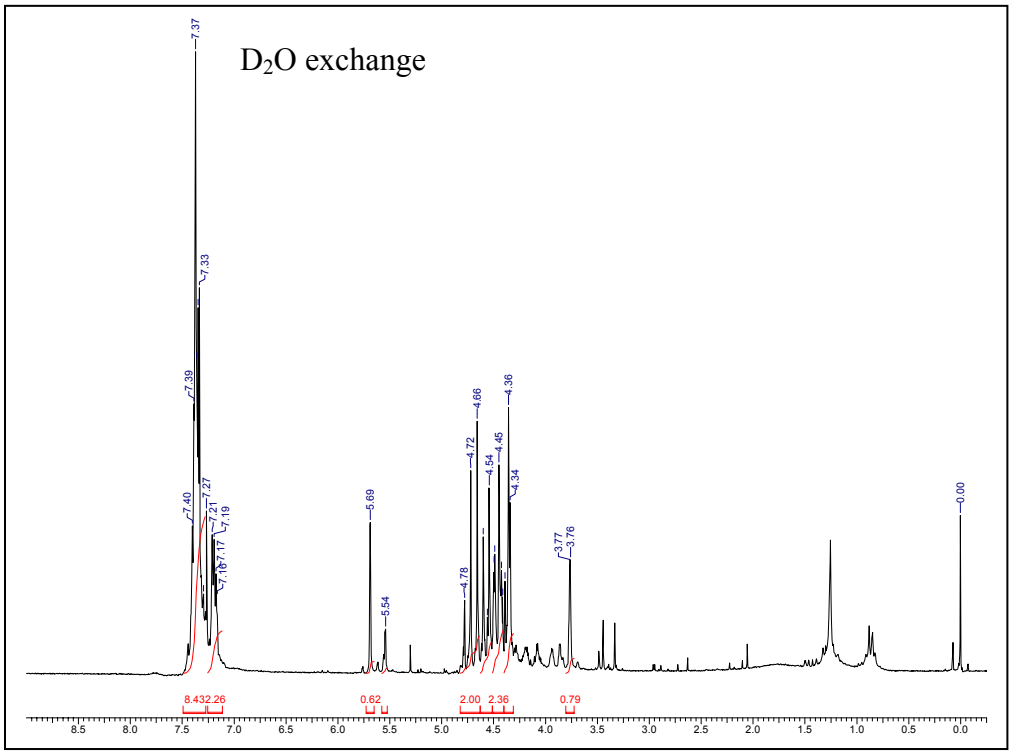
D2O exchange
7.37
7.33
7.39
7.40
7.27
7.21
7.19
7.17
7.16
5.69
5.54
4.78
4.72
4.66
4.54
4.45
4.36
4.34
3.77
3.76
0.00
8.43
2.26
0.62
2.00
2.36
0.79

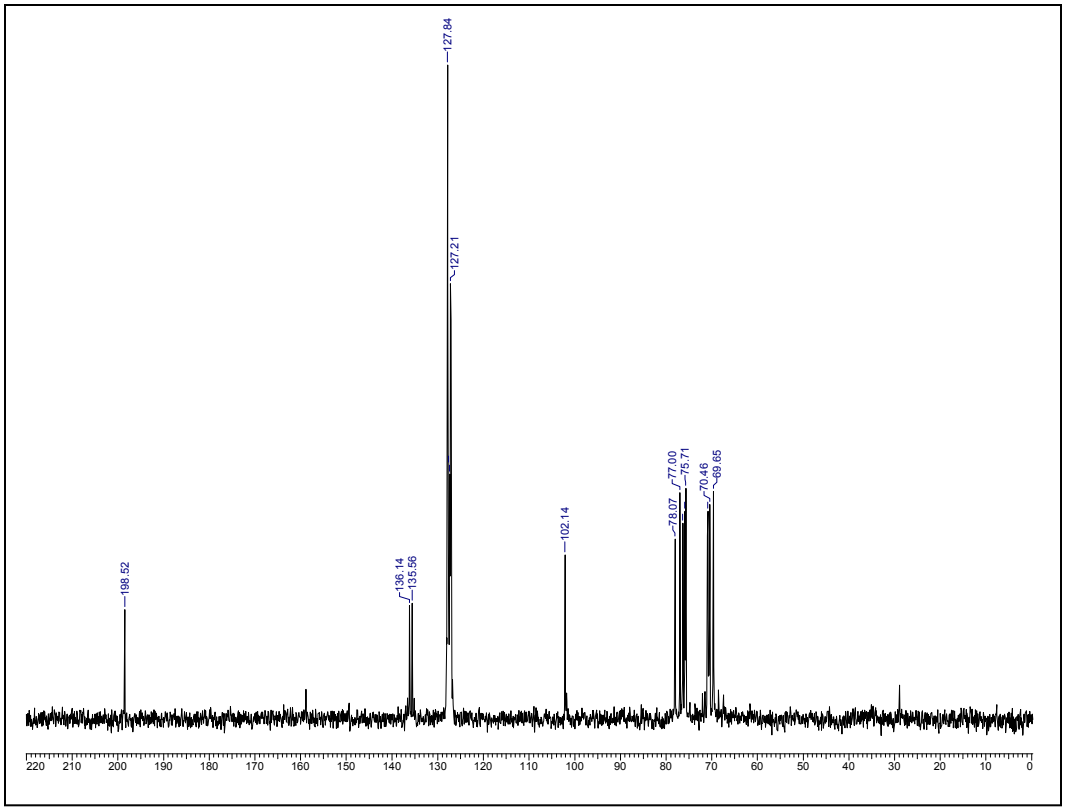
127.84
127.21
198.52
136.14
135.56
102.14
78.07
77.00
75.71
70.46
69.85
220 210 200 190 180 170 160 150 140 130 120 110 100 90 80 70 60 50 40 30 20 10 0

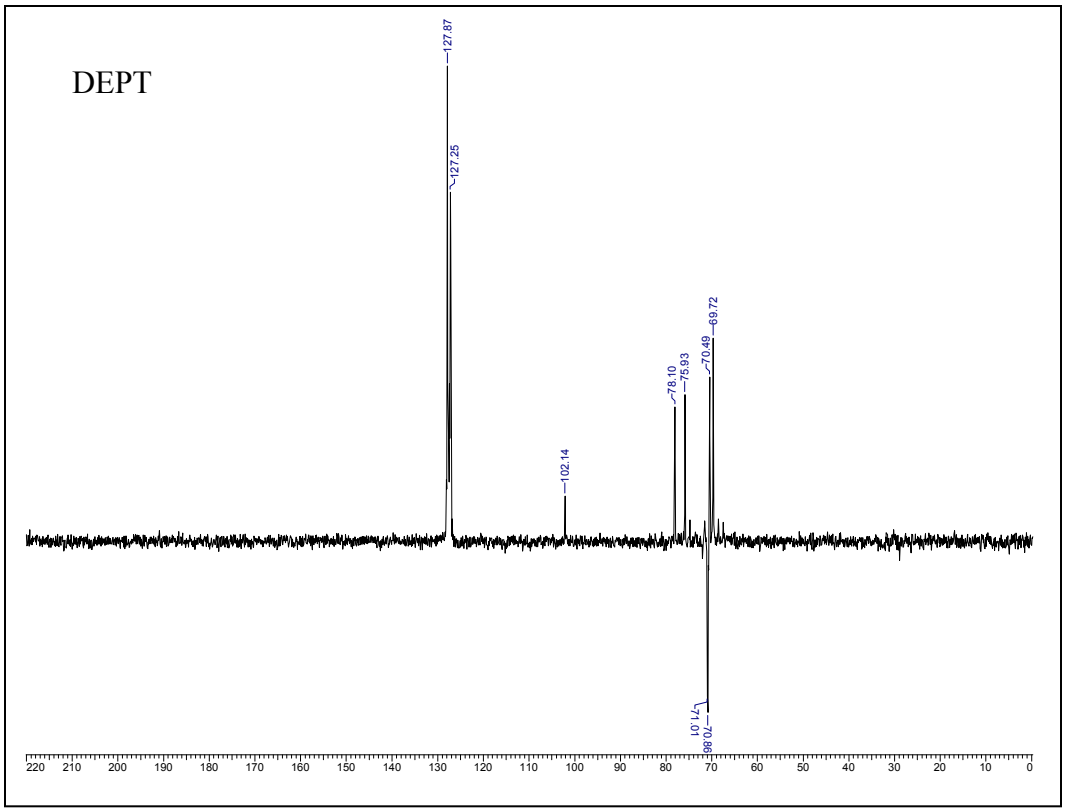
DEPT
127.87
127.25
102.14
78.10
75.93
70.49
69.72
71.01
70.86
220 210 200 190 180 170 160 150 140 130 120 110 100 90 80 70 60 50 40 30 20 10 0

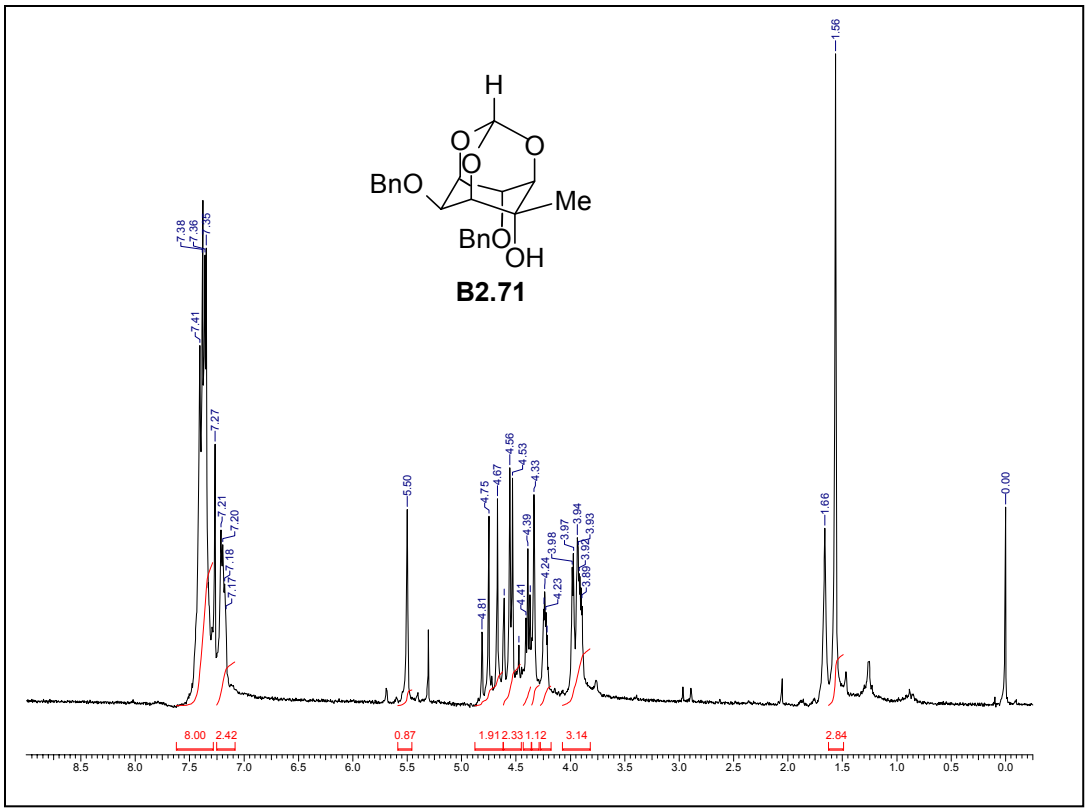
H
O
O
O
BnO
Me
BnO
OH
B2.71
1.56
7.38
7.36
7.35
7.41
7.27
7.21
7.20
7.18
7.17
5.50
4.75
4.67
4.56
4.53
4.33
4.39
3.98
3.97
3.94
3.93
3.92
4.24
4.23
4.41
4.81
3.89
1.66
0.00
8.00
2.42
0.87
1.91
2.33
1.12
3.14
2.84

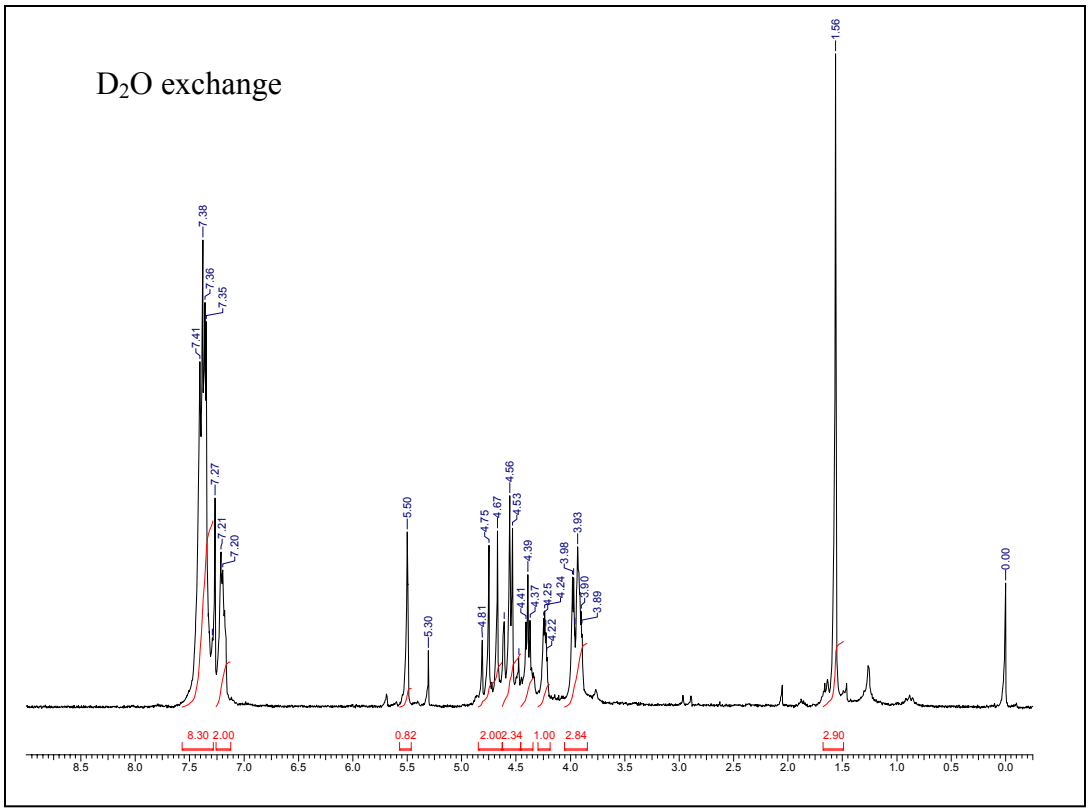
D2O exchange
1.56
7.38
7.36
7.35
7.41
7.27
7.21
7.20
5.50
5.30
4.75
4.67
4.56
4.53
4.39
4.81
4.41
4.37
4.25
4.24
4.22
3.98
3.93
3.90
3.88
0.00
8.30
2.00
0.82
2.00
2.34
1.00
2.84
2.90

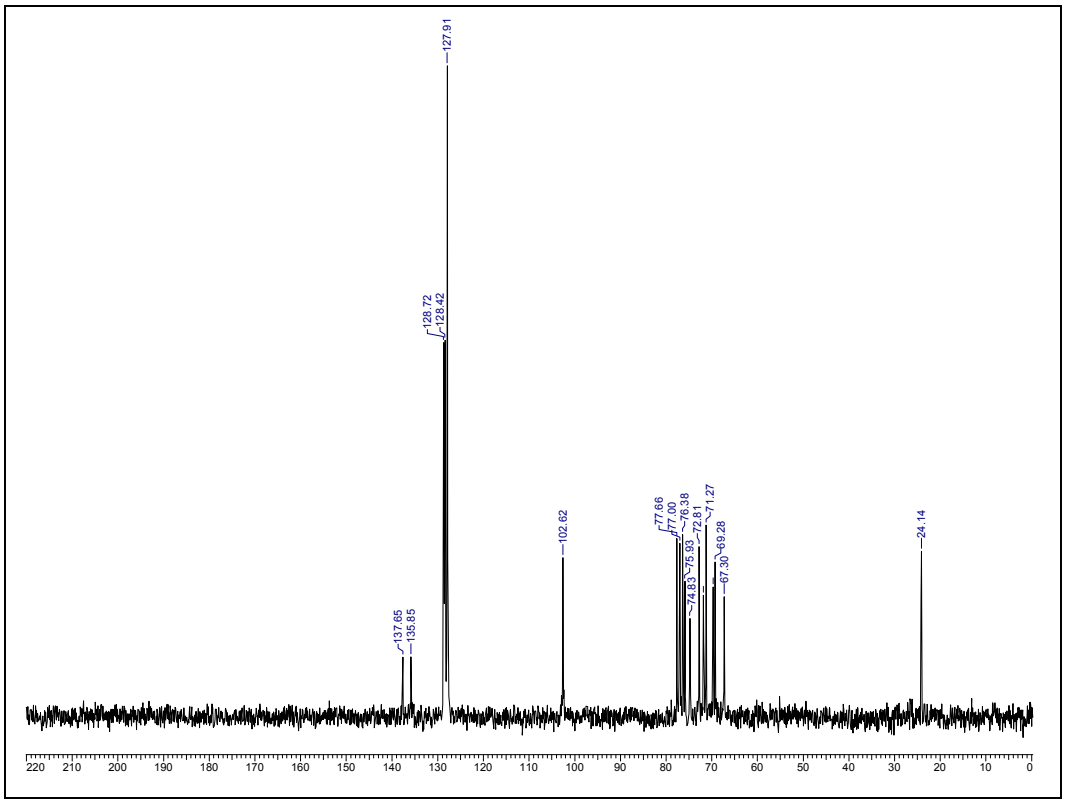
127.91
128.72
128.42
137.65
135.85
102.62
77.66
77.00
76.38
75.83
74.83
72.81
71.27
69.28
67.30
24.14
220 210 200 190 180 170 160 150 140 130 120 110 100 90 80 70 60 50 40 30 20 10 0

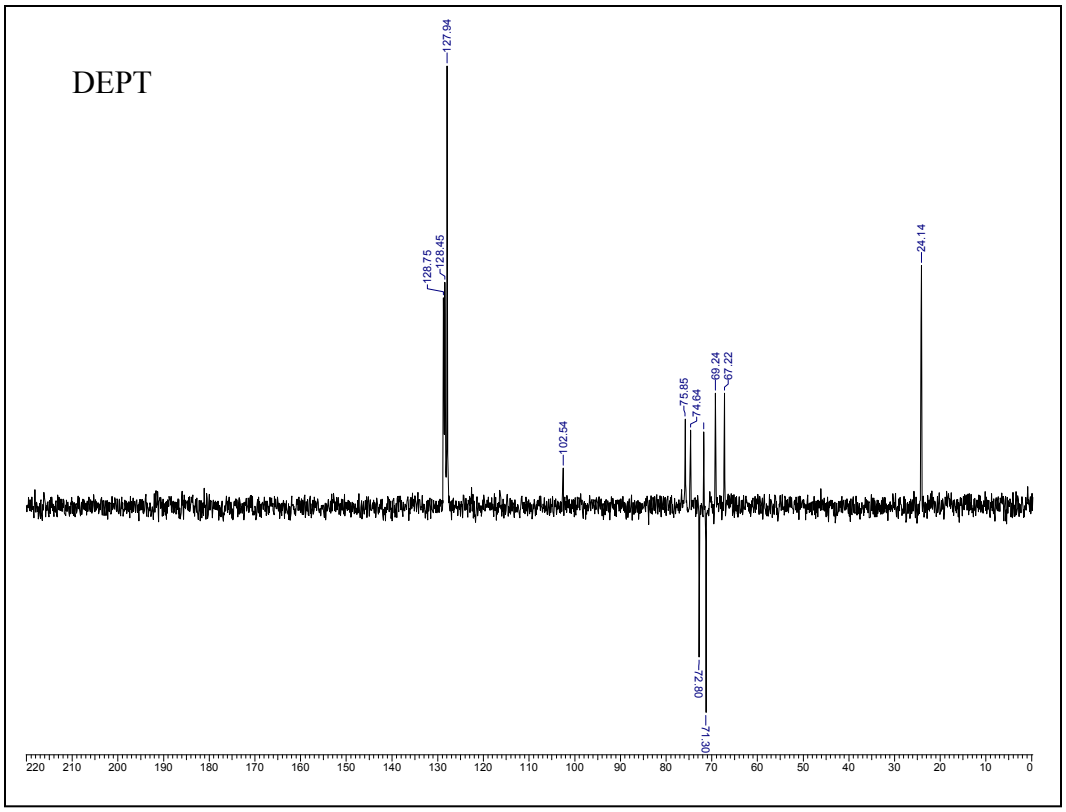
DEPT
127.94
128.75
128.45
102.54
75.85
74.64
69.24
67.22
72.80
71.30
24.14
220 210 200 190 180 170 160 150 140 130 120 110 100 90 80 70 60 50 40 30 20 10 0

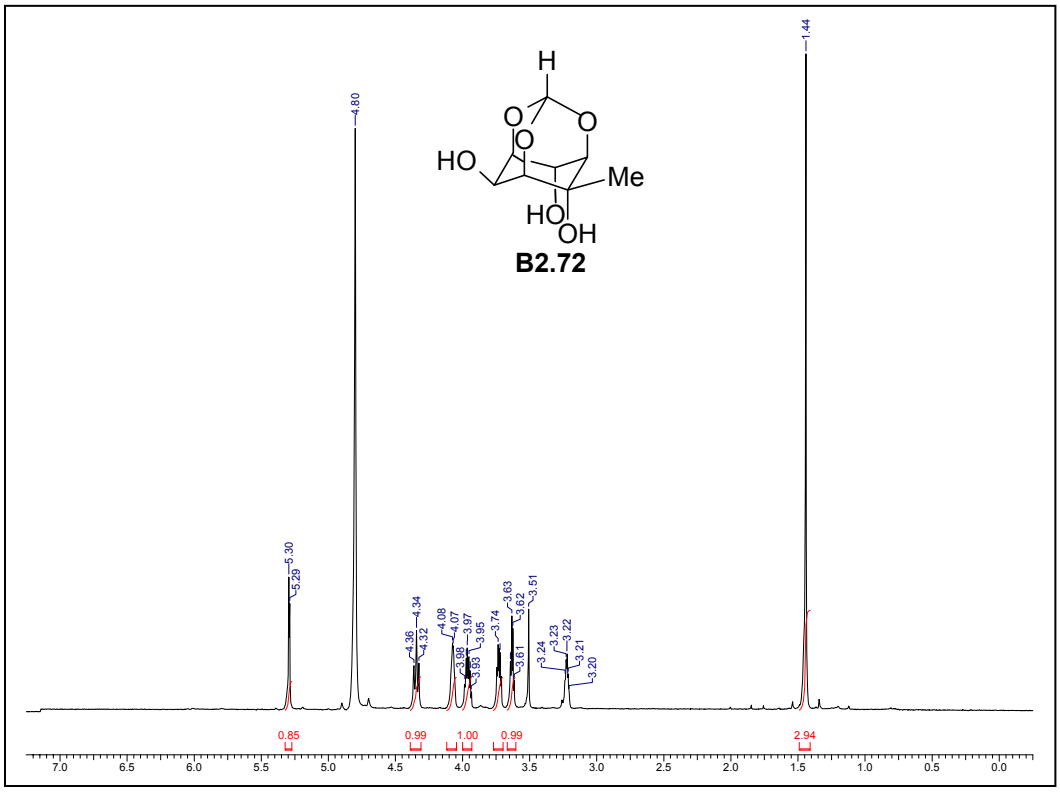
H
O
O
O
HO
Me
HO
OH
B2.72
1.44
4.80
5.30
5.29
4.36
4.34
4.32
4.08
4.07
3.97
3.95
3.93
3.98
3.74
3.63
3.62
3.61
3.51
3.24
3.23
3.22
3.21
3.20
0.85
0.99
1.00
0.99
2.94
7.0
6.5
6.0
5.5
5.0
4.5
4.0
3.5
3.0
2.5
2.0
1.5
1.0
0.5
0.0

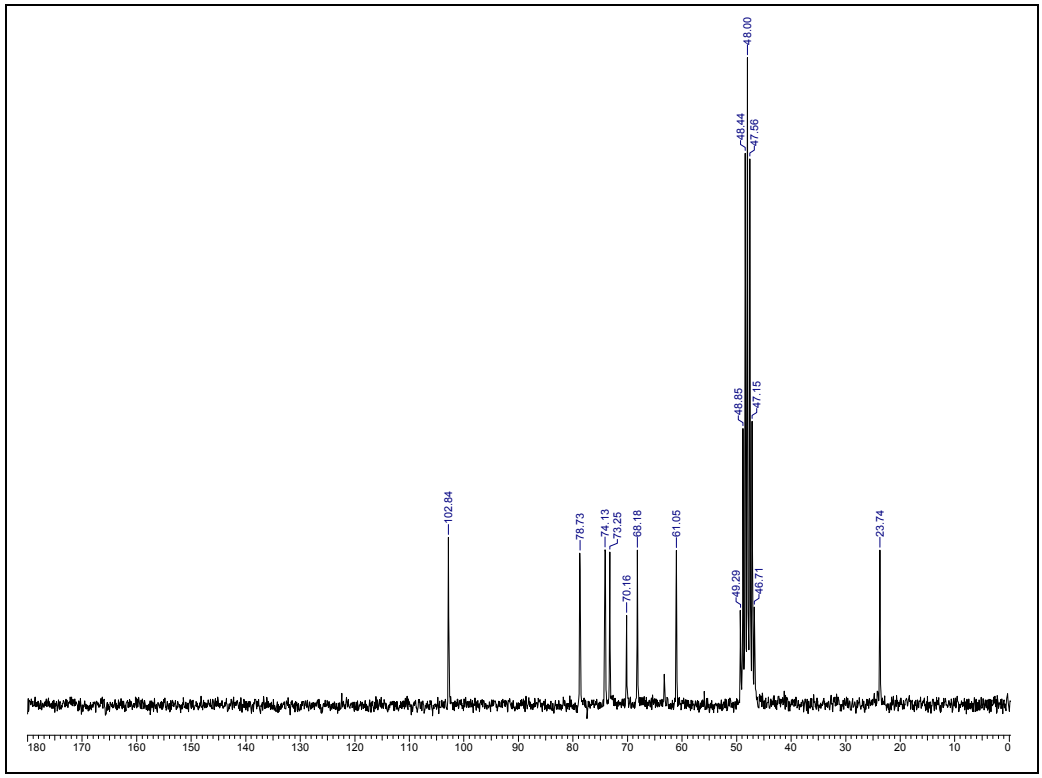
48.00
48.44
47.56
48.85
47.15
102.84
78.73
74.13
73.25
68.18
61.05
70.16
49.29
46.71
23.74
180 170 160 150 140 130 120 110 100 90 80 70 60 50 40 30 20 10 0

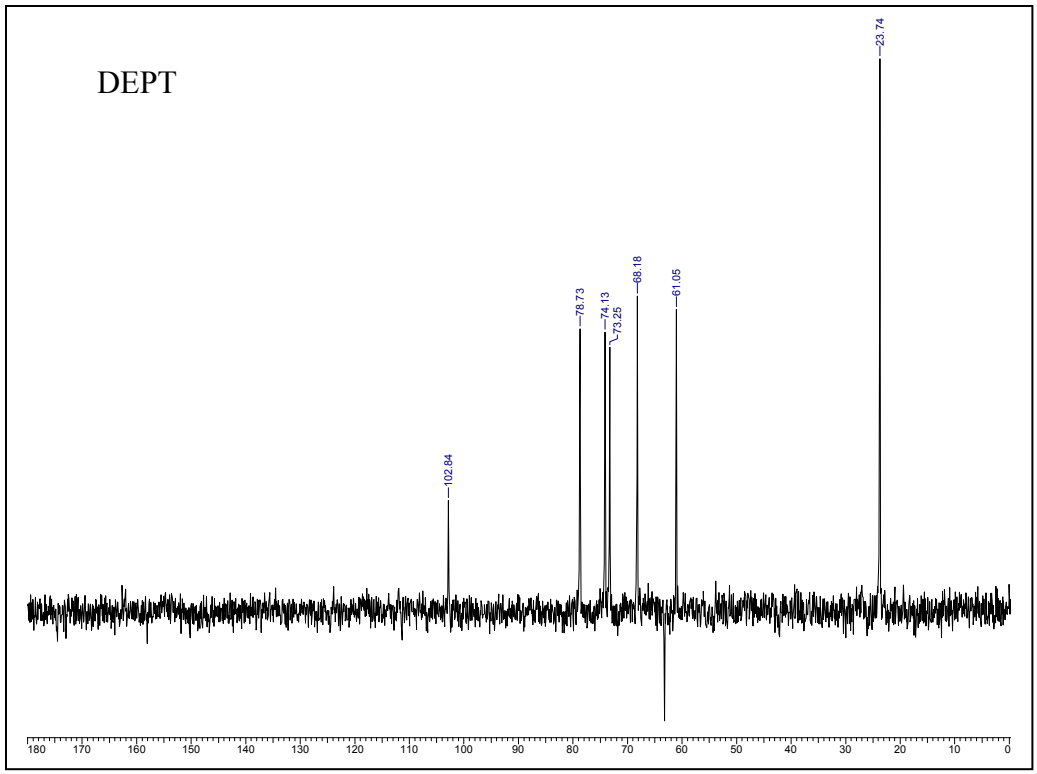
DEPT
23.74
78.73
74.13
73.25
68.18
61.05
102.84
180 170 160 150 140 130 120 110 100 90 80 70 60 50 40 30 20 10 0

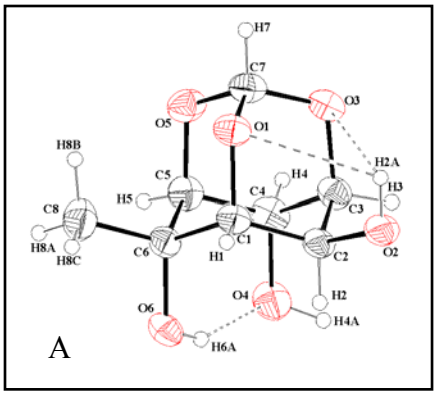

ORTEPs of **B2.72,** (A) from ethyl acetate (B) from Methanol

Crystal data table of **B2.72**

Identification code	**B2.72** (from EtOAc)	**B2.72** (from MeOH)
Empirical formula, formula weight	$C_8H_{12}O_6$, 204.18	$C_8H_{12}O_6$, 204.18
Crystal form, colour	Needle, colourless	Plate, colourless
Crystal size (mm)	0.62 × 0.25 × 0.22	0.57 × 0.27 × 0.22
Wavelength	0.71073 Å	0.71073 Å
Temperature (K)	293(2) K	293(2) K
Crystal system, space group	Monoclinic, $P2_1/n$	Orthorhombic, $Pna2_1$
Unit cell dimensions	a = 7.7470(7) Å b = 11.4780 (11) Å c = 9.2812 (9) Å β = 92.905(2)º	a = 11.722(5) Å b = 9.029(4) Å c = 8.155(4) Å
Volume	824.22(13) $Å^3$	863.1(6) $Å^3$
Z, calculated density	4, 1.645 Mg / m^3	4, 1.571 Mg / m^3
F(000)	432	432
Absorption coefficient (μ)	0.143 mm^{-1}	0.136 mm^{-1}
Max. and min. transmission	0.9692 and 0.9165	0.9706 and 0.9263
Refle^n collected / unique / observed	5750 / 1442 / 1337	3847 / 1230 / 1211
θ range for data collections	2.82–25.00º	4.15-25.00º
Limiting indices	-9⇐h⇒9 -13⇐k⇒13 -11⇐l⇒11	-13⇐h⇒6 -10⇐k⇒9 -6⇐l⇒9
Goodness-of-fit on F^2	1.063	1.073
Final R indices [I >2σ(I)]	R1 = 0.0337, wR2 = 0.0887	R1 = 0. 0282, wR2 = 0. 0734
R indices [all data]	R1 = 0.0356, wR2 = 0.0907	R1 = 0.0285, wR2 = 0.0738
Data / restraints / parameters	1442/ 0 / 164	1230 / 0 / 175
H-atom treatment	From difference Fourier map	From difference Fourier map
Largest diff. peak and hole ($\rho_{max,}$ & ρ_{min})	0.228 & -0.204 $eÅ^{-3}$	0.154 & -0.162 $eÅ^{-3}$

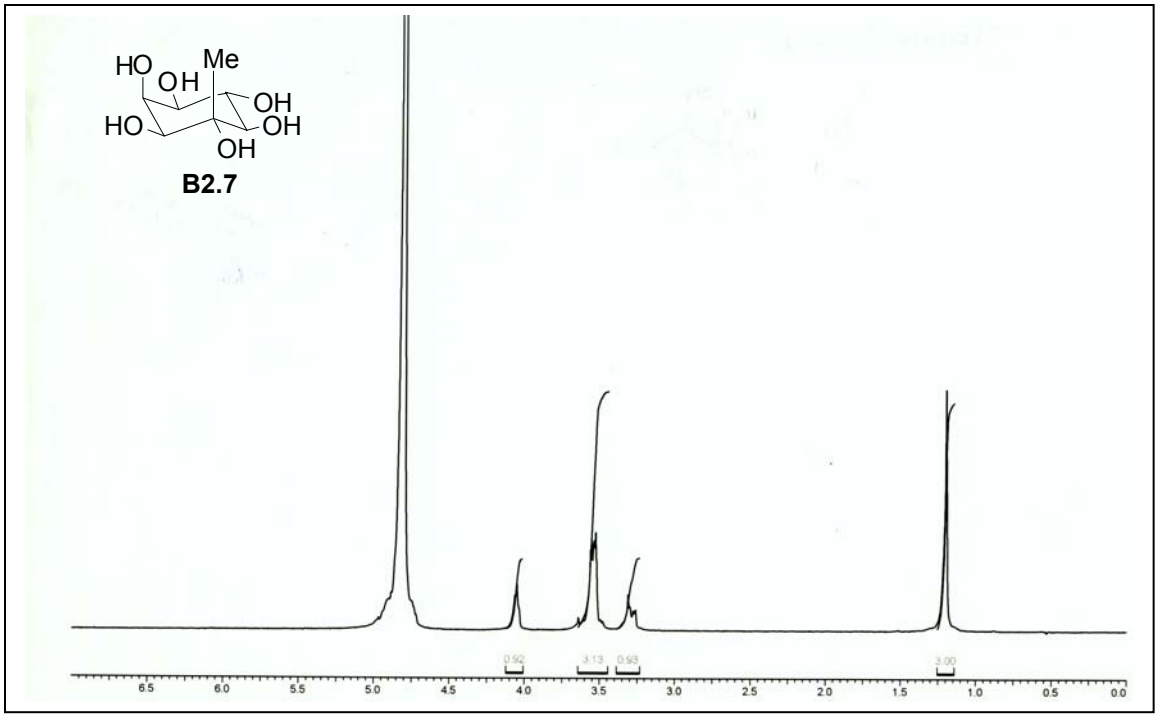
HO
OH
Me
OH
HO
OH
OH
B2.7
0.92
3.13
0.93
3.00
6.5
6.0
5.5
5.0
4.5
4.0
3.5
3.0
2.5
2.0
1.5
1.0
0.5
0.0

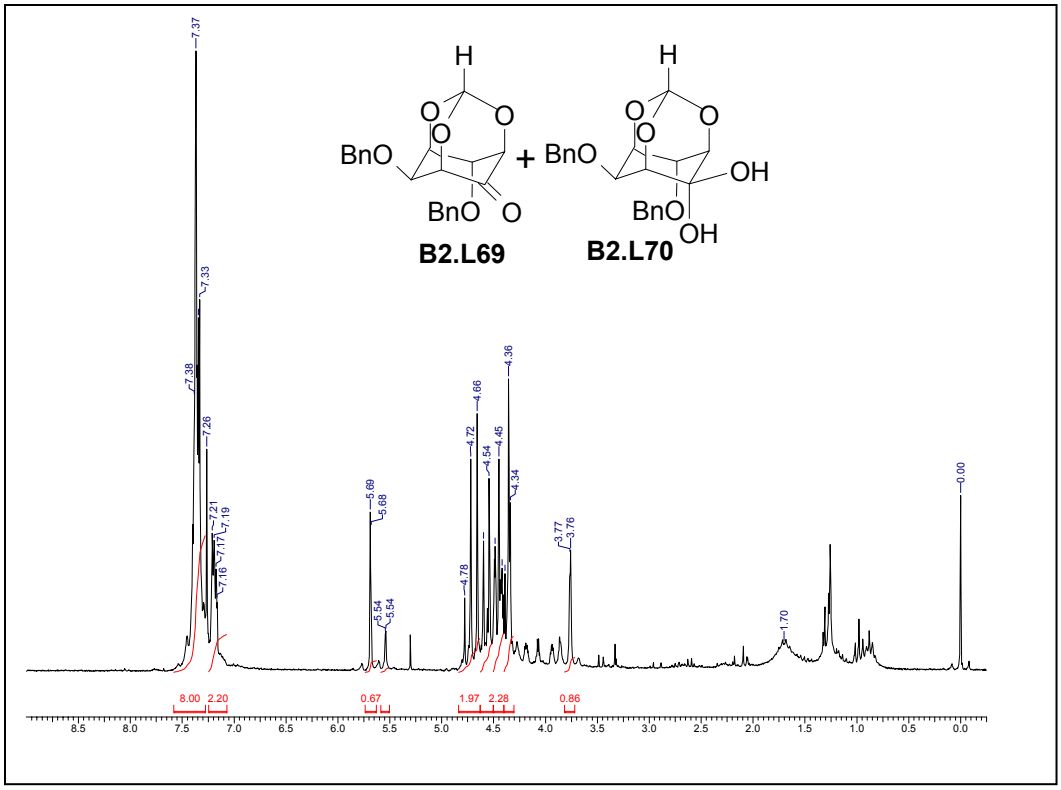
H
O
O
O
BnO
BnO
O
B2.L69
+
H
O
O
O
BnO
OH
BnO
OH
B2.L70
7.37
7.33
7.38
7.26
7.21
7.19
7.17
7.16
5.69
5.68
5.54
5.54
4.78
4.72
4.66
4.54
4.45
4.36
4.34
3.77
3.76
1.70
0.00
8.00
2.20
0.67
1.97
2.28
0.86

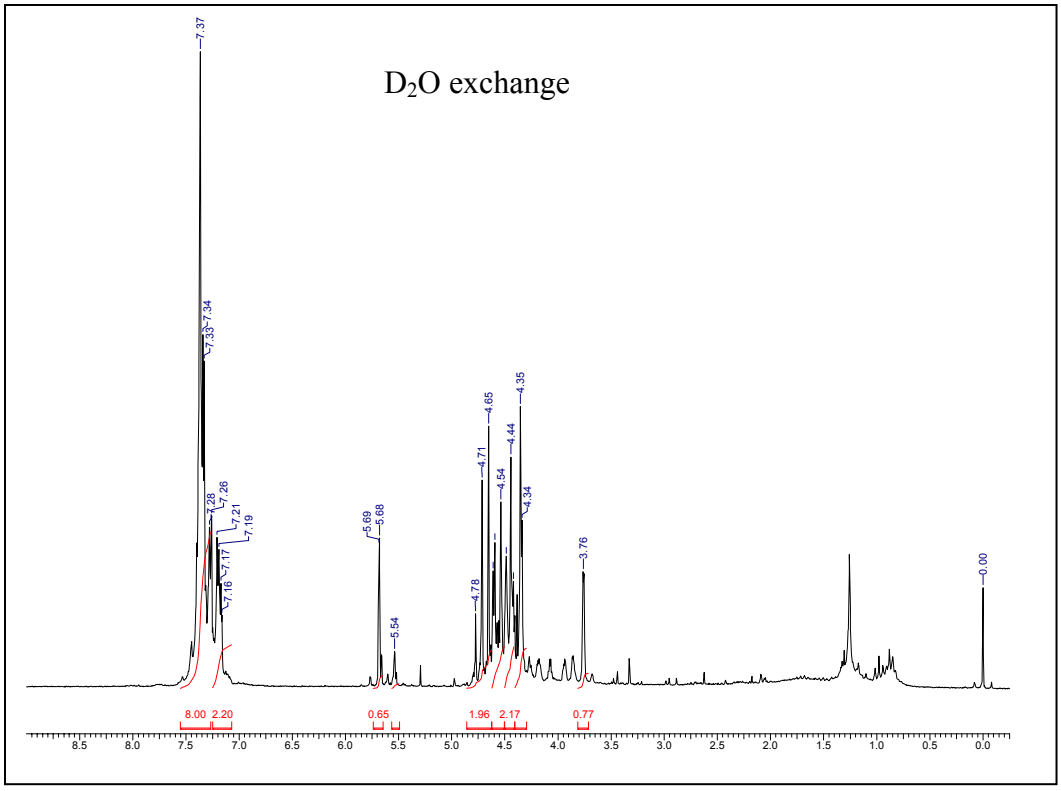
D2O exchange
7.37
7.34
7.33
7.28
7.26
7.21
7.19
7.17
7.16
5.69
5.68
5.54
4.78
4.71
4.65
4.54
4.44
4.35
4.34
3.76
0.00
8.00
2.20
0.65
1.96
2.17
0.77

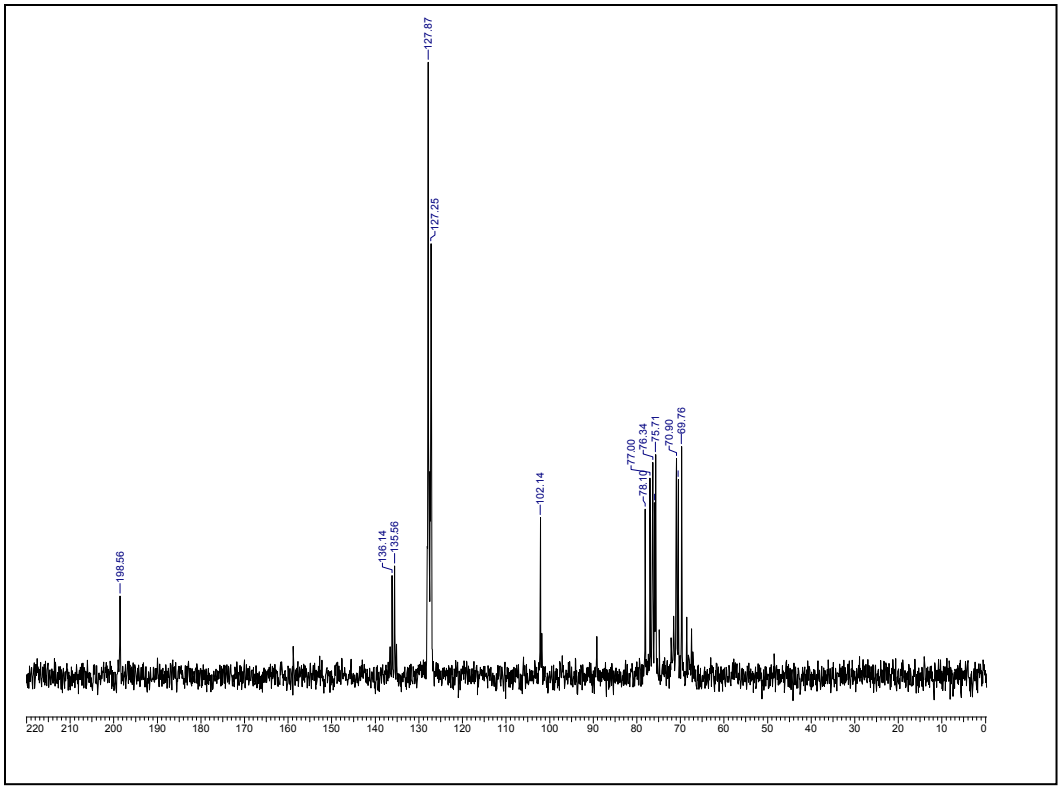
127.87
127.25
102.14
77.00
76.34
75.71
70.90
69.76
78.10
136.14
135.56
198.56
220 210 200 190 180 170 160 150 140 130 120 110 100 90 80 70 60 50 40 30 20 10 0

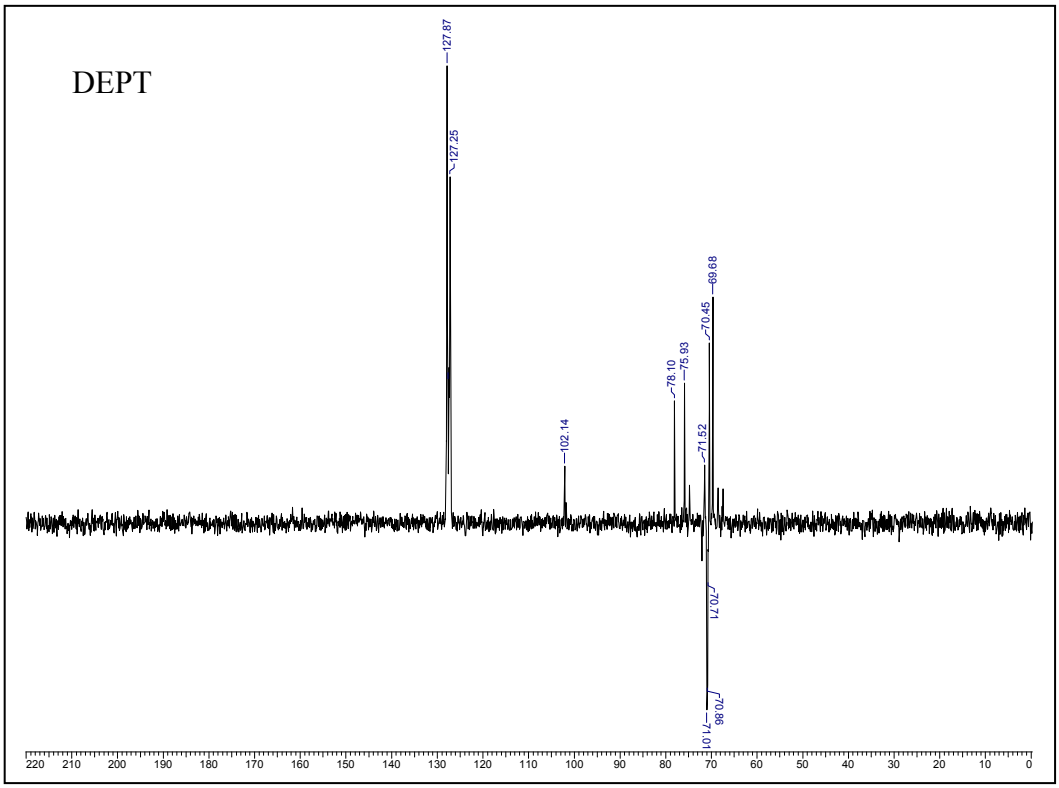
DEPT
127.87
127.25
102.14
78.10
75.93
71.52
70.45
69.68
70.71
70.86
71.01
220 210 200 190 180 170 160 150 140 130 120 110 100 90 80 70 60 50 40 30 20 10 0

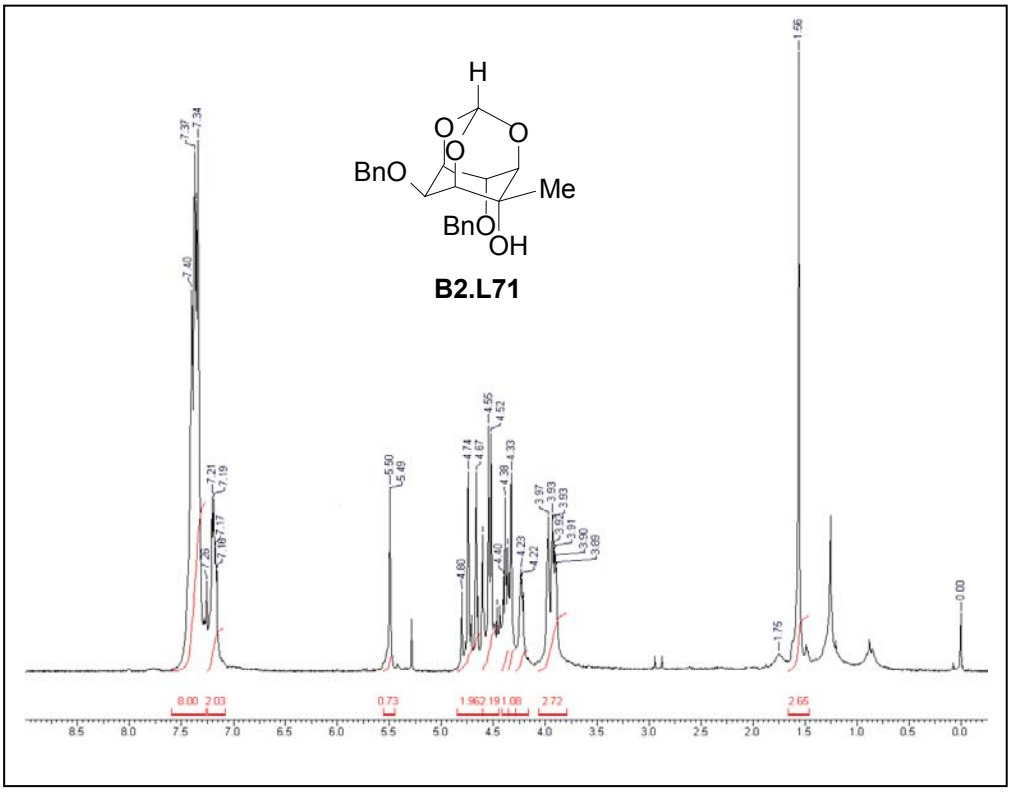
H
O
O
O
O
BnO
Me
BnO
OH
B2.L71

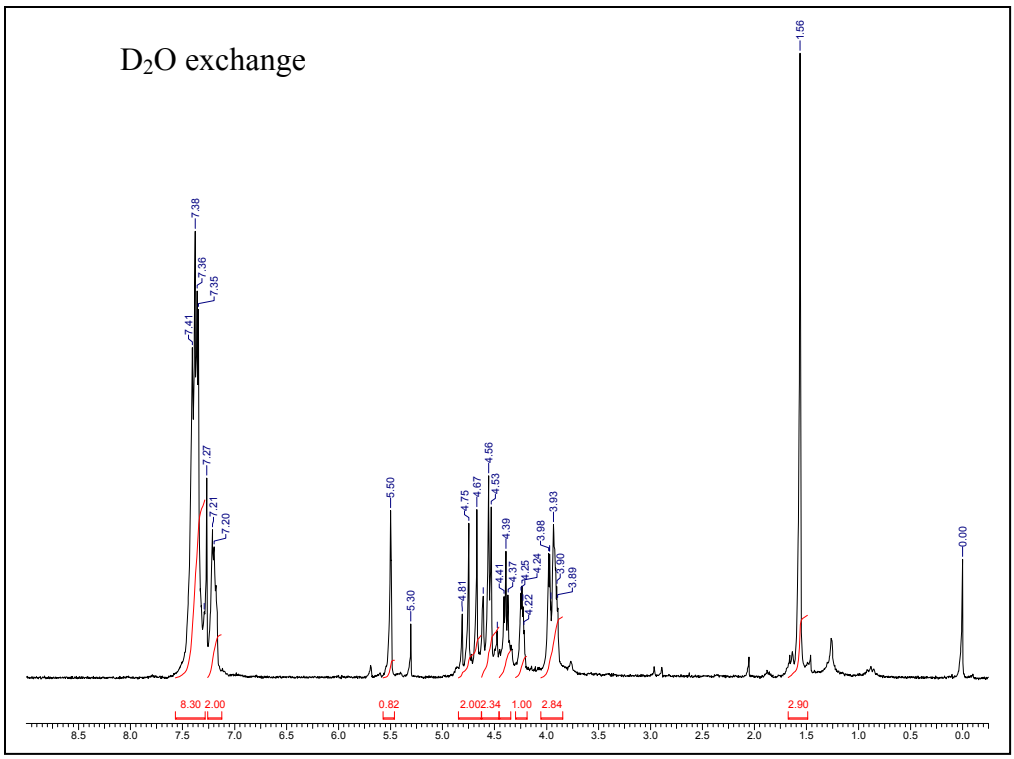
D2O exchange

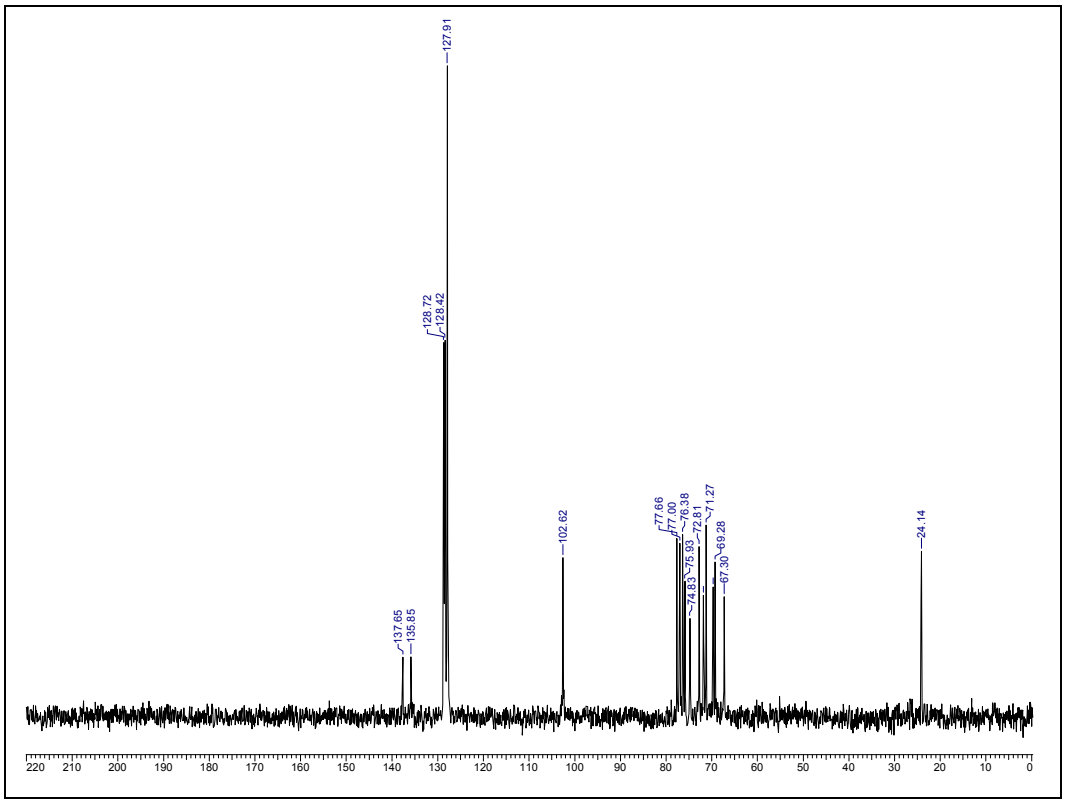
127.91
128.72
128.42
137.65
135.85
102.62
77.66
77.00
76.38
72.81
75.93
74.83
71.27
69.28
67.30
24.14
220 210 200 190 180 170 160 150 140 130 120 110 100 90 80 70 60 50 40 30 20 10 0

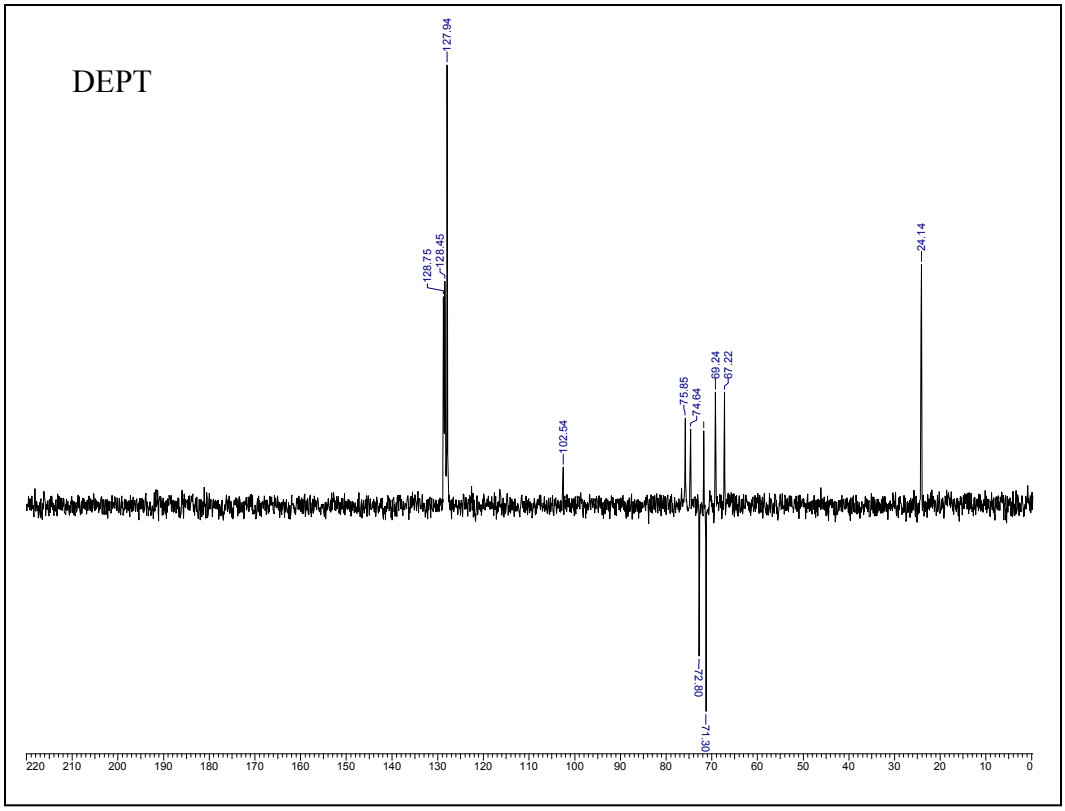
DEPT
127.94
128.75
128.45
24.14
102.54
75.85
74.64
69.24
67.22
72.80
71.30
220 210 200 190 180 170 160 150 140 130 120 110 100 90 80 70 60 50 40 30 20 10 0

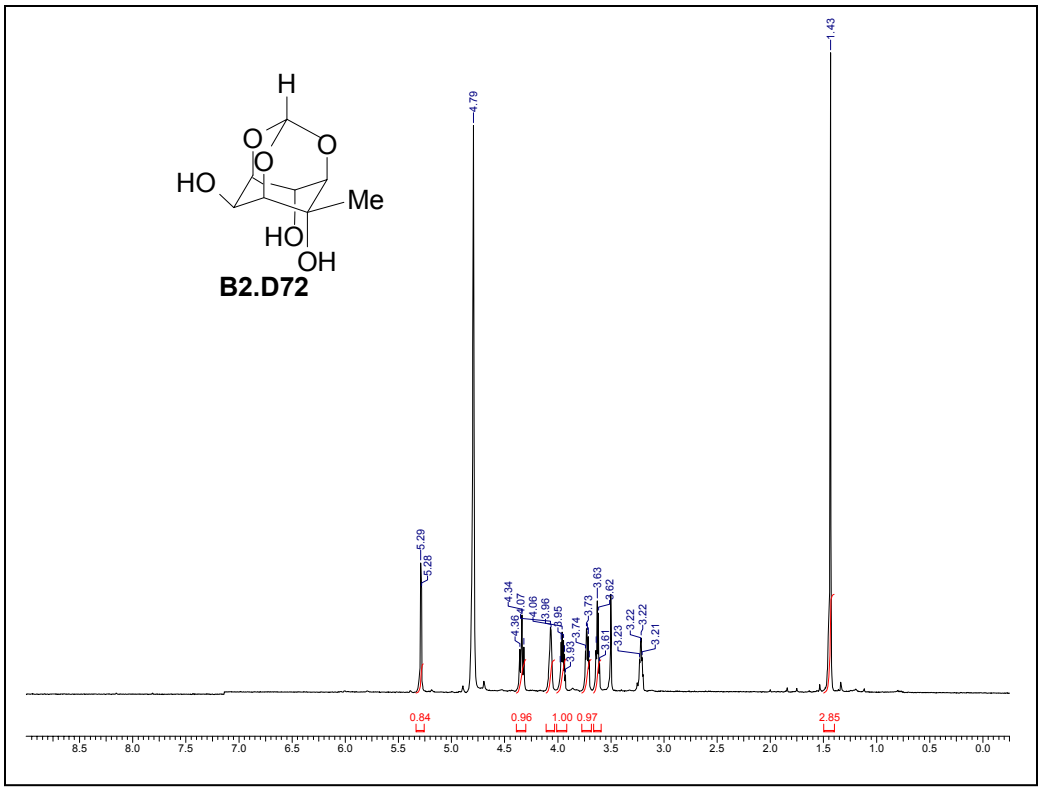
H
O
O
O
HO
Me
HO
OH
B2.D72
1.43
4.79
5.29
5.28
4.34
4.07
4.06
3.96
3.95
3.74
3.73
3.63
3.62
3.23
3.22
3.22
3.21
0.84
0.96
1.00
0.97
2.85

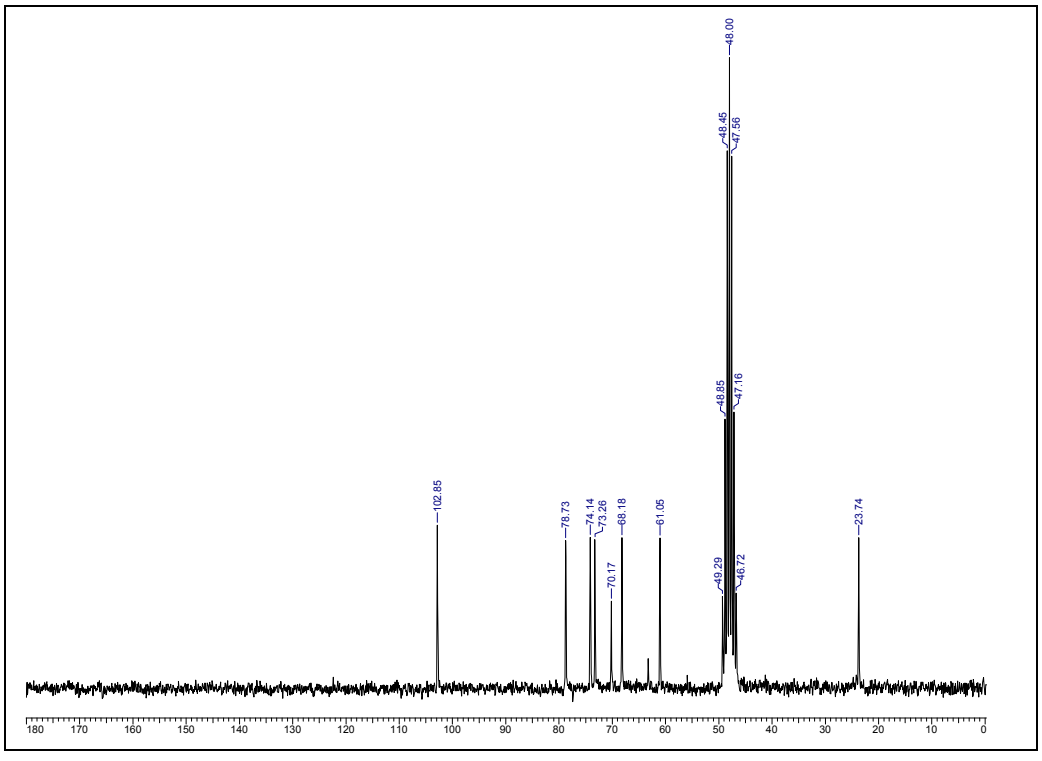
48.00
48.45
47.56
48.85
47.16
102.85
78.73
74.14
73.26
68.18
61.05
49.29
46.72
70.17
23.74

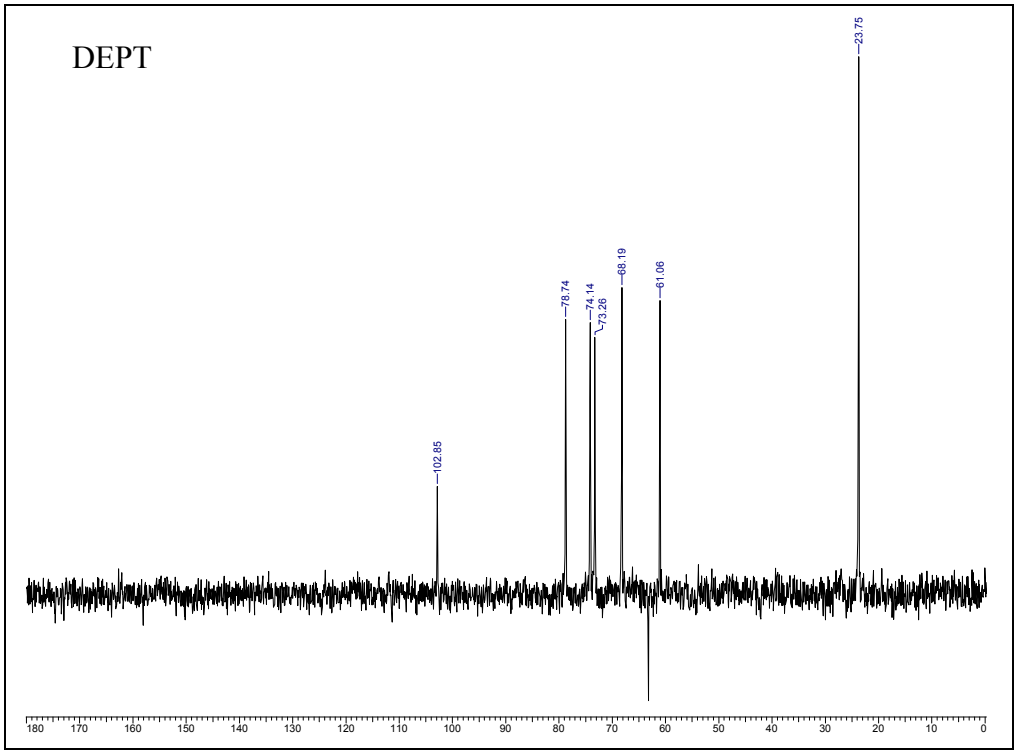
DEPT
23.75
78.74
74.14
73.26
68.19
61.06
102.85
180 170 160 150 140 130 120 110 100 90 80 70 60 50 40 30 20 10 0

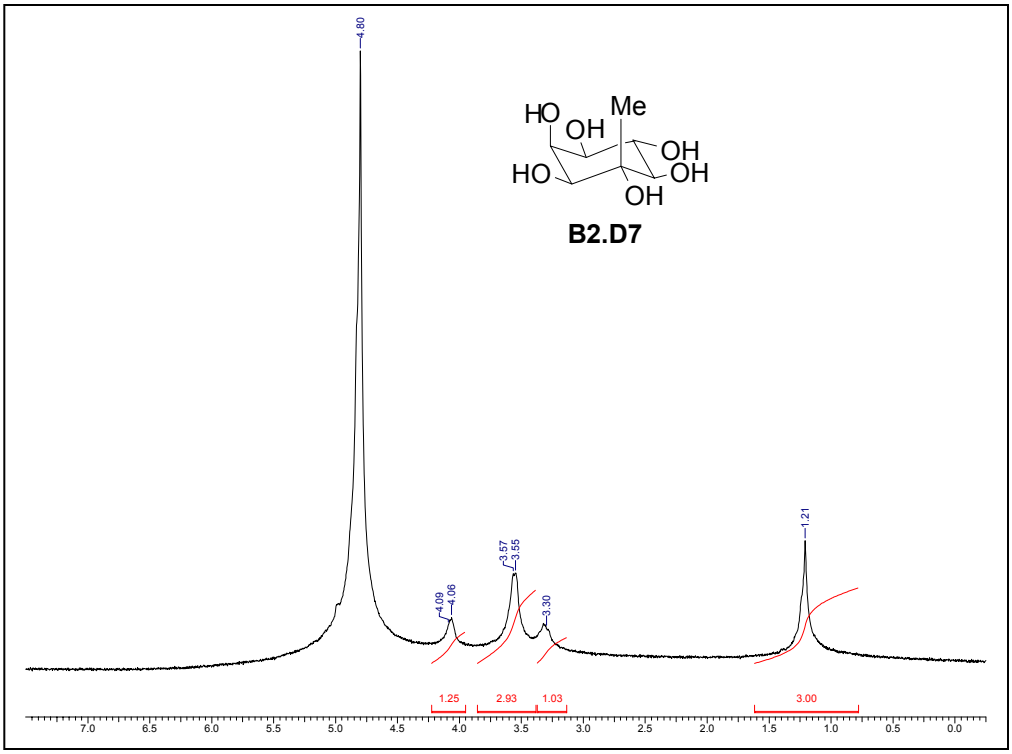
4.80
HO
OH
Me
OH
HO
OH
OH
B2.D7
4.09
4.06
3.67
3.55
3.30
1.21
1.25
2.93
1.03
3.00
7.0 6.5 6.0 5.5 5.0 4.5 4.0 3.5 3.0 2.5 2.0 1.5 1.0 0.5 0.0

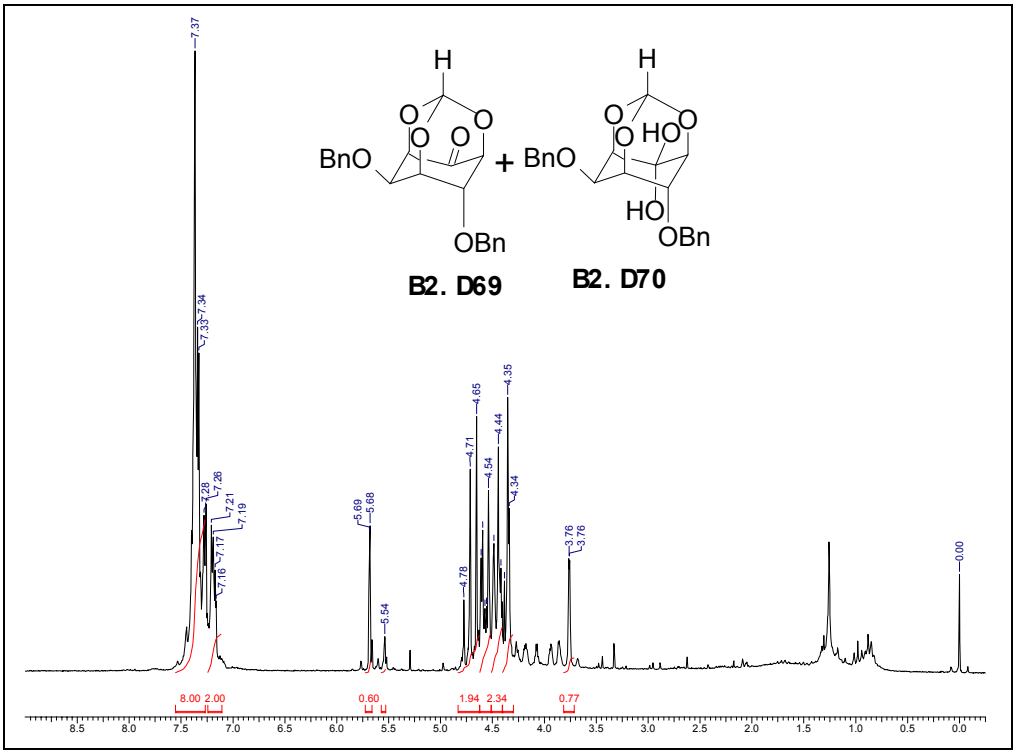
BnO
OBn
+
BnO
HO
HO
OBn
B2. D69
B2. D70

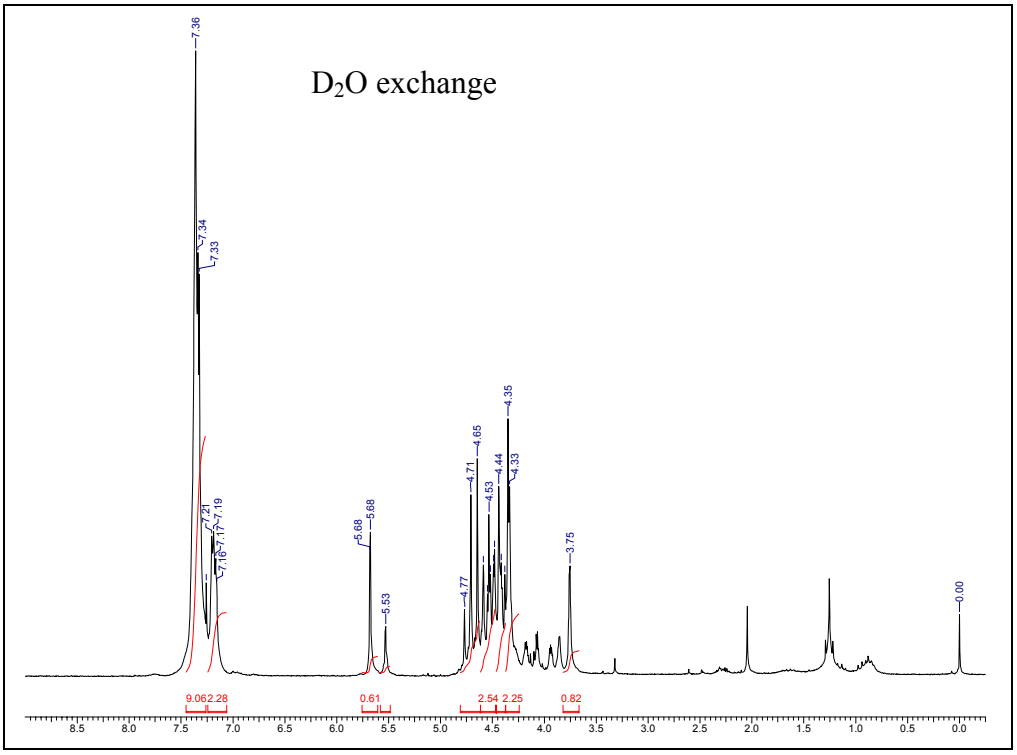
D2O exchange

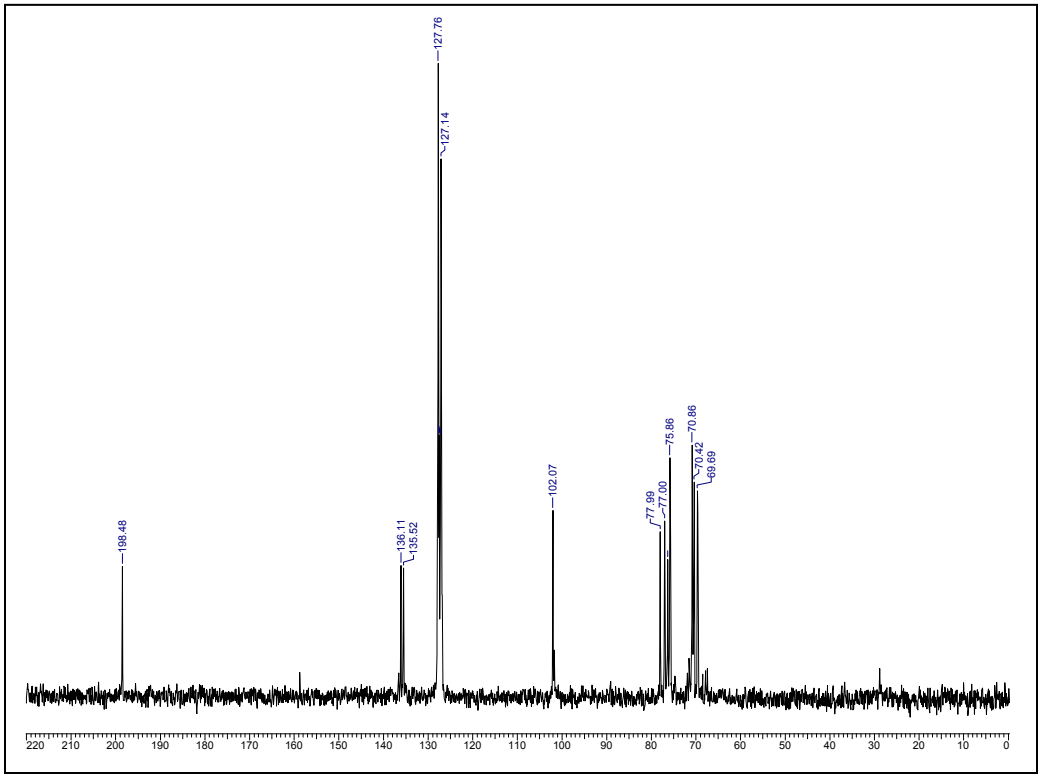
127.76
127.14
198.48
136.11
135.52
102.07
77.99
77.00
75.86
70.86
70.42
69.69
220 210 200 190 180 170 160 150 140 130 120 110 100 90 80 70 60 50 40 30 20 10 0

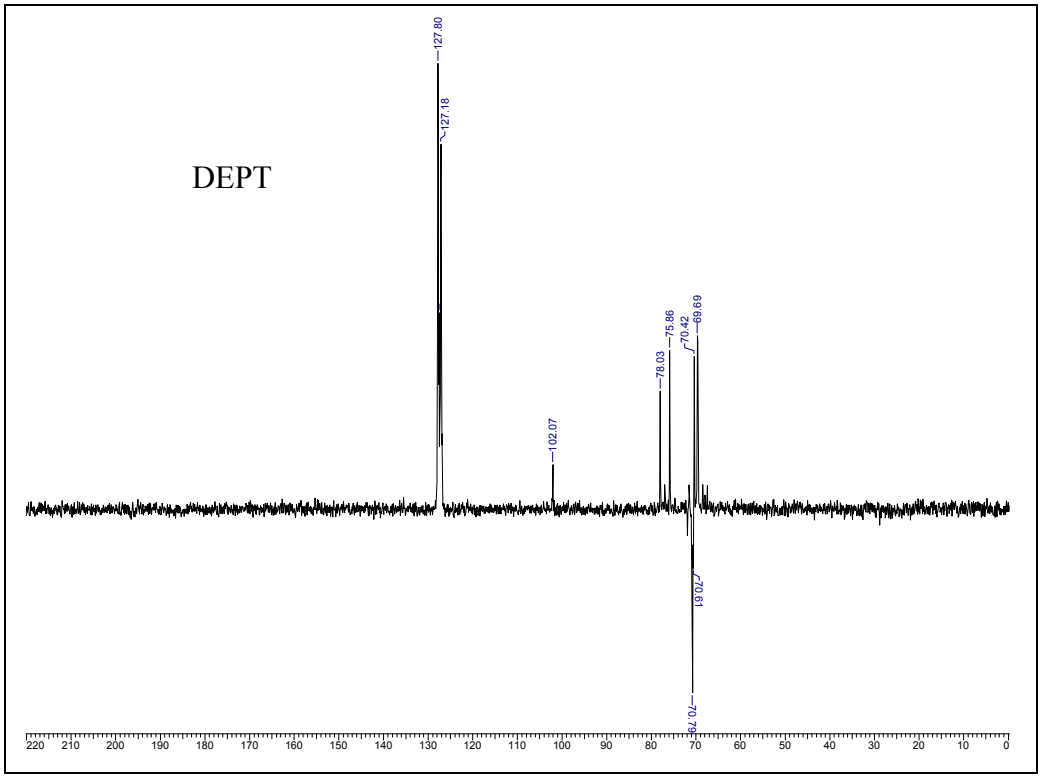
DEPT
127.80
127.18
102.07
78.03
75.86
70.42
69.69
70.61
70.28
220 210 200 190 180 170 160 150 140 130 120 110 100 90 80 70 60 50 40 30 20 10 0

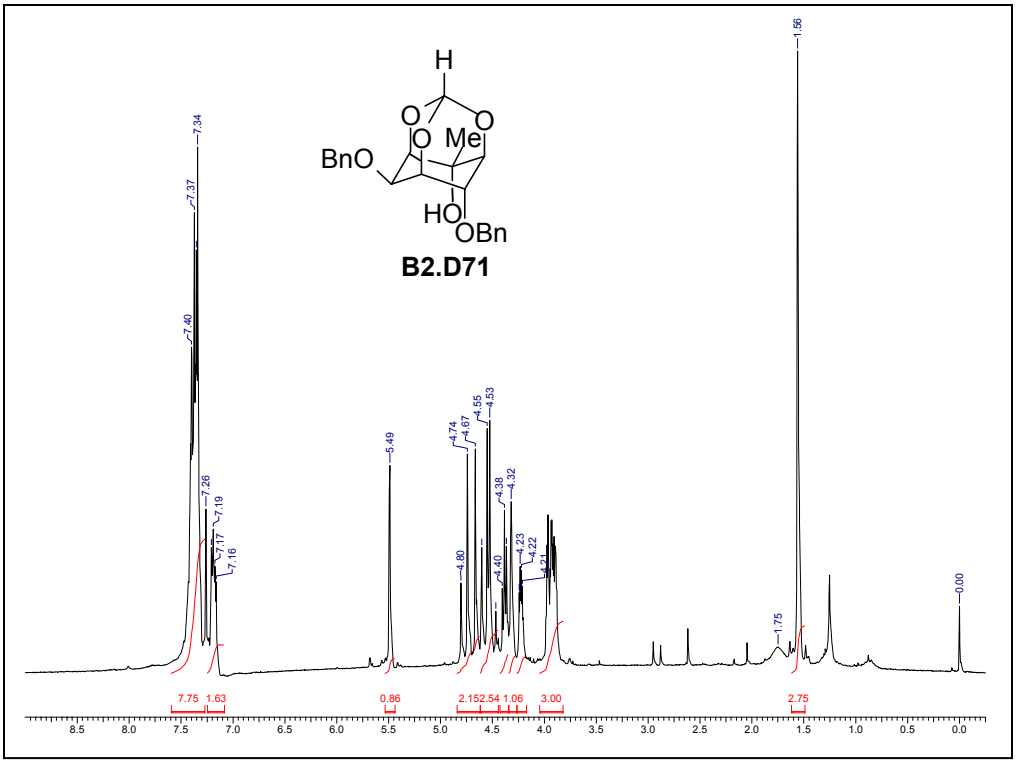
H
O
O
O
Me
BnO
HO
OBn
B2.D71
7.34
7.37
7.40
7.26
7.19
7.17
7.16
5.49
4.74
4.67
4.55
4.53
4.38
4.32
4.80
4.40
4.23
4.22
1.56
1.75
0.00
7.75
1.63
0.86
2.15
2.54
1.06
3.00
2.75

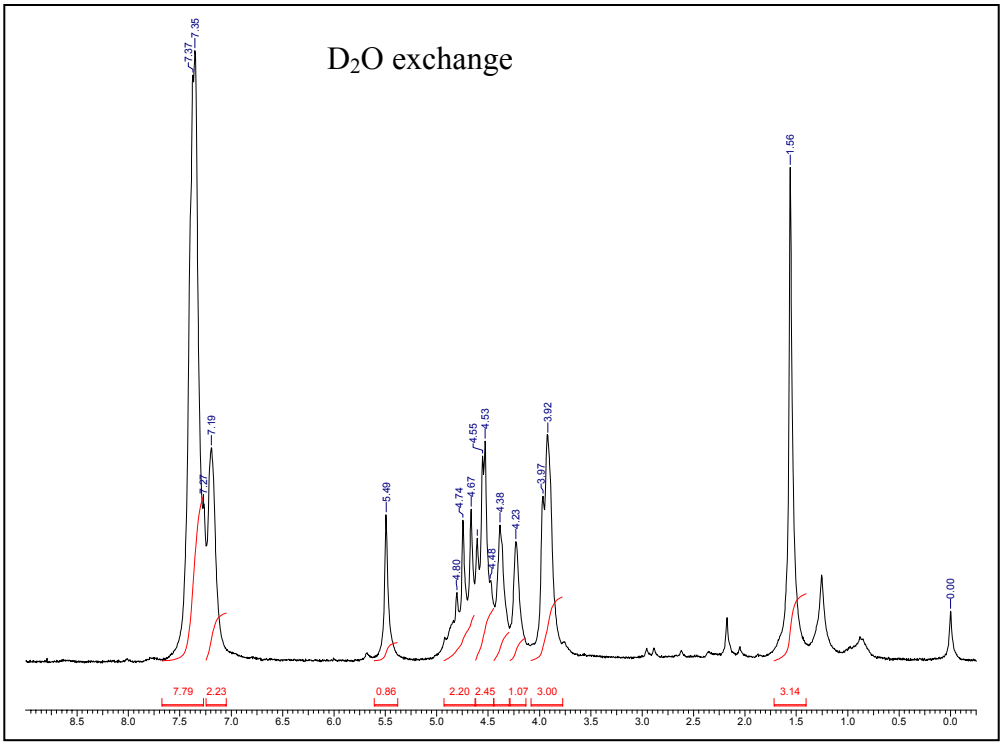
D2O exchange
7.35
7.37
7.19
7.47
5.49
4.74
4.67
4.55
4.53
4.38
4.23
4.80
4.46
3.92
3.87
1.56
0.00
7.79
2.23
0.86
2.20
2.45
1.07
3.00
3.14

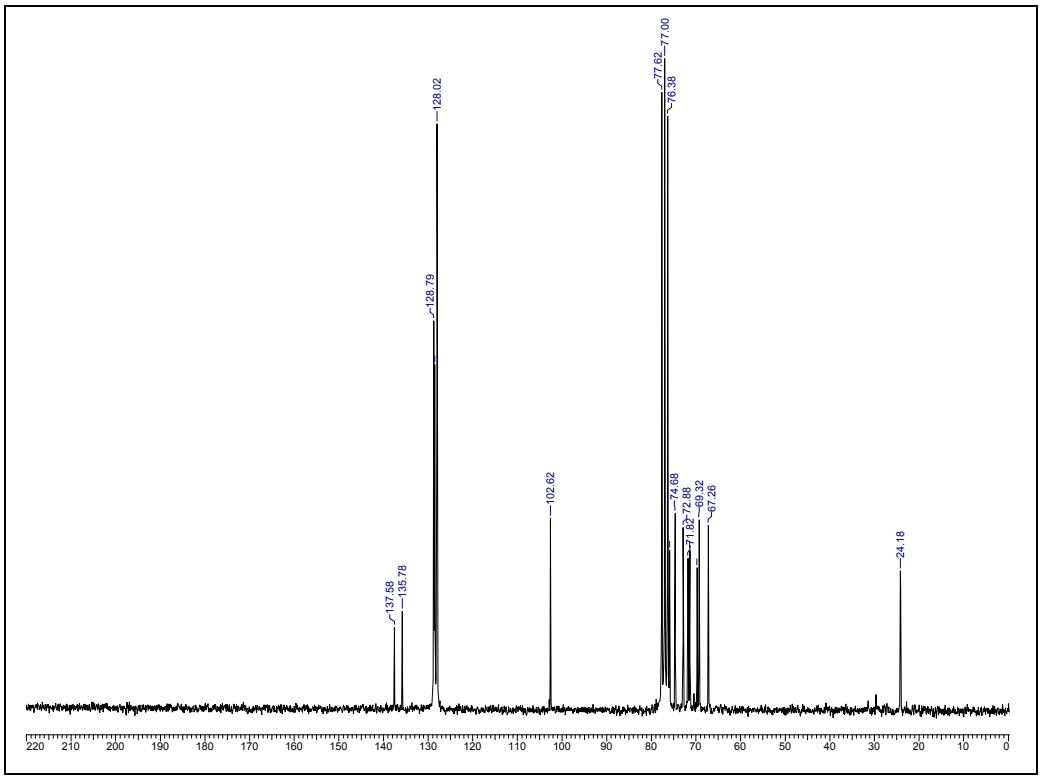
137.58
135.78
128.79
128.02
102.62
77.62
77.00
76.38
74.68
72.88
71.32
69.32
67.26
24.18
220 210 200 190 180 170 160 150 140 130 120 110 100 90 80 70 60 50 40 30 20 10 0

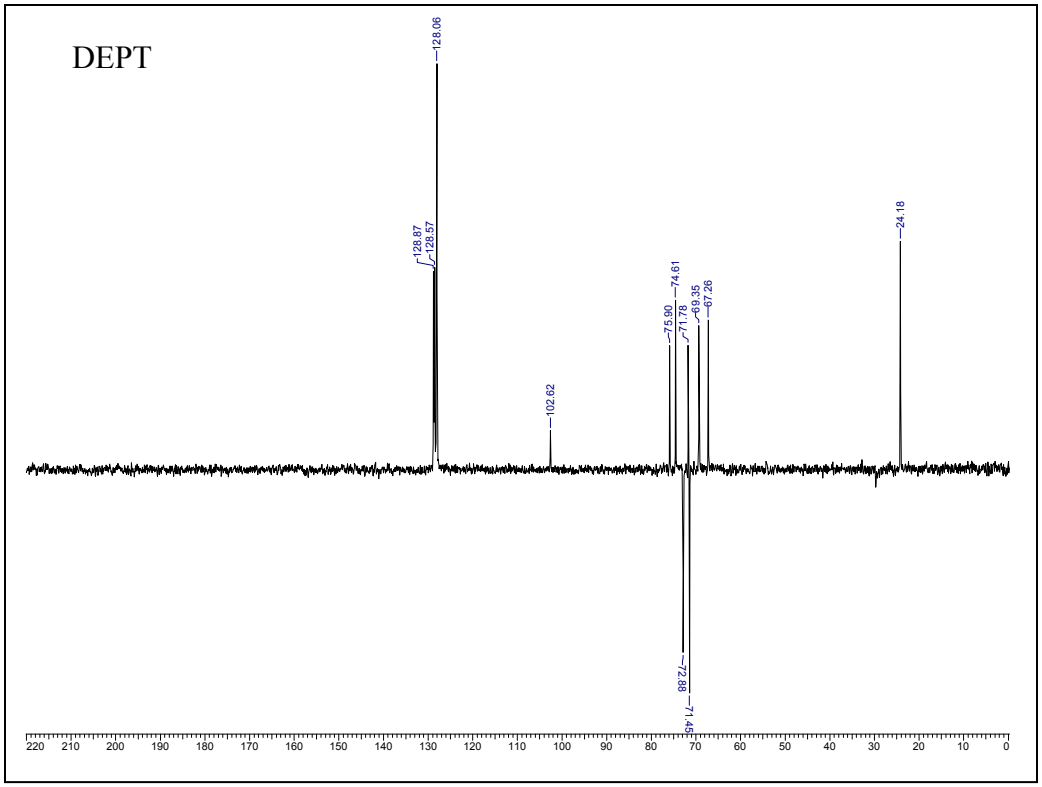
DEPT
128.87
128.57
128.06
102.62
75.90
74.61
71.78
69.35
67.26
72.88
71.45
24.18
220 210 200 190 180 170 160 150 140 130 120 110 100 90 80 70 60 50 40 30 20 10 0

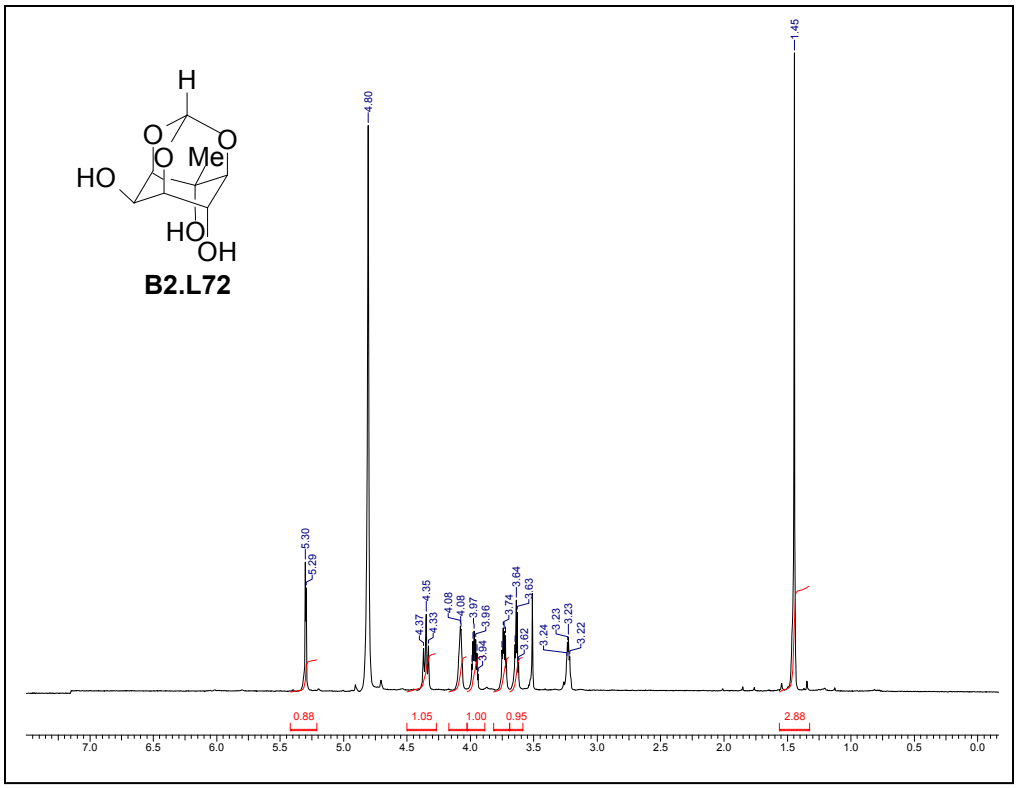
H
O
O
O
Me
HO
HO
OH
B2.L72
1.45
4.80
5.30
5.29
4.37
4.35
4.33
4.08
4.08
3.97
3.96
3.94
3.74
3.64
3.63
3.62
3.24
3.23
3.23
3.22
0.88
1.05
1.00
0.95
2.88
7.0
6.5
6.0
5.5
5.0
4.5
4.0
3.5
3.0
2.5
2.0
1.5
1.0
0.5
0.0

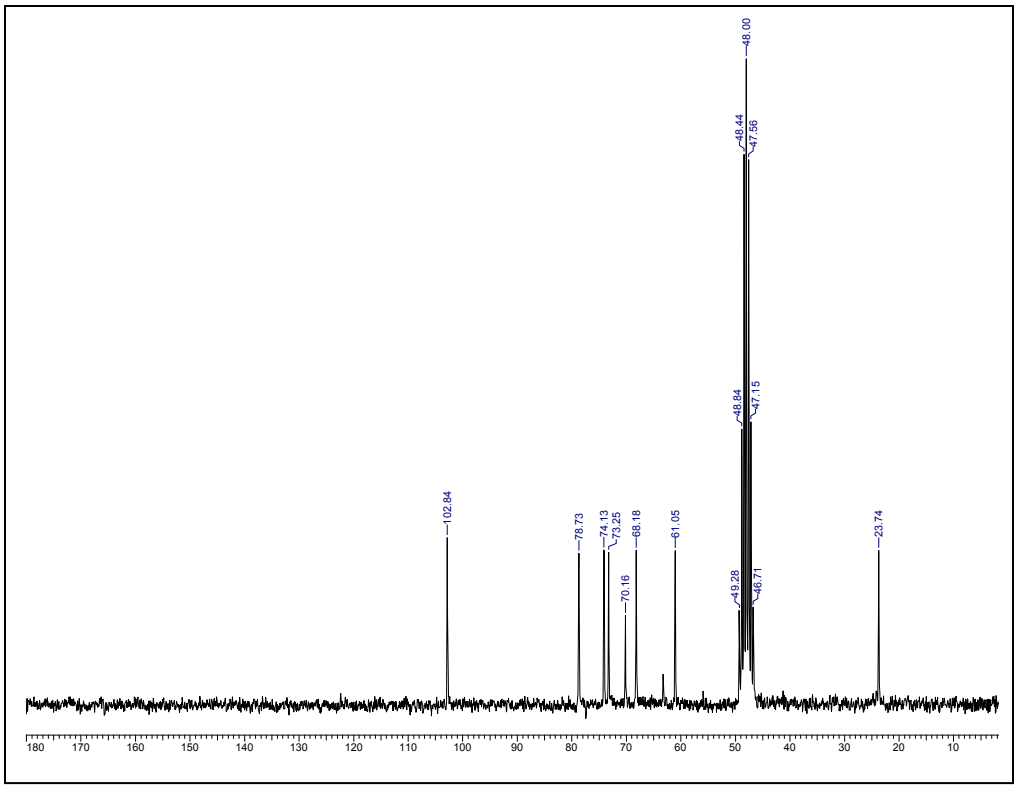
48.00
48.44
47.56
48.84
47.15
102.84
78.73
74.13
73.25
68.18
61.05
70.16
49.28
46.71
23.74
180
170
160
150
140
130
120
110
100
90
80
70
60
50
40
30
20
10

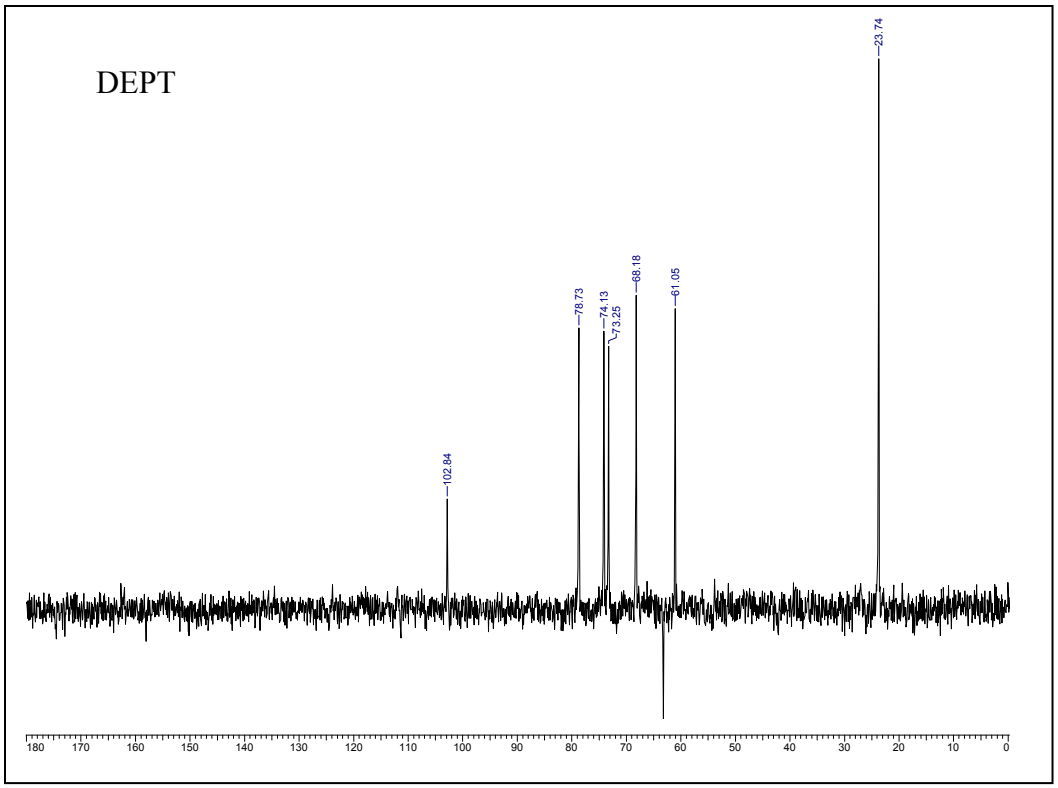
DEPT
23.74
78.73
74.13
73.25
68.18
61.05
102.84
180 170 160 150 140 130 120 110 100 90 80 70 60 50 40 30 20 10 0

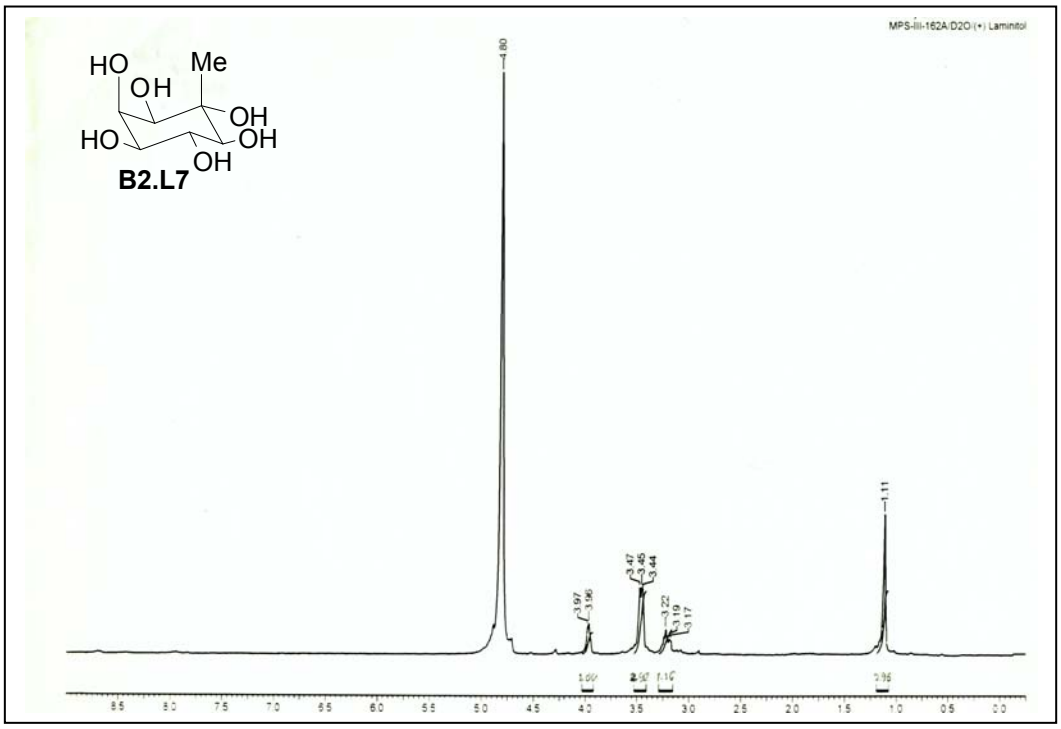
HO
Me
OH
OH
HO
OH
OH
B2.L7
MPS-III-162A/D2O/(+) Laminitol
4.80
3.97
3.96
3.47
3.45
3.44
3.22
3.19
3.17
1.11
8.5 8.0 7.5 7.0 6.5 6.0 5.5 5.0 4.5 4.0 3.5 3.0 2.5 2.0 1.5 1.0 0.5 0.0

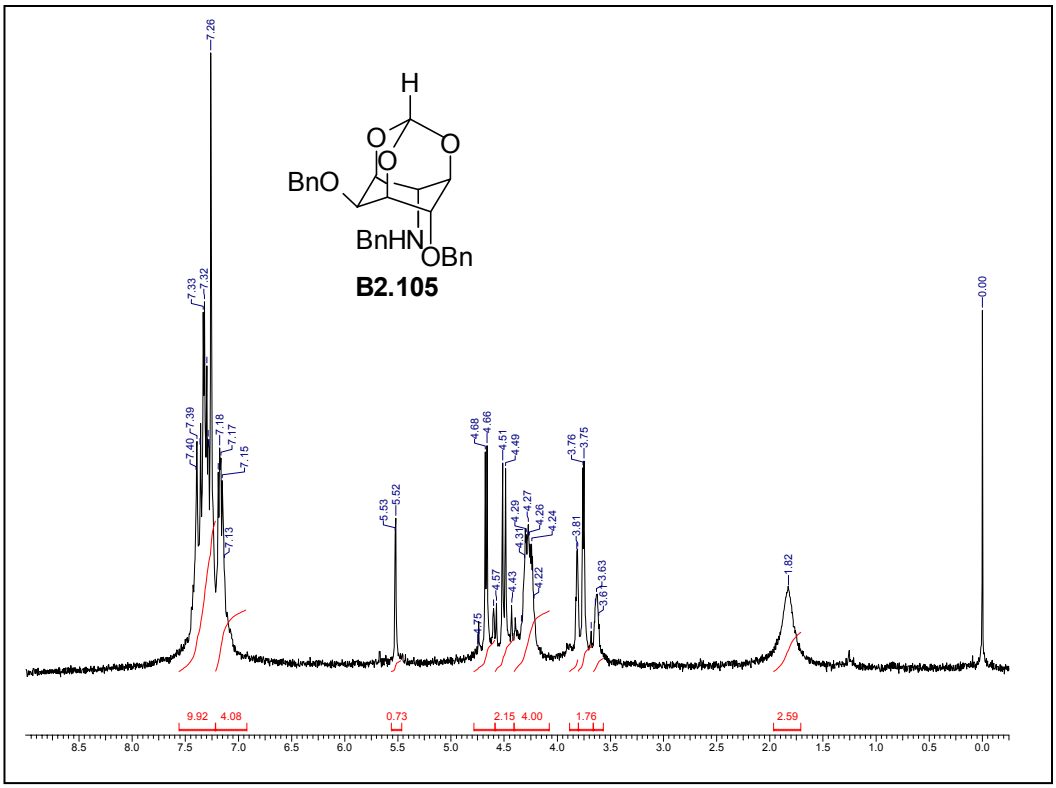
H
O
O
O
BnO
BnHN
OBn
B2.105
7.26
7.33
7.32
7.39
7.40
7.18
7.17
7.15
7.13
5.53
5.52
4.68
4.66
4.51
4.49
4.29
4.27
4.26
4.24
4.31
4.22
4.57
4.43
4.75
3.76
3.75
3.81
3.63
3.61
1.82
0.00
9.92
4.08
0.73
2.15
4.00
1.76
2.59

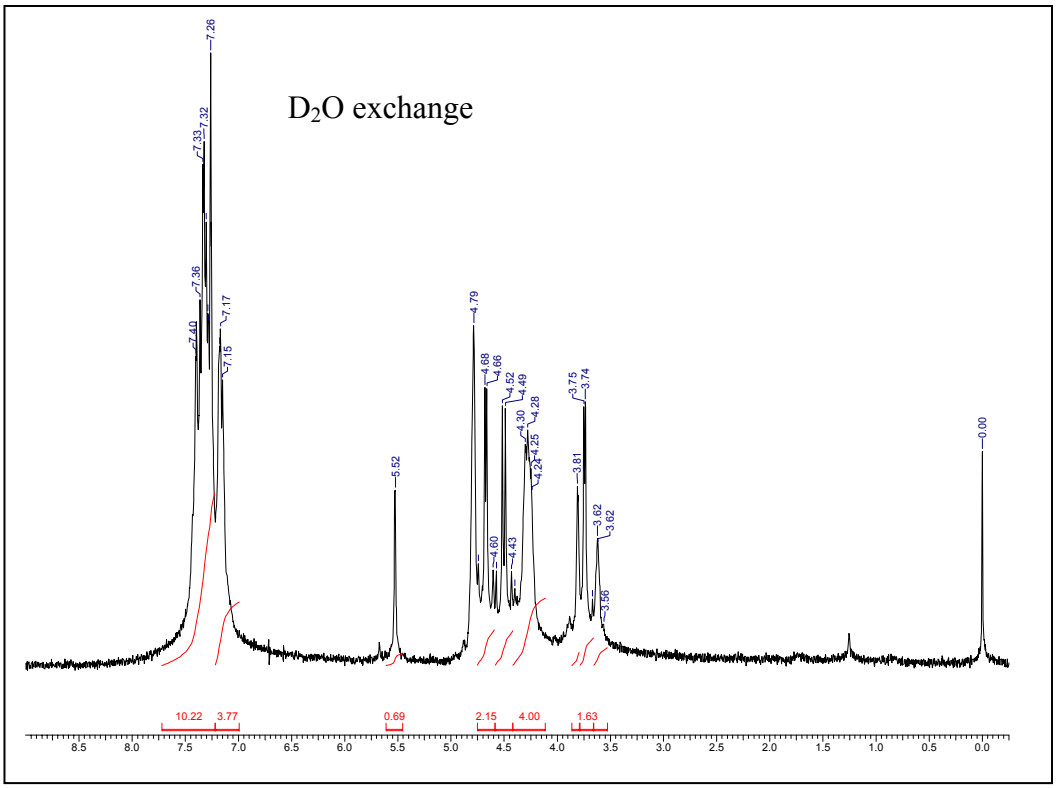
D2O exchange
7.26
7.33
7.32
7.36
7.40
7.17
7.15
5.52
4.79
4.68
4.66
4.52
4.49
4.30
4.28
4.25
4.24
4.60
4.43
3.75
3.74
3.81
3.62
3.62
3.56
0.00
10.22
3.77
0.69
2.15
4.00
1.63

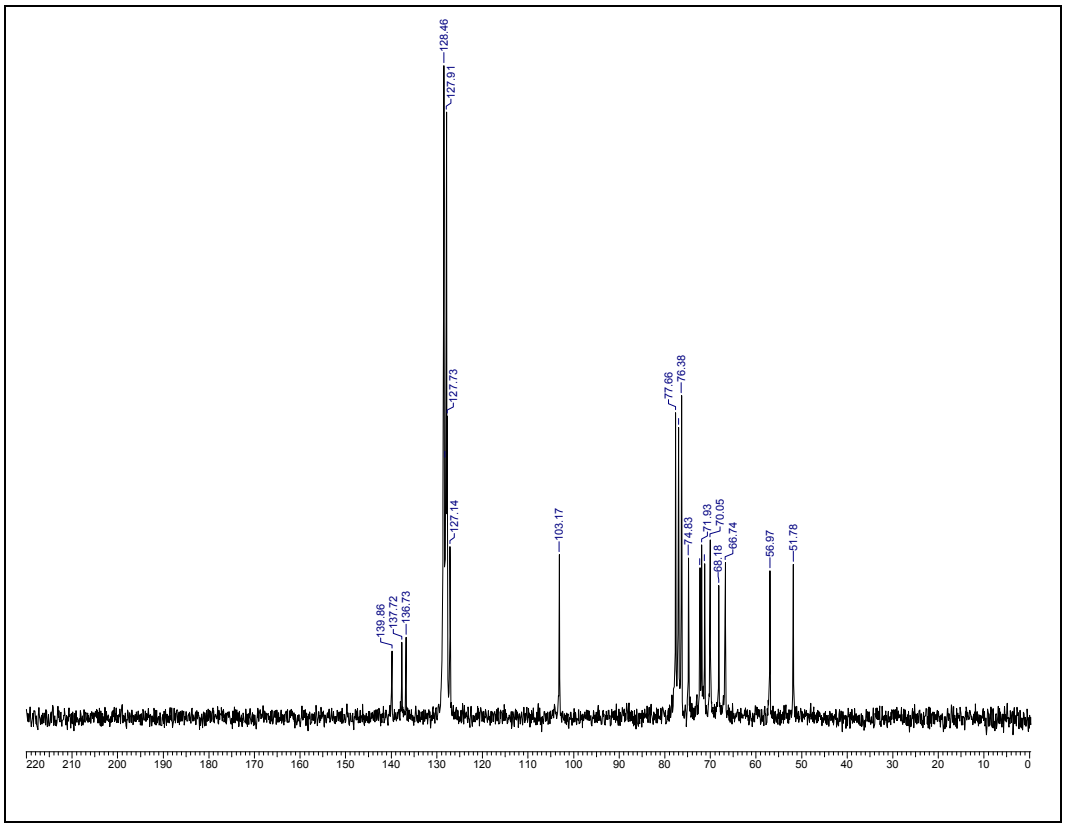
128.46
127.91
127.73
127.14
103.17
77.66
76.38
74.83
71.93
70.05
68.18
66.74
56.97
51.78
139.86
137.72
136.73
220 210 200 190 180 170 160 150 140 130 120 110 100 90 80 70 60 50 40 30 20 10 0

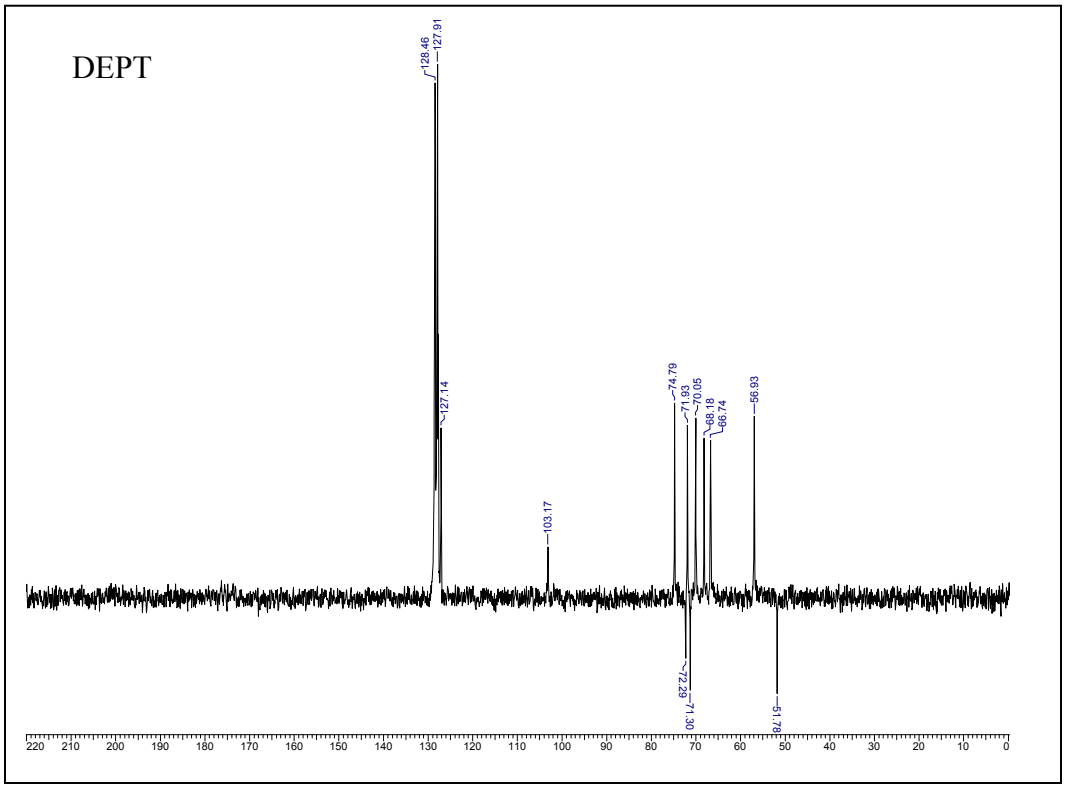
DEPT
128.46
127.91
127.14
103.17
74.79
71.93
70.05
68.18
66.74
56.93
72.29
71.30
51.78
220 210 200 190 180 170 160 150 140 130 120 110 100 90 80 70 60 50 40 30 20 10 0

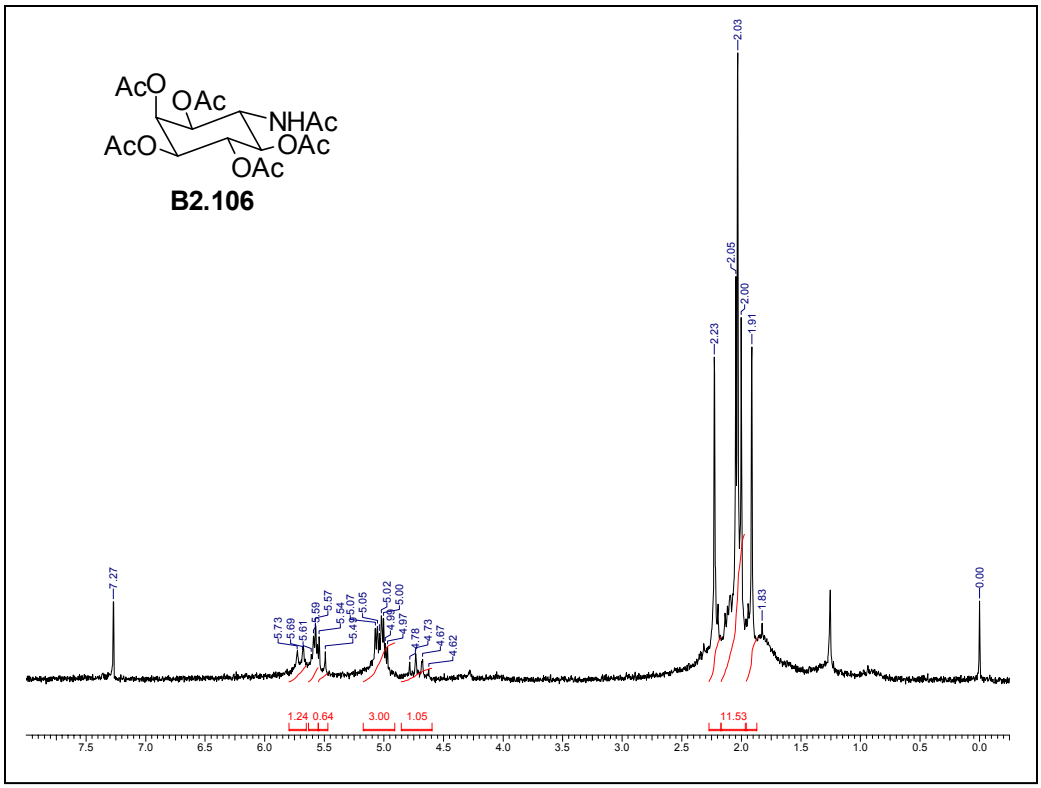
AcO
OAc
NHAc
AcO
OAc
OAc
B2.106
7.27
5.73
5.69
5.61
5.59
5.57
5.54
5.49
5.07
5.05
5.02
5.00
4.99
4.97
4.78
4.73
4.67
4.62
2.03
2.05
2.00
1.91
2.23
1.83
0.00
1.24
0.64
3.00
1.05
11.53

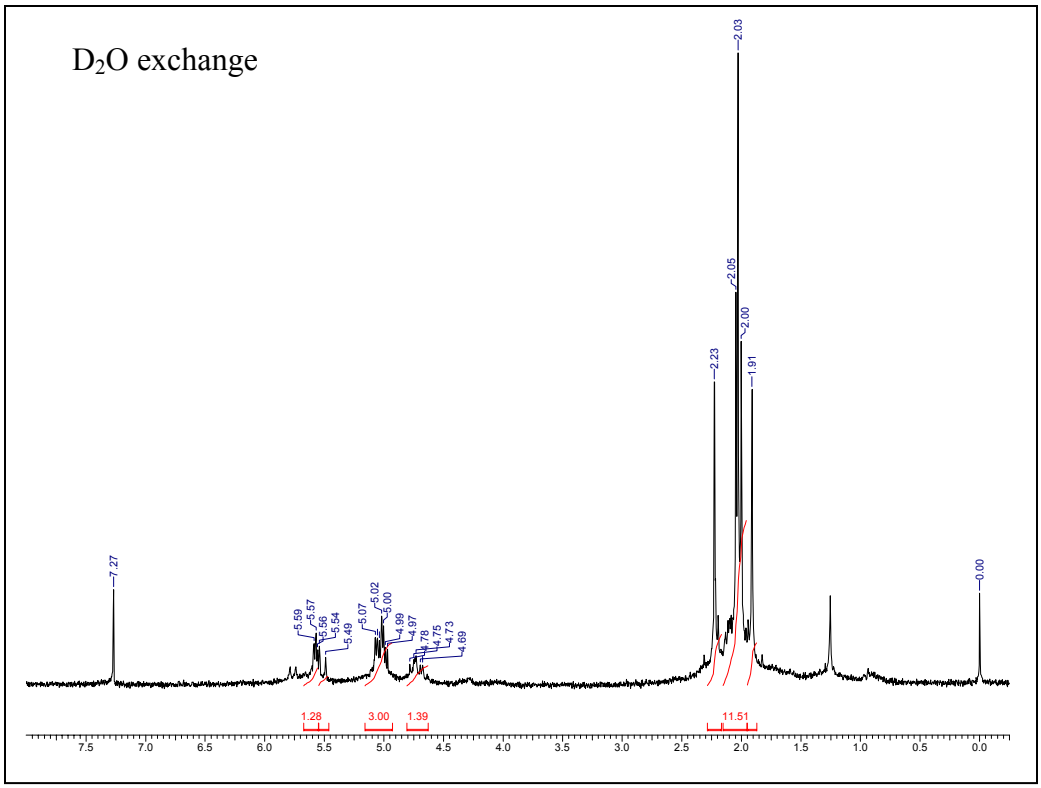
D2O exchange
7.27
5.59
5.57
5.56
5.54
5.49
5.07
5.02
5.00
4.99
4.97
4.78
4.75
4.73
4.69
2.03
2.05
2.00
1.91
2.23
0.00
1.28
3.00
1.39
11.51

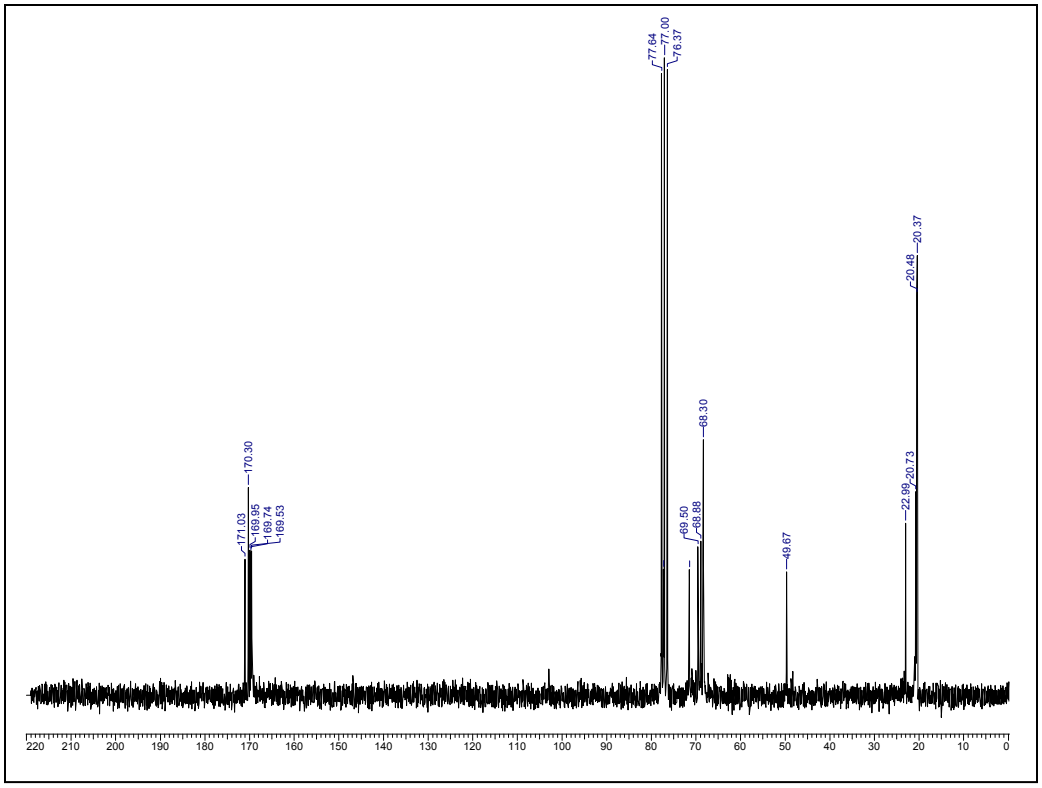
77.64
77.00
76.37
20.48
20.37
68.30
170.30
171.03
169.95
169.74
169.53
69.50
68.88
22.99
20.73
49.67
220 210 200 190 180 170 160 150 140 130 120 110 100 90 80 70 60 50 40 30 20 10 0

DEPT

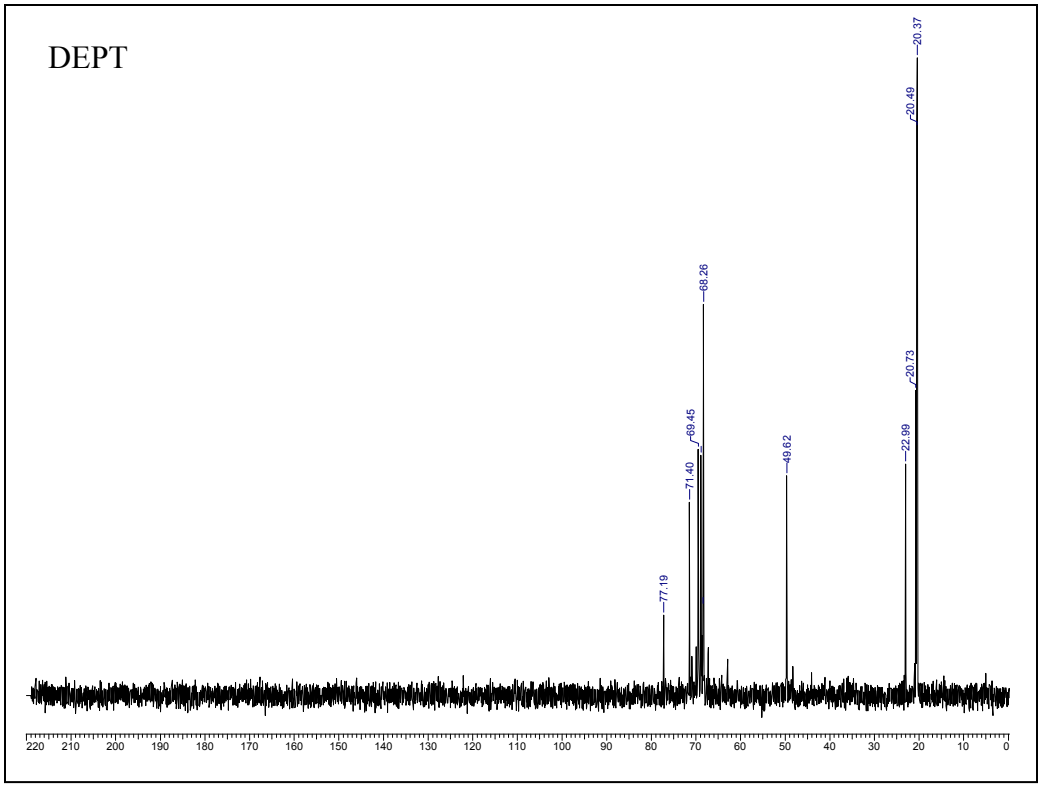
20.37
20.49
68.26
20.73
69.45
71.40
49.62
22.99
77.19
220 210 200 190 180 170 160 150 140 130 120 110 100 90 80 70 60 50 40 30 20 10 0

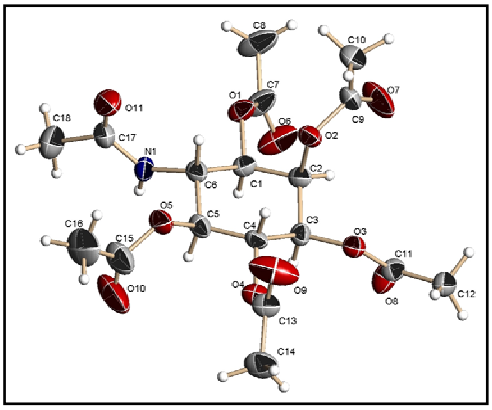

ORTEP of **B2.106**

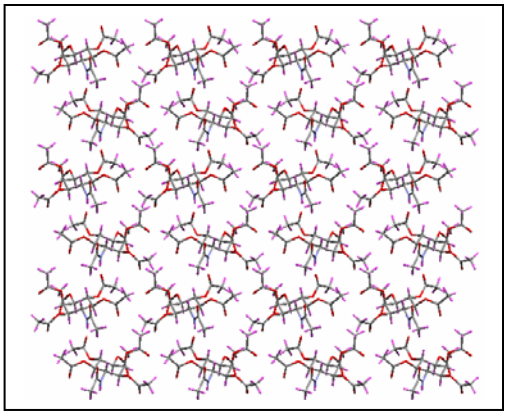

Packing of **B2.106** down the a-axis

Crystal data table of **B2.106**

Identification code	**B2.106** (crystallized from chloroform-light petroleum mixture)
Empirical formula	$C_{18}H_{25}O_{11}N$
Formula weight	431.39
Temperature	566(2) K
Wavelength	0.71073 Å
Crystal system, space group	Monoclinic, *C*c
Unit cell dimensions	a = 8.935(4) Å; α = 90º b = 20.921(9) Å; β = 100.524(9)º c = 12.365(6) Å; γ = 90º
Volume	2272.6(18) $Å^3$
Z, Calculated density	4, 1.261 Mg/m^3
Absorption coefficient	0.106 mm^{-1}
F(000)	912
Crystal size	0.35 x 0.10 x 0.02 mm
θ range for data collection	2.51 to 25.00º
Limiting indices	-10<=h<=10; -24<=k<=24; -14<=l<=14
Reflections collected / unique	10850 / 4008 [R(int) = 0.0611]
Completeness to θ = 25.00	100 %
Max. and min. transmission	0.9982 and 0.9640
Refinement method	Full-matrix least-squares on F^2
Data / restraints / parameters	4008 / 2 / 277
Goodness-of-fit on F^2	0.977
Final R indices [I>2σ (I)]	R1 = 0.0632, wR2 = 0.1236
R indices (all data)	R1 = 0.1542, wR2 = 0.1535
Extinction coefficient	none
Largest diff. peak and hole (ρ_{max} & ρ_{min})	0.159 and -0.109 e. $Å^{-3}$

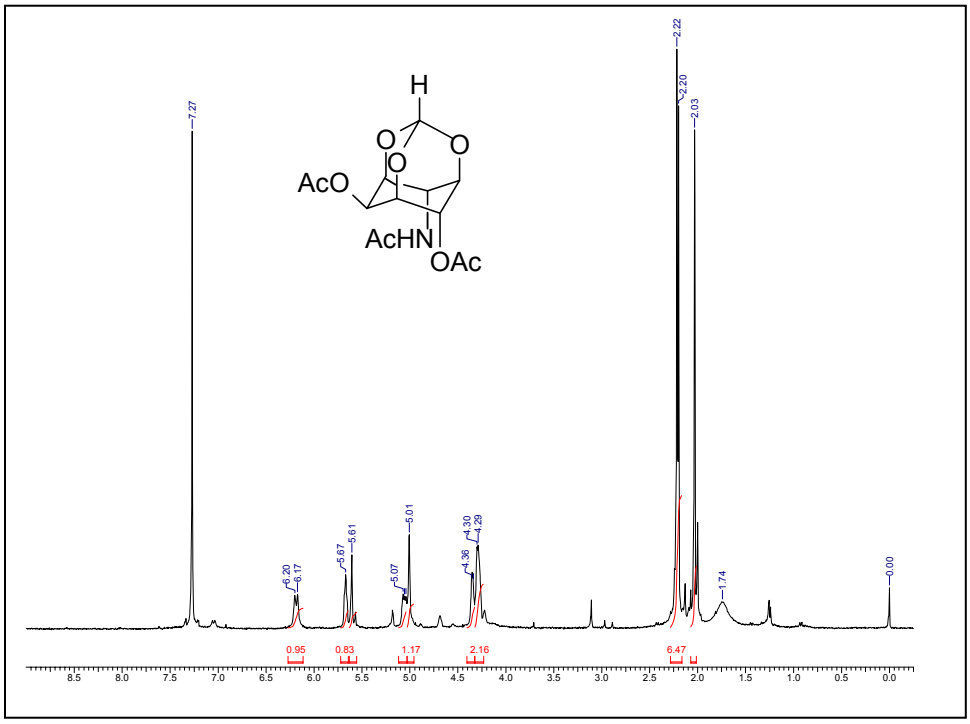
H
O
O
O
AcO
AcHN
OAc
7.27
6.20
6.17
5.67
5.61
5.07
5.01
4.36
4.30
4.29
2.22
2.20
2.03
1.74
0.00
0.95
0.83
1.17
2.16
6.47

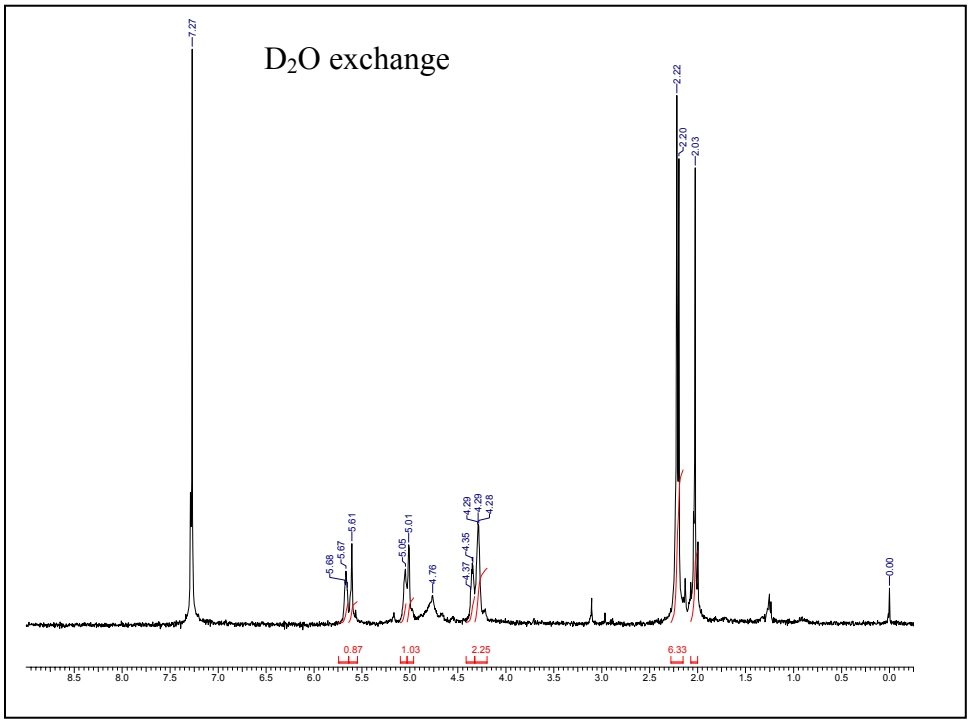
D2O exchange
7.27
5.68
5.67
5.61
5.05
5.01
4.76
4.37
4.35
4.29
4.29
4.28
2.22
2.20
2.03
0.00
0.87
1.03
2.25
6.33

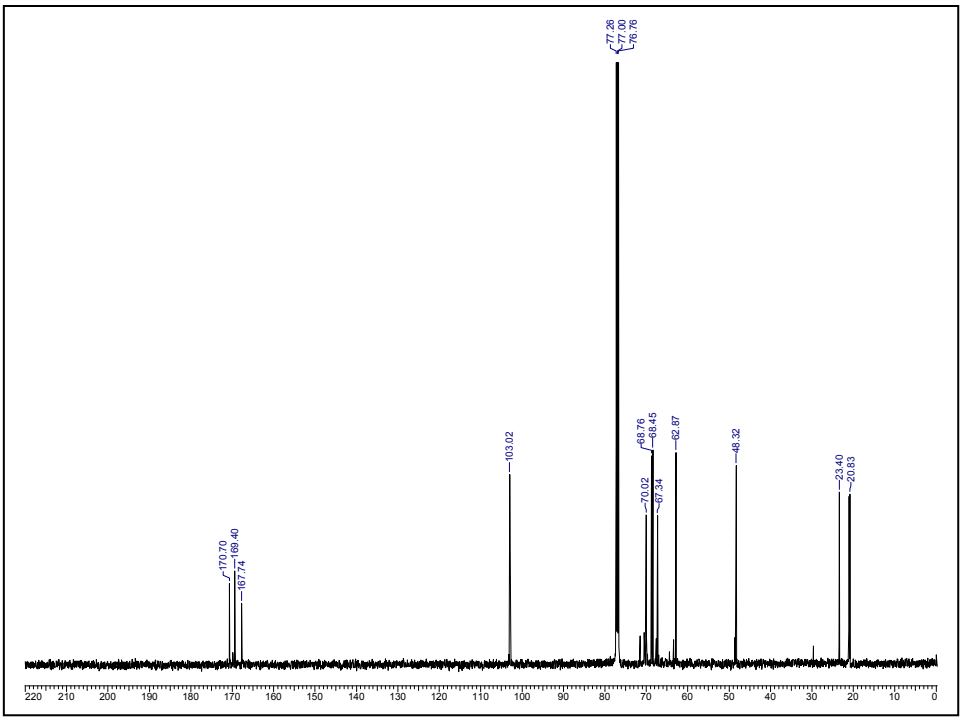
77.26
77.00
76.76
170.70
169.40
167.74
103.02
68.76
68.45
62.87
70.02
67.34
48.32
23.40
20.83
220 210 200 190 180 170 160 150 140 130 120 110 100 90 80 70 60 50 40 30 20 10 0

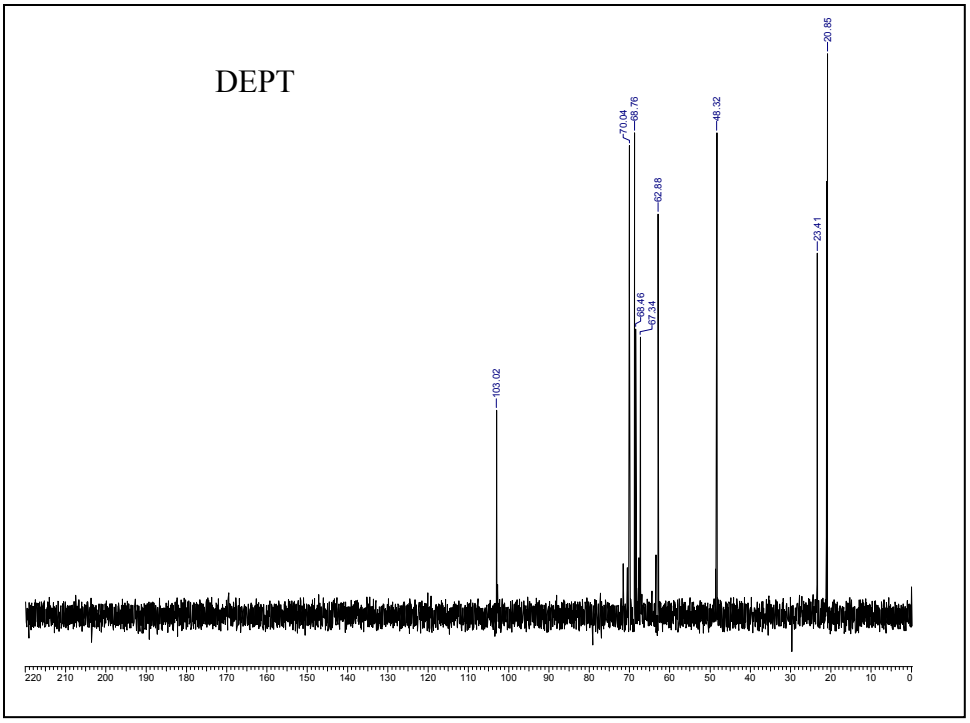
DEPT
20.85
70.04
68.76
48.32
62.88
23.41
68.46
67.34
103.02
220 210 200 190 180 170 160 150 140 130 120 110 100 90 80 70 60 50 40 30 20 10 0

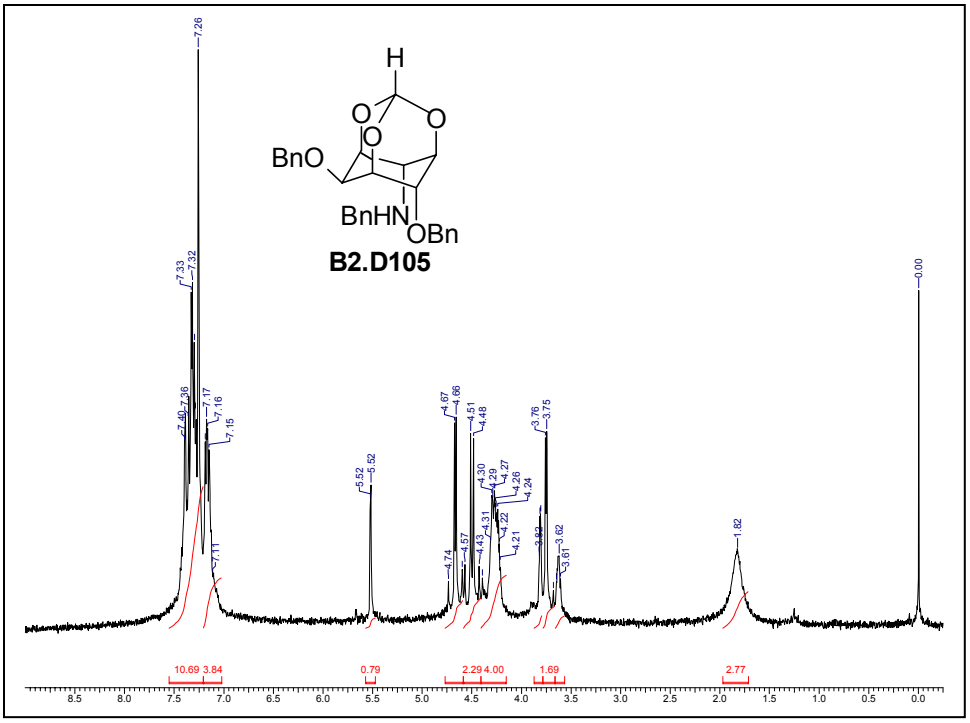
H
O
O
O
BnO
BnHN
OBn
B2.D105

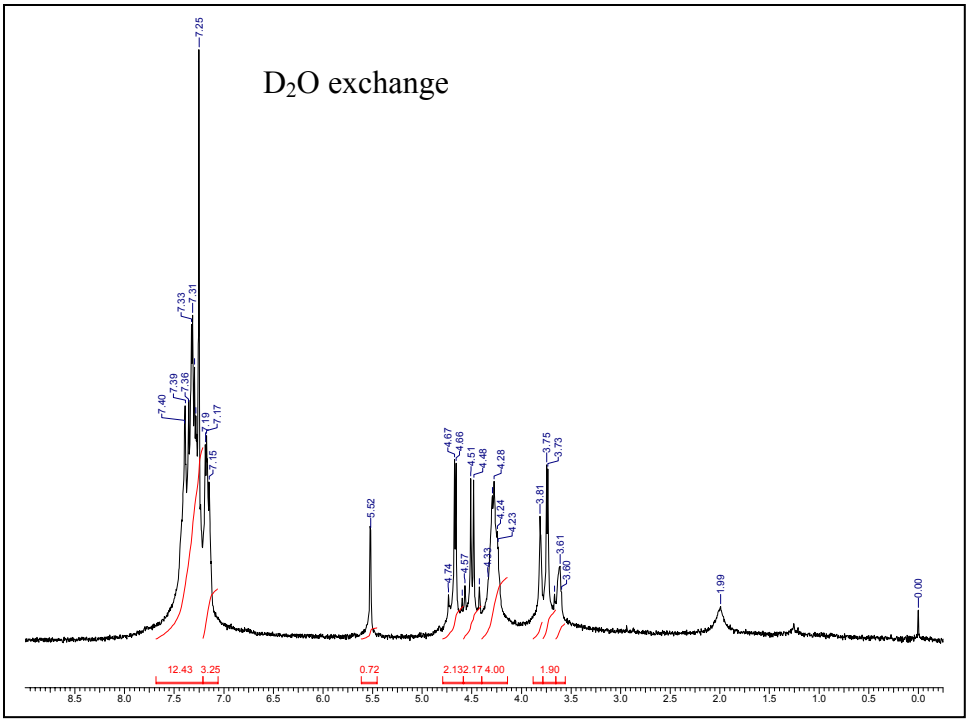
D2O exchange

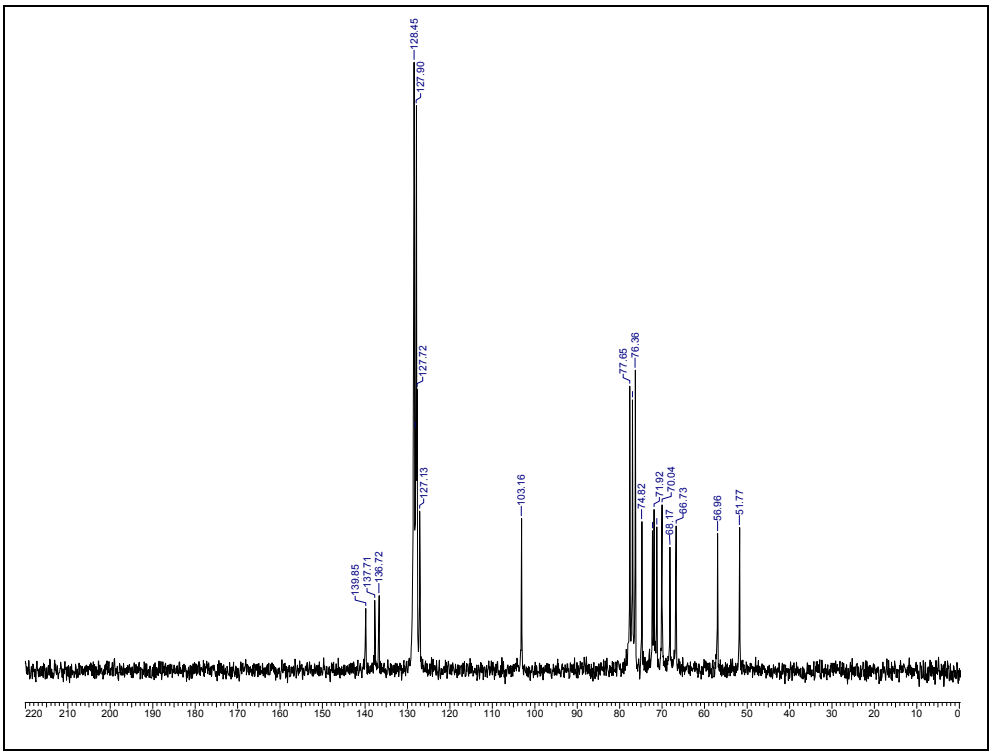
128.45
127.90
127.72
127.13
103.16
77.65
76.36
74.82
71.92
70.04
68.17
66.73
56.96
51.77
139.85
137.71
136.72

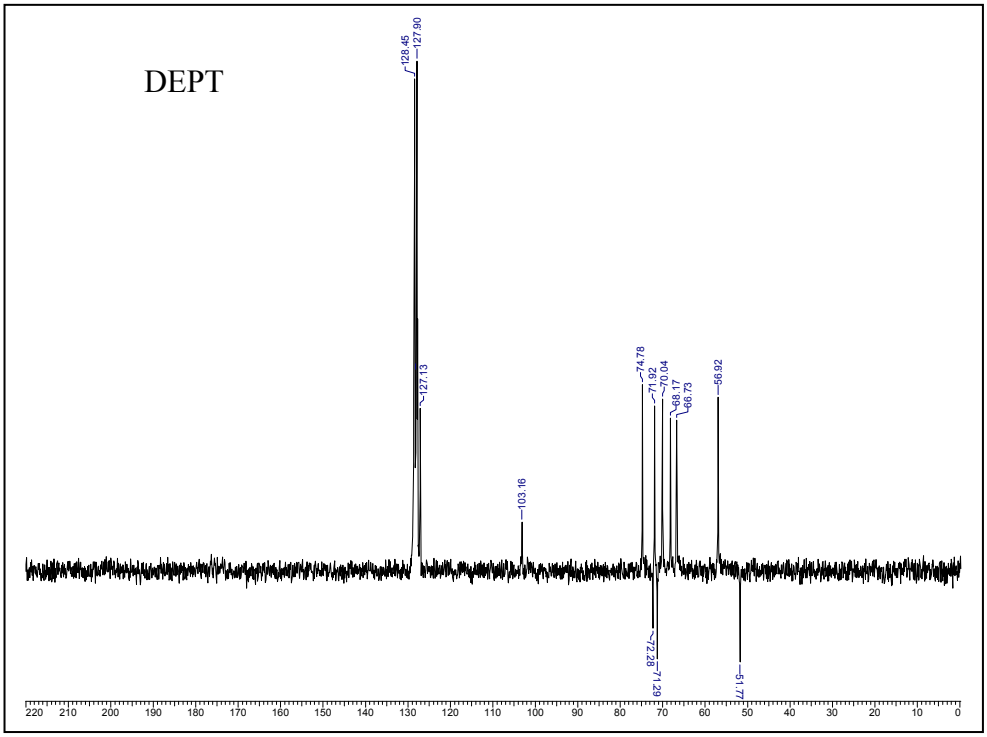
DEPT
128.45
127.90
127.13
103.16
74.78
71.92
70.04
68.17
66.73
56.92
72.28
72.03
51.77

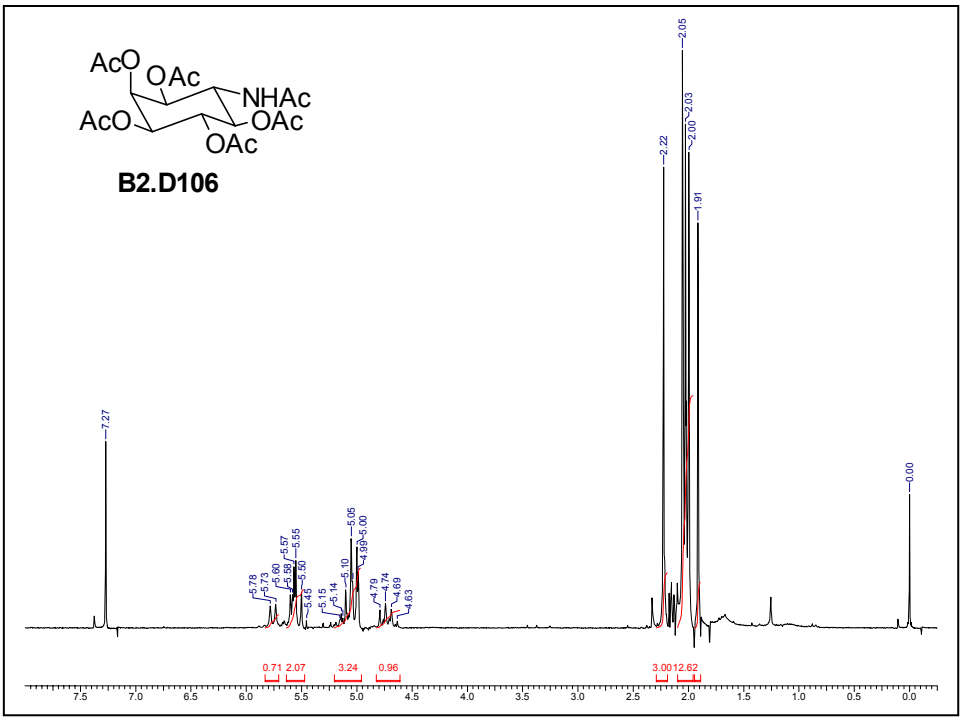
AcO
OAc
NHAc
AcO
OAc
OAc
B2.D106
2.05
2.22
2.03
2.00
1.91
7.27
0.00
5.78
5.73
5.60
5.59
5.57
5.55
5.50
5.45
5.15
5.14
5.10
5.05
5.00
4.99
4.79
4.74
4.69
4.63
0.71
2.07
3.24
0.96
3.00
12.62

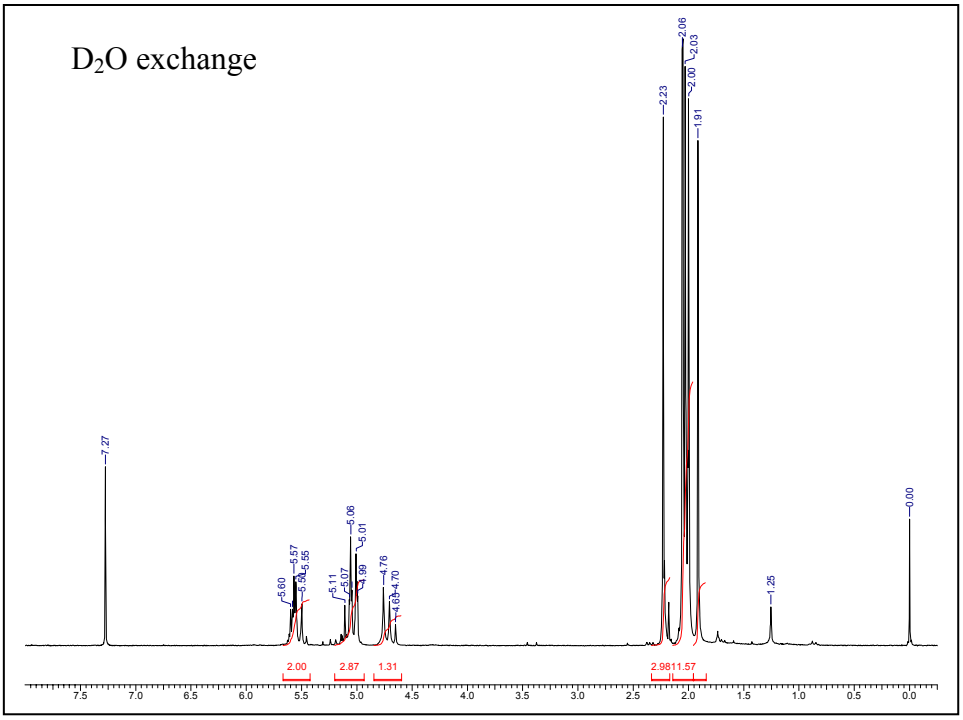
D2O exchange
2.06
2.03
2.00
2.23
1.91
7.27
0.00
1.25
5.60
5.57
5.55
5.11
5.07
5.06
5.01
4.99
4.76
4.70
4.63
2.00
2.87
1.31
2.98
11.57

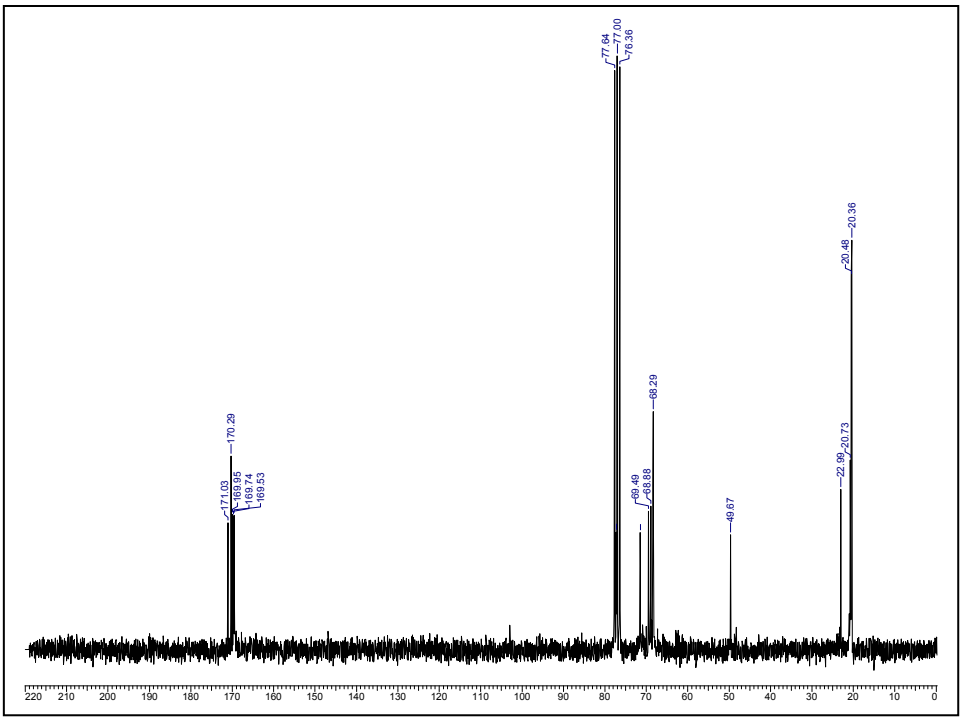
77.64
77.00
76.36
20.48
20.36
68.29
170.29
20.73
22.99
171.03
169.95
169.74
169.53
69.49
68.88
49.67

DEPT

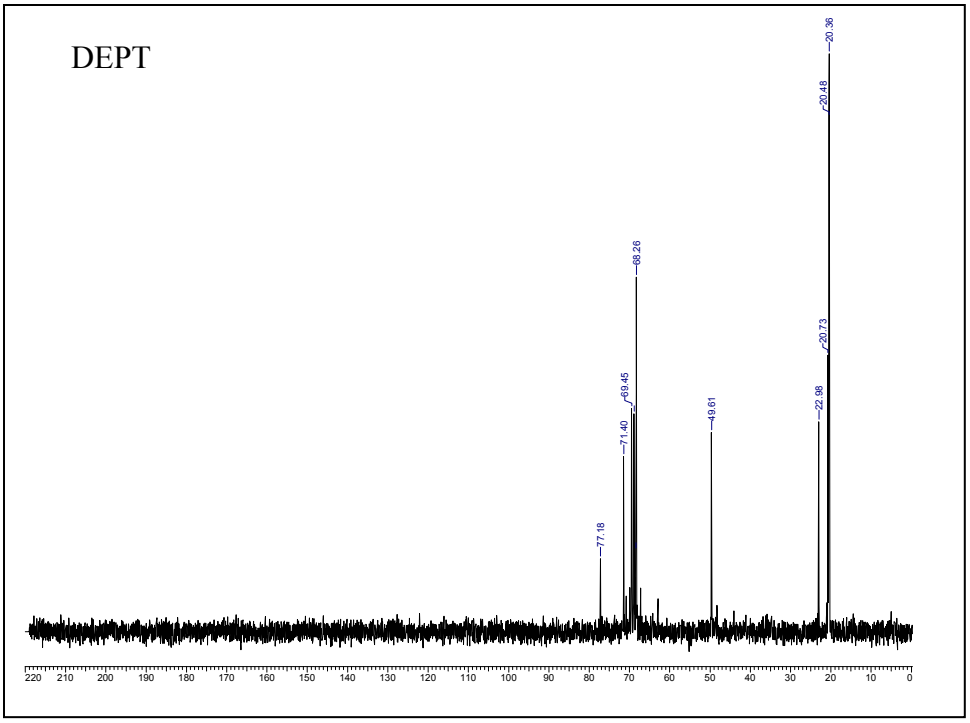
20.36
20.48
68.26
20.73
69.45
71.40
49.61
22.98
77.18

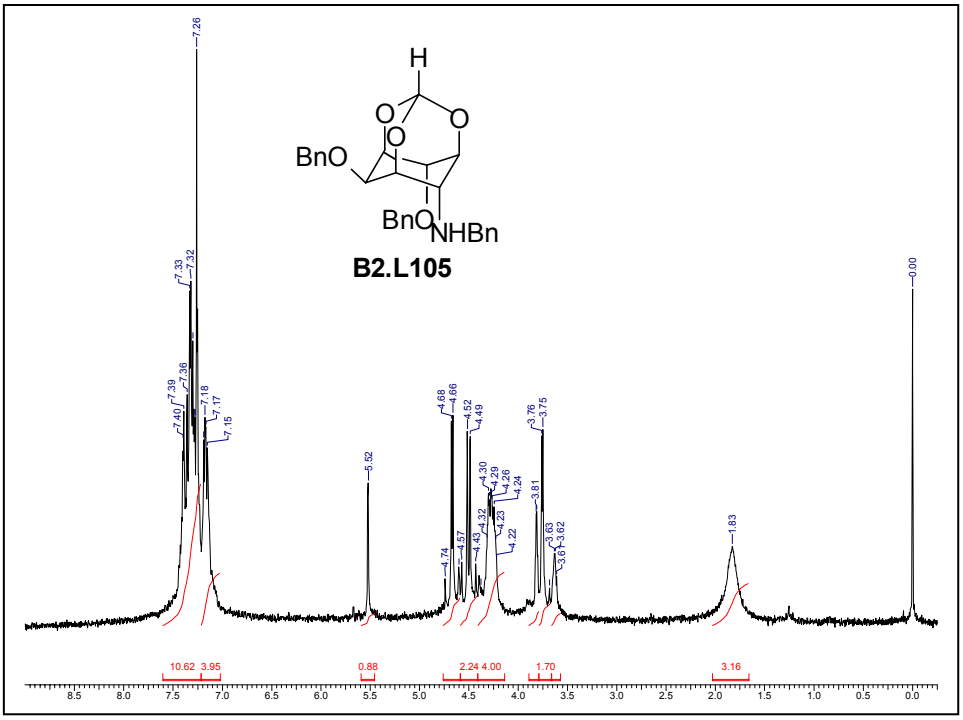
H
O
O
O
BnO
BnO
NHBn
B2.L105
7.26
7.33
7.32
7.39
7.36
7.40
7.18
7.17
7.15
5.52
4.68
4.66
4.52
4.49
4.30
4.29
4.26
4.24
4.32
4.28
4.23
4.22
4.74
4.57
4.43
3.76
3.75
3.81
3.63
3.62
3.61
1.83
0.00
10.62
3.95
0.88
2.24
4.00
1.70
3.16

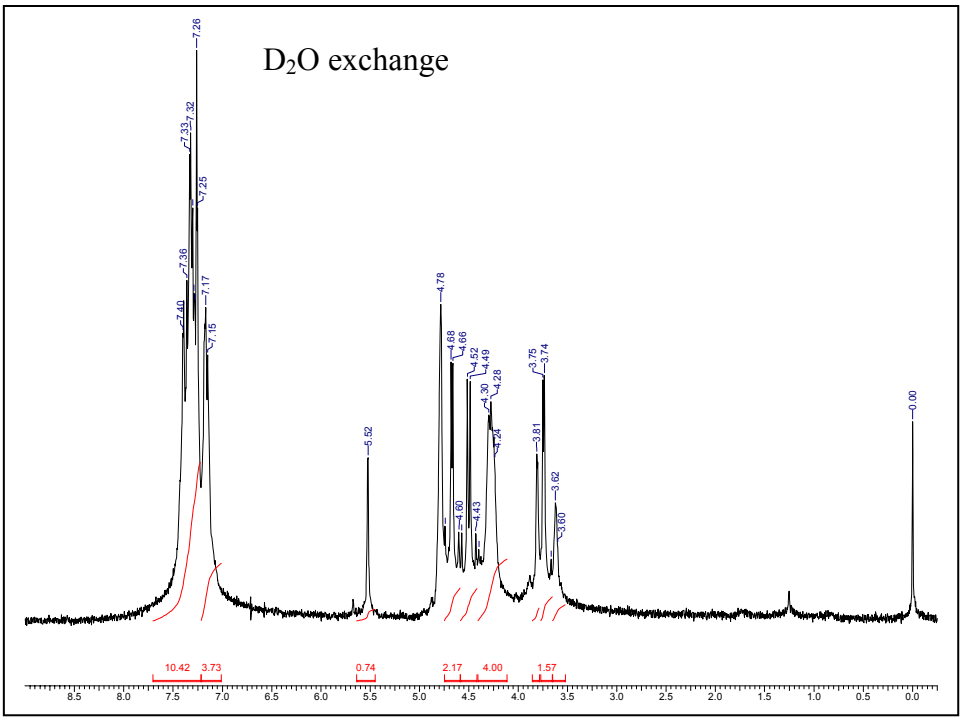
D2O exchange
7.26
7.33
7.32
7.25
7.36
7.40
7.17
7.15
4.78
4.68
4.66
4.52
4.49
4.30
4.28
4.26
5.52
3.75
3.74
3.81
3.62
3.60
4.60
4.43
0.00
10.42
3.73
0.74
2.17
4.00
1.57

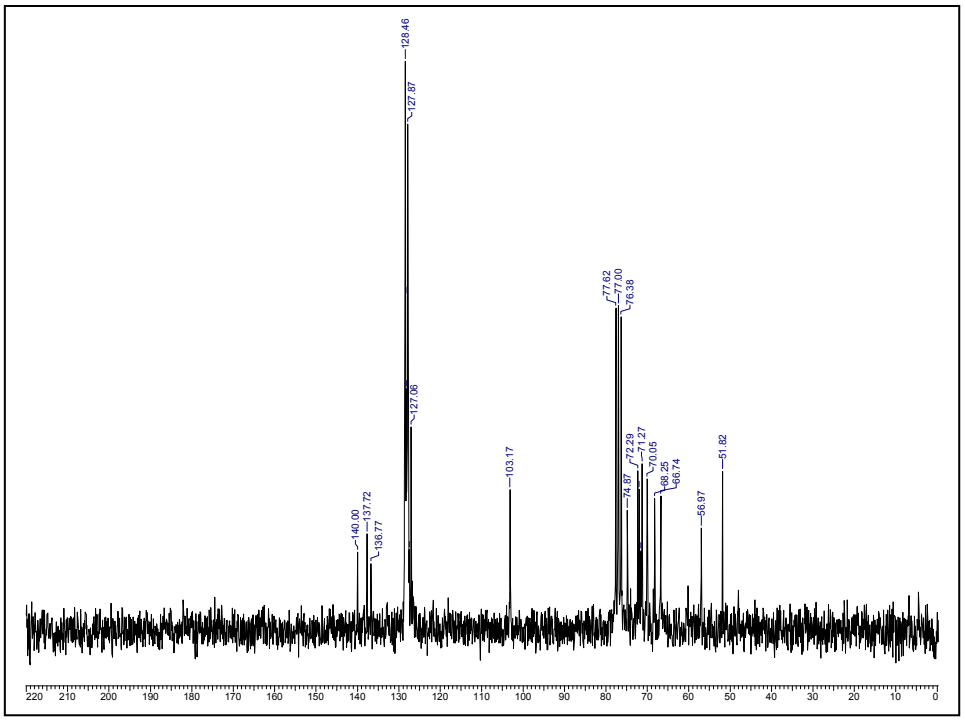
128.46
127.87
77.62
77.00
76.38
127.06
103.17
72.29
71.27
70.05
68.25
66.74
56.97
51.82
140.00
137.72
136.77

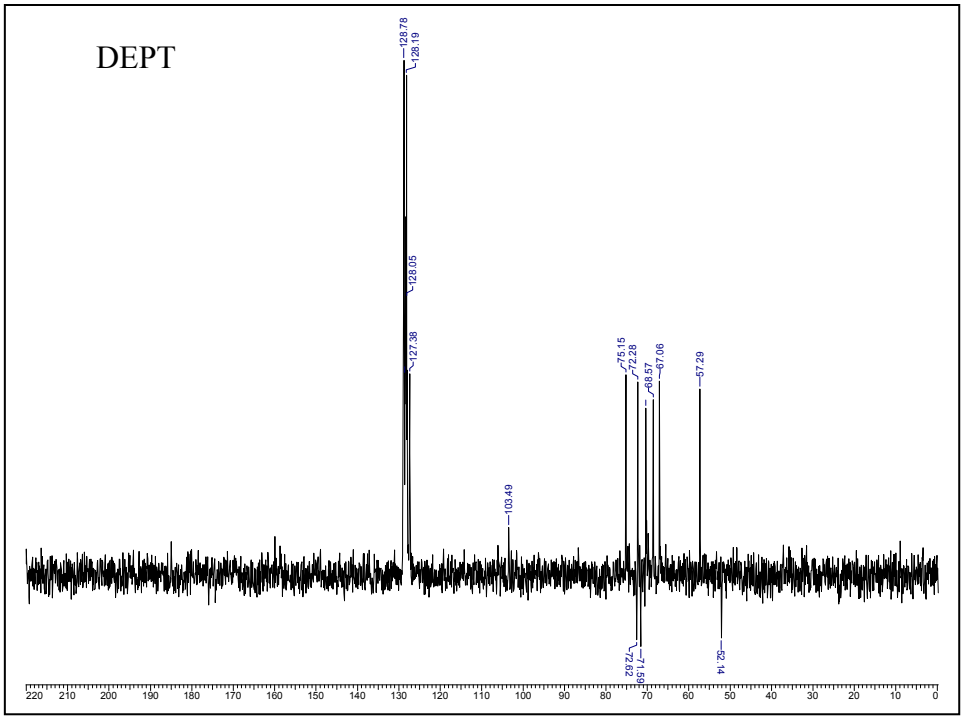
DEPT
128.78
128.19
128.05
127.38
103.49
75.15
72.28
68.57
67.06
57.29
72.62
71.56
52.14

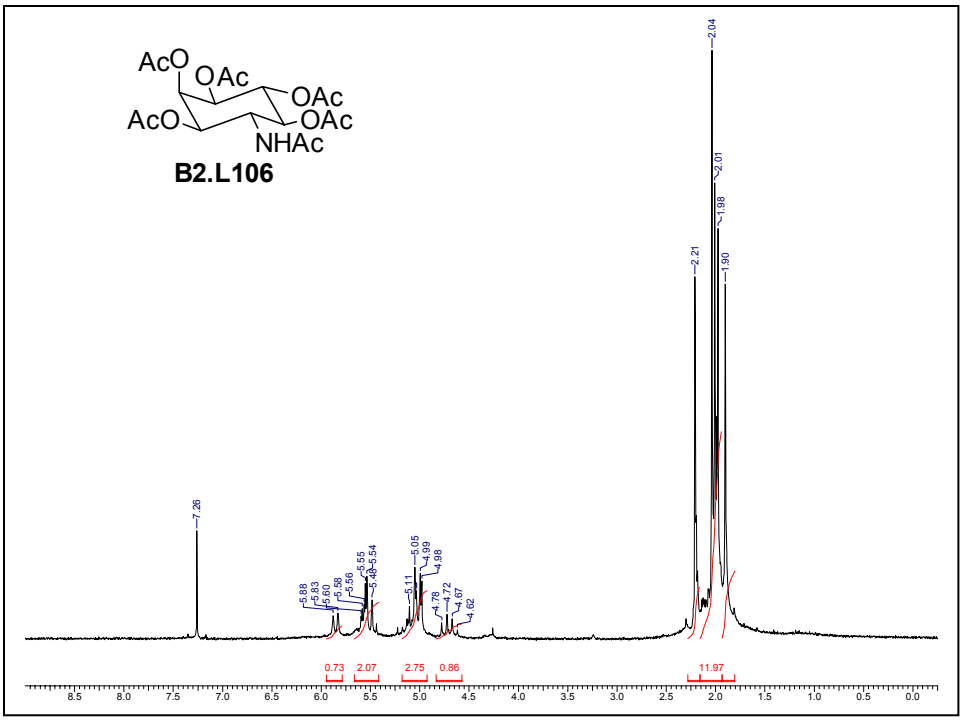
AcO
OAc
OAc
AcO
OAc
NHAc
B2.L106
7.26
5.88
5.83
5.60
5.58
5.55
5.54
5.11
5.05
4.99
4.98
4.78
4.72
4.67
4.62
2.21
2.04
2.01
1.98
1.90
0.73
2.07
2.75
0.86
11.97

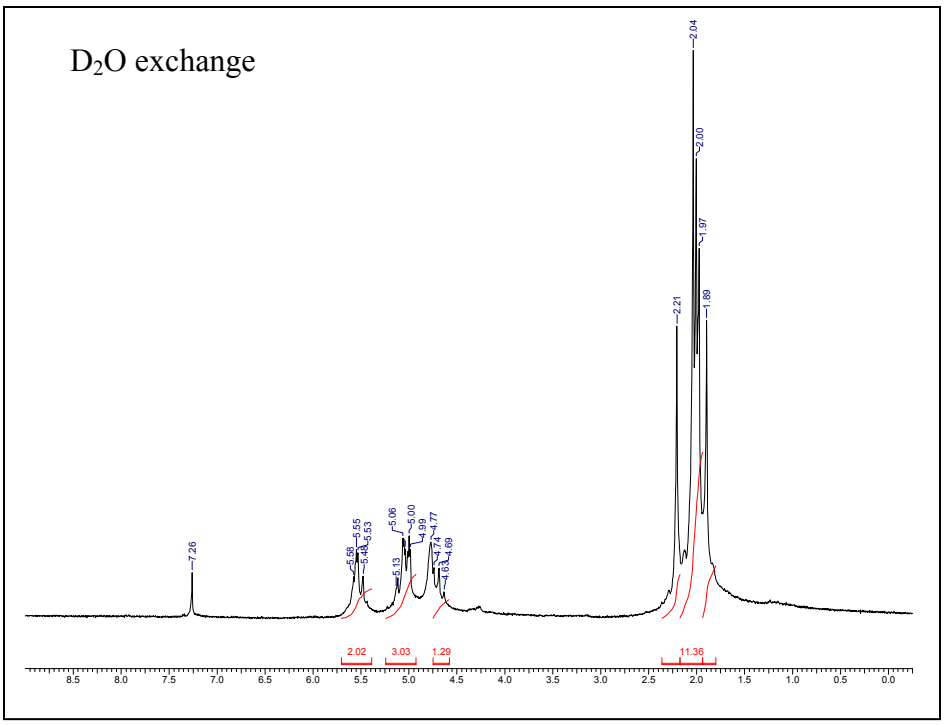
D2O exchange
7.26
5.55
5.53
5.06
5.00
4.99
4.77
4.74
4.69
2.21
2.04
2.00
1.97
1.89
2.02
3.03
1.29
11.36

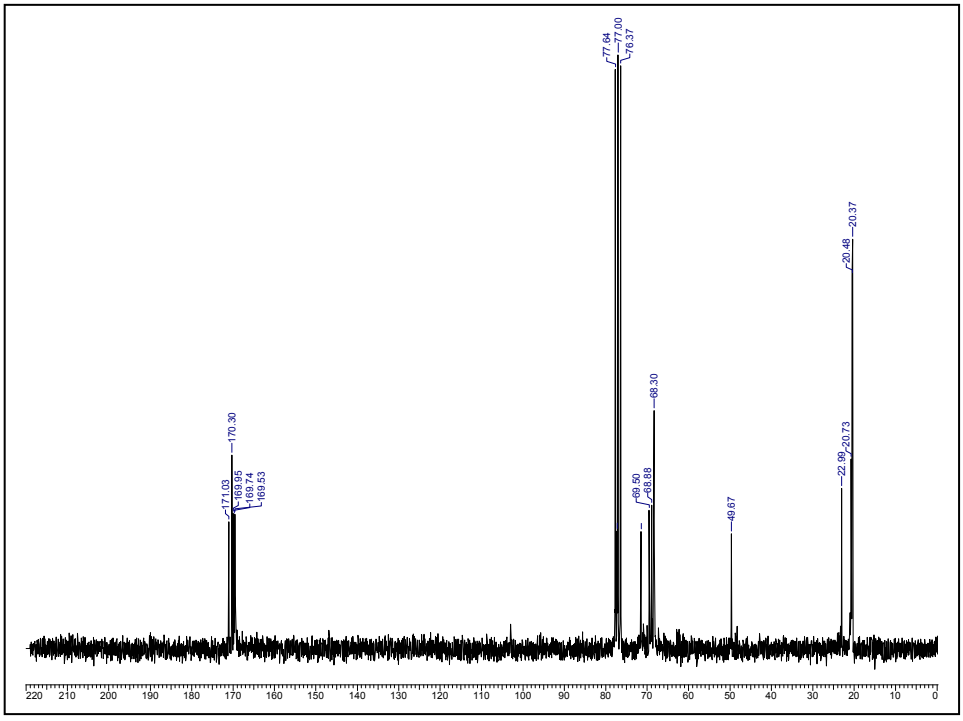
77.64
77.00
76.37
68.30
20.48
20.37
170.30
171.03
169.95
169.74
169.53
69.50
68.68
49.67
22.99
20.73
220 210 200 190 180 170 160 150 140 130 120 110 100 90 80 70 60 50 40 30 20 10 0

DEPT

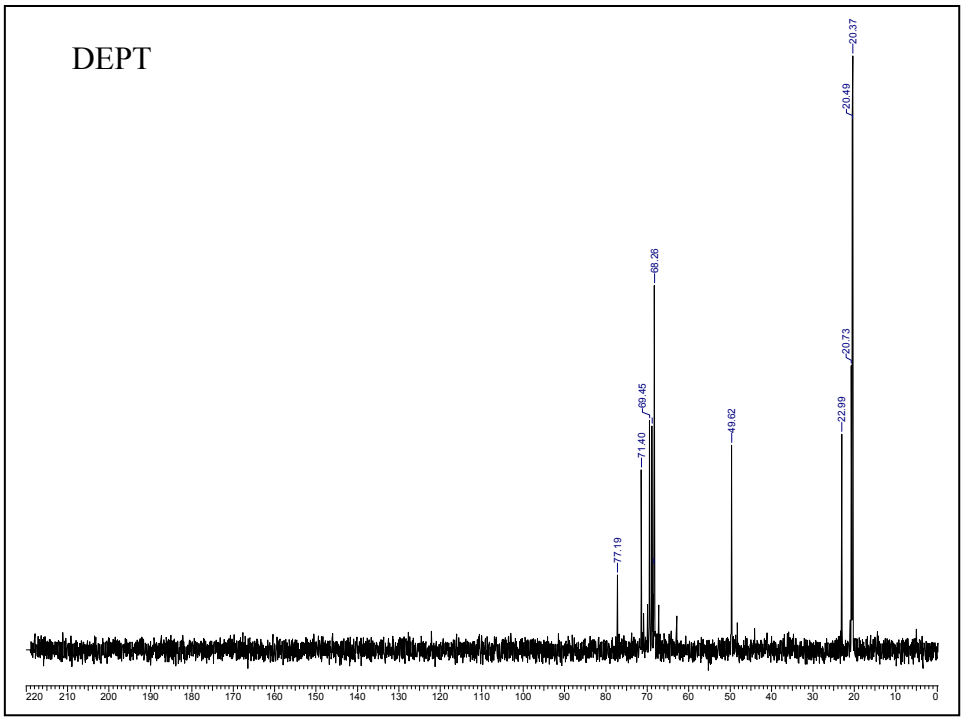
20.37
20.49
68.26
20.73
69.45
71.40
49.62
22.99
77.19
220 210 200 190 180 170 160 150 140 130 120 110 100 90 80 70 60 50 40 30 20 10 0

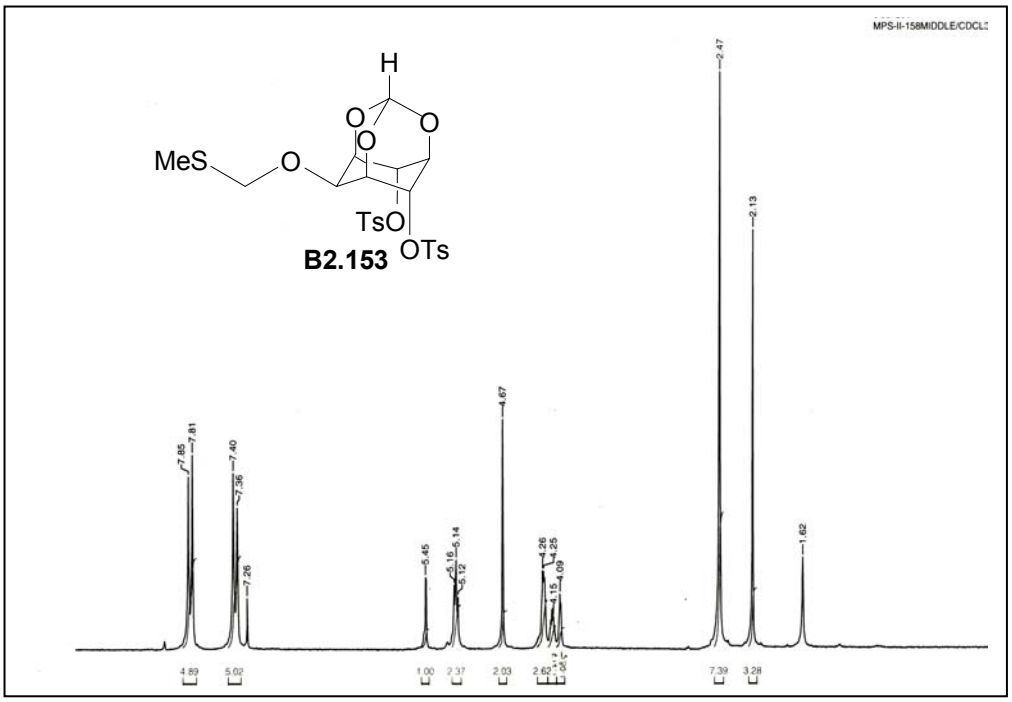
MPS-II-158MIDDLE/CDCL3
H
O
O
O
O
MeS
O
TsO
OTs
B2.153
7.85
7.81
7.40
7.36
7.26
5.45
5.16
5.14
5.12
4.67
4.26
4.25
4.15
4.09
2.47
2.13
1.62
4.89
5.02
1.00
2.37
2.03
2.62
7.39
3.28

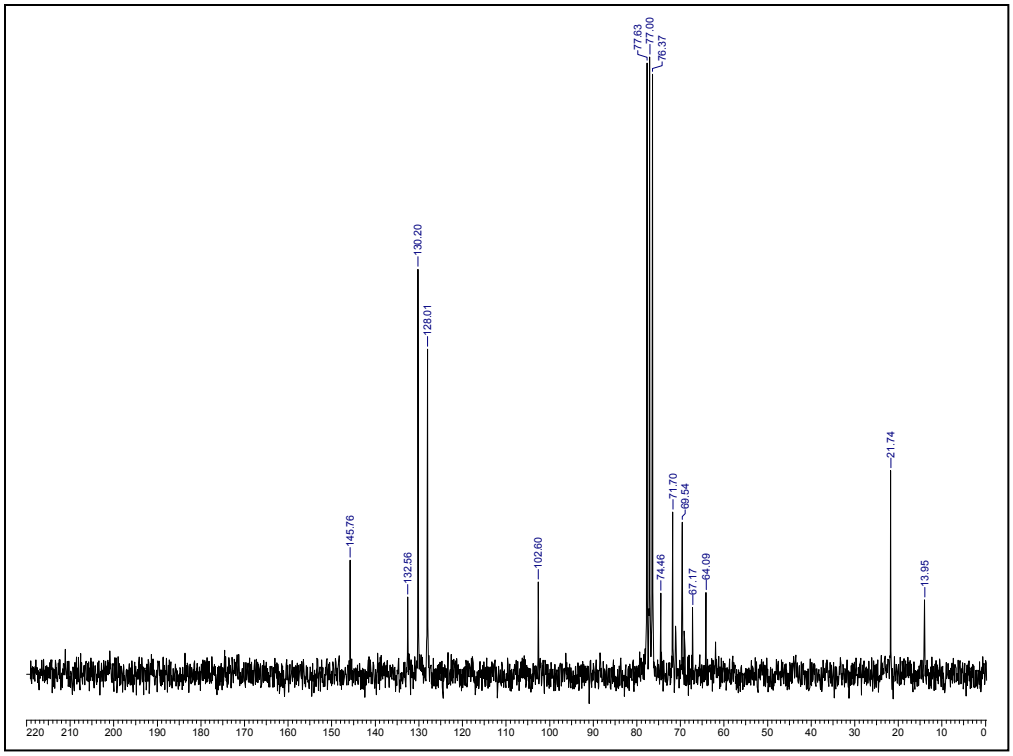
77.63
77.00
76.37
130.20
128.01
145.76
132.56
102.60
74.46
71.70
69.54
67.17
64.09
21.74
13.95
220 210 200 190 180 170 160 150 140 130 120 110 100 90 80 70 60 50 40 30 20 10 0

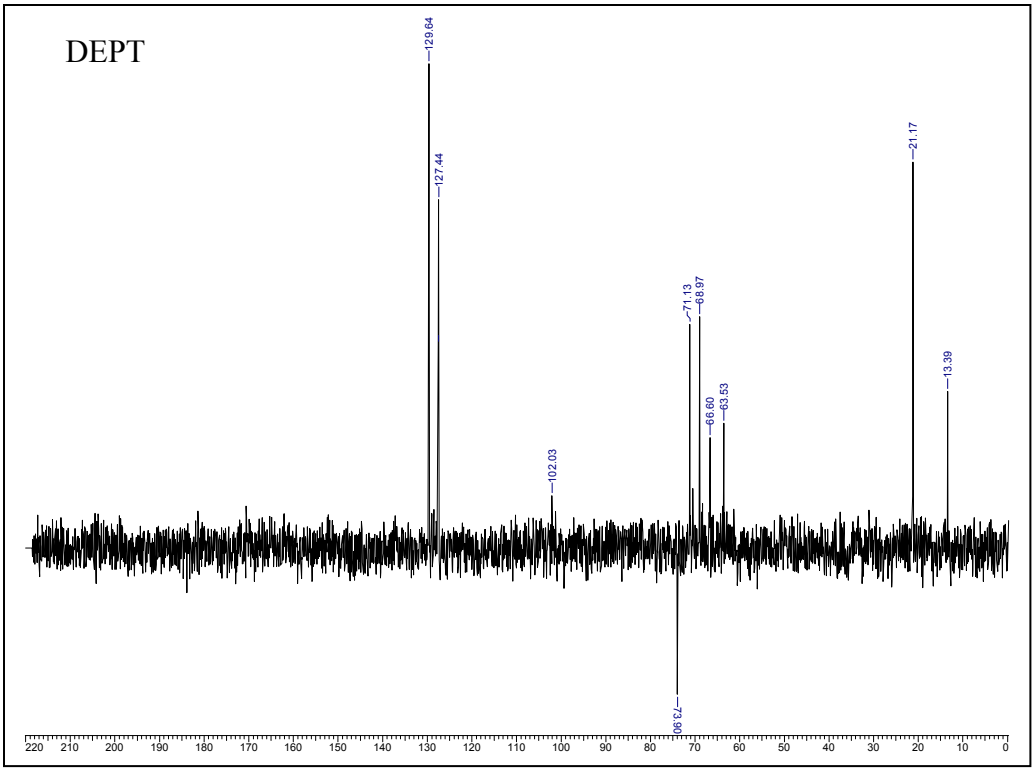
DEPT
129.64
127.44
102.03
73.90
71.13
68.97
66.60
63.53
21.17
13.39

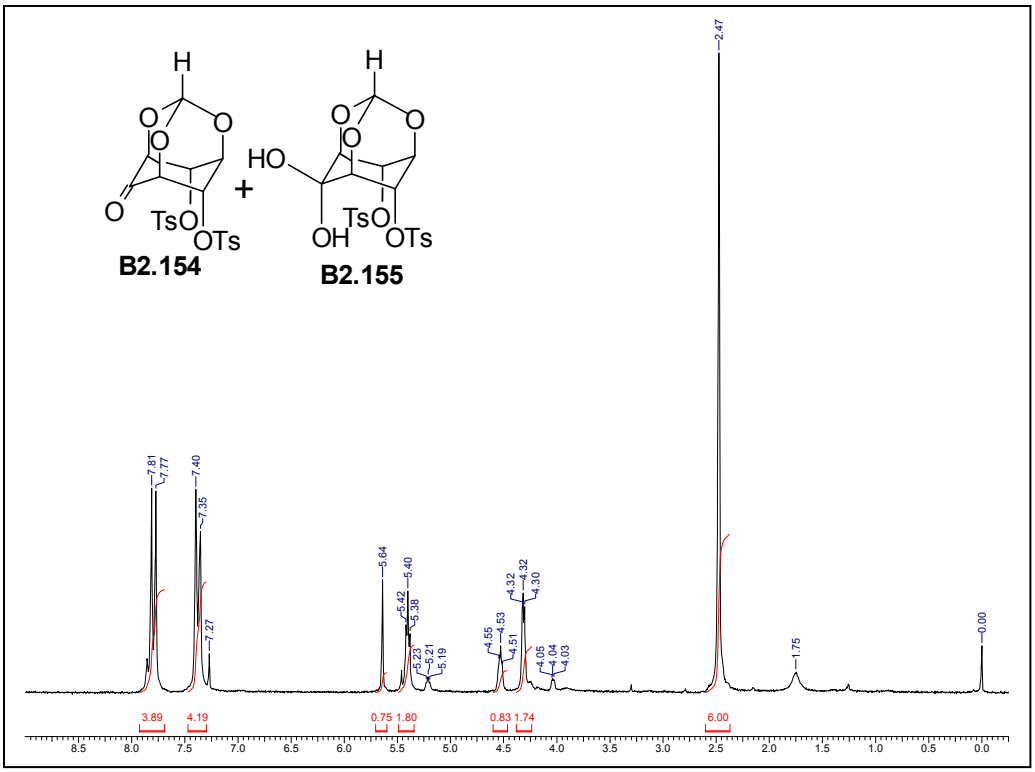
B2.154
B2.155
7.81
7.77
7.40
7.35
7.27
5.64
5.42
5.40
5.38
5.23
5.21
5.19
4.55
4.53
4.51
4.32
4.32
4.30
4.05
4.04
4.03
2.47
1.75
0.00
3.89
4.19
0.75
1.80
0.83
1.74
6.00

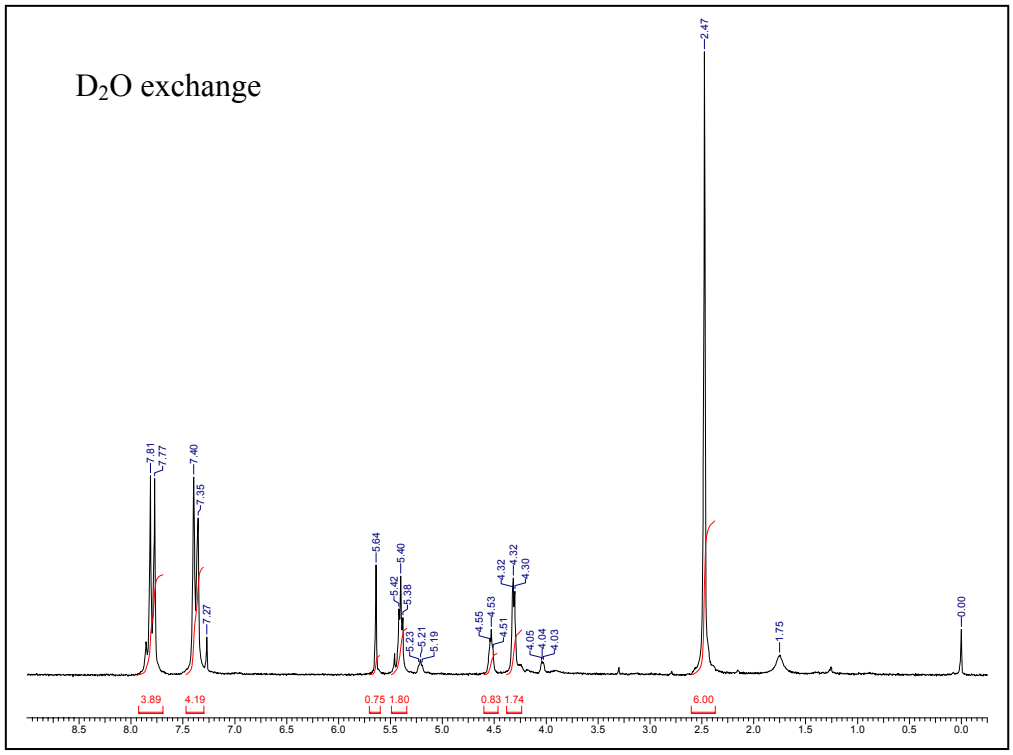
D2O exchange
2.47
7.81
7.77
7.40
7.35
7.27
5.64
5.42
5.40
5.38
5.23
5.21
5.19
4.55
4.53
4.51
4.32
4.32
4.30
4.05
4.04
4.03
1.75
0.00
3.89
4.19
0.75
1.80
0.83
1.74
6.00

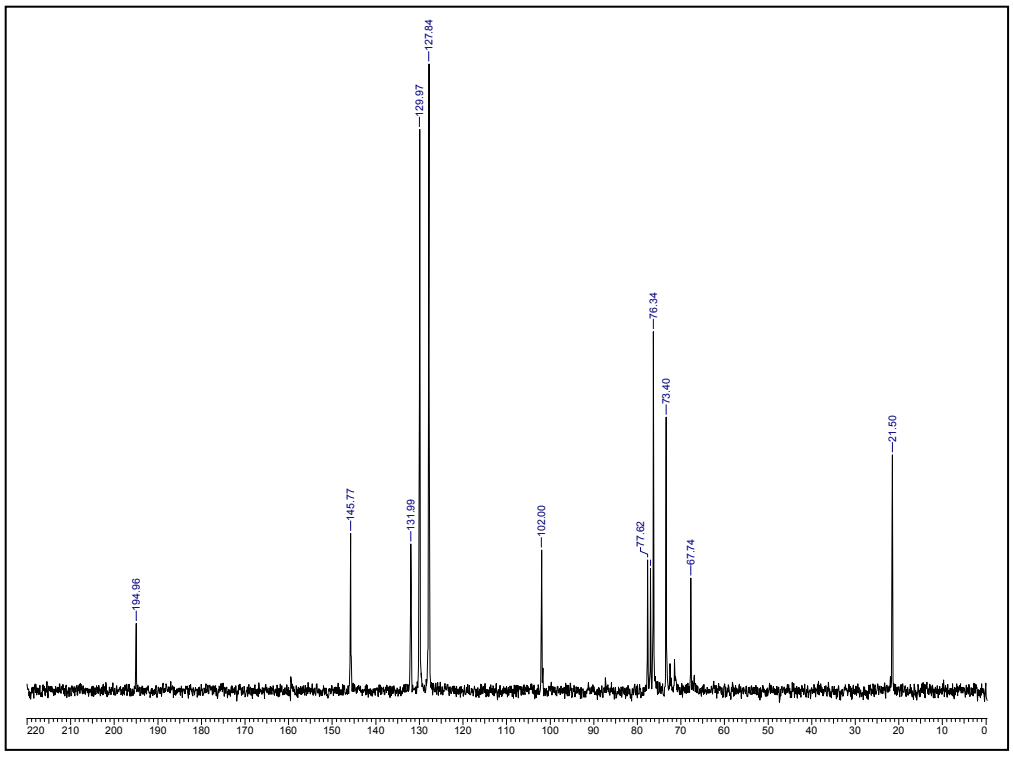
194.96
145.77
131.99
129.97
127.84
102.00
77.62
76.34
73.40
67.74
21.50

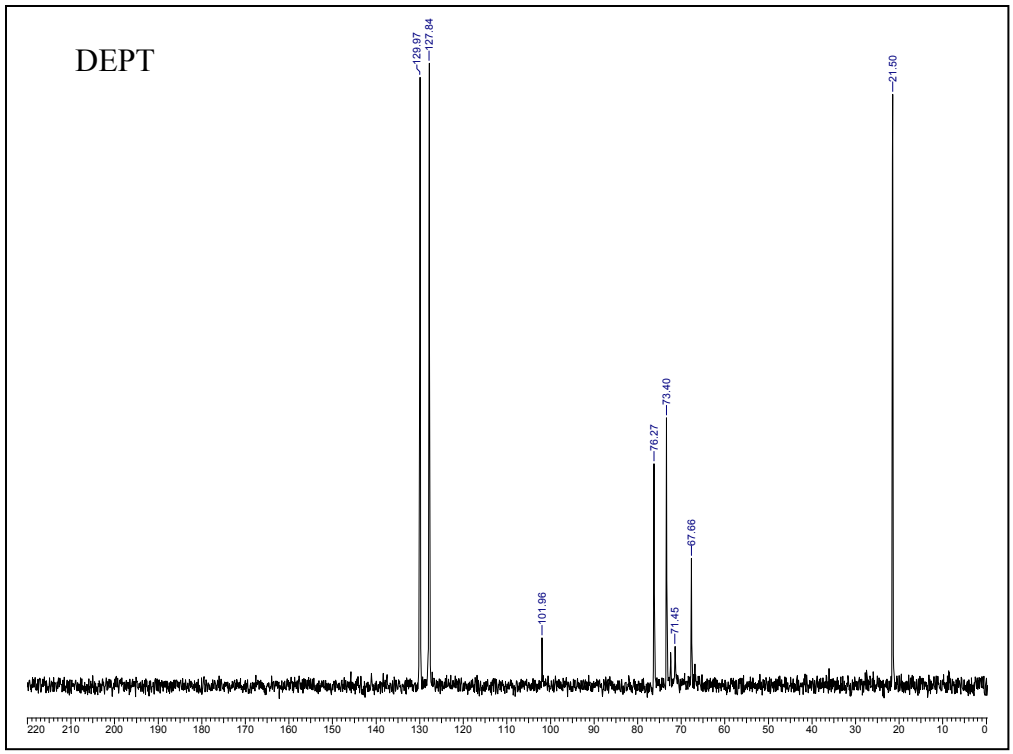

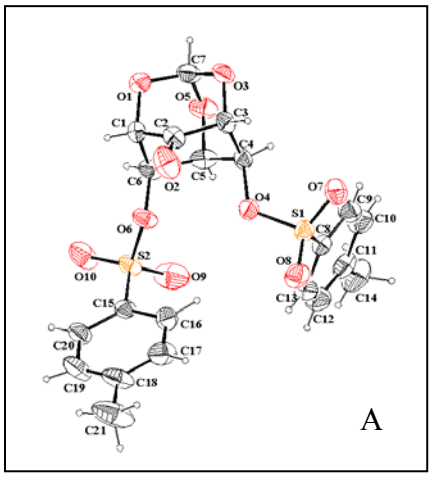

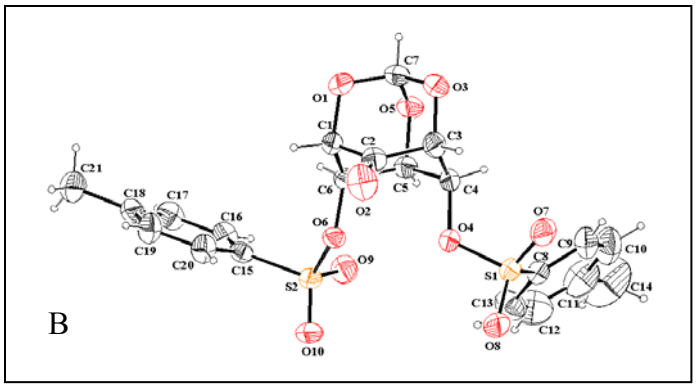

ORTEPs of **B2.154,** (A) from chloroform (B) from dichloromethane

Crystal data table of **B2.154**

Identification code	**B2.154** (from chloroform)	**B2.154** (from dichloromethane)
Empirical formula	$C_{21}H_{20}O_{10}S_2$	$C_{21}H_{20}O_{10}S_2$
Formula weight	496.49	496.49
Temperature	293(2) K	293(2) K
Wavelength	0.71073 Å	0.71073 Å
Crystal system, space group	Monoclinic, *P*2(1)/c	Orthorhombic, *P*bcn
Unit cell dimensions	a = 15.604(5) Å; α = 90º b = 12.949(4) Å; β = 108.270(5)º c = 11.554(4) Å; γ = 90º	a = 16.976(10) Å; α = 90º b = 17.134(13) Å; β = 90º c = 16.088(11) Å; γ = 90º
Volume	2217.0(13) $Å^3$	4679(5) $Å^3$
Z, Calculated density	4, 1.488 Mg/m^3	8, 1.410 Mg/m^3
Absorption coefficient	0.296 mm^{-1}	0.281 mm^{-1}
F(000)	1032	2064
Crystal size	0.37 x 0.29 x 0.08 mm	0.55 x 0.41 x 0.06 mm
θ range for data collection	2.49 to 25.00º	1.69 to 25.25º
Limiting indices	-18<=h<=18, -15<=k<=15, -13<=l<=13	-20<=h<=20; -19<=k<=20; -19<=l<=19
Reflections collected / unique	20329 / 3894 [R(int) = 0.0424]	31738 / 4232 [R(int) = 0.0546]
Completeness to θ = 25.00	99.6 %	99.7 %
Max. and min. transmission	0.9770 and 0.8972	0.9842 and 0.8620
Refinement method	Full-matrix least-squares on F^2	Full-matrix least-squares on F^2
Data / restraints / parameters	3894 / 0 / 356	4232 / 0 / 340
Goodness-of-fit on F^2	1.143	1.141
Final R indices [I>2σ (I)]	R1 = 0.0763, wR2 = 0.1908	R1 = 0.0360, wR2 = 0.1246
R indices (all data)	R1 = 0.0898, wR2 = 0.2007	R1 = 0.0920, wR2 = 0.1359
Extinction coefficient	none	none
Largest diff. peak and hole (ρ_{max} & ρ_{min})	1.229 and -0.227 e. $Å^{-3}$	0.291 and -0.173 e. $Å^{-3}$

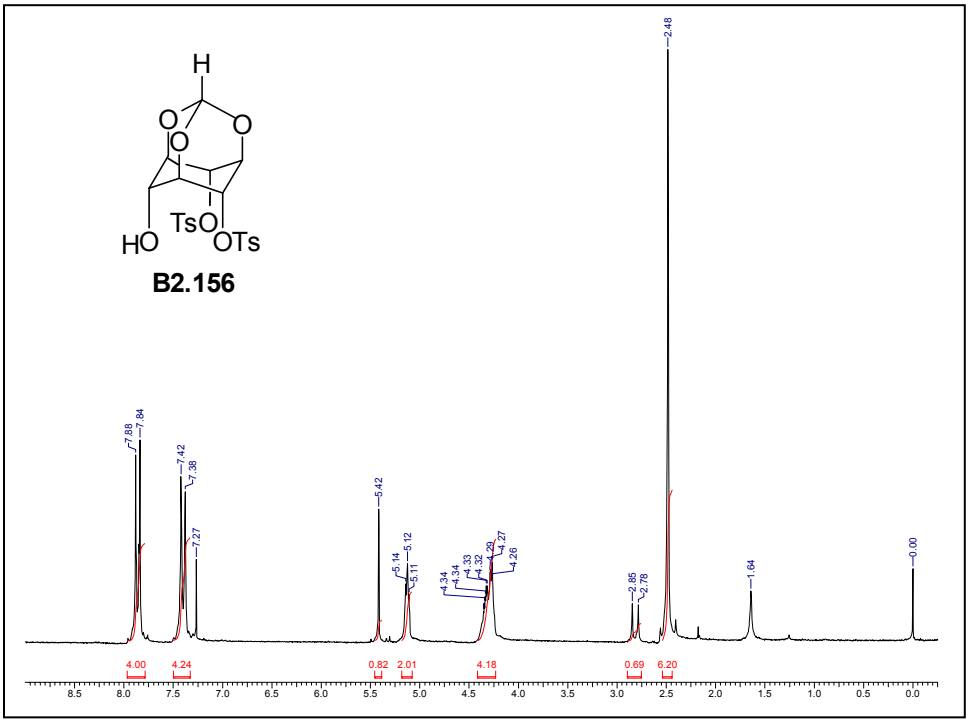
H
O
O
O
O
HO
TsO
OTs
B2.156
7.88
7.84
7.42
7.38
7.27
5.42
5.14
5.12
5.11
4.34
4.33
4.32
4.29
4.27
4.26
2.85
2.78
2.48
1.64
0.00
4.00
4.24
0.82
2.01
4.18
0.69
6.20

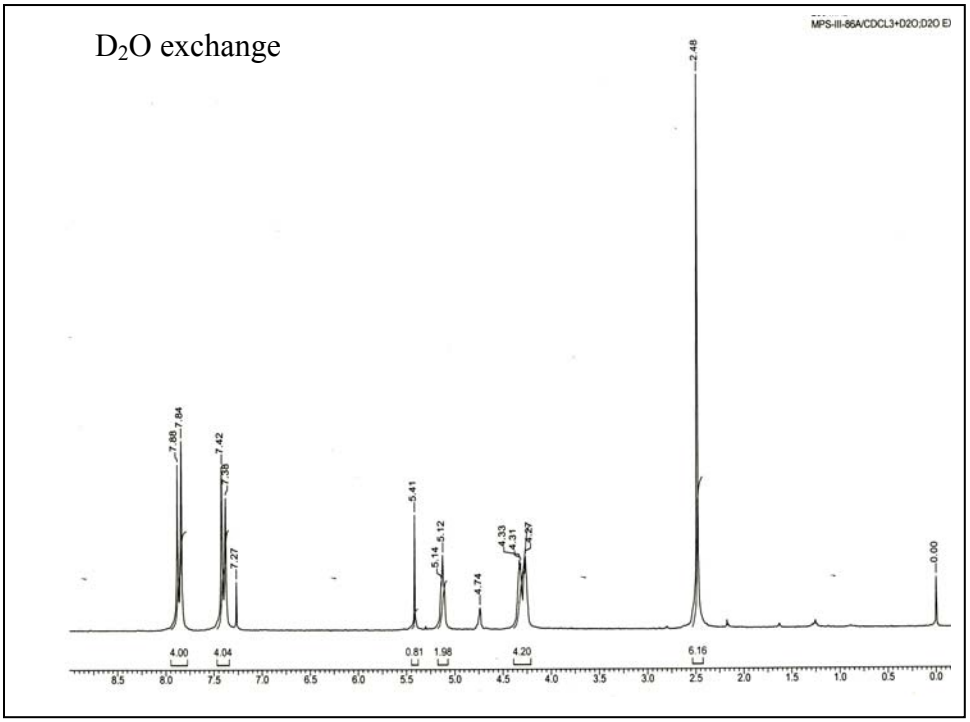
D2O exchange
MPS-III-86A/CDCL3+D2O;D2O E)
7.88
7.84
7.42
7.38
7.27
5.41
5.14
5.12
4.74
4.33
4.31
4.27
2.48
0.00
4.00
4.04
0.81
1.98
4.20
6.16

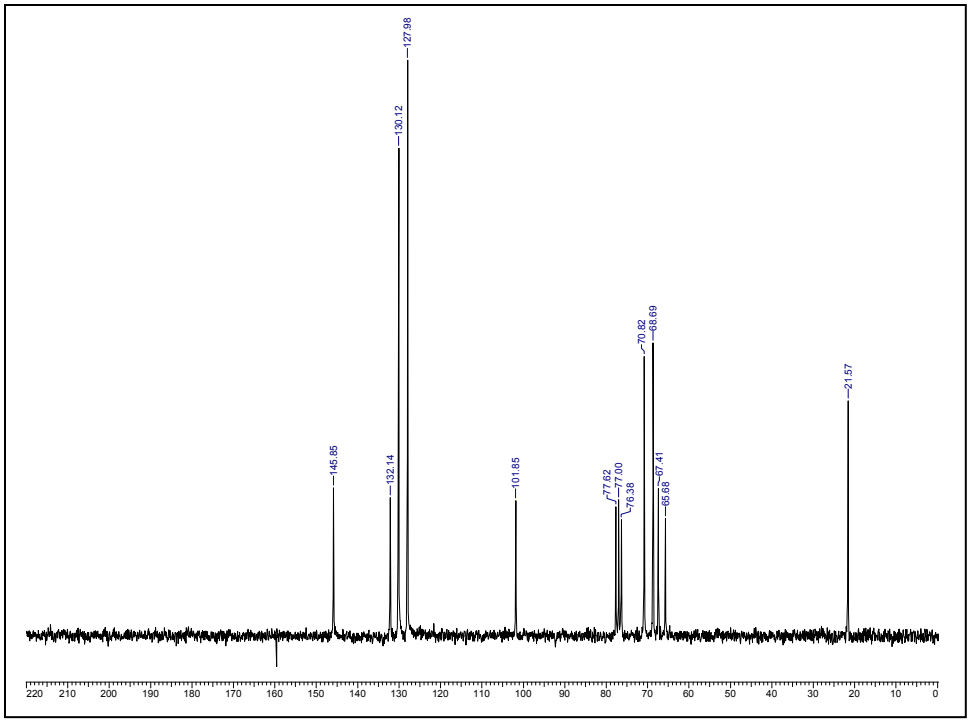
127.98
130.12
70.82
68.69
21.57
145.85
132.14
101.85
77.62
77.00
76.38
67.41
65.68
220 210 200 190 180 170 160 150 140 130 120 110 100 90 80 70 60 50 40 30 20 10 0

DEPT

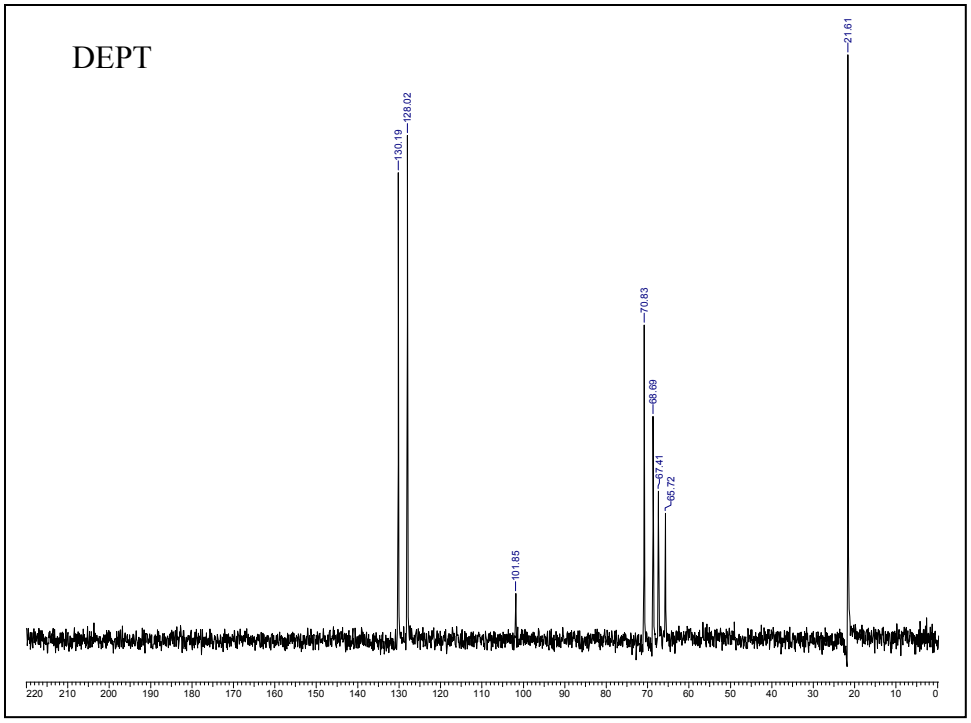
21.61
130.19
128.02
70.83
68.69
67.41
65.72
101.85
220 210 200 190 180 170 160 150 140 130 120 110 100 90 80 70 60 50 40 30 20 10 0

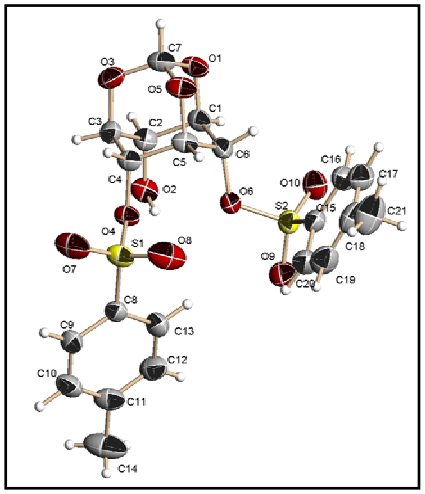

ORTEP of **B2.156**

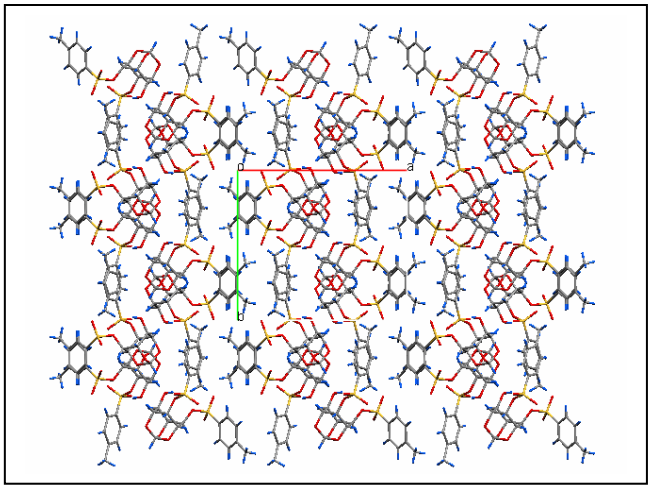

Packing of **B2.156** down the c-axis

Crystall data table of **B2.156**

Identification code	**B2.156** (crystallized from dichloromethane)
Empirical formula	$C_{21}H_{22}O_{10}S_2$
Formula weight	498.51
Temperature	566(2) K
Wavelength	0.71073 Å
Crystal system, space group	Monicliniic, $P2_1/c$
Unit cell dimensions	a = 15.5096(13) Å; α = 90º b = 13.0347(11) Å; β = 100.8320(10)º c = 11.4245(10) Å; γ = 90º
Volume	2198.7(3) $Å^3$
Z, Calculated density	4, 1.506 Mg/m^3
Absorption coefficient	0.299 mm^{-1}
F(000)	1040
Crystal size	0.66 x 0.57 x 0.32 mm
θ range for data collection	2.08 to 25.00º
Limiting indices	-18<=h<=18;-15<=k<=15; -3<=l<=13
Reflections collected / unique	15490 / 3874 [R(int) = 0.0188]
Completeness to θ = 25.00	99.9 %
Max. and min. transmission	0.9104 and 0.8282
Refinement method	Full-matrix least-squares on F^2
Data / restraints / parameters	3874 / 0 / 386
Goodness-of-fit on F^2	1.023
Final R indices [I>2σ (I)]	R1 = 0.0369, wR2 = 0.1056
R indices (all data)	R1 = 0.0410, wR2 = 0.1104
Extinction coefficient	none
Largest diff. peak and hole (ρ_{max} & ρ_{min})	0.245 and -0.279 e. $Å^{-3}$

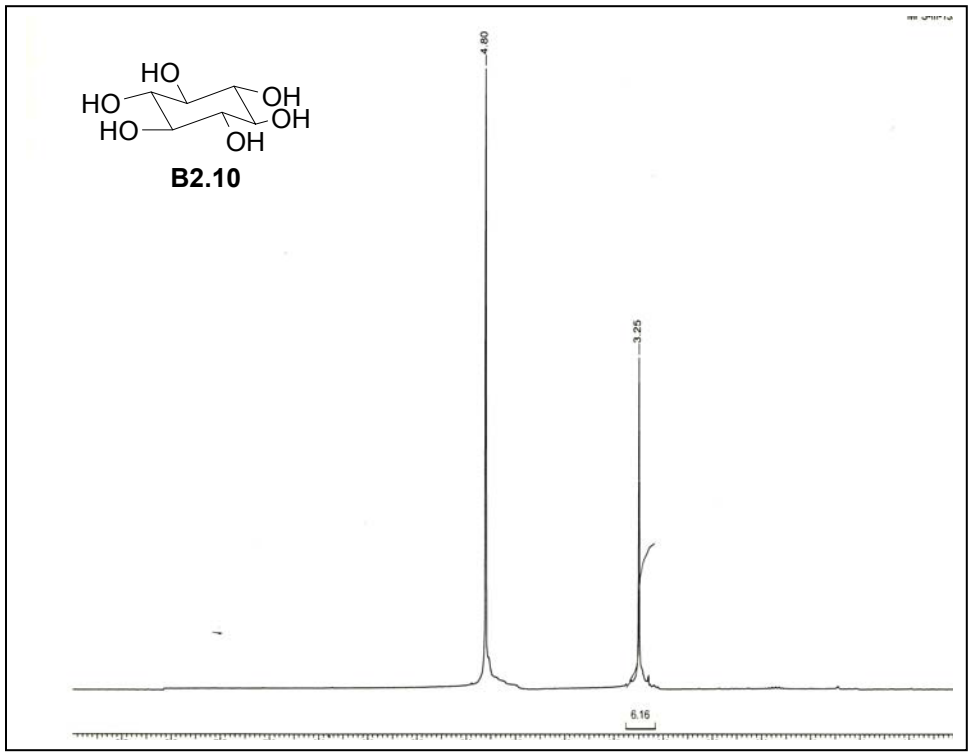
HO
HO
HO
OH
OH
OH
B2.10
4.80
3.25
6.16

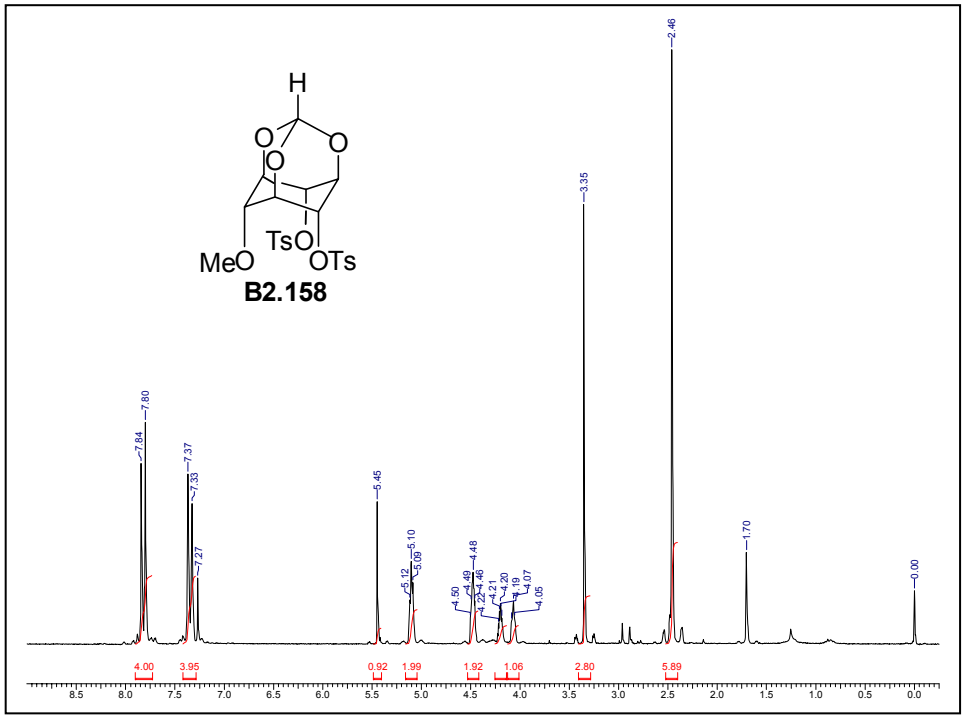
H
O
O
O
MeO
TsO
OTs
B2.158
2.46
3.35
7.80
7.84
7.37
7.33
7.27
5.45
5.12
5.10
5.08
4.50
4.48
4.46
4.22
4.20
4.19
4.07
4.05
1.70
0.00
4.00
3.95
0.92
1.99
1.92
1.06
2.80
5.89

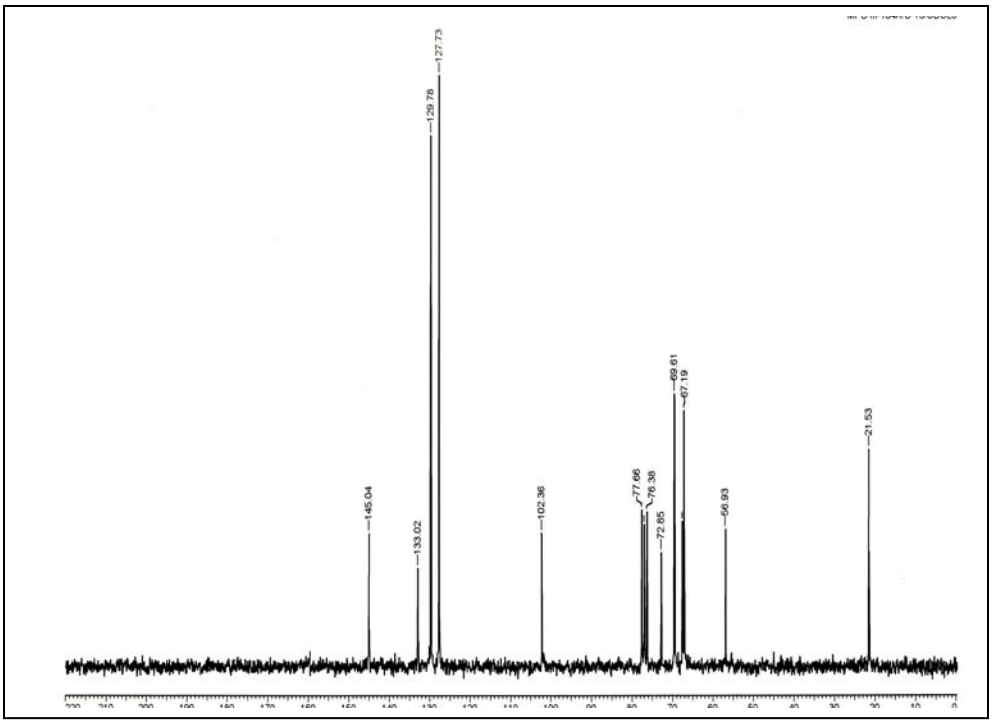
145.04
133.02
129.78
127.73
102.36
77.66
76.38
72.85
69.61
67.19
56.93
21.53

DEPT

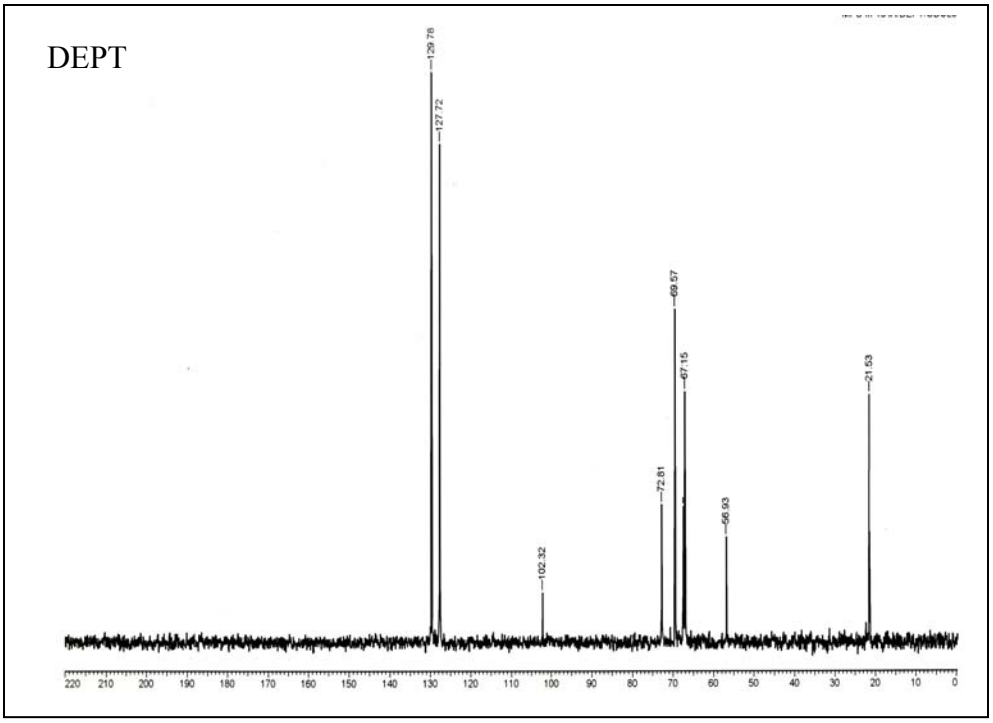
129.78
127.72
102.32
72.81
69.57
67.15
56.93
21.53
220 210 200 190 180 170 160 150 140 130 120 110 100 90 80 70 60 50 40 30 20 10 0

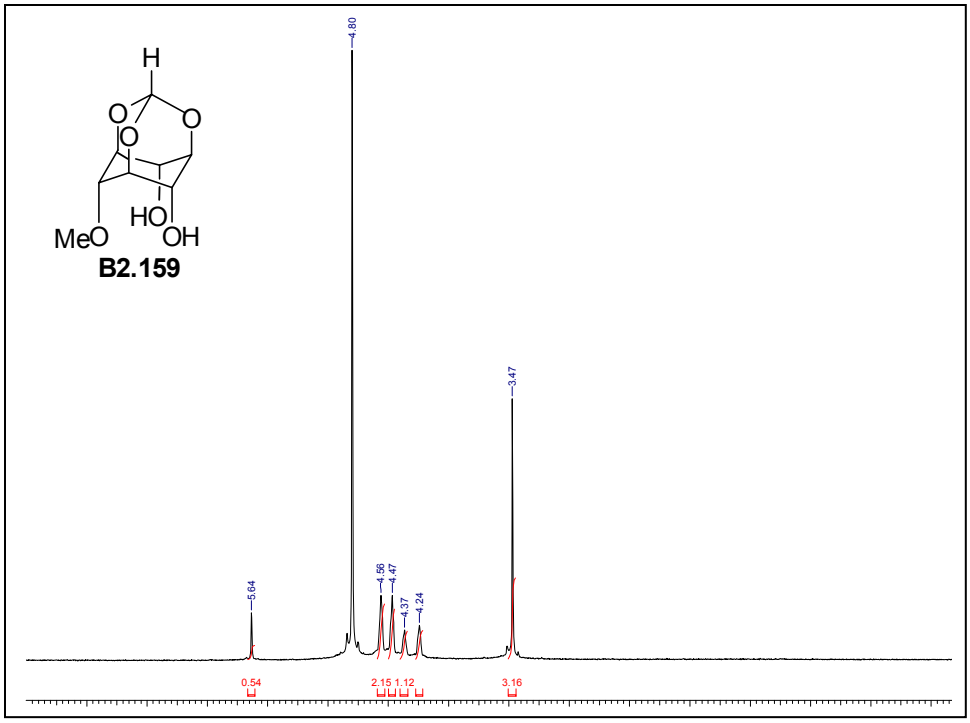
H
O
O
O
HO
MeO
OH
B2.159
4.80
3.47
5.64
4.56
4.47
4.37
4.24
0.54
2.15
1.12
3.16

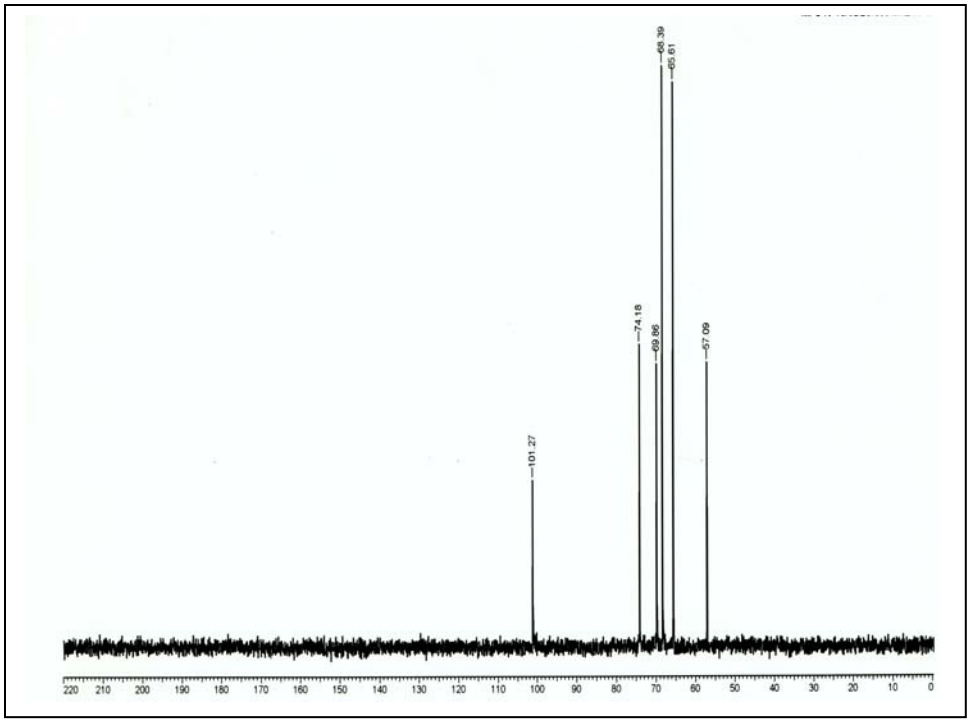
68.39
65.61
74.18
69.86
57.09
101.27
220
210
200
190
180
170
160
150
140
130
120
110
100
90
80
70
60
50
40
30
20
10
0

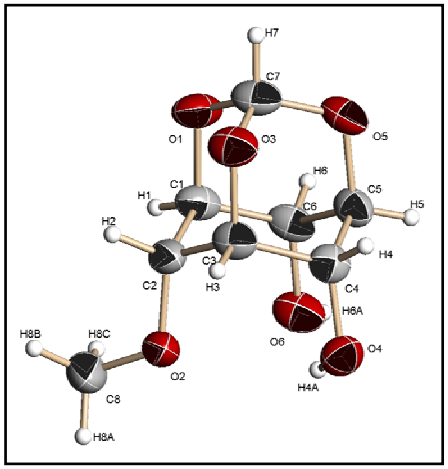

ORTEP of **B2.159**

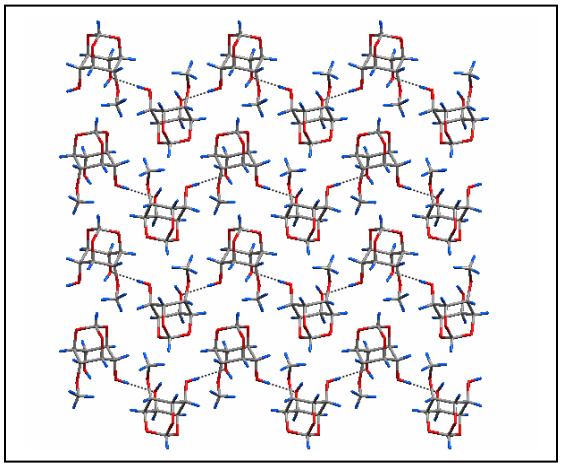

Packing of **B2.159** down c-axis

Crystal data table of **B2.159**

Identification code	**B2.159** (methanol crystals)
Empirical formula	$C_8H_{12}O_6$
Formula weight	208.18
Temperature	566(2) K
Wavelength	0.71073 Å
Crystal system, space group	Orthorhombic, *F*dd2
Unit cell dimensions	a = 19.452(8) Å; α = 90º b = 26.690(10) Å; β = 90º c = 6.496(2) Å; γ = 90º
Volume	3372(2) $Å^3$
Z, Calculated density	16, 1.609 Mg/m^3
Absorption coefficient	0.140 mm^{-1}
F(000)	1728
Crystal size	0.77 × 0.25 × 0.24 mm
θ range for data collection	2.59 to 23.31º
Limiting indices	-17<=h<=21;-27<=k<=29; -7<=l<=7
Reflections collected / unique	3470 / 1198 [R(int) = 0.0310]
Completeness to θ = 25.00	98.8 %
Max. and min. transmission	0.9672 and 0.9000
Refinement method	Full-matrix least-squares on F^2
Data / restraints / parameters	1198 / 1 / 176
Goodness-of-fit on F^2	1.105
Final R indices [I>2σ (I)]	R1 = 0.0243, wR2 = 0.0621
R indices (all data)	R1 = 0.0248, wR2 = 0.0628
Extinction coefficient	None
Largest diff. peak and hole (ρ_{max} & ρ_{min})	0.093 and -0.134 e. $Å^{-3}$

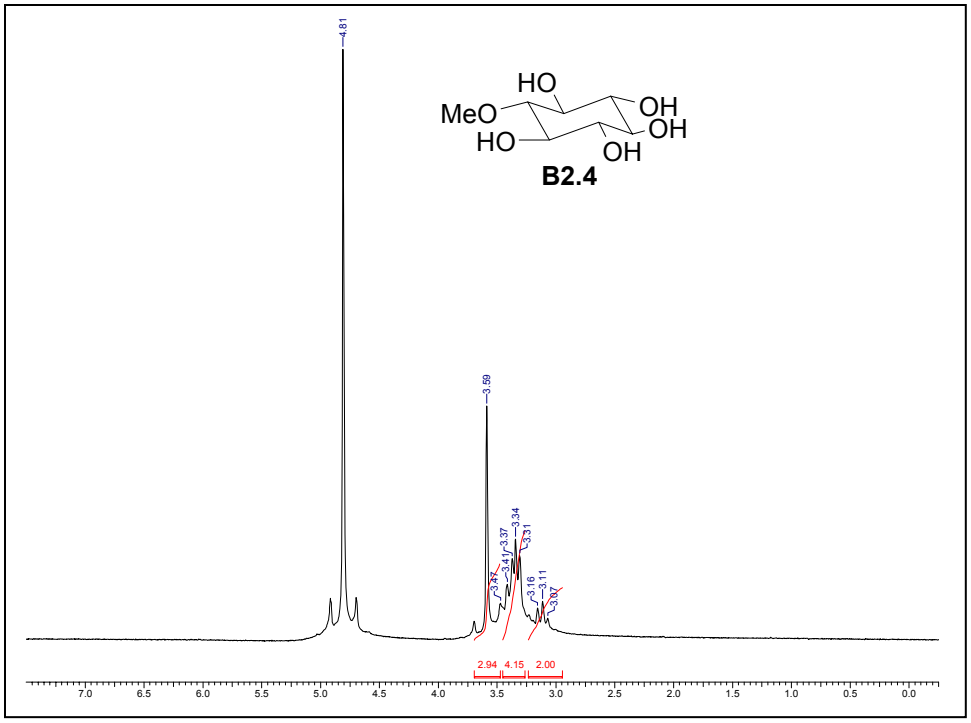
4.81
HO
MeO
HO
OH
OH
OH
B2.4
3.59
3.37
3.34
3.31
3.16
3.11
3.07
2.94
4.15
2.00
7.0
6.5
6.0
5.5
5.0
4.5
4.0
3.5
3.0
2.5
2.0
1.5
1.0
0.5
0.0

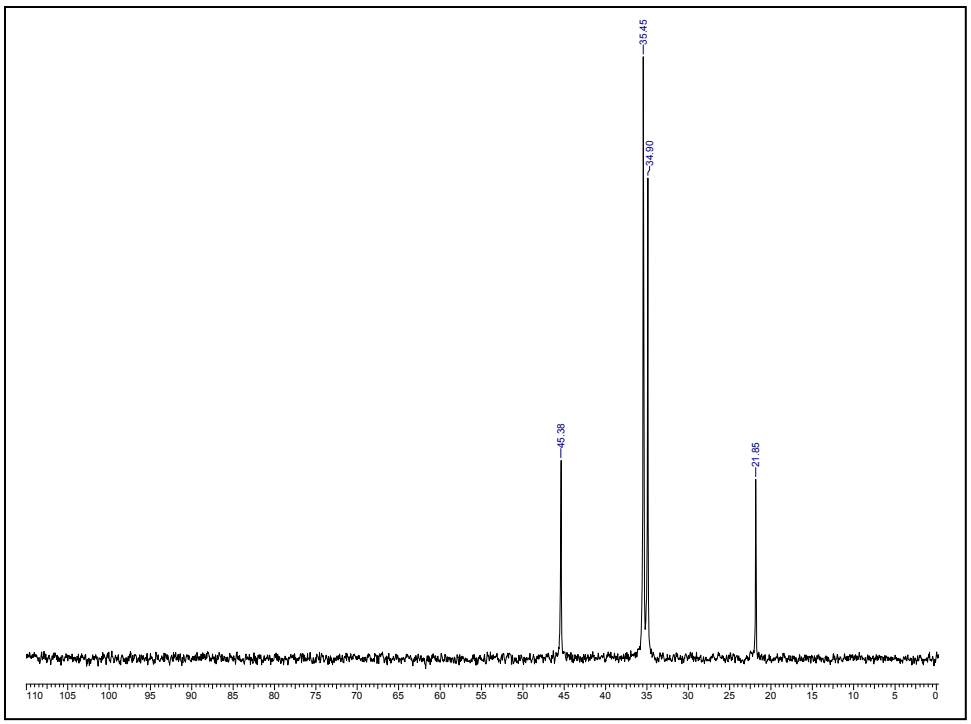
35.45
34.90
45.38
21.85
110
105
100
95
90
85
80
75
70
65
60
55
50
45
40
35
30
25
20
15
10
5
0

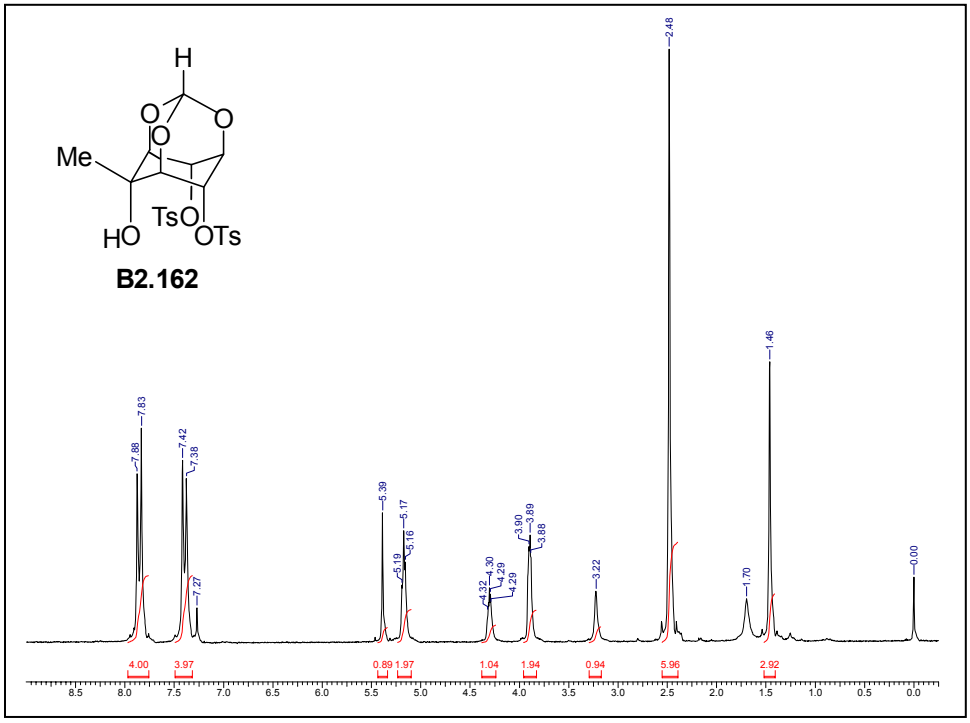
H
O
O
O
Me
TsO
HO
OTs
B2.162
2.48
1.46
7.83
7.88
7.42
7.38
7.27
5.39
5.17
5.16
5.19
4.32
4.30
4.29
3.90
3.89
3.88
3.22
1.70
0.00
4.00
3.97
0.89
1.97
1.04
1.94
0.94
5.96
2.92

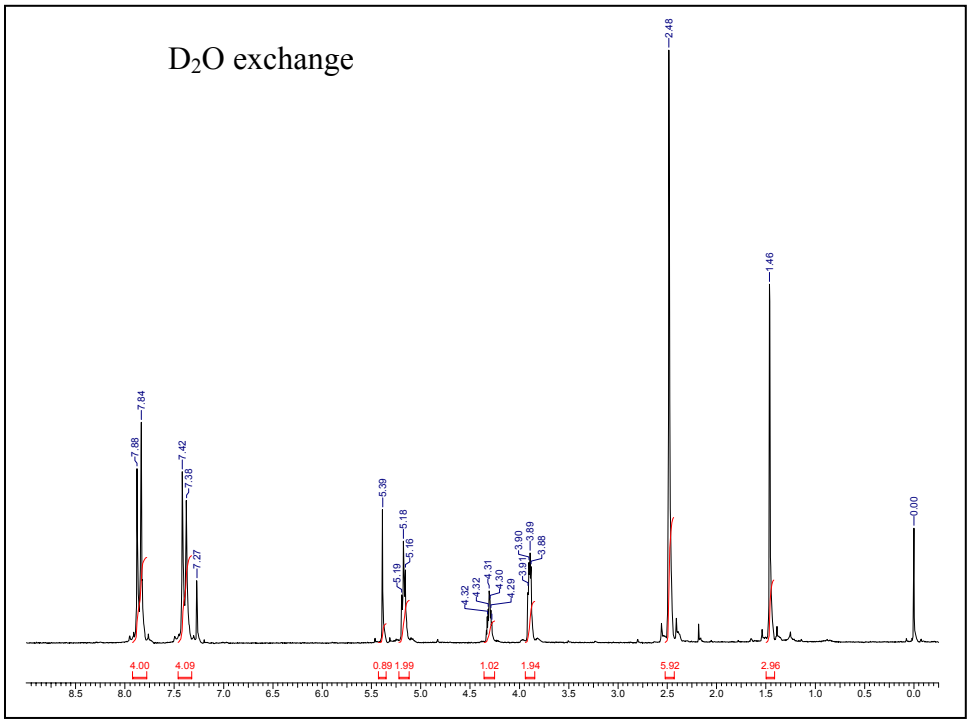
D2O exchange
2.48
1.46
7.84
7.88
7.42
7.38
7.27
5.39
5.18
5.16
5.19
4.32
4.31
4.30
4.29
3.91
3.90
3.89
3.88
0.00
4.00
4.09
0.89
1.99
1.02
1.94
5.92
2.96

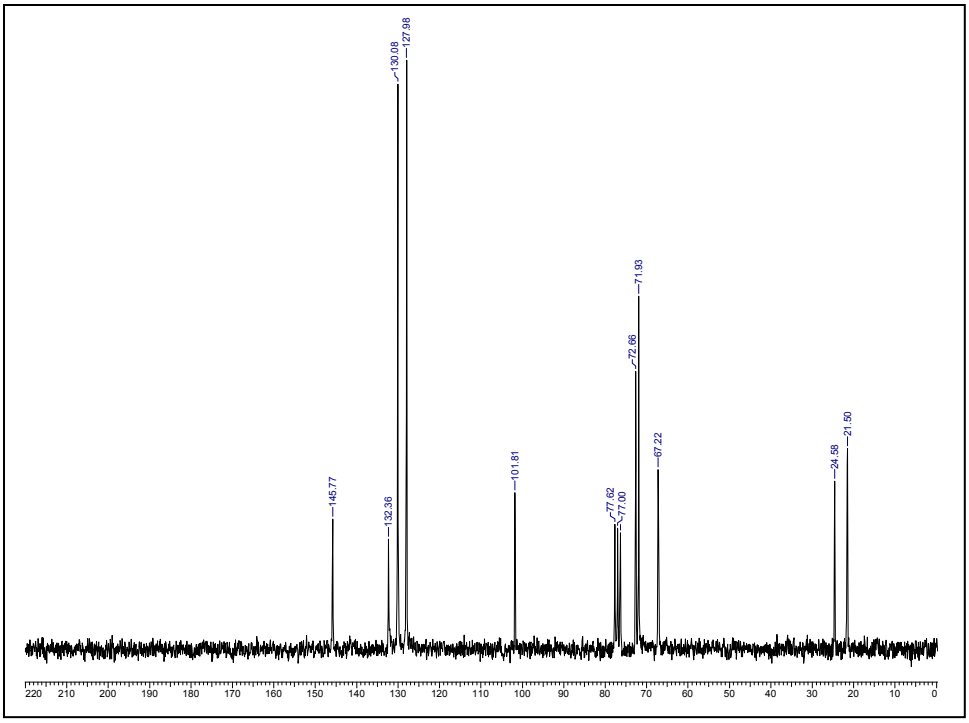
130.08
127.98
71.93
72.66
67.22
21.50
24.58
101.81
145.77
132.36
77.62
77.00
220 210 200 190 180 170 160 150 140 130 120 110 100 90 80 70 60 50 40 30 20 10 0

DEPT

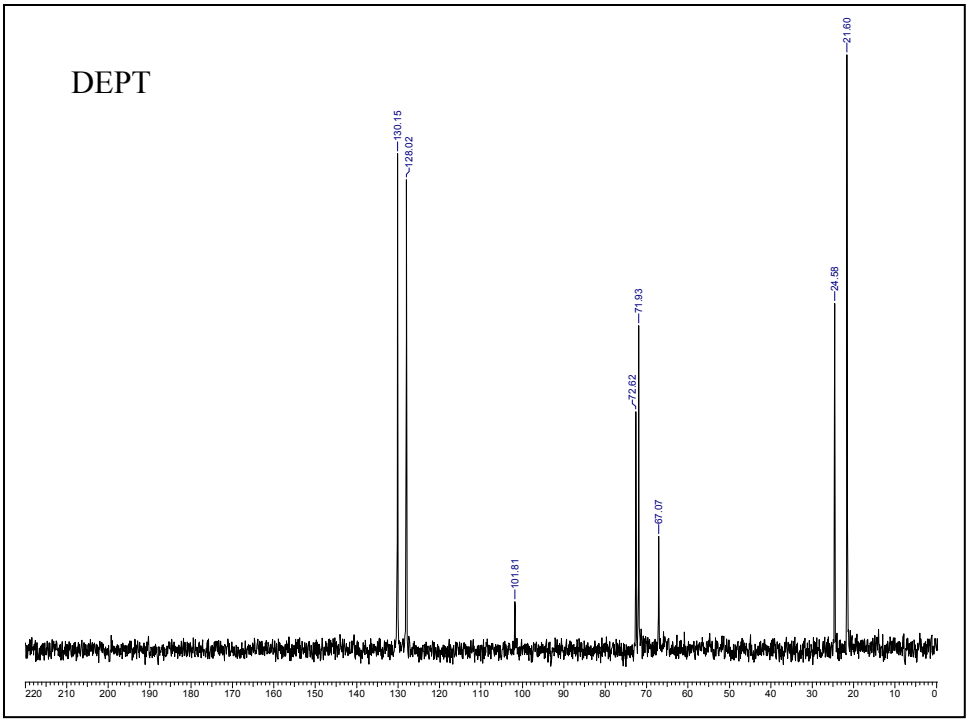
21.60
130.15
128.02
24.58
71.93
72.62
67.07
101.81
220 210 200 190 180 170 160 150 140 130 120 110 100 90 80 70 60 50 40 30 20 10 0

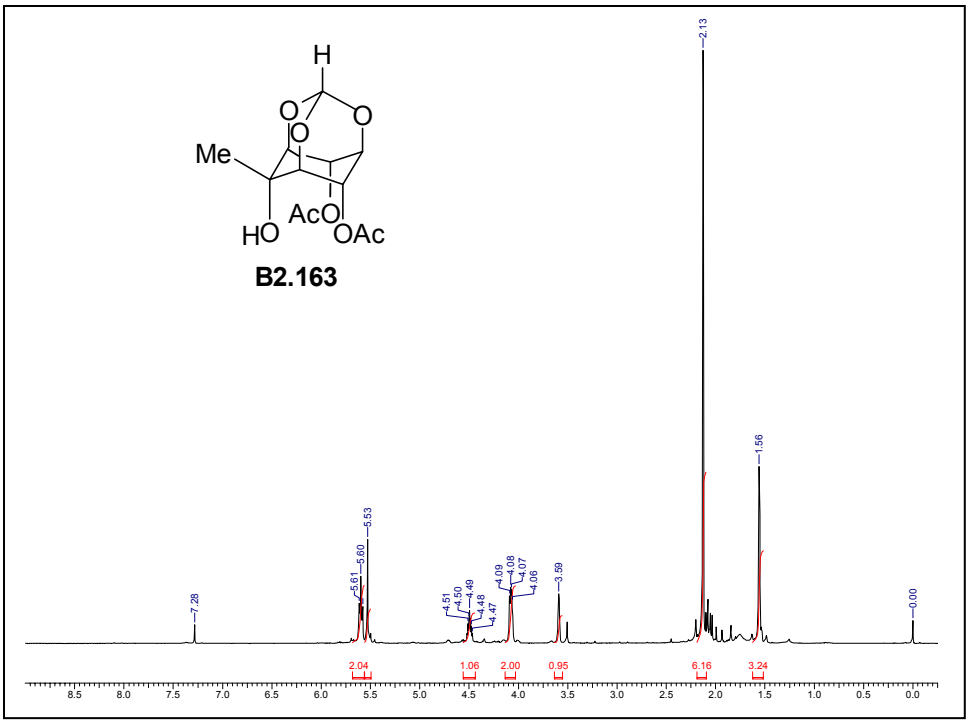
H
O
O
O
Me
HO
AcO
OAc
B2.163
2.13
1.56
5.53
5.61
5.60
4.51
4.50
4.49
4.48
4.47
4.09
4.08
4.07
4.06
3.59
7.28
0.00
2.04
1.06
2.00
0.95
6.16
3.24

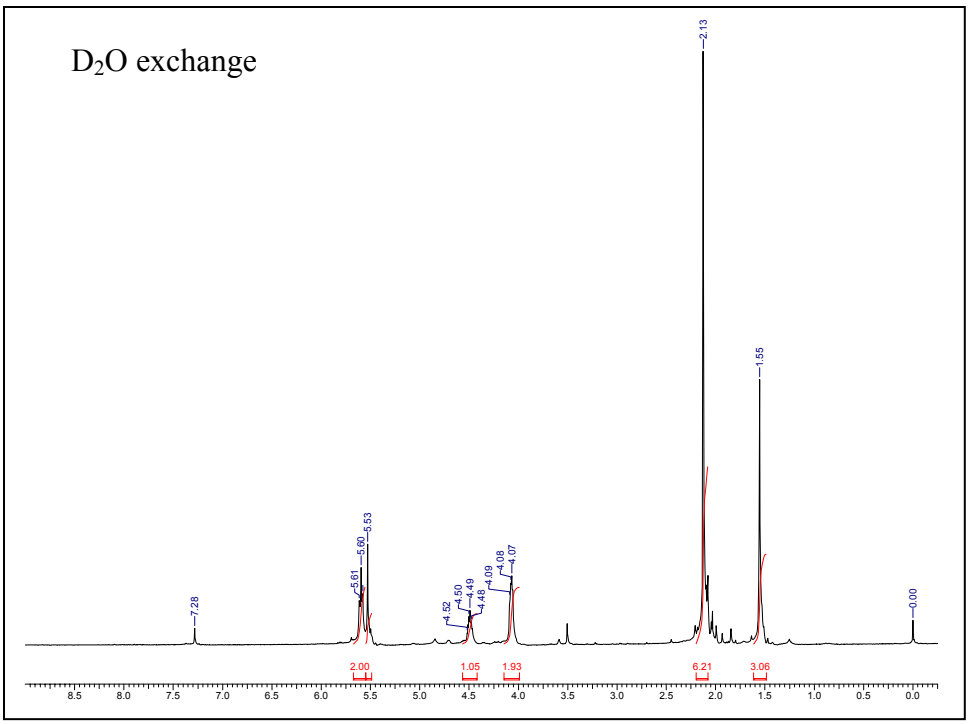
D2O exchange
2.13
1.55
5.53
5.61
5.60
4.52
4.50
4.49
4.48
4.09
4.08
4.07
7.28
0.00
2.00
1.05
1.93
6.21
3.06

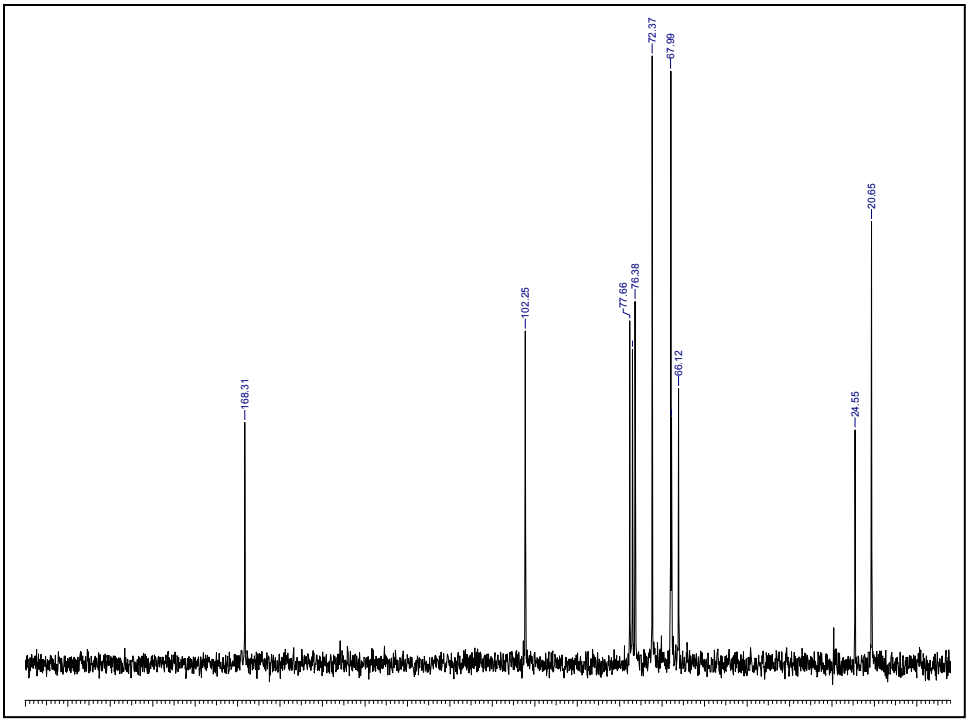
168.31
102.25
77.66
76.38
72.37
67.99
66.12
24.55
20.65

DEPT

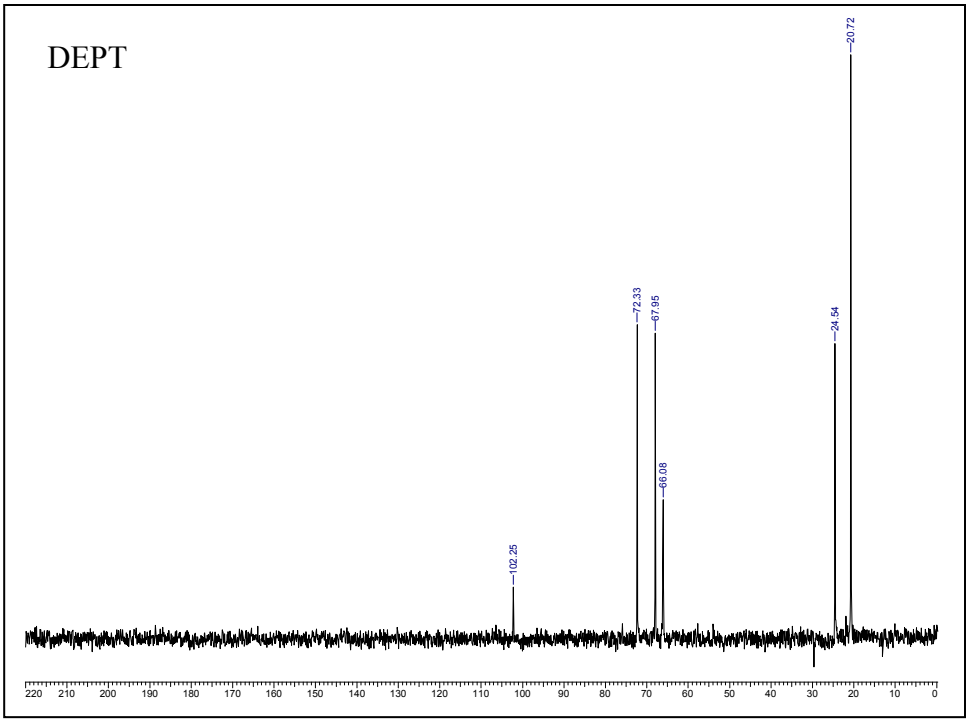
102.25
72.33
67.95
66.08
24.54
20.72
220 210 200 190 180 170 160 150 140 130 120 110 100 90 80 70 60 50 40 30 20 10 0

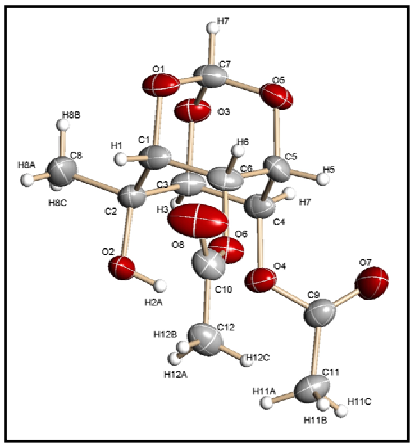

ORTEP of **B2.163**

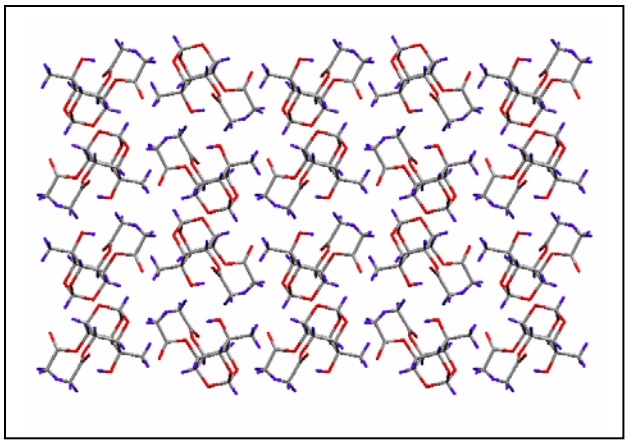

Molecular packing of **B2.163** down the a-axis

Crystal data table of **B2.163**

Identification code	**B2.163**(crystallized from chloroform-light petroleum mixture)
Empirical formula	$C_{12}H_{16}O_8$
Formula weight	288.25
Temperature	293(2) K
Wavelength	0.71073 Å
Crystal system, space group	Monoclinic, $P2_1/n$
Unit cell dimensions	a = 8.019(3) Å; α = 90º b = 14.251(5) Å; β = 106.583(5)º c = 11.837(4) Å; γ = 90º
Volume	1296.4(8) $Å^3$
Z, Calculated density	4, 1.477 Mg/m^3
Absorption coefficient	0.126 mm^{-1}
F(000)	608
Crystal size	0.58 × 0.48 × 0.37 mm
θ range for data collection	2.29º - 25.00º
Limiting indices	-9<=h<=9; -16<=k<=16; -14<=l<=14
Reflections collected / unique	11785 / 2269 [R(int) = 0.0587]
Completeness to θ = 25.00	99.5%
Max. and min. transmission	0.9306 and 0.9548
Refinement method	Full-matrix least-squares on F^2
Data / restraints / parameters	2269/0/213
Goodness-of-fit on F^2	1.134
Final R indices [I>2σ (I)]	R1 = 0.0587, wR2 = 0.1444
R indices (all data)	R1 = 0.0597, wR2 = 0.1454
Extinction coefficient	none
Largest diff. peak and hole (ρ_{max} & ρ_{min})	0.309 and -0.157 e. $Å^{-3}$

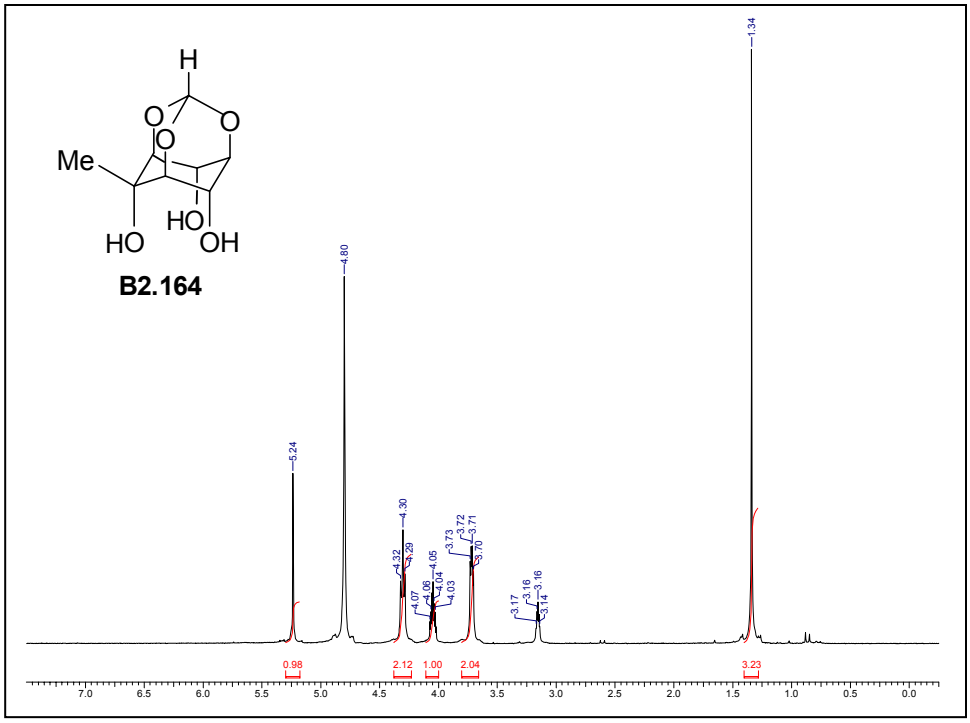
H
O
O
O
Me
HO
HO
OH
B2.164
1.34
4.80
5.24
4.30
4.32
4.29
4.07
4.06
4.05
4.04
4.03
3.73
3.72
3.71
3.70
3.17
3.16
3.16
3.14
0.98
2.12
1.00
2.04
3.23
7.0
6.5
6.0
5.5
5.0
4.5
4.0
3.5
3.0
2.5
2.0
1.5
1.0
0.5
0.0

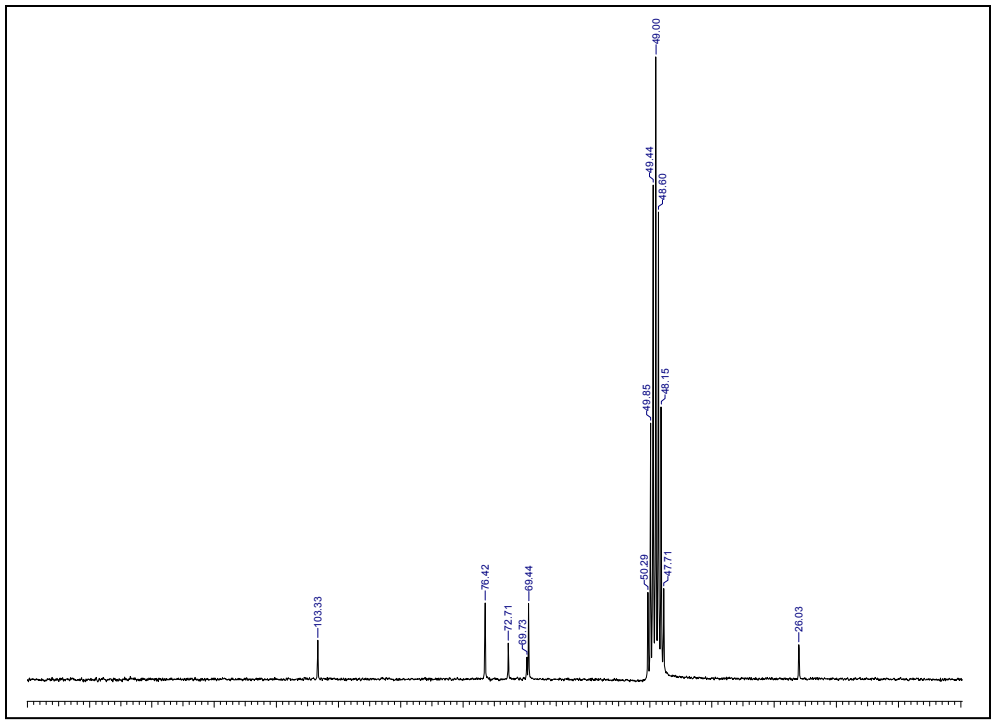
49.00
49.44
48.60
49.85
48.15
50.29
47.71
76.42
69.44
72.71
69.73
103.33
26.03

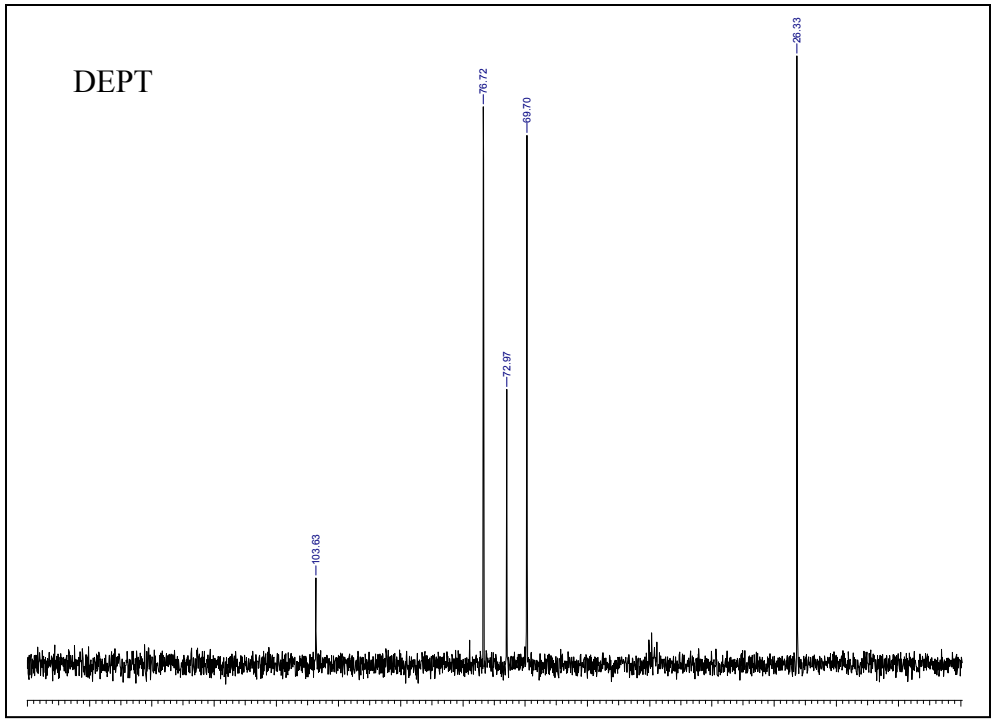
DEPT
26.33
76.72
69.70
72.97
103.63

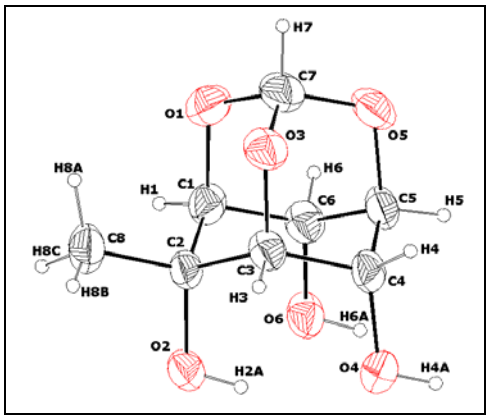

ORTEP of **B2.164**

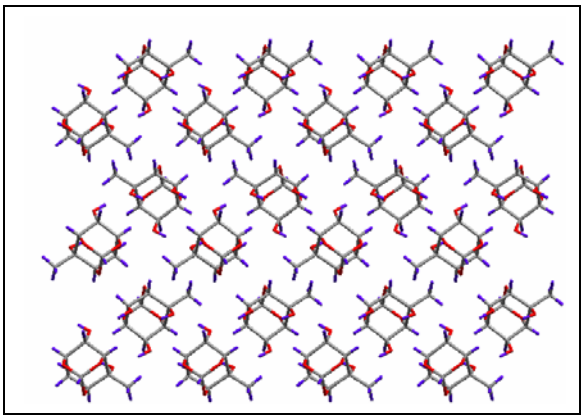

Packing of **B2.164** down the c-axis

Crystal data table of **B2.164**

Identification code	**B2.164**(Crystallized from methanol)
Empirical formula	$C_8H_{12}O_6$
Formula weight	208.18
Temperature	293(2) K
Wavelength	0.71073 Å
Crystal system, space group	Monoclinic, $P2_1/c$
Unit cell dimensions	a = 7.399(5) Å; α = 90° b = 7.500(5) Å; β = 90.399(12)° c = 14.595(10) Å; γ = 90°
Volume	829.8(10) $Å^3$
Z, Calculated density	4, 1.634 Mg/m^3
Absorption coefficient	0.142 mm^{-1}
F(000)	432
Crystal size	0.54 × 0.32 × 0.18 mm
θ range for data collection	2.75 to 25.49°
Limiting indices	-8<=h<=8;-4<=k<=9; -18<=l<=18
Reflections collected / unique	3865 / 1525 [R(int) = 0.0956]
Completeness to θ = 25.00	99.1%
Max. and min. transmission	0.9748 and 0.9272
Refinement method	Full-matrix least-squares on F^2
Data / restraints / parameters	1525 / 0 / 175
Goodness-of-fit on F^2	1.109
Final R indices [I>2σ (I)]	R1 = 0.0608, wR2 = 0.1599
R indices (all data)	R1 = 0.0763, wR2 = 0.1720
Extinction coefficient	None
Largest diff. peak and hole (ρ_{max} & ρ_{min})	0.332 and -0.351 e. $Å^{-3}$

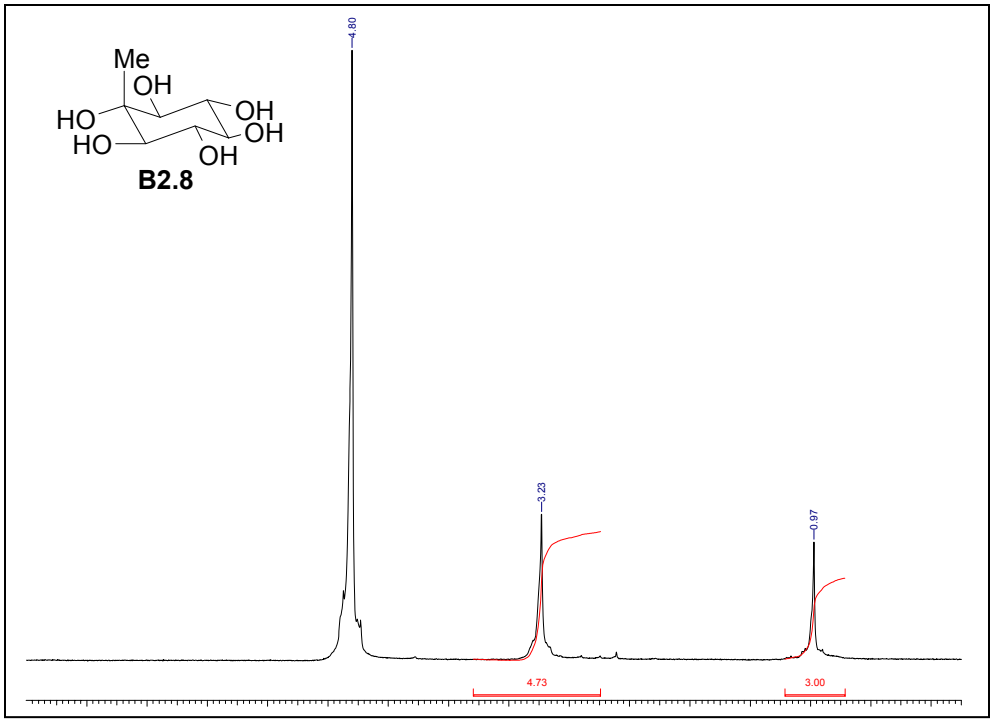
Me
OH
HO
HO
OH
OH
OH
B2.8
4.80
3.23
0.97
4.73
3.00

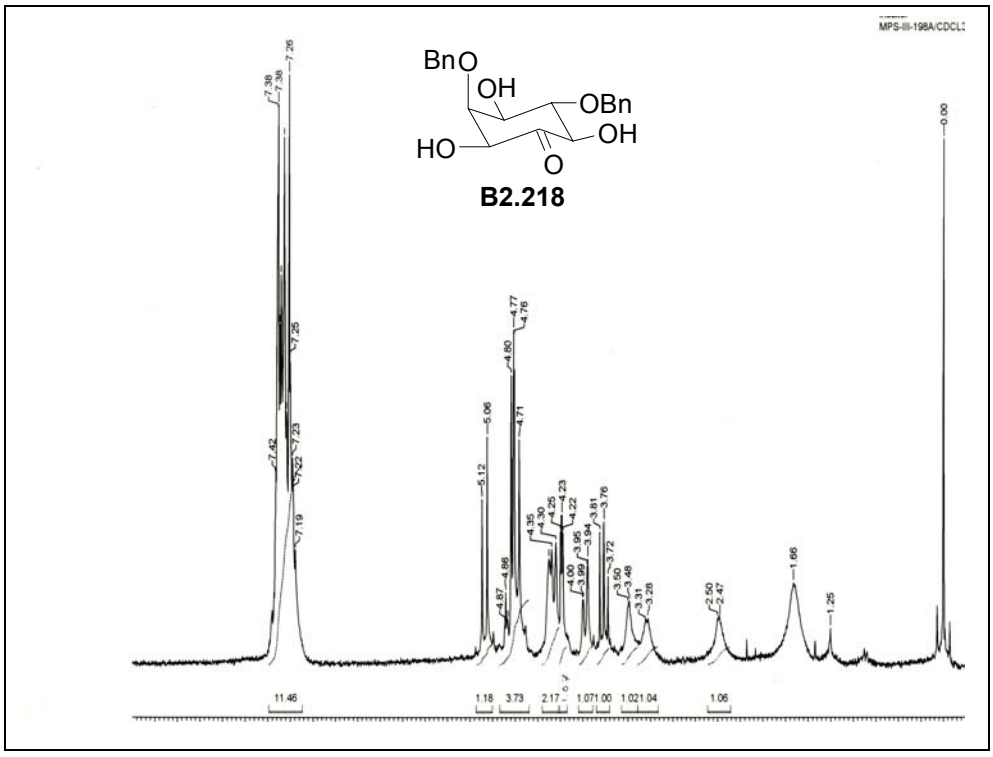
BnO
OH
OBn
HO
OH
O
B2.218
11.46
1.18
3.73
2.17
1.07
1.00
1.02
1.04
1.06

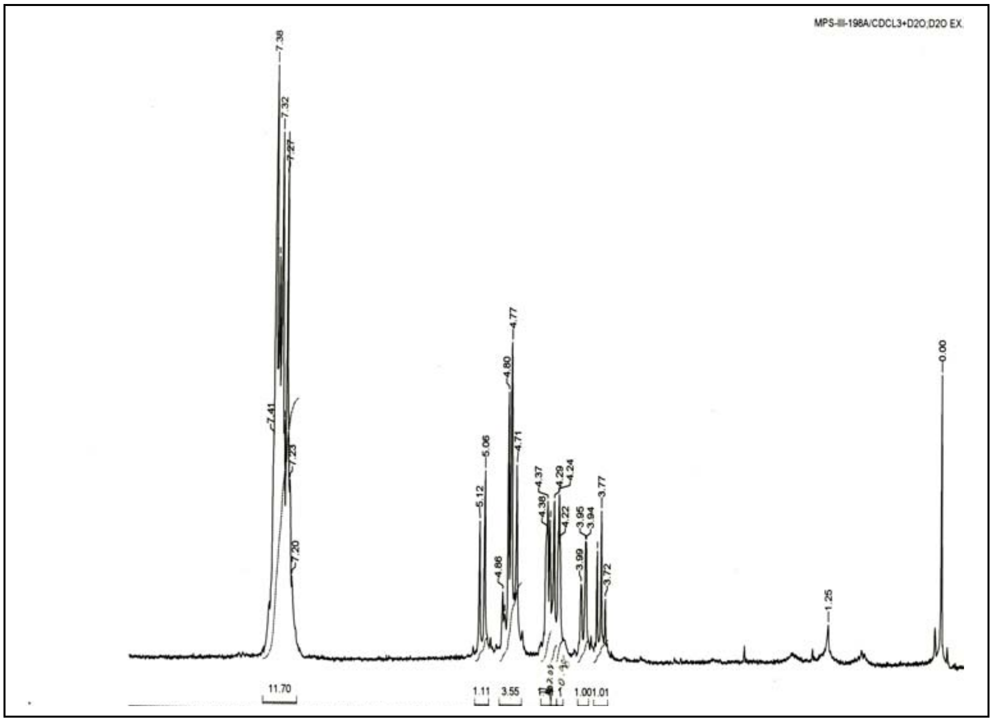
MPS-III-198A/CDCL3+D2O;D2O EX.
7.38
7.32
7.27
7.41
7.23
7.20
4.77
4.80
5.06
4.71
5.12
4.86
4.37
4.38
4.29
4.24
4.22
3.95
3.94
3.99
3.77
3.72
1.25
0.00
11.70
1.11
3.55
1.00
1.01

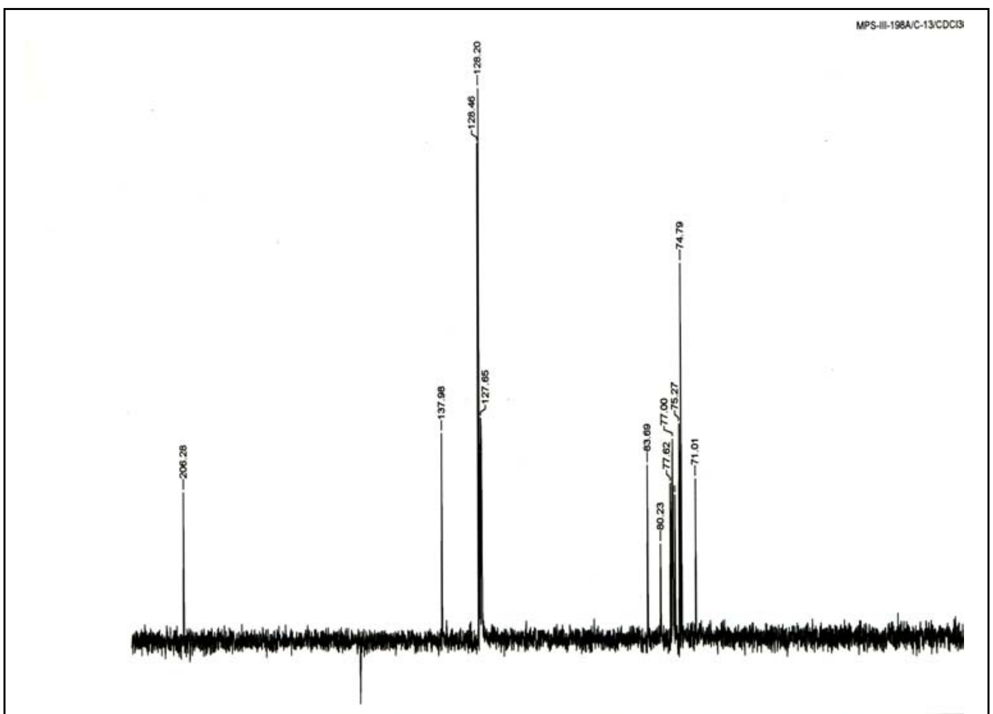
MPS-III-198A/C-13/CDCl3
128.20
128.46
127.65
137.98
206.28
74.79
75.27
77.00
77.62
83.69
80.23
71.01

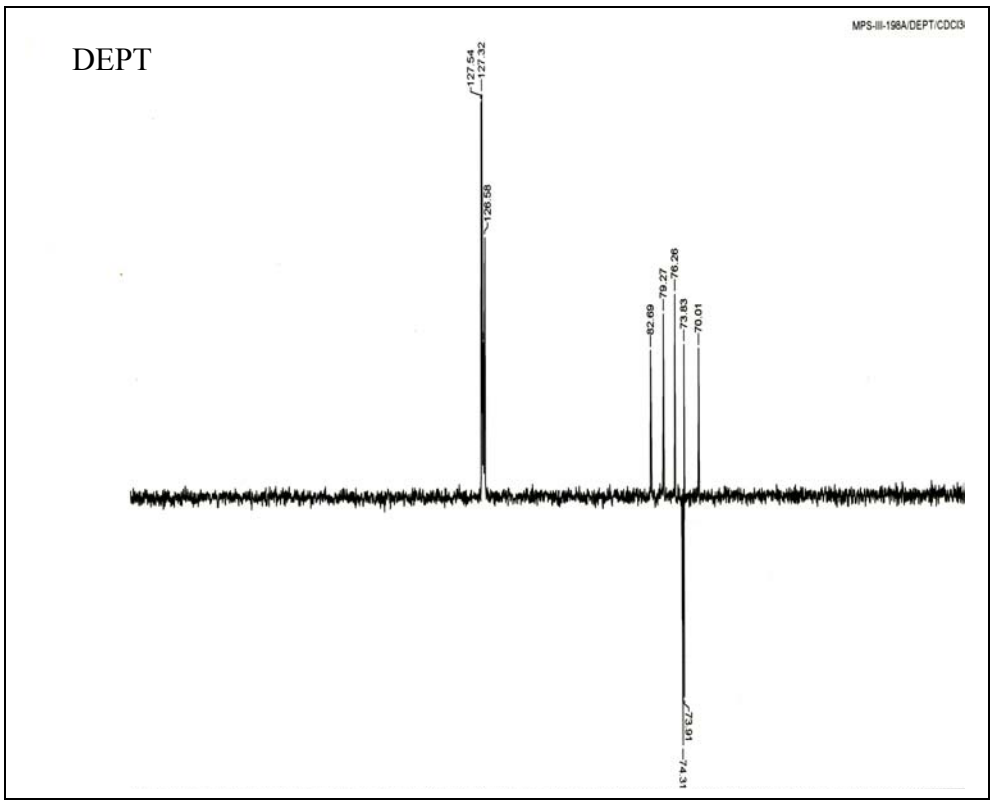
DEPT
MPS-III-198A/DEPT/CDCl3
127.54
127.32
126.58
82.69
79.27
76.26
73.83
70.01
73.91
74.31

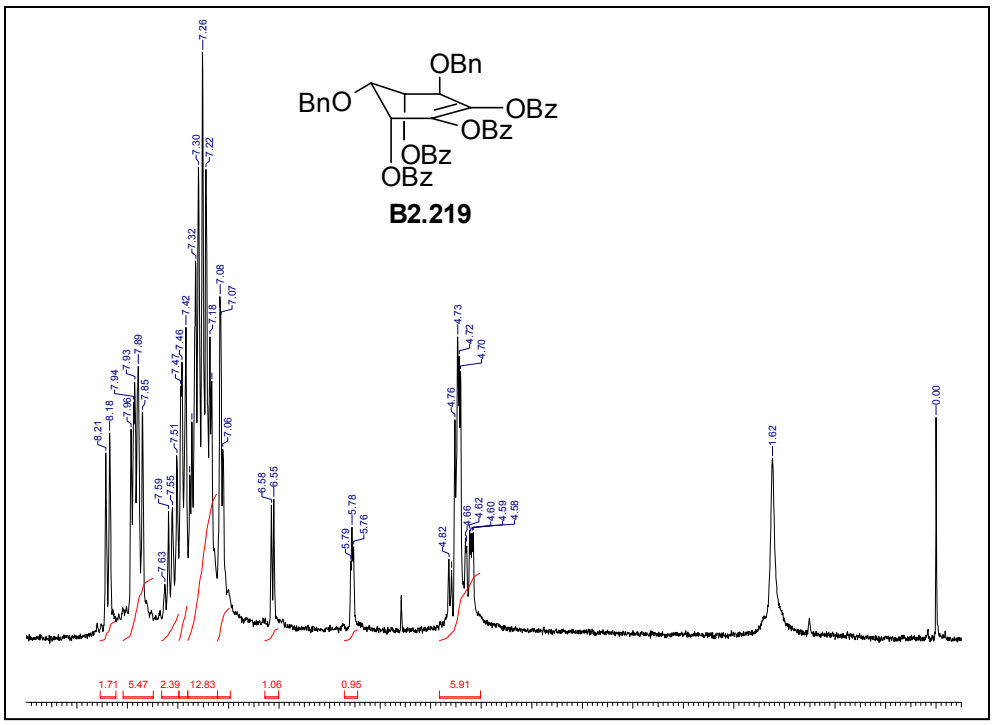
OBn
BnO
OBz
OBz
OBz
OBz
B2.219
8.21
8.18
7.94
7.93
7.89
7.86
7.85
7.59
7.55
7.51
7.47
7.46
7.42
7.32
7.30
7.26
7.22
7.18
7.08
7.07
7.06
7.03
6.58
6.55
5.78
5.76
5.73
4.82
4.76
4.73
4.72
4.70
4.66
4.62
4.60
4.59
4.58
1.62
0.00
1.71
5.47
2.39
12.83
1.06
0.95
5.91

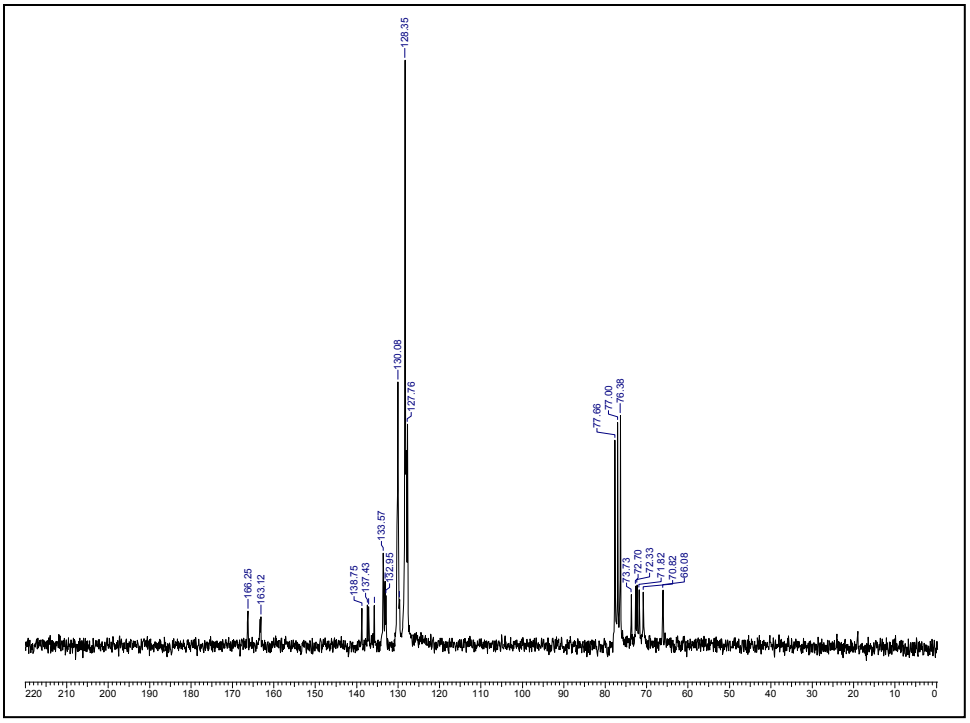
128.35
130.08
127.76
77.66
77.00
76.38
166.25
163.12
138.75
137.43
133.57
132.95
73.73
72.70
72.33
71.82
70.82
66.08
220 210 200 190 180 170 160 150 140 130 120 110 100 90 80 70 60 50 40 30 20 10 0

DEPT

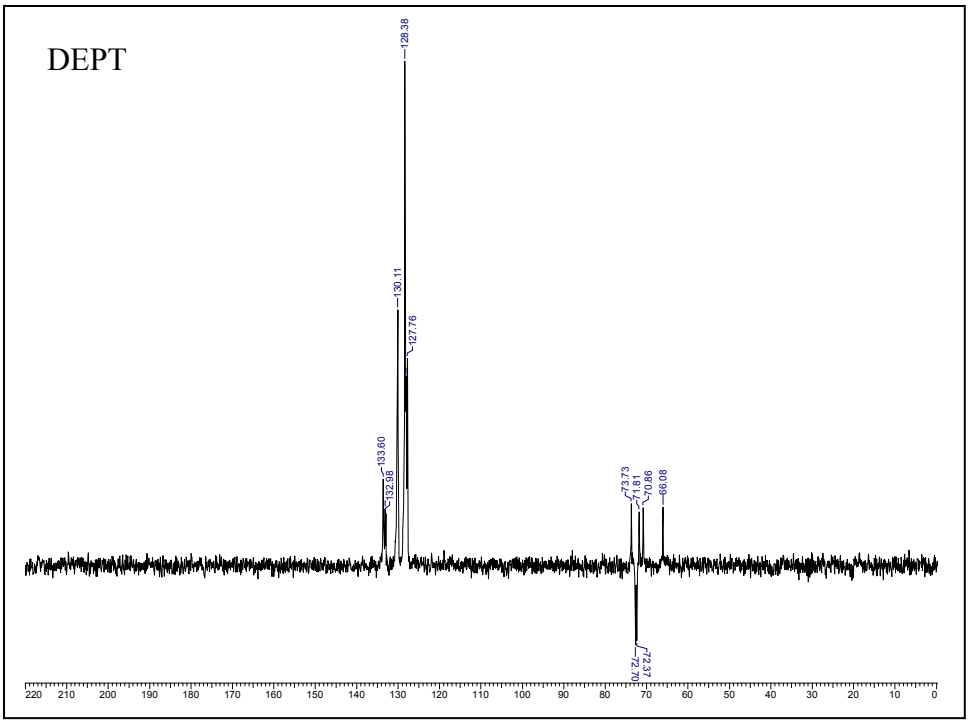
128.38
130.11
127.76
133.60
132.98
73.73
71.81
70.86
66.08
72.37
72.70
220 210 200 190 180 170 160 150 140 130 120 110 100 90 80 70 60 50 40 30 20 10 0

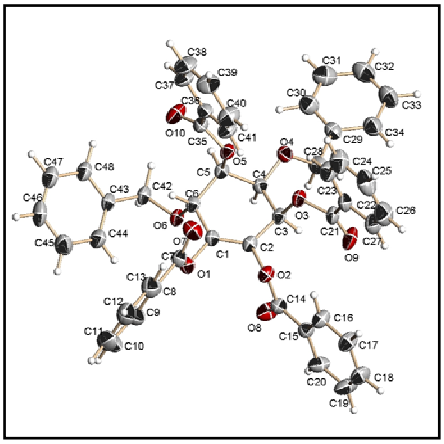

ORTEP of **B2.219**

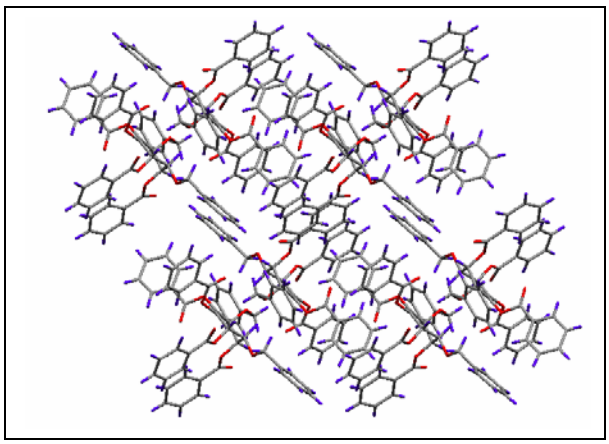

Packing of **B2.219** down the b-axis

Crystal data table of **B2.219**

Identification code	**B2.219** (chloroform-light petroleum crystals)
Empirical formula	$C_{32}H_{25.33}O_{6.76}$
Formula weight	516.52
Temperature	293(2) K
Wavelength	0.71073 Å
Crystal system, space group	Triclinic, *P*-1
Unit cell dimensions	a = 12.640(4) Å; α = 69.402(5)° b = 13.600(4) Å; β = 64.625(4)° c = 13.835(4) Å; γ = 81.265(5)°
Volume	2011.5(10) $Å^3$
Z, Calculated density	3, 1.279 Mg/m^3
Absorption coefficient	0.090 mm^{-1}
F(000)	812
Crystal size	0.24 × 0.17 × 0.15 mm
θ range for data collection	1.60 to 25.00°
Limiting indices	-15<=h<=15; -16<=k<=16;-6<=l<=16
Reflections collected / unique	19324 / 7070 [R(int) = 0.0276]
Completeness to θ = 25.00	99.7%
Max. and min. transmission	0.9869 and 0.9787
Refinement method	Full-matrix least-squares on F^2
Data / restraints / parameters	7070 / 0 / 675
Goodness-of-fit on F^2	1.013
Final R indices [I>2σ (I)]	R1 = 0.0442, wR2 = 0.0997
R indices (all data)	R1 = 0.0776, wR2 = 0.1143
Extinction coefficient	None
Largest diff. peak and hole (ρ_{max} & ρ_{min})	0.208 and -0.127 e. $Å^{-3}$

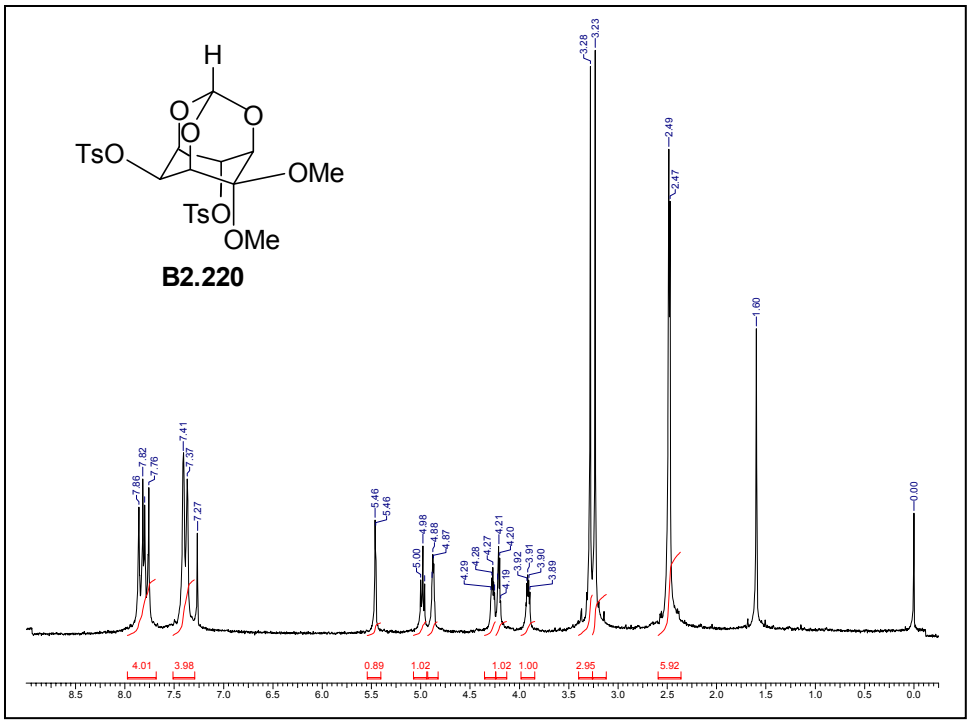
H
O
O
O
TsO
OMe
TsO
OMe
B2.220
7.86
7.82
7.76
7.41
7.37
7.27
5.46
5.46
5.00
4.98
4.88
4.87
4.29
4.28
4.27
4.21
4.20
3.92
3.91
3.90
3.89
3.28
3.23
2.49
2.47
1.60
0.00
4.01
3.98
0.89
1.02
1.02
1.00
2.95
5.92

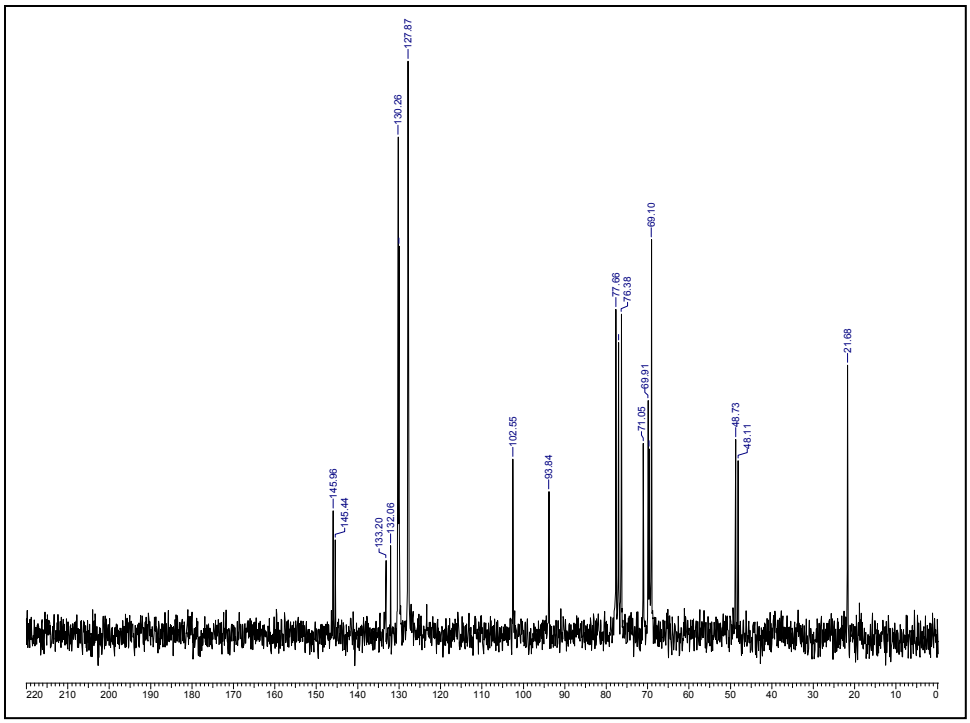
127.87
130.26
77.66
76.38
69.10
69.91
71.05
21.68
102.55
93.84
48.73
48.11
145.96
145.44
133.20
132.06
220 210 200 190 180 170 160 150 140 130 120 110 100 90 80 70 60 50 40 30 20 10 0

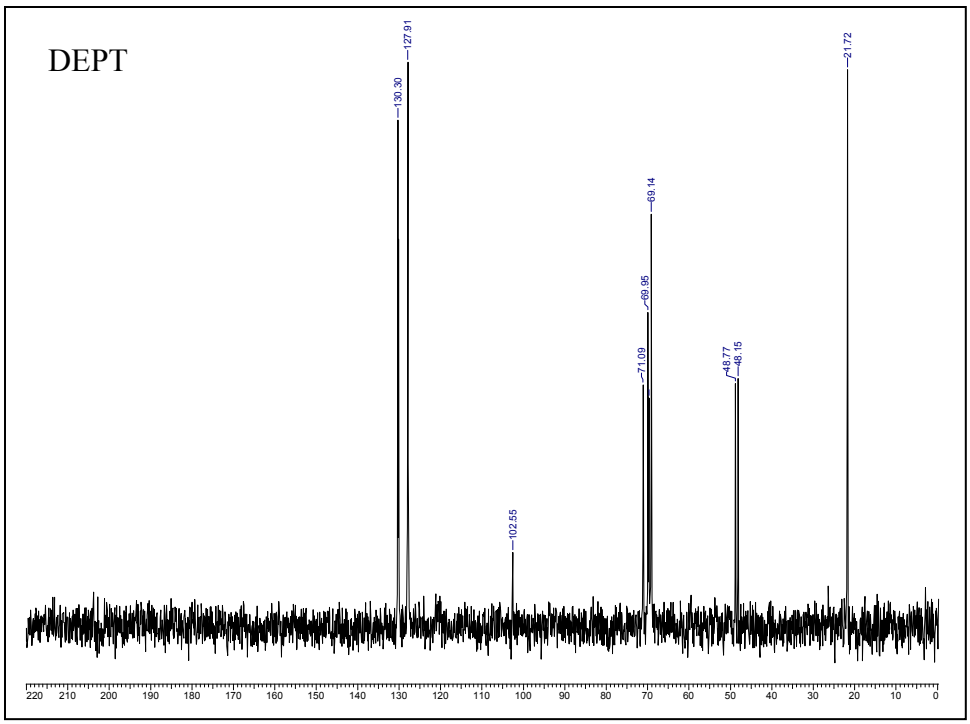
DEPT
127.91
130.30
21.72
69.14
69.95
71.09
48.77
48.15
102.55
220 210 200 190 180 170 160 150 140 130 120 110 100 90 80 70 60 50 40 30 20 10 0

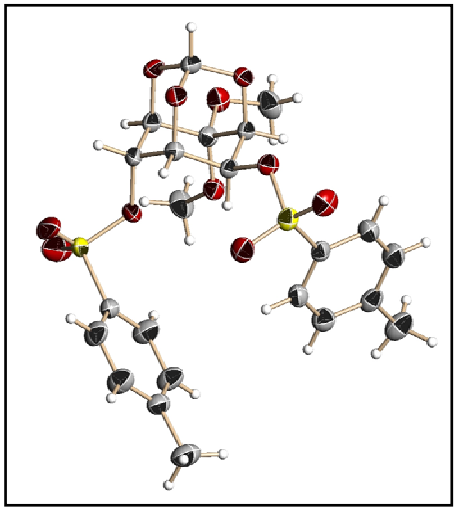

ORTEP of **B2.220**

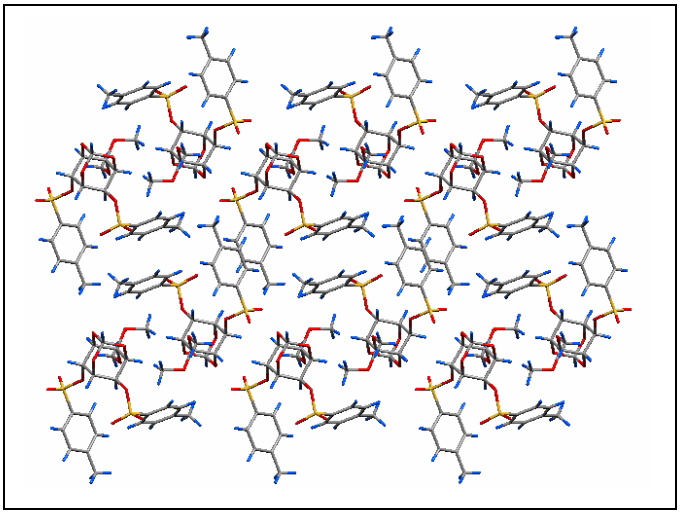

Packing of **B2.220** down the a-axis

Crystal data table of **B2.220**

Identification code	**B2.220** (Crystallized from chloroform-light petroleum)
Empirical formula	$C_{23}H_{26}O_{11}S_2$
Formula weight	542.56
Temperature	556(2) K
Wavelength	0.71073 Å
Crystal system, space group	Triclinic, *P*-1
Unit cell dimensions	a = 8.342(3) Å; α = 86.414(7)° b = 12.026(5) Å; β = 76.133(8)° c = 12.683(5) Å; γ = 88.602(10)°
Volume	1232.8(8) $Å^3$
Z, Calculated density	2, 1.462 Mg/m^3
Absorption coefficient	0.276 mm^{-1}
F(000)	568
Crystal size	0.52 × 0.20 × 0.09 mm
θ range for data collection	1.66 to 25.00°
Limiting indices	-9<=h<=9; -14<=k<=14; -15<=l<=15
Reflections collected / unique	11766 / 4318 [R(int) = 0.0210]
Completeness to θ = 25.00	99.7%
Max. and min. transmission	0.9753 and 0.8706
Refinement method	Full-matrix least-squares on F^2
Data / restraints / parameters	4318 / 0 / 429
Goodness-of-fit on F^2	1.040
Final R indices [I>2σ (I)]	R1 = 0.0417, wR2 = 0.1106
R indices (all data)	R1 = 0.0532, wR2 = 0.1172
Extinction coefficient	None
Largest diff. peak and hole (ρ_{max} & ρ_{min})	0.276 and -0.128 e. $Å^{-3}$

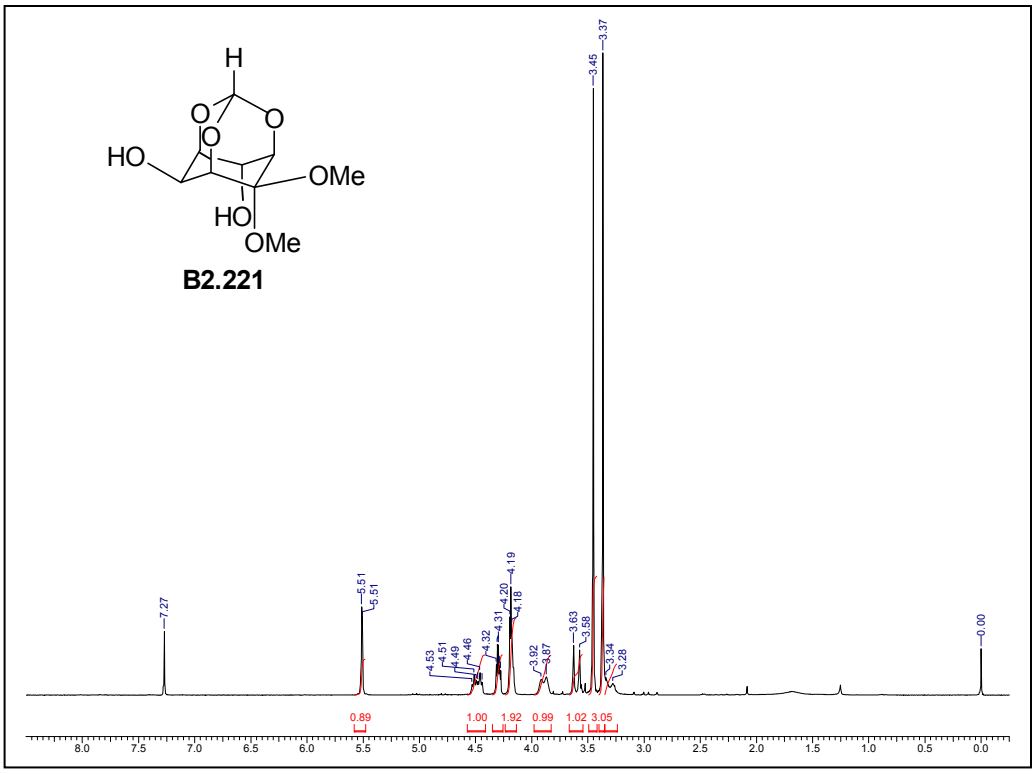
H
O
O
O
HO
OMe
HO
OMe
B2.221
3.45
3.37
7.27
5.51
5.51
4.53
4.51
4.49
4.46
4.32
4.31
4.20
4.19
4.18
3.92
3.87
3.63
3.58
3.34
3.28
0.00
0.89
1.00
1.92
0.99
1.02
3.05
8.0
7.5
7.0
6.5
6.0
5.5
5.0
4.5
4.0
3.5
3.0
2.5
2.0
1.5
1.0
0.5
0.0

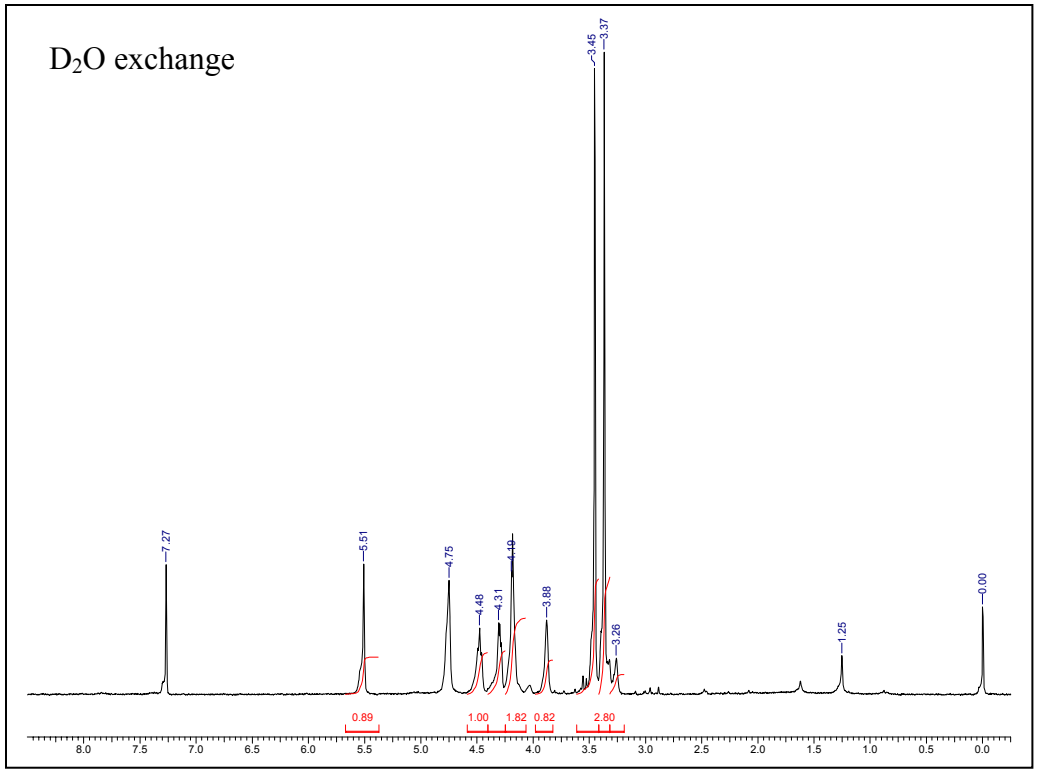
D2O exchange
3.45
3.37
7.27
5.51
4.75
4.48
4.31
4.19
3.88
3.26
1.25
0.00
0.89
1.00
1.82
0.82
2.80
8.0
7.5
7.0
6.5
6.0
5.5
5.0
4.5
4.0
3.5
3.0
2.5
2.0
1.5
1.0
0.5
0.0

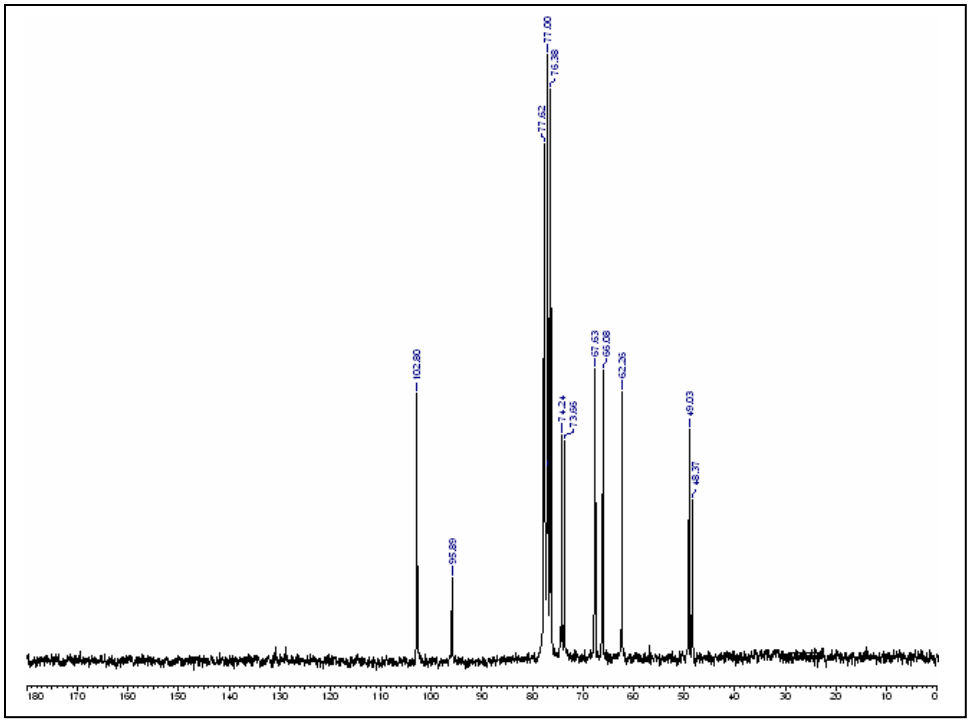
77.00
76.38
77.62
102.80
95.89
67.63
66.08
62.35
74.24
73.66
49.03
48.37
180 170 160 150 140 130 120 110 100 90 80 70 60 50 40 30 20 10 0

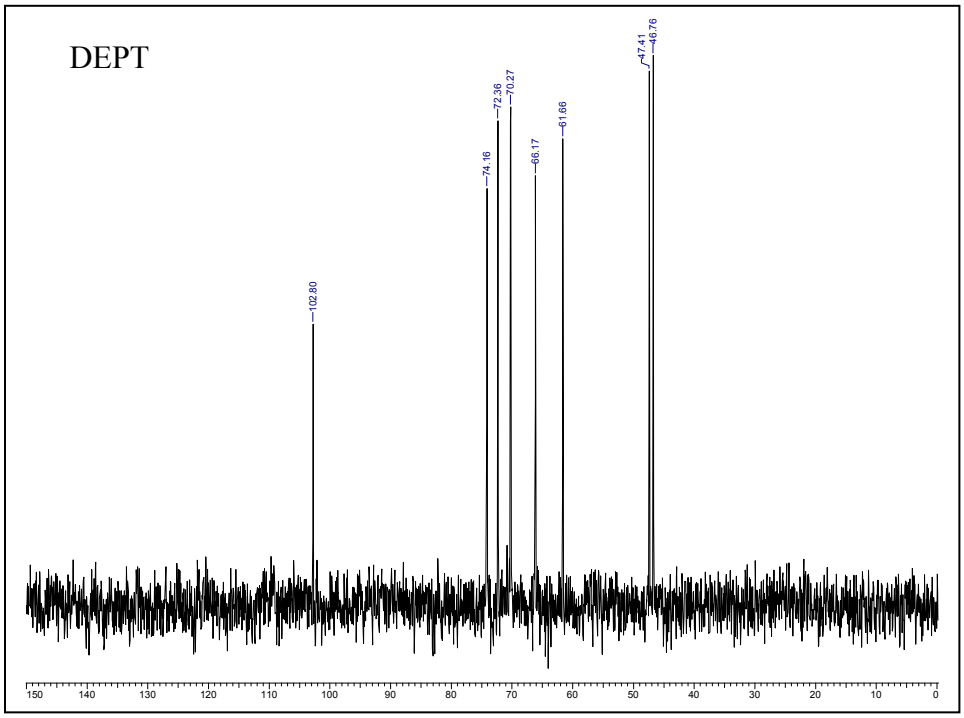
DEPT
47.41
46.76
72.36
70.27
74.16
66.17
61.66
102.80
150 140 130 120 110 100 90 80 70 60 50 40 30 20 10 0

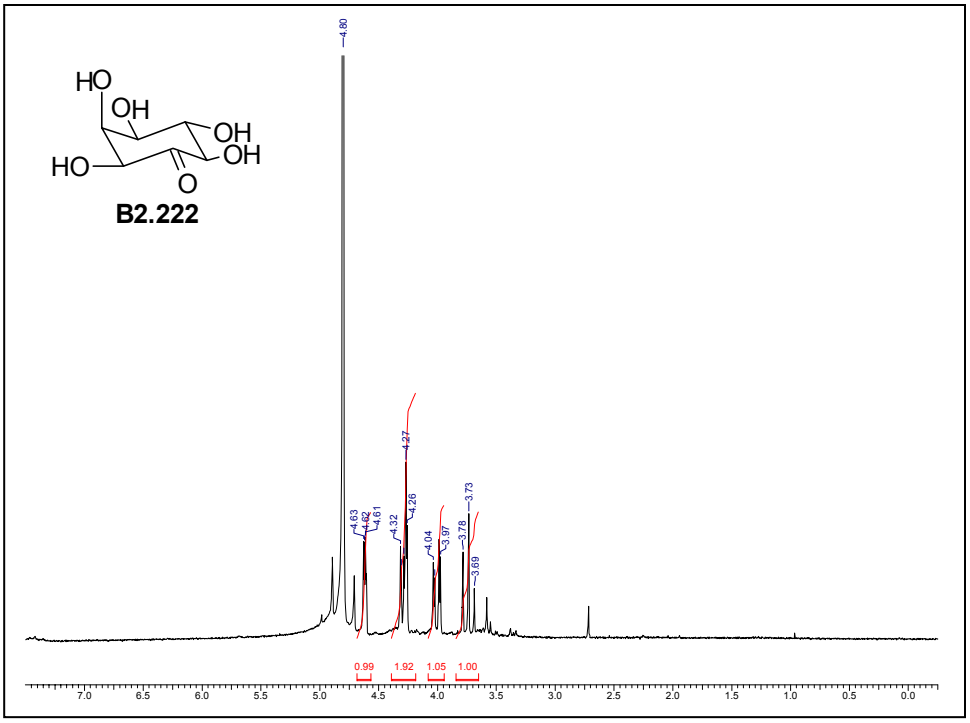
HO
OH
OH
OH
HO
O
B2.222
4.80
4.63
4.62
4.61
4.32
4.27
4.26
4.04
3.97
3.78
3.73
3.69
0.99
1.92
1.05
1.00
7.0
6.5
6.0
5.5
5.0
4.5
4.0
3.5
3.0
2.5
2.0
1.5
1.0
0.5
0.0